UNITED STATES PATENT AND TRADEMARK OFFICE

BEFORE THE PATENT TRIAL AND APPEAL BOARD

APPLE INC.,
Petitioner,

v.

MASIMO CORPORATION,
Patent Owner.

Case IPR2022-01291
U.S. Patent 10,687,745

DECLARATION OF ANNE KOCH BALAND

I, ANNE KOCH BALAND, hereby declare the following:

1. I am over the age of 18, have personal knowledge of the facts set forth herein, and am competent to testify to the same. I am a document delivery librarian in the library department of Fish & Richardson P.C. (hereafter "FR Library").

2. I earned a Master of Library Science (MLIS) from Dominican University in 2007. I have over 15 years of experience in the library/information science field.

3. I am experienced in library cataloging. My responsibilities at the FR Library include, among other things, accessing and securing copies of documents requested by attorneys and other staff at FR.

I. **Exhibit 1039**

4. On or around September 8, 2023, I personally retrieved and viewed ITC Inv. No. 337-TA-1276 Exhibit RX-0504, which is a copy of a document entitled "Optimization of Reflectance-Mode Pulse Oximeter Sensors" by Austin Wareing, included below as Appendix A. I accessed the website of Lexis® CourtLink® at https://www.lexisnexis.com/en-us/products/courtlink.page and searched for and located the referenced ITC exhibit. Comparing Exhibit 1039 to

the document attached as Appendix A to this declaration, I certify that Exhibit 1039 is a true and correct copy of ITC Inv. No. 337-TA-1276 Exhibit RX-0504.

II. Exhibit 1040

5. On or around September 8, 2023, I personally retrieved and viewed ITC Inv. No. 337-TA-1276 Exhibit RX-0508, which is a copy of a paper entitled "Stimulating Student Learning with a Novel 'In-House' Pulse Oximeter Design" by Jianchu Yao and Steve Warren, included below as Appendix B. I accessed the website of Lexis® CourtLink® at https://www.lexisnexis.com/en-us/products/courtlink.page and searched for and located the referenced ITC exhibit. Comparing Exhibit 1040 to the document attached as Appendix B to this declaration, I certify that Exhibit 1040 is a true and correct copy of ITC Inv. No. 337-TA-1276 Exhibit RX-0508.

III. Exhibit 1041

6. On or around September 8, 2023, I personally retrieved and viewed ITC Inv. No. 337-TA-1276 Exhibit RX-0632, included below as Appendix C. I accessed the website of Lexis® CourtLink® at https://www.lexisnexis.com/en-us/products/courtlink.page and searched for and located the referenced ITC exhibit. Comparing Exhibit 1041 to the document attached as Appendix C to this declaration, I certify that Exhibit 1041 is a true and correct copy of ITC Inv. No. 337-TA-1276 Exhibit RX-0632.

IV. Exhibit 1043

7. I personally obtained and viewed an excerpt including the definition of "correspond" from The American Heritage Dictionary of the English Language, Fifth Edition (Houghton Mifflin Harcourt Publishing Company 2011), included below as Appendix D. The excerpt was obtained from Retriev-It (https://www.retrievit.com), a document retrieval company, on or around September 8, 2023. Comparing Exhibit 1043 to the document attached as Appendix D to this declaration, I certify that Exhibit 1043 is a true and correct copy of the excerpt from The American Heritage Dictionary of the English Language, Fifth Edition (Houghton Mifflin Harcourt Publishing Company 2011) obtained from Retriev-It.

V. Exhibit 1044

8. I personally obtained and viewed the excerpt including the definition of "correspond" from Collins Dictionary (HarperCollins Publishers 2010), included below as Appendix E. The excerpt was obtained from Retriev-It (https://www.retrievit.com), on or around September 8, 2023. Comparing Exhibit 1044 to the document attached as Appendix E to this declaration, I certify that Exhibit 1044 is a true and correct copy of the excerpt from Collins Dictionary (HarperCollins Publishers 2010) obtained from Retriev-It.

VI. Exhibit 1045

9. I personally obtained and viewed an excerpt including the definition of "correspond" from Merriam-Webster's Collegiate Dictionary, Eleventh Edition (Merriam-Webster, Incorporated 2014), included below as Appendix F. The excerpt was obtained from Retriev-It (https://www.retrievit.com), on or around September 8, 2023. Comparing Exhibit 1045 to the document attached as Appendix F to this declaration, I certify that Exhibit 1045 is a true and correct copy of the excerpt from Merriam-Webster's Collegiate Dictionary, Eleventh Edition (Merriam-Webster, Incorporated 2014) obtained from Retriev-It.

VII. Exhibit 1046

10. I personally obtained and viewed an excerpt from the publication titled "The Biomedical Engineering Handbook" by Joseph D. Bronzino (CRC Press, Inc. 1995), included below as Appendix G. The publication was obtained from Research Solutions (https://www.researchsolutions.com), a document retrieval company, on or around September 8, 2023. Comparing Exhibit 1046 to the document attached as Appendix G to this declaration, I certify that Exhibit 1046 is a true and correct copy of the excerpt from "The Biomedical Engineering Handbook" by Joseph D. Bronzino (CRC Press, Inc. 1995) obtained from Research Solutions.

VIII. Exhibit 1048

11. On or around September 8, 2023, I personally retrieved and viewed the paper entitled "Recent Developments in Pulse Oximetry," by John W. Severinghaus and Joseph F. Kelleher published in Anesthesiology, Vol. 76, No. 6 (June 1992), included below as Appendix H. I accessed the website of Anesthesiology at https://pubs.asahq.org/anesthesiology and searched for and located the referenced publication. Comparing Exhibit 1048 to the document attached as Appendix H to this declaration, I certify that Exhibit 1048 is a true and correct copy of "Recent Developments in Pulse Oximetry," by John W. Severinghaus and Joseph F. Kelleher published in Anesthesiology, Vol. 76, No. 6 (June 1992).

IX. Exhibit 1049

12. On or around September 8, 2023, I personally retrieved and viewed the article entitled "MIO Alpha BLE Review" by Jill Duffy published on the PC Magazine website (Jan. 28, 2013), included below as Appendix I. I accessed the website of PC Magazine at https://www.pcmag.com/reviews/mio-alpha-ble to retrieve the referenced article. Comparing Exhibit 1049 to the document attached as Appendix I to this declaration, I certify that Exhibit 1049 is a true and correct copy of "MIO Alpha BLE Review" by Jill Duffy published on the PC Magazine website (Jan. 28, 2013).

X. Exhibit 1050

13. I personally retrieved and viewed the publication entitled "A Neo-Reflective Wrist Pulse Oximeter," by Grantham Pang and Chao Ma published by IEEE in IEEE Access, Volume 2 (January 12, 2015), included below as Appendix J. I accessed the website of IEEE Xplore at https://ieeexplore.ieee.org/Xplore/home.jsp and searched for and located the referenced publication. Comparing Exhibit 1050 to the document attached as Appendix J to this declaration, Exhibit 1050 is a true and correct copy of "A Neo-Reflective Wrist Pulse Oximeter," by Grantham Pang and Chao Ma.

XI. Exhibit 1051

14. I personally retrieved and viewed the publication entitled "A Wireless Reflectance Pulse Oximeter With Digital Baseline Control for Unfiltered Photoplethysmograms" by Kejia Li and Steve Warren published in IEEE Transactions on Biomedical Circuits and Systems, Vol. 6, No. 3 (June 2012), included below as Appendix K. I accessed the website of IEEE Xplore at https://ieeexplore.ieee.org/Xplore/home.jsp and searched for and located the referenced publication on or around September 8, 2023. Comparing Exhibit 1051 to the document attached as Appendix K to this declaration, I certify that Exhibit 1051 is a true and correct copy "A Wireless Reflectance Pulse Oximeter With

Digital Baseline Control for Unfiltered Photoplethysmograms" by Kejia Li and Steve Warren.

XII. Exhibit 1052

15. On or around September 8, 2023, I personally retrieved and viewed U.S. Patent Application Publication No. 2006/0253010 issued to Brady et al., included below as Appendix L. I accessed the website of Patsnap at https://www.patsnap.com, accessed a user account, and searched for and located the referenced publication. Comparing Exhibit 1052 to the document attached as Appendix L to this declaration, I certify that Exhibit 1052 is a true and correct copy of U.S. Patent Application Publication No. 2006/0253010 to Brady et al.

XIII. Exhibit 1053

16. On or around September 8, 2023, I personally retrieved and viewed the publication entitled "Implementation of a Wireless Pulse Oximeter Based on Wrist Band Sensor" by Cai et al. published for the 3rd International Conference on Biomedical Engineering and Informatics (BMEI 2010), included below as Appendix M. I accessed the website of IEEE Xplore at https://ieeexplore.ieee.org/Xplore/home.jsp and searched for and located the referenced publication. Comparing Exhibit 1053 to the document attached as Appendix M to this declaration, I certify that Exhibit 1053 is a true and correct

copy of "Implementation of a Wireless Pulse Oximeter Based on Wrist Band Sensor" by Cai et al.

XIV. Exhibit 1054

17. I personally retrieved and viewed International Publication No. WO 2001/17421 by Lindberg et al, included below as Appendix N. I accessed the website of Patsnap at https://www.patsnap.com, accessed a user account, and searched for and located the referenced publication on or around September 8, 2023. Comparing Exhibit 1054 to the document attached as Appendix N to this declaration, I certify that Exhibit 1054 is a true and correct copy of International Publication No. WO 2001/17421 by Lindberg et al.

XV. Exhibit 1055

18. I personally retrieved and viewed the publication entitled, "Optimum Place for Measuring Pulse Oximeter Signal in Wireless Sensor-Belt or Wrist-Band" by Maattala et al. published for the 2007 International Conference on Convergence Information Technology by the Institute of Electrical and Electronics Engineers (IEEE) (2007), included below as Appendix O. I accessed the website of IEEE Xplore at https://ieeexplore.ieee.org/Xplore/home.jsp and searched for and located the referenced publication on or around September 8, 2023. Comparing Exhibit 1055 to the document attached as Appendix O to this declaration, I certify

that Exhibit 1055 is a true and correct copy of "Optimum Place for Measuring Pulse Oximeter Signal in Wireless Sensor-Belt or Wrist-Band," by Maattala et al.

XVI. Exhibit 1056

19. I personally retrieved and viewed the publication entitled "Reflectance-Based Pulse Oximeter for the Chest and Wrist" by Fontaine et al. submitted to the Worchester Polytechnic Institute, included below as Appendix P. I accessed the website of the Worcester Polytechnic Institute at https://www.wpi.edu and searched for and located the referenced publication on or around September 8, 2023. Comparing Exhibit 1056 to the document attached as Appendix P to this declaration, I certify that Exhibit 1056 is a true and correct copy of "Reflectance-Based Pulse Oximeter for the Chest and Wrist" by Fontaine et al.

XVII. Exhibit 1058

20. I personally retrieved and viewed U.S. Patent No. 7,468,036 issued to Rulkov et al., included below as Appendix Q. I accessed the website of Patsnap at https://www.patsnap.com, accessed a user account, and searched for and located the referenced publication on or around September 8, 2023. Comparing Exhibit 1058 to the document attached as Appendix Q to this declaration, I certify that Exhibit 1058 is a true and correct copy of U.S. Patent No. 7,468,036 issued to Rulkov et al.

XVIII. Exhibit 1069

21. I personally retrieved and viewed the publication entitled "Optical Oximetry Sensors for Whole Blood and Tissue" by Setsuo Takatani and Jian Ling published in IEEE Engineering in Medicine and Biology (June/July 1994), included below as Appendix R. I accessed the website of IEEE Xplore at https://ieeexplore.ieee.org/Xplore/home.jsp and searched for and located the referenced publication on or around September 8, 2023. Comparing Exhibit 1069 to the document attached as Appendix R to this declaration, I certify that Exhibit 1069 is a true and correct copy of "Optical Oximetry Sensors for Whole Blood and Tissue" by Setsuo Takatani and Jian Ling.

XIX. Exhibit 1076

22. I personally retrieved and viewed the web page entitled "Beam Shaping with Cylindrical Lenses" published by Newport Corporation at https://www.newport.com/n/beam-shaping-with-cylindrical-lenses, included below as Appendix S. I accessed the web page https://www.newport.com/n/beam-shaping-with-cylindrical-lenses of Newport Corporation's website and retrieved the referenced web page on or around September 8, 2023. Comparing Exhibit 1076 to the document attached as Appendix S to this declaration, I certify that Exhibit 1076 is a true and correct copy of "Beam Shaping with Cylindrical Lenses," by the Newport Corporation.

XX. Exhibit 1077

23. On or around September 12, 2003, I personally retrieved and viewed the publication entitled "Laser Beam Shaping Theory and Techniques, Second Edition" by Fred M. Dickey published by Taylor & Francis Group, LLC (2014). I accessed the website of Amazon at www.amazon.com, accessed a user account, and searched for, located, and purchased the Kindle version of the referenced publication; a receipt of the purchase and screenshots of the Kindle version are attached as Appendix T. Comparing Exhibit 1077 to the document attached as Appendix T to this declaration, Exhibit 1077 is a true and correct copy of "Laser Beam Shaping Theory and Techniques, Second Edition" by Fred M. Dickey.

XXI. Exhibit 1078

24. On or around September 8, 2023, I personally retrieved and viewed the publication entitled "Micro-LED Technologies and Applications" by Lee et al. published in Information Display (June 2016), included below as Appendix U. I accessed the website of The Society for Information Display at https://sid.onlinelibrary.wiley.com and searched for and located the referenced publication. Comparing Exhibit 1078 to the document attached as Appendix U to this declaration, I certify Exhibit 1078 is a true and correct copy of "Micro-LED Technologies and Applications" by Lee et al.

26. I hereby declare that all statements made herein of my own knowledge are true and that all statements made on information and belief are believed to be true; and further that these statements were made with the knowledge that willful false statements and the like so made are punishable by fine or imprisonment, or both, under Section 1001 of Title 18 of the United States Code.

Respectfully submitted,

/Anne Koch Baland/

Date: September 12, 2023

Anne Koch Baland

APPENDIX A

Optimization of Reflectance-Mode Pulse Oximeter Sensors

Austin Wareing, B.S.

Sponsor: National Science Foundation Research Experiences for Undergraduates Program; Advisor: Steve Warren, Ph.D.

Pulse oximeters provide physiological information such as heart rate and blood oxygen saturation. These devices acquire measurements using red and infrared light that passes through the patients skin and underlying tissue. Pulse oximeter sensors can either be transmission-mode, where light passes completely through the tissue and is collected on an opposing skin surface, or reflection-mode, where light is reflected back towards the sensor and collected in the same region as the incident light. Reflectance-mode sensors offer more measurement-site flexibility since they are only mounted on one side of the skin. However, these sensors are at a disadvantage since they collect only a fraction of the light reflected from tissue, which is primarily forward scattering. Increasing the reliability and quality of reflectance-mode signals will make these sensors a more attractive alternative to traditional transmission-mode designs.

Previous Design

- One photodiode collects reflected red and infrared signals, resulting in poor efficiency and a smaller signal-to-noise ratio.
- Hard plastic material does not conform to most skin surfaces.
- More ambient light noise due to holes in plastic and inability to mold to a curved surface.

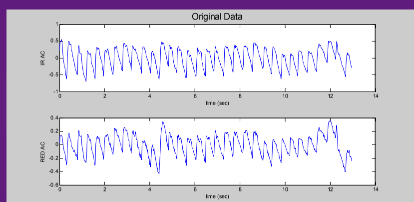

- Signal-to-noise ratio is highly dependent on sensor movement.
- Signal is often difficult to obtain, requiring several attempts to collect viable data.

Optimized Design

- Multiple photodiodes collect more of the reflected light, forming a radial pattern around the source(s).
- Pliable material allows the sensor to conform to the measurement site.
- Less susceptible to ambient noise due to opaque material and flexible design.

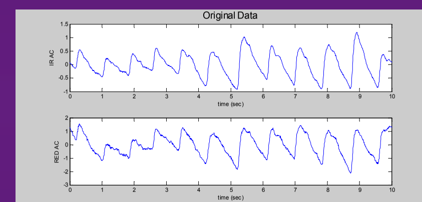

- Output signal exhibits greater signal-to-noise ratio.
- Signal is also more reliable than with the previous design; less effort is required to collect viable data.

Pulse Oximeter Sensor

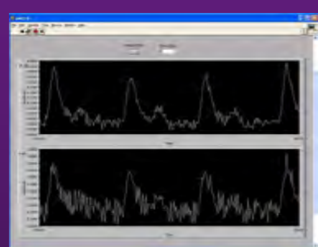

- Small, Lightweight components are unimposing to the wearer.
- Provides time-domain plethysmograms that can be used to calculate different physiological parameters.

Measurement Site Comparison

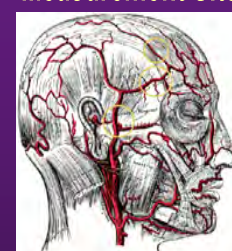

Viable and Unobtrusive Measuring Sites

- Middle temporal artery (in front of ear)
- Frontal branch (along hair line)
- Wrist

Finger

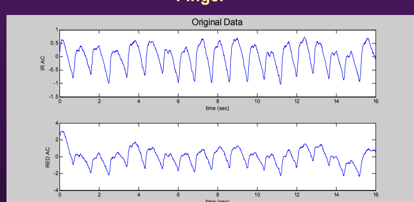

Middle Temporal Artery

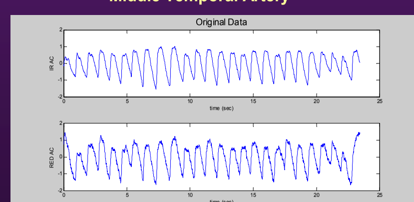

- Measurements from sites on the head are similar to those collected from sites on the finger.
- Head-mounted sensors have also proven to be less obtrusive since they do not impede movement or use of the hands.

This material is based upon work supported by the National Science Foundation under grants BES–0440183 and BES–0093916. Opinions, findings, conclusions, or recommendations expressed in this material are those of the author(s) and do not necessarily reflect the views of the NSF.

APPENDIX B

Stimulating Student Learning with a Novel "In-House" Pulse Oximeter Design

Jianchu Yao, M.S. and Steve Warren, Ph.D.
Department of Electrical & Computer Engineering, Kansas State University
Manhattan, KS 66506, USA

Abstract

This paper addresses the design of a plug-and-play pulse oximeter and its application to a biomedical instrumentation laboratory and other core Electrical Engineering courses. The low-cost, microcontroller-based unit utilizes two light-emitting diodes as excitation sources, acquires reflectance data with a photodiode, and sends these raw photo-plethysmographic data to a personal computer via an RS-232 serial link. A LabVIEW interface running on the personal computer processes these raw data and stores the results to a file. The design of this pulse oximeter is unique in two ways: the excitation sources are driven just hard enough to always keep the photodiode active (meaning the sensor can be used in ambient light), and the hardware separates out the derivatives of the red and infrared photo-plethysmograms so that it can amplify the pulsatile component of each signal to fill the range of the analog-to-digital converter. Unlike commercial pulse oximeters whose packaging hides the hardware configuration from the students, the open, unpackaged design stimulates student interest and encourages dialogue with the developer; the in-house nature of the design appeals to students. Moreover, most pulse oximeters on the market are expensive and provide users with a front panel that displays only percent oxygen saturation and heart rate. This low-cost unit provides unfiltered pulsatile data, allowing students to investigate tradeoffs between different oxygen saturation calculation methods, test different filtering approaches (e.g., for motion artifact reduction), and extract other biomedical parameters (e.g., respiration rate and biometric indicators). Time-domain data from these units have been used in linear systems and scientific computing courses to teach filtering techniques, illustrate discrete Fourier transform applications, introduce time-frequency principles, and test data fitting algorithms.

I. Introduction

An optical pulse oximeter measures the intensity of light passing through heterogeneous tissue and uses variations in this light intensity (primarily resulting from the fractional volume variation of arterial blood) to calculate blood oxygen saturation. Due to its non-invasive nature, high precision in its operational range, and reasonable cost, optical pulse oximetry is widely adopted as a standard patient monitoring technique. Although its foundations date back more than fifty years,[1] many facets of this technology still attract researchers. Current interest areas include motion artifact reduction,[2, 3] power consumption optimization,[4] low-perfusion measurements,[5, 6] and issues germane to various application environments (e.g., wearability for battlefield and home care monitors).[7-9] It is important for biomedical engineering students to understand the principles of pulse oximetry, hardware/software design issues, and signal processing approaches.

Pulse oximeter design addresses engineering areas such as optical component selection, mechanical layout, circuit design, microprocessor control, digital communication, and signal processing. Therefore, a pulse oximeter not only serves as an excellent study vehicle that allows students to learn techniques such as photoplethysmographic signal processing; it also provides a platform where students can acquire hands-on experience in practical device design. In addition, the real-time data that a pulse oximeter offers gives instructors flexibility when assigning projects and homework to students of various educational levels (graduate and undergraduate) and backgrounds (e.g., electrical engineering or biology).

Many commercial pulse oximeters display calculated parameters (i.e., percent oxygen saturation and heart rate) on their front panels, hiding the original unfiltered data from which these calculations were made. In this paper, we present an "in-house" pulse oximeter that provides raw sensor data for use in the classroom. The device is utilized in bioinstrumentation laboratory sessions, and its data provide real-world signals to other core Electrical Engineering courses.

This paper first briefly describes the theory behind photoplethysmographic (PPG) pulse oximetry. It then presents the development of a pulse oximeter, emphasizing design features that enable its application to education. These features include (a) a stand-alone pulse oximeter module with a novel circuit design, an open form-factor, and multiple signal outputs, (b) a personal computer station with a flexible, user friendly LabVIEW interface and a variety of signal processing options, and (c) the production of raw data that can be used for parameter extraction exercises. The paper describes how this device and it features have been applied in classroom environments to stimulate student learning. Several examples are introduced in detail, including (a) a pulse oximetry laboratory/lecture pair for a bioinstrumentation course sequence, (b) data sources for course projects in Linear Systems (EECE 512) and Scientific Computing (EECE 840), and (c) a platform upon which undergraduate honors research students can build. This approach can be extended to other devices and classes.

II. Theory – Principles of Pulse Oximetry

PPG pulse oximetry relies on the fractional change in light absorption due to arterial pulsations. In a typical configuration, light at two different wavelengths illuminating one side of tissue (e.g., a finger) will be detected on the same side (reflectance mode) or the opposing side (transmission mode) after traversing the vascular tissues between the source and the detector.[10] When a fingertip is simplified as a hemispherical volume that is a homogenous mixture of blood (arterial and venous) and tissue, the detected light intensity is described by the Beer-Lambert law: [11]

$$I_t = I_0 \left(e^{-\mu_{at}T}\right)\left(e^{-\mu_{av}V}\right)\left(e^{-\mu_{aa}A}\right) \tag{1}$$

where I_0 is the incident light intensity, I_t is the light intensity detected by the photodetector, and μ_{at}, μ_{av}, and μ_{aa} are the absorption coefficients of the bloodless tissue layer, the venous blood layer, and the arterial blood layer, respectively, in units of cm^{-1}.

The heart's pumping action generates arterial pulsations that result in relative changes in arterial blood volume, represented by *dA*, which adds an "ac" component to the detected intensity:

$$dI_t = -I_0 \mu_{aa} \left(e^{-\mu_{at}T}\right)\left(e^{-\mu_{av}V}\right)\left(e^{-\mu_{aa}A}\right) dA \tag{2}$$

Multiple elements contribute to the attenuation of light traveling through tissue, and arterial pulsation has only a small relative effect on the amount of light detected (on the order of one percent or less; see Figure 1).

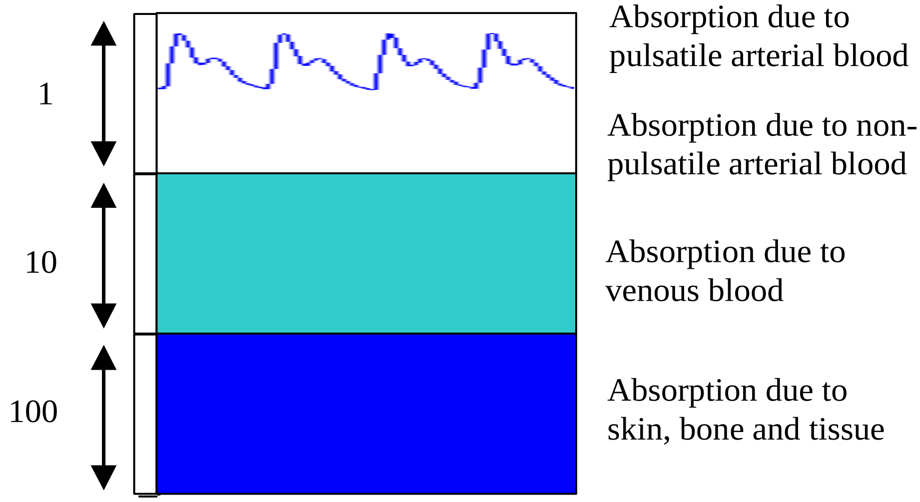

Figure 1. Breakdown of the components in the detected photo-plethysmographic signal.[12]

Dividing this change by the dc value normalizes this variation:

$$\frac{I_{ac}}{I_{dc}} = \frac{dI_t}{I_t} = -\mu_{aa} dA \tag{3}$$

The ratio of the above ratio for two wavelengths ('r' for red, 'IR' for infrared) is given by

$$R = \frac{(dI_t / I_t)_r}{(dI_t / I_t)_{IR}} = \frac{\mu_{a,r}}{\mu_{a,IR}}, \tag{4}$$

where $\mu_{a,i}$ can be expressed as a function of S_aO_2,[13] arterial oxygen saturation:

$$\mu_{a,i} = \frac{H}{v_i}\left[S_aO_2\sigma_a^{100\%} + (1 - S_aO_2)\sigma_a^{0\%}\right] \tag{5}$$

Here, $i = r, IR$, while $\sigma_a^{100\%}$ and $\sigma_a^{0\%}$ are the wavelength-dependent optical absorption cross sections of the red blood cells containing totally oxygenated and totally deoxygenated hemoglobin, respectively. One can therefore calculate arterial oxygen saturation using

$$S_aO_2 = \frac{R\sigma_{a,IR}^{0\%} - \sigma_{a,r}^{0\%}}{\left(\sigma_{a,r}^{100\%} - \sigma_{a,r}^{0\%}\right) + R\left(\sigma_{a,IR}^{0\%} - \sigma_{a,IR}^{100\%}\right)} \tag{6}$$

Equation (6) provides the desired relationship between the experimentally-determined ratio *R* and the arterial oxygen saturation S_aO_2. Researchers assume this relationship applies to monochromatic light sources. In reality, commonly available LEDs are used as light sources and typically have spectral widths of 20 to 50 nm. Therefore, the standard molar absorption coefficient for hemoglobin cannot be used directly in (6). Furthermore, the simplified mathematical description above only approximates a real system that incorporates inhomogeneities and mechanical movement. Consequently, (6) is often represented empirically by fitting clinical data to the following generalized function:

$$S_aO_2 = k_1R + k_2 \tag{7}$$

where, e.g., k_1= -25.6, k_2= 118.8[14] or k_1= -25, k_2= 110.[15]

III. Methods

A. Pulse Oximeter Development

As shown in the functional block diagram in Figure 2, a pulse oximeter consists of three main units: (1) an optical probe, (2) a circuit module that hosts an analog amplifier, signal conditioning element, and microcontroller, and (c) a personal computer that receives data from the circuit module and processes, displays, and stores these data.

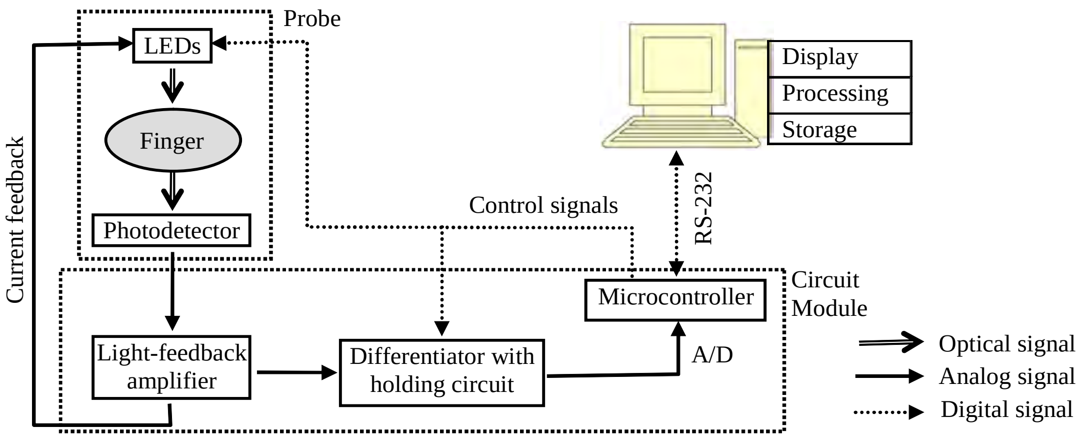

Figure 2. Functional block diagram of the pulse oximeter.

The analog portion of the pulse oximeter consists of a light-feedback amplifier and an analog differentiator with a specialized sample and hold circuit. The current feedback design adjusts the light level at the excitation LEDs such that the detected light intensity is constant, keeping the photodiode centered in its active region. To improve the stability of this feedback loop, a photodiode with smaller gain, rather than a phototransistor, is used as a photodetector. Two LEDs with wavelengths of 660 nm and 940 nm were selected as excitation sources.

As discussed earlier, the “ac” component resulting from arterial blood volume variation is very small. If A/D conversion is performed on the overall signal, this tiny “ac” component will be buried in the “huge” “dc” component after conversion. A differentiator addresses this issue. It removes the “dc” component by subtracting the previous signal voltage-level from the present signal voltage-level and amplifies this difference, yielding the “ac” component. A hold circuit is added to store voltage-levels from the previous sample cycle. The differentiator improves signal resolution by allowing one to take advantage of the full range of the A/D converter.

This circuitry is coordinated by a PIC microcontroller. Three output lines control the operation of the circuitry, and two A/D inputs sample the desired signal. Two outputs modulate the two light sources and switch the charging and discharging of their corresponding hold capacitors. The other output operates the differentiator. The two A/D inputs acquire and digitize two signals: the "dc" signal when the differentiator is turned off (it is actually the original signal that includes both "dc" and "ac" components) and the amplified difference of the present and previous voltage level when the differentiator is turned on.

The PIC microcontroller also operates an RS-232 port to a personal computer running a LabVIEW interface. Digitized data are sent to the PC over this RS-232 interface. Because the sensor module and personal computer communicate asynchronously, and 8 bytes (two bytes for each signal) are sent in each RS-232 packet, a handshaking protocol is used to synchronize the two devices. The PC generates an acknowledgement after successfully receiving each data packet so that the pulse oximeter module can transmit the next data packet.

On the PC, LabVIEW virtual instruments (a) reconstruct the differentiated data, (b) filter the pulsatile signal with motion artifact reduction algorithms, (c) display the differentiated and reconstructed waveforms, (d) compute and display values for heart rate and blood oxygen saturation (see Figure 4), and (e) store the original and processed data to a text file for follow-up analysis. The data in the file are in columnar format:

Column 1 – Time in milliseconds,
Column 2 – $d(I_{ac})_{ir}/dt$ (derivative of the near-infrared signal)
Column 3 – $(I_{dc})_{ir}$
Column 4 – $d(I_{ac})_{red}/dt$ (derivative of the red signal)
Column 5 – $(I_{dc})_{red}$
Column 6 – $(I_{ac})_{ir}/dt$ (reconstructed near-infrared signal)
Column 7 – $(I_{dc})_{red}$ (reconstructed red signal)

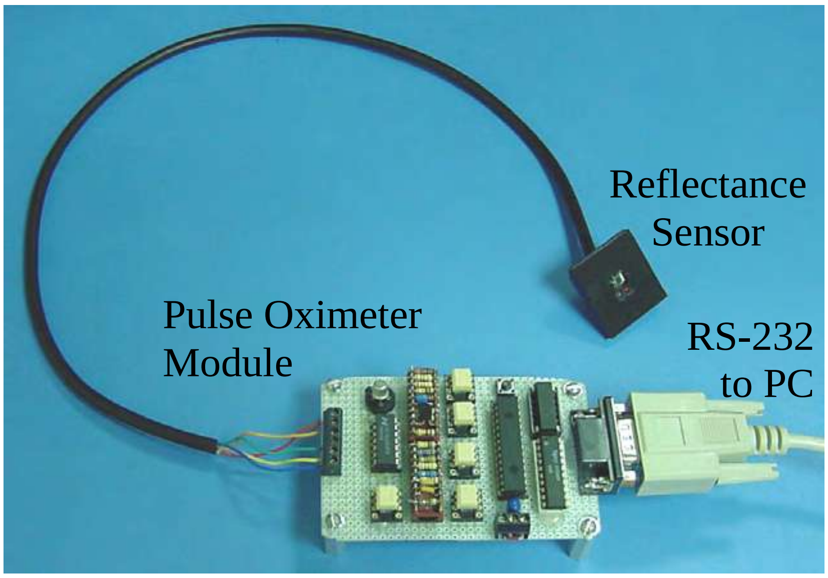

Figure 3. Pulse oximeter module and reflectance probe.

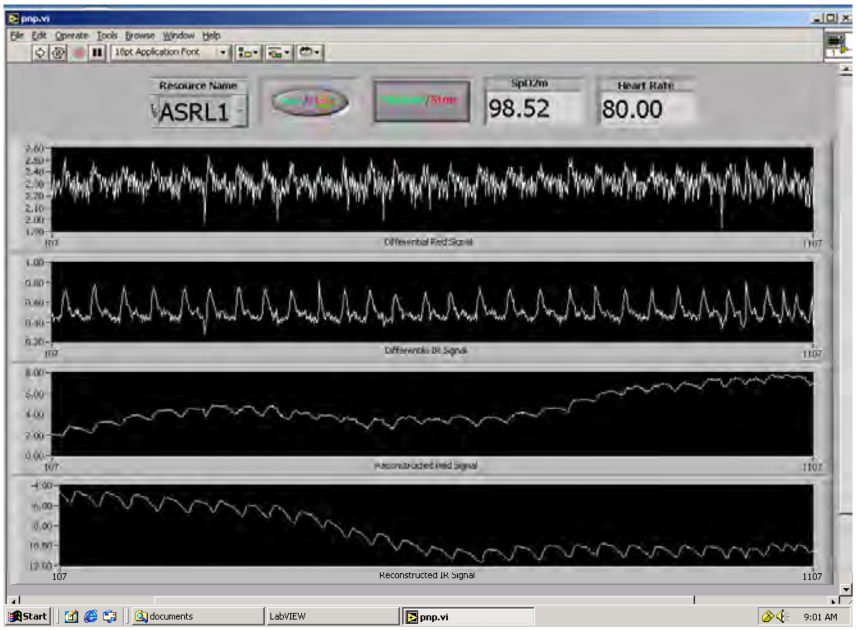

Figure 4. LabVIEW virtual instrument for the pulse oximeter. In addition to heart rate and blood oxygen saturation (%), the interface displays the red and infrared derivative data (top two waveforms) and the red and infrared reconstructed data (bottom two waveforms).

B. A Pulse Oximetry Lecture/Laboratory Pair

At Kansas State University, the 4-credit-hour Bioinstrumentation course sequence (URL: http://www.eece.ksu.edu/~eece772/) consists of three courses instructed by faculty from the Department of Electrical & Computer Engineering (EECE) and the Department of Anatomy and Physiology (AP). These courses are EECE 772 (Theory and Techniques of Bioinstrumentation, 2 hours), EECE 773 (Bioinstrumentation Design Laboratory, 1 hour), and AP 773 (Bioinstrumentation Laboratory, 1 hour). These courses can be taken for either undergraduate or graduate credit. The two laboratory hours provide hands-on experience and are intended to help students obtain a deeper understanding of concepts learned in lectures.

The pulse oximeter discussed earlier serves as a basis for a lecture/laboratory pair in the Bioinstrumentation course sequence. In order to improve the quality of the laboratory, the second author designed a laboratory session for AP 773 that uses the pulse oximeter developed by the first author. Four sets of devices were constructed and have been used as teaching tools in these laboratory sessions. The **learning objectives** of this laboratory (i.e., what a student should be able to do upon completion of the laboratory) are the following:

- Explain the physiological origin of a photoplethysmogram
- Describe the hardware and software components required to determine blood oxygen saturation using light-based sensors
- Calculate blood oxygen saturation given a set of red/infrared plethysmograms
- Assess the character and spectral content of the time-varying signals

- Extract physiological data from a photoplethysmogram
- Describe person-to-person variations in plethysmographic signal data
- Calculate calibration coefficients using different approaches
- Counteract the effects of mild motion artifact

During the laboratory, the class is divided into groups of 2~3 students. Each group is equipped with a collection of components: a reflectance probe, a circuit module, a serial cable, and a personal computer with the LabVIEW interface installed. The students are first taught how to use the modules properly. They then gather PPG data from their team members at different body locations and save these data to files for later signal processing.

Figure 5. Two students acquire photoplethysmographic data in the AP 773 pulse oximetry laboratory (Fall 2002).

These data are processed using Microsoft Excel or MATLAB. In addition to observing and analyzing time domain data, the students are also required to interpret and understand the spectral components of the signal by performing Fast Fourier Transforms (FFTs) on the data sets. They implement different methods for calculating the “ac/dc” ratios required to obtain arterial oxygen saturation. Two calculation methods are used to compute these ratios. The methods correspond to Equations 3 and 4, which supply a parameter for Equation 7. The ‘peak/valley’ method considers the peak-to-valley amplitude of the reconstructed signal as I_{ac} when calculating the “ac/dc” ratio. This method is evaluated with two different filtering techniques: a sliding average filter and a sliding median filter. The FFT method uses the spectral peaks of the red and near-infrared signals to represent I_{ac} in the calculations. The students are then asked to compare the calculation methods and choose the best one.

Students are also encouraged to experiment with other noise reduction filters. Additionally, by observing and analyzing waveforms acquired from different team members, students can realize that factors such as skin color and perfusion affect the quality of acquired PPG data. They are also asked to evaluate the differences between PPG signals acquired at different body locations (e.g., wrist, forehead, or ear lobe) that have noticeably different vascular profiles.

C. Pulse Oximeter Applied to Other Educational Venues

In addition to the lecture/laboratory pair noted in the previous section, the pulse oximeter design and the signal data gathered from various implementations of this design have been applied in multiple undergraduate (*EECE 499 – Honors Research*; *EECE 512 – Linear Systems*) and graduate (*EECE 840 – Scientific Computing*) educational venues. The **signals** acquired from this platform have been used in the following ways:

- data for time-domain smoothing algorithms (see Figure 6),
- signals for time- and frequency-domain filtering projects (see Figure 7 and Figure 8),
- waveforms for Fourier series reconstruction projects (see Figure 9), and
- signals for time-frequency spectrogram projects (see Figure 10).

The **modules** have also been used as starting points for various undergraduate honors research projects, as depicted in Figure 11.

Course Projects. In the smoothing exercises (see Figure 6), students are asked to perform signal processing exercises to 'smooth out' variations in signals corrupted with noise. Two of the common techniques are illustrated here. Polynomials, by their nature, are smooth curves whose numbers of peaks and valleys correspond to the order of the polynomial. In this figure, a polynomial of order 12 provides a reasonable representation of the original data set. Note that the behavior of the fitting polynomial is unpredictable outside of the original bounds. Sliding average and median filters are also a smoothing approach that can be implemented by a young student without much programming experience (the graph on the right in Figure 6 was produced with an Excel spreadsheet). For this photoplethysmograph (sampled at 160 Hz), a 7-wide sliding window appears to provide a reasonable job of smoothing out the noise while retaining the fundamental shape of the waveform.

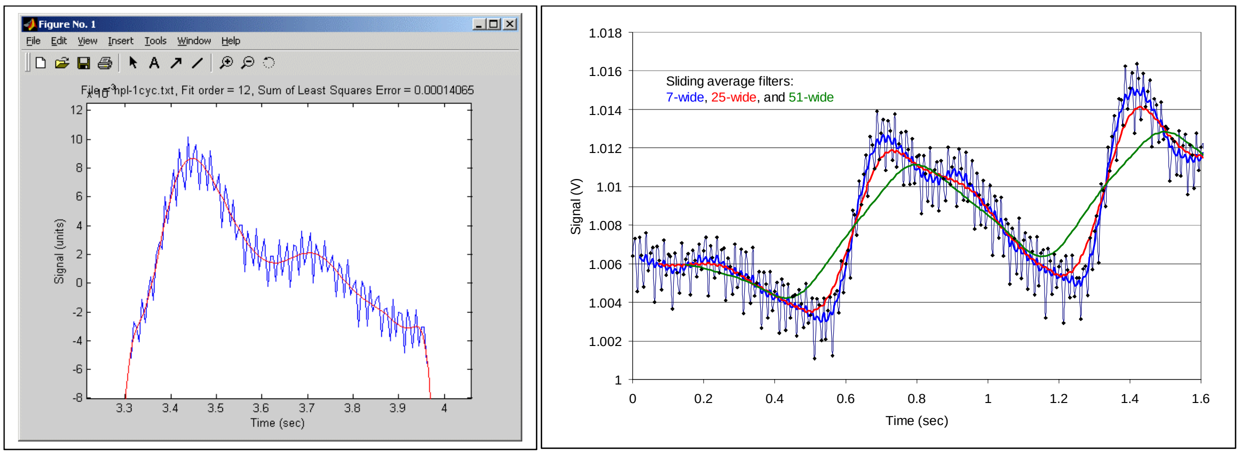

Figure 6. Data smoothing algorithms (polynomial fits and sliding average filters) applied to photoplethysmographic data. These exercises were assigned in EECE 772 (Bioinstrumentation) and EECE 840 (Scientific Computing).

In the EECE 512 project depicted in Figure 7, a student's code (1) loads a signal from an input ASCII text file, (2) performs a convolution (i.e., filtering operation) between the input signal and a cascade of 2^{nd}-order Butterworth lowpass and highpass filters (which can be combined to create lowpass, highpass, or bandpass filters), (3) saves the output signal to disk, and (4) plots the original and filtered signals to the screen. Input signals for these simulations include both ideal signals (e.g., pulses, square waves, and sinusoids) and real-world signals (e.g., biomedical signals such as electrocardiograms and light reflectance signals from the pulse oximeter modules presented here).

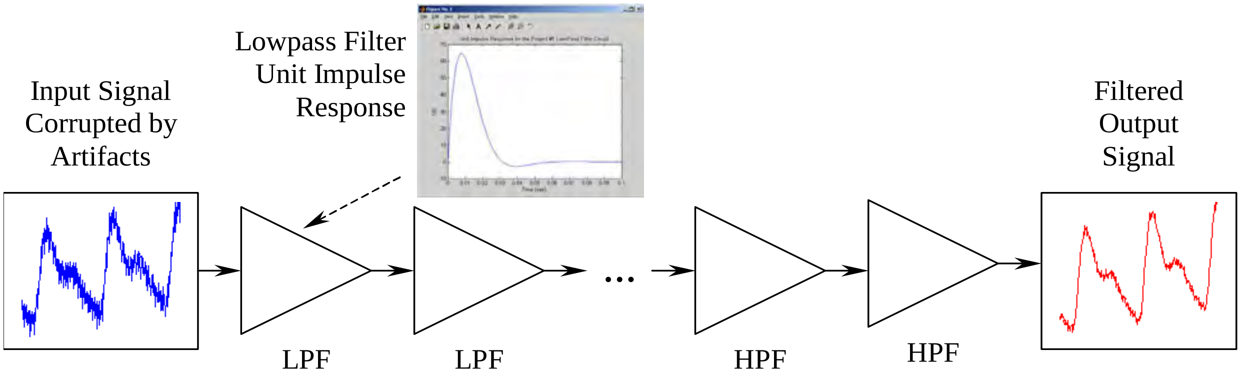

Figure 7. Multi-stage filtering of photoplethysmographic data via time-domain convolution in EECE 512 (Linear Systems). Stages: 2^{nd}-order lowpass and highpass filters.

Frequency-domain filters are also an important part of a signals and systems course. In these projects, a student's program typically (1) loads an input signal from a file and calculates its Fourier transform, (2) calculates the frequency response of a filter chosen by the user, and (3) performs a frequency-domain filtering operation on the input signal: it multiplies the input signal spectrum by the spectrum of the filter and then takes the inverse Fourier transform of the result. The program then saves the input/output signals, their spectra, and the filter spectra to a set of ASCII text files and creates a plotting script that can be called by MATLAB or GNUPLOT. In the example illustrated in Figure 8, an ideal bandpass filter with a low cutoff of 0.3 Hz and a high cutoff or 15 Hz was used to remove the drift and 60 Hz noise present in the original plethysmographic signal.

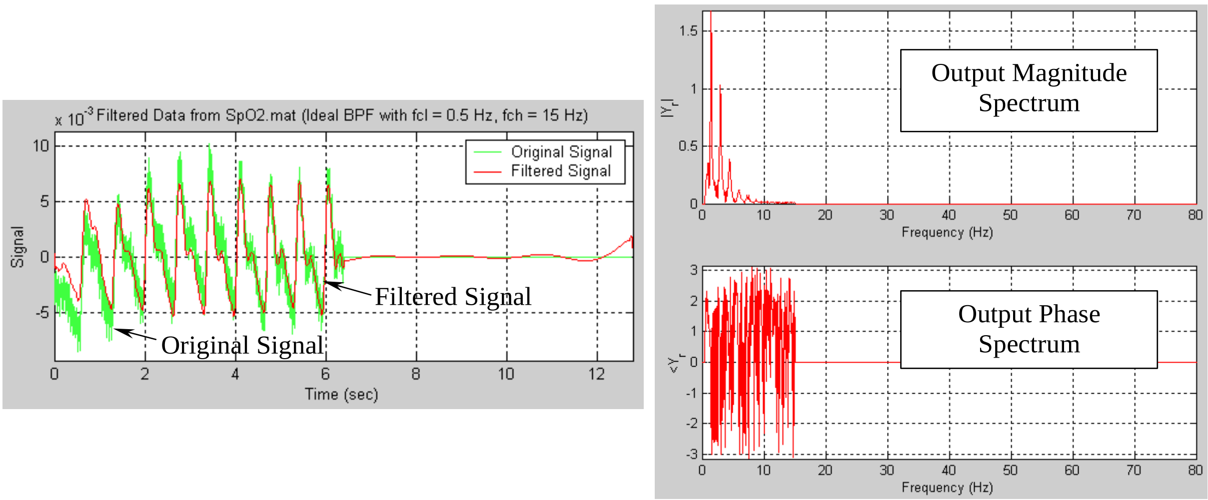

Figure 8. Frequency-domain filtering of pulsatile light reflectance data to remove signal drift and 60 Hz noise. Course: EECE 512 (Linear Systems).

Figure 9 illustrates the use of light reflectance signals in a Fourier series project. In the left part of Figure 9, the top set of axes displays a PPG signal and its Fourier series reconstruction. The middle and bottom axes plot the magnitude and phase coefficients, respectively, that were calculated for the reconstruction. Note that 45 harmonics (or cosines with different magnitudes and phases) were required to replicate the shape of the initial signal. In the canine electrocardiogram depicted on the right hand side of the figure, 125 harmonics produced a good reconstruction. This is due to the higher frequency components present in each QRS complex.

Human Pulse Plethysmogram

Canine Electrocardiogram

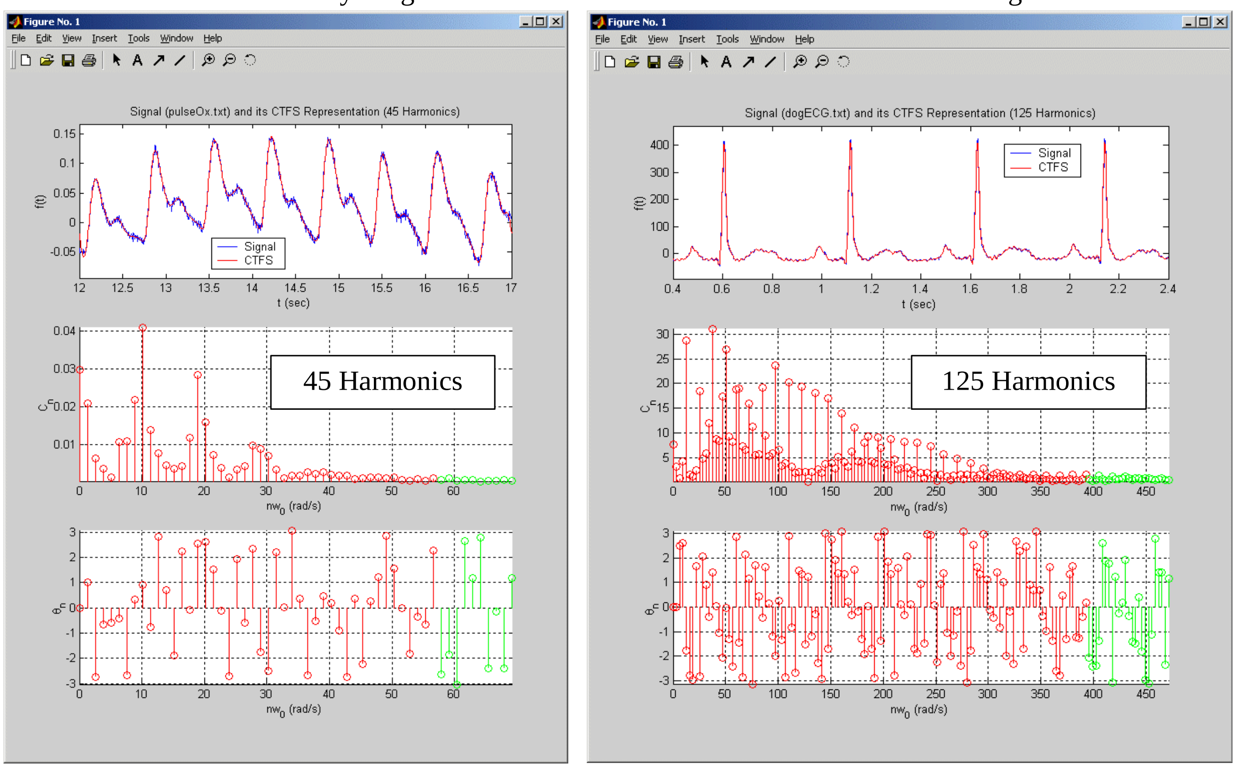

Figure 9. Reconstruction of biomedical signal data (human finger photoplethysmogram and canine electrocardiogram) using Fourier series. Class: EECE 512 (Linear Systems).

It can be helpful to understand how a signal's spectral character changes as a function of time. Figure 10 presents an example of a MATLAB interface that would be written by a student in a graduate scientific computing course. In this figure, the upper left set of axes plots the time-domain plethysmogram, while the lower left set of axes displays the spectrum of the signal versus time. The plots on the right depict the magnitude and phase spectrum of the input signal at the time denoted by the vertical line that occurs at ~55 seconds (see the upper left trace). The fields on the right side of the interface depict parameters that can be chosen by the user.

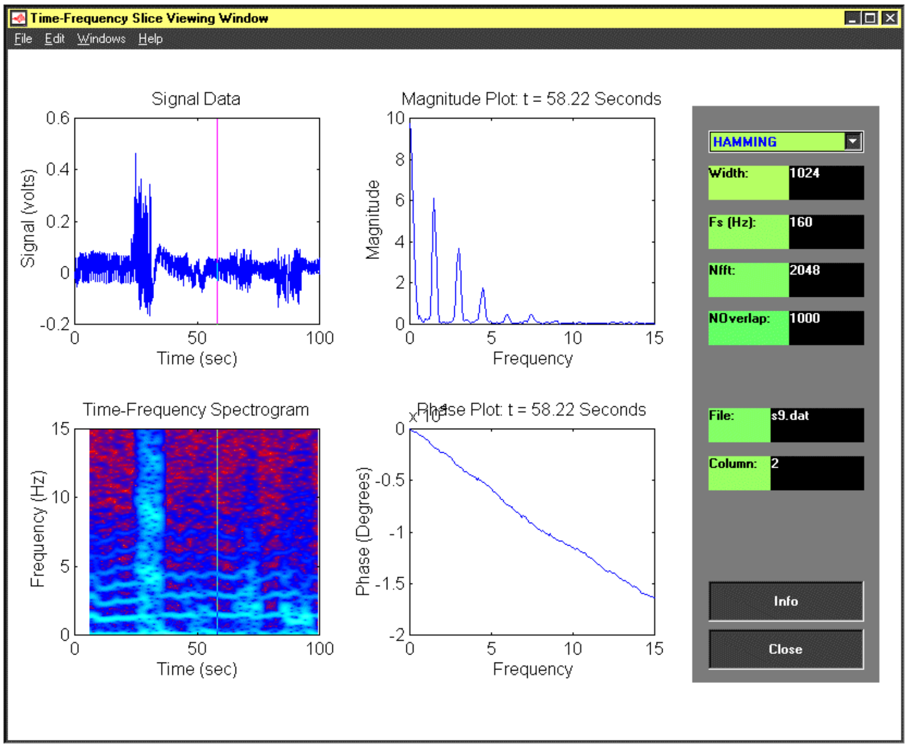

Figure 10. Time-frequency analysis of reflectance data in EECE 840 (Scientific Computing).

Honors Research Projects. The undergraduate Electrical & Computer Engineering curriculum at KSU allows high achieving students to perform research for course credit. The pulse oximeter modules presented in this paper have contributed to five EECE 499 (Honors Research) projects to date (see Figure 11). For the project shown at the top of the figure, Ben Young developed a system based upon the pulse oximeter module that acquired light reflectance data from the forehead using sensors mounted on a firefighter helmet. The goal of this project was to establish whether meaningful blood oxygen saturation measurements could be acquired continuously on an individual that needed to use their hands freely and could be exposed to dangerous levels of carbon monoxide. The second project from the top, managed by Shelly Allison and Craig Nelson, involved gathering light reflectance data from normal and hypertensive elderly subjects. These data will be analyzed for correlations between spectral behavior and the measured blood pressure of the subjects. The goal is to find a comfortable, noninvasive way to replicate the information normally provided by often painful blood pressure cuffs.

As noted in Figure 11, Jonathan Hicks investigated a method to use a patient's light reflectance data as a biometric indicator. This capability would allow a home monitoring system to authenticate the identity of a patient prior to uploading the patient's physiological data to a remote electronic patient record. The benefits of this approach are two-fold: (1) no interaction is required on the part of the patient and (2) the data are independently verified prior to submission. The plots in Figure 11 show a representative light reflectance signal for a patient and the single-period template used to represent that time-varying signal. Two other representative templates are also depicted in the figure to show how these wave shapes vary from person to person. This method uses a statistical test to determine whether a patient's current data are similar to the single-period template stored for the patient. Finally, Austin Wareing was supported by an NSF Research Experience for Undergraduates grant to optimize the light reflectance sensor design and improve the interaction between the pulse oximeter and the host LabVIEW program. His radial sensor design and a resulting set of waveforms are depicted at the bottom of Figure 11.

Ben Young: Forehead Measurements of Blood Oxygen Saturation for Use with Fire Fighter Helmets

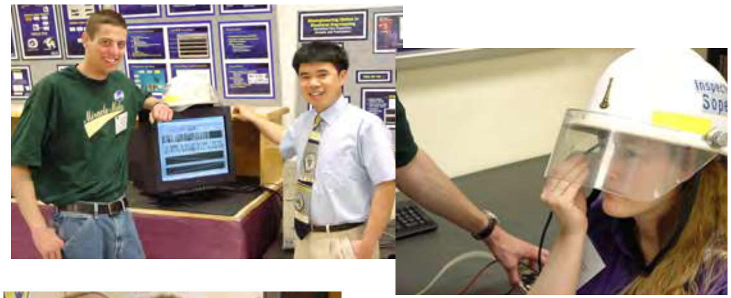

Shelly Allison and Craig Nelson: Light-Based Indicators for Hypertension

Jonathan Hicks: Photoplethysmographic Signals as Biometric Authenticators

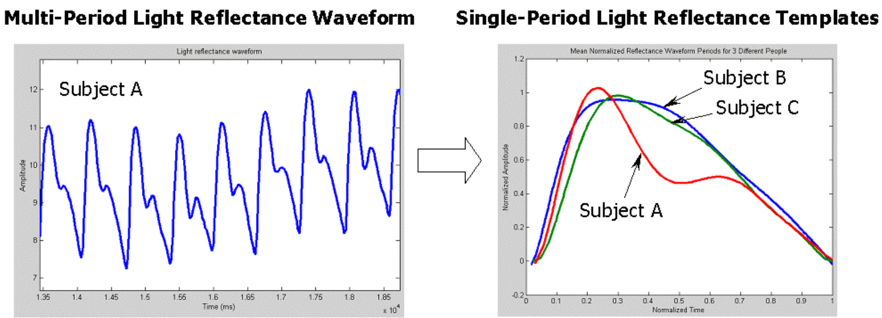

Austin Wareing: Optimization of Light Reflectance Sensors

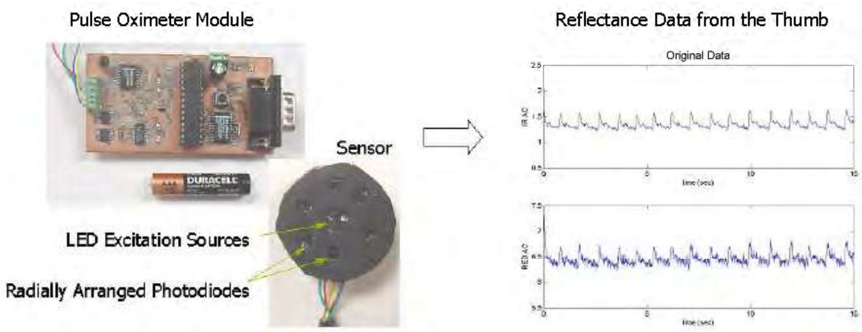

Figure 11. Honors research projects that have benefited from the pulse oximeter design.

IV. Discussion and Conclusion

This paper presented initial efforts to apply an in-house pulse oximeter design to multiple secondary education venues. These efforts have indicated that students enjoy instructional experiences that utilize real-world devices, especially when they can manipulate elements of the design such as the signal processing algorithms that would normally be hidden from the user. The pulse oximeter modules have been used in four Fall offerings of the AP 773 laboratory (2001~2004). Because these home-grown pulse oximeters offer improved data access as compared to commercial products, instructors can experience far greater flexibility when assigning homework, which is especially appreciated when the background and educational experiences of the students vary significantly.

Each laboratory session that utilized these modules has been supported by device developers. Interactions between the device developers and the students (users) lead to experiences that are hard to replicate with packaged, off-the-shelf units. These interactions help the students appreciate the concepts discussed in lecture and allow them to become more familiar with the device development process.

As noted in the body of the paper, several other undergraduate and graduate courses have benefited from the data availability offered by these pulse oximeters. When asked, “What part of the project did you like the most” (on the survey for the Spring 2003 Linear Systems project depicted in Figure 7) one student responded, “Being able to see the ECG and pulse oximeter signals with the noise filtered out.” Many other individuals in this class of 65 students had similar opinions about working with data provided by a device in a nearby laboratory. Processing real-world signals stimulated the students’ interest the most, followed by the excitement of simply getting their code to work. The same Linear Systems student, when asked the question, “How could a project of this nature be improved?,” responded with, “More realistic signals to filter − that is what made me feel like this was a realistic project.”

The inexpensive hardware, plug-and-play features, and information-rich signals offered by these pulse oximeters have also provided starter platforms for honors students that wish to perform innovative research. These experiences not only help them to apply knowledge learned from their courses and understand recent developments; more importantly, they may also motivate these capable students to pursue careers in an expanding biomedical industry.

Acknowledgements

The authors wish to acknowledge Jerry T. Love, Sandia National Laboratories (retired), for the original design of the light feedback circuit. Portions of this material are based upon work supported by the National Science Foundation under grant BES–0093916. Opinions, findings, conclusions, or recommendations expressed in this material are those of the author(s) and do not necessarily reflect the views of the NSF. All studies addressed in this paper that involve human subjects have been approved by the Human Studies Board at Kansas State University under protocol #2211.

References

[1] Brinkman, R. and W. G. Zijlstra. "Determination and continuous registration of the percentage oxygen saturation in clinical conditions," *Arch. Chir. Neurol.*, vol. 1, pp. 177-183.

[2] Swedlow, D. B. "Oximeter with motion detection for alarm modification," International Patent Application WO 94y22360 ~13, 1994, pp.

[3] Yao, J., and S. Warren. "A Novel Algorithm to Separate Motion Artifacts from the Photoplethysmographic Signal for a Pulse Oximeter," presented at 4th Joint EMBS-BMES Conf., San Francisco, CA, 2004.

[4] Rhee, Sokwoo, B.-H. Yang, and H. H. Asada,. "Artifact-resistant power-efficient design of finger-ring plethysmographic sensors," *IEEE Transactions on Biomedical Engineering*, vol. 48, May, pp. 795-805.

[5] Mannheimer, P.D., J.R. Cascini, M.E. Fein, and S.L. Nierlich. "Wavelength selection for low-saturation pulse oximetry," *IEEE Transactions on Biomedical Engineering*, vol. 44, March, pp. 148 - 158.

[6] Zonios, G., U. Shankar, and V.K. Iyer. "Pulse oximetry theory and calibration for low saturations," *IEEE Transactions on Biomedical Engineering*, vol. 51, May, pp. 818 - 822.

[7] Warren, S., J. Yao, and G. E., Barnes. "Wearable Sensors and Component-Based Design for Home Health Care," presented at 2nd Joint EMBS-BMES Conf., Houston, TX, 2002.

[8] Johnston, W.S., P.C. Branche, C.J. Pujary, and Y. Mendelson. "Effects of motion artifacts on helmet-mounted pulse oximeter sensors," presented at Proceedings of the IEEE 30th Annual Northeast Bioengineering Conference, 2004, 2004.

[9] Crilly, P.B., E.T. Arakawa, D.L. Hedden, and T.L. Ferrell. "An integrated pulse oximeter system for telemedicine applications," presented at Proceedings of the IEEE Instrumentation and Measurement Technology Conference, 1997, 1997.

[10] Bronzino, Joseph D. *IEEE Biomedical Engineering Handbook*: CRC Press, IEEE Press, 1995, 0-8493-8346-3.

[11] Yoshiya, Y. Shimada, and K. Tanaka. "Spectrophotometric monitoring of arterial oxygen saturation in the fingertip," *Med. Biol. Eng. Comput.*, vol. 18, pp. 27-32.

[12] Peck, Y., S. Cheang, and Peter R Smith. "An Overview of Non-Contact Photoplethysmography," *Electronic systems and control division research*, pp. 53~59.

[13] Schmitt, J. M. "Simple photon diffusion analysis of the effects of multiple scattering on pulse oximetry," *IEEE Transaction on Biomedical Engineering*, vol. 38, December, pp. 1194-1203.

[14] Mendelson, Yitzak, Peter W. Cheung, Michael R. Neuman, David G. Fleming, and Stephan D. Cahn. "Spectrophotometric Investigation of Pulsatile Blood Flow for Transcutaneous Reflection Oximetry," *Advances in Experimental Medicine and Biology*, vol. 159, pp. 93-102.

[15] Love, Jerry T., S. Warren, G. R. Laguna , and T. J. Miller. " Personal Status Monitor," Sandia National Lab SAND97-0418, 1997.

Biographical Information

Jianchu Yao is a doctoral candidate in Electrical Engineering at Kansas State University. Prior to his study at KSU, Mr. Yao worked on real-time embedded controls for five years in the continuous manufacturing processes and robotics industry. His current research interests include bioinstrumentation, sensor networking, and plug-and-play devices.

Steve Warren is an Associate Professor of Electrical & Computer Engineering at Kansas State University. He teaches courses in linear systems, computer graphics, biomedical instrumentation, and scientific computing. Dr. Warren manages the KSU *Medical Component Design Laboratory*, and his research focuses on plug-and-play, wearable systems for telemedicine.

APPENDIX C

RX-0632

APPENDIX D

The American Heritage® dictionary of the English Language

FIFTH EDITION

Houghton Mifflin Harcourt
BOSTON NEW YORK

Visit our website at www.ahdictionary.com
or www.youareyourwords.com.

Library of Congress Cataloging-in-Publication Data

The American Heritage dictionary of the English language. -- 5th ed.
p. cm.
Previous ed.: 2000.
ISBN 978-0-547-04101-8
1. English language--Dictionaries.
PE1628.A623 2011
423--dc22

2011004777

Manufactured in the United States of America

1 2 3 4 5 6 7 8 9 10–QGV–15 14 13 12 11

Navy, serving either with the Navy or the Marines, who has been trained to give first aid and basic medical treatment, especially in combat situations. **2.** A member of a government-sponsored group designated as a corps: *Peace Corpsmen.*

cor·pu·lence (kôr′pyə-ləns) *n.* The condition of being excessively fat; obesity. [Middle English, corporality < Latin *corpulentia*, corpulence < *corpulentus*, corpulent < *corpus*, body; see **kʷrep-** in App. I.]

cor·pu·lent (kôr′pyə-lənt) *adj.* Having an abundance or excess of flesh or fat. See Synonyms at **fat.**

cor pul·mo·na·le (kôr′ po͝ol′mə-nä′lē, -năl′ē, pŭl′-) *n.* Acute strain or hypertrophy of the right ventricle caused by a disorder of the lungs or of the pulmonary blood vessels. [New Latin *cor pulmōnāle* : Latin *cor*, heart + New Latin *pulmōnāle*, neuter of *pulmōnālis*, of the lungs.]

cor·pus (kôr′pəs) *n., pl.* **-po·ra** (-pər-ə) **1.** A large collection of writings of a specific kind or on a specific subject. **2.** A collection of writings or recorded remarks used for linguistic analysis. **3.** *Economics* **a.** The capital or principal amount, as of an estate or trust. **b.** The principal of a bond. **4.** *Anatomy* **a.** The main part of a bodily structure or organ. **b.** A distinct bodily mass or organ having a specific function. **5.** The overall length of a violin. [Middle English < Latin; see **kʷrep-** in App. I.]

corpus al·bi·cans (ăl′bĭ-kănz′) *n.* The white fibrous scar tissue in an ovary that results after the involution and regression of the corpus luteum. [New Latin *corpus albicāns* : Latin *corpus*, body + New Latin *albicāns*, whitening.]

corpus cal·lo·sum (kə-lō′səm) *n., pl.* **corpora cal·lo·sa** (kə-lō′sə) The arched bridge of nervous tissue that connects the two cerebral hemispheres, allowing communication between the right and left sides of the brain. [New Latin *corpus callōsum* : Latin *corpus*, body + Latin *callōsum*, neuter of *callōsus*, callous.]

Cor·pus Chris·ti¹ (kôr′pəs krĭs′tē) A city of southern Texas on **Corpus Christi Bay**, an arm of the Gulf of Mexico at the mouth of the Nueces River. Founded as a trading post in 1839, the city developed as a port.

Cor·pus Chris·ti² (kôr′pəs krĭs′tē) *n.* A Christian feast in honor of the Eucharist, observed on the first Thursday or the first Sunday after Trinity Sunday. [Middle English < Medieval Latin *Corpus Christi*, body of Christ : Latin *corpus*, body + Latin *Christī*, genitive of *Christus*, Christ.]

cor·pus·cle (kôr′pə-səl, -pŭs′əl) *n.* **1a.** An unattached body cell, such as a blood or lymph cell. **b.** A rounded globular mass of cells, such as the pressure receptor on certain nerve endings. **2.** A discrete particle, such as a photon or an electron. **3.** A minute globular particle. [Latin *corpusculum*, diminutive of *corpus*, body; see **kʷrep-** in App. I.] **—cor·pus′cu·lar** (kôr-pŭs′kyə-lər) *adj.*

corpus de·lic·ti (dĭ-lĭk′tī′) *n.* **1.** *Law* The corroborating evidence that shows that a crime has been committed, other than a confession or an alleged accomplice's statement. **2.** A corpse. [New Latin *corpus dēlictī* : Latin *corpus*, body, collection of facts + Latin *dēlictī*, genitive of *dēlictum*, crime.]

corpus lu·te·um (lo͞o′tē-əm) *n., pl.* **corpora lu·te·a** (lo͞o′tē-ə) A yellow, progesterone-secreting mass of cells that forms from an ovarian follicle after the release of a mature egg. Also called *yellow body.* [New Latin *corpus lūteum* : Latin *corpus*, body + Latin *lūteum*, neuter of *lūteus*, yellow.]

corpus stri·a·tum (strī-ā′təm) *n., pl.* **corpora stri·a·ta** (strī-ā′tə) Either of two gray and white striated bodies of nerve fibers located in the lower lateral wall of each cerebral hemisphere. [New Latin *corpus striātum* : Latin *corpus*, body + Latin *striātum*, neuter of *striātus*, striated.]

cor·rade (kə-rād′) *tr. & intr.v.* **-rad·ed, -rad·ing, -rades** To erode or be eroded by abrasion. [Latin *corrādere*, to scrape together : *com-*, com- + *rādere*, to scrape; see **rēd-** in App. I.] **—cor·ra′sion** (-rā′zhən) *n.* **—cor·ra′sive** (-sĭv, -zĭv) *adj.*

cor·ral (kə-răl′) *n.* **1.** An enclosure for confining livestock. **2.** An enclosure formed by a circle of wagons for defense against attack during an encampment. ❖ *tr.v.* **-ralled, -ral·ling, -rals 1.** To drive into and hold in a corral. **2.** To arrange (wagons) in a corral. **3.** To take control or possession of. **4.** To gather; garner: *"difficult for congressional leadership to corral a majority of votes"* (Don J. Pease). [Spanish < Vulgar Latin **currāle*, enclosure for carts < Latin *currus*, cart < *currere*, to run; see **kers-** in App. I.]

cor·rect (kə-rĕkt′) *v.* **-rect·ed, -rect·ing, -rects** *—tr.* **1a.** To make or put right: *correct a mistake; correct a misunderstanding.* **b.** To remove the errors or mistakes from: *corrected her previous testimony.* **c.** To indicate or mark the errors in: *correct an exam.* **2a.** To speak to or communicate with (someone) in order to point out a mistake or error. **b.** To scold or punish so as to improve or reform. **3.** To remedy or counteract (a defect, for example): *The new glasses corrected his blurry vision.* **4.** To adjust so as to meet a required standard or condition: *correct the wheel alignment on a car.* *—intr.* **1.** To make corrections. **2.** To make adjustments; compensate: *correcting for the effects of air resistance.* ❖ *adj.* **1.** Free from error or fault; true or accurate. **2.** Conforming to standards; proper: *correct behavior.* [Middle English *correcten* < Latin *corrigere*, *corrēct-* : *com-*, intensive pref.; see **com–** + *regere*, to rule; see **reg-** in App. I.] **—cor·rect′a·ble, cor·rect′i·ble** *adj.* **—cor·rect′ly** *adv.* **—cor·rect′ness** *n.* **—cor·rec′tor** *n.*

✦**SYNONYMS** *correct, rectify, remedy, redress, revise, amend* These verbs mean to make right what is wrong. *Correct* refers to eliminating faults, errors, or defects: *I corrected the spelling mistakes. The new design corrected the flaws in the earlier version. Rectify* stresses the idea of bringing something into conformity with a standard of what is right: *"It is dishonest to claim that we can rectify racial injustice without immediate cost"* (Mari J. Matsuda). *Remedy* involves removing or counteracting something considered a cause of harm, damage, or discontent: *He took courses to remedy his abysmal ignorance. Redress* refers to setting right something considered immoral or unethical and usually involves some kind of recompense: *"They said he had done very little to redress the abuses that the army had committed against the civilian population"* (Daniel Wilkinson). *Revise* suggests change that results from careful reconsideration: *The agency revised its safety recommendations in view of the new findings. Amend* implies improvement through alteration or correction: *"Whenever* [the people] *shall grow weary of the existing government, they can exercise their constitutional right of amending it, or their revolutionary right to dismember or overthrow it"* (Abraham Lincoln).

cor·rec·tion (kə-rĕk′shən) *n.* **1.** The act or process of correcting. **2.** Something offered or substituted for a mistake or fault: *made corrections in the report.* **3a.** Punishment intended to rehabilitate or improve. **b. corrections** The treatment of offenders through a system of penal incarceration, rehabilitation, probation, and parole, or the administrative system by which these are effectuated. **4.** An amount or quantity added or subtracted in order to correct. **5.** A decline in stock-market activity or prices following a period of increases. **—cor·rec′tion·al** *adj.*

cor·rec·ti·tude (kə-rĕk′tĭ-to͞od′, -tyo͞od′) *n.* Appropriate manners and behavior; propriety.

cor·rec·tive (kə-rĕk′tĭv) *adj.* Tending or intended to correct: *corrective lenses.* ❖ *n.* An agent that corrects. **—cor·rec′tive·ly** *adv.*

Cor·reg·gio (kə-rĕj′ō, kō-rĕd′jō), **Antonio Allegri da** 1494?–1534. Italian Renaissance painter known for his use of chiaroscuro. Among his works are devotional pictures, including *Holy Night*, and frescoes, such as those in the convent of San Paolo in Parma (1518).

Cor·reg·i·dor (kə-rĕg′ĭ-dôr′, kôr-rĕ′hē-dôr′) A island of the northern Philippines at the entrance to Manila Bay. After a prolonged siege and bombardment, Filipino and US troops surrendered the fortified island to Japan in May 1942. US paratroopers recaptured it in March 1945.

cor·re·late (kôr′ə-lāt′, kŏr′-) *v.* **-lat·ed, -lat·ing, -lates** *—tr.* To establish or demonstrate as having a correlation: *correlated drug abuse and crime.* *—intr.* To be related by a correlation. ❖ *adj.* (-lĭt, -lāt′) Related by a correlation, especially having corresponding characteristics. ❖ *n.* (-lĭt, -lāt′) Either of two correlate entities; a correlative. [Back-formation < CORRELATION.] **—cor′re·lat′a·ble** *adj.* **—cor′re·la′tor** *n.*

cor·re·la·tion (kôr′ə-lā′shən, kŏr′-) *n.* **1.** A relationship or connection between two things based on co-occurrence or pattern of change: *a correlation between drug abuse and crime.* **2.** *Statistics* The tendency for two values or variables to change together, in either the same or opposite way: *As cigarette smoking increases, so does the incidence of lung cancer, indicating a positive correlation.* **3.** An act of correlating or the condition of being correlated. [Medieval Latin *correlātiō*, *correlātiōn-* : Latin *com-*, com- + Latin *relātiō*, relation, report (< *relātus*, past participle of *referre*, to carry back; see RELATE).] **—cor′re·la′tion·al** *adj.*

correlation coefficient *n.* A measure of the interdependence of two random variables that ranges in value from −1 to +1, indicating perfect negative correlation at −1, absence of correlation at zero, and perfect positive correlation at +1. Also called *coefficient of correlation.*

cor·rel·a·tive (kə-rĕl′ə-tĭv) *adj.* **1.** Related; corresponding. **2.** *Grammar* Indicating a reciprocal or complementary relationship: *a correlative conjunction.* ❖ *n.* **1.** Either of two correlative entities; a correlate. **2.** *Grammar* A correlative word or expression. **—cor·rel′a·tive·ly** *adv.*

correlative conjunction *n.* Either of a pair of conjunctions, such as *either . . . or* or *both . . . and*, that connect two parts of a sentence and are not used adjacent to each other. The second of the pair is always a coordinating conjunction.

cor·re·spond (kôr′ĭ-spŏnd′, kŏr′-) *intr.v.* **-spond·ed, -spond·ing, -sponds 1.** To be in agreement, harmony, or conformity. **2.** To be similar or equivalent in character, quantity, origin, structure, or function: *English* navel *corresponds to Greek* omphalos. **3.** To communicate by letter, usually over a period of time. [French *correspondre* < Medieval Latin *correspondēre* : Latin *com-*, com- + *respondēre*, to respond; see RESPOND.]

✦**SYNONYMS** *correspond, conform, harmonize, coincide, accord, agree* These verbs all indicate a compatibility between people or things. *Correspond* refers to similarity in form, nature, function, character, or structure: *"Scientific statements may or may not correspond to the facts of the physical world"* (George Soros). *Conform* stresses correspondence in essence or basic characteristics, sometimes to an ideal or established standard: *"Home was the place where I was forced to conform to someone else's image of who and what I should be"* (bell hooks). *Harmonize* implies the combination or arrangement of elements in a pleasing whole: *The print on the curtains harmonized with the striped sofa. Coincide* stresses exact agreement: *"His interest happily coincided with his duty"* (Edward A. Freeman). *Accord* implies harmony, unity, or consistency, as in essential nature: *"The creed* [upon which America was founded] *was widely seen as both progressive and universalistic: It accorded with the future, and it was open to all"* (Everett Carll Ladd). *Agree* may indicate mere lack of incongruity or discord, although it often suggests acceptance of ideas or actions and thus accommodation: *We finally agreed on a price for the house.* See also synonyms at **assent.**

cor·re·spon·dence (kôr′ĭ-spŏn′dəns, kŏr′-) *n.* **1.** The act, fact, or state of agreeing or conforming: *The correspondence of the witness's statement with the known facts suggests that he is telling the truth.* **2.** A similarity, connection, or equivalence: *Is there a correspondence between corporal punishment in children and criminal behavior in adults?* **3a.** Communication by the exchange of letters, e-mails, or other forms of written messages. **b.** The messages sent or received.

ă	pat	oi	boy
ā	pay	ou	out
âr	care	o͝o	took
ä	father	o͝or	lure
ĕ	pet	o͞o	boot
ē	be	ŭ	cut
ĭ	pit	ûr	urge
ī	bite	th	thin
îr	pier	*th*	this
ŏ	pot	zh	vision
ō	toe	ə	about,
ô	paw		item
ôr	core		

Stress marks: **′** (primary); ′ (secondary), as in **dictionary** (dĭk′shə-nĕr′ē)

correspondence course *n.* An educational course offered by a correspondence school.

correspondence principle *n.* The principle that predictions of quantum theory approach those of classical physics in the limit of large quantum numbers.

correspondence school *n.* A school that offers instruction by mail, sending lessons and examinations to a student.

cor·re·spon·den·cy (kôr′ĭ-spŏn′dən-sē, kŏr′-) *n., pl.* **-cies** Correspondence.

cor·re·spon·dent (kôr′ĭ-spŏn′dənt, kŏr′-) *n.* **1.** One who communicates by means of letters, e-mails, or other forms of written messages. **2.** One employed by the print or broadcast media to supply news stories or articles: *a foreign correspondent.* **3.** One that has regular business dealings with another, especially at a distance. **4.** Something that corresponds; a correlative. ❖ *adj.* Corresponding. **—cor′re·spon′dent·ly** *adv.*

cor·re·spond·ing (kôr′ĭ-spŏn′dĭng, kŏr′-) *adj.* **1.** Having the same or nearly the same relationship. **2.** Accompanying another: *a high corporate position and its corresponding problems.* **3a.** Having been assigned the responsibility of written communications: *a corresponding secretary.* **b.** Participating at a distance from the rest of a group: *a corresponding member of the bar association.* **—cor′re·spond′ing·ly** *adv.*

cor·re·spon·sive (kôr′ĭ-spŏn′sĭv, kŏr′-) *adj.* Jointly responsive. **—cor′re·spon′sive·ly** *adv.*

cor·ri·da (kō-rē′də, -dä) *n.* A bullfight, especially a program in which six bulls aged at least four years old are engaged. [Spanish *corrida (de toros)*, running (of the bulls), bullfight < past participle of *correr*, to run < Latin *currere*; see **kers-** in App. I.]

cor·ri·do (kō-rē′dō) *n., pl.* **-dos** A Mexican ballad or folk song. [American Spanish < Spanish, ballad < past participle of *correr*, to run < Old Spanish < Latin *currere*; see **kers-** in App. I.]

cor·ri·dor (kôr′ĭ-dər, -dôr′, kŏr′-) *n.* **1.** A narrow hallway, passageway, or gallery, often with rooms or apartments opening onto it. **2a.** A tract of land designated or used for a specific purpose, as for railroad lines, highways, or pipelines. **b.** A route designated for a specific purpose: *a hazardous material corridor; a sea corridor for shipping; a flight corridor.* **c.** A route or tract of land used by migrating animals. **3.** A thickly populated strip of land connecting two or more urban areas: *people who live in the Boston-Washington corridor.* **—*idiom:* corridors of power** The places or positions from which people in authority wield power. [French < Italian *corridore* < *correre*, to run < Latin *currere*; see **kers-** in App. I.]

cor·rie (kôr′ē, kŏr′ē) *n.* A round hollow in a hillside; a cirque. [Scottish Gaelic *coire*, hollow, cauldron < Old Irish, cauldron, whirlpool.]

Cor·rie·dale (kôr′ē-dāl′) *n.* **1.** A hornless sheep of a breed developed in New Zealand and Australia, raised for its meat and dense wool. **2.** The wool of this sheep. [After *Corriedale*, the sheep run in New Zealand where development of the breed was begun in the 1860s.]

Cor·ri·gan (kôr′ĭ-gən, kŏr′-), **Mairead** Born 1944. Irish peace activist. She shared the 1976 Nobel Peace Prize for work in Northern Ireland's peace movement.

cor·ri·gen·dum (kôr′ə-jĕn′dəm, kŏr′-) *n., pl.* **-da** (-də) **1.** An error to be corrected, especially a printer's error. **2. corrigenda** A list of errors in a book along with their corrections. [Latin, neuter gerundive of *corrigere*, to correct; see CORRECT.]

cor·ri·gi·ble (kôr′ĭ-jə-bəl, kŏr′-) *adj.* Capable of being corrected, reformed, or improved. [Middle English < Old French < Medieval Latin *corrigibilis* < Latin *corrigere*, to correct; see CORRECT.] **—cor′ri·gi·bil′i·ty** *n.* **—cor′ri·gi·bly** *adv.*

cor·ri·val (kə-rī′vəl, kō-) *n.* A rival or opponent. [French < Latin *corrīvālis* : *com-*, intensive pref.; see COM- + *rīvālis*, rival; see RIVAL.] **—cor·ri′val** *adj.* **—cor·ri′val·ry** (-rē) *n.*

cor·rob·o·rant (kə-rŏb′ər-ənt) *adj. Archaic* Producing or stimulating physical vigor. Used of a medicine.

cor·rob·o·rate (kə-rŏb′ə-rāt′) *tr.v.* **-rat·ed, -rat·ing, -rates** To strengthen or support with other evidence; make more certain. See Synonyms at **confirm.** [Latin *corrōborāre, corrōborāt-* : *com-*, com- + *rōborāre*, to strengthen (< *rōbur, rōbor-*, strength; see **reudh-** in App. I).] **—cor·rob′o·ra′tion** *n.* **—cor·rob′o·ra′tive** (-ə-rā′tĭv, -ər-ə-tĭv), **cor·rob′o·ra·to′ry** (-ər-ə-tôr′ē) *adj.* **—cor·rob′o·ra′tor** *n.*

cor·rob·o·ree (kə-rŏb′ə-rē) *n.* **1.** An Australian Aboriginal dance festival held at night, especially in celebration of an important event. **2.** *Australian* **a.** A large, noisy celebration. **b.** A great tumult; a disturbance. [< Dharuk *garabari.*]

cor·rode (kə-rōd′) *v.* **-rod·ed, -rod·ing, -rodes** *—tr.* **1.** To destroy a metal or alloy gradually, especially by oxidation or chemical action: *acid corroding metal.* **2.** To impair steadily; deteriorate: *"Doubt and mistrust could creep into our lives, corroding personal and professional relationships"* (Philip Taubman). *—intr.* To be eaten or worn away. [Middle English *corroden* < Latin *corrōdere*, to gnaw away : *com-*, intensive pref.; see COM- + *rōdere*, to gnaw; see **rēd-** in App. I.] **—cor·rod′i·ble, cor·ro′si·ble** (-rō′sə-bəl) *adj.*

Hernando Cortés

cor·ro·sion (kə-rō′zhən) *n.* **1a.** The act or process of corroding. **b.** The condition produced by corroding. **2.** A substance, such as rust, formed by corroding. [Middle English *corosioun*, corrosion of tissue < Old French *corrosion* < Medieval Latin *corrōsiō, corrōsiōn-*, the act of gnawing < Latin *corrōsus*, past participle of *corrōdere*, to gnaw away; see CORRODE.]

cor·ro·sive (kə-rō′sĭv, -zĭv) *adj.* **1.** Having the capability or tendency to cause corrosion: *a corrosive acid.* **2.** Gradually destructive; steadily harmful: *corrosive anxiety; corrosive increases in prices; a corrosive narcotics trade.* **3.** Spitefully sarcastic: *corrosive criticism; corrosive wit.* ❖ *n.* A substance having the capability or tendency to cause corrosion. **—cor·ro′sive·ly** *adv.* **—cor·ro′sive·ness** *n.*

corrosive sublimate *n.* See **mercuric chloride.**

cor·ru·gate (kôr′ə-gāt′, kŏr′-) *v.* **-gat·ed, -gat·ing, -gates** *—tr.* To shape into folds or parallel and alternating ridges and grooves. *—intr.* To become shaped into such folds or ridges and grooves: *"Now the immense ocean . . . sensed the change. Its surface rippled and corrugated where sweeping cloud shadows touched it"* (John Updike). [Latin *corrūgāre, corrūgāt-*, to wrinkle up : *com-*, com- + *rūgāre*, to wrinkle (< *rūga*, wrinkle).] **—cor′ru·gate′, cor′ru·gat′ed** (-gā′tĭd) *adj.*

corrugated iron *n.* A structural sheet iron, usually galvanized, shaped in parallel furrows and ridges for rigidity.

cor·ru·ga·tion (kôr′ə-gā′shən, kŏr′-) *n.* **1a.** The act or process of corrugating. **b.** The state of being corrugated. **2.** A groove or ridge on a corrugated surface.

cor·rupt (kə-rŭpt′) *adj.* **1.** Marked by immorality and perversion; depraved. **2.** Venal or dishonest: *a corrupt mayor.* **3.** Containing errors or alterations, especially ones that prevent proper understanding or use: *a corrupt translation; a corrupt computer file.* **4.** *Archaic* Tainted; putrid. ❖ *v.* **-rupt·ed, -rupt·ing, -rupts** *—tr.* **1.** To ruin morally; pervert: *"The argument that modern life consists of a menu of horrors by which we are corrupted . . . is a founding idea of the critique of modernity"* (Susan Sontag). **2.** To destroy or subvert the honesty or integrity of, as by offering bribes: *"Our politics has been corrupted by money and suffused with meanness"* (Peter Edelman). **3a.** To cause to become rotten; spoil: *"There was a strange smell in the room, high and slightly sweet, like perfume corrupted in the bottle"* (Bella Bathurst). **b.** *Archaic* To render impure; contaminate. **4a.** To alter from original or proper form: *"Strangers named them the Chippewa, which was corrupted to Ojibway"* (Paul Theroux). **b.** *Computers* To damage (data) in a file or on a disk. *—intr.* To become corrupt. [Middle English < Latin *corruptus*, past participle of *corrumpere*, to destroy : *com-*, intensive pref.; see COM- + *rumpere*, to break; see **reup-** in App. I.] **—cor·rupt′er, cor·rup′tor** *n.* **—cor·rup′tive** *adj.* **—cor·rupt′ly** *adv.* **—cor·rupt′ness** *n.*

❖**SYNONYMS** *corrupt, debase, debauch, deprave, pervert, vitiate* These verbs mean to ruin utterly in character or quality: *was corrupted by power; debased himself by taking the bribe; a youth debauched by drugs; led a life depraved by sensual indulgence; perverted her talent by her pursuit of commercial success; a laudable goal vitiated by dishonest means.*

cor·rupt·i·ble (kə-rŭp′tə-bəl) *adj.* Capable of being corrupted: *corruptible judges.* **—cor·rupt′i·bil′i·ty** *n.* **—cor·rupt′i·bly** *adv.*

cor·rup·tion (kə-rŭp′shən) *n.* **1a.** The act or process of corrupting. **b.** The state of being corrupt. **2.** Decay; rot.

cor·rup·tion·ist (kə-rŭp′shə-nĭst) *n.* One who defends or practices corruption, particularly in politics.

cor·sage (kôr-säzh′, -säj′) *n.* **1.** A small bouquet of flowers worn at the shoulder or waist or on the wrist. **2.** The bodice or waist of a dress. [Middle English, torso < Old French < *cors*, body < Latin *corpus*; see **kʷrep-** in App. I.]

cor·sair (kôr′sâr′) *n.* **1.** A pirate, especially along the Barbary Coast. **2.** A swift pirate ship, often operating with official sanction. [French *corsaire* < Old Provençal *corsari* < Old Italian *corsaro* < Medieval Latin *cursārius* < *cursus*, plunder < Latin, run, course; see COURSE.]

corse (kôrs) *n. Archaic* A corpse. [Middle English *cors* < Old French < Latin *corpus*; see **kʷrep-** in App. I.]

corse·let (kôrs′lĭt) *n.* **1.** also **cors·let** (kôrs′lĭt) Body armor, especially a breastplate. **2.** also **cor·se·lette** (kôr′sə-lĕt′) An undergarment that is a combination of a light corset and a brassiere. [French, diminutive of Old French *cors*, body; see CORSET.]

cor·set (kôr′sĭt) *n.* **1.** A close-fitting undergarment, often reinforced by stays, worn to support and shape the waistline, hips, and breasts. **2.** A medieval outer garment, especially a laced jacket or bodice. ❖ *tr.v.* **-set·ed, -set·ing, -sets** To enclose in or as if in a corset. [Middle English, bodice < Old French, diminutive of *cors*, body < Latin *corpus*; see **kʷrep-** in App. I.]

cor·se·tiere (kôr′sĭ-tîr′) *n.* One who makes, fits, or sells corsets, brassieres, girdles, and similar undergarments. [French *corsetière*, feminine of *corsetier*, corset-maker < *corset*, corset < Old French; see CORSET.]

Cor·si·ca (kôr′sĭ-kə) An island of France in the Mediterranean Sea north of Sardinia. Napoleon Bonaparte was born on the island, which was ceded to France by Genoa in 1768. **—Cor′si·can** *adj. & n.*

cors·let (kôrs′lĭt) *n.* Variant of **corselet** (sense 1).

cor·tege also **cor·tège** (kôr-tĕzh′) *n.* **1.** A train of attendants, as of a distinguished person; a retinue. **2a.** A ceremonial procession. **b.** A funeral procession. [French *cortège* < Old Italian *corteggio* < *corteggiare*, to pay honor < *corte*, court < Latin *cohors, cohort-*, throng; see **gher-**[1] in App. I.]

Cor·tés (kôr-tĕz′, -tĕs′), **Hernando** or **Hernán** 1485–1547. Spanish explorer and conquistador who conquered Aztec Mexico for Spain.

cor·tex (kôr′tĕks′) *n., pl.* **-ti·ces** (-tĭ-sēz′) or **-tex·es 1.** *Anatomy* **a.** The outer layer of an internal organ or body structure, as of the kidney or adrenal gland. **b.** The outer layer of gray matter that covers the surface of the cerebral hemisphere. **2.** *Botany* The region of tissue in a root or stem lying between the epidermis and the vascular tissue. **3.** An external layer, such as bark or rind. [Latin, bark; see **sker-**[1] in App. I.]

cor·ti·cal (kôr′tĭ-kəl) *adj.* **1.** Of, relating to, derived from, or consisting of cortex. **2.** Of, relating to, associated with, or depending on the cerebral cortex. **—cor′ti·cal·ly** *adv.*

cor·ti·cate (kôr′tĭ-kĭt, -kāt′) also **cor·ti·cat·ed** (-kā′tĭd) *adj.* Having a cortex or a similar specialized outer layer.

cortico– or **cortic–** *pref.* Cortex: *corticotropin.* [< Latin *cortex, cortic-*, bark, rind; see CORTEX.]

APPENDIX E

Collins

175 YEARS OF DICTIONARY PUBLISHING

Dictionary

Collins

HarperCollins Publishers
Westerhill Road
Bishopbriggs
Glasgow
G64 2QT

Tenth edition 2009
REISSUED WITH REVISED SUPPLEMENT 2010

Reprint 10 9 8 7 6 5 4 3 2 1 0

UK QUARTERBOUND EDITION
ISBN 978-0-00-738233-0

UK STANDARD EDITION
ISBN 978-0-00-732119-3

AUSTRALIAN QUARTERBOUND EDITION
ISBN 978-0-7322-9009-2

AUSTRALIAN STANDARD EDITION
ISBN 978-0-7322-9008-5

NEW ZEALAND QUARTERBOUND EDITION
ISBN 978-0-00-732114-8

NEW ZEALAND STANDARD EDITION
ISBN 978-0-00-732115-5

www.collinslanguage.com

A catalogue record for this book is available from the British Library

Designed by Wolfgang Homola

Typeset by Davidson Pre-Press, Glasgow

Printed in India by Gopsons Papers Ltd

Acknowledgements
We would like to thank those authors and publishers who kindly gave permission for copyright material to be used in the Collins corpus. We would also like to thank Times Newspapers Ltd for providing valuable data.

About the type
This dictionary is typeset in CollinsFedra, a special version of the Fedra family of types designed by Peter Bil'ak. CollinsFedra has been customized especially for Collins dictionaries; it includes both sans serif (for headwords) and serif (entries) versions, in several different weights. Its large x-height, its open 'eye', and its basis in the tradition of humanist letterforms make CollinsFedra both familiar and easy to read at small sizes. It has been designed to use the minimum space without sacrificing legibility, as well as including a number of characters and signs that are specific to dictionary typography. Its companion phonetic type is the first of its kind to be drawn according to the same principles as the regular typeface, rather than assembled from rotated and reflected characters from other types. Peter Bil'ak (born 1973, Slovakia) is a graphic and type designer living in the Netherlands. He is the author of two books, Illegibility and Transparency. As well as the Fedra family, he has designed several other typefaces including Eureka. His typotheque.com website has become a focal point for research and debate around contemporary type design.

corrective (kəˈrɛktɪv) *adj* **1** tending or intended to correct ▷ *n* **2** something that tends or is intended to correct > **corˈrectively** *adv*

Corregidor (kəˈrɛgɪˌdɔː) *n* an island at the entrance to Manila Bay, in the Philippines: site of the defeat of American forces by the Japanese (1942) in World War II

correlate (ˈkɒrɪˌleɪt) *vb* **1** to place or be placed in a mutual, complementary, or reciprocal relationship **2** (*tr*) to establish or show a correlation ▷ *adj* **3** having a mutual, complementary, or reciprocal relationship ▷ *n* **4** either of two things mutually or reciprocally related > ˈ**correˌlatable** *adj*

correlation (ˌkɒrɪˈleɪʃən) *n* **1** a mutual or reciprocal relationship between two or more things **2** the act or process of correlating or the state of being correlated **3** *statistics* the extent of correspondence between the ordering of two variables. Correlation is positive or direct when two variables move in the same direction and negative or inverse when they move in opposite directions > ˌ**correˈlational** *adj*

● **ETYMOLOGY** C16: from Medieval Latin *correlātiō*, from *com-* together + *relātiō*, RELATION

correlation coefficient *n* *statistics* a statistic measuring the degree of correlation between two variables as by dividing their covariance by the square root of the product of their variances. The closer the correlation coefficient is to 1 or –1 the greater the correlation; if it is random, the coefficient is zero. See also **Pearson's correlation coefficient, Spearman's rank-order coefficient**

correlative (kɒˈrɛlətɪv) *adj* **1** in mutual, complementary, or reciprocal relationship; corresponding **2** denoting words, usually conjunctions, occurring together though not adjacently in certain grammatical constructions, as for example *neither* and *nor* in such sentences as *he neither ate nor drank* ▷ *n* **3** either of two things that are correlative **4** a correlative word > **corˈrelatively** *adv* > **corˈrelativeness** *or* **corˌrelaˈtivity** *n*

correspond (ˌkɒrɪˈspɒnd) *vb* (*intr*) **1** (usually foll by *with* or *to*) to conform, be in agreement, or be consistent or compatible (with); tally (with) **2** (usually foll by *to*) to be similar or analogous in character or function **3** (usually foll by *with*) to communicate by letter > ˌ**correˈspondingly** *adv*

● **ETYMOLOGY** C16: from Medieval Latin *correspondēre*, from Latin *respondēre* to RESPOND

correspondence (ˌkɒrɪˈspɒndəns) *n* **1** the act or condition of agreeing or corresponding **2** similarity or analogy **3** agreement or conformity **4 a** communication by the exchange of letters **b** the letters so exchanged

correspondence column *n* a section of a newspaper or magazine in which are printed readers' letters to the editor

correspondence school *n* an educational institution that offers tuition (**correspondence courses**) by post

correspondent (ˌkɒrɪˈspɒndənt) *n* **1** a person who communicates by letter or by letters **2** a person employed by a newspaper, etc, to report on a special subject or to send reports from a foreign country **3** a person or firm that has regular business relations with another, esp one in a different part f the country or abroad **4** something that corresponds to another ▷ *adj* **5** similar or analogous

Corrèze (*French* kɔrɛz) *n* a department of central France, in Limousin region. Capital: Tulle. Pop: 234 144 (2003 est). Area: 5888 sq km (2296 sq miles)

corrida (koˈrriða) *n* the Spanish word for **bullfight**

● **ETYMOLOGY** Spanish, from the phrase *corrida de toros*, literally: a running of bulls, from *correr* to run, from Latin *currere*

corridor (ˈkɒrɪˌdɔː) *n* **1** a hallway or passage connecting parts of a building **2** a strip of land or airspace along the route of a road or river: *the M1 corridor* **3** a strip of land or airspace that affords access, either from a landlocked country to the sea (such as the **Polish corridor**, 1919–39, which divided Germany) or from a state to an exclave (such as the **Berlin corridor**, 1945–90, which passed through the former East Germany) **4** a passageway connecting the compartments of a railway coach **5 corridors of power** the higher echelons of government, the Civil Service, etc, considered as the location of power and influence **6** a flight path that affords safe access for intruding aircraft **7** the path that a spacecraft must follow when re-entering the atmosphere, above which lift is insufficient and below which heating effects are excessive

● **ETYMOLOGY** C16: from Old French, from Old Italian *corridore*, literally: place for running, from *correre* to run, from Latin *currere*

corridor of uncertainty *n* **1** *cricket* an area of a wicket just outside a batsman's off stump, so located that the batsman will have difficulty in deciding whether or not to play a ball bowled into it **2** *soccer* an area of the pitch between the defenders and the goalkeeper, in which it is not clear who should take the responsibility of dealing with a ball played into it **3** any situation in which the right course of action is not clear

corrie (ˈkɒrɪ) *n* *geology* another name for **cirque** (sense 1)

● **ETYMOLOGY** C18: from Gaelic *coire* cauldron, kettle

Corriedale (ˈkɒrɪˌdeɪl) *n* a breed of sheep reared for both wool and meat, originally developed in New Zealand and Australia

corrie-fisted (ˌkɒrɪˈfɪstɪd) *adj* *Scot dialect* left-handed

● **ETYMOLOGY** C20: from earlier *car*, *ker* left hand or side, from Gaelic *cearr* left or wrong hand

Corrientes (*Spanish* koˈrrjentes) *n* a port in NE Argentina, on the Paraná River. Pop: 340 000 (2005 est)

corrigendum (ˌkɒrɪˈdʒɛndəm) *n, pl* **-da** (-də) **1** an error to be corrected **2** Also called: **erratum** (*sometimes plural*) a slip of paper inserted into a book after printing, listing errors and corrections

● **ETYMOLOGY** C19: from Latin: that which is to be corrected, from *corrigere* to CORRECT

corrigible (ˈkɒrɪdʒɪbᵊl) *adj* **1** capable of being corrected **2** submissive or submitting to correction > ˌ**corrigiˈbility** *n* > ˈ**corrigibly** *adv*

● **ETYMOLOGY** C15: from Old French, from Medieval Latin *corrigibilis*, from Latin *corrigere* to set right, CORRECT

corrival (kəˈraɪvᵊl) *n, vb* a rare word for **rival** > **corˈrivalry** *n*

● **ETYMOLOGY** C16: from Old French, from Late Latin *corrīvālis*, from Latin *com-* together, mutually + *rīvālis* RIVAL

corroborant (kəˈrɒbərənt) *adj* *archaic* **1** serving to corroborate **2** strengthening

corroborate *vb* (kəˈrɒbəˌreɪt) **1** (*tr*) to confirm or support (facts, opinions, etc), esp by providing fresh evidence: *the witness corroborated the accused's statement* ▷ *adj* (kəˈrɒbərɪt) *archaic* **2** serving to corroborate a fact, an opinion, etc **3** (of a fact) corroborated > **corˌroboˈration** *n* > **corroborative** (kəˈrɒbərətɪv) *or* **corˈroboˌratory** *adj* > **corˈroboratively** *adv* > **corˈroboˌrator** *n*

● **ETYMOLOGY** C16: from Latin *corrōborāre* to invigorate, from *rōborāre* to make strong, from *rōbur* strength, literally: oak

corroboree (kəˈrɒbərɪ) *n* *Austral* **1** a native assembly of sacred, festive, or warlike character **2** *informal* any noisy gathering

● **ETYMOLOGY** C19: from a native Australian language

corrode (kəˈrəʊd) *vb* **1** to eat away or be eaten away, esp by chemical action as in the oxidation or rusting of a metal **2** (*tr*) to destroy gradually; consume: *his jealousy corroded his happiness* > **corˈrodant** *or* **corˈrodent** *n* > **corˈroder** *n* > **corˈrodible** *adj* > **corˌrodiˈbility** *n*

● **ETYMOLOGY** C14: from Latin *corrōdere* to gnaw to pieces, from *rōdere* to gnaw; see RODENT, RAT

corrody (ˈkɒrədɪ) *n, pl* **-dies** a variant spelling of **corody**

corrosion (kəˈrəʊʒən) *n* **1** a process in which a solid, esp a metal, is eaten away and changed by a chemical action, as in the oxidation of iron in the presence of water by an electrolytic process **2** slow deterioration by being eaten or worn away **3** the condition produced by or the product of corrosion

corrosive (kəˈrəʊsɪv) *adj* **1** (esp of acids or alkalis) capable of destroying solid materials **2** tending to eat away or consume **3** cutting; sarcastic: *a corrosive remark* ▷ *n* **4** a corrosive substance, such as a strong acid or alkali > **corˈrosively** *adv* > **corˈrosiveness** *n*

corrosive sublimate *n* another name for **mercuric chloride**

corrugate *vb* (ˈkɒrʊˌgeɪt) **1** (*usually tr*) to fold or be folded into alternate furrows and ridges ▷ *adj* (ˈkɒrʊgɪt, -ˌgeɪt) **2** folded into furrows and ridges; wrinkled > ˌ**corruˈgation** *n*

● **ETYMOLOGY** C18: from Latin *corrūgāre*, from *rūga* a wrinkle

corrugated iron *n* a thin structural sheet made of iron or steel, formed with alternating ridges and troughs

corrugated paper *n* a packaging material made from layers of heavy paper, the top layer of which is grooved and ridged

corrugator (ˈkɒrʊˌgeɪtə) *n* a muscle whose contraction causes wrinkling of the brow

corrupt (kəˈrʌpt) *adj* **1** lacking in integrity; open to or involving bribery or other dishonest practices: *a corrupt official; corrupt practices in an election* **2** morally depraved **3** putrid or rotten **4** contaminated; unclean **5** (of a text or manuscript) made meaningless or different in meaning from the original by scribal errors or alterations **6** (of computer programs or data) containing errors ▷ *vb* **7** to become or cause to become dishonest or disloyal **8** to debase or become debased morally; deprave **9** (*tr*) to infect or contaminate; taint **10** (*tr*) to cause to become rotten **11** (*tr*) to alter (a text, manuscript, etc) from the original **12** (*tr*) *computing* to introduce errors into (data or a program) > **corˈrupter** *or* **corˈruptor** *n* > **corˈruptive** *adj* > **corˈruptively** *adv* > **corˈruptly** *adv* > **corˈruptness** *n*

● **ETYMOLOGY** C14: from Latin *corruptus* spoiled, from *corrumpere* to ruin, literally: break to pieces, from *rumpere* to break

corruptible (kəˈrʌptəbᵊl) *adj* susceptible to corruption; capable of being corrupted > **corˌruptiˈbility** *or* **corˈruptibleness** *n* > **corˈruptibly** *adv*

corruption (kəˈrʌpʃən) *n* **1** the act of corrupting or state of being corrupt **2** moral perversion; depravity **3** dishonesty, esp bribery **4** putrefaction or decay **5** alteration, as of a manuscript **6** an altered form of a word > **corˈruptionist** *n*

corsac (ˈkɔːsæk) *n* a fox, *Vulpes corsac*, of central Asia

● **ETYMOLOGY** C19: from a Turkic language

corsage (kɔːˈsɑːʒ) *n* **1** a flower or small bunch of flowers worn pinned to the lapel, bosom, etc, or sometimes carried by women **2** the bodice of a dress

● **ETYMOLOGY** C15: from Old French, from *cors* body, from Latin *corpus*

corsair (ˈkɔːsɛə) *n* **1** a pirate **2** a privateer, esp of the Barbary Coast

● **ETYMOLOGY** C15: from Old French *corsaire* pirate, from Medieval Latin *cursārius*, from Latin *cursus* a running, COURSE

corse (kɔːs) *n* an archaic word for **corpse**

Corse (kɔrs) *n* the French name for **Corsica**

corselet (ˈkɔːslɪt) *n* **1** a piece of armour for the top part of the body. Also spelt: **corslet** **2** a one-piece foundation garment, usually combining a brassiere and a corset

● **ETYMOLOGY** C15: from Old French, from *cors* bodice of a garment, from Latin *corpus* body

corset (ˈkɔːsɪt) *n* **1 a** a stiffened, elasticated, or laced foundation garment, worn esp by women, that usually extends from below the chest to the hips, providing support for the spine and stomach and shaping the figure **b** a similar garment worn because of injury, weakness, etc, by either sex **2** *informal* a restriction or limitation, esp government control of bank lending **3** a stiffened outer bodice worn by either sex, esp in the 16th century ▷ *vb* **4** (*tr*) to dress or enclose in, or as in, a corset

● **ETYMOLOGY** C14: from Old French, literally: a little bodice; see CORSELET

corsetier (ˌkɔːsɪˈtɪə) *n* a man who makes and fits corsets

corsetière (ˌkɔːsɛtɪˈɛə, kɔːˌsɛt-) *n* a woman who makes and fits corsets

APPENDIX F

Merriam-Webster's Collegiate® Dictionary

ELEVENTH EDITION

Merriam-Webster, Incorporated
Springfield, Massachusetts, U.S.A.

A GENUINE MERRIAM-WEBSTER

The name *Webster* alone is no guarantee of excellence. It is used by a number of publishers and may serve mainly to mislead an unwary buyer.

Merriam-Webster™ is the name you should look for when you consider the purchase of dictionaries or other fine reference books. It carries the reputation of a company that has been publishing since 1831 and is your assurance of quality and authority.

Library of Congress Cataloging in Publication Data

Merriam-Webster's collegiate dictionary. — Eleventh ed.
p. cm.
Includes index.
ISBN 978-0-87779-807-1 (Laminated unindexed : alk. paper)
ISBN 978-0-87779-808-8 (Jacketed hardcover unindexed : alk. paper)
ISBN 978-0-87779-809-5 (Jacketed hardcover with digital download : alk. paper)
ISBN 978-0-87779-810-1 (Leatherlook with digital download : alk. paper)
ISBN 978-0-87779-811-8 (Luxury Leather)
ISBN 978-0-87779-813-2 (Canadian)
ISBN 978-0-87779-814-9 (International)
1. English language—Dictionaries. I. Title: Collegiate dictionary. II. Merriam-Webster, Inc.
PE1628.M36 2003
423—dc21 2003003674
CIP

Made in the United States of America

19th Printing Quad Graphics Versailles KY December 2014

persons associated together or acting under common direction; *esp* : a body of persons having a common activity or occupation ⟨the press ~⟩ **3** : CORPS DE BALLET

corps de bal·let \ˌkȯr-də-(ˌ)ba-ˈlā\ *n, pl* **corps de ballet** *same or* ˌkȯrz-də-\ [F] (1818) : the ensemble of a ballet company

corps d'elite \ˌkȯr-dā-ˈlēt\ *n, pl* **corps d'elite** *same or* ˌkȯrz-dā-\ [F *corps d'élite*] (1832) **1** : a body of picked troops **2** : a group of the best people in a category

corpse \ˈkȯrps\ *n* [ME *corps,* fr. AF *cors, corps,* fr. L *corpus*] (13c) **1** *archaic* : a human or animal body whether living or dead **2 a** : a dead body esp. of a human being **b** : the remains of something discarded or defunct ⟨the ~*s* of rusting cars⟩

corps·man \ˈkȯr(z)-mən\ *n* (1901) **1** : an enlisted man trained to give first aid and minor medical treatment **2** : a member of a government-sponsored service corps

cor·pu·lence \ˈkȯr-pyə-lən(t)s\ *n* (1547) : the state of being corpulent

cor·pu·len·cy \-lən(t)-sē\ *n, pl* **-cies** (1577) : CORPULENCE

cor·pu·lent \-lənt\ *adj* [ME, fr. L *corpulentus,* fr. *corpus*] (14c) : having a large bulky body : OBESE — **cor·pu·lent·ly** *adv*

cor pul·mo·na·le \ˌkȯr-ˌpu̇l-mə-ˈnā-lē, -ˌpəl-, -ˈna-\ *n, pl* **cor·dia pul·mo·na·lia** \ˈkȯr-dē-ə-ˌpu̇l-mə-ˈnā-lē-ə, -ˌpəl-, -ˈna-\ [NL, lit., pulmonary heart] (1857) : disease of the heart characterized by hypertrophy and dilatation of the right ventricle and secondary to disease of the lungs or their blood vessels

cor·pus \ˈkȯr-pəs\ *n, pl* **cor·po·ra** \-p(ə-)rə\ [ME, fr. L] (15c) **1** : the body of a human or animal esp. when dead **2 a** : the main part or body of a bodily structure or organ ⟨the ~ of the uterus⟩ **b** : the main body or corporeal substance of a thing; *specif* : the principal of a fund or estate as distinct from income or interest **3 a** : all the writings or works of a particular kind or on a particular subject; *esp* : the complete works of an author **b** : a collection or body of knowledge or evidence; *esp* : a collection of recorded utterances used as a basis for the descriptive analysis of a language

corpus al·la·tum \-ə-ˈlā-təm, -ˈlā-\ *n, pl* **corpora al·la·ta** \-ˈlā-tə, -ˈlā-tə\ [NL, lit., applied body] (1947) : one of a pair of separate or fused bodies in many insects that are sometimes closely associated with the corpora cardiaca and that secrete hormones (as juvenile hormone)

corpus cal·lo·sum \-ka-ˈlō-səm\ *n, pl* **corpora cal·lo·sa** \-sə\ [NL, lit., callous body] (1677) : the great band of commissural fibers uniting the cerebral hemispheres of higher mammals including humans — see BRAIN illustration

corpus car·di·a·cum \-kär-ˈdī-ə-kəm\ *n, pl* **corpora car·di·a·ca** \-ə-kə\ [NL, lit., cardiac body] (1960) : one of a pair of separate or fused bodies of nervous tissue in many insects that lie posterior to the brain and function in the storage and secretion of brain hormone

Cor·pus Chris·ti \ˈkȯr-pəs-ˈkris-tē\ *n* [ME, fr. ML, lit., body of Christ] (14c) : the Thursday after Trinity observed as a Roman Catholic festival in honor of the Eucharist

cor·pus·cle \ˈkȯr-(ˌ)pə-səl\ *n* [L *corpusculum,* dim. of *corpus*] (1660) **1** : a minute particle **2 a** : a living cell; *esp* : one (as a red or white blood cell or a cell in cartilage or bone) not aggregated into continuous tissues **b** : any of various small circumscribed multicellular bodies — **cor·pus·cu·lar** \kȯr-ˈpəs-kyə-lər\ *adj*

cor·pus de·lic·ti \ˈkȯr-pəs-di-ˈlik-ˌtī, -(ˌ)tē\ *n, pl* **corpora delicti** [NL, lit., body of the crime] (1818) **1** : the substantial and fundamental fact necessary to prove the commission of a crime **2** : the material substance (as the body of the victim of a murder) upon which a crime has been committed

corpus lu·te·um \-ˈlü-tē-əm\ *n, pl* **corpora lu·tea** \-tē-ə\ [NL, lit., yellowish body] (1788) : a yellowish mass of progesterone-secreting endocrine tissue that forms immediately after ovulation from the ruptured graafian follicle in the mammalian ovary

corpus stri·a·tum *n, pl* **corpora stri·a·ta** [NL, lit., striated body] (1851) : either of a pair of masses of nervous tissue within the brain that contain two large nuclei of gray matter separated by sheets of white matter

corr *abbr* **1** correct; corrected; correction **2** correspondence; correspondent; corresponding **3** corrupt; corruption

cor·rade \kə-ˈrād\ *vb* **cor·rad·ed; cor·rad·ing** [L *corradere* to scrape together, fr. *com-* + *radere* to scrape — more at RODENT] *vt* (1646) : to wear away by abrasion ~ *vi* : to crumble away through abrasion — **cor·ra·sion** \-ˈrā-zhən\ *n* — **cor·ra·sive** \-ˈrā-siv, -ziv\ *adj*

[1]**cor·ral** \kə-ˈral, -ˈrel\ *n* [Sp, fr. VL **currale* enclosure for vehicles, fr. L *currus* cart, fr. *currere* to run — more at CAR] (1582) **1** : a pen or enclosure for confining or capturing livestock **2** : an enclosure made with wagons for defense of an encampment

[2]**corral** *vt* **cor·ralled; cor·ral·ling** (1847) **1** : to enclose in a corral **2** : to arrange (wagons) so as to form a corral **3** : COLLECT, GATHER ⟨*corralling* votes for the upcoming election⟩

[1]**cor·rect** \kə-ˈrekt\ *vt* [ME, fr. L *correctus,* pp. of *corrigere,* fr. *com-* + *regere* to lead straight — more at RIGHT] (14c) **1 a** : to make or set right : AMEND ⟨~ an error⟩ **b** : COUNTERACT, NEUTRALIZE ⟨~ a harmful tendency⟩ **c** : to alter or adjust so as to bring to some standard or required condition ⟨~ a lens for spherical aberration⟩ **2 a** : to punish (as a child) with a view to reforming or improving **b** : to point out usu. for amendment the errors or faults of ⟨spent the day ~*ing* tests⟩ — **cor·rect·able** \-ˈrek-tə-bəl\ *adj* — **cor·rec·tor** \-ˈrek-tər\ *n*

syn CORRECT, RECTIFY, EMEND, REMEDY, REDRESS, AMEND, REFORM, REVISE mean to make right what is wrong. CORRECT implies taking action to remove errors, faults, deviations, defects ⟨*correct* your spelling⟩. RECTIFY implies a more essential changing to make something right, just, or properly controlled or directed ⟨*rectify* a misguided policy⟩. EMEND specif. implies correction of a text or manuscript ⟨*emend* a text⟩. REMEDY implies removing or making harmless a cause of trouble, harm, or evil ⟨set out to *remedy* the evils of the world⟩. REDRESS implies making compensation or reparation for an unfairness, injustice, or imbalance ⟨*redress* past social injustices⟩. AMEND, REFORM, REVISE imply an improving by making corrective changes, AMEND usu. suggesting slight changes ⟨*amend* a law⟩, REFORM implying drastic change ⟨plans to *reform* the court system⟩, and REVISE suggesting a careful examination of something and the making of necessary changes ⟨*revise* the schedule⟩. *syn* see in addition PUNISH

[2]**correct** *adj* [ME, corrected, fr. L *correctus,* fr. pp. of *corrigere*] (1668) **1** : conforming to an approved or conventional standard ⟨~ behavior⟩ **2** : conforming to or agreeing with fact, logic, or known truth ⟨a ~ response⟩ **3** : conforming to a set figure ⟨enclosed the ~ return postage⟩ **4** : conforming to the strict requirements of a specific ideology or set of beliefs or values ⟨environmentally ~⟩ ⟨spiritually ~⟩ — **cor·rect·ly** \kə-ˈrek(t)-lē\ *adv* — **cor·rect·ness** \-ˈrek(t)-nəs\ *n*

syn CORRECT, ACCURATE, EXACT, PRECISE, NICE, RIGHT mean conforming to fact, standard, or truth. CORRECT usu. implies freedom from fault or error ⟨*correct* answers⟩ ⟨socially *correct* dress⟩. ACCURATE implies fidelity to fact or truth attained by exercise of care ⟨an *accurate* description⟩. EXACT stresses a very strict agreement with fact, standard, or truth ⟨*exact* measurements⟩. PRECISE adds to EXACT an emphasis on sharpness of definition or delimitation ⟨*precise* calibration⟩. NICE stresses great precision and delicacy of adjustment or discrimination ⟨makes *nice* distinctions⟩. RIGHT is close to CORRECT but has a stronger positive emphasis on conformity to fact or truth rather than mere absence of error or fault ⟨the *right* thing to do⟩.

corrected time *n* (ca. 1891) : a boat's elapsed time less its time allowance in yacht racing

cor·rec·tion \kə-ˈrek-shən\ *n* (14c) **1** : the action or an instance of correcting: as **a** : AMENDMENT, RECTIFICATION **b** : REBUKE, PUNISHMENT **c** : a bringing into conformity with a standard **d** : NEUTRALIZATION, COUNTERACTION ⟨~ of acidity⟩ **2** : a decline in market price or business activity following and counteracting a rise **3 a** : something substituted in place of what is wrong ⟨marking ~*s* on the students' papers⟩ **b** : a quantity applied by way of correcting (as for adjustment of an instrument) **4** : the treatment and rehabilitation of offenders through a program involving penal custody, parole, and probation; *also* : the administration of such treatment as a matter of public policy — usu. used in pl. — **cor·rec·tion·al** \-shnəl, -shə-nᵊl\ *adj*

correction fluid *n* (1968) : a liquid used to paint over typing or writing errors

cor·rec·ti·tude \kə-ˈrek-tə-ˌtüd, -ˌtyüd\ *n* [blend of *correct* and *rectitude*] (1893) : correctness or propriety of conduct

cor·rec·tive \kə-ˈrek-tiv\ *adj* (1531) : intended to correct ⟨~ lenses⟩ ⟨~ punishment⟩ — **corrective** *n* — **cor·rec·tive·ly** *adv*

[1]**cor·re·late** \ˈkȯr-ə-lət, ˈkär-, -ˌlāt\ *n* [back-formation fr. *correlation*] (1643) **1** : either of two things so related that one directly implies or is complementary to the other (as husband and wife) **2** : a phenomenon that accompanies another phenomenon, is usu. parallel to it, and is related in some way to it ⟨precise electrical ~*s* of conscious thinking in the human brain —Bayard Webster⟩ — **correlate** *adj*

[2]**cor·re·late** \-ˌlāt\ *vb* **-lat·ed; -lat·ing** *vi* (ca. 1742) : to bear reciprocal or mutual relations : CORRESPOND ~ *vt* **1 a** : to establish a mutual or reciprocal relation between ⟨~ activities in the lab and the field⟩ **b** : to show correlation or a causal relationship between **2** : to present or set forth so as to show relationship ⟨he ~*s* the findings of the scientists, the psychologists, and the mystics —Eugene Exman⟩ — **cor·re·lat·able** \-ˌlā-tə-bəl\ *adj* — **cor·re·lat·or** \-ˌlā-tər\ *n*

cor·re·la·tion \ˌkȯr-ə-ˈlā-shən, ˌkär-\ *n* [ML *correlation-, correlatio,* fr. L *com-* + *relation-, relatio* relation] (1561) **1** : the state or relation of being correlated; *specif* : a relation existing between phenomena or things or between mathematical or statistical variables which tend to vary, be associated, or occur together in a way not expected on the basis of chance alone ⟨the obviously high positive ~ between scholastic aptitude and college entrance —J. B. Conant⟩ **2** : the act of correlating — **cor·re·la·tion·al** \-shnəl, -shə-nᵊl\ *adj*

correlation coefficient *n* (1895) : a number or function that indicates the degree of correlation between two sets of data or between two random variables and that is equal to their covariance divided by the product of their standard deviations

cor·rel·a·tive \kə-ˈre-lə-tiv\ *adj* (1530) **1** : naturally related : CORRESPONDING **2** : reciprocally related **3** : regularly used together but typically not adjacent ⟨the ~ conjunctions *either . . . or*⟩ — **correlative** *n* — **cor·rel·a·tive·ly** *adv*

cor·re·spond \ˌkȯr-ə-ˈspänd, ˌkär-\ *vi* [MF or ML; MF *correspondre,* fr. ML *correspondēre,* fr. L *com-* + *respondēre* to respond] (1529) **1 a** : to be in conformity or agreement ⟨the ideal failed . . . to ~ with the reality —J. R. Sutherland⟩ **b** : to compare closely : MATCH — usu. used with *to* or *with* **c** : to be equivalent or parallel **2** : to communicate with a person by exchange of letters

cor·re·spon·dence \-ˈspän-dən(t)s\ *n* (15c) **1 a** : the agreement of things with one another **b** : a particular similarity **c** : a relation between sets in which each member of one set is associated with one or more members of the other — compare FUNCTION 5a **2 a** : communication by letters; *also* : the letters exchanged **b** : the news, information, or opinion contributed by a correspondent to a newspaper or periodical

correspondence course *n* (1902) : a course offered by a correspondence school

correspondence school *n* (1889) : a school that teaches nonresident students by mailing them lessons and exercises which upon completion are returned to the school for grading

cor·re·spon·den·cy \ˌkȯr-ə-ˈspän-dən(t)-sē, ˌkär-\ *n, pl* **-cies** (1589) : CORRESPONDENCE

[1]**cor·re·spon·dent** \ˌkȯr-ə-ˈspän-dənt, ˌkär-\ *adj* [ME, fr. MF or ML; MF, fr. ML *correspondent-, correspondens,* prp. of *correspondēre*] (15c) **1** : CORRESPONDING **2** : FITTING, CONFORMING — used with *with* or *to* ⟨the outcome was entirely ~ with my wishes⟩

[2]**correspondent** *n* (ca. 1630) **1 a** : one who communicates with another by letter **b** : one who has regular commercial relations with another **c** : one who contributes news or commentary to a publication (as a newspaper) or a radio or television network often from a distant place ⟨a war ~⟩ **2** : something that corresponds

corresponding *adj* (1579) **1 a** : having or participating in the same relationship (as kind, degree, position, correspondence, or function) esp. with regard to the same or like wholes (as geometric figures or sets) ⟨~ parts of similar triangles⟩ **b** : RELATED, ACCOMPANYING ⟨all rights carry with them ~ responsibilities —W. P. Paepcke⟩ **2 a** : charged with the duty of writing letters ⟨~ secretary⟩ **b** : participating or serving at a distance and by mail ⟨a ~ member of the society⟩ — **cor·re·spond·ing·ly** \-ˈspän-diŋ-lē\ *adv*

corresponding angles *n pl* (1784) : any pair of angles each of which is on the same side of one of two lines cut by a transversal and on the same side of the transversal

cor·re·spon·sive \ˌkȯr-ə-ˈspän(t)-siv, ˌkär-\ *adj* (1606) : mutually responsive

cor·ri·da \kō-ˈrē-t͟hə\ *n* [Sp, lit., act of running] (1802) : BULLFIGHT

cor·ri·dor \ˈkȯr-ə-dər, ˈkär-, -ˌdȯr\ *n* [MF, fr. It dial. (N Italy) *corridore*, fr. *correre* to run, fr. L *currere* — more at CAR] (1719) **1 a** : a passageway (as in a hotel or office building) into which compartments or rooms open **b** : a place or position in which esp. political power is wielded through discussion and deal-making ⟨was excluded from the ~*s* of power after losing the election⟩ **2** : a usu. narrow passageway or route: as **a** : a narrow strip of land through foreign-held territory **b** : a restricted lane for air traffic **c** : a land path used by migrating animals **3 a** : a densely populated strip of land including two or more major cities ⟨the Northeast ~ stretching from Washington into New England —S. D. Browne⟩ **b** : an area or stretch of land identified by a specific common characteristic or purpose ⟨a ~ of liberalism⟩ ⟨the city's industrial ~⟩

cor·rie \ˈkȯr-ē, ˈkär-ē\ *n* [ScGael *coire*, lit., kettle] (1795) : CIRQUE 3

Cor·rie·dale \-ˌdāl\ *n* [*Corriedale*, ranch in New Zealand] (1902) : any of a breed of rather large usu. hornless sheep developed in New Zealand and raised for mutton and wool

cor·ri·gen·dum \ˌkȯr-ə-ˈjen-dəm, ˌkär-\ *n, pl* **-da** \-də\ [L, neut. of *corrigendus*, gerundive of *corrigere* to correct] (1823) : an error in a printed work discovered after printing and shown with its correction on a separate sheet

cor·ri·gi·ble \ˈkȯr-ə-jə-bəl, ˈkär-\ *adj* [ME, fr. MF, fr. ML *corrigibilis*, fr. L *corrigere*] (15c) : capable of being set right : REPARABLE ⟨a ~ defect⟩ — **cor·ri·gi·bil·i·ty** \ˌkȯr-ə-jə-ˈbi-lə-tē, ˌkär-\ *n*

cor·ri·val \kə-ˈrī-vəl, kō-, kō-\ *n* [MF, fr. L *corrivalis*, fr. *com-* + *rivalis* rival] (1579) : RIVAL, COMPETITOR — **corrival** *adj*

cor·rob·o·rant \kə-ˈrä-bə-rənt\ *adj* (1626) *archaic* : having an invigorating effect — used of a medicine

cor·rob·o·rate \kə-ˈrä-bə-ˌrāt\ *vt* **-rat·ed; -rat·ing** [L *corroboratus*, pp. of *corroborare*, fr. *com-* + *robor-*, *robur* strength] (1529) : to support with evidence or authority : make more certain **syn** see CONFIRM — **cor·rob·o·ra·tion** \-ˌrä-bə-ˈrā-shən\ *n* — **cor·rob·o·ra·tive** \-ˈrä-bə-ˌrā-tiv, -ˈrä-b(ə-)rə-\ *adj* — **cor·rob·o·ra·tor** \-ˈrä-bə-ˌrā-tər\ *n* — **cor·rob·o·ra·to·ry** \-ˈrä-b(ə-)rə-ˌtȯr-ē\ *adj*

cor·rob·o·ree \kə-ˈrä-bə-rē, -ˈrä-\ *n* [Dharuk (Australian aboriginal language of the Port Jackson area) *garaabara*] (1811) **1** : a nocturnal festivity with songs and symbolic dances by which the Australian aborigines celebrate events of importance **2** *Austral* **a** : a noisy festivity **b** : TUMULT

cor·rode \kə-ˈrōd\ *vb* **cor·rod·ed; cor·rod·ing** [ME, fr. L *corrodere* to gnaw to pieces, fr. *com-* + *rodere* to gnaw — more at RODENT] *vt* (14c) **1** : to eat away by degrees as if by gnawing; *esp* : to wear away gradually usu. by chemical action ⟨the metal was *corroded* beyond repair⟩ **2** : to weaken or destroy gradually : UNDERMINE ⟨manners and miserliness that ~ the human spirit —Bernard De Voto⟩ ~ *vi* : to undergo corrosion — **cor·rod·ible** \-ˈrō-də-bəl\ *adj*

corrody *var of* CORODY

cor·ro·sion \kə-ˈrō-zhən\ *n* [ME, fr. LL *corrosion-*, *corrosio* act of gnawing, fr. L *corrodere*] (14c) **1** : the action, process, or effect of corroding **2** : a product of corroding

cor·ro·sive \-ˈrō-siv, -ziv\ *adj* (14c) **1** : tending or having the power to corrode ⟨~ acids⟩ ⟨~ action⟩ ⟨the ~ effects of alcoholism⟩ **2** : bitingly sarcastic ⟨~ satire⟩ — **corrosive** *n* — **cor·ro·sive·ly** *adv* — **cor·ro·sive·ness** *n*

corrosive sublimate *n* (ca. 1747) : MERCURIC CHLORIDE

cor·ru·gate \ˈkȯr-ə-ˌgāt, ˈkär-\ *vb* **-gat·ed; -gat·ing** [L *corrugatus*, pp. of *corrugare*, fr. *com-* + *ruga* wrinkle; prob. akin to Lith *raukas* wrinkle — more at ROUGH] *vt* (1620) : to form or shape into wrinkles or folds or into alternating ridges and grooves : FURROW ~ *vi* : to become corrugated

corrugated *adj* (1590) : having corrugations ⟨~ paper⟩; *also* : made of corrugated material (as cardboard) ⟨~ boxes⟩

cor·ru·ga·tion \ˌkȯr-ə-ˈgā-shən, ˌkär-\ *n* (1528) **1** : the act of corrugating **2** : a ridge or groove of a surface that has been corrugated

[1]**cor·rupt** \kə-ˈrəpt\ *vb* [ME, fr. L *corruptus*, pp. of *corrumpere*, fr. *com-* + *rumpere* to break — more at REAVE] *vt* (14c) **1 a** : to change from good to bad in morals, manners, or actions; *also* : BRIBE **b** : to degrade with unsound principles or moral values **2** : ROT, SPOIL **3** : to subject (a person) to corruption of blood **4** : to alter from the original or correct form or version ⟨the file was ~*ed*⟩ ~ *vi* **1 a** : to become tainted or rotten **b** : to become morally debased **2** : to cause disintegration or ruin **syn** see DEBASE — **cor·rupt·er** *also* **cor·rup·tor** \-ˈrəp-tər\ *n* — **cor·rupt·ibil·i·ty** \-ˌrəp-tə-ˈbi-lə-tē\ *n* — **cor·rupt·ible** \-ˈrəp-tə-bəl\ *adj* — **cor·rupt·ibly** \-blē\ *adv*

[2]**corrupt** *adj* [ME, fr. AF or L; AF, fr. L *corruptus*] (14c) **1 a** : morally degenerate and perverted : DEPRAVED **b** : characterized by improper conduct (as bribery or the selling of favors) ⟨~ judges⟩ **2** : PUTRID, TAINTED **3** : adulterated or debased by change from an original or correct condition ⟨a ~ version of the text⟩ **syn** see VICIOUS — **cor·rupt·ly** \-ˈrəp(t)-lē\ *adv* — **cor·rupt·ness** \-ˈrəp(t)-nəs\ *n*

cor·rup·tion \kə-ˈrəp-shən\ *n* (14c) **1 a** : impairment of integrity, virtue, or moral principle : DEPRAVITY **b** : DECAY, DECOMPOSITION **c** : inducement to wrong by improper or unlawful means (as bribery) **d** : a departure from the original or from what is pure or correct **2** *archaic* : an agency or influence that corrupts **3** *chiefly dial* : PUS

cor·rup·tion·ist \-sh(ə-)nist\ *n* (1810) : one who practices or defends corruption esp. in politics

corruption of blood (1563) : the effect of an attainder which bars a person from inheriting, retaining, or transmitting any estate, rank, or title

cor·rup·tive \kə-ˈrəp-tiv\ *adj* (15c) : producing or tending to produce corruption — **cor·rup·tive·ly** *adv*

cor·sage \kȯr-ˈsäzh, -ˈsäj, ˈkȯr-ˌ\ *n* [F, bust, bodice, fr. OF, bust, fr. *cors* body, fr. L *corpus*] (1830) **1** : the waist or bodice of a dress **2** : an arrangement of flowers worn as a fashion accessory

cor·sair \ˈkȯr-ˌser, kȯr-ˈ\ *n* [MF & Olt; MF *corsaire* pirate, fr. Old Occitan *corsari*, fr. OIt *corsaro*, fr. ML *cursarius*, fr. L *cursus* course — more at COURSE] (1549) : PIRATE; *esp* : a privateer of the Barbary Coast

corse \ˈkȯrs\ *n* [ME *cors*, fr. AF] (13c) *archaic* : CORPSE

corse·let *for 1* ˈkȯr-slət, *for 2* ˌkȯr-sə-ˈlet\ *n* (1563) **1** *or* **cors·let** [MF, dim. of *cors* body, bodice] : a piece of armor covering the trunk **2** *or* **cor·se·lette** [fr. *Corselette*, a trademark] : an undergarment combining girdle and brassiere

[1]**cor·set** \ˈkȯr-sət\ *n* [ME, fr. AF, dim. of *cors*] (13c) **1** : a usu. close-fitting and often laced medieval jacket **2** : a woman's close-fitting boned supporting undergarment that is often hooked and laced and that extends from above or beneath the bust or from the waist to below the hips and has garters attached

[2]**corset** *vt* (1845) **1** : to dress in or fit with a corset **2** : to restrict closely : control rigidly

cor·se·tiere \ˌkȯr-sə-ˈtir, -ˈtyer\ *n* [F *corsetière*, fem. of *corsetier*, fr. *corset*] (1848) : one who makes, fits, or sells corsets, girdles, or brassieres

cor·set·ry \ˈkȯr-sə-trē\ *n* (1904) : underwear (as corsets, girdles, and brassieres) meant to shape a woman's body

cor·tege *also* **cor·tège** \kȯr-ˈtezh, ˈkȯr-ˌ\ *n* [F *cortège*, fr. It *corteggio*, fr. *corteggiare* to court, fr. *corte* court, fr. L *cohort-*, *cohors* enclosure — more at COURT] (1648) **1** : a train of attendants : RETINUE **2** : PROCESSION; *esp* : a funeral procession

cor·tex \ˈkȯr-ˌteks\ *n, pl* **cor·ti·ces** \ˈkȯr-tə-ˌsēz\ *or* **cor·tex·es** [L *cortic-*, *cortex* bark — more at CUIRASS] (1677) **1 a (1)** : the outer or superficial part of an organ or bodily structure (as the kidney, adrenal gland, or cerebellum or a bone); *esp* : CEREBRAL CORTEX **(2)** : the proteinaceous usu. pigmented layer of a hair below the cuticle **b** : the outer part of some organisms (as paramecia) **2** : a plant bark or rind (as cinchona) used medicinally **3 a** : the typically parenchymatous layer of tissue external to the vascular tissue and internal to the corky or epidermal tissues of a green plant; *broadly* : all tissues external to the xylem **b** : an outer or investing layer of various algae, lichens, or fungi

cor·ti·cal \ˈkȯr-ti-kəl\ *adj* (1671) **1** : of, relating to, or consisting of cortex **2** : involving or resulting from the action or condition of the cerebral cortex — **cor·ti·cal·ly** \-k(ə-)lē\ *adv*

cortico- *comb form* : cortex ⟨*cortico*tropin⟩

cor·ti·coid \ˈkȯr-ti-ˌkȯid\ *n* (1941) : CORTICOSTEROID — **corticoid** *adj*

cor·ti·co·ste·roid \ˌkȯr-ti-kō-ˈstir-ˌȯid *also* -ˈster-\ *n* (1944) : any of various adrenal-cortex steroids (as corticosterone, cortisone, and aldosterone) used medically esp. as anti-inflammatory agents — compare GLUCOCORTICOID, MINERALOCORTICOID

cor·ti·co·ste·rone \ˌkȯr-tə-ˈkäs-tə-ˌrōn, -ti-kō-stə-ˈ; ˌkȯr-ti-kō-ˈstir-ˌōn, -ˈster-\ *n* (1937) : a colorless crystalline corticosteroid $C_{21}H_{30}O_4$ that is important in protein and carbohydrate metabolism

cor·ti·co·tro·pin \ˌkȯr-ti-kō-ˈtrō-pən\ *also* **cor·ti·co·tro·phin** \-fən\ *n* (1946) : ACTH; *also* : a preparation of ACTH that is used esp. in the treatment of rheumatoid arthritis and rheumatic fever

cor·ti·sol \ˈkȯr-tə-ˌsȯl, -ˌzȯl, -ˌsōl, -ˌzōl\ *n* [cortisone + [3]-*ol*] (1951) : a glucocorticoid $C_{21}H_{30}O_5$ produced by the adrenal cortex upon stimulation by ACTH that mediates various metabolic processes (as gluconeogenesis), has anti-inflammatory and immunosuppressive properties, and whose levels in the blood may become elevated in response to physical or psychological stress — called also *hydrocortisone*

cor·ti·sone \-ˌsōn, -ˌzōn\ *n* [alter. of *corticosterone*] (1949) : a glucocorticoid $C_{21}H_{28}O_5$ of the adrenal cortex used in synthetic form esp. as an anti-inflammatory agent (as for rheumatoid arthritis)

Cort·land \ˈkȯrt-lənd\ *n* [prob. fr. *Cortland* Co., New York] (1935) : a juicy apple having red skin and crisp mildly tart white flesh

co·run·dum \kə-ˈrən-dəm\ *n* [Tamil *kuruntam*; akin to Skt *kuruvinda* ruby] (1804) : a very hard mineral that consists of aluminum oxide occurring in massive and crystalline forms, that can be synthesized, and that is used for gemstones (as ruby and sapphire) and as an abrasive

co·rus·cant \kə-ˈrəs-kənt\ *adj* (15c) : SHINING, GLITTERING

cor·us·cate \ˈkȯr-ə-ˌskāt, ˈkär-\ *vi* **-cat·ed; -cat·ing** [L *coruscatus*, pp. of *coruscare* to flash] (1705) **1** : to give off or reflect light in bright beams or flashes : SPARKLE **2** : to be brilliant or showy in technique or style

cor·us·ca·tion \ˌkȯr-ə-ˈskā-shən, ˌkär-\ *n* (15c) **1** : GLITTER, SPARKLE **2** : a flash of wit

cor·vée \ˈkȯr-ˌvā, kȯr-ˈ\ *n* [F, fr. ML *corrogata*, fr. L, fem. of *corrogatus*, pp. of *corrogare* to collect, requisition, fr. *com-* + *rogare* to ask — more at RIGHT] (14c) **1** : unpaid labor (as toward constructing roads) due from a feudal vassal to his lord **2** : labor exacted in lieu of taxes by public authorities esp. for highway construction or repair

corves *pl of* CORF

cor·vette \kȯr-ˈvet\ *n* [F, fr. MF, prob. fr. MD *corf*, a kind of ship, lit., basket — more at CORF] (1636) **1** : a warship ranking in the old sailing navies next below a frigate **2** : a highly maneuverable armed escort ship that is smaller than a destroyer

cor·vid \ˈkȯr-vəd\ *n* [NL *Corvidae*, fr. *Corvus*, genus name, fr. L, raven] (ca. 1909) : any of a family (Corvidae) of stout-billed passerine birds including the crows, jays, magpies, and the raven

cor·vi·na \kȯr-ˈvē-nə\ *n* [AmerSp, fr. Sp — more at CORBINA] (1787) : any of several marine bony fishes (genus *Cynoscion* of the family Sciaenidae) of the Pacific coast of No. America

cor·vine \ˈkȯr-ˌvīn\ *adj* [L *corvinus*, fr. *corvus* raven — more at RAVEN] (ca. 1656) : of or relating to the crows : resembling a crow

Cor·vus \ˈkȯr-vəs\ *n* [L (gen. *Corvi*), lit., raven] (1658) : a small constellation adjoining Virgo on the south

Cor·y·bant \ˈkȯr-ə-ˌbant, ˈkär-\ *n, pl* **Cor·y·bants** \-ˌban(t)s\ *or* **Cor·y·ban·tes** \ˌkȯr-ə-ˈban-tēz, ˌkär-\ [MF *Corybante*, fr. L *Corybas*, fr. Gk *Korybas*] (14c) : one of the attendants or priests of Cybele noted for wildly emotional processions and rites

cor·y·ban·tic \ˌkȯr-ē-ˈban-tik, ˌkär-\ *adj* (1642) : being in the spirit or manner of a Corybant; *esp* : WILD, FRENZIED ⟨~ dancing⟩

co·ryd·a·lis \kə-ˈri-də-ləs\ *n* [NL, genus name, fr. Gk *korydallis* crested lark (*Galerida cristata*), fr. *korydos* crested lark] (1818) : any of a large

\ə\ abut \ᵊ\ kitten, F table \ər\ further \a\ ash \ā\ ace \ä\ mop, mar \au̇\ out \ch\ chin \e\ bet \ē\ easy \g\ go \i\ hit \ī\ ice \j\ job \ŋ\ sing \ō\ go \ȯ\ law \ȯi\ boy \th\ thin \t͟h\ the \ü\ loot \u̇\ foot \y\ yet \zh\ vision, beige \k, ⁿ, œ, ue, ʸ\ see Guide to Pronunciation

APPENDIX G

THE Biomedical Engineering HANDBOOK

Editor-in-Chief
JOSEPH D. BRONZINO
Trinity College
Hartford, Connecticut

CRC PRESS
IEEE PRESS
A CRC Handbook Published in Cooperation with IEEE Press

Library of Congress Cataloging-in-Publication Data

The biomedical engineering handbook / editor-in-chief, Joseph D. Bronzino.
p. cm. — (The electrical engineering handbook series)
Includes bibliographical references and index.
ISBN 0-8493-8346-3
1. Biomedical engineering—Handbooks, manuals, etc. I. Bronzino,
Joseph D., 1937– . II. Series.
[DNLM: 1. Biomedical Engineering—handbooks. QT 29 B615 1995]
R856.15.B86 1995
610'.28—dc20
DNLM/DLC
For Library of Congress 95-6294
CIP

International Standard Book Number 0-8493-8346-3
Library of Congress Card Number 95-6294
Printed in the United States of America 1 2 3 4 5 6 7 8 9 0
Printed on acid-free paper

Introduction

In the 20th century, technological innovation has progressed at such an accelerated pace that it has permeated almost every facet of our lives. This is especially true in the field of medicine and the delivery of health care services. Today, in most developed countries, the modern hospital has emerged as the center of a technologically sophisticated health care system serviced by an equally technologically sophisticated staff.

With almost continual technological innovation driving medical care, engineering professionals have become intimately involved in many medical ventures. As a result, the discipline of biomedical engineering has emerged as an integrating medium for two dynamic professions, medicine and engineering. In the process, biomedical engineers have become actively involved in the design, development, and utilization of materials, devices (such as ultrasonic lithotripsy, pacemakers, etc.), and techniques (such as signal and image processing, artificial intelligence, etc.) for clinical research, as well as the diagnosis and treatment of patients. Thus many biomedical engineers now serve as members of health care delivery teams seeking new solutions for the difficult health care problems confronting our society. The purpose of this handbook is to *provide a central core of knowledge from those fields encompassed by the discipline of biomedical engineering*. Before presenting this detailed information, it is important to provide a sense of the evolution of the modern health care system and identify the diverse activities biomedical engineers perform to assist in the diagnosis and treatment of patients.

Evolution of the Modern Health Care System

Before 1900, medicine had little to offer the average citizen, since its resources consisted mainly of the physician, his education, and his "little black bag." In general, physicians seemed to be in short supply, but the shortage had rather different causes than the current crisis in the availability of health care professionals. Although the costs of obtaining medical training were relatively low, the demand for doctors' services also was very small, since many of the services provided by the physician also could be obtained from experienced amateurs in the community. The home was typically the site for treatment and recuperation, and relatives and neighbors constituted an able and willing nursing staff. Babies were delivered by midwives, and those illnesses not cured by home remedies were left to run their natural, albeit frequently fatal, course. The contrast with contemporary health care practices, in which specialized physicians and nurses located within the hospital provide critical diagnostic and treatment services, is dramatic.

The changes that have occurred within medical science originated in the rapid developments that took place in the applied sciences (chemistry, physics, engineering, microbiology, physiology, pharmacology, etc.) at the turn of the century. This process of development was characterized by intense interdisciplinary cross-fertilization, which provided an environment in which medical research was able to take giant strides in developing techniques for the diagnosis and treatment of disease. For example, in 1903, Willem Einthoven, the Dutch physiologist, devised the first electrocardiograph to measure the electrical activity of the heart. In applying discoveries in the physical sciences to the analysis of a biologic process, he initiated a new age in both cardiovascular medicine and electrical measurement techniques.

New discoveries in medical sciences followed one another like intermediates in a chain reaction. However, the most significant innovation for clinical medicine was the development of x-rays. These "new kinds of rays," as their discoverer W. K. Roentgen described them in 1895, opened the "inner man" to medical inspection. Initially, x-rays were used to diagnose bone fractures and dislocations, and in the process, x-ray machines became commonplace in most urban hospitals. Separate departments of radiology were established, and their influence spread to other departments throughout the hospital. By the 1930s, x-ray visualization of practically all organ systems of the body had been made possible through the use of barium salts and a wide variety of radiopaque materials.

X-ray technology gave physicians a powerful tool that, for the first time, permitted accurate diagnosis of a wide variety of diseases and injuries. Moreover, since x-ray machines were too cumbersome and expensive for local doctors and clinics, they had to be placed in health care centers or hospitals. Once there, x-ray technology essentially triggered the transformation of the hospital from a passive receptacle for the sick to an active curative institution for all members of society.

For economic reasons, the centralization of health care services became essential because of many other important technological innovations appearing on the medical scene. However, hospitals remained institutions to dread, and it was not until the introduction of sulfanilamide in the mid-1930s and penicillin in the early 1940s that the main danger of hospitalization, i.e., cross-infection among patients, was significantly reduced. With these new drugs in their arsenals, surgeons were permitted to perform their operations without prohibitive morbidity and mortality due to infection. Furthermore, even though the different blood groups and their incompatibility were discovered in 1900 and sodium citrate was used in 1913 to prevent clotting, full development of blood banks was not practical until the 1930s, when technology provided adequate refrigeration. Until that time, "fresh" donors were bled and the blood transfused while it was still warm.

Once these surgical suites were established, the employment of specifically designed pieces of medical technology assisted in further advancing the development of complex surgical procedures. For example, the Drinker respirator was introduced in 1927 and the first heart-lung bypass in 1939. By the 1940s, medical procedures heavily dependent on medical technology, such as cardiac catheterization and angiography (the use of a cannula threaded through an arm vein and into the heart with the injection of radiopaque dye for the x-ray visualization of lung and heart vessels and valves), were developed. As a result, accurate diagnosis of congenital and acquired heart disease (mainly valve disorders due to rheumatic fever) became possible, and a new era of cardiac and vascular surgery was established.

Following World War II, technological advances were spurred on by efforts to develop superior weapon systems and establish habitats in space and on the ocean floor. As a by-product of these efforts, the development of medical devices accelerated and the medical profession benefited greatly from this rapid surge of "technological finds." Consider the following examples:

1. Advances in solid-state electronics made it possible to map the subtle behavior of the fundamental unit of the central nervous system—the neuron—as well as to monitor various physiologic parameters, such as the electrocardiogram, of patients in intensive care units.
2. New prosthetic devices became a goal of engineers involved in providing the disabled with tools to improve their quality of life.
3. Nuclear medicine—an outgrowth of the atomic age—emerged as a powerful and effective approach in detecting and treating specific physiologic abnormalities.

4. Diagnostic ultrasound based on sonar technology became so widely accepted that ultrasonic studies are now part of the routine diagnostic workup in many medical specialties.
5. "Spare parts" surgery also became commonplace. Technologists were encouraged to provide cardiac assist devices, such as artificial heart valves and artificial blood vessels, and the artificial heart program was launched to develop a replacement for a defective or diseased human heart.
6. Advances in materials have made the development of disposable medical devices, such as needles and thermometers, as well as implantable drug delivery systems, a reality.
7. Computers similar to those developed to control the flight plans of the *Apollo* capsule were used to store, process, and cross-check medical records, to monitor patient status in intensive care units, and to provide sophisticated statistical diagnoses of potential diseases correlated with specific sets of patient symptoms.
8. Development of the first computer-based medical instrument, the computerized axial tomography scanner, revolutionized clinical approaches to noninvasive diagnostic imaging procedures, which now include magnetic resonance imaging and positron emission tomography as well.

The impact of these discoveries and many others has been profound. The health care system consisting primarily of the "horse and buggy" physician is gone forever, replaced by a technologically sophisticated clinical staff operating primarily in "modern" hospitals designed to accommodate the new medical technology. This evolutionary process continues, with advances in biotechnology and tissue engineering altering the very nature of the health care delivery system itself.

The Field of Biomedical Engineering

Today, many of the problems confronting health professionals are of extreme interest to engineers because they involve the design and practical application of medical devices and systems—processes that are fundamental to engineering practice. These medically related design problems can range from very complex large-scale constructs, such as the design and implementation of automated clinical laboratories, multiphasic screening facilities (i.e., centers that permit many clinical tests to be conducted), and hospital information systems, to the creation of relatively small and "simple" devices, such as recording electrodes and biosensors, that may be used to monitor the activity of specific physiologic processes in either a research or clinical setting. They encompass the many complexities of remote monitoring and telemetry, including the requirements of emergency vehicles, operating rooms, and intensive care units. The American health care system, therefore, encompasses many problems that represent challenges to certain members of the engineering profession called *biomedical engineers.*

Biomedical Engineering: A Definition

Although what is included in the field of biomedical engineering is considered by many to be quite clear, there are some disagreements about its definition. For example, consider the terms *biomedical engineering, bioengineering,* and *clinical* (or *medical*) *engineering* which have been defined in Pacela's *Bioengineering Education Directory* [Quest Publishing Co., 1990]. While Pacela defines *bioengineering* as the broad umbrella term used to describe this entire field, *bioengineering* is usually defined as a basic research–oriented activity closely related to biotechnology and genetic engineering, i.e., the modification of animal or plant cells, or parts of cells, to improve plants or animals or to develop new microorganisms for beneficial ends. In the food industry, for example, this has meant the improvement of strains of yeast for fermentation. In agriculture, bioengineers may be concerned with the improvement of crop yields by treatment of plants with organisms to reduce frost damage. It is clear that bioengineers of the future will have a tremendous impact on the quality of human life, the potential of this specialty is difficult to imagine. Consider the following activities of bioengineers:

- Development of improved species of plants and animals for food production
- Invention of new medical diagnostic tests for diseases
- Production of synthetic vaccines from clone cells
- Bioenvironmental engineering to protect human, animal, and plant life from toxicants and pollutants
- Study of protein-surface interactions
- Modeling of the growth kinetics of yeast and hybridoma cells
- Research in immobilized enzyme technology
- Development of therapeutic proteins and monoclonal antibodies

In reviewing the above-mentioned terms, however, *biomedical engineering* appears to have the most comprehensive meaning. Biomedical engineers apply electrical, mechanical, chemical, optical, and other engineering principles to understand, modify, or control biologic (i.e., human and animal) systems, as well as design and manufacture products that can monitor physiologic functions and assist in the diagnosis and treatment of patients. When biomedical engineers work within a hospital or clinic, they are more properly called *clinical engineers.*

Activities of Biomedical Engineers

The breadth of activity of biomedical engineers is significant. The field has moved significantly from being concerned primarily with the development of medical devices in the 1950s and 1960s and to include a more wide-ranging set of activities. As illustrated below, the field of biomedical engineering now includes many new career areas, each of which is presented in this *Handbook*. These areas include

- Application of engineering system analysis (physiologic modeling, simulation, and control) to biologic problems
- Detection, measurement, and monitoring of physiologic signals (i.e., *biosensors* and *biomedical instrumentation*)
- Diagnostic interpretation via signal-processing techniques of bioelectric data
- Therapeutic and rehabilitation procedures and devices (rehabilitation engineering)
- Devices for replacement or augmentation of bodily functions (*artificial organs*)
- Computer analysis of patient-related data and clinical decision making (i.e., medical informatics and artificial intelligence)
- Medical imaging, i.e., the graphic display of anatomic detail or physiologic function
- The creation of new biologic products (i.e., *biotechnology* and *tissue engineering*)

Typical pursuits of biomedical engineers, therefore, include

- Research in new materials for implanted artificial organs
- Development of new diagnostic instruments for blood analysis
- Computer modeling of the function of the human heart
- Writing software for analysis of medical research data
- Analysis of medical device hazards for safety and efficacy
- Development of new diagnostic imaging systems
- Design of telemetry systems for patient monitoring
- Design of biomedical sensors for measurement of human physiologic systems variables
- Development of expert systems for diagnosis of diseases
- Design of closed-loop control systems for drug administration

- Modeling of the physiologic systems of the human body
- Design of instrumentation for sports medicine
- Development of new dental materials
- Design of communication aids for the handicapped
- Study of pulmonary fluid dynamics
- Study of the biomechanics of the human body
- Development of material to be used as replacement for human skin

Biomedical engineering, then, is an interdisciplinary branch of engineering that ranges from theoretical, nonexperimental undertakings to state-of-the-art applications. It can encompass research, development, implementation, and operation. Accordingly, like medical practice itself, it is unlikely that any single person can acquire expertise that encompasses the entire field. Yet, because of the interdisciplinary nature of this activity, there is considerable interplay and overlapping of interest and effort between them. For example, biomedical engineers engaged in the development of biosensors may interact with those interested in prosthetic devices to develop a means to detect and use the same bioelectric signal to power a prosthetic device. Those engaged in automating the clinical chemistry laboratory may collaborate with those developing expert systems to assist clinicians in making decisions based on specific laboratory data. The possibilities are endless.

Perhaps a greater potential benefit occurring from the use of biomedical engineering is identification of the problems and needs of our present health care system that can be solved using existing engineering technology and systems methodology. Consequently, the field of biomedical engineering offers hope in the continuing battle to provide high-quality health care at a reasonable cost; and if properly directed toward solving problems related to preventive medical approaches, ambulatory care services, and the like, biomedical engineers can provide the tools and techniques to make our health care system more effective and efficient.

Joseph D. Bronzino
Editor-in-Chief

The Discipline of Biomedical Engineering

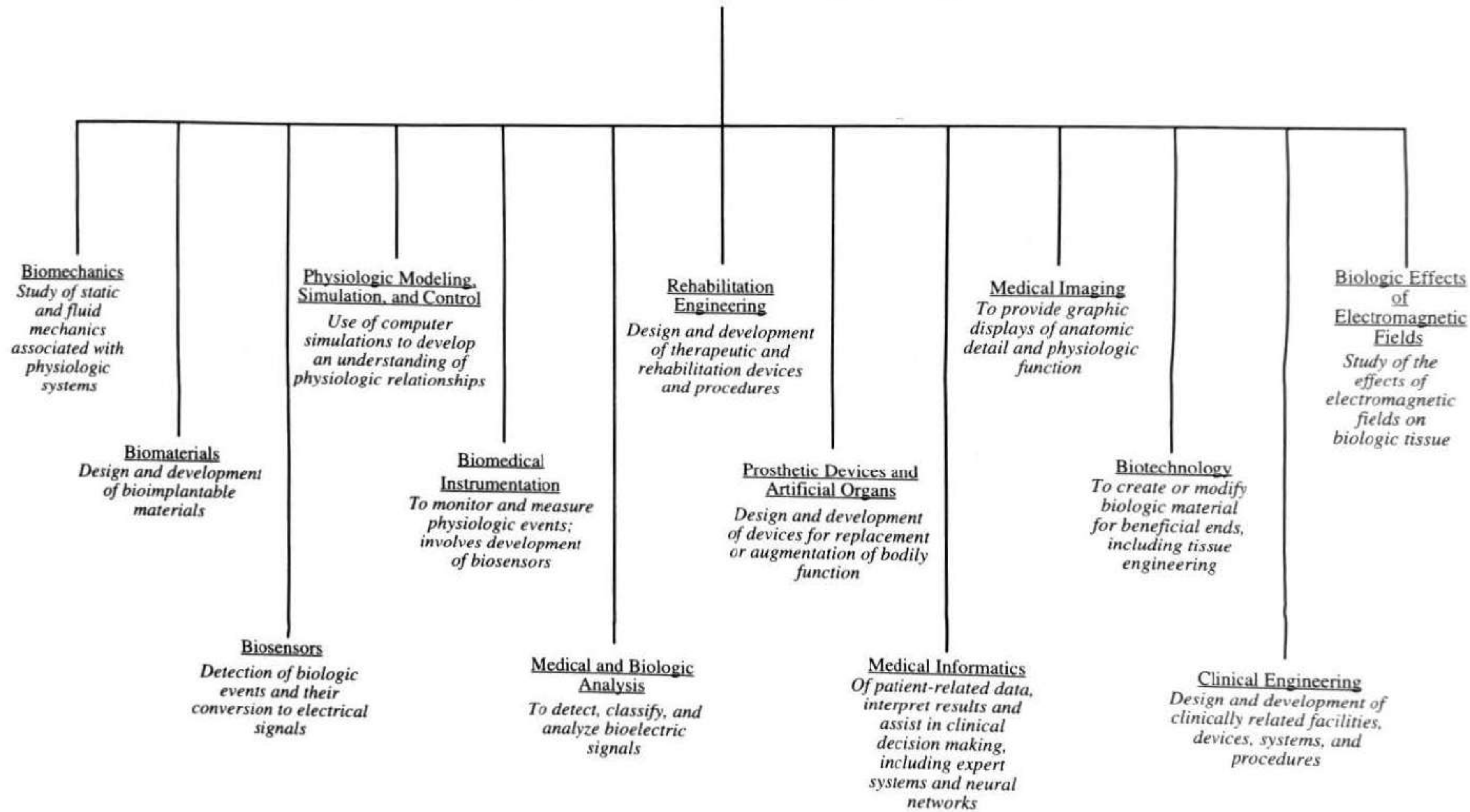

THE Biomedical Engineering HANDBOOK

Editor-in-Chief

JOSEPH D. BRONZINO

Trinity College

Hartford, Connecticut

CRC PRESS IEEE PRESS

A CRC Handbook Published in Cooperation with IEEE Press

Library of Congress Cataloging-in-Publication Data

The biomedical engineering handbook / editor-in-chief, Joseph D. Bronzino.
p. cm. — (The electrical engineering handbook series)
Includes bibliographical references and index.
ISBN 0-8493-8346-3
1. Biomedical engineering—Handbooks, manuals, etc. I. Bronzino, Joseph D., 1937– . II. Series.
[DNLM: 1. Biomedical Engineering—handbooks. QT 29 B615 1995]
R856.15.B86 1995
610′.28—dc20
DNLM/DLC
For Library of Congress 95-6294
CIP

No claim to original U.S. Government works
International Standard Book Number 0-8493-8346-3
Library of Congress Card Number 95-6294
Printed in the United States of America 1 2 3 4 5 6 7 8 9 0
Printed on acid-free paper

52

Optical Sensors

Yitzhak Mendelson
Worcester Polytechnic Institute

Optical methods are among the oldest and best-established techniques for sensing biochemical analytes. Instrumentation for optical measurements generally consists of a light source, a number of optical components to generate a light beam with specific characteristics and to direct this light to some modulating agent, and a photodetector for processing the optical signal. The central part of an optical sensor is the modulating component, and a major part of this chapter will focus on how to exploit the interaction of an analyte with optical radiation in order to obtain essential biochemical information.

The number of publications in the field of optical sensors for biomedical applications has grown significantly during the past two decades. Numerous scientific reviews and historical perspectives have been published, and the reader interested in this rapidly growing field is advised to consult these sources for additional details. This chapter will emphasize the basic concept of typical optical sensors intended for continuous in vivo monitoring of biochemical variables, concentrating on those sensors which have generally progressed beyond the initial feasibility stage and reached the promising stage of practical development or commercialization.

Optical sensors are usually based on optical fibers or on planar waveguides. Generally, there are three distinctive methods for quantitative optical sensing at surfaces:

1. The analyte directly affects the optical properties of a waveguide, such as evanescent waves (electromagnetic waves generated in the medium outside the optical waveguide when light is reflected from within) or surface plasmons (resonances induced by an evanescent wave in a thin film deposited on a waveguide surface).
2. An optical fiber is used as a plain transducer to guide light to a remote sample and return light from the sample to the detection system. Changes in the intrinsic optical properties of the medium itself are sensed by an external spectrophotometer.
3. An indicator or chemical reagent placed inside, or on, a polymeric support near the tip of the optical fiber is used as a mediator to produce an observable optical signal. Typically, conventional techniques, such as absorption spectroscopy and fluorimetry, are employed to measure changes in the optical signal.

0-8493-8346-3/95/$0.00+$.50

52.1 Instrumentation

The actual implementation of instrumentation designed to interface with optical sensors will vary greatly depending on the type of optical sensor used and its intended application. A block diagram of a generic instrument is illustrated in Fig. 52.1. The basic building blocks of such an instrument are the light source, various optical elements, and photodetectors.

Light Source

A wide selection of light sources are available for optical sensor applications. These include: highly coherent gas and semiconductor diode lasers, broad spectral band incandescent lamps, and narrow-band, solid-state, light-emitting diodes (LEDs). The important requirement of a light source is obviously good stability. In certain applications, for example in portable instrumentation, LEDs have significant advantages over other light sources because they are small and inexpensive, consume low power, produce selective wavelengths, and are easy to work with. In contrast, tungsten lamps produce a broader range of wavelengths, higher intensity, and better stability but require a sizable power supply and can cause heating problems inside the apparatus.

Optical Elements

Various optical elements are used routinely to manipulate light in optical instrumentation. These include lenses, mirrors, light choppers, beam splitters, and couplers for directing the light from the light source into the small aperture of a fiber optic sensor or a specific area on a waveguide surface and collecting the light from the sensor before it is processed by the photodetector. For wavelength selection, optical filters, prisms, and diffraction gratings are the most common components used to provide a narrow bandwidth of excitation when a broadwidth light source is utilized.

Photodetectors

In choosing photodetectors for optical sensors, a number of factors must be considered. These include sensitivity, detectivity, noise, spectral response, and response time. Photomultipliers and

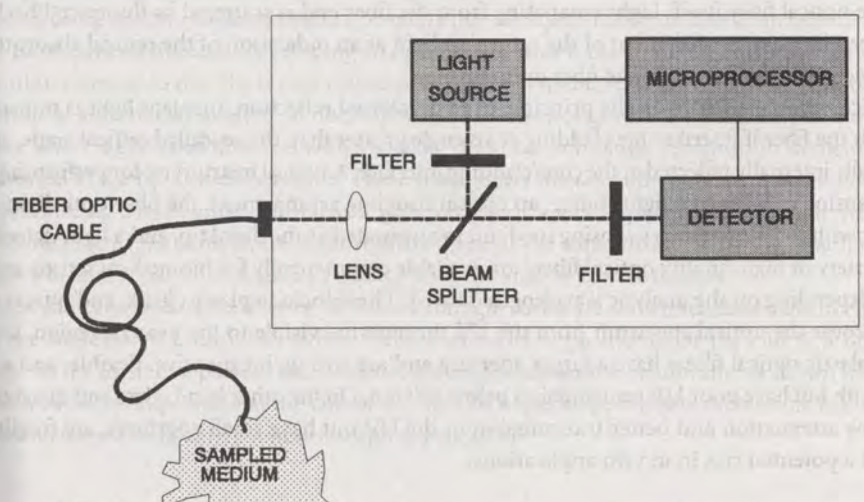

FIGURE 52.1 General diagram representing the basic building blocks of an optical instrument for optical sensor applications.

semiconductor quantum photodetectors, such as photoconductors and photodiodes, are both suitable. The choice, however, is somewhat dependent on the wavelength region of interest. Generally, both give adequate performance. Photodiodes are usually more attractive because of the compactness and simplicity of the circuitry involved.

Typically, two photodetectors are used in optical instrumentation because it is often necessary to include a separate reference detector to track fluctuations in source intensity and temperature. By taking a ratio between the two detector readings, whereby a part of the light that is not affected by the measurement variable is used for correcting any optical variations in the measurement system, a more accurate and stable measurement can be obtained.

Signal Processing

Typically, the signal obtained from a photodetector provides a voltage or a current proportional to the measured light intensity. Therefore, either simple analog computing circuitry (e.g., a current-to-voltage converter) or direct connection to a programmable gain voltage stage is appropriate. Usually, the output from a photodetector is connected directly to a preamplifier before it is applied to sampling and analog-to-digital conversion circuitry residing inside a computer.

Quite often two different wavelengths of light are utilized to perform a specific measurement. One wavelength is usually sensitive to changes in the species being measured, and the other wavelength is unaffected by changes in the analyte concentration. In this manner, the unaffected wavelength is used as a reference to compensate for fluctuations in instrumentation over time. In other applications, additional discriminations, such as pulse excitation or electronic background subtraction utilizing synchronized lock-in amplifier detection, are useful, allowing improved selectivity and enhanced signal-to-noise ratio.

52.2 Optical Fibers

Several types of biomedical measurements can be made by using either plain optical fibers as a remote device for detecting changes in the spectral properties of tissue and blood or optical fibers tightly coupled to various indicator-mediated transducers. The measurement relies either on direct illumination of a sample through the endface of the fiber or by excitation of a coating on the side wall surface through evanescent wave coupling. In both cases, sensing takes place in a region outside the optical fiber itself. Light emanating from the fiber end is scattered or fluoresced back into the fiber, allowing measurement of the returning light as an indication of the optical absorption or fluorescence of the sample at the fiber optic tip.

Optical fibers are based on the principle of total internal reflection. Incident light is transmitted through the fiber if it strikes the cladding at an angle greater than the so-called critical angle, so that it is totally internally reflected at the core/cladding interface. A typical instrument for performing fiber optic sensing consists of a light source, an optical coupling arrangement, the fiber optic light guide with or without the necessary sensing medium incorporated at the distal tip, and a light detector.

A variety of high-quality optical fibers are available commercially for biomedical sensor applications, depending on the analytic wavelength desired. These include plastic, glass, and quartz fibers which cover the optical spectrum from the UV through the visible to the near IR region. On one hand, plastic optical fibers have a larger aperture and are strong, inexpensive, flexible, and easy to work with but have poor UV transmission below 400 nm. On the other hand, glass and quartz fibers have low attenuation and better transmission in the UV but have small apertures, are fragile, and present a potential risk in in vivo applications.

Probe Configurations

There are many different ways to implement fiber optic sensors. Most fiber optic chemical sensors employ either a single-fiber configuration, where light travels to and from the sensing tip in one fiber, or a double-fiber configuration, where separate optical fibers are used for illumination and detection. A single fiber optic configuration offers the most compact and potentially least expensive implementation. However, additional challenges in instrumentation are involved in separating the illuminating signal from the composite signal returning for processing.

The design of intravascular catheters require special considerations related to the sterility and biocompatibility of the sensor. For example, intravascular fiberoptic sensors must be sterilizable and their material nonthrombogenic and resistant to platelet and protein deposition. Therefore, these catheters are typically made of materials covalently bound with heparin or antiplatelet agents. The catheter is normally introduced into the jugular vein via a peripheral cut-down and a slow heparin flush is maintained until it is removed from the blood.

Optical Fiber Sensors

Advantages cited for fiber optic sensors include their small size and low cost. In contrast to electrical measurements, where the difference of two absolute potentials must be measured, fiber optics are self-contained and do not require an external reference signal. Because the signal is optical, there is no electrical risk to the patient, and there is no direct interference from surrounding electric or magnetic fields. Chemical analysis can be performed in real-time with almost an instantaneous response. Furthermore, versatile sensors can be developed that respond to multiple analytes by utilizing multiwavelength measurements.

Despite these advantages, optical fiber sensors exhibit several shortcomings. Sensors with immobilized dyes and other indicators have limited long-term stability, and their shelf life degrades over time. Moreover, ambient light can interfere with the optical measurement unless optical shielding or special time-synchronous gating is performed.

Indicator-Mediated Transducers

Only a limited number of biochemical analytes have an intrinsic optical absorption that can be measured with sufficient selectivity directly by spectroscopic methods. Other species, particularly hydrogen, oxygen, carbon dioxide, and glucose, which are of primary interest in diagnostic applications, are not susceptible to direct photometry. Therefore, indicator-mediated sensors have been developed using specific reagents that are properly immobilized on the surface of an optical sensor.

The most difficult aspect of developing an optical biosensor is the coupling of light to the specific recognition element so that the sensor can respond selectively and reversibly to a change in the concentration of a particular analyte. In fiber-optic-based sensors, light travels efficiently to the end of the fiber where it exits and interacts with a specific chemical or biologic recognition element that is immobilized at the tip of the fiber optic. These transducers may include indicators and ionophores (i.e., ion-binding compounds) as well as a wide variety of selective polymeric materials. After the light interacts with the sample, the light returns through the same or a different optical fiber to a detector which correlates the degree of change with the analyte concentration.

Typical indicator-mediated fiber-optic-sensor configurations are shown schematically in Fig. 52.2. In (*a*) the indicator is immobilized directly on a membrane positioned at the end of a fiber. An indicator in the form of a powder can be either glued directly onto a membrane, as shown in (*b*), or physically retained in position at the end of the fiber by a special permeable membrane (*c*), a tubular capillary/membrane (*d*), or a hollow capillary tube (*e*).

52.3 General Principles of Optical Sensing

Two major optical techniques are commonly available to sense optical changes at sensor interfaces. These are usually based on evanescent wave and surface plasmon resonance principles.

Evanescent Wave Spectroscopy

When light propagates along an optical fiber, it is not confined to the core region but penetrates to some extent into the surrounding cladding region. In this case, an electromagnetic component of the light penetrates a characteristic distance (on the order of one wavelength) beyond the reflecting surface into the less optically dense medium where it is attenuated exponentially according to Beer-Lambert's law (Fig. 52.3).

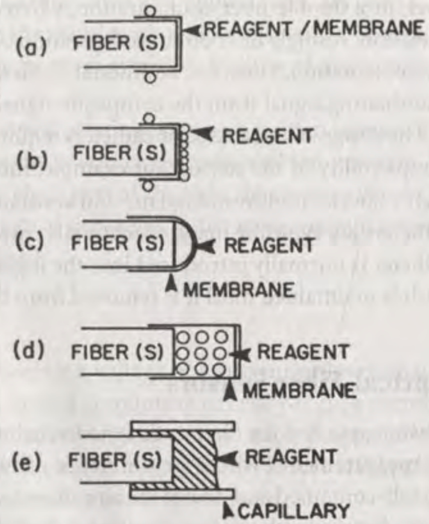

FIGURE 52.2 Typical configuration of different indicator-mediated fiber optic sensor tips (from Otto S. Wolfbeis, Fiber Optic Chemical Sensors and Biosensors, vol. 1, CRC Press, Boca Raton, 1990).

The evanescent wave depends on the angle of incidence and the incident wavelength. This phenomenon has been widely exploited to construct different types of optical sensors for biomedical applications. Because of the short penetration depth and the exponential decay of the intensity, the evanescent wave is absorbed mainly by absorbing compounds very close to the surface. In the case of particularly weak absorbing analytes, sensitivity can be enhanced by combining the evanescent wave principle with multiple internal reflections along the sides of an unclad portion of a fiber optic tip.

Instead of an absorbing species, a fluorophore can also be used. Light is absorbed by the fluorophore emitting detectable fluorescent light at a higher wavelength, thus providing improved sensitivity. Evanescent wave sensors have been applied successfully to measure the fluorescence of indicators in solution, for pH measurement, and in immunodiagnostics.

Surface Plasmon Resonance

Instead of the dielectric/dielectric interface used in evanescent wave sensors, it is possible to arrange a dielectric/metal/dielectric sandwich layer such that when monochromatic polarized light (e.g., from a laser source) impinges on a transparent medium having a metallized (e.g., Ag or Au) surface, light is absorbed within the plasma formed by the conduction electrons of the metal. This results in a phenomenon known as *surface plasmon resonance* (SPR). When SPR is induced, the effect is

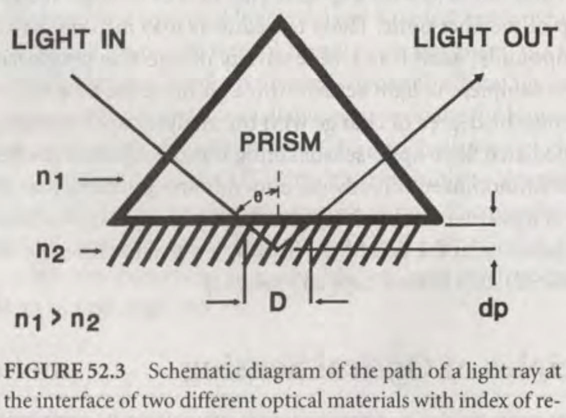

FIGURE 52.3 Schematic diagram of the path of a light ray at the interface of two different optical materials with index of refraction n_1 and n_2. The ray penetrates a fraction of a wavelength (*dp*) beyond the interface into the medium with the smaller refractive index.

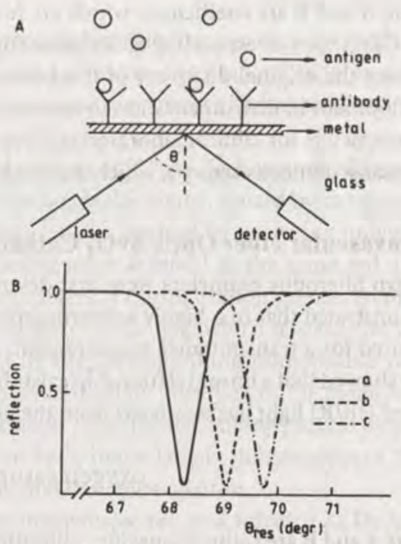

FIGURE 52.4 Surface plasmon resonance at the interface between a thin metallic surface and a liquid (A). A sharp decrease in the reflected light intensity can be observed in (B). The location of the resonance angle is dependent on the refractive index of the material present at the interface.

observed as a minimum in the intensity of the light reflected off the metal surface.

As is the case with the evanescent wave, an SPR is exponentially decaying into solution with a penetration depth of about 20 nm. The resonance between the incident light and the plasma wave depends on the angle, wavelength, and polarization state of the incident light and the refractive indices of the metal film and the materials on either side of the metal film. A change in the dielectric constant or the refractive index at the surface causes the resonance angle to shift, thus providing a highly sensitive means of monitoring surface reactions.

The method of SPR is generally used for sensitive measurement of variations in the refractive index of the medium immediately surrounding the metal film. For example, if an antibody is bound to or absorbed into the metal surface, a noticeable change in the resonance angle can be readily observed because of the change of the refraction index at the surface, assuming all other parameters are kept constant (Fig. 52.4). The advantage of this concept is the improved ability to detect the direct interaction between antibody and antigen as an interfacial measurement.

SPR has been used to analyze immunochemicals and to detect gases. The main limitations of SPR, however, is that the sensitivity depends on the optical thickness of the adsorbed layer, and, therefore, small molecules cannot be measured in very low concentrations.

52.4 Applications

Oximetry

Oximetry refers to the colorimetric measurement of the degree of oxygen saturation, that is, the relative amount of oxygen carried by the hemoglobin in the erythrocytes, by recording the variation in the color of deoxyhemoglobin (Hb) and oxyhemoglobin (HbO_2). A quantitative method for measuring blood oxygenation is of great importance in assessing the circulatory and respiratory status of a patient.

Various optical methods for measuring the oxygen saturation of arterial (SaO_2) and mixed venous (SvO_2) blood have been developed, all based on light transmission through, or reflecting from, tissue and blood. The measurement is performed at two specific wavelengths: λ_1, where there is a large difference in light absorbance between Hb and HbO_2 (e.g., 660 nm red light), and λ_2, which can be an isobestic wavelength (e.g., 805 nm infrared light), where the absorbance of light is independent of blood oxygenation, or a different wavelength in the infrared region > 805 nm, where the absorbance of Hb is slightly smaller than that of HbO_2.

Assuming for simplicity that a hemolyzed blood sample consists of a two-component homogeneous mixture of Hb and HbO_2, and that light absorbance by the mixture of these two components is additive, a simple quantitative relationship can be derived for computing the oxygen saturation of blood:

$$\text{Oxygen saturation} = A - B\left[\frac{OD(\lambda_1)}{OD(\lambda_2)}\right]$$

where A and B are coefficients which are functions of the specific absorptivities of Hb and HbO_2, and OD is the corresponding absorbance (optical density) of the blood.

Since the original discovery of this phenomenon over 50 years ago, there has been progressive development in instrumentation to measure oxygen saturation along three different paths: bench-top oximeters for clinical laboratories, fiber optic catheters for invasive intravascular monitoring, and transcutaneous sensors, which are noninvasive devices placed against the skin.

Intravascular Fiber Optic SvO_2 Catheters

In vivo fiberoptic oximeters were first described in the early 1960s by Polanyi and Heir [1]. They demonstrated that in a highly scattering medium such as blood, where a very short path length is required for a transmittance measurement, a reflectance measurement was practical. Accordingly, they showed that a linear relationship exists between oxygen saturation and the ratio of the infrared-to-red (IR/R) light backscattered from the blood

$$\text{oxygen saturation} = \mathbf{a} - \mathbf{b}(\text{IR/R})$$

where **a** and **b** are catheter-specific calibration coefficients.

Fiber optic SvO_2 catheters consist of two separate optical fibers. One fiber is used for transmitting the light to the flowing blood, and a second fiber directs the backscattered light to a photodetector. In some commercial instruments (e.g., Oximetrix), automatic compensation for hematocrit is employed utilizing three, rather than two, infrared reference wavelengths. Bornzin and coworkers [2] and Mendelson and coworkers [3] described a 5-lumen, 7.5F thermodilution catheter that is comprised of three unequally spaced optical fibers, each fiber 250 μm in diameter, and provides continuous SvO_2 reading with automatic corrections for hematocrit variations (Fig. 52.5).

Intravenous fiberoptic catheters are utilized in monitoring SvO_2 in the pulmonary artery and can be used to indicate the effectiveness of the cardiopulmonary system during cardiac surgery and in the ICU. Several problems limit the wide clinical application of intravascular fiberoptic oximeters. These include the dependence of the individual red and infrared backscattered light intensities and their ratio on hematocrit (especially for SvO_2 below 80%), blood flow, motion artifacts due to catheter tip "whipping" against the blood vessel wall, blood temperature, and pH.

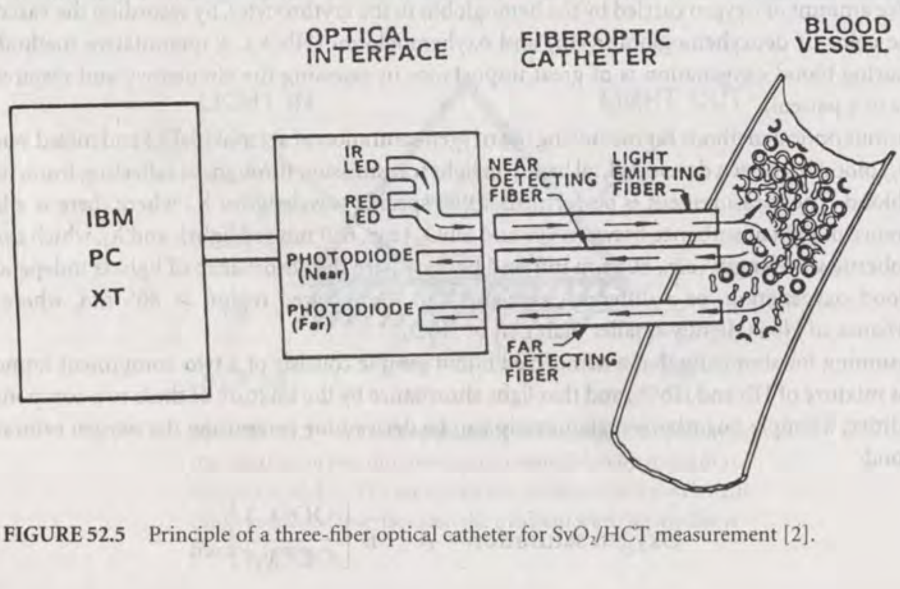

FIGURE 52.5 Principle of a three-fiber optical catheter for SvO_2/HCT measurement [2].

Noninvasive Pulse Oximetry

Noninvasive monitoring of SaO_2 by pulse oximetry is a rapidly growing practice in many fields of clinical medicine [4]. The most important advantage of this technique is the capability to provide continuous, safe, and effective monitoring of blood oxygenation at the patient's bedside without the need to calibrate the instrument before each use.

Pulse oximetry, which was first suggested by Aoyagi and colleagues [5] and Yoshiya and colleagues [6], relies on the detection of the time-variant photoplethysmographic signal, caused by changes in arterial blood volume associated with cardiac contraction. SaO_2 is derived by analyzing only the time-variant changes in absorbance caused by the pulsating arterial blood at the same red and infrared wavelengths used in conventional invasive type oximeters. A normalization process is commonly performed by which the pulsatile (*ac*) component at each wavelength, which results from the expansion and relaxation of the arterial bed, is divided by the corresponding nonpulsatile (*dc*) component of the photoplethysmogram, which is composed of the light absorbed by the blood-less tissue and the nonpulsatile portion of the blood compartment. This effective scaling process results in a normalized red/infrared ratio which is dependent on SaO_2 but is largely independent of the incident light intensity, skin pigmentation, skin thickness, and tissue vasculature.

Pulse oximeter sensors consist of a pair of small and inexpensive red and infrared LEDs and a single, highly sensitive, silicone photodetector. These components are mounted inside a reusable rigid spring-loaded clip, a flexible probe, or a disposable adhesive wrap (Fig. 52.6). The majority of the commercially available sensors are of the transmittance type in which the pulsatile arterial bed, e.g., ear lobe, fingertip, or toe, is positioned between the LEDs and the photodetector. Other probes are available for reflectance (backscatter) measurement where both the LEDs and photodetector are mounted side-by-side facing the skin [7, 8].

Noninvasive Cerebral Oximetry

Another substance whose optical absorption in the near infrared changes corresponding to its reduced and oxidized state is cytochrome aa3, the terminal member of the respiratory chain. Although the concentration of cytochrome aa3 is considerably lower than that of hemoglobin, advanced instrumentation including time-resolved spectroscopy and differential measurements is being used successfully to obtain noninvasive measurements of hemoglobin saturation and cytochrome aa3 by transilluminating areas of the neonatal brain [9–11].

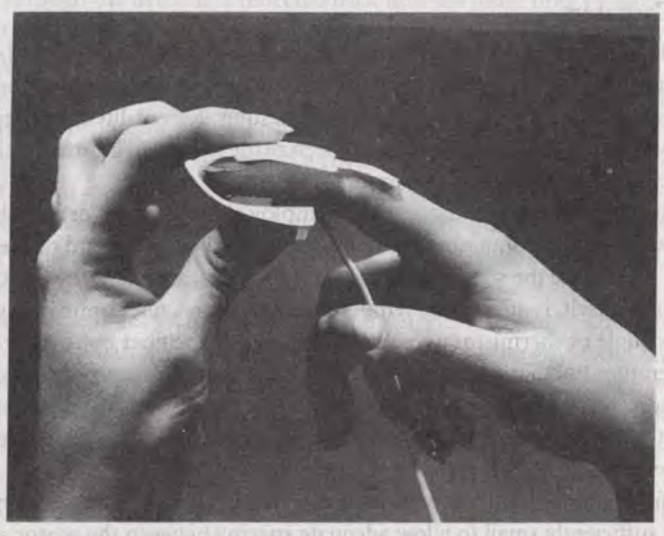

FIGURE 52.6 Disposable finger probe of a noninvasive pulse oximeter.

Blood Gases

Frequent measurement of blood gases, i.e., oxygen partial pressure (pO_2), carbon dioxide partial pressure (pCO_2), and pH, is essential to clinical diagnosis and management of respiratory and metabolic problems in the operating room and the ICU. Considerable effort has been devoted over the last two decades to developing disposable extracorporeal and in particular intravascular fiber optic sensors which can be used to provide continuous information on the acid-base status of a patient.

In the early 1970s, Lubbers and Opitz [12] originated what they called *optodes* (from the Greek, *optical path*) for measurements of important physiologic gases in fluids and in gases. The principle upon which these sensors was designed was a closed cell containing a fluorescent indicator in solution, with a membrane permeable to the analyte of interest (either ions or gases) constituting one of the cell walls. The cell was coupled by optical fibers to a system that measured the fluorescence in the cell. The cell solution would equilibrate with the pO_2 or pCO_2 of the medium placed against it, and the fluorescence of an indicator reagent in the solution would correspond to the partial pressure of the measured gas.

Extracorporeal Measurement

Following the initial feasibility studies of Lubbers and Opitz, Cardiovascular Devices (CDI, USA) developed a GasStat extracorporeal system suitable for continuous online monitoring of blood gases ex vivo during cardiopulmonary bypass operations. The system consists of a disposable plastic sensor connected inline with a blood loop through a fiber optic cable. Permeable membranes separate the flowing blood from the sensor chemistry. The CO_2-sensitive indicator consists of a fine emulsion of a bicarbonate buffer in a two-component silicone. The pH-sensitive indicator is a cellulose material to which hydroxypyrene trisulfonate (HPTS) is bonded covalently. The O_2-sensitive chemistry is composed of a solution of oxygen-quenching decacyclene in a one-component silicone covered with a thin layer of black PTFE for optical isolation and to render the measurement insensitive to the halothane anesthetic.

The extracorporeal device has two channels, one for arterial blood and the other for venous blood, and is capable of recording the temperature of the blood for correcting the measurements to 37°C. Several studies have been conducted comparing the specifications of the GasStat with that of intermittent blood samples analyzed on bench-top blood gas analyzers [13–15].

Intravascular Catheters

During the past decade, numerous efforts have been made to develop integrated fiber optic sensors for intravascular monitoring of blood gases. A few commercial systems for monitoring blood gases and pH are currently undergoing extensive clinical testing. Recent literature reports of sensor performance show that considerable progress has been made mainly in improving the accuracy and reliability of these intravascular blood gas sensors [16–19].

Most fiber optic intravascular blood gas sensors employ either a single- or a double-fiber configuration. Typically, the matrix containing the indicator is attached to the end of the optical fiber as illustrated in Fig. 52.7. Since the solubility of O_2 and CO_2 gases, as well as the optical properties of the sensing chemistry itself, is affected by temperature variations, fiber optic intravascular sensors include a thermocouple or thermistor wire running alongside the fiber optic cable to monitor and correct for temperature fluctuations near the sensor tip. A nonlinear response is characteristic of most chemical indicator sensors, so they are designed to match the concentration region of the intended application. Also, the response time of the optode is somewhat slower compared to electrochemical sensors.

Intravascular fiber optic blood gas sensors are normally placed inside a standard 20-gauge catheter, which is sufficiently small to allow adequate spacing between the sensor and the catheter wall. The resulting lumen is large enough to permit the withdrawal of blood samples, introduction

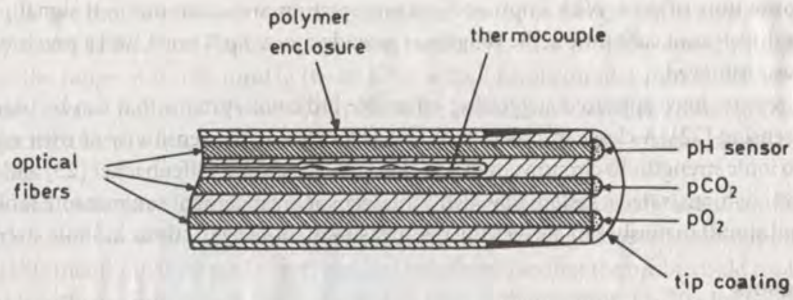

FIGURE 52.7 Principle diagram of an integrated fiber optic blood gas catheter (from Otto S. Wolfbeis, Fiber Optic Chemical Sensors and Biosensors, vol. 2, CRC Press, Boca Raton, 1990).

of a continuous heparin flush, and the recording of a blood pressure waveform. In addition, the optical fibers are encased in a protective tubing to contain any fiber fragments in case they break off.

pH Sensors

In 1976, Peterson and coworkers [20] originated the development of the first fiber optic chemical sensor for physiological pH measurement. The basic idea was to contain a reversible color-changing indicator at the end of a pair of optical fibers. The indicator, phenol red, was covalently bound to a hydrophilic polymer in the form of water-permeable microbeads. This technique stabilized the indicator concentration. The indicator beads were contained in a sealed hydrogen-ion-permeable envelope made out of a hollow cellulose tubing. In effect, this formed a miniature spectrophotometric cell at the end of the fibers and represented an early prototype of a fiber optic chemical sensor.

The phenol red dye indicator is a weak organic acid, and the acid form (un-ionized) and base form (ionized) are present in a concentration ratio determined by the ionization constant of the acid and the pH of the medium according to the familiar Henderson-Hasselbalch equation. The two forms of the dye have different optical absorption spectra, so the relative concentration of one of the forms, which varies as a function of pH, can be measured optically and related to variations in pH. In the pH sensor, green (560 nm) and red (longer than 600 nm) light emerging form the end of one fiber passes through the dye and is reflected back into the other fiber by light-scattering particles. The green light is absorbed by the base form of the indicator. The red light is not absorbed by the indicator and is used as an optical reference. The ratio of green to red light is measured and is related to pH by an *S*-shaped curve with an approximate high-sensitivity linear region where the equilibrium constant (*pK*) of the indicator matches the pH of the solution.

The same principle can also be used with a reversible fluorescent indicator, in which case the concentration of one of the indicator forms is measured by its fluorescence rather than absorbance intensity. Light in the blue or UV wavelength region excites the fluorescent dye to emit longer wavelength light, and the two forms of the dye may have different excitation or emission spectra to allow their distinction.

The original instrument design for a pH measurement was very simple and consisted of a tungsten lamp for fiber illumination, a rotating filter wheel to select the green and red light returning from the fiber optic sensor, and signal processing instrumentation to give a pH output based on the green-to-red ratio. This system was capable of measuring pH in the physiologic range between 7.0–7.4 with an accuracy and precision of 0.01 pH units. The sensor was susceptible to ionic strength variation in the order of 0.01 pH unit per 11% change in ionic strength.

Further development of the pH probe for practical use was continued by Markle and colleagues [21]. They designed the fiber optic probe in the form of a 25-gauge (0.5 mm o.d.) hypodermic needle, with an ion-permeable side window, using 75-mm-diameter plastic optical fibers. The sensor had a

90% response time of 30 s. With improved instrumentation and computerized signal processing, and with a three-point calibration, the range was extended to ± 3 pH units, and a precision of 0.001 pH units was achieved.

Several reports have appeared suggesting other dye indicator systems that can be used for fiber optic pH sensing [22]. A classic problem with dye indicators is the sensitivity of their equilibrium constant to ionic strength. To circumvent this problem, Wolfbeis and Offenbacher [23] and Opitz and Lubbers [24] demonstrated a system in which a dual sensor arrangement can measure ionic strength and pH and simultaneously can correct the pH measurement for variations in ionic strength.

pCO_2 Sensors

The pCO_2 of a sample is typically determined by measuring changes in the pH of a bicarbonate solution which is isolated from the sample by a CO_2-permeable membrane but remains in equilibrium with the CO_2. The bicarbonate and CO_2, as carbonic acid, form a pH buffer system, and, by the Henderson-Hasselbalch equation, hydrogen ion concentration is proportional to the pCO_2 in the sample. This measurement is done with either a pH electrode or a dye indicator in solution.

Vurek [25] demonstrated that the same techniques can be used also with a fiber optic sensor. In his design, one plastic fiber carries light to the transducer, which is made of a silicone rubber tubing about 0.6 mm in diameter and 1.0 mm long, filled with a phenol red solution in a 35-mM bicarbonate. Ambient pCO_2 controls the pH of the solution which changes the optical absorption of the phenol red dye. The CO_2 permeates through the rubber to equilibrate with the indicator solution. A second optical fiber carries the transmitted signal to a photodetector for analysis. The design by Zhujun and Seitz [26] uses a pCO_2 sensor based on a pair of membranes separated from a bifurcated optical fiber by a cavity filled with bicarbonate buffer. The external membrane is made of silicone, and the internal membrane is HPTS immobilized on an ion-exchange membrane.

pO_2 Sensors

The development of an indicator system for fiber optic pO_2 sensing is challenging because there are very few known ways to measure pO_2 optically. Although a color-changing indicator would have been desirable, the development of a sufficiently stable indicator has been difficult. The only principle applicable to fiber optics appears to be the quenching effect of oxygen on fluorescence.

Fluorescence quenching is a general property of aromatic molecules, dyes containing them, and some other substances. In brief, when light is absorbed by a molecule, the absorbed energy is held as an excited electronic state of the molecule. It is then lost by coupling to the mechanical movement of the molecule (heat), reradiated from the molecule in a mean time of about 10 ns (fluorescence), or converted into another excited state with much longer mean lifetime and then reradiated (phosphorescence). Quenching reduces the intensity of fluorescence and is related to the concentration of the quenching molecules, such as O_2.

A fiber optic sensor for measuring pO_2 using the principle of fluorescence quenching was developed by Peterson and colleagues [27]. The dye is excited at around 470 nm (blue) and fluoresces at about 515 nm (green) with an intensity that depends on the pO_2. The optical information is derived from the ratio of green fluorescence to the blue excitation light, which serves as an internal reference signal. The system was chosen for visible light excitation, because plastic optical fibers block light transmission at wavelengths shorter than 450 nm, and glass fibers were not considered acceptable for biomedical use.

The sensor was similar in design to the pH probe continuing the basic idea of an indicator packing in a permeable container at the end of a pair of optical fibers. A dye perylene dibutyrate, absorbed on a macroreticular polystyrene adsorbent, is contained in a oxygen-permeable porous polystyrene envelope. The ratio of green to blue intensity was processed according to the Stren-Volmer equation

$$\frac{I_0}{I} = 1 + K\,pO_2$$

where I and I_0 are the fluorescence emission intensities in the presence and absence of quencher, respectively, and K is the Stern-Volmer quenching coefficient. This provides a nearly linear readout of pO_2 over the range of 0–150 mmHg (0–20 kPa), with a precision of 1 mm Hg (0.13 kPa). The original sensor was 0.5 mm in diameter, but it can be made much smaller. Although its response time in a gas mixture is a fraction of a second, it is slower in an aqueous system, about 1.5 min for 90% response.

Wolfbeis and coworkers [28] designed a system for measuring the widely used halothane anesthetic which interferes with the measurement of oxygen. This dual-sensor combination had two semipermeable membranes (one of which blocked halothane) so that the probe could measure both oxygen and halothane simultaneously. The response time of their sensor, 15–20 s for halothane and 10–15 s for oxygen, is considered short enough to allow gas analysis in the breathing circuit. Potential applications of this device include the continuous monitoring of halothane in breathing circuits and in the blood.

Glucose Sensors

Another important principle that can be used in fiber optic sensors for measurements of high sensitivity and specificity is the concept of competitive binding. This was first described by Schultz, Mansouri, and Goldstein [29] to construct a glucose sensor. In their unique sensor, the analyte (glucose) competes for binding sites on a substrate (the lectin concanavalin A) with a fluorescent indicator-tagged polymer [fluorescein isothiocyanate (FITC)-dextran]. The sensor, which is illustrated in Fig. 52.8, is arranged so that the substrate is fixed in a position out of the optical path of the fiber end. The substrate is bound to the inner wall of a glucose-permeable hollow fiber tubing (300 μ O.D.×200 μ I.D.) and fastened to the end of an optical fiber. The hollow fiber acts as the container and is impermeable to the large molecules of the fluorescent indicator. The light beam that extends from the fiber "sees" only the unbound indicator in solution inside the hollow fiber but not the indicator bound on the container wall. Excitation light passes through the fiber and into the solution, fluorescing the unbound indicator, and the fluorescent light passes back along the same fiber to a measuring system. The fluorescent indicator and the glucose are in competitive binding equilibrium with the substrate. The interior glucose concentration equilibrates with its concentration exterior to the probe. If the glucose concentration increases, the indicator is driven off the substrate to increase the concentration of the indicator. Thus, fluorescence intensity as seen by the optical fiber follows the glucose concentration.

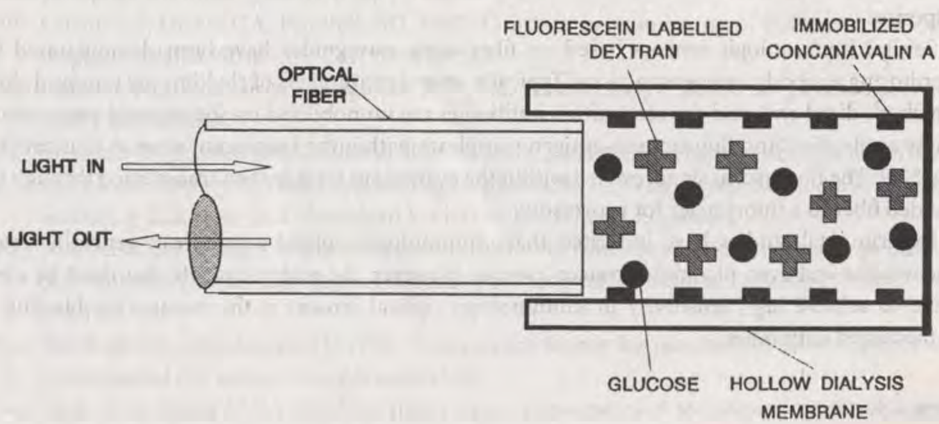

FIGURE 52.8 Schematic diagram of a competitive binding fluorescence affinity sensor for glucose measurement [29].

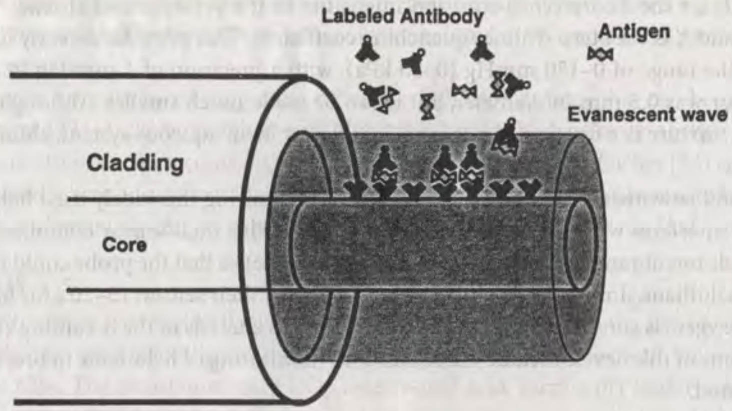

FIGURE 52.9 Basic principle of a fiber optic antigen-antibody sensor [33].

The response time of the sensor was found to be about 5 min. In vivo studies demonstrated fairly close correspondence between the sensor output and actual blood glucose levels. A time lag of about 5 min was found and is believed to be due to the diffusion of glucose across the hollow fiber membrane and the diffusion of FTIC-dextran within the tubing.

In principle, the concept of competitive binding can be applied to any analysis for which a specific reaction can be devised. However, long-term stability of these sensors remains the major limiting factor that needs to be solved.

Immunosensors

Immunologic techniques offer outstanding selectivity and sensitivity through the process of antibody-antigen interaction. This is the primary recognition mechanism by which the immune system detects and fights foreign matter and has therefore allowed the measurement of many important compounds at trace levels in complex biologic samples.

In principle, it is possible to design competitive binding optical sensors utilizing immobilized antibodies as selective reagents and detecting the displacement of a labeled antigen by the analyte. Therefore, antibody-based immunologic optical sensors have been the subject of considerable research in the past few years [30–34]. In practice, however, the strong binding of antigens to antibodies and vice versa causes difficulties in constructing reversible sensors with fast dynamic responses.

Several immunologic sensors based on fiber optic waveguides have been demonstrated for monitoring antibody-antigen reactions. Typically, several centimeters of cladding are removed along the fiber's distal end, and the recognition antibodies are immobilized on the exposed core surface. These antibodies bind fluorophore-antigen complexes within the evanescent wave as illustrated in Fig. 52.9. The fluorescent signal excited within the evanescent wave is then transmitted through the cladded fiber to a fluorimeter for processing.

Experimental studies have indicated that immunologic optical sensors can generally detect micromolar and even picomolar concentrations. However, the major obstacle that must be overcome to achieve high sensitivity in immunologic optical sensors is the nonspecific binding of immobilized antibodies.

References

1. Polanyi ML, Heir RM. 1962. In vivo oximeter with fast dynamic response. Rev Sci Instrum 33:1050.

2. Bornzin GA, Mendelson Y, Moran BL, et al. 1987. Measuring oxygen saturation and hematocrit using a fiberoptic catheter. Proc 9th Ann Conf Eng Med Bio Soc 807–809.
3. Mendelson Y, Galvin JJ, Wang Y. 1990. In vitro evaluation of a dual oxygen saturation/hematocrit intravascular fiberoptic catheter. Biomed Instrum Tech 24:199.
4. Mendelson Y. 1992. Pulse oximetry: Theory and applications for noninvasive monitoring. Clin Chem 28(9): 1601.
5. Aoyagi T, Kishi M, Yamaguchi K, et al. 1974. Improvement of the earpiece oximeter. Jpn Soc Med Electron Biomed Eng 90–91.
6. Yoshiya I, Shimada Y, Tanaka K. 1980. Spectrophotometric monitoring of arterial oxygen saturation in the fingertip. Med Biol Eng Comput 18:27.
7. Mendelson Y, Solomita MV. 1992. The feasibility of spectrophotometric measurements of arterial oxygen saturation from the scalp utilizing noninvasive skin reflectance pulse oximetry. Biomed Instrum Technol 26:215.
8. Mendelson Y, McGinn MJ. 1991. Skin reflectance pulse oximetry: In vivo measurements from the forearm and calf. J Clin Monit 7:7.
9. Chance B, Leigh H, Miyake H, et al. 1988. Comparison of time resolved and un-resolved measurements of deoxyhemoglobin in brain. Proc Nat Acad Sci 85:4971.
10. Jobsis FF, Keizer JH, LaManna JC, et al. 1977. Reflection spectrophotometry of cytochrome aa3 in vivo. Appl Physiol: Respirat Environ Excerc Physiol 43(5): 858.
11. Kurth CD, Steven IM, Benaron D, et al. 1993. Near-infrared monitoring of the cerebral circulation. J Clin Monit 9:163.
12. Lubbers DW, Opitz N. 1975. The pCO_2/pO_2-optode: A new probe for measurement of pCO_2 or pO_2 in fluids and gases. Z Naturforsch C: Biosci 30C:532.
13. Clark CL, O'Brien J, McCulloch J, et al. 1986. Early clinical experience with GasStat. J Extra Corporeal Technol 18:185.
14. Hill AG, Groom RC, Vinansky RP, et al. 1985. On-line or off-line blood gas analysis: Cost vs. time vs. accuracy. Proc Am Acad Cardiovasc Perfusion 6:148.
15. Siggaard-Andersen O, Gothgen IH, Wimberley, et al. 1988. Evaluation of the GasStat fluorescence sensors for continuous measurement of pH, pCO_2 and pO_2 during CPB and hypothermia. Scand J Clin Lab Invest 48 (Suppl. 189):77.
16. Zimmerman JL, Dellinger RP. 1993. Initial evaluation of a new intra-arterial blood gas system in humans. Crit Care Med 21(4):495.
17. Gottlieb A. 1992. The optical measurement of blood gases—approaches, problems and trends: Fiber optic medical and fluorescent sensors and applications. Proc SPIE 1648:4.
18. Barker SL, Hyatt J. 1991. Continuous measurement of intraarterial pHa, $PaCO_2$, and PaO_2 in the operation room. Anesth Analg 73:43.
19. Larson CP, Divers GA, Riccitelli SD. 1991. Continuous monitoring of PaO_2 and $PaCO_2$ in surgical patients. Abstr Crit Care Med 19:525.
20. Peterson JI, Goldstein SR, Fitzgerald RV. 1980. Fiber optic pH probe for physiological use. Anal Chem 52:864.
21. Markle DR, McGuire DA, Goldstein SR, et al. 1981. A pH measurement system for use in tissue and blood, employing miniature fiber optic probes, In DC Viano (ed), Advances in Bioengineering, p 123, New York, American Society of Mechanical Engineers.
22. Wolfbeis OS, Furlinger E, Kroneis H, et al. 1983. Fluorimetric analysis: 1. A study on fluorescent indicators for measuring near neutral (physiological) pH values. Fresenius' Z Anal Chem 314:119.
23. Wolfbeis OS, Offenbacher H. 1986. Fluorescence sensor for monitoring ionic strength and physiological pH values. Sens Actuators 9:85.
24. Opitz N, Lubbers DW. 1983. New fluorescence photomatrical techniques for simultaneous and continuous measurements of ionic strength and hydrogen ion activities. Sens Actuators 4:473.

25. Vurek GG, Feustel PJ, Severinghaus JW. 1983. A fiber optic pCO_2 sensor. Ann Biomed Eng 11:499.
26. Zhujun Z, Seitz WR. 1984. A carbon dioxide sensor based on fluorescence. Anal Chim Acta 160:305.
27. Peterson JI, Fitzgerald RV, Buckhold DK. 1984. Fiber-optic probe for in vivo measurement of oxygen partial pressure. Anal Chem 56:62.
28. Wolfbeis OS, Posch HE, Kroneis HW. 1985. Fiber optical fluorosensor for determination of halothane and/or oxygen. Anal Chem 57:2556.
29. Schultz JS, Mansouri S, Goldstein IJ. 1982. Affinity sensor: A new technique for developing implantable sensors for glucose and other metabolites. Diabetes Care 5:245.
30. Andrade JD, Vanwagenen RA, Gregonis DE, et al. 1985. Remote fiber optic biosensors based on evanescent-excited fluoro-immunoassay: Concept and progress. IEEE Trans Electron Devices ED-32: 1175.
31. Sutherland RM, Daehne C, Place JF, et al. 1984. Optical detection of antibody-antigen reactions at a glass-liquid interface. Clin Chem 30:1533.
32. Hirschfeld TE, Block MJ. 1984. Fluorescent immunoassay employing optical fiber in a capillary tube. US Patent No. 4,447,546.
33. Anderson GP, Golden JP, Ligler FS. 1994. An evanescent wave biosensor: Part I. Fluorescent signal acquisition from step-etched fiber optic probes. IEEE Trans Biomes Eng 41(6):578.
34. Golden JP, Anderson GP, Rabbany SY, et al. 1994. An evanescent wave biosensor: Part II. Fluorescent signal acquisition from tapered fiber optic probes. IEEE Trans Biomed Eng 41(6):585.

53
Bioanalytic Sensors

Richard P. Buck
University of North Carolina

53.1 Classification of Biochemical Reactions in the Context of Sensor Design and Development

Introduction and Definitions

Since sensors generate a measurable material property, they belong in some grouping of transducer devices. Sensors specifically contain a recognition process that is characteristic of a material sample at the molecular-chemical level, and a sensor incorporates a transduction process (step) to create a useful signal. Biomedical sensors include a whole range of devices that may be chemical sensors, physical sensors, or some kind of mixed sensor.

Chemical sensors use chemical processes in the recognition and transduction steps. Biosensors are also chemical sensors, but they use particular classes of biological recognition/transduction processes. A pure physical sensor generates and transduces a parameter that does not depend on the chemistry per se but is a result of the sensor responding as an aggregate of point masses or charges. All these when used in a biologic system (biomatrix) may be considered *bioanalytic* sensors without regard to the chemical, biochemical, or physical distinctions. They provide an "analytic signal of the biologic system" for some further use.

The chemical recognition process focuses on some molecular-level chemical entity, usually a kind of chemical structure. In classical analysis this structure may be a simple functional group: SiO^- in a glass electrode surface, a chromophore in an indicator dye, or a metallic surface structure, such as silver metal that recognizes Ag^+ in solution. In recent times, the biologic recognition processes have been better understood, and the general concept of recognition by *receptor* or *chemoreceptor* has come into fashion. Although these are often large molecules bound to cell membranes, they contain specific structures that permit a wide variety of different molecular recognition steps including recognition of large and small species and of charged and uncharged species. Thus, *chemoreceptor* appears in the sensor literature as a generic term for the principal entity doing the recognition. For a history and examples, see references [1–6].

0-8493-8346-3/95/$0.00+$.50

Biorecognition in biosensors has especially stressed "receptors" and their categories. Historically, application of receptors has not necessarily meant measurement directly of the receptor. Usually there are coupled chemical reactions, and the transduction has used measurement of the subsidiary products: change of pH, change of dissolved 0_2, generation of H_2O_2, changes of conductivity, changes of optical adsorption, and changes of temperature. Principal receptors are enzymes because of their extraordinary selectivity. Other receptors can be the more subtle species of biochemistry: antibodies, organelles, microbes, and tissue slices, not to mention the trace level "receptors" that guide ants such as pheromones and other unusual species. A sketch of a generic bioanalytic sensor is shown in Fig. 53.1.

Classification of Recognition Reactions and Receptor Processes

The concept of *recognition* in chemistry is universal. It almost goes without saying that all chemical reactions involved recognition and selection on the basis of size, shape, and charge. For the purpose of constructing sensors, general recognition based on these factors is not usually enough. Frequently in inorganic chemistry a given ion will react indiscriminantly with similar ions of the same size and charge. Changes in charge from unity to two, for example, do change the driving forces of some ionic reactions. By control of dielectric constant of phases, heterogeneous reactions can often be "tailored" to select divalent ions over monovalent ions and to select small versus large ions or vice versa.

Shape, however, has more special possibilities, and natural synthetic methods permit product control. Nature manages to use shape together with charge to build organic molecules, called enzymes, that have acquired remarkable selectivity. It is in the realm of biochemistry that these natural constructions are investigated and catalogued. Biochemistry books list large numbers of enzymes and other selective materials that direct chemical reactions. Many of these have been tried as the basis of selective sensors for bioanalytic and biomedical purposes. The list in Table 53.1 shows how some of these materials can be grouped into lists according to function and to analytic substrate, both organic and inorganic. The principles seem general, so there is no reason to discriminate against the inorganic substrates in favor or the organic substrates. All can be used in biomedical analysis.

53.2 Classification of Transduction Processes—Detection Methods

Some years ago, the engineering community addressed the topic of sensor classification—Richard M. White in IEEE Trans. Ultra., Ferro., Freq. Control (UFFC), UFFC-34 (1987) 124, and Wen E. Ko in IEEE/EMBS Symposium Abstract T.1.1 84CH2068-5 (1984). It is interesting because the physical

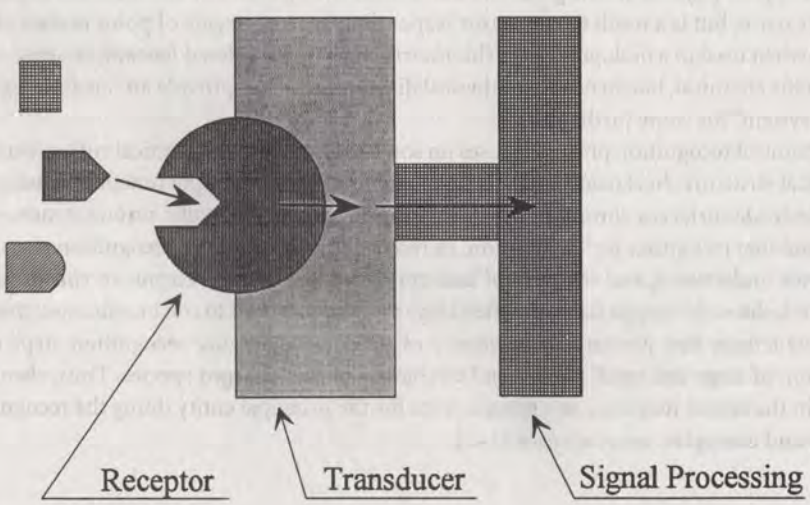

FIGURE 53.1 Generic bioanalytic sensor.

TABLE 53.1 Recognition Reactions and Receptor Processes

1. Insoluble salt-based sensors

a. $$S^{+} + R^{-} \rightleftharpoons \text{(insoluble salt)}$$

Ion exchange with crystalline SR (homogeneous or heterogeneous crystals)

	chemical signal S^{+n}	receptor R^{-n}
	inorganic cations	inorganic anions
examples:	Ag^{+}, Hg_2^{2+}, Pb^{2+}, Cd^{2+}, Cu^{2+}	$S^{=}$, $Se^{2=}$, SCN^{-}, I^{-}, Br^{-}, Cl^{-}

b. $$S^{-n} + R^{+n} \rightleftharpoons \text{SR (insoluble salt)}$$

Ion exchange with crystalline SR (homogeneous or heterogeneous crystals)

	chemical signal S^{-n}	receptor R^{+n}
	inorganic anions	inorganic cations
examples:	F^{-}, $S^{=}$, $Se^{2=}$, SCN^{-}, I^{-}, Br^{-}, Cl^{-}	LaF_2^{+}, Ag^{+}, Hg_2^{2+}, Pb^{2+}, Cd^{2+}, Cu^{2+}

2. Solid ion exchangers

a. $$S^{+n} + R^{-n}\text{ (sites)} \rightleftharpoons S^{+n}R^{-n} = \text{SR (in ion exchanger phase)}$$

Ion exchange with synthetic ion exchangers containing negative fixed sites (homogeneous or heterogeneous, inorganic or organic materials)

	chemical signal S^{+n}	receptor R^{-n}
	inorganic and organic ions	inorganic and organic ion sites
examples:	H^{+}, Na^{+}, K^{+}	silicate glass $Si\text{-}0^{-}$
	H^{+}, Na^{+}, K^{+}, other M^{+n}	synthetic sulfonated, phosphorylated, EDTA-substituted polystyrenes

b. $$S^{-n} + R^{+n}\text{(sites)} \rightleftharpoons S^{-n}R^{+n} = \text{SR (in ion exchanger phase)}$$

Ion exchange with synthetic ion exchangers containing positive fixed sites (homogeneous or heterogeneous, inorganic or organic materials)

	chemical signal S^{-n}	receptor R^{+n}
	organic and inorganic ions	organic and inorganic ion sites
examples:	hydrophobic anions	quaternized polystyrene

3. Liquid ion exchanger sensors with electrostatic selection

a. $$S^{+n} + R^{-n}\text{(sites)} \rightleftharpoons S^{+n}R^{-n} = \text{SR (in ion exchanger phase)}$$

Plasticized, passive membranes containing mobile, trapped negative fixed sites (homogeneous or heterogeneous, inorganic or organic materials)

	chemical signal S^{+n}	receptor R^{-n}
	inorganic and organic ions	inorganic and organic ion sites
examples:	Ca^{2+}	diester of phosphoric acid or monoester of a phosphonic acid
	M^{+n}	dinonylnaphthalene sulfonate and other organic, hydrophobic anions
	$R_1R_2R_3R_4N^{+}$ and bis-Quaternary Cations cationic drugs tetrasubstituted arsonium^{+}	tetraphenylborate anion or substituted derivatives

b. $$S^{-n} + R^{+n}\text{(sites)} \rightleftharpoons S^{-n}R^{+n} = \text{SR (in ion exchanger phase)}$$

Plasticized, passive membranes containing mobile, trapped negative fixed sites (homogeneous or heterogeneous, inorganic or organic materials)

	chemical signal S^{-n}	receptor R^{+n}
	inorganic and organic ions	inorganic and organic ion sites
examples:	anions, simple Cl^{-}, Br^{-}, ClO_4^{-}	quaternary ammonium cations: e.g. tridodecylmethyl-ammonium
anions, complex, drugs		quaternary ammonium cations: e.g. tridodecylmethyl-ammonium

4. Liquid ion exchanger sensors with neutral (or charged) carrier selection

a. $$S^{+n} + X \text{ and } R^{-n}\text{(sites)} \rightleftharpoons S^{+n}X\,R^{-n} = \text{SXR (in ion exchanger phase)}$$

Plasticized, passive membranes containing mobile, trapped negative fixed sites (homogeneous or heterogeneous, inorganic or organic materials)

	chemical signal S^{+n}	receptor R^{-n}
	inorganic and organic ions	inorganic and organic ion sites
examples:	Ca^{2+}	X = synthetic ionophore complexing agent selective to Ca^{2+}
		R^{-n} usually a substituted tetra phenylborate salt
	Na^{+}, K^{+}, H^{+}	X = selective ionophore complexing agent

(continued)

TABLE 53.1 Recognition Reactions and Receptor Processes *(continued)*

b.	$S^{-n} + X$ and R^{+n}(sites) $\rightleftharpoons$ $S^{-n}X\,R^{+n} = SXR$ (in ion exchanger phase)	
Plasticized, passive membranes containing mobile, trapped negative fixed sites (homogeneous or heterogeneous, inorganic or organic materials)		
	chemical signal S^{-n}	receptor R^{+n}
	inorganic and organic ions	inorganic and organic ion sites
examples:	HPO_4^{2-}	R^{+n} = quaternary ammonium salt X = synthetic ionophore complexing agent: aryl organotin compound or suggested cyclic polyamido-polyamines
	HCO_3^-	X = synthetic ionophore: trifluoro acetophenone
	Cl^-	X = aliphatic organotin compound
5. Bioaffinity sensors based on change of local electron densities		
	$S + R \rightleftharpoons SR$	
	chemical signal S	receptor R
	protein	dyes
	saccharide	lectin
	glycoprotein	
	substrate	enzyme
	inhibitor	
		Transferases Hydrolases (peptidases, esterases, etc.) Lyases Isomerases Ligases
	prosthetic group	apoenzyme
	antigen	antibody
	hormone	"receptor"
	sustrate analogue	transport system
6. Metabolism sensors based on substrate consumption and product formation		
	$S + R \rightleftharpoons SR \rightarrow P + R$	
	chemical signal S	receptor R
	substrate	enzyme
examples:	lactate (SH_2) $SH_2 + A \rightleftharpoons S + AH_2$ lactate + NAD^+	hydrogenases catalyze hydrogen transfer from S to acceptor A (not molecular oxygen!) reversibly pyruvate + NADH + H^+ using lactate dehydrogenase
	glucose (SH_2) $SH_2 + \frac{1}{2}O_2 \rightleftharpoons S + H_2O$ or $SH_2 + O_2 \rightleftharpoons S + H_2O_2$ glucose + $O_2 \rightleftharpoons$ gluconolactone + H_2O_2	oxidases catalyze hydrogen transfer to molecular oxygen using glucose oxidase
	reducing agents (S) $2S + 2H^+ + H_2O_2 \rightleftharpoons 2S^+ + 2H_2O$ $Fe^{2+} + H_2O_2 + 2H^+ \rightleftharpoons Fe^{3+} + 2H_2O$	peroxidases catalyze oxidation of a substrate by H_2O_2 using horseradish peroxidase
	reducing agents L-lactate + $O_2 \rightleftharpoons$ acetate + CO_2 + H_2O	oxygenases catalyze substrate oxidations by molecular O_2
	cofactor	organelle
	inhibitor	microbe
	activator	tissue slice
	enzyme activity	
7. Coupled and hybrid systems using sequences, competition, anti-interference and amplification concepts and reactions		
8. Biomimetic sensors		
	chemical signal S	receptor R
	sound stress light	carrier-enzyme

Source: Adapted from [2, 6].

and chemical properties are given equal weight. There are many ideas given here that remain without embodiment. This list is reproduced as Table 53.2. Of particular interest in this section are "detection means used in sensors" and "sensor conversion phenomena." At present the principle transduction schemes use electrochemical, optical, and thermal detection effects and principles.

TABLE 53.2 Detection Means and Conversion Phenomena Used in Sensors

Detection means
Biologic
Chemical
Electric, magnetic, or electromagnetic wave
Heat, temperature
Mechanical displacement of wave
Radioactivity, radiation
Other
Conversion phenomena
Biologic
Biochemical transformation
Physical transformation
Effect on test organism
Spectroscopy
Other
Chemical
Chemical transformation
Physical transformation
Electrochemical process
Spectroscopy
Other
Physical
Thermoelectric
Photoelectric
Photomagnetic
Magnetoelectric
Elastomagnetic
Thermoelastic
Elastoelectric
Thermomagnetic
Thermooptic
Photoelastic
Other

Calorimetric, Thermometric, and Pyroelectric Transducers

Especially useful for enzymatic reactions, the generation of heat (enthalpy change) can be used easily and generally. The enzyme provides the selectivity and the reaction enthalpy cannot be confused with other reactions from species in a typical biologic mixture. The ideal aim is to measure total evolved heat, i.e., to perform a calorimetric measurement. In real systems there is always heat loss, i.e., heat is conducted away by the sample and sample container so that the process cannot be adiabatic as required for a total heat evolution measurement. As a result, temperature difference before and after evolution is measured most often. It has to be assumed that the heat capacity of the specimen and container is constant over the small temperature range usually measured.

The simplest transducer is a thermometer coated with the enzyme that permits the selected reaction to proceed. Thermistors are used rather than thermometers or thermocouples. The change of resistance of certain oxides is much greater than the change of length of a mercury column or the microvolt changes of thermocouple junctions.

Pyroelectric heat flow transducers are relatively new. Heat flows from a heated region to a lower temperature region, controlled to occur in one dimension. The lower temperature side can be coated with an enzyme. When the substrate is converted, the lower temperature side is warmed. The pyroelectric material is from a category of materials that develops a spontaneous voltage difference in a thermal gradient. If the gradient is disturbed by evolution or adsorption of heat, the voltage temporarily changes.

In biomedical sensing, some of the solid-state devices based on thermal sensing cannot be used effectively. The reason is that the sensor itself has to be heated or is heated quite hot by catalytic surface reactions. Thus pellistors (oxides with catalytic surfaces and embedded platinum wire thermometer), chemiresistors, and "Figaro" sensor "smoke" detectors have not found many biologic applications.

Optical, Optoelectronic Transducers

Most optical detection systems for sensors are small, i.e., they occupy a small region of space because the sample size and volume are themselves small. This means that common absorption spectrophotometers and photofluorometers are not used with their conventional sample-containing cells or with their conventional beam-handling systems. Instead light-conducting *optical fibers* are used to connect the sample with the more remote monochromator and optical readout system. The techniques still remain absorption spectrophotometry, fluorimetry including fluorescence quenching, and reflectometry.

The most widely published optical sensors use a miniature reagent contained or immobilized at the tip of an optical fiber. In most systems a permselective membrane coating allows the detected species to penetrate the dye region. The corresponding absorption change, usually at a sensitive externally preset wavelength, is changed and correlated with the sample concentration. Similarly, fluorescence can be stimulated by the higher-frequency external light source and the lower-frequency emission detected. Some configurations are illustrated in references [1, 2]. Fluorimetric detection of coenzyme A, $NAD^+/NADH$, is involved in many so-called pyridine-linked enzyme systems. The fluorescence of NADH contained or immobilized can be a convenient way to follow these reactions. Optodes, miniature encapsulated dyes, can be placed in vivo. Their fluorescence can be enhanced or quenched and used to detect acidity, oxygen, and other species.

A subtle form of optical transduction uses the "peeled" optical fiber as a multiple reflectance cell. The normal fiber core glass has a refractive index greater than that of the exterior coating; there is a range of angles of entry to the fiber so that *all* the light beam remains inside the core. If the coating is removed and materials of lower index of refraction are coated on the exterior surface, there can be absorption by multiple reflections, since the evanescent wave can peretrate the coating. Chemical reagent can be added externally to create selective layers on the optical fiber.

Ellipsometry is a reflectance technique that depends on the optical constants and thickness of surface layer. For colorless layers, a polarized light beam will change its plane of polarization upon reflection by the surface film. The thickness can sometimes be determined when optical constants are known or approximated by constants of the bulk material. Antibody-antigen surface reaction can be detected this way.

Piezoelectric Transducers

Cut quartz crystals have characteristic modes of vibration that can be induced by painting electrodes on the opposite surfaces and applying a megaHertz ac voltage. The frequency is searched until the crystal goes into a resonance. The resonant frequency is very stable. It is a property of the material and maintains a value to a few parts per hundred million. When the surface is coated with a stiff mass, the frequency is altered. The shift in frequency is directly related to the surface mass for thin, stiff layers. The reaction of a substrate with this layer changes the constants of the film and further shifts the resonant frequency. These devices can be used in air, in vacuum, or in electrolyte solutions.

Electrochemical Transducers

Electrochemical transducers are commonly used in the sensor field. The main forms of electrochemistry used are potentiometry [zero-current cell voltage (potential difference measurements)], amperometry (current measurement at constant applied voltage at the working electrode), and ac conductivity of a cell.

Potentiometric Transduction

The classical generation of an activity-sensitive voltage is spontaneous in a solution containing both nonredox ions and redox ions. Classical electrodes of types 1, 2, and 3 respond by ion exchange directly or indirectly to ions of the same material as the electrode. Inert metal electrodes (sometimes called *type 0*)—Pt, Ir, Rh, and occasionally carbon C—respond by electron exchange from redox pairs in solution. Potential differences are interfacial and reflect ratios of activities of oxidized to reduced forms.

Amperometric Transduction

For dissolved species that can exchange electrons with an inert electrode, it is possible to force the transfer in one direction by applying a voltage very oxidizing (anodic) or reducing (cathodic). When the voltage is fixed, the species will be, by definition, out of equilibrium with the electrode at its present applied voltage. Locally, the species (regardless of charge) will oxidize or reduce by moving from bulk solution to the electrode surface where they react. Ions do not move like electrons. Rather they diffuse from high to low concentration and do not usually move by drift or migration. The reason is that the electrolytes in solutions are at high concentrations, and the electric field is virtually eliminated from the bulk. The field drops through the first 1000 Angstroms at the electrode surface. The concentration of the moving species is from high concentration in bulk to zero at the electrode surface where it reacts. This process is called *concentration polarization.* The current flowing is limited by mass transport and so is proportional to the bulk concentration.

Conductometric Transducers

Ac conductivity (impedance) can be purely resistive when the frequency is picked to be about 1000 to 10,000 Hz. In this range the transport of ions is sufficiently slow that they never lose their uniform concentration. They simply quiver in space and carry current forward and backward each half cycle. In the lower and higher frequencies, the cell capacitance can become involved, but this effect is to be avoided.

53.3 Tables of Sensors from the Literature

The longest and most consistently complete references to the chemical sensor field is the review issue of *Analytical Chemistry Journal.* In the 1970s and 1980s these appeared in the April issue, but more recently they appear in the June issue. The editors are Jiri Janata and various colleagues [7–10]. Not all possible or imaginable sensors have been made according to the list in Table 53.2. A more realistic table can be constructed from the existing literature that describes actual devices. This list is Table 53.3. Book references are listed in Table 53.4 in reverse time order to about 1986. This list covers

TABLE 53.3 Chemical Sensors and Properties Documented in the Literature

I. General topics including items II-V: selectivity, fabrication, data processing
II. Thermal sensors
III. Mass sensors
  - Gas sensors
  - Liquid sensors

IV. Electrochemical sensors
  - Potentiometric sensors
    - References electrodes
    - Biomedical electrodes
    - Applications to cations, anions
    - Coated wire/hybrids
    - ISFETs and related
    - Biosensors
    - Gas sensors
  - Amperometric sensors
    - Modified electrodes
    - Gas sensors
    - Biosensors
      - Direct electron transfer
      - Mediated electron transfer
      - Biomedical
  - Conductimetric sensors
    - Semiconducting oxide sensors
    - Zinc oxide-based
    - Chemiresistors
    - Dielectrometers

V. Optical sensors
  - Liquid sensors
  - Biosensors
  - Gas sensors

most of the major source books and many of the symposium proceedings volumes. The reviews [7–10] are a principal source of references to the published research literature.

53.4 Applications of Microelectronics in Sensor Fabrication

The reviews of sensors since 1988 cover fabrication papers and microfabrication methods and examples [7–10]. A recent review by two of the few *chemical* sensor scientists (chemical engineers) who

TABLE 53.4 Books and Long Reviews Keyed to Items in Table 53.3 (Reviewed since 1988 in reverse time sequence)

I. Yamauchi S (ed). 1992. Chemical Sensor Technology, vol 4, Tokyo, Kodansha Ltd.
Flores JR, Lorenzo E. 1992. Amperometric Biosensors, In MR Smyth, JG Vos (eds), Comprehensive Analytical Chemistry Amsterdam, Elsevier.
Vaihinger S, Goepel W. 1991. Multicomponent analysis in chemical sensing. In W Goepel, J Hesse, J Zemel (eds), Sensors vol 2 Part 1, pp 191–237, Weinheim, Germany, VCH Publishers.
Wise DL (ed). 1991. Bioinstrumentation and Biosensors, New York, Marcel Dekker.
Scheller F, Schubert F. 1989. Biosensors, Basel, Switzerland, Birkhauser Verlag, see also [2].
Madou M, Morrison SR. 1989. Chemical Sensing with Solid State Devices, New York, Academic Press.
Janata J. 1989. Principles of Chemical Sensors, New York, Plenum Press.
Edmonds TE (ed). 1988. Chemical Sensors, Glasgow, Blackie.
Yoda K. 1988. Immobilized enzyme cells. Methods Enzymology, 137:61.
Turner APF, Karube I, Wilson GS eds. 1987. Biosensors: Fundamentals and Applications, Oxford, Oxford University Press.
Seiyama T (ed). 1986. Chemical Sensor Technology, Tokyo, Kodansha Ltd.

II. Thermal Sensor
There are extensive research and application papers and these are mentioned in books listed under I. However, the up-to-date lists of papers are given in references 7–10.

III. Mass Sensors
There are extensive research and application papers and these are mentioned in books listed under I. However, the up-to-date lists of papers are given in references 7–10. Fundamentals of this rapidly expanding field are recently reviewed:
Buttry DA, Ward MD. 1992. Measurement of Interfacial processes at Electrode Surfaces with the Electrochemical Quartz Crystal Microbalance, Chemical Reviews 92:1355.
Grate JW, Martin SJ, White RM. 1993. Acoustic Wave Microsensors, part 1, Analyt Chem 65:940A; part 2, Analyt Chem 65:987A.
Ricco AT. 1994. SAW Chemical Sensors, The Electrochemical Society Interface Winter: 38–44.

IVA. Electrochemical Sensors—Liquid Samples
Scheller F, Schmid RD (eds). 1992. Biosensors: Fundamentals, Technologies and Applications, GBF Monograph Series, New York, VCH Publishers.
Erbach R, Vogel A, Hoffmann B. 1992. Ion-sensitive field-effect structures with Langmuir-Blodgett membranes, In F Scheller, RD Schmid (eds). Biosensors: Fundamentals, Technologies, and Applications, GBF Monograph 17, pp 353–357, New York, VCH Publishers.
Ho May YK, Rechnitz GA. 1992. An Introduction to Biosensors, In RM Nakamura, Y Kasahara, GA Rechnitz (eds), Immunochemical Assays and Biosensors Technology, pp 275–291, Washington DC, American Society Microbiology.
Mattiasson B, Haakanson H. Immunochemically-based assays for process control, 1992. Advances in Biochemical Engineering and Biotechnology 46:81.
Maas AH, Sprokholt R. 1990. Proposed IFCC Recommendations for electrolyte measurements with ISEs in clinical chemistry, In A Ivaska, A Lewenstam, R Sara (eds), Contemporary Electroanalytical Chemistry, Proceedings of the ElectroFinnAnalysis International Conference on Electroanalytical Chemistry, pp 311–315, New York, Plenum.
Vanrolleghem P, Dries D, Verstreate W. RODTOX: Biosensor for rapid determination of the biochemical oxygen demand, 1990. In C Christiansen, L Munck, J Villadsen, (eds), Proceedings of the 5th European Congress Biotechnology, vol 1, pp 161–164, Copenhagen, Denmark, Munksgaard.
Cronenberg C, Van den Heuvel H, Van den Hauw M, Van Groen B. Development of glucose microelectrodes for measurements in biofilms, 1990. In C Christiansen, L Munck, J Villadsen J, (eds), Proceedings of the 5th European Congress Biotechnology, vol 1, pp 548–551, Copenhagen, Denmark, Munksgaard.
Wise DL (ed). 1989. Bioinstrumentation Research, Development and Applications, Boston, MA, Butterworth-Heinemann.

Pungor E (ed). 1989. Ion-Selective Electrodes—Proceedings of the 5th Symposium (Matrafured, Hungary 1988), Oxford, Pergamon.
Wang J (ed). 1988. Electrochemical Techniques in Clinical Chemistry and Laboratory Medicine, New York, VCH Publishers.
Evans A. 1987. Potentiometry and Ion-selective Electrodes, New York, Wiley.
Ngo TT (ed) 1987. Electrochemical Sensors in Immunological Analysis, New York, Plenum.
IVB. Electrochemical Sensors—Gas Samples
Sberveglieri G (ed). 1992. Gas Sensors, Dordrecht, The Netherlands, Kluwer.
Moseley PT, Norris JOW, Williams DE. 1991. Technology and Mechanisms of Gas Sensors, Bristol, U.K., Hilger.
Moseley PT, Tofield BD (eds). 1989. Solid State Gas Sensors, Philadelphia, Taylor and Francis, Publishers.
V. Optical Sensors
Coulet PR, Blum LJ. Luminescence in Biosensor Design, 1991. In DL Wise, LB Wingard, Jr (eds). Biosensors with Fiberoptics, pp 293–324, Clifton, N.J., Humana.
Wolfbeis OS. 1991. Spectroscopic Techniques, In OS Wolfbeis (ed). Fiber Optic Chemical Sensors and Biosensors, vol 1, pp 25–60. Boca Raton, Fla, CRC Press.
Wolfbeis OS. 1987. Fibre-optic sensors for chemical parameters of interest in biotechnology, In RD Schmidt (ed). GBF (Gesellschaft fur Biotechnologische Forschung) Monogr. Series, vol 10, pp 197–206, New York, VCH Publishers.

---

also operate a microfabrication laboratory is C. C. Liu, Z.-R. Zhang. 1992. Research and development of chemical sensors using microfabrication techniques. Selective Electrode Rev 14:147.

References

1. Janata J. 1989. Principles of Chemical Sensors, New York, Plenum.
2. Scheller F, Schubert F. 1989. Biosensors, #18 in Advances in Research Technologies (Beitrage zur Forschungstechnologie), Berlin, Akademie-Verlag, Amsterdam, Elsevier (English translation).
3. Turner APF, Karube I, Wilson GS. 1987. Biosensors: Fundamentals and Applications, Oxford, Oxford University Press.
4. Hall EAH. 1990. Biosensors, Milton Keynes, England, Open University Press.
5. Eddoes MJ. 1990. Theoretical Methods for Analyzing Biosensor Performance. In AEG Cass (ed), Biosensor—A Practical Approach, Oxford, IRL Press at Oxford University Ch. 9 pp 211–262.
6. Cosofret VV, Buck RP. 1992. Pharmaceutical Applications of Membrane Sensors, Boca Raton, Fla, CRC Press.
7. Janata J, Bezegh A. 1988. Chemical sensors, Analyt Chem 60:62R.
8. Janata J. 1990. Chemical sensors, Analyt Chem 62:33R.
9. Janata J. 1992. Chemical sensors, Analyt Chem 66:196R.
10. Janata J, Josowicz M, DeVaney M. 1994. Chemical Sensors, Analyt Chem 66:207R.

THE
Biomedical Engineering
HANDBOOK

Editor-in-Chief
JOSEPH D. BRONZINO
Trinity College
Hartford, Connecticut

CRC PRESS
IEEE PRESS
A CRC Handbook Published in Cooperation with IEEE Press

Library of Congress Cataloging-in-Publication Data

The biomedical engineering handbook / editor-in-chief, Joseph D. Bronzino.
p. cm. — (The electrical engineering handbook series)
Includes bibliographical references and index.
ISBN 0-8493-8346-3
1. Biomedical engineering—Handbooks, manuals, etc. I. Bronzino, Joseph D., 1937– . II. Series.
[DNLM: 1. Biomedical Engineering—handbooks. QT 29 B615 1995]
R856.15.B86 1995
610'.28—dc20
DNLM/DLC
For Library of Congress 95-6294
CIP

This book contains information obtained from authentic and highly regarded sources. Reprinted material is quoted with permission, and sources are indicated. A wide variety of references are listed. Reasonable efforts have been made to publish reliable data and information, but the author and the publisher cannot assume responsibility for the validity of all materials or for the consequences of their use.

Direct all inquiries to CRC Press, Inc., 2000 Corporate Blvd. N.W., Boca Raton, Florida 33431.

International Standard Book Number 0-8493-8346-3
Library of Congress Card Number 95-6294
Printed in the United States of America 1 2 3 4 5 6 7 8 9 0
Printed on acid-free paper

55

Digital Biomedical Signal Acquisition and Processing

Luca T. Mainardi
Polytechnic University, Milan

Anna M. Bianchi
St. Raffaele Hospital, Milan

Sergio Cerutti
Polytechnic University, Milan

Biologic signals carry information that is useful for comprehension of the complex pathophysiologic mechanisms underlying the behavior of living systems. Nevertheless, such information cannot be available directly from the raw recorded signals; it can be masked by other biologic signals contemporaneously detected (endogenous effects) or buried in some additive noise (exogenous effects). For such reasons, some additional processing is usually required to enhance the relevant information and to extract from it parameters that quantify the behavior of the system under study, mainly for physiologic studies, or that define the degree of pathology for routine clinical procedures (diagnosis, therapy, or rehabilitation).

Several processing techniques can be used for such purposes (they are also called *preprocessing techniques*): time- or frequency-domain methods including filtering, averaging, spectral estimation, and others. Even if it is possible to deal with continuous time waveforms, it is usually convenient to convert them into a numerical form before processing. The recent progress of digital technology, in terms of both hardware and software, makes more efficient and flexible digital rather than analog processing. Digital techniques have several advantages: Their performance is generally powerful, being able to easily implement even complex algorithms, and accuracy depends only on the truncation and round-off errors, whose effects can be predicted and controlled by the designer and are largely unaffected by other unpredictable variables such as component aging and temperature, which can degrade the performances of analog devices. Moreover, design parameters can be more easily changed because they involve software rather than hardware modifications.

A few basic elements of signal acquisition and processing will be presented in the following; our aim is to stress mainly the aspects connected with acquisition and analysis of biologic signals, leaving to the cited literature a deeper insight into the various subjects for both the fundamentals of digital signal processing and the applications.

55.1 Acquisition

A schematic representation of a general acquisition system is shown in Fig. 55.1. Several physical magnitudes are usually measured from biologic systems. They include electromagnetic quantities

0-8493-8346-3/95/$0.00+$.50

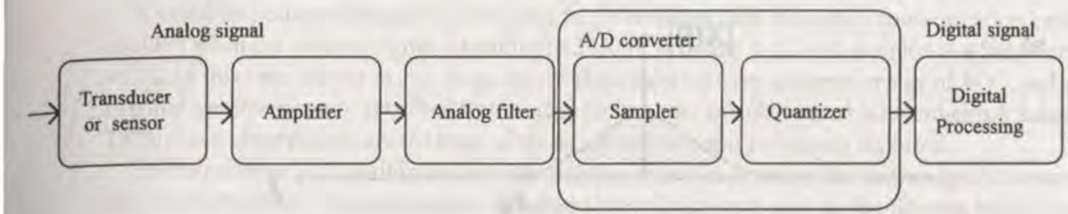

FIGURE 55.1 General block diagram of the acquisition procedure of a digital signal.

(currents, potential differences, field strengths, etc.), as well as mechanical, chemical, or generally nonelectrical variables (pressure, temperature, movements, etc.). Electric signals are detected by *sensors* (mainly electrodes), while nonelectric magnitudes are first converted by *transducers* into electric signals that can be easily treated, transmitted, and stored. Several books of biomedical instrumentation give detailed descriptions of the various transducers and the hardware requirements associated with the acquisition of the different biologic signals [Cobbold, 1988; Tompkins & Webster, 1981; Webster, 1992].

An analog preprocessing block is usually required to amplify and filter the signal (in order to make it satisfy the requirements of the following hardware such as the dynamic of the analog-to-digital converter), to compensate some unwanted sensor characteristics, or to reduce the portion of undesired noise. Moreover, the continuous-time signal should be bandlimited before analog-to-digital (A/D) conversion. Such an operation is needed to reduce the effect of aliasing induced by sampling, as will be described in the next section. Here it is important to remember that the acquisition procedure should preserve the information contained in the original signal waveform. This is a crucial point when recording biologic signals, whose characteristics often may be considered by physicians as indices of some underlying pathologies (i.e., the ST-segment displacement on an ECG signal can be considered a marker of ischemia, the peak-and-wave pattern on an EEG tracing can be a sign of epilepsy, and so on). Thus the acquisition system should not introduce any form of distortion that can be misleading or can destroy real pathologic alterations. For this reason, the analog prefiltering block should be designed with *constant modulus* and *linear phase* (or zero-phase) frequency response, at least in the passband, over the frequencies of interest. Such requirements make the signal arrive undistorted up to the A/D converter.

The analog waveform is then A/D converted into a digital signal; i.e., it is transformed into a series of numbers discretized both in time and amplitude that can be easily managed by digital processors. The A/D conversion ideally can be divided in two steps, as shown in Fig. 55.1: the *sampling* process, which converts the continuous signal in a discrete-time series and whose elements are named *samples,* and a *quantization* procedure, which assigns the amplitude value of each sample within a set of determined discrete values. Both processes modify the characteristics of the signal, and their effects will be discussed in the following sections.

The Sampling Theorem

The advantages of processing a digital series instead of an analog signal have been reported previously. Furthermore, the basic property when using a sampled series instead of its continuous waveform lies in the fact that the former, under certain hypotheses, is completely representative of the latter. When this happens, the continuous waveform can be perfectly reconstructed just from the series of sampled values. This is known as the *sampling theorem* (or *Shannon theorem*) [Shannon, 1949]. It states that a continuous-time signal can be completely recovered from its samples if, and only if, the sampling rate is greater than twice the signal bandwidth.

In order to understand the assumptions of the theorem, let us consider a continuous band-limited signal $x(t)$ (up to f_b) whose Fourier transform $X(f)$ is shown in Fig. 55.2*a* and suppose to uni-

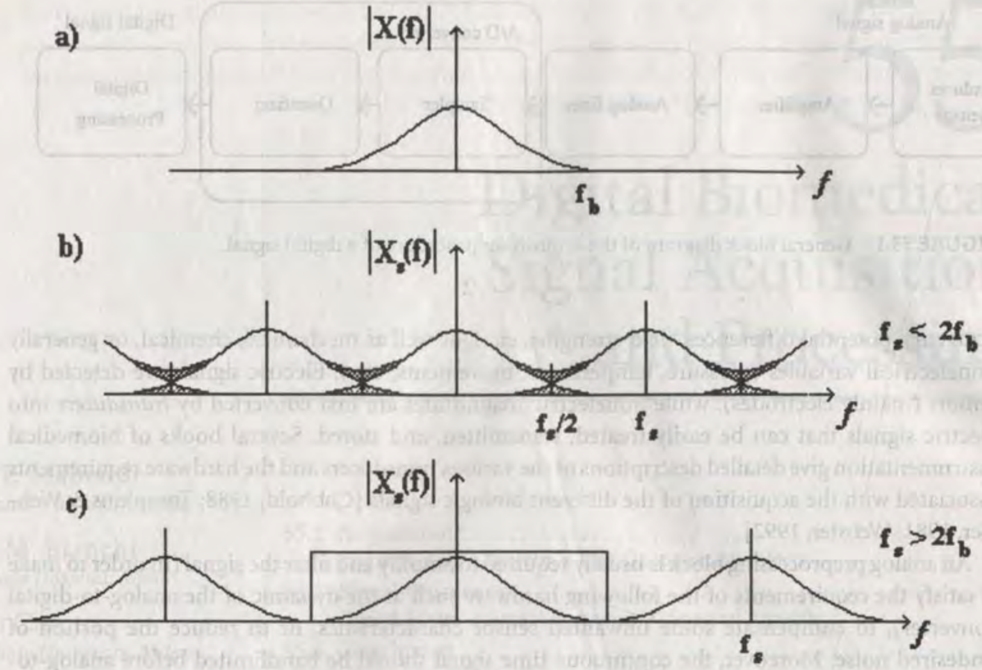

FIGURE 55.2 Effect of sampling frequency (f_s) on a band-limited signal (up to frequency f_b). Fourier transform of the original time signal (*a*), of the sampled signal when $f_s < 2f_b$ (*b*), and when $f_s > 2f_b$ (*c*). The dark areas in part *b* indicate the aliased frequencies.

formly sample it. The sampling procedure can be modeled by the multiplication of $x(t)$ with an impulse train

$$i(t) = \sum_{k=-\infty,\infty} \delta(t - kT_s) \tag{55.1}$$

where $\delta(t)$ is the delta (Dirac) function, k is an integer, and T_s is the sampling interval. The sampled signal becomes

$$x_s(t) = x(t) \cdot i(t) = \sum_{k=-\infty,\infty} x(t) \cdot \delta(t - kT_s) \tag{55.2}$$

Taking into account that multiplication in time domain implies convolution in frequency domain, we obtain

$$X_s(f) = X(f) * I(f) = X(f) * \frac{1}{T_s} \sum_{k=-\infty,\infty} \delta(f - kf_s) = \frac{1}{T_s} \sum_{k=-\infty,\infty} X(f - kf_s) \tag{55.3}$$

where $f_s = 1/T_s$ is the sampling frequency.

Thus $X_s(f)$, i.e., the Fourier transform of the sampled signal, is periodic and consists of a series of identical repeats of $X(f)$ centered around multiples of the sampling frequency, as depicted in Fig. 55.2*b*,*c*. It is worth noting in Fig. 55.2*b* that the frequency components of $X(f)$ placed above $f_s/2$ appears, when $f_s < 2f_b$, as folded back, summing up to the lower-frequency components. This phenomenon is known as *aliasing* (higher components look "alias" lower components). When aliasing occurs, the original information (Fig. 55.2*a*) cannot be recovered because the frequency components of the original signal are irreversibly corrupted by the overlaps of the shifted versions of $X(f)$.

A visual inspection of Fig. 55.2 allows one to observe that such frequency contamination can be avoided when the original signal is bandlimited [$X(f) = 0$ for $f > f_b$] and sampled at a frequency $f_s \geq 2f_b$. In this case, shown in Fig. 55.2*c*, no overlaps exist between adjacent replay of $X(f)$, and the original waveform can be retrieved by low-pass filtering the sampled signal [Oppenheim & Schafer, 1975]. Such observations are the basis of the sampling theorem previously reported.

The hypothesis of a bandlimited signal is hardly verified in practice, due to the signal characteristics or to the effect of superimposed wideband noise. It is worth noting that filtering before sampling is always needed even if we assume the incoming signal to be bandlimited. Let us consider the following example of an EEG signal whose frequency content of interest ranges between 0 and 40 Hz (the usual diagnostic bands are δ, 0 to 3.5 Hz; ϑ, 4 to 7 Hz; α, 8 to 13 Hz; β, 14 to 40 Hz). We may decide to sample it at 80 Hz, thus literarily respecting the Shannon theorem. If we do it without prefiltering, we could find some unpleasant results. Typically, the 50-Hz mains noise will replicate itself in the signal band (30 Hz, i.e., the β band), thus corrupting irreversibly the information, which is of great interest from a physiologic and clinical point of view. The effect is shown in Fig. 55.3*a* (before sampling) and Fig. 55.3*b* (after sampling). Generally, it is advisable to sample at a frequency greater than $2f_b$ [Gardenhire, 1964] in order to take into account the nonideal behaviour of the filter or the other preprocessing devices. Therefore, the prefiltering block of Fig. 55.1 is always required to bandlimit the signal before sampling and to avoid aliasing errors.

The Quantization Effects

The quantization produces a discrete signal, whose samples can assume only certain values according to the way they are coded. Typical step functions for a uniform quantizer are reported in Fig. 55.4*a,b*, where the quantization interval Δ between two quantization levels is evidenced in two cases: rounding and truncation, respectively.

Quantization is a heavily nonlinear procedure, but fortunately, its effects can be statistically modeled. Figure 55.4*c,d* shows it; the nonlinear quantization block is substituted by a statistical model in which the error induced by quantization is treated as an additive noise $e(n)$ (**quantization error**) to the signal $x(n)$. The following hypotheses are considered in order to deal with a simple mathematical problem:

1. $e(n)$ is supposed to be a white noise with uniform distribution.
2. $e(n)$ and $x(n)$ are uncorrelated.

First of all, it should be noted that the probability density of $e(n)$ changes according to the adopted coding procedure. If we decide to round the real sample to the nearest quantization level, we have

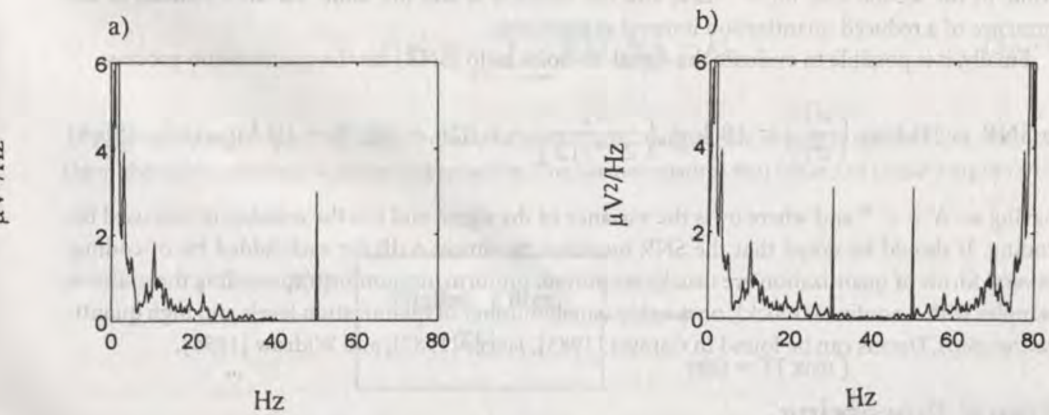

FIGURE 55.3 Power spectrum of an EEG signal (originally bandlimited up to 40 Hz). The presence of 50-Hz mains noise (*a*) causes aliasing error in the 30-Hz component (i.e., in the β diagnostic band) in the sampled signal (*b*) if $f_s = 80$ Hz.

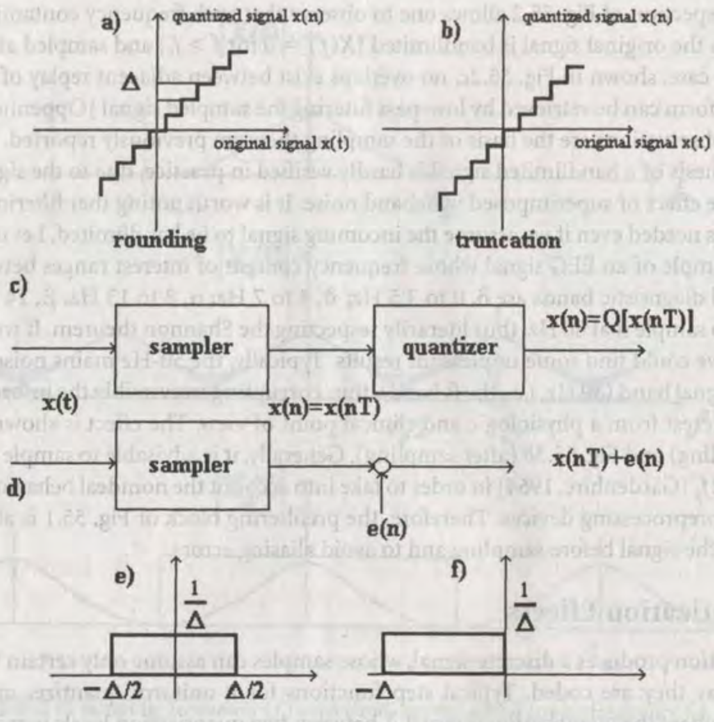

FIGURE 55.4 Nonlinear relationships for rounding (*a*) and truncation (*b*) quantization procedures. Description of quantization block (*c*) by a statistical model (*d*) and probability densities for the quantization noise $e(n)$ for rounding (*e*) and truncation (*f*). Δ is the quantization interval.

$-\Delta/2 \leq e(n) < \Delta/2$, while if we decide to truncate the sample amplitude, we have $-\Delta \leq e(n) < 0$. The two probability densities are plotted in Fig. 55.4*e,f*.

The two ways of coding yield processes with different statistical properties. In the first case the mean and variance value of $e(n)$ are

$$m_e = 0 \quad \sigma_e^2 = \Delta^2/12$$

while in the second case $m_e = -\Delta/2$, and the variance is still the same. Variance reduces in the presence of a reduced quantization interval as expected.

Finally, it is possible to evaluate the signal-to-noise ratio (SNR) for the quantization process:

$$\mathrm{SNR} = 10\log_{10}\left(\frac{\sigma_x^2}{\sigma_e^2}\right) = 10\log_{10}\left(\frac{\sigma_x^2}{2^{-2b}/12}\right) = 6.02b + 10.79 + 10\log_{10}(\sigma_x^2) \quad (55.4)$$

having set $\Delta = 2^{-2b}$ and where σ_x^2 is the variance of the signal and b is the number of bits used for coding. It should be noted that the SNR increases by almost 6 dB for each added bit of coding. Several forms of quantization are usually employed: uniform, nonuniform (preceding the uniform sampler with a nonlinear block), or roughly (small number of quantization levels and high quantization step). Details can be found in Carassa [1983], Jaeger [1982], and Widrow [1956].

55.2 Signal Processing

A brief review of different signal-processing techniques will be given in this section. They include traditional filtering, averaging techniques, and spectral estimators.

Only the main concepts of analysis and design of digital filters are presented, and a few examples are illustrated in the processing of the ECG signal. Averaging techniques will then be described briefly and their usefulness evidenced when noise and signal have similar frequency contents but different statistical properties; an example for evoked potentials enhancement from EEG background noise is illustrated. Finally, different spectral estimators will be considered and some applications shown in the analysis of RR fluctuations [i.e., the heart rate variability (HRV) signal].

Digital Filters

A *digital filter* is a discrete-time system that operates some transformation on a digital input signal $x(n)$ generating an output sequence $y(n)$, as schematically shown by the block diagram in Fig. 55.5. The characteristics of transformation $T[\cdot]$ identify the filter. The filter will be *time-variant* if $T[\cdot]$ is a function of time or *time-invariant* otherwise, while is said to be *linear* if, and only if, having $x_1(n)$ and $x_2(n)$ as inputs producing $y_1(n)$ and $y_2(n)$, respectively, we have

$$T[ax_1 + bx_2] = aT[x_1] + bT[x_2] = ay_1 + by_2. \tag{55.5}$$

In the following, only linear, time-invariant filters will be considered, even if several interesting applications of nonlinear [Glaser & Ruchkin, 1976; Tompkins, 1993] or time-variant [Cohen, 1983; Huta & Webster, 1973; Thakor, 1987; Widrow et al., 1975] filters have been proposed in the literature for the analysis of biologic signals.

The behavior of a filter is usually described in terms of input-output relationships. They are usually assessed by exciting the filter with different inputs and evaluating which is the response (output) of the system. In particular, if the input is the impulse sequence $\delta(n)$, the resulting output, the impulse response, has a relevant role in describing the characteristic of the filter. Such a response can be used to determine the response to more complicated input sequences. In fact, let us consider a generic input sequence $x(n)$ as a sum of weighed and delayed impulses

$$x(n) = \sum_{k=-\infty,\infty} x(k) \cdot \delta(n-k) \tag{55.6}$$

and let us identify the response to $\delta(n-k)$ as $h(n-k)$. If the filter is time-invariant, each delayed impulse will produce the same response, but time-shifted; due to the linearity property, such responses will be summed at the output:

$$y(n) = \sum_{k=-\infty,\infty} x(k) \cdot h(n-k). \tag{55.7}$$

This convolution product links input and output and defines the property of the filter. Two of them should be recalled: *stability* and *causality*. The former ensures that bounded (finite) inputs will

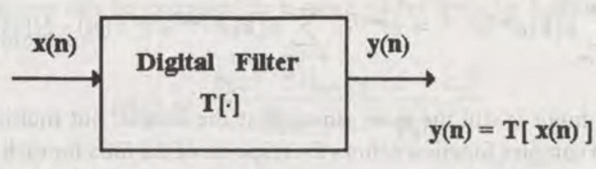

FIGURE 55.5 General block diagram of a digital filter. The output digital signal $y(n)$ is obtained from the input $x(n)$ by means of a transformation $T[\cdot]$ which identifies the filter.

produce bounded outputs. Such a property can be deduced by the impulse response; it can be proved that the filter is stable if and only if

$$\sum_{k=-\infty,\infty} |h(k)| < \infty \tag{55.8}$$

Causality means that the filter will not respond to an input before the input is applied. This is in agreement with our physical concept of a system, but it is not strictly required for a digital filter that can be implemented in a noncausal form. A filter is causal if and only if

$$h(k) = 0 \qquad \text{for } k < 0$$

Even if relation (55.7) completely describes the properties of the filter, most often it is necessary to express the input-output relationships of linear discrete-time systems under the form of the z-transform operator, which allows one to express relation (55.7) in a more useful, operative, and simpler form.

The z-Transform

The z-transform of a sequence $x(n)$ is defined by [Rainer et al., 1972]

$$X(z) = \sum_{k=-\infty,\infty} x(k) \cdot z^{-k} \tag{55.9}$$

where z is a complex variable. This series will converge or diverge for different z values. The set of z values which makes Eq. (55.9) converge is the region of convergence, and it depends on the series $x(n)$ considered.

Among the properties of the z-transform, we recall

- The delay (shift) property:
  If $\quad w(n) = x(n - T) \quad$ then $\quad W(z) = X(z) \cdot z^{-T}$
- The product of convolution:
  If $\quad w(n) = \sum_{k=-\infty,\infty} x(k) \cdot y(n-k) \quad$ then $\quad W(z) = X(z) \cdot Y(z)$

The Transfer Function in the z-Domain

Thanks to the previous property, we can express Eq. (55.7) in the z-domain as a simple multiplication:

$$Y(z) = H(z) \cdot X(z) \tag{55.10}$$

where $H(z)$, known as *transfer function* of the filter, is the z-transform of the impulse response. $H(z)$ plays a relevant role in the analysis and design of digital filters. The response to input sinusoids can be evaluated as follows: Assume a complex sinusoid $x(n) = e^{j\omega n T_s}$ as input, the correspondent filter output will be

$$y(n) = \sum_{k=0,\infty} h(k) e^{j\omega T_s (n-k)} = e^{j\omega n T_s} \sum_{k=0,\infty} h(k) e^{-j\omega k T_s} = x(n) \cdot H(z)|_{z=e^{j\omega T_s}} \tag{55.11}$$

Then a sinusoid in input is still the same sinusoid at the output, but multiplied by a complex quantity $H(\omega)$. Such complex function defines the response of the filter for each sinusoid of ω pulse in input, and it is known as the frequency response of the filter. It is evaluated in the complex z plane by computing $H(z)$ for $z = e^{j\omega T_s}$, namely, on the point locus that describes the unitary circle on the z plane ($|e^{j\omega T_s}| = 1$). As a complex function, $H(\omega)$ will be defined by its module $|H(\omega)|$ and by its phase $\angle H(\omega)$ functions, as shown in Fig. 55.6 for a moving average filter of order 5. The figure indicates that the lower-frequency components will come through the filter almost unaffected, while the higher-frequency components will be drastically reduced. It is usual to express the horizontal axis of frequency response from 0 to π. This is obtained because only pulse frequencies up to $\omega_s/2$ are reconstructable (due to the Shannon theorem), and therefore, in the horizontal axis, the value of ωT_s is reported which goes from 0 to π. Furthermore, Fig. 55.6*b* demonstrates that the phase is piecewise linear, and in correspondence with the zeroes of $|H(\omega)|$, there is a change in phase of π value. According to their frequency response, the filters are usually classified as (1) low-pass, (2) high-pass, (3) bandpass, or (4) bandstop filters. Figure 55.7 shows the ideal frequency response for such filters with the proper low- and high-frequency cutoffs.

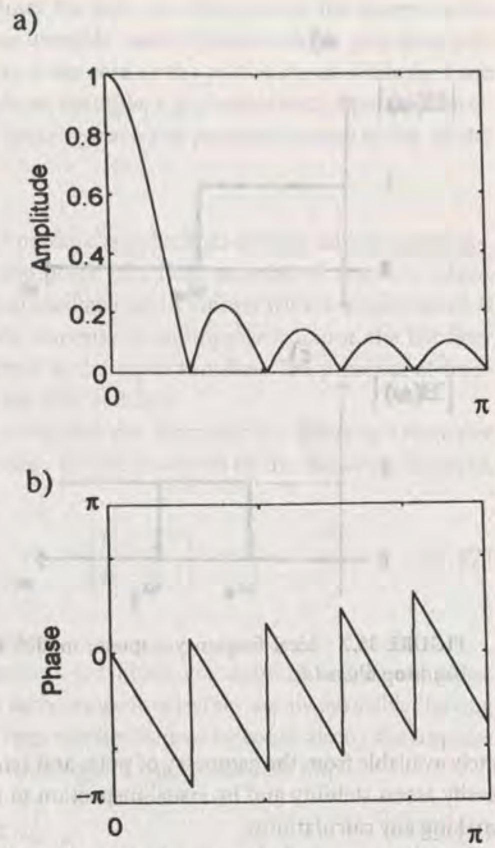

FIGURE 55.6 Modulus (*a*) and phase (*b*) diagrams of the frequency response of a moving average filter of order 5. Note that the frequency plots are depicted up to π. In fact, taking into account that we are dealing with a sampled signal whose frequency information is up to $f_s/2$, we have $\omega_{max} = 2\pi f_s/2 = \pi f_s$ or $\omega_{max} = \pi$ if normalized with respect to the sampling rate.

For a large class of linear, time-invariant systems, $H(z)$ can be expressed in the following general form:

$$H(z) = \frac{\sum\limits_{m=0,M} b_m z^{-m}}{1 + \sum\limits_{k=1,N} a_k z^{-k}} \tag{55.12}$$

which describes in the z domain the following *difference equation* in the discrete time domain:

$$y(n) = -\sum_{k=1,N} a_k y(n-k) + \sum_{m=0,M} b_m x(n-m) \tag{55.13}$$

When at least one of the a_k coefficient is different from zero, some output values contribute to the current output. The filter contains some feedback, and it is said to be implemented in a *recursive* form. On the other hand, when the a_k values are all zero, the filter output is obtained only from the current or previous inputs, and the filter is said to be implemented in a *nonrecursive* form.

The transfer function can be expressed in a more useful form by finding the roots of both numerator and denominator:

$$H(z) = \frac{b_0 z^{N-M} \prod_{m=1,M}(z - z_m)}{\prod_{k=1,N}(z - p_k)} \tag{55.14}$$

where z_m are the zeroes and p_k are the poles. It is worth nothing that $H(z)$ presents $N - M$ zeros in correspondence with the origin of the z plane and M zeroes elsewhere (N zeroes totally) and N poles. The pole-zero form of $H(z)$ is of great interest because several properties of the filter are immedi-

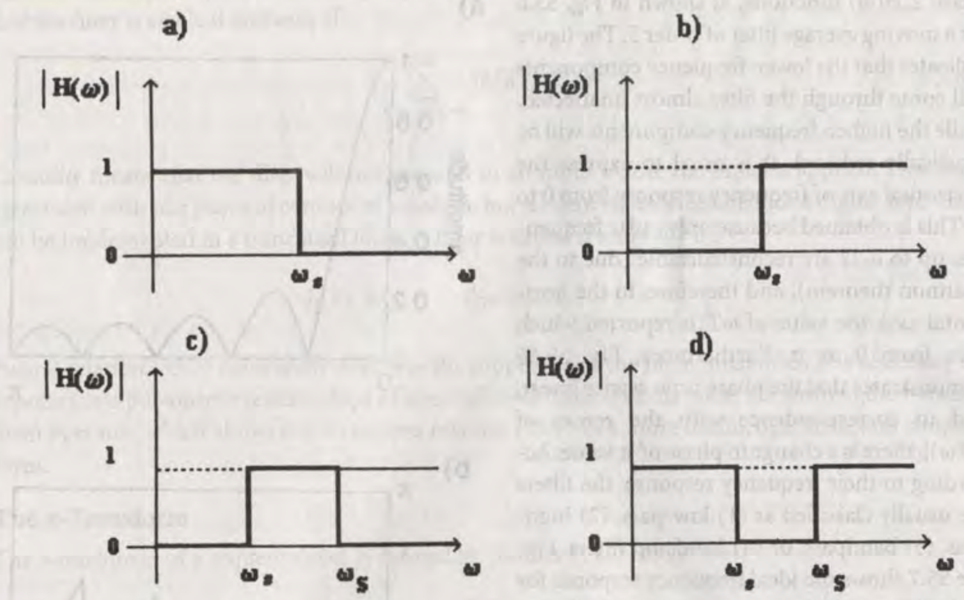

FIGURE 55.7 Ideal frequency-response moduli for low-pass (*a*), high-pass (*b*), bandpass (*c*), and bandstop filters (*d*).

ately available from the geometry of poles and zeroes in the complex z plane. In fact, it is possible to easily assess stability and by visual inspection to roughly estimate the frequency response without making any calculations.

Stability is verified when all poles lie inside the unitary circle, as can be proved by considering the relationships between the z-transform and the Laplace s-transform and by observing that the left side of the s plane is mapped inside the unitary circle [Jackson, 1986; Oppenheim & Schafer, 1975].

The frequency response can be estimated by noting that $(z - z_m)|_{z=e^{j\omega T_s}}$ is a vector joining the mth zero with the point on the unitary circle identified by the angle ωT_s. Defining

$$\begin{aligned}\vec{B}_m &= (z - z_m)|_{z=e^{j\omega T_s}}\\ \vec{A}_k &= (z - p_k)|_{z=e^{j\omega T_s}}\end{aligned} \tag{55.15}$$

we obtain

$$\begin{aligned}|H(\omega)| &= \frac{b_0\Pi_{m=1,M}|\vec{B}_m|}{\Pi_{k=1,N}|\vec{A}_k|}\\ \angle H(\omega) &= \sum_{m=1,M}\angle\vec{B}_m - \sum_{k=1,N}\angle\vec{A}_k + (N-M)\omega T_s.\end{aligned} \tag{55.16}$$

Thus the modulus of $H(\omega)$ can be evaluated at any frequency $\omega°$ by computing the distances between poles and zeroes and the point on the unitary circle corresponding to $\omega = \omega°$, as evidenced by Fig. 55.8, where a filter with two pairs of complex poles and three zeros is considered.

To obtain the estimate of $H(\omega)$, we move around the unitary circle and roughly evaluate the effect of poles and zeroes by keeping in mind a few rules [Challis & Kitney, 1982]: (1) when we are close to a zero, $|H(\omega)|$ will approach zero, and a positive phase shift will appear in $\angle H(\omega)$ as the vector from the zero reverses its angle; (2) when we are close to a pole, $|H(\omega)|$ will tend to peak, and a negative phase change is found in $\angle H(\omega)$ (the closer the pole to unitary circle, the sharper is the peak until it reaches infinite and the filter becomes unstable); and (3) near a closer pole-zero pair, the response modulus will tends to zero or infinity if the zero or the pole is closer, while far from this pair, the modulus can be considered unitary. As an example, it is possible to compare the modulus and phase diagram of Fig. 55.8*b,c* with the relative geometry of poles and zeroes of Fig. 55.8*a*.

FIR and IIR Filters

A common way of classifying digital filters is based on the characteristics of their impulse response. For finite impulse response (FIR) filters, $h(n)$ is composed of a finite number of nonzero values, while for infinite impulse response (IIR) filters, $h(n)$ oscillates up to infinity with nonzero values. It is clearly evident that in order to obtain an infinite response to an impulse in input, the IIR filter must contain some feedback that sustains the output as the input vanishes. The presence of feedback paths requires to put particular attention to the filter stability.

Even if FIR filters are usually implemented in a nonrecursive form and IIR filters in a recursive form, the two ways of classification are not coincident. In fact, as shown by the following example, a FIR filter can be expressed in a recursive form

$$H(z) = \sum_{k=0,N-1} z^{-k} = \sum_{k=0,N-1} z^{-k}\frac{(1-z^{-1})}{(1-z^{-1})} = \frac{1-z^{-N}}{1-z^{-1}} \tag{55.17}$$

for a more convenient computational implementation.

As shown previously, two important requirements for filters are stability and linear phase response. FIR filters can be easily designed to fulfill such requirements; they are always stable (having no poles outside the origin); and the linear phase response is obtained by constraining the impulse response coefficients to have symmetry around their midpoint. Such constrain implies

$$b_m = \pm\, b^{*}_{M-m} \tag{55.18}$$

where the b_m are the M coefficients of an FIR filter. The sign + or − stays in accordance with the symmetry (even or odd) and M value (even or odd). This is a necessary and sufficient condition for FIR filters to have linear phase response. Two cases of impulse response that yield a linear phase filter are shown in Fig. 55.9.

It should be noted that condition (55.18) imposes geometric constrains to the zero locus of $H(z)$. Taking into account Eq. (55.12), we have

$$z^M H(z) = H\left(\frac{1}{z^*}\right) \tag{55.19}$$

Thus, both z_m and $1/z_m^*$ must be zeros of $H(z)$. Then the zeroes of linear phase FIR filters must lie on the unitary circle, or they must appear in pairs and with inverse moduli.

Design Criteria

In many cases, the filter is designed in order to satisfy some requirements, usually on the frequency response, which depend on the characteristic of the particular application the filter is intended for. It is known that ideal filters, like those reported in Fig. 55.7, are not physically realizable (they would require an infinite number of coefficients of impulse response); thus we can design FIR or IIR filters that can only mimic, with an acceptable error, the ideal response. Figure 55.10 shows a frequency response of a not ideal low-pass filter. Here, there are ripples in passband and in stopband, and there is a transition band from passband to stopband, defined by the interval $\omega_s - \omega_p$.

Several design techniques are available, and some of them require heavy computational tasks, which are capable of developing filters with defined specific requirements. They include window technique, frequency-sampling method, or equiripple design for FIR filters. Butterworth, Chebychev, elliptical design, and impulse-invariant or bilinear transformation are instead employed for IIR filters. For detailed analysis of digital filter techniques, see Antoniou [1979], Cerutti [1983], and Oppenheim and Schafer [1975].

Examples

A few examples of different kinds of filters will be presented in the following, showing some applications on ECG signal processing. It is known that the ECG contains relevant information over a wide range of frequencies; the lower-frequency contents should be preserved for correct measurement of the slow ST displacements, while higher-frequency contents are needed to correctly estimate amplitude and duration of the faster contributions, mainly at the level of the QRS complex. Unfortunately, several sources of noise are present in the same frequency band, such as, for example, higher-frequency noise due to muscle contraction (EMG noise), the lower-frequency noise due to motion artifacts (baseline wandering), the effect of respiration or the low-frequency noise in the skin-electrode interface, and others.

In the first example, the effect of two different low-pass filters will be considered. An ECG signal corrupted by an EMG noise (Fig. 55.11*a*) is low-pass filtered by two different low-pass filters whose frequency responses are shown in Fig. 55.11*b,c*. The two FIR filters have cutoff frequencies at 40 and 20 Hz, respectively, and were designed through window techniques (Weber-Cappellini window, filter length = 256 points) [Cappellini et al., 1978].

The output signals are shown in Fig. 55.11*d,e*. Filtering drastically reduces the superimposed noise but at the same time alters the original ECG waveform. In particular, the R wave amplitude is progressively reduced by decreasing the cutoff frequency, and the QRS width is progressively increased as well. On the other hand, P waves appears almost unaffected, having frequency components generally lower than 20 to 30 Hz. At this point, it is worth noting that an increase in QRS duration is generally associated with various pathologies, such as ventricular hypertrophy or bundle-branch block. It is therefore necessary to check that an excessive band limitation does not introduce a false-positive indication in the diagnosis of the ECG signal.

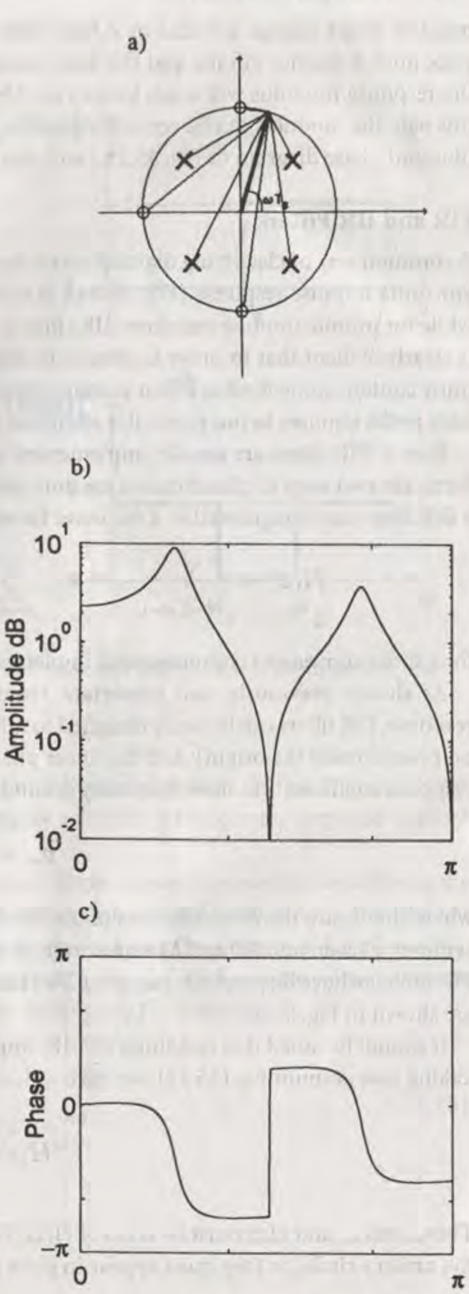

FIGURE 55.8 Poles and zeroes geometry (*a*) and relative frequency response modulus (*b*) and phase (*c*) characteristics. Moving around the unitary circle a rough estimation of $|H(\omega)|$ and $\angle H(\omega)$ can be obtained. Note the zeros' effects at π and $\pi/2$ and modulus rising in proximity of the poles. Phase shifts are cleary evident in part *c* closer to zeros and poles.

a)

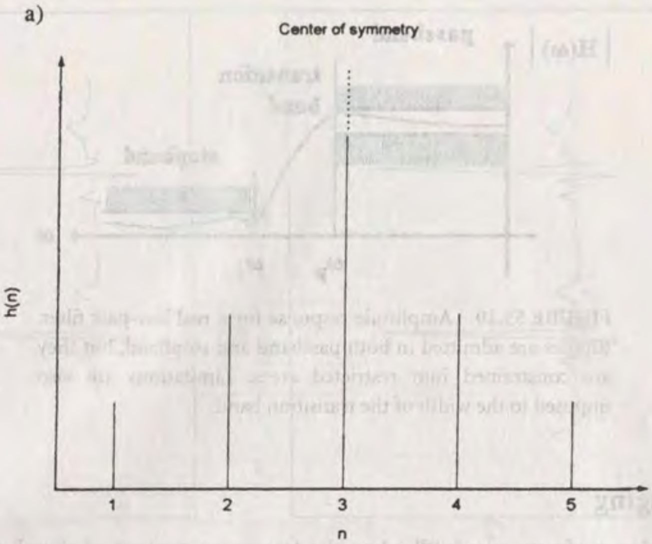

b)

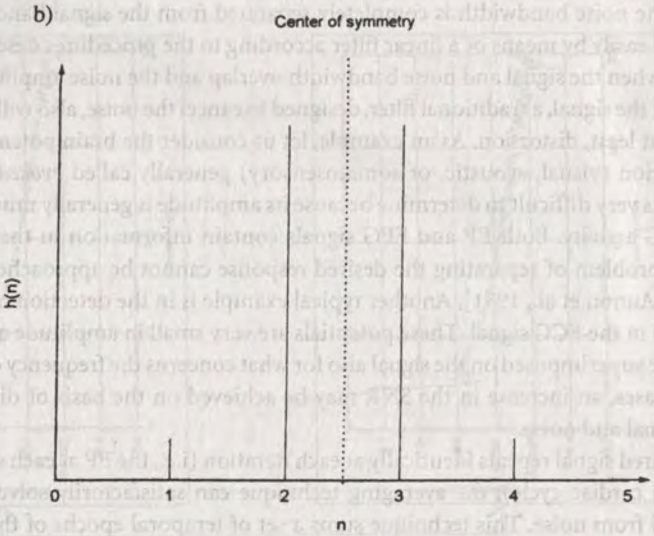

FIGURE 55.9 Examples of impulse response for linear phase FIR filters: odd (*a*) and even (*b*) number of coefficients.

An example of an application for stopband filters (notch filters) is presented in Fig. 55.12. It is used to reduce the 50-Hz mains noise on the ECG signal, and it was designed by placing a zero in correspondence of the frequency we want to suppress.

Finally, an example of a high-pass filter is shown for the detection of the QRS complex. Detecting the time occurrence of a fiducial point in the QRS complex is indeed the first task usually performed in ECG signal analysis. The QRS complex usually contains the higher-frequency components with respect to the other ECG waves, and thus such components will be enhanced by a high-pass filter. Figure 55.13 shows how QRS complexes (Fig. 55.13*a*) can be identified by a derivative high-pass filter with a cutoff frequency to decrease the effect of the noise contributions at high frequencies (Fig. 55.13*b*). The filtered signal (Fig. 55.13*c*) presents sharp and well-defined peaks that are easily recognized by a threshold value.

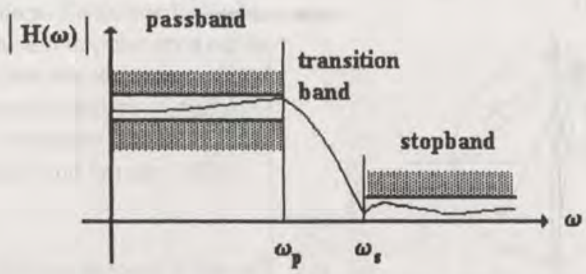

FIGURE 55.10 Amplitude response for a real low-pass filter. Ripples are admitted in both passband and stopband, but they are constrained into restricted areas. Limitations are also imposed to the width of the transition band.

Signal Averaging

Traditional filtering performs very well when the frequency content of signal and noise do not overlap. When the noise bandwidth is completely separated from the signal bandwidth, the noise can be decreased easily by means of a linear filter according to the procedures described earlier. On the other hand, when the signal and noise bandwidth overlap and the noise amplitude is enough to seriously corrupt the signal, a traditional filter, designed to cancel the noise, also will introduce signal cancellation or, at least, distortion. As an example, let us consider the brain potentials evoked by a sensory stimulation (visual, acoustic, or somatosensory) generally called *evoked potentials* (EP). Such a response is very difficult to determine because its amplitude is generally much lower than the background EEG activity. Both EP and EEG signals contain information in the same frequency range; thus the problem of separating the desired response cannot be approached via traditional digital filtering [Aunon et al., 1981]. Another typical example is in the detection of ventricular late potentials (VLP) in the ECG signal. These potentials are very small in amplitude and are comparable with the noise superimposed on the signal also for what concerns the frequency content [Simson, 1981]. In such cases, an increase in the SNR may be achieved on the basis of different statistical properties of signal and noise.

When the desired signal repeats identically at each iteration (i.e., the EP at each sensory stimulus, the VLP at each cardiac cycle), the averaging technique can satisfactorily solve the problem of separating signal from noise. This technique sums a set of temporal epochs of the signal together with the superimposed noise. If the time epochs are properly aligned, through efficient trigger-point recognition, the signal waveforms directly sum together. If the signal and the noise are characterized by the following statistical properties:

1. All the signal epochs contain a deterministic signal component $x(n)$ that does not vary for all the epochs.
2. The superimposed noise $w(n)$ is a broadband stationary process with zero mean and variance σ^2 so that

$$\begin{aligned} E[w(n)] &= 0 \\ E[w^2(n)] &= \sigma^2 \end{aligned} \tag{55.20}$$

3. Signal $x(n)$ and noise $w(n)$ are uncorrelated so that the recorded signal $y(n)$ at the ith iteration can be expressed as

$$y(n)_i = x(n) + w_i(n), \tag{55.21}$$

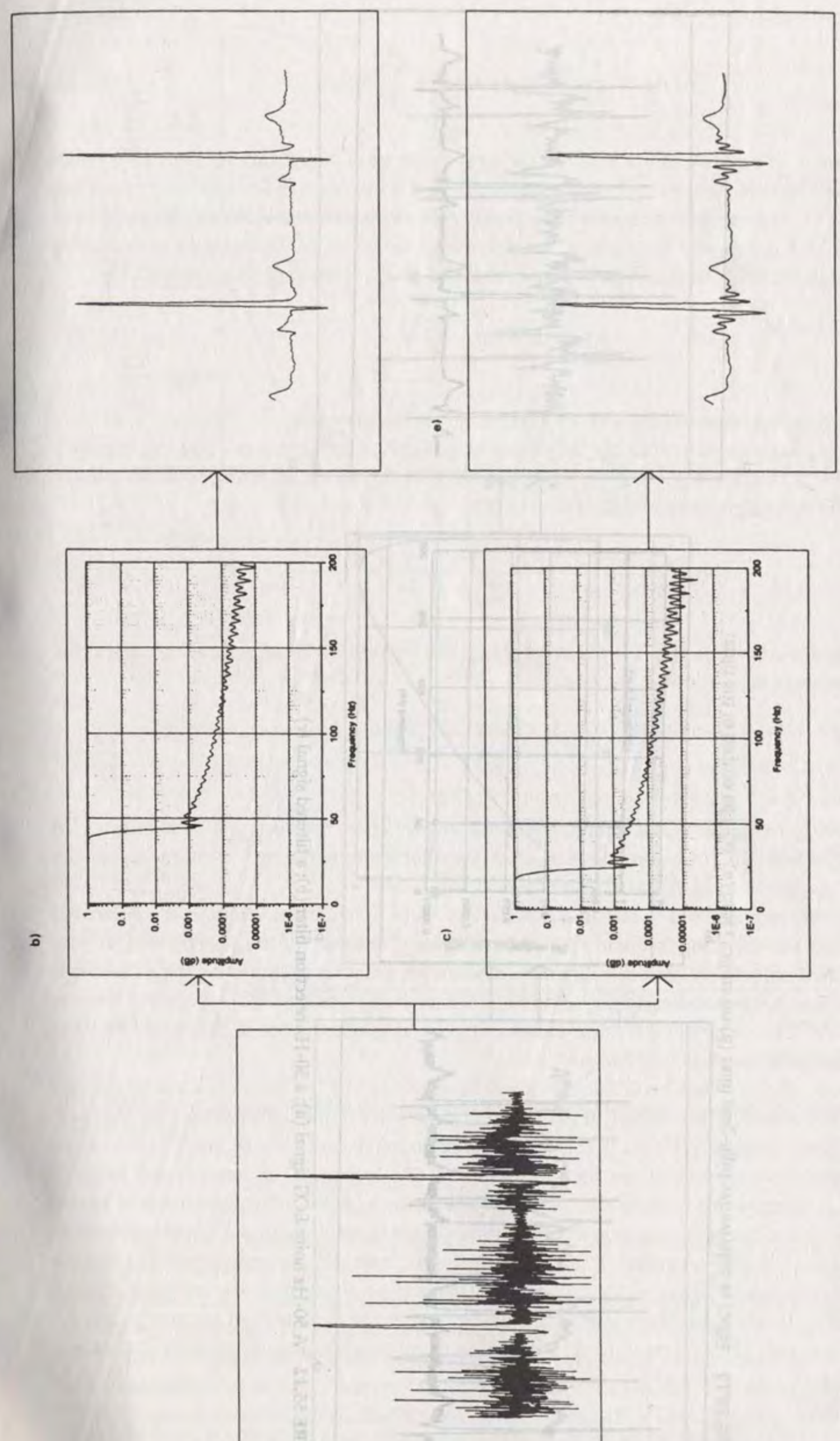

FIGURE 55.11 Effects of two different low-pass filters (*b*) and (*c*) on an ECG trace (*a*) corrupted by EMG noise. Both amplitude reduction and variation in the QRS width induced by too drastic lowpass filtering are evidenced.

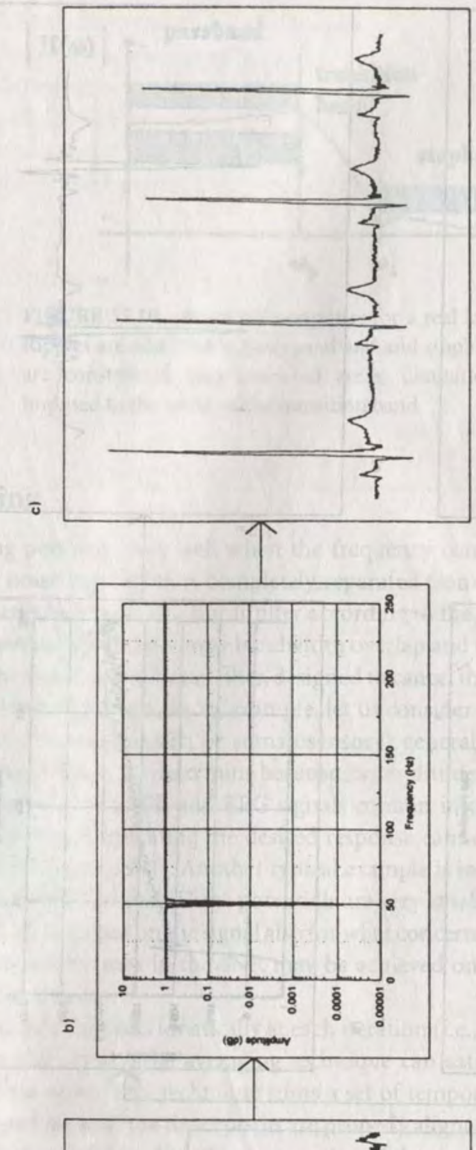

FIGURE 55.12 A 50-Hz noisy ECG signal (*a*); a 50-Hz rejection filter (*b*); a filtered signal (*c*).

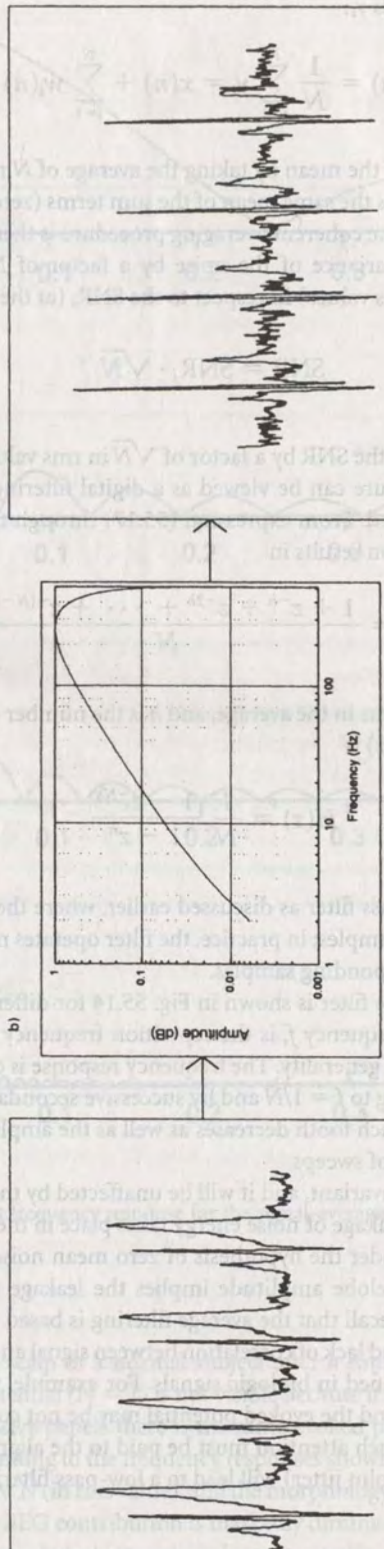

FIGURE 55.13 Effect of a derivative high-pass filter (*b*) on an ECG lead (*a*) (*c*) The output of the filter.

Then the averaging process yields y_t:

$$y_t(n) = \frac{1}{N}\sum_{i=1}^{N} y_i = x(n) + \sum_{i=1}^{N} w_i(n) \tag{55.22}$$

The noise term is an estimate of the mean by taking the average of N realizations. Such an average is a new random variable that has the same mean of the sum terms (zero in this case) and which has variance of σ^2/N. The effect of the coherent averaging procedure is then to maintain the amplitude of the signal and reduce the variance of the noise by a factor of N. In order to evaluate the improvement in the SNR (in rms values) in respect to the SNR$_i$ (at the generic ith sweep):

$$\mathrm{SNR} = \mathrm{SNR}_i \cdot \sqrt{N} \tag{55.23}$$

Thus signal averaging improves the SNR by a factor of $\sqrt{N}$ in rms value.

A coherent averaging procedure can be viewed as a digital filtering process, and its frequency characteristics can be investigated. From expression (55.17) through the z-transform, the transfer function of the filtering operation results in

$$H(z) = \frac{1 + z^{-h} + z^{-2h} + \cdots + z^{-(N-1)h}}{N} \tag{55.24}$$

where N is the number of elements in the average, and h is the number of samples in each response. An alternative expression for $H(z)$ is

$$H(z) = \frac{1}{N}\,\frac{1 - z^{-Nh}}{1 - z^{h}} \tag{55.25}$$

This is a moving average low-pass filter as discussed earlier, where the output is a function of the preceding value with a lag of h samples; in practice, the filter operates not on the time sequence but in the sweep sequence on corresponding samples.

The frequency response of the filter is shown in Fig. 55.14 for different values of the parameter N. In this case, the sampling frequency f_s is the repetition frequency of the sweeps, and we may assume it to be 1 without loss of generality. The frequency response is characterized by a main lobe with the first zero corresponding to $f = 1/N$ and by successive secondary lobes separated by zeroes at intervals $1/N$. The width of each tooth decreases as well as the amplitude of the secondary lobes when increasing the number N of sweeps.

The desired signal is sweep-invariant, and it will be unaffected by the filter, while the broadband noise will be decreased. Some leakage of noise energy takes place in the center of the sidelobes and, of course, at zero frequency. Under the hypothesis of zero mean noise, the dc component has no effect, and the diminishing sidelobe amplitude implies the leakage to be not relevant for high frequencies. It is important to recall that the average filtering is based on the hypothesis of broadband distribution of the noise and lack of correlation between signal and noise. Unfortunately, these assumptions are not always verified in biologic signals. For example, the assumption of independence of the background EEG and the evoked potential may be not completely realistic [Gevins & Remond, 1987]. In addition, much attention must be paid to the alignment of the sweeps; in fact, slight misalignments (fiducial point jitter) will lead to a low-pass filtering effect of the final result.

Example

As mentioned previously, one of the fields in which signal-averaging technique is employed extensively is in the evaluation of cerebral evoked response after a sensory stimulation. Figure 55.15*a* shows

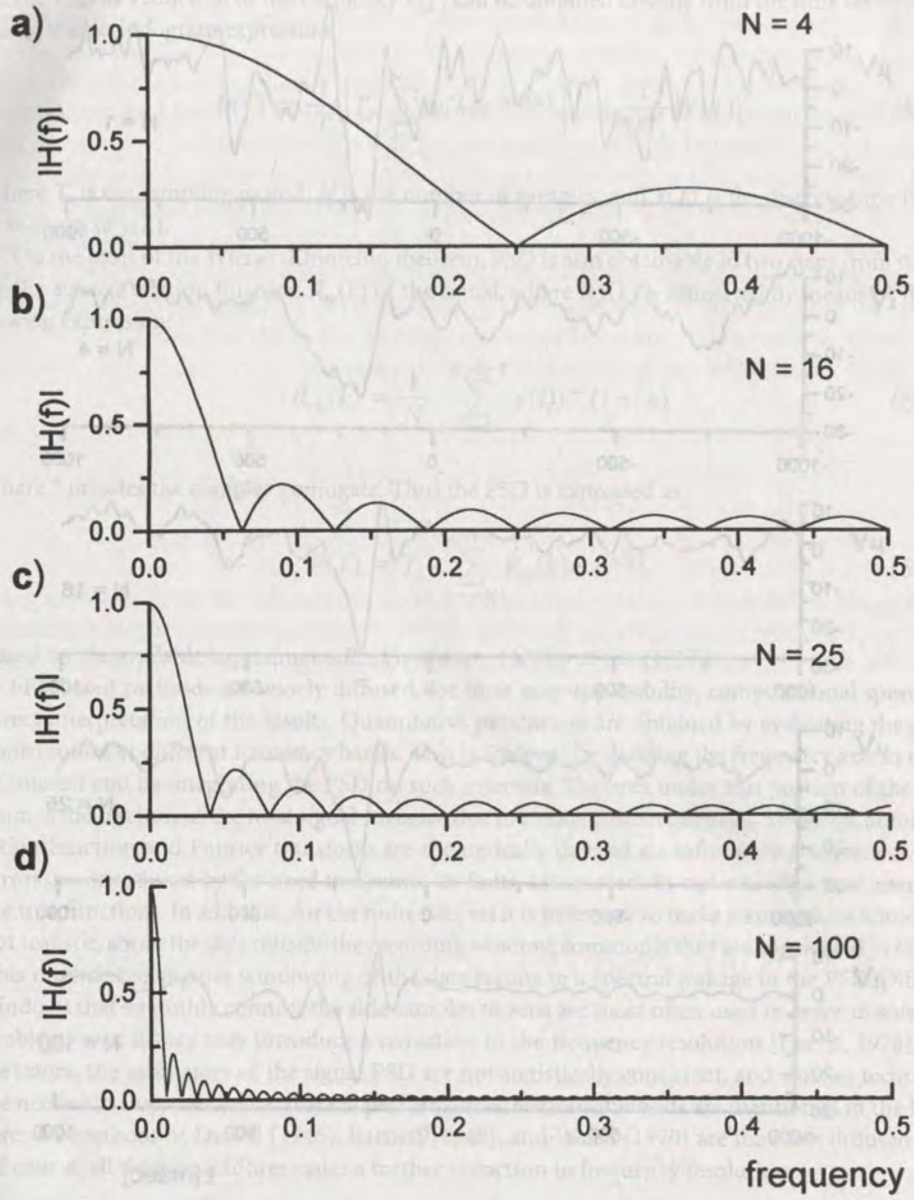

FIGURE 55.14 Equivalent frequency response for the signal-averaging procedure for different values of N (see text).

the EEG recorded from the scalp of a normal subject after a somatosensory stimulation released at time $t = 0$. The evoked potential ($N = 1$) is not visible because it is buried in the background EEG (upper panel). In the successive panels there is the same evoked potential after averaging different numbers of sweeps corresponding to the frequency responses shown in Fig. 55.14. As N increases, the SNR is improved by a factor $\sqrt{N}$ (in rms value), and the morphology of the evoked potential becomes more recognizable while the EEG contribution is markedly diminished. In this way it is easy to evaluate the quantitative indices of clinical interest, such as the amplitude and the latency of the relevant waves.

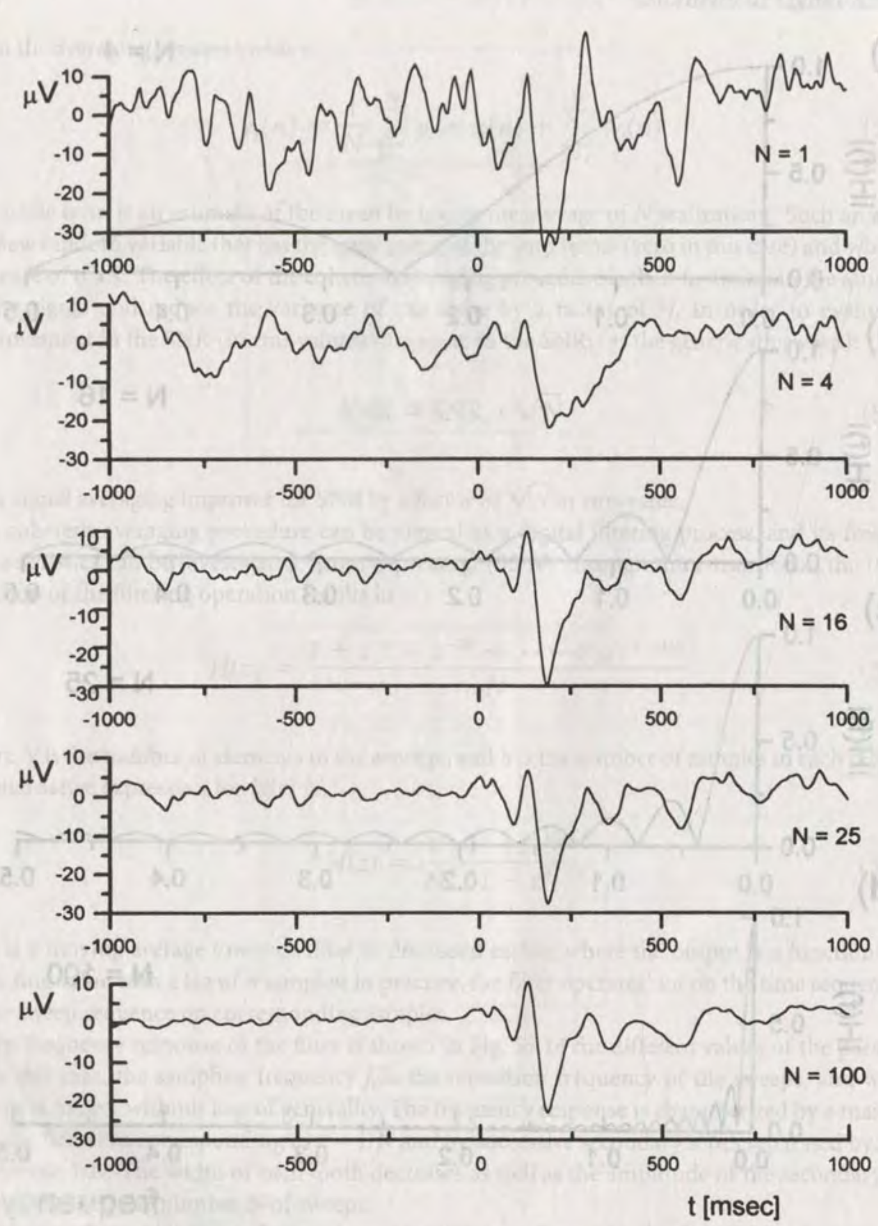

FIGURE 55.15 Enhancement of evoked potential (EP) by means of averaging technique. The EEG noise is progressively reduced, and the EP morphology becomes more recognizable as the number of averaged sweeps (N) is increased.

Spectral Analysis

The various methods to estimate the power spectrum density (PSD) of a signal may be classified as *nonparametric* and *parametric*.

Nonparametric Estimators of PSD

This is a traditional method of frequency analysis based on the Fourier transform that can be evaluated easily through the fast Fourier transform (FFT) algorithm [Marple, 1987]. The expression of the PSD as a function of the frequency $P(f)$ can be obtained directly from the time series $y(n)$ by using the periodogram expression

$$P(f) = \frac{1}{T_s}\left|T_s \sum_{k=0}^{N-1} y(k)e^{-j2\pi fkT_s}\right|^2 = \frac{1}{NT_s}|Y(f)|^2 \tag{55.26}$$

where T_s is the sampling period, N is the number of samples, and $Y(f)$ is the discrete time Fourier transform of $y(n)$.

On the basis of the Wiener-Khintchin theorem, PSD is also obtainable in two steps from the FFT of the autocorrelation function $R_{yy}(k)$ of the signal, where $R_{yy}(k)$ is estimated by means of the following expression:

$$\hat{R}_{yy}(k) = \frac{1}{N} \sum_{i=0}^{N-k-1} y(i)y^*(i+k) \tag{55.27}$$

where * denotes the complex conjugate. Thus the PSD is expressed as

$$P(f) = T_s \cdot \sum_{k=-N}^{N} \hat{R}_{yy}(k)e^{-j2\pi fkT_s} \tag{55.28}$$

based on the available lag estimates $\hat{R}_{yy}(k)$, where $-(1/2T_s) \leq f \leq (1/2T_s)$

FFT-based methods are widely diffused, for their easy applicability, computational speed, and direct interpretation of the results. Quantitative parameters are obtained by evaluating the power contribution at different frequency bands. This is achieved by dividing the frequency axis in ranges of interest and by integrating the PSD on such intervals. The area under this portion of the spectrum is the fraction of the total signal variance due to the specific frequencies. However, autocorrelation function and Fourier transform are theoretically defined on infinite data sequences. Thus errors are introduced by the need to operate on finite data records in order to obtain estimators of the true functions. In addition, for the finite data set it is necessary to make assumptions, sometimes not realistic, about the data outside the recording window; commonly they are considered to be zero. This implicit rectangular windowing of the data results in a spectral leakage in the PSD. Different windows that smoothly connect the side samples to zero are most often used in order to solve this problem, even if they may introduce a reduction in the frequency resolution [Harris, 1978]. Furthermore, the estimators of the signal PSD are not statistically consistent, and various techniques are needed to improve their statistical performances. Various methods are mentioned in the literature; the methods of Dariell [1946], Bartlett [1948], and Welch [1970] are the most diffused ones. Of course, all these procedures cause a further reduction in frequency resolution.

Parametric Estimators

Parametric approaches assume the time series under analysis to be the output of a given mathematical model, and no drastic assumptions are made about the data outside the recording window. The PSD is calculated as a function of the model parameters according to appropriate expressions. A critical point in this approach is the choice of an adequate model to represent the data sequence. The model is completely independent of the physiologic, anatomic, and physical characteristics of the biologic system but provides simply the input-output relationships of the process in the so-called black-box approach.

Among the numerous possibilities of modeling, linear models, characterized by a rational transfer function, are able to describe a wide number of different processes. In the most general case, they are represented by the following linear equation that relates the input-driving signal $w(k)$ and the output of an autoregressive moving average (ARMA) process:

$$y(k) = -\sum_{i=1}^{p} a_i y(k-i) + \sum_{j=1}^{q} b_j w(k-j) + w(k) \tag{55.29}$$

where $w(k)$ is the input white noise with zero mean value and variance λ^2, p and q are the orders of AR and MA parts, respectively, and a_i and b_j are the proper coefficients.

The ARMA model may be reformulated as an AR or an MA if the coefficients b_j or a_i are, respectively, set to zero. Since the estimation of the AR parameters results in linear equations, AR models are usually employed in place of ARMA or MA models, also on the basis of the Wold decomposition theorem [Marple, 1987] that establishes that any stationary ARMA or MA process of finite variance can be represented as a unique AR model of appropriate order, even infinite; likewise, any ARMA or AR process can be represented by an MA model of sufficiently high order.

The AR PSD is then obtained from the following expression:

$$P(f) = \frac{\lambda^2 T_s}{\left|1 + \sum_{i=1}^{p} a_i z^{-i}\right|^2_{z=\exp(j2\pi f T_s)}} = \frac{\lambda^2 T_s}{\left|\prod_{l=1}^{p} (z - z_l)\right|^2_{z=\exp(j2\pi f T_s)}} \tag{55.30}$$

The right side of the relation puts into evidence the poles of the transfer function that can be plotted in the z-transform plane. Figure 55.16b shows the PSD function of the HRV signal depicted in Fig. 55.16a, while Fig. 55.16c displays the corresponding pole diagram obtained according to the procedure described in the preceding section.

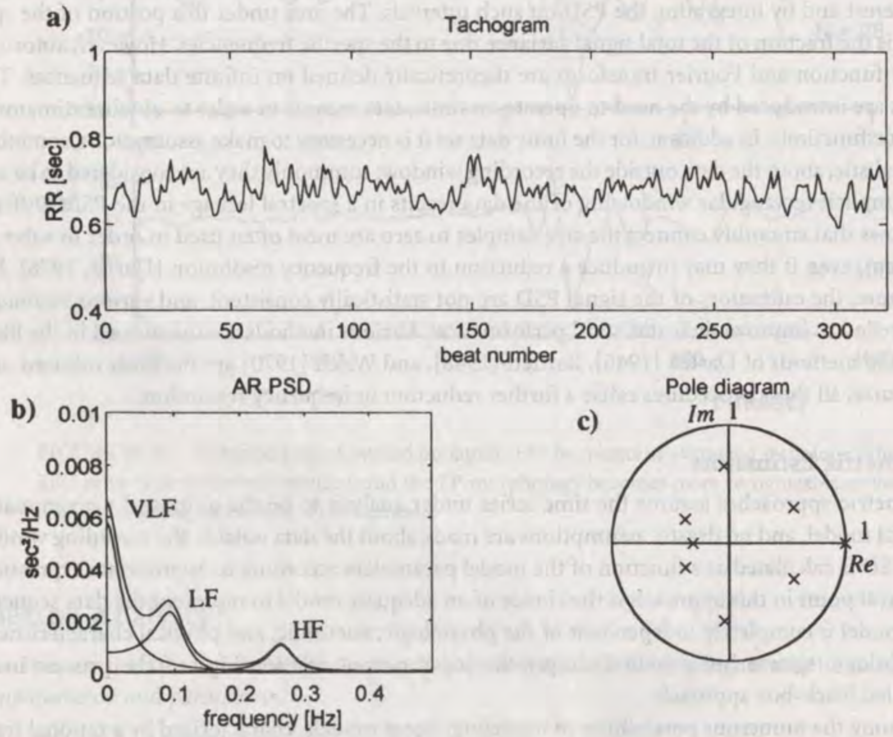

FIGURE 55.16 (a) Interval tachogram obtained from an ECG recording as the sequence of the RR time intervals expressed in seconds as a function of the beat number. (b) PSD of the signal (a) evaluated by means of an AR model (see text). (c) Pole diagram of the PSD shown in (b).

Parametric methods are methodologically and computationally more complex than the nonparametric ones, since they require an a priori choice of the structure and of the order of the model of the signal-generation mechanism. Some tests are required a posteriori to verify the whiteness of the prediction error, such as the Anderson test (autocorrelation test) [Box & Jenkins, 1976] in order to test the reliability of the estimation. Postprocessing of the spectra can be performed as well as for nonparametric approaches by integrating the $P(f)$ function in predefined frequency ranges; however, the AR modeling has the advantage of allowing a spectral decomposition for a direct and automatic calculation of the power and frequency of each spectral component. In the z-transform domain, the autocorrelation function (ACF) $R(k)$ and the P(z) of the signal are related by the following expression:

$$R(k) = \frac{1}{2\pi j}\int_{|z|=1} P(z)z^{k-1}\,dz \qquad (55.31)$$

If the integral is calculated by means of the residual method, the ACF is decomposed into a sum of dumped sinusoids, each one related to a pair of complex conjugate poles, and of dumped exponential functions, related to the real poles [Zetterberg, 1969]. The Fourier transform of each one of these terms gives the expression of each spectral component that fits the component related to the relevant pole or pole pair. The argument of the pole gives the central frequency of the component, while the ith spectral component power is the residual γ_i in case of real poles and $2Re(\gamma_i)$ in case of conjugate pole pairs. γ_i is computed from the following expression:

$$\gamma_i = z^{-1}(z - z_i)P(z)|_{z=z_i} \qquad (55.32)$$

It is advisable to point out the basic characteristics of the two approaches that have been described above: the nonparametric and the parametric. The latter (parametric) has evident advantages with respect to the former, which can be summarized in the following:

- It has a more statistical consistency even on short segments of data; i.e., under certain assumptions, a spectrum estimated through autoregressive modeling is a maximum entropy spectrum (MES).
- The spectrum is more easily interpretable with an "implicit" filtering of what is considered random noise.
- An easy and more reliable calculation of the spectral parameters (postprocessing of the spectrum), through the spectral decomposition procedure, is possible. Such parameters are directly interpretable from a physiologic point of view.
- There is no need to window the data in order to decrease the spectral leakage.
- The frequency resolution does not depend on the number of data.

On the other hand, the parametric approach

- Is more complex from a methodologic and computational point of view.
- Requires an a priori definition of the kind of the model (AR, MA, ARMA, or other) to be fitted and mainly its complexity defined (i.e., the number of parameters).

Some figures of merit introduced in literature may be of help in determining their value [Akaike, 1974]. Still, this procedure may be difficult in some cases.

Example

As an example, let us consider the frequency analysis of the heart rate variability (HRV) signal. In Fig. 55.16*a*, the time sequence of the RR intervals obtained from an ECG recording is shown. The RR intervals are expressed in seconds as a function of the beat number in the so-called interval tachogram. It is worth noting that the RR series is not constant but is characterized by oscillations of up to the 10% of its mean value. These oscillations are not casual but are the effect of the action of the autonomic nervous system in controlling heart rate. In particular, the frequency analysis of such a signal (Fig. 55.16*b* shows the PSD obtained by mean of an AR model) has evidenced three principal contributions in the overall variability of the HRV signal. A very low frequency (VLF) component is due to the long-term regulation mechanisms that cannot be resolved by analyzing a few minutes of signal (3 to 5 minutes are generally studied in the traditional spectral analysis of the HRV signal). Other techniques are needed for a complete understanding of such mechanisms. The low-frequency (LF) component is centered around 0.1 Hz, in a range between 0.03 and 0.15 Hz. An increase in its power has always been observed in relation to sympathetic activations. Finally, the high-frequency (HF) component, in synchrony with the respiration rate, is due to the respiration activity mediated by the vagus nerve; thus it can be a marker of vagal activity. In particular, LF and HF power, both in absolute and in normalized units (i.e., as percentage value on the total power without the VLF contribution), and their ratio LF/HF are quantitative indices widely employed for the quantification of the sympathovagal balance in controlling heart rate [Malliani et al., 1991].

55.3 Conclusion

The basic aspects of signal acquisition and processing have been illustrated, intended as fundamental tools for the treatment of biologic signals. A few examples also were reported relative to the ECG signal, as well as EEG signals and EPs. Particular processing algorithms have been described that use digital filtering techniques, coherent averaging, and power spectrum analysis as reference examples on how traditional or innovative techniques of digital signal processing may impact the phase of informative parameter extraction from biologic signals. They may improve the knowledge of many physiologic systems as well as help clinicians in dealing with new quantitative parameters that could better discriminate between normal and pathologic cases.

Defining Terms

Aliasing: Phenomenon that takes place when, in A/D conversion, the sampling frequency f_s is lower than twice the frequency content f_b of the signal; frequency components above $f_s/2$ are folded back and are summed to the lower-frequency components, distorting the signal.

Averaging: Filtering technique based on the summation of N stationary waveforms buried in casual broadband noise. The SNR is improved by a factor of $\sqrt{N}$.

Frequency response: A complex quantity that, multiplied by a sinusoid input of a linear filter, gives the output sinusoid. It completely characterizes the filter and is the Fourier transform of the impulse response.

Impulse response: Output of a digital filter when the input is the impulse sequence $\delta(n)$. It completely characterizes linear filters and is used for evaluating the output corresponding to different kinds of inputs.

Notch filter: A stopband filter whose stopped band is very sharp and narrow.

Parametric methods: Spectral estimation methods based on the identification of a signal generating model. The power spectral density is a function of the model *parameters*.

Quantization error: Error added to the signal, during the A/D procedure, due to the fact that the analog signal is represented by a digital signal that can assume only a limited and predefined set of values.

Region of convergence: In the *z*-transform plane, the ensemble containing the *z*-complex points that makes a series converge to a finite value.

References

Akaike H. 1974. A new look at the statistical model identification. IEEE Trans Autom Contr (AC-19):716.

Antoniou A. 1979. Digital Filters: Analysis and Design. New York, McGraw-Hill.

Aunon JL, McGillim CD, Childers DG. 1981. Signal processing in evoked potential research: Averaging and modeling. CRC Crit Rev Bioing 5:323.

Bartlett MS. 1948. Smoothing priodograms from time series with continuous spectra. Nature 61:686.

Box GEP, Jenkins GM. 1976. Time Series Analysis: Forecasting and Control. San Francisco, Holden-Day.

Cappellini V, Constantinides AG, Emiliani P. 1978. Digital Filters and Their Applications. London, Academic Press.

Carassa F. 1983. Comunicazioni Elettriche. Torino, Boringhieri.

Cerutti S. 1983. Filtri numerici per l'eleborazione di segnali biologici. Milano, CLUP.

Challis RE, Kitney RI. 1982. The design of digital filters for biomedical signal processing: 1. Basic concepts. J Biomed Eng 5:267.

Cobbold RSC. 1988. Transducers for Biomedical Measurements. New York, Wiley.

Cohen A. 1983. Biomedical Signal Processing: Time and Frequency Domains Analysis. Boca Raton, Fla, CRC Press.

Dariell PJ. 1946. On the theoretical specification and sampling properties of autocorrelated time-series (discussion). JR Stat Soc 8:88.

Gardenhire LW. 1964. Selecting sample rate. ISA J 4:59.

Gevins AS, Remond A (eds). 1987. Handbook of Electrophysiology and Clinical Neurophysiology. Amsterdam, Elsevier.

Glaser EM, Ruchkin DS. 1976. Principles of Neurophysiological Signal Processing. New York, Academic Press.

Harris FJ, 1978. On the use of windows for harmonic analysis with the discrete Fourier transform. Proc IEEE 64(1):51.

Huta K, Webster JG. 1973. 60-Hz interference in electrocardiography. IEEE Trans Biomed Eng 20(2):91.

Jackson LB. 1986. Digital Signal Processing. Hingham, Mass, Kluer Academic.

Jaeger RC. 1982. Tutorial: Analog data acquisition technology: II. Analog to digital conversion. IEEE Micro 8:46.

Malliani A, Pagani M, Lombardi F, Cerutti S. 1991. Cardiovascular neural regulation explored in the frequency domain. Circulation 84:482.

Marple SL. 1987. Digital Spectral Analysis with Applications. Englewood Cliff, NJ, Prentice-Hall.

Oppenheim AV, Schafer RW. 1975. Digital Signal Processing. Englewood Cliffs, NJ, Prentice-Hall.

Rainer LR, Cooley JW, Helms HD, et al. 1972. Terminology in digital signal processing. IEEE Trans Audio Electroac AU-20:322.

Shannon CE. 1949. Communication in presence of noise. Proc IRE 37:10.

Simson MB. 1981. Use of signals in the terminal QRS complex to identify patients with ventricular tachycardia after myocardial infarction. Circulation 64:235.

Thakor NV. 1987. Adaptive filtering of evoked potential. IEEE Trans Biomed Eng 34:1706.

Tompkins WJ (ed). 1993. Biomedical Digital Signal Processing. Englewood Cliffs, NJ, Prentice-Hall.

Tompkins WJ, Webster JG (eds). 1981. Design of Microcomputer-Based Medical Instrumentation. Englewood Cliffs, NJ, Prentice-Hall.

Webster JG (ed). 1992. Medical Instrumentation, 2d ed. Boston, Houghton-Mufflin.

Welch DP. 1970. The use of fast Fourier transform for the estimation of power spectra: A method based on time averaging over short modified periodograms. IEEE Trans Acoust AU-15:70.

Widrow B. 1956. A study of rough amplitude quantization by means of Nyquist sampling theory. IRE Trans Cric Theory 3:266.

Widrow B, Glover JRJ, Kaunitz J, et al. 1975. Adaptive noise cancelling: Principles and applications. Proc IEEE 63(12):1692.

Zetterberg LH. 1969. Estimation of parameters for a linear difference equation with application to EEG analysis. Math Biosci 5:227.

Further Information

A book that provides a general overview of basic concepts in biomedical signal processing is *Digital Biosignal Processing,* by Rolf Weitkunat (ed) (Elsevier Science Publishers, Amsterdam, 1991). Contributions by different authors provide descriptions of several processing techniques and many applicative examples on biologic signal analysis. A deeper and more specific insight of actual knowledge and future perspectives on ECG analysis can be found in *Electrocardiography: Past and Future,* by Philippe Coumel and Oscar B. Garfein (eds) (Annals of the New York Academy Press, vol 601, 1990). Advances in signal processing are monthly published in the journal *IEEE Transactions on Signal Processing,* while the *IEEE Transaction on Biomedical Engineering* provides examples of applications in biomedical engineering fields.

THE Biomedical Engineering HANDBOOK

Editor-in-Chief
JOSEPH D. BRONZINO
Trinity College
Hartford, Connecticut

CRC PRESS   IEEE PRESS

A CRC Handbook Published in Cooperation with IEEE Press

Library of Congress Cataloging-in-Publication Data

The biomedical engineering handbook / editor-in-chief, Joseph D. Bronzino.
p. cm. — (The electrical engineering handbook series)
Includes bibliographical references and index.
ISBN 0-8493-8346-3
1. Biomedical engineering—Handbooks, manuals, etc. I. Bronzino, Joseph D., 1937– . II. Series.
[DNLM: 1. Biomedical Engineering—handbooks. QT 29 B615 1995]
R856.15.B86 1995
610'.28—dc20
DNLM/DLC
For Library of Congress 95-6294
CIP

This book contains information obtained from authentic and highly regarded sources. Reprinted material is quoted with permission, and sources are indicated. A wide variety of references are listed. Reasonable efforts have been made to publish reliable data and information, but the author and the publisher cannot assume responsibility for the validity of all materials or for the consequences of their use.

Direct all inquiries to CRC Press, Inc., 2000 Corporate Blvd. N.W., Boca Raton, Florida 33431.

International Standard Book Number 0-8493-8346-3
Library of Congress Card Number 95-6294
Printed in the United States of America 1 2 3 4 5 6 7 8 9 0
Printed on acid-free paper

88

Noninvasive Optical Monitoring

Ross Flewelling
Nellcor Incorporated

Optical measures of physiologic status are attractive because they can provide a simple, noninvasive, yet real-time assessment of medical condition. Noninvasive optical monitoring is here taken to mean the use of visible or near-infrared light to directly assess the internal physiologic status of a person without the need of extracting a blood or tissue sample or using a catheter. Liquid water strongly absorbs ultraviolet and infrared radiation, and thus these spectral regions are useful only for analyzing thin surface layers or respiratory gases, neither of which will be the subject of this review. Instead, it is the visible and near-infrared portions of the electromagnetic spectrum that provide a unique "optical window" into the human body, opening new vistas for noninvasive monitoring technologies.

Various molecules in the human body possess distinctive spectral absorption characteristics in the visible or near-infrared spectral regions and therefore make optical monitoring possible. The most strongly absorbing molecules at physiologic concentrations are the hemoglobins, myoglobins, cytochromes, melanins, carotenes, and bilirubin (see Fig. 88.1 for some examples). Perhaps less appreciated are the less distinctive and weakly absorbing yet ubiquitous materials possessing spectral characteristics in the near-infrared: water, fat, proteins, and sugars. Simple optical methods are now available to quantitatively and noninvasively measure some of these compounds directly in intact tissue. The most successful methods to date have used hemoglobins to assess the oxygen content of blood, cytochromes to assess the respiratory status of cells, and possibly near-infrared to assess endogenous concentrations of metabolytes, including glucose.

88.1 Oximetry and Pulse Oximetry

Failure to provide adequate oxygen to tissues—*hypoxia*—can in a matter of minutes result in reduced work capacity of muscles, depressed mental activity, and ultimately cell death. It is therefore of considerable interest to reliably and accurately determine the amount of oxygen in blood or tissues. *Oximetry* is the determination of the oxygen content of blood or tissues, normally by optical means. In the clinical laboratory the oxygen content of whole blood can be determined by a bench-top cooximeter or blood gas analyzer. But the need for timely clinical information and the desire to

0-8493-8346-3/95/$0.00+$.50

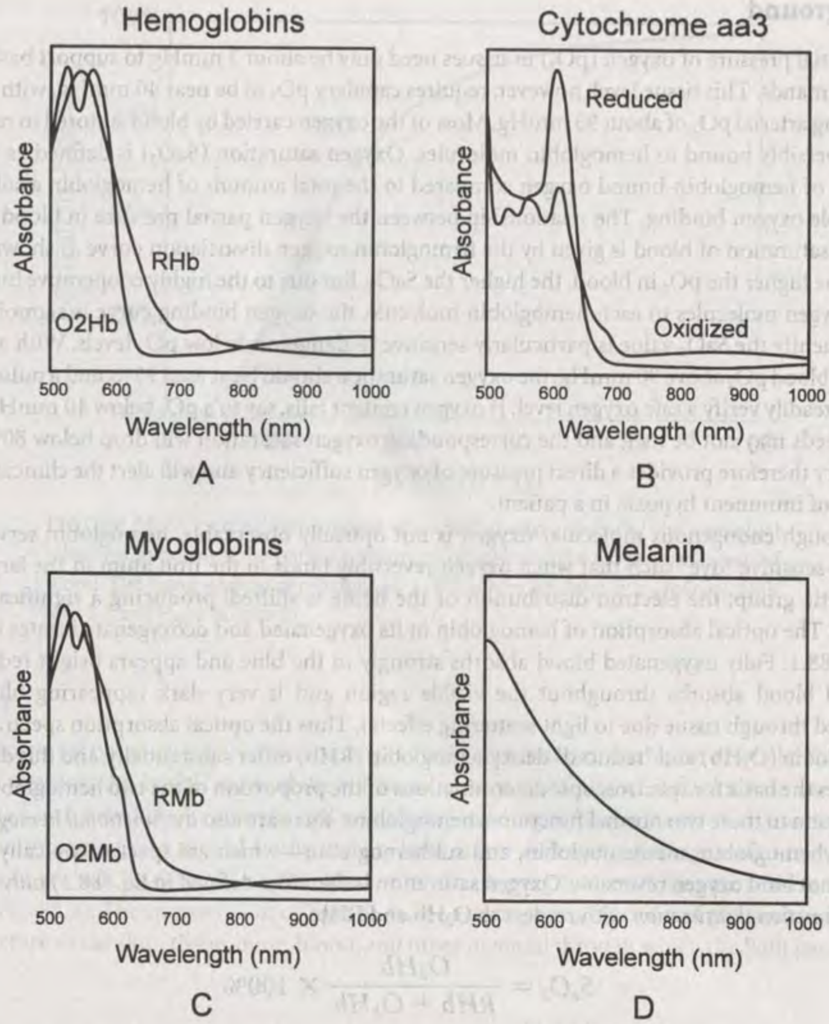

FIGURE 88.1 Absorption spectra of some endogenous biologic materials (*a*) hemoglobins, (*b*) cytochrome *aa3*, (*c*) myoglobins, and (*d*) melanin.

minimize the inconvenience and cost of extracting a blood sample and later analyze it in the lab has led to the search for alternative noninvasive optical methods. Since the 1930s, attempts have been made to use multiple wavelengths of light to arrive at a complete spectral characterization of a tissue. These approaches, although somewhat successful, have remained of limited utility owing to the awkward instrumentation and unreliable results.

It was not until the invention of *pulse oximetry* in the 1970s and its commercial development and application in the 1980s that noninvasive oximetry became practical. Pulse oximetry is an extremely easy-to-use, noninvasive, and accurate measurement of real-time arterial oxygen saturation. Pulse oximetry is now used routinely in clinical practice, has become a standard of care in all U.S. operating rooms, and is increasingly used wherever critical patients are found. The explosive growth of this new technology and its considerable utility led John Severinghaus and Poul Astrup [1986] in an excellent historical review to conclude that pulse oximetry was "arguably the most significant technological advance ever made in monitoring the well-being and safety of patients during anesthesia, recovery and critical care."

Background

The partial pressure of oxygen (pO_2) in tissues need only be about 3 mmHg to support basic metabolic demands. This tissue level, however, requires capillary pO_2 to be near 40 mmHg, with a corresponding arterial pO_2 of about 95 mmHg. Most of the oxygen carried by blood is stored in red blood cells reversibly bound to hemoglobin molecules. Oxygen saturation (SaO_2) is defined as the percentage of hemoglobin-bound oxygen compared to the total amount of hemoglobin available for reversible oxygen binding. The relationship between the oxygen partial pressure in blood and the oxygen saturation of blood is given by the hemoglobin oxygen dissociation curve as shown in Fig. 88.2. The higher the pO_2 in blood, the higher the SaO_2. But due to the highly cooperative binding of four oxygen molecules to each hemoglobin molecule, the oxygen binding curve is sigmoidal, and consequently the SaO_2 value is particularly sensitive to dangerously low pO_2 levels. With a normal arterial blood pO_2 above 90 mmHg, the oxygen saturation should be at least 95%, and a pulse oximeter can readily verify a safe oxygen level. If oxygen content falls, say to a pO_2 below 40 mmHg, metabolic needs may not be met, and the corresponding oxygen saturation will drop below 80%. Pulse oximetry therefore provides a direct measure of oxygen sufficiency and will alert the clinician to any danger of imminent hypoxia in a patient.

Although endogenous molecular oxygen is not optically observable, hemoglobin serves as an oxygen-sensitive "dye" such that when oxygen reversibly binds to the iron atom in the large heme prosthetic group, the electron distribution of the heme is shifted, producing a significant color change. The optical absorption of hemoglobin in its oxygenated and deoxygenated states is shown in Fig. 88.1. Fully oxygenated blood absorbs strongly in the blue and appears bright red; deoxygenated blood absorbs throughout the visible region and is very dark (appearing blue when observed through tissue due to light scattering effects). Thus the optical absorption spectra of oxyhemoglobin (O_2Hb) and "reduced" deoxyhemoglobin (RHb) differ substantially, and this difference provides the basis for spectroscopic determinations of the proportion of the two hemoglobin states. In addition to these two normal functional hemoglobins, there are also *dysfunctional hemoglobins*—carboxyhemoglobin, methemoglobin, and sulfhemoglobin—which are spectroscopically distinct but do not bind oxygen reversibly. Oxygen saturation is therefore defined in Eq. (88.1) only in terms of the *functional saturation* with respect to O_2Hb and RHb:

$$S_aO_2 = \frac{O_2Hb}{RHb + O_2Hb} \times 100\% \tag{88.1}$$

Cooximeters are bench-top analyzers that accept whole blood samples and utilize four or more wavelengths of monochromatic light, typically between 500 and 650 nm, to spectroscopically determine the various individual hemoglobins in the sample. If a blood sample can be provided, this spectroscopic method is accurate and reliable. Attempts to make an equivalent quantitative analysis noninvasively through intact tissue have been fraught with difficulty. The problem has been to contend with the wide variation in scattering and nonspecific absorption properties of very complex heterogeneous tissue. One of the more successful approaches, marketed by Hewlett-Packard, used eight optical wavelengths transmitted through the pinna of the ear. In this approach a "bloodless" measurement is first obtained by squeezing as much blood as possible from an area of tissue; the arterial blood is then allowed to flow back, and the oxygen saturation is determined by analyzing the change in the spectral absorbance characteristics of the tissue. While this method works fairly well, it is cumbersome, operator dependent, and does not always work well on poorly perfused or highly pigmented subjects.

In the early 1970s, Takuo Aoyagi recognized that most of the interfering nonspecific tissue effects could be eliminated by utilizing only the change in the signal during an arterial pulse. Although an early prototype was built in Japan, it was not until the refinements in implementation and application by Biox (now Ohmeda) and Nellcor Incorporated in the 1980s that the technology became widely adopted as a safety monitor for critical care use.

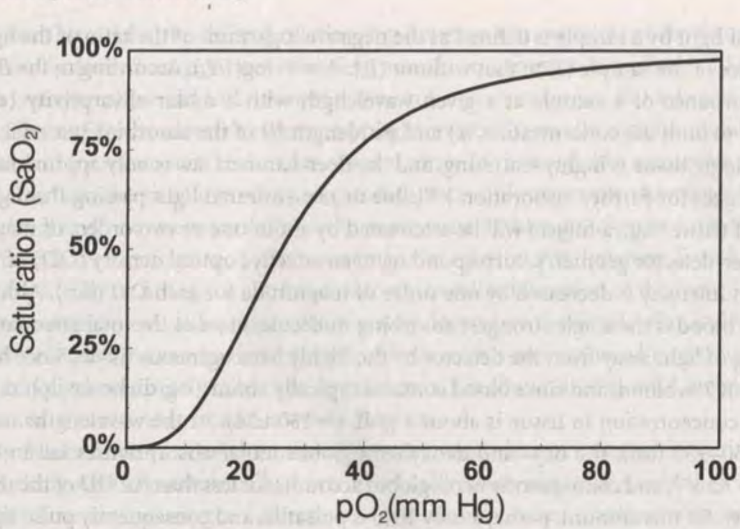

FIGURE 88.2 Hemoglobin oxygen dissociation curve showing the sigmoidal relationship between the partial pressure of oxygen and the oxygen saturation of blood. The curve is given approximately by $\%SaO_2 = 100\%/[1 + P_{50}/pO_2)^n]$, with $n = 2.8$ and $P_{50} = 26$ mm Hg.

Theory

Pulse oximetry is based on the fractional change in light transmission during an arterial pulse at two different wavelengths. In this method the fractional change in the signal is due only to the arterial blood itself, and therefore the complicated nonpulsatile and highly variable optical characteristics of tissue are eliminated. In a typical configuration, light at two different wavelengths illuminating one side of a finger will be detected on the other side, after having traversed the intervening vascular tissues (Fig. 88.3). The transmission of light at each wavelength is a function of the thickness, color, and structure of the skin, tissue, bone, blood, and other material through which the light passes. The

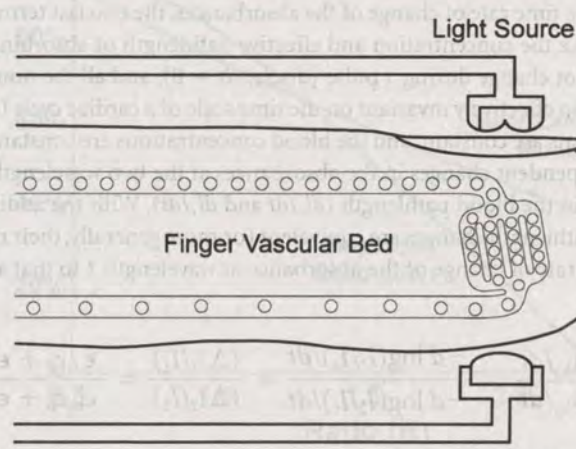

FIGURE 88.3 Typical pulse oximeter sensing configuration on a finger. Light at two different wavelengths is emitted by the source, diffusely scattered through the finger, and detected on the opposite side by a photodetector.

absorbance of light by a sample is defined as the negative logarithm of the ratio of the light intensity in the presence of the sample (I) to that without (I_o): $A = -\log(I/I_o)$. According to the *Beer-Lambert law*, the absorbance of a sample at a given wavelength with a molar absorptivity (ϵ) is directly proportional to both the concentration (c) and pathlength (l) of the absorbing material: $A = \epsilon cl$. (In actuality, biologic tissue is highly scattering, and the Beer-Lambert law is only approximately correct; see the references for further elaboration.) Visible or near-infrared light passing through about one centimeter of tissue (e.g., a finger) will be attenuated by about one or two orders of magnitude for a typical emitter-detector geometry, corresponding to an effective optical density (OD) of 1–2 OD (the detected light intensity is decreased by one order of magnitude for each OD unit). Although hemoglobin in the blood is the single strongest absorbing molecule, most of the total attenuation is due to the scattering of light away from the detector by the highly heterogeneous tissue. Since human tissue contains about 7% blood, and since blood contains typically about 14 g/dL hemoglobin, the effective hemoglobin concentration in tissue is about 1 g/dL (~150 uM). At the wavelengths used for pulse oximetry (650–950 nm), the oxy- and deoxyhemoglobin molar absorptivities fall in the range of 100–1000 $M^{-1}cm^{-1}$, and consequently hemoglobin accounts for less than 0.2 OD of the total observed optical density. Of this amount, perhaps only 10% is pulsatile, and consequently pulse signals of only about a few percent are ultimately measured, at times even one-tenth of this.

A mathematical model for pulse oximetry begins by considering light at two wavelengths, λ_1 and λ_2, passing through tissue and being detected at a distant location as in Fig. 88.3. At each wavelength the total light attenuation is described by four different component absorbances: oxyhemoglobin in the blood (concentration c_o, molar absorptivity ϵ_o, and effective pathlength l_o), "reduced" deoxyhemoglobin in the blood (concentration c_r, molar absorptivity ϵ_r, and effective pathlength l_r), specific variable absorbances that are not from the arterial blood (concentration c_x, molar absorptivity ϵ_x, and effective pathlength l_x), and all other non-specific sources of optical attenuation, combined as A_y, which can include light scattering, geometric factors, and characteristics of the emitter and detector elements. The total absorbance at the two wavelengths can then be written:

$$\begin{cases} A_{\lambda_1} = \epsilon_{o_1} c_o l_o + \epsilon_{r_1} c_r l_r + \epsilon_{x_1} c_x l_x + A_{y_1} \\ A_{\lambda_2} = \epsilon_{o_2} c_o l_o + \epsilon_{r_2} c_r l_r + \epsilon_{x_2} c_x l_x + A_{y_2} \end{cases} \quad (88.2)$$

The blood volume change due to the arterial pulse results in a modulation of the measured absorbances. By taking the time rate of change of the absorbances, the two last terms in each equation are effectively zero, since the concentration and effective pathlength of absorbing material outside the arterial blood do not change during a pulse [$d(c_x l_x)/dt = 0$], and all the nonspecific effects on light attenuation are also effectively invariant on the time scale of a cardiac cycle ($dA_y/dt = 0$). Since the extinction coefficients are constant, and the blood concentrations are constant on the time scale of a pulse, the time-dependent changes in the absorbances at the two wavelengths can be assigned entirely to the change in the blood pathlength (dl_o/dt and dl_r/dt). With the additional assumption that these two blood pathlength changes are equivalent (or more generally, their ratio is a constant), the ratio R of the time rate of change of the absorbance at wavelength *1* to that at wavelength *2* reduces to the following:

$$R = \frac{dA_{\lambda_1}/dt}{dA_{\lambda_2}/dt} = \frac{-d\log(I_1/I_o)/dt}{-d\log(I_2/I_o)/dt} = \frac{(\Delta I_1/I_1)}{(\Delta I_2/I_2)} = \frac{\epsilon_{o_1} c_o + \epsilon_{r_1} c_r}{\epsilon_{o_2} c_o + \epsilon_{r_2} c_r} \quad (88.3)$$

Observing that functional oxygen saturation is given by $S = c_o/(c_o + c_r)$, and that $(1-S) = c_r/(c_o + c_r)$, the oxygen saturation can then be written in terms of the ratio R as follows:

$$S = \frac{\epsilon_{r1} - \epsilon_{r2} R}{(\epsilon_{r1} - \epsilon_{o1}) - (\epsilon_{r2} - \epsilon_{o2}) R} \quad (88.4)$$

Equation (88.4) provides the desired relationship between the experimentally determined ratio R and the clinically desired oxygen saturation S. In actual use, commonly available LEDs are used as the light sources, typically a red LED near 660 nm and a near-infrared LED selected in the range 890–950 nm. Such LEDs are not monochromatic light sources, typically with bandwidths between 20 and 50 nm, and therefore standard molar absorptivities for hemoglobin cannot be used directly in Eq. (88.4). Further, the simple model presented above is only approximately true; for example, the two wavelengths do not necessarily have the exact same pathlength changes, and second-order scattering effects have been ignored. Consequently the relationship between S and R is instead determined empirically by fitting the clinical data to a generalized function of the form $S = (a - bR)/(c - dR)$. The final empirical calibration will ultimately depend on the details of an individual sensor design, but these variations can be determined for each sensor and included in unique calibration parameters. A typical empirical calibration for R versus S is shown in Fig. 88.4, together with the curve that standard molar absorptivities would predict.

In this way the measurement of the ratio of the fractional change in signal intensity of the two LEDs is used along with the empirically determined calibration equation to obtain a beat-by-beat measurement of the arterial oxygen saturation in a perfused tissue—continuously, noninvasively, and to an accuracy of a few percent.

Applications and Future Directions

Pulse oximetry is now routinely used in nearly all operating rooms and critical care areas in the United States and increasingly throughout the world. It has become so pervasive and useful that it is now being called the "fifth" vital sign (for an excellent review of practical aspects and clinical applications of the technology see Kelleher [1989]).

The principal advantages of pulse oximetry are that it provides continuous, accurate, and reliable monitoring of arterial oxygen saturation on nearly all patients, utilizing a variety of convenient sensors, reusable as well as disposable. Single-patient-use adhesive sensors can easily be applied to fingers for adults and children and to arms or legs for neonates. Surface reflectance sensors have also

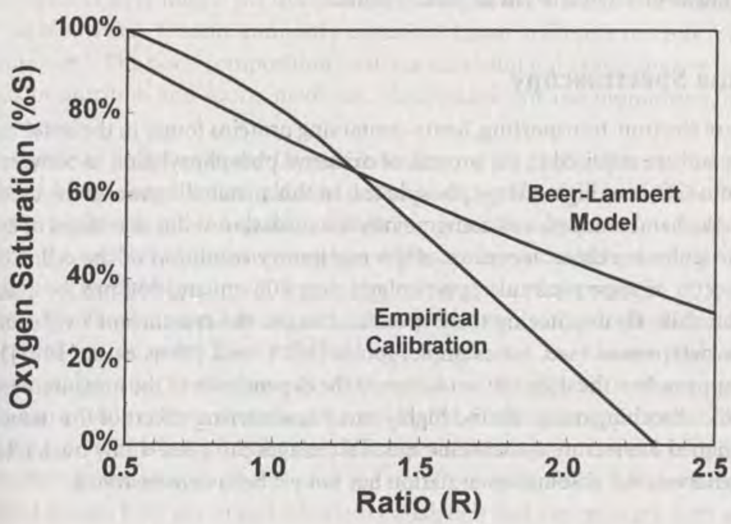

FIGURE 88.4 Relationship between the measured ratio of fractional changes in light intensity at two wavelengths, R, and the oxygen saturation S. Beer-Lambert model is from Eq. (88.4) with $\epsilon_{o_1} = 100$, $\epsilon_{o_2} = 300$, $\epsilon_{r_1} = 800$, and $\epsilon_{r_2} = 200$. Empirical calibration is based on $\%S = 100\% \times (a - bR)/(c - dR)$ with $a = 1000$, $b = 550$, $c = 900$, and $d = 350$, with a linear extrapolation below 70%.

been developed based on the same principles and offer a wider choice for sensor location, though they tend to be less accurate and prone to more types of interference.

Limitations of pulse oximetry include sensitivity to high levels of optical or electric interference, errors due to high concentrations of dysfunctional hemoglobins (methemoglobin or carboxyhemoglobin) or interference from physiologic dyes (such as methylene blue). Other important factors, such as total hemoglobin content, fetal hemoglobin, or sickle cell trait, have little or no effect on the measurement except under extreme conditions. Performance can also be compromised by poor signal quality, as may occur for poorly perfused tissues with weak pulse amplitudes or by motion artifact.

Hardware and software advances continue to provide more sensitive signal detection and filtering capabilities, allowing pulse oximeters to work better on more ambulatory patients. Already some pulse oximeters incorporate ECG synchronization for improved signal processing. A pulse oximeter for use in labor and delivery is currently under active development by several research groups and companies. A likely implementation may include use of a reflectance surface sensor for the fetal head to monitor the adequacy of fetal oxygenation. This application is still in active development, and clinical utility remains to be demonstrated.

88.2 Nonpulsatile Spectroscopy

Background

Nonpulsatile optical spectroscopy has been used for more than half a century for noninvasive medical assessment, such as in the use of multiwavelength tissue analysis for oximetry and skin reflectance measurement for bilirubin assessment in jaundiced neonates. These early applications have found some limited use, but with modest impact. Recent investigations into new nonpulsatile spectroscopy methods for assessment of deep-tissue oxygenation (e.g., cerebral oxygen monitoring), for evaluation of respiratory status at the cellular level, and for the detection of other critical analytes, such as glucose, may yet prove more fruitful. The former applications have led to spectroscopic studies of cytochromes in tissues, and the latter has led to considerable work into new approaches in near-infrared analysis of intact tissues.

Cytochrome Spectroscopy

Cytochromes are electron-transporting, heme-containing proteins found in the inner membranes of mitochondria and are required in the process of oxidative phosphorylation to convert metabolytes and oxygen into CO_2 and high-energy phosphates. In this metabolic process the cytochromes are reversibly oxidized and reduced, and consequently the oxidation-reduction states of cytochromes c and aa_3 in particular are direct measures of the respiratory condition of the cell. Changes in the absorption spectra of these molecules, particularly near 600 nm and 830 nm for cytochrome aa_3, accompany this shift. By monitoring these spectral changes, the cytochrome oxidation state in the tissues can be determined (see, for example, Jöbsis [1977] and Jöbsis et al. [1977]). As with all nonpulsatile approaches, the difficulty is to remove the dependence of the measurement on the various nonspecific absorbing materials and highly variable scattering effects of the tissue. To date, instruments designed to measure cytochrome spectral changes can successfully track relative changes in brain oxygenation, but absolute quantitation has not yet been demonstrated.

Near-Infrared Spectroscopy and Glucose Monitoring

Near-infrared (NIR), the spectral region between 780 nm and 3000 nm, is characterized by broad and overlapping spectral peaks produced by the overtones and combinations of infrared vibrational modes. Figure 88.5 shows typical NIR absorption spectra of fat, water, and starch. Exploitation of

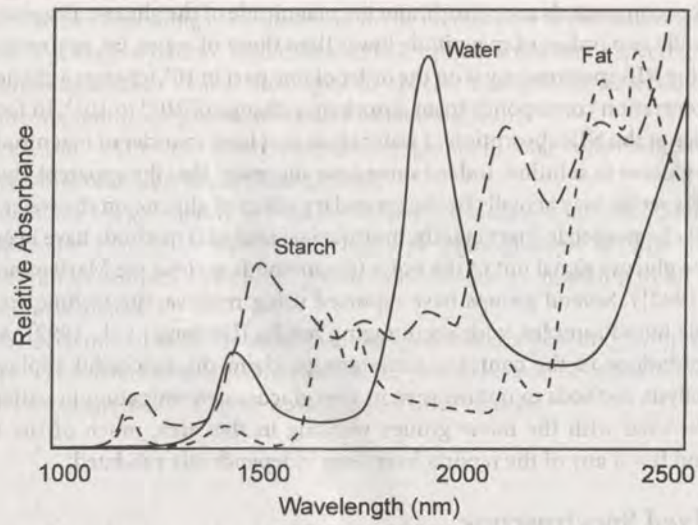

FIGURE 88.5 Typical near-infrared absorption spectra of several biologic materials.

this spectral region for *in vivo* analysis has been hindered by the same complexities of nonpulsatile tissue spectroscopy described above and is further confounded by the very broad and indistinct spectral features characteristic of the NIR. Despite these difficulties, NIR spectroscopy has garnered considerable attention, since it may enable the analysis of common analytes.

Karl Norris and coworkers pioneered the practical application of NIR spectroscopy, using it to evaluate water, fat, and sugar content of agricultural products (see Osborne et al. [1993] and Burns and Cuirczak [1992]). The further development of sophisticated *multivariate analysis* techniques, together with new scattering models (e.g., Kubelka-Munk theory) and high-performance instrumentation, further extended the application of NIR methods. Over the past decade, many research groups and companies have touted the use of NIR techniques for medical monitoring, such as for determining the relative fat, protein, and water content of tissue, and more recently for noninvasive glucose measurement. The body composition analyses are useful but crude and are mainly limited to applications in nutrition and sports medicine. Noninvasive glucose monitoring, however, is of considerable interest.

More than 2 million diabetics in the United States lance their fingers three to six times a day to obtain a drop of blood for chemical glucose determination. The ability of these individuals to control their glucose levels, and the quality of their life generally, would dramatically improve if a simple, noninvasive method for determining blood glucose levels could be developed. Among the noninvasive optical methods proposed for this purpose are optical rotation, NIR analysis, and raman spectroscopy. The first two have received the most attention. Optical rotation methods aim to exploit the small optical rotation of polarized light by glucose. To measure physiologic glucose levels in a 1-cm thick sample to an accuracy of 25 mg/dL would require instrumentation that can reliably detect an optical rotation of at least 1 millidegree. Finding an appropriate in vivo optical path for such measurements has proved most difficult, with most approaches looking to use either the aqueous humor or the anterior chamber of the eye [Coté et al., 1992; Rabinovitch et al., 1982]. Although several groups have developed laboratory analyzers that can measure such a small effect, so far in vivo measurement has not been demonstrated, due both to unwanted scattering and optical activity of biomaterials in the optical path and to the inherent difficulty in developing a practical instrument with the required sensitivity.

NIR methods for noninvasive glucose determination are particularly attractive, although the task is formidable. Glucose has spectral characteristics near 1500 nm and in the 2000–2500 nm band where many other compounds also absorb, and the magnitude of the glucose absorbance in biologic samples is typically two orders of magnitude lower than those of water, fat, or protein. The normal detection limit for NIR spectroscopy is on the order of one part in 10^3, whereas a change of 25 mg/dL in glucose concentration corresponds to an absorbance change of 10^{-4} to 10^{-5}. In fact, the temperature dependence of the NIR absorption of water alone is at least an order of magnitude greater than the signal from glucose in solution. Indeed some have suggested that the apparent glucose signature in complex NIR spectra may actually be the secondary effect of glucose on the water.

Sophisticated chemometric (particularly, multivariate analysis) methods have been employed to try to extract the glucose signal out of the noise (for methods reviews see Martens and Næs [1989] and Haaland [1992]). Several groups have reported using multivariate techniques to quantitate glucose in whole blood samples, with encouraging results [Haaland et al., 1992]. And despite all theoretical disputations to the contrary, some groups claim the successful application of these multivariate analysis methods to noninvasive in vivo glucose determination in patients [Robinson et al., 1992]. Yet even with the many groups working in this area, much of the work remains unpublished, and few if any of the reports have been independently validated.

Time-Resolved Spectroscopy

The fundamental problem in making quantitative optical measurements through intact tissue is dealing with the complex scattering phenomena. This scattering makes it difficult to determine the effective pathlength for the light, and therefore attempts to use the Beer-Lambert law, or even to determine a consistent empirical calibration, continue to be thwarted. Application of new techniques in time-resolved spectroscopy may be able to tackle this problem. Thinking of light as a packet of photons, if a single packet from a light source is sent through tissue, then a distant receiver will detected a photon distribution over time—the photons least scattered arriving first and the photons most scattered arriving later. In principle, the first photons arriving at the detector passed directly through the tissue. For these first photons the distance between the emitter and the detector is fixed and known, and the Beer-Lambert law should apply, permitting determination of an *absolute* concentration for an absorbing component. The difficulty in this is, first, that the measurement time scale must be on the order of the photon transit time (subnanosecond), and second, that the number of photons getting through without scattering will be extremely small, and therefore the detector must be exquisitely sensitive. Although these considerable technical problems have been overcome in the laboratory, their implementation in a practical instrument applied to a real subject remains to be demonstrated. This same approach is also being investigated for noninvasive optical imaging, since the unscattered photons should produce sharp images (see Chance et al., [1988], Chance [1991], and Yoo and Alfano [1989]).

88.3 Conclusions

The remarkable success of pulse oximetry has established noninvasive optical monitoring of vital physiologic functions as a modality of considerable value. Hardware and algorithm advances in pulse oximetry are beginning to broaden its use outside the traditional operating room and critical care areas. Other promising applications of noninvasive optical monitoring are emerging, such as for measuring deep tissue oxygen levels, determining cellular metabolic status, or for quantitative determination of other important physiologic parameters such as blood glucose. Although these latter applications are not yet practical, they may ultimately impact noninvasive clinical monitoring just as dramatically as pulse oximetry.

Defining Terms

Beer-Lambert law: Principle stating that the optical absorbance of a substance is proportional to both the concentration of the substance and the pathlength of the sample.

Cytochromes: Heme-containing proteins found in the membranes of mitochondria and required for oxidative phosphorylation, with characteristic optical absorbance spectra.

Dysfunctional hemoglobins: Those hemoglobin species that cannot reversibly bind oxygen (carboxyhemoglobin, methemoglobin, and sulfhemoglobin).

Functional saturation: The ratio of oxygenated hemoglobin to total nondysfunctional hemoglobins (oxyhemoglobin plus deoxyhemoglobin).

Hypoxia: Inadequate oxygen supply to tissues necessary to maintain metabolic activity.

Multivariate analysis: Empirical models developed to relate multiple spectral intensities from many calibration samples to known analyte concentrations, resulting in an optimal set of calibration parameters.

Oximetry: The determination of blood or tissue oxygen content, generally by optical means.

Pulse oximetry: The determination of functional oxygen saturation of pulsatile arterial blood by ratiometric measurement of tissue optical absorbance changes.

References

Burns DA, Ciurczak EW (eds). 1992. Handbook of Near-Infrared Analysis. New York, Marcel Dekker.

Chance B. 1991. Optical method. Annu Rev Biophys Biophys Chem 20:1.

Chance B, Leigh JS, Miyake H, et al. 1988. Comparison of time-resolved and -unresolved measurements of deoxyhemoglobin in brain. Proc Natl Acad Sci USA 85(14):4971.

Coté GL, Fox MD, Northrop RB. 1992. Noninvasive optical polarimetric glucose sensing using a true phase measurement technique. IEEE Trans Biomed Eng 39(7):752.

Haaland DM. 1992. Multivariate calibration methods applied to the quantitative analysis of infrared spectra. In PC Jurs (ed), Computer-Enhanced Analytical Spectroscopy, vol 3, pp 1–30. New York Plenum.

Haaland DM, Robinson MR, Koepp GW, et al. 1992. Reagentless near-infrared determination of glucose in whole blood using multivariate calibration. Appl Spectros 46(10):1575.

Jöbsis FF. 1977. Noninvasive, infrared monitoring of cerebral and myocardial oxygen sufficiency and circulatory parameters. Science 198(4323):1264.

Jöbsis FF, Keizer JH, LaManna JC, et al. 1977. Reflectance spectrophotometry of cytochrome aa_3 in vivo. J Appl Physiol 43(5):858.

Kelleher JF. 1989. Pulse oximetry. J Clin Monit 5(1):37.

Martens H, Næs T. 1989. Multivariate Calibration. New York, John Wiley.

Osborne BG, Fearn T, Hindle PH. 1993. Practical NIR Spectroscopy with Applications in Food and Beverage Analysis. Essex, England, Longman Scientific & Technical.

Payne JP, Severinghaus JW (eds). 1986. Pulse Oximetry. New York, Springer-Verlag.

Rabinovitch B, March WF, Adams RL. 1982. Noninvasive glucose monitoring of the aqueous humor of the eye: Part I. Measurement of very small optical rotations. Diabetes Care 5(3):254.

Robinson MR, Eaton RP, Haaland DM, et al. 1992. Noninvasive glucose monitoring in diabetic patients: a preliminary evaluation. Clin Chem 38(9):1618.

Severinghaus JW, Astrup PB. 1986. History of blood gas analysis. VI. Oximetry. J Clin Monit 2(4):270.

Severinghaus JW, Honda Y. 1987*a*. History of blood gas analysis. VII. Pulse oximetry. J Clin Monit 3(2):135.

Severinghaus JW, Honda Y. 1987*b*. Pulse oximetry. Int Anesthesiol Clin 25(4):205.

Severinghaus JW, Kelleher JF. 1992. Recent developments in pulse oximetry. Anesthesiology 76(6):1018.

Tremper KK, Barker SJ. 1989. Pulse oximetry. Anesthesiology 70(1):98.

Wukitsch MW, Petterson MT, Tobler DR, et al. 1988. Pulse oximetry: Analysis of theory, technology, and practice. J Clin Monit 4(4):290.

Yoo KM, Alfano RR. 1989. Photon localization in a disordered multilayered system. Phys Rev B 39(9):5806.

Further Information

Two collections of papers on pulse oximetry include a book edited by J. P. Payne and J. W. Severinghaus, *Pulse Oximetry* (New York, Springer-Verlag, 1986), and a journal collection—International Anesthesiology Clinics [25(4), 1987]. For technical reviews of pulse oximetry, see J. A. Pologe's 1987 "Pulse Oximetry" [Int Anesthesiol Clin 25(3):137], Kevin K. Tremper and Steven J. Barker's 1989 "Pulse Oximetry" [Anesthesiology 70(1):98], and Michael W. Wukitsch, Michael T. Patterson, David R. Tobler, and coworkers' 1988 "Pulse Oximetry: Analysis of Theory, Technology, and Practice" [J Clin Monit 4(4):290].

For a review of practical and clinical applications of pulse oximetry, see the excellent review by Joseph F. Kelleher [1989] and John Severinghaus and Joseph F. Kelleher [1992]. John Severinghaus and Yoshiyuki Honda have written several excellent histories of pulse oximetry [1987*a*, 1987*b*].

For an overview of applied near-infrared spectroscopy, see Donald A. Burns and Emil W. Ciurczak [1992] and B. G. Osborne, T. Fearn, and P. H. Hindle [1993]. For a good overview of multivariate methods, see Harald Martens and Tormod Næs [1989].

THE

Biomedical Engineering

HANDBOOK

Editor-in-Chief
JOSEPH D. BRONZINO
Trinity College
Hartford, Connecticut

CRC PRESS IEEE PRESS
A CRC Handbook Published in Cooperation with IEEE Press

Library of Congress Cataloging-in-Publication Data

The biomedical engineering handbook / editor-in-chief, Joseph D. Bronzino.
p. cm. — (The electrical engineering handbook series)
Includes bibliographical references and index.
ISBN 0-8493-8346-3
1. Biomedical engineering—Handbooks, manuals, etc. I. Bronzino, Joseph D., 1937– . II. Series.
[DNLM: 1. Biomedical Engineering—handbooks. QT 29 B615 1995]
R856.15.B86 1995
610'.28—dc20
DNLM/DLC
For Library of Congress 95-6294
CIP

International Standard Book Number 0-8493-8346-3
Library of Congress Card Number 95-6294
Printed in the United States of America 1 2 3 4 5 6 7 8 9 0
Printed on acid-free paper

89

Medical Instruments and Devices Used in the Home

Bruce R. Bowman
EdenTec Corporation

Edward Schuck
EdenTec Corporation

89.1 Scope of the Market for Home Medical Devices

The market for medical devices used in the home and alternative sites has increased dramatically in the last 10 years and has reached an overall estimated size of more than $1.6 billion [FIND/SVP, 1992]. In the past, hospitals have been thought of as the only places to treat sick patients. But with the major emphasis on reducing healthcare costs, increasing numbers of sicker patients move from hospitals to their homes. Treating sicker patients outside the hospital places additional challenges on medical device design and patient use. Equipment designed for hospital use can usually rely on trained clinical personnel to support the devices. Outside the hospital, the patient and/or family members must be able to use the equipment, requiring these devices to have a different set of design and safety features. This chapter will identify some of the major market segments using medical devices in the home and discuss important design considerations associated with home use.

Table 89.1 outlines market segments where devices and products are used to treat patients outside the hospital [FIND/SVP, 1992]. The durable medical equipment market is the most established market providing aids for patients to improve access and mobility. These devices are usually not life supporting or sustaining, but in many cases they can make the difference in allowing a patient to be able to function outside a hospital or nursing or skilled facility. Other market segments listed employ generally more sophisticated solutions to clinical problems. These will be discussed by category of use.

The incontinence and ostomy area of products is one of the largest market segments and is growing in direct relationship to our aging society. Whereas sanitary pads and colostomy bags are not very "high-tech," well-designed aids can have a tremendous impact on the comfort and independence of these patients. Other solutions to incontinence are technically more sophisticated, such as use of electric stimulation of the sphincter muscles through an implanted device or a miniature stimulator inserted as an anal or vaginal plug to maintain continence [Wall et al., 1993].

Many forms of equipment are included in the Respiratory segment. These devices include those that maintain life support as well as those that monitor patients' respiratory function. These patients,

0-8493-8346-3/95/$0.00+$.50

TABLE 89.1 Major Market Segments Outside Hospitals

Market Segment	Estimated Equipment Size 1991	Device Examples
Durable medical equipment	$373 M*	Specialty beds, wheelchairs, toilet aids, ambulatory aids
Incontinence and ostomy products	$600 M*	Sanitary pads, electrical stimulators, colostomy bags
Respiratory equipment	$180 M*	Oxygen therapy, portable ventilators, nasal CPAP, monitors, apnea monitors
Drug infusion, drug measurement	$300 M	Infusion pumps, access ports, patient-controlled analgesia (PCA), glucose measurement, implantable pumps
Pain control and functional stimulation	$140 M	Transcutaneous electrical nerve stimulation (TENS), functional electrical nerve stimulation (FES)

**Source:* FIND/SVP [1992].

with proper medical support, can function outside the hospital at a significant reduction in cost and increased patient comfort [Pierson, 1994]. One area of this segment, infant apnea monitors, provides parents or caregivers the cardio/respiratory status of an at-risk infant so that intervention (CPR etc.) can be initiated if the baby has a life-threatening event. The infant monitor shown in Fig. 89.1 is an example of a patient monitor designed for home use and will be discussed in more detail later in this chapter. Pulse oximetry monitors are also going home with patients. They are used to measure noninvasively the oxygen level of patients receiving supplemental oxygen or ventilator-dependent patients to determine if they are being properly ventilated.

Portable infusion pumps are an integral part of providing antibiotics, pain management, chemotherapy, and parenteral and enteral nutrition. The pump shown in Fig. 89.2 is an example of technology that allows the patient to move about freely while receiving sometimes lengthy drug therapy. Implantable drug pumps are also available for special long-term therapy needs.

Pain control using electric stimulation in place of drug therapy continues to be an increasing market. The delivery of small electric impulses to block pain is continuing to gain medical accep-

FIGURE 89.1 Infant apnea monitor used in a typical home setting (photo courtesy of EdenTec Corporation).

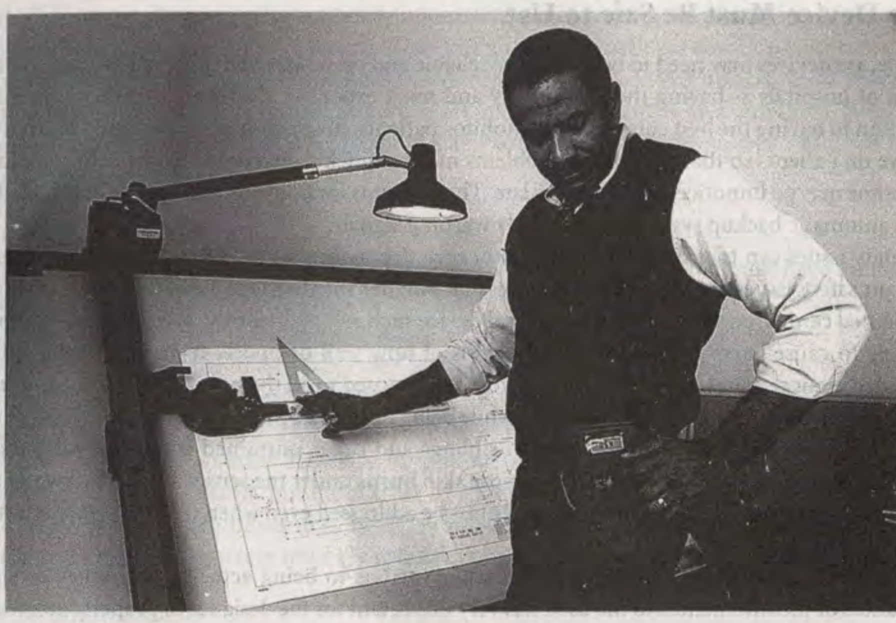

FIGURE 89.2 Portable drug pump used throughout the day (photo courtesy of Pharmacia Deltec Inc.).

tance for treatment outside the hospital setting. A different form of electric stimulation called functional electric stimulation (FES) applies short pulses of electric current to the nerves that control weak or paralyzed muscles. This topic is covered as a separate chapter in this book.

Growth of the homecare business has created problems in overall healthcare costs since a corresponding decrease in hospital utilization has not yet occurred. In the future, however, increased homecare will necessarily result in reassessment and downsizing in the corresponding hospital segment. There will be clear areas of growth and areas of consolidation in the new era of healthcare reform. It would appear, however, that homecare has a bright future of continued growth.

89.2 Unique Challenges to the Design and Implementation of High-Tech Homecare Devices

What are some of the unique requirements of devices that could allow more sophisticated equipment to go home with ordinary people of varied educational levels without compromising their care? Even though each type of clinical problem has different requirements for the equipment that must go home with the patient, certain common qualities must be inherent in most devices used in the home. Three areas to consider when equipment is used outside of the hospital are that the device (1) must provide a positive clinical outcome, (2) must be safe and easy to use, and (3) must be user-friendly enough so that it will be used.

The Device Must Provide a Positive Clinical Outcome

Devices cannot be developed any longer just because new technology becomes available. They must solve the problem for which they were intended and make a significant clinical difference in the outcome or management of the patient while saving money. These realities are being driven by those who reimburse for devices, as well as by the FDA as part of the submission for approval to market a new device.

The Device Must Be Safe to Use

Homecare devices may need to be even *more* reliable and even *safer* than hospital devices. We often think of hospitals as having the best quality and most expensive devices that money can buy. In addition to having the best equipment to monitor patients, hospitals have nurses and aids that keep an eye on patients so that equipment problems may be quickly discovered by the staff. A failure in the home may go unnoticed until it is too late. Thus systems for home use really need extra reliability with automatic backup systems and/or early warning signals.

Safety issues can take on a different significance depending on the intended use of the device. Certain safety issues are important regardless of whether the device is a critical device such as an implanted cardiac pacemaker or a noncritical device such as a bed-wetting alarm. No device should be able to cause harm to the patient regardless of how well or poorly it may be performing its intended clinical duties. Devices must be safe when exposed to all the typical environmental conditions to which the device could be exposed while being operated by the entire range of possible users of varied education and while exposed to siblings and other untrained friends or relatives. For instance, a bed-wetting alarm should not cause skin burns under the sensor if a glass of water spills on the control box. This type of safety issue must be addressed even when it significantly affects the final cost to the consumer.

Other safety issues are not obviously differentiated as to being actual safety issues or simply nuisances or inconveniences to the user. It is very important for the designer to properly define these issues; although some safety features can be included with little or no extra cost, other safety features may be very costly to implement. It may be a nuisance for the patient using a TENS pain control stimulator to have the device inadvertently turned off when its on/off switch is bumped while watching TV. In this case, the patient only experiences a momentary cessation of pain control until the unit is turned back on. But it could mean injuries or death to the same patient driving an automobile who becomes startled when his TENS unit inadvertently turns on and he causes an accident.

Reliability issues can also be mere inconveniences or major safety issues. Medical devices should be free of design and materials defects so that they can perform their intended functions reliably. Once again, reliability does not necessarily need to be expensive and often can be obtained with good design. Critical devices, i.e., devices that could cause death or serious injury if they stopped operating properly, may need to have redundant systems for backup, which likely will increase cost.

The Device Must Be Designed So That It *Will* Be Used

A great deal of money is being spent in healthcare on device for patients that end up not being used. There are numerous reasons for this happening including that the wrong device was prescribed for the patient's problem in the first place; the device works, but it has too many false alarms; the device often fails to operate properly; it is cumbersome to use or difficult to operate or too uncomfortable to wear.

Ease of Use

User-friendliness is one of the most important features in encouraging a device to be used. Technological sophistication may be just as necessary in areas that allow ease of use as in attaining accuracy and reliability in the device. The key is that the technologic sophistication be transparent to the user so that the device does not intimidate the user. Transparent features such as automatic calibration or automatic sensitivity adjustment may help allow successful use of a device that would otherwise be too complicated.

Notions of what makes a device easy to use, however, need to be thoroughly tested with the patient population intended for the device. Caution needs to be taken in defining what "simple" means to different people. A VCR may be simple to the designer because all features can be programmed with one button, but it may not be simple to users if they have to remember that it takes two long pushes and one short to get into the clock-setting program.

Convenience for the user is also extremely important in encouraging use of a device. Applications that require devices to be portable must certainly be light enough to be carried. Size is almost always important for anything that must fit within the average household. Either a device must be able to be left in place in the home or it must be easy to set up, clean, and put away. Equipment design can make the difference between the patient appropriately using the equipment or deciding that it is just too much hassle to bother.

Reliability

Users must also have confidence in the reliability of the device being used and must have confidence that if it is not working properly, the device will tell them that something is wrong. Frequent breakdowns or false alarms will result in frustration and ultimately in reduced compliance. Eventually patients will stop using the device altogether. Most often, reliability can be designed into a product with little or no extra cost in manufacturing, and everything that can be done at no cost to enhance reliability should be done. It is very important, however, to understand what level of additional reliability involving extra cost is necessary for product acceptance. Reliability can always be added by duplicated backup systems, but the market or application may not warrant such an approach. Critical devices which are implanted, such as cardiac pacemakers, have much greater reliability requirements, since they involve not only patient frustration but also safety.

Cost Reimbursement

Devices must be paid for before the patient can realize the opportunity to use new, effective equipment. Devices are usually paid for by one of two means. First, they are covered on an American Medical Association Current Procedural Terminology Code (CPT-code) which covers the medical, surgical, and diagnostic services provided by physicians. The CPT-codes are usually priced out by Medicare to establish a baseline reimbursement level. Private carriers usually establish a similar or different level of reimbursement based on regional or other considerations. Gaining new CPT-codes for new devices can take a great deal of time and effort. The second method is to cover the procedure and device under a capitated fee where the hospital is reimbursed a lump sum for a procedure including the device, hospital, homecare, and physician fees.

Every effort should be made to design devices to be low cost. Device cost is being scrutinized more and more by those who reimburse. It is easy to state, however, that a device needs to be inexpensive. Unfortunately the reality is that healthcare reforms and new regulations by FDA are making medical devices more costly to develop, to obtain regulatory approvals for [FDA, 1993], and to manufacture.

Professional Medical Service Support

The more technically sophisticated a device is, the more crucial that homecare support and education be a part of a program. In fact, in many cases, such support and education are as important as the device itself.

Medical service can be offered by numerous homecare service companies. Typically these companies purchase the equipment instead of the patient, and a monthly fee is charged for use of the equipment along with all the necessary service. The homecare company then must obtain reimbursement from third-party payers. Some of the services offered by the homecare company include training on how to use the equipment, CPR training, transporting the equipment to the home, servicing/repairing equipment, monthly visits, and providing on-call service 24 hours a day. The homecare provider must also be able to provide feedback to the treating physician on progress of the treatment. This feedback may include how well the equipment is working, the patient's medical status, and compliance of the patient.

89.3 Infant Monitor Example

Many infants are being monitored in the home using apnea monitors because they have been identified with breathing problems [Kelly, 1992]. Theses include newborn premature babies who have apnea of prematurity [Henderson-Smart, 1992; NIH, 1987], siblings of babies who have died of sudden infant death syndrome (SIDS) [Hunt, 1992; NIH, 1987], or infants who have had an apparent life-threatening episode (ALTE) related to lack of adequate respiration [Kahn et al. 1992; NIH, 1987]. Rather than keeping infants in the hospital for a problem that they may soon outgrow (1–6 months), doctors often discharge them from the hospital with an infant apnea monitor that measures the duration of breathing pauses and heart rate and sounds an alarm if either parameter crosses limits prescribed by the doctor.

Infant apnea monitors are among the most sophisticated devices used routinely in the home. These devices utilize microprocessor control, sophisticated breath-detection and artifact rejection firmware algorithms, and internal memory that keeps track of use of the device as well as recording occurrence of events and the physiologic waveforms associated with the events. The memory contents can be downloaded directly to computer or sent via modem remotely where a complete 45-day report can be provided to the referring physician (see Fig. 89.3).

Most apnea monitors measure breathing effort through impedance pneumography. A small (100–200 uA) high-frequency (25–100 kHz) constant-current train of pulses is applied across the chest between a pair of electrodes. The voltage needed to drive the current is measured, and thereby the effective impedance between the electrodes can be calculated. Impedance across the chest increases as the chest expands and decreases as the chest contracts with each breath. The impedance change with each breath can be as low as 0.2 ohms on top of an electrode base impedance of 2000 ohms, creating some interesting signal-to-noise challenges. Furthermore, motion artifact and blood volume changes in the heart and chest can cause impedance changes of 0.6 ohms or more that can look just like breathing. Through the same pair of electrodes, heart rate is monitored by picking up the electrocardiogram (ECG) [AAMI, 1988].

Because the impedance technique basically measures motion of the chest, this technique can only be used to monitor central apnea or lack of breathing effort. Another less common apnea in infants called obstructive apnea results when an obstruction of the airway blocks air from flowing in spite of breathing effort. Obstructive apnea can not be monitored using impedance pneumography [Kelly, 1992].

There is a very broad socioeconomic and educational spectrum of parents or caregivers who may be monitoring their infants with an apnea monitor. This places an incredible challenge for the design of the device so that it is easy enough to be used by a variety of caregivers. It also puts special requirements on the homecare service company that must be able to respond to these patients within a matter of minutes, 24 hours a day.

The user-friendly monitor shown in Fig. 89.1 uses a two-button operation, the on/off switch, and a reset switch. The visual alarm indicators are invisible behind a back-lit panel except when an actual alarm occurs. A word describing the alarm then appears. By not showing all nine possible alarm conditions unless an alarm occurs, parent confusion and anxiety is minimized. Numerous safety features are built into the unit, some of which are noticeable but many of which are internal to the operation of the monitor. One useful safety feature is the self-check. When the device is turned on, each alarm LED lights in sequence, and the unit beeps once indicating that the self-check was completed successfully. This gives users the opportunity to confirm that all the alarm visual indicators and the audible indicator are working and provides added confidence for users leaving their baby on the monitor. A dual-level battery alarm gives an early warning that the battery will soon need charging. The weak battery alarm allows users to reset the monitor and continue monitoring their babies for several more hours before depleting the battery to the charge battery level where the monitor must be attached to the ac battery charger/adapter. This allows parents the freedom to leave their homes for a few hours knowing that their child can continue to be monitored.

A multistage alarm reduces the risk of parents sleeping through an alarm. Most parents are sleep-deprived with a new baby. Consequently, it can be easy for parents in a nearby room to sleep through a monitor alarm even when the monitor sounds at 85 dB. A three-stage alarm helps to reduce this risk. After 10 seconds of sounding at 1 beep per second, the alarm switches to 3 beeps per second for

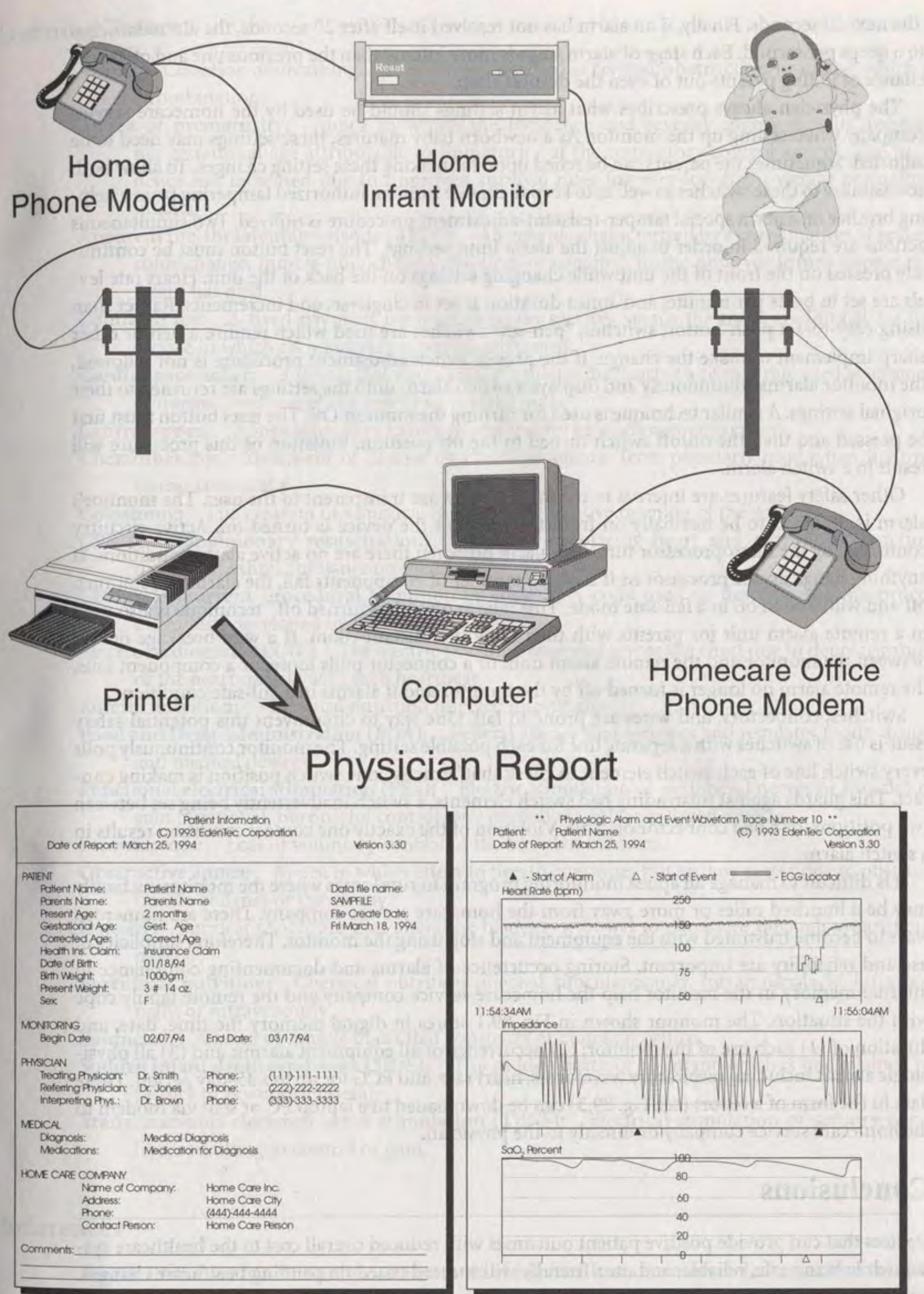

FIGURE 89.3 Infant apnea monitor with memory allows data to be sent by modem to generate physician report (drawing courtesy of EdenTec Corporation).

the next 10 seconds. Finally, if an alarm has not resolved itself after 20 seconds, the alarm switches to 6 beeps per second. Each stage of alarm sounds more intense than the previous one and offers the chance of jolting parents out of even the deepest sleep.

The physician always prescribes what alarm settings should be used by the homecare service company when setting up the monitor. As a newborn baby matures, these settings may need to be adjusted. Sometimes the parents can be relied upon for making these setting changes. To allow both accessibility to these switches as well as to keep them safe from unauthorized tampering from a helping brother or sister, a special tamper-resistant-adjustment procedure is utilized. Two simultaneous actions are required in order to adjust the alarm limit settings. The reset button must be continually pressed on the front of the unit while changing settings on the back of the unit. Heart rate levels are set in beats per minute, and apnea duration is set in single-second increments. Rather than using easy-to-set push-button switches, "pen-set" switches are used which require a pen or other sharp implement to make the change. If the proper switch adjustment procedure is not followed, the monitor alarms continuously and displays a switch alarm until the settings are returned to their original settings. A similar technique is used for turning the monitor Off. The reset button must first be pressed and then the on/off switch turned to the off position. Violation of this procedure will result in a switch alarm.

Other safety features are internal to the monitor and are transparent to the user. The monitor's alarm is designed to be normally on from the moment the device is turned on. Active circuitry controlled by the microprocessor turns the alarm off when there are no active alarm conditions. If anything hangs up the processor or if any of a number of components fail, the alarm will not turn off and will remain on in a fail-safe mode. This "alarm on unless turned off" technique is also used in a remote alarm unit for parents with their baby in a distant room. If a wire breakage occurs between the monitor and the remote alarm unit, or a connector pulls loose, or a component fails, the remote alarm no longer is turned off by the monitor and it alarms in a fail-safe condition.

Switches, connectors, and wires are prone to fail. One way to circumvent this potential safety issue is use of switches with a separate line for each possible setting. The monitor continuously polls every switch line of each switch element to check that "exactly" one switch position is making contact. This guards against misreading bad switch elements, a switch inadvertently being set between two positions, or a bad connector or cable. Violation of the exactly one contact condition results in a switch alarm.

It is difficult to manage an apnea monitoring program in rural areas where the monitoring family may be a hundred miles or more away from the homecare service company. There are numerous ways to become frustrated with the equipment and stop using the monitor. Therefore, simplicity of use and reliability are important. Storing occurrence of alarms and documenting compliance in internal memory in the monitor help the homecare service company and the remote family cope with the situation. The monitor shown in Fig. 89.1 stores in digital memory the time, date, and duration of (1) each use of the monitor; (2) occurrence of all equipment alarms; and (3) all physiologic alarms including respiratory waveforms, heart rate, and ECG for up to a 45-day period. These data in the form of a report (see Fig. 89.3) can be downloaded to a laptop PC or sent via modem to the homecare service company or directly to the physician.

89.4 Conclusions

Devices that can provide positive patient outcomes with reduced overall cost to the healthcare system while being safe, reliable, and user-friendly will succeed based on pending healthcare changes. Future technology in areas of sensors, communications, and memory capabilities should continue to increase the potential effectiveness of homecare management programs by using increasingly sophisticated devices. The challenge for the medical device designer is to provide cost-effective, reliable, and easy-to-use solutions that can be readily adopted by the multidisciplinary aspects of homecare medicine while meeting FDA requirements.

Defining Terms

Apnea: Cessation of breathing. Apnea can be classified as **central, obstructive,** or mixed, which is a combination.

Apnea of prematurity: Apnea in which the incidence and severity increases with decreasing gestational age attributable to immaturity of the respiratory control system. The incidence has increased due to improved survival rates for very-low-birth-weight premature infants.

Apparent life-threatening episode (ALTE): An episode characterized by a combination of apnea, color change, muscle tone change, choking, or gagging. To the observer it may appear the infant has died.

Capitated fee: A fixed payment for *total* program services versus the more traditional fee for service in which each individual service is charged.

Cardiac pacemaker: A device that electrically stimulates the heart at a certain rate used in absence of normal function of the heart's sino-atrial node.

Central apnea: Apnea secondary to lack of respiratory or diaphragmatic effort.

Chemotherapy: Treatment of disease by chemical agents. Term popularly used when fighting cancer chemically.

Colostomy: The creation of a surgical hole as an alternative opening of the colon.

CPR (cardiopulmonary resuscitation): Artificially replacing heart and respiration function through rhythmic pressure on the chest.

CPT-code (current procedural terminology code): A code used to describe specific procedures/tests developed by the AMA.

Electrocardiogram (ECG): The electric potential recorded across the chest due to depolarization of the heart muscle with each heartbeat.

Enteral nutrition: Chemical nutrition injected intestinally.

Food and Drug Administration (FDA): Federal agency that oversees and regulates foods, drugs, and medical devices.

Functional electrical stimulation (FES): Electric stimulation of peripheral nerves or muscles to gain functional, purposeful control over partially or fully paralyzed muscles.

Incontinence: Loss of voluntary control of the bowel or bladder.

Obstructive apnea: Apnea in which effort to breath continues but airflow ceases due to obstruction or collapse of the airway.

Ostomy: Surgical procedure that alters the bladder or bowel to eliminate through an artificial passage.

Parenteral nutrition: Chemical nutrition injected subcutaneously, intramuscularly, intrasternally, or intravenously.

Sphincter: A band of muscle fibers that constricts or closes an orifice.

Sudden infant death syndrome (SIDS): The sudden death of an infant which is unexplained by history or postmortem exam.

Transcutaneous electrical nerve stimulation (TENS): Electrical stimulation of sensory nerve fibers resulting in control of pain.

References

AAMI. 1988. Association for the Advancement of Medical Instrumentation Technical Information Report: Apnea Monitoring by Means of Thoracic Impedance Pneumography, Arlington, Virg.

FDA. November 1993. Reviewers Guidance for Premarket Notification Submissions (Draft), Anesthesiology and Respiratory Device Branch. Division of Cardiovascular, Respiratory, and Neurological Devices. Food and Drug Administration. Washington DC.

FIND/SVP. 1992. The Market for Home Care Products, a Market Intelligence Report. New York.

Henderson-Smart, DJ. 1992. Apnea of prematurity. In R Beckerman, R Brouillette, C Hunt (eds), Respiratory Control Disorders in Infants and Children, pp 161–177, Baltimore, Williams and Wilkins.

Hunt, CE. 1992. Sudden infant death syndrome. In R Beckerman, R Brouillette, C Hunt (eds), Respiratory Control Disorders in Infants and Children, pp 190–211, Baltimore, Williams and Wilkins.

Kahn A, Rebuffat E, Franco P, et al. 1992. Apparent life-threatening events and apnea of infancy. In R Beckerman, R Brouillette, C Hunt (eds), Respiratory Control Disorders in Infants and Children, pp 178–189, Baltimore, Williams and Wilkins.

Kelly DH. 1992. Home monitoring. In R Beckerman, R Brouillette, C Hunt (eds), Respiratory Control Disorders in Infants and Children, pp 400–412, Baltimore, Williams and Wilkins.

NIH. 1987. Infantile Apnea and Home Monitoring, Report of NIH Consensus Development Conference, US Department of Health and Human Services, NIH publication 87-2905.

Pierson DJ. 1994. Controversies in home respiratory care: Conference summary. Respir Care 39(4):294.

Wall LL, Norton PA, Dehancey JOL. 1993. Practical Urology, Baltimore, Williams and Wilkins.

APPENDIX H

REVIEW ARTICLE
Julien F. Biebuyck, M.B., D.Phil., Editor

Anesthesiology
76:1018–1038, 1992

Recent Developments in Pulse Oximetry

John W. Severinghaus, M.D., Joseph F. Kelleher, M.D., M.A.†*

CONTENTS

Pulse oximeters now occupy most critical care arenas and virtually every operating room in the United States. They are manufactured by more than 35 firms, with 1989 annual world wide sales estimated at 65,000 units valued at $200 million.

In January 1989, two comprehensive reviews of pulse oximetry were published. One gave relative emphasis to theory of operation and other technical aspects,[1] while the other focused primarily on clinical issues.[2] Since the reviews of 1989 were completed, more than 500 additional publications have described methods, uses, problems, progress, and effects of pulse oximetry—135 of them in the 6-month period prior to the end date of this review (October 1, 1991). The past 3 yr have seen a variety of other reviews concerning some recent developments[3–12] as well as the history of pulse oximetry.[13,14]

The purpose of this article is to summarize the literature on pulse oximetry that has appeared since the major reviews of early 1989. Expressions such as "before 1988" and "since 1988," unless otherwise indicated, refer herein to the mid-1988 cutoff date for the references appearing in those reviews.

Methodological Developments

There is relatively little to report as to methodological advance in pulse oximetry since 1988. A potential exception is surface reflectance ("surface") oximetry, which has received significant recent experimental attention but does not appear ready for widespread clinical use. In 1988, a review of pulse oximetry[2] could dismiss the topic of reflectance oximetry by observing that it was "one desirable possibility for the future of pulse oximetry . . . in which measurements of reflected light would allow monitoring at nontransilluminable sites, such as the fetal presenting part during labor." With the possible exception of its use in labor, reflectance oximetry is still largely investigational. Some models now couple the oximeter to the ECG (see "Limitations of Pulse Oximetry: Motion

* Department of Anesthesia and Cardiovascular Research Institute, University of California, San Francisco, California.

† Anesthesia Service Medical Group, Inc., San Diego, California.
Received from the Department of Anesthesia and Cardiovascular Research Institute, University of California, San Francisco and the Anesthesia Service Medical Group, Inc., San Diego, California. Accepted for publication January 21, 1992.

This review contains portions of Severinghaus JW: Oximetry: Uses and limitations. ASA Refresher Courses in Anesthesiology 19:139–152, 1991.

Address reprint requests to Dr. Severinghaus: 1386HSE, UCSF, San Francisco, California 94143.

Key words: Blood: oxygen measurement; oxygen saturation. Complications: hypoxia; postoperative hypoxia; respiratory problems. Equipment: optical; oximeters. Monitoring: oximetry.

Artifact"). Probe design has been evolving toward reduced size and greater comfort. Two recent reviews discussed the technology of pulse oximetry,[15,16] although it must be noted that by and large this technology has not changed since 1988.

Equipment is now available to permit central nursing stations to monitor several patients remotely (Novametrix Inc). Pan and James[17] reported trials of a telemetric pulse oximetry network for use in monitoring of patients on a ward (after caesarean section). Their study was concerned primarily with false alarms (see "Limitations of Pulse Oximetry: False Alarms and False Nonalarms").

Uses of Pulse Oximetry

Clinical uses of pulse oximetry may be divided into the oximetric and the plethysmographic.[2] The oximetric applications are largely concerned with detecting and quantitating hypoxemia in various settings, but considerable attention and controversy have surrounded oximetry's use in avoiding neonatal hyperoxia as well.

In 1988, the detection of hypoxemia in perioperative and critical-care settings was an established use for the pulse oximeter; its utility as the sole monitor for neonatal hyperoxia was controversial at best; and a large number of plethysmographic uses had been suggested anecdotally, relatively few of which had been submitted to more rigorous examination.[1,2] All three of these generalizations still hold, despite worthwhile developments in each area.

The time-honored, if not ideally rigorous, technique of "citation analysis" (used memorably in Keats's 1983 Rovenstine Lecture,[18] among other publications) helps to illustrate where current clinical interest in pulse oximetry is directed. It is clear from table 1 that pulse oximetry, having entrenched itself in the bank of operating-room monitors, is now under active scrutiny for the recovery room and for outpatient settings such as the endoscopy suite, the dentist's office, and the sleep laboratory. Table 2 lists recent active topics of investigation into performance or limitations of pulse oximetry, independent of clinical setting.

TABLE 1. Uses of Pulse Oximeters: Topical Analysis by Frequency of Publication from May 1988 to October 1991

Subject	Number of Papers
Endoscopy	26
Postoperative recovery	22
Neonatal intensive care unit	21
Oral surgery and dentistry	14
Airway management	13
Sleep studies	13
Hypotension, poor perfusion	12
Premedication	11
Pediatric anesthesia	10
Transport	10
Emergency	9
Chronic obstructive pulmonary disease, lung disease	8
Adequacy of circulatory tests	8
Anesthesia, adult	8

Topics reported in three to seven papers include croup; infection; fetal monitoring; magnetic resonance imaging; exercise; epidural morphine; altitude studies; mechanical ventilation; caesarean section; intensive care units; hypothermia; embolism; one-lung anesthesia; positioning problems; heart surgery; and anemia. Other uses discussed in one or two papers include home monitoring of sudden infant death syndrome patients; weaning from a ventilator; hypoxemia during labor; seizures; asthma; induction of anesthesia with jet ventilation; obesity and apnea; hemodialysis; pneumothorax; pulmonary edema; aspiration; malignant hyperthermia; efficacy of cardiopulmonary resuscitation; effect of sickle cell disease; application in ear, nose, and throat practice; and home O_2 therapy control.

TABLE 2. Performance and Limitations of Pulse Oximetry: Topical Analysis by Frequency of Publication from May 1988 to October 1991

Subject	Number of Papers
Effects of methemoglobin, carboxyhemoglobin	19
Tests of accuracy	18
Sites for probes	13
Failure with hypoperfusion	12
Standards and legal issues	7
Motion artifact	6
Skin pigments	6
Uses in animals	6
Models for *in vitro* testing	5
Palmar circulation (Allen's test)	5

Other publications described oximetry in burn patients; comparisons with transcutaneous P_{O_2}; use in tissue revascularization and transplantation; effect on use of arterial blood gas analysis; reports of finger burns by probes; blood pressure measurement; and cost–benefit ratio estimations.

The Detection of Hypoxemia

The high prevalence of clinically unsuspected hypoxemia is perhaps the most famous disclosure that pulse oximetry has made. The incidence of hypoxemia was studied intraoperatively in a single-blind study of 296 adult anesthetics by Moller *et al.*[19] In 53%, mild hypoxemia (86–90%) was seen. Severe hypoxemia, with hemoglobin (Hb) oxygen saturation measured by pulse oximetry (Sp_{O_2}) as < 81%, was recorded in 20% of the patients; 70% of these severe episodes were not detected by the anesthetist. McKay and Noble[20] found that 6% of a series of nearly 5,000 anesthetics involved critical incidents, of which 29 involved Sp_{O_2} readings < 75%. Coté *et al.*,[21] in a single-blind study of 402 pediatric cases, separately examined the effect of withholding oximeter and/or capnograph data from the anesthesia team. They identified 59 major desaturation events ($Sp_{O_2} < 85\%$ for > 30 s) in 43 patients and 130 minor desaturations (< 95% for > 60 s). Of the major events, 41 (≃ 70%) were first diagnosed by oximetry, 13 by the anesthesiologist and 5 by the capnograph. Blinding the oximeter data increased the number of patients experiencing major desaturation events from 12 to 31 ($P = 0.003$). Infants ≤ 6 months of age had the highest incidence of major desaturation events. Blinding the capnograph data altered neither the frequency of desaturation events nor the incidence of major capnograph events but did increase the number of patients with minor capnograph events ($P = 0.0026$). The authors concluded: "1) The pulse oximeter is far superior to either the capnograph or clinical judgment in providing the earliest warning of desaturation events. 2) Capnography can provide an early warning to potentially life-threatening problems, but such problems often result in desaturation . . . ."[21]

In a less-controlled study of 91 pediatric anesthesia cases, Schulz *et al.*[22] found hypoxic episodes ($Sp_{O_2} < 95\%$) in 52% and major desaturations ($Sp_{O_2} < 85\%$) in 54% of newborn infants. They reported that "desaturation was more likely to occur in intubated children than in those with a mask ($p < 0.05$)" (reflecting problems with the processes of intubation and extubation).

These last 3 yr have seen the investigative focus turn from the operating room and intensive care unit, where unanticipated hypoxemia is relatively rare, to the postanesthesia recovery period, clearly demonstrating the high incidence of hypoxemia due to the effects of anesthetic, sedative, relaxant, and especially opioid drugs.[23–36] In Copenhagen, a single-blind study[32] of 202 adults in the recovery room following elective operations, found decreases to $Sp_{O_2} < 91\%$ in 55% of all patients at some time before discharge, despite administration of nasal oxygen in more than half of these hypoxic episodes, and to $Sp_{O_2} < 80\%$ in 13%. Patients who had undergone regional anesthesia had a lower risk of hypoxemia. A randomized study by Lampe *et al.*[31] of 141 patients for carotid endarterectomy or hip replacement noted postoperative $Sp_{O_2} < 90\%$ in 63% and <86% in 21%; they monitored that portion of the postoperative period included in "a 24-hour period beginning just after induction of anesthesia." Use of oxygen during the first postoperative night reduced the incidence of hypoxemia from 29% to 0%.

During recovery from anesthesia studied in Sydney, Australia[34] with routine use of nasal oxygen as judged appropriate by nurses, 80% of patients' saturations decreased to < 90% Sp_{O_2} and 26% decreased to < 80% Sp_{O_2} during the first 15 min of recovery. Sixty-four percent decreased to < 90% even while the patients received nasal oxygen. On the other hand, in Boston, Morris *et al.*[23] showed that only 14% of inpatients developed at least transient hypoxemia during recovery, and only 1% of outpatients became hypoxic in the recovery room. The amounts of premedication and injected sedatives and opioids were not significantly different between inpatients and outpatients.

Canet *et al.*[36] not only demonstrated postoperative hypoxemia in 44% of more than 200 patients and showed that 35% oxygen prevented hypoxemia, but also reviewed other evidence that supported the routine administration of oxygen and the concomitant use of pulse oximetry.

The incidence of hypoxemia has been investigated in various outpatient or "office" procedures accompanied by sedation without professional anesthesia assistance. The greatest attention has centered on bronchoscopy and endoscopy. Schnapf[37] demonstrated > 5% desaturation in 80% of 36 children aged 6–142 months during fiberoptic bronchoscopy in a pediatric special care unit or pulmonary laboratory, with higher incidence in the youngest patients.

Pulse oximetry has shown potentially dangerous desaturation to be present in 45% of patients undergoing endoscopy under sedation.[38] A prospective study by Moore *et al.*[39] in surgical intensive care disclosed hypoxic episodes in 21% of patients in the surgical intensive care unit, mostly during mechanical ventilation. In a recent review with 63 references, Bell[40] suggests that during gastrointestinal endoscopy, hypoxic problems are common, with 60% of deaths during endoscopy attributed to cardiopulmonary complications. Al-Hadeedi and Leaper[41] observe that the 1:5,000 mortality during upper gastrointestinal endoscopy—itself "several fold" lower than that for endoscopic retrograde cholangiopancreatography—still "does not compare favorably with the much lower perioperative mortality directly attributed to anesthesia." In 132 patients undergoing endoscopic retrograde cholangiopancreatography under sedation, they found that Sp_{O_2} decreased from 95.7 ± 2.4% (mean ± standard deviation) to 88.9 ± 6.4%. The largest decreases occurred after positioning of the endoscope (rather than after administration of the sedative or completion of the procedure). In 57 patients between the ages of 6 weeks and 36 months undergoing 60 flexible upper intestinal endoscopies with parenteral sedation only, 7 patients showed oxygen desaturation to < 90% after sedation but before insertion of the endoscope without overt clinical evidence of complications.[42] The British Society of Gastroenterology recommended and approved guidelines for use of pulse oximetry as a standard during all procedures and also suggested that oxygen be administered.[43]

Sedation and anesthesia are commonly used without professional anesthesia assistance in oral surgery and dentistry. In view of the potentially high incidence of hypoxia, pulse oximetry has been strongly recommended,[44] although Wilson[45] suggested that 87–90% of desaturation episodes in his study of 22 sedated children were due to motion artifacts.

Marjot and Valentine[46] found an 80% incidence of hypoxemia ("persistent desaturation to S_aO_2 less than 90%") following premedication with lorazepam, morphine, and droperidol for cardiac surgery, accompanied in 33% by ECG changes, previously unsuspected and easily corrected by oxygen administration. Hypoxemia ($Sa_{O_2} < 90\%$) was documented in 10 of 15 women in labor, 7 of whom had received opioids.[47]

Oximetry has also been used to demonstrate that periodic breathing in premature and newborn infants is unrelated to the occurrence of apneic spells.[48] Oximetry may reduce the need for intensive care in low-risk groups. In 30 patients during emergency field rescue operations, Sp_{O_2} was compared with arterial blood oxyhemoglobin (O_2Hb) and found to correlate with r = 0.898 and bias ($Sp_{O_2} - O_2Hb$) of -0.3 ± 2.4.[49]

Airway management problems aided by oximetry include evaluation of the performance of experimental rescue devices such as the "glossopalatinal tube,"[50] detection of obstructed[51] or misplaced[52–54] endotracheal tubes, assessment of readiness for removal of tracheostomy,[55] foreign body removal,[56] and effectiveness of use of helium.[57] Oximetry is especially useful in managing one-lung anesthesia.[58]

Use of oximetry and end-tidal P_{CO_2} instead of arterial blood gas in assessing a patient's ability to be separated from mechanical ventilation was studied in 60 patients by Withington *et al.*[59] After assessing noninvasive method reliability in 20 subjects, they demonstrated the success of the method in the next 40. Pulse oximetry has been used in optimizing continuous positive airway pressure and positive end-expiratory pressure[60] and, for quantitative purposes, pulse oximetry has been a documented help in a variety of procedures, such as determination of the needed oxygen flow rate or concentration in ventilator-dependent patients.[61]

When epidural morphine came into general use for pain relief, there was concern about possible unobserved apnea on wards. Choi *et al.*[62] demonstrated in 20 post–caesarean section women that half of the patients experience desaturation to < 85% over the 15-h monitoring period, whether they were given morphine parenterally or epidurally, but the desaturation occurred within 3 h with parenteral morphine and at 13.7 ± 5.9 h with epidural morphine.

In a study in general hospital (non–critical-care) units, Bowton *et al.*[63] found that 75% of patients monitored for 36 h had at least one episode of desaturation to < 90% and 58% had at least one episode of desaturation to < 85%. Few of these episodes were documented, and even the availability of monitoring had little effect on care.

The use of oximetry in emergency care situations was reviewed.[64] Patients transported by ambulance, helicopter, and aircraft are increasingly monitored by pulse oximetry because the vibration makes most other methods of ventilatory and circulatory monitoring ineffective.[65] Short *et al.* compared seven oximeters during helicopter transport, and reported three to be subject to vibration interference or otherwise unacceptable.[66]

Pulse oximetry is used (in connection with periodic arterial blood gas determination) to help adjust the flow rates and periods of use of home oxygen therapy of patients with chronic obstructive pulmonary disease, *e.g.* in response to increased needs with exercise and rapid–eye-movement sleep. A review of this field by Tiep (110 references) suggests that the involvement of physician and oxygen supplier may have increased in the effort to tailor oxygen supply to demand and to reduce possible excessive oxygenation (and respiratory depression).[67]

In summary, pulse oximetry is now well-established—both inside and outside the operating room and intensive care unit— as a useful and sensitive detector of hypoxemia. Its acceptance as a supplement to clinical detection for hypoxia is clearly apparent. Equally apparent, however, is the role of motion artifact in limiting its specificity, especially in certain populations (see "Limitations of Pulse Oximetry: Motion Artifact"). Furthermore, outcome studies are generally lacking for the above-mentioned applications, leaving open the question of whether pulse oximetry reduces morbidity and mortality (see "Does Pulse Oximetry Increase Patient Safety?").

Monitoring Circulation

The pulse oximeter's plethysmographic capability has been proposed as a monitor of circulatory adequacy. By 1988, a number of anecdotal applications of this type had been reported.[2] This list is now longer (below), but an earlier caution[2] still holds true: the pulsatile perfusion required to generate a pulse signal on a given pulse oximeter in not *a priori* either necessary or sufficient to guarantee adequacy of circulation for a given application. Machine characteristics, intersubject variability, and intrasubject variability all are involved. Only controlled studies can resolve these issues; by and large, these have not been done for plethysmographic applications of the pulse oximeter.

The best-studied use of this type is Allen's test. In 1988 there was no consensus among those who had investigated pulse oximeter plethysmography as a measure of palmar collateral circulation.[2] Several others have now tried and recommended it without controlled testing.[68,69] Levinsohn *et al.*,[70] taking digital cuff sphygmomanometry as the "gold standard," showed laser Doppler to be equally accurate and easier to use, and found the classic ("subjective") Allen's test to be sensitive but not very specific ("a good screening test"). But they found pulse oximetry to indicate false adequacy of collateral circulation in two of three hands with abnormal digital systolic pressure.

In contrast, Pillow and Herrick[71] found that laser Doppler agreed with pulse oximetry in 109 of 109 patients with respect to both ulnar collateral flow (100 sufficient, 9 insufficient) and radial collateral flow (108 sufficient, 1 insufficient). They were unable to account for the contrary results of Glavin and Jones,[72] who rejected pulse oximetry for this test 2 yr earlier, in 1989, except to speculate that the thumb may be a more sensitive site than the index finger for monitoring ulnar collateral flow. Despite the further study, this issue appears no more settled than it was three yr ago.

Systolic blood pressure may be accurately determined by reappearance of the pulsatile waveform during cuff deflation in instruments that display the waveform (tested with Ohmeda 3700)[73,74] or, perhaps more accurately, by waveform disappearance during slow cuff inflation.[75–77] Comparison of pulse amplitudes on the finger and the toe demonstrated toe vasodilation due to sympathetic blockade with spinal anesthesia.[78] The waveform response to a Valsalva maneuver can detect patients with autonomic dysfunction or blockade.[79]

Other new reported uses include determining ductus arteriosus patency,[80] assessing the level of ischemia in peripheral vascular disease (in which it is claimed to be more sensitive than either transcutaneous P_{O_2} [tcP_{O_2}] or Doppler flowmetry[81]), assuring patency of major arterial grafts,[82] testing viability of the bowel,[83,84] indicating artery compression in shoulder arthroscopy[85] or fracture manipulation,[86] determining limb vascularity,[87] assessing circulatory adequacy of the arm when an unconscious patient is placed in the lateral or prone position or with arms elevated or hyperabducted for surgery,[88] and monitoring circulation of reimplanted digits or grafts.[89] In general, these are anecdotal uses, not verified by controlled studies.

Role in Preventing Retinopathy of Prematurity

In premature infants, the administration of supplemental oxygen is associated with retinopathy of prematurity (ROP).[90,91] The duration, concentration, and pattern of oxygen toxicity all are implicated—as are gestational age, hypercapnia (possibly *via* a vasodilatory increase in oxygen delivery to the retinal vasculature[92]), the state of the ductus arteriosus (open[93] or closed[94]), light,[95] and literally dozens of other factors, which may or may not be confounding.[91] Indeed, premature infants can develop ROP despite persistent hypoxemia.[96]

Empirical recommendations for arterial oxygen saturation (Sa_{O_2}) in infants at risk for ROP generally fall into the 90%–95% range.[2,97] The pulse oximeter has obvious application here, but its main use is in preventing hypoxemia, not hyperoxia. It is generally agreed that pulse oximetry is not adequate for evaluating hyperoxia in this setting—not only because its inherent inaccuracy of 2–3% looms so large in the region of the Hb–oxygen dissociation curve above Sa_{O_2} 90%, but also, and more fundamentally, because there is no consensus on an acceptable safe upper limit for Sa_{O_2}.

A recent "consensus report" on neonatal pulse oximetry,[98] definitive enough in its other recommendations, was able to recommend "further research" only after "long and complex" discussion of a safe upper limit. The current uncertainty about this issue is illustrated by the various definitions of hyperoxia used in recent investigations into neonatal pulse oximetry; they include $P_{O_2} > 80$ mmHg,[99] $P_{O_2} > 90$ mmHg,[100] and $P_{O_2} > 100$ mmHg.[98]

Hay *et al.*[101] noted that when an Ohmeda 3800 displayed $Sp_{O_2} = 92 \pm 3\%$ in neonates, the Pa_{O_2} was between 40 and 100 mmHg 100% of the time—but they added that, while keeping $Sp_{O_2} = 92 \pm 3\%$ "seems prudent and safe, . . . this conclusion is arbitrary and not tested."

Bucher *et al.*[100] recently concluded that the Nellcor N-100 and the Ohmeda Biox 3700 are highly (95%) sensitive for hyperoxic episodes ($P_{O_2} > 90$ mmHg) but have only mediocre specificity (38% and 52%, respectively); this 95% sensitivity was achieved by choosing an Sp_{O_2} upper limit of 96% for the Nellcor N-100 but of only 89% for the Ohmeda Biox 3700. Findings like these suggest that caution is required in interpreting blanket recommendations on safe upper limits, such as Hay's "consensus" of Sp_{O_2} 94–95%,[98] that do not make reference to a specific pulse oximeter brand and model.

On the other hand, Reynolds and Yu,[99] also using the Ohmeda Biox 3700 and studying 175 readings in 12 neonates with pulmonary compromise, recommended an Sp_{O_2} upper limit of 90% to avoid $P_{O_2} > 80$ mmHg. If nothing else, the incongruity between this result and that of Bucher *et al.*[100] underscores that the prevention of ROP may involve more than just control of Sa_{O_2} or Pa_{O_2}. Indeed, the recent slowdown in published investigations into a safe upper limit of Sa_{O_2} for neonates—in contrast to a veritable spate of such studies *circa* 1987—may signal a conceptual retrenching as the multifactorial nature of ROP is acknowledged in practice.

What is certain is that pulse oximetry cannot currently be recommended as the sole monitor of oxygenation for the neonate at risk for ROP. The prevention of ROP is probably best accomplished by either intermittent arterial blood gas analysis or continuous tcP_{O_2} monitoring, with pulse oximetry as a supplementary modality.

As Sa_{O_2} decreases, because of the steepening dissociation curve, oximetry becomes progressively more dependable than tcP_{O_2} measurement in assessing, controlling, and maintaining some defined level of oxygenation. In an infant with mostly fetal Hb, a 5-mmHg change in P_{O_2} at 70 mmHg ($\simeq 97\%$ Sa_{O_2}) is equivalent to only about

0.6% change of Sa_{O_2}, but the same 5 mmHg change at 40 mmHg ($\simeq$ 87% Sa_{O_2}) accompanies a 5% change in Sa_{O_2}. Fetal Hb is not distinguishable from adult Hb by pulse oximeters.[102] For this reason, at $Sa_{O_2} < 90\%$, some investigators[99,103,104] believe oximetry to be more reliable than transcutaneous monitoring, but not even they seem to believe that it can supplant other forms of monitoring. The relative merits of tcP_{O_2} monitoring and pulse oximetry have been reviewed.[105–107]

Investigative Uses

Cardiopulmonary resting and exercise tests,[108,109] hypoxic ventilatory response studies,[110] and sleep abnormality studies[111–116] are now more easily and accurately done with oximetry. The rate of decrease of Sp_{O_2} during apnea after 5 min of preoxygenation was shown by Jense *et al.*[117] to be twice as fast in morbidly obese patients, with Sp_{O_2} decreasing to 90% in 163 ± 15 s in the obese subjects.

Using oximetry, Brodsky *et al.* reassessed diffusion hypoxia after discontinuation of nitrous oxide.[118] In ASA physical status I and II patients breathing unspecified concentrations of isoflurane in 3:2 nitrous oxide/oxygen (at 5 $l \cdot min^{-1}$), a transient Sp_{O_2} decrease of 4% was seen 3 min after discontinuation of nitrous oxide, whereas no corresponding drop was seen in patients breathing isoflurane in 100% oxygen.

Oximetry has been used to test exposure to and acclimatization at high altitude[119–123] and to study breath-holding in the diving women of Korea and Japan.[124] Pulse oximeters have been successfully used in laboratory animals such as the dog,[125] sheep,[126,127] pig,[128] horse,[129] rabbit,[130] and rat.[131] The sites used have been the ear, cheek, tongue, and tail.

Limitations of Pulse Oximetry

Incidence of Failure

In a prospective intraoperative study at the University of Washington, Freund *et al.* reported a 1.12% failure rate in 11,046 anesthetics.[132] Failure was defined conservatively as "the inability to obtain any pulse oximetry reading for a cumulative period of 30 minutes or greater after all mechanical problems . . . had been eliminated and all possible sites had been tried . . ." (*e.g.*, other digits, ear, nose). Curiously, the failure rates differed by hospital: they were 0.78% at the University Hospital, 0.56% at the Harborview Hospital, and 0.56% at the Children's Hospital, but 4.24% at the Veterans' hospital. When a failure occurred, it persisted for 32% of total anesthesia time.

In a retrospective study of 1,403 patients in a postanesthesia care unit at the University of Washington Hospital, Gillies *et al.*[133] found a comparable failure rate of 1.1% (two or more 15-min periods when no values were noted). About 90% of failures were at the beginning of the stay in the postanesthesia care unit.

Low Signal-to-noise Ratio

Probably a majority of the factors that interfere with pulse oximetry can be explained as either too little signal (low-perfusion state, improper probe placement) or too much "noise" (motion, ambient light, electrocautery, venous pressure waves). When arterial pulsation decreases below some fraction of total transmitted light (about 0.2% for the Ohmeda units), the signal is judged unacceptable by the computer program, which may display a "low quality signal" message, display a blank, or set the display to zero. This lower limit for default varies between manufacturers. Instruments that continue to display Sp_{O_2} at lower pulse pressures may be more prone to providing erroneous data at low signal levels.[7,134–136] If artificial "pulsations" are present (due to some interfering process such as mechanical movement or ventilation), the processor may either default to zero or display an incorrect Sp_{O_2} with an erroneous heart rate. The inappropriate heart rate can often alert the user that a problem exists.

Probe Position

Kelleher and Ruff documented that finger probes, when withdrawn partially beyond the fingertip, exhibit what they called a "penumbra effect,"[137] often causing a false low reading before failure occurs. (The authors speculated that this might also cause a false high reading if Sa_{O_2} is < 85%.) The mechanism probably involves light shunt either edgewise through superficial finger tissue or through air, lowering the signal-to-noise ratio. The erroneous values are more common with warm than with cold fingers.

Vasoconstrictors

Cold vasoconstriction combined with a low pulse pressure (*e.g.*, after cardiac bypass) or an increase in venous pressure often precludes detection of Sp_{O_2} from fingers or at least delays detection of hypoxemia.[138] In ten pediatric patients deliberately surface-cooled to 25° C, the arterial oxygen saturation was overestimated by the pulse oximeter between 30° and 36° C and was underestimated below 30° C when the initial saturation was low.[139] Vasoconstriction in shock or cold may essentially stop flow through fingers without eliminating pulsatility in arterioles. This may result in gradual desaturation of the arterial blood remaining in the fingertips, either by diffusion through arterial walls or by movement in and out of sinusoids or capillaries. An example was noted in a cachectic

70-yr-old woman during hemorrhagic shock, initially treated with ephedrine.[77] Sp_{O_2} decreased from 98% to 45% while the heart rate detected by the oximeter continued to be correct at radial arterial P_{O_2} = 550 mmHg. Local finger desaturation has been confirmed during experimental hypotension and vasoconstriction.[77]

Finger vasoconstriction can prevent detection of the changes clearly shown with an ear probe.[140] Anecdotal reports suggest that a finger block with 0.25 ml 1% lidocaine on each side at the base of the finger may restore circulation and oximeter detection in the face of vasoconstriction induced by cold or hypotension. Grayson and Bourke[141] were able to restore oximetry signals for 1.5–2 h in five of five patients in whom finger signal had disappeared using 2 ml 2% lidocaine. Topical nitroglycerin paste on the finger has been used to reverse vasoconstriction, but with variable results. Spinal anesthesia strongly increased the pulse amplitude detected in the toe.[78,140]

Low-perfusion Limits

The low-perfusion limits of pulse oximetry were relatively unexplored in 1988. Since then, the low-pressure and -flow limits at which oximeters fail have been extensively investigated.[7,77,134–136,142] In volunteers, Severinghaus and Spellman[77] induced hand hypotension or vasoconstriction by several methods such as arm elevation in the lateral decubitus position (a nitroprusside infusion was required in several instances to induce signal detection failure), application of a carpenter's C-clamp slowly over the antecubital brachial artery, inflation of a brachial cuff, and intraarterial injection of norepinephrine. The three pulse oximeters tested were the Nellcor N200, the Ohmeda 3740, and the Criticare 504US. The mean systolic pressure at the threshold of function (mean of failure with decreasing pressure and recovery with increasing pressure) was 29.7 ± 12.8 mmHg with elevation, a test in which pulse pressure remains normal. No difference was found among the three oximeters. However, with partial clamping of the brachial artery, the Nellcor threshold was 47.1 ± 13.5 mmHg, significantly higher than those of the other two (38.7 ± 14.5 with Criticare, 36.0 ± 3.4 with Ohmeda). Norepinephrine injection further increased the thresholds. A potentially significant observation was that when pressure was just above threshold, detection of an induced hypoxic transient was delayed, in one case by 6 min. Also noted was a decrease of Sp_{O_2} despite normoxia in the awake volunteers, reaching on average 88.8 ± 11.5% Sp_{O_2} just before failure. The authors suggested that pulsation may continue to be detected in the absence of flow, such that oxygen may diffuse from either arteriole or capillary to finger tissue, causing an actual decrease in the pulsating blood oxygen saturation. These failure thresholds were considerably lower than those often seen clinically, suggesting that clinical failure is more often due to finger vasoconstriction than to hypotension.

The brachial arterial C-clamp method was also used by Falconer and Robinson[134] to compare failure and error rates in 13 pulse oximeters in volunteers at reduced pulse pressures during steady mild hypoxemia (80 < Sa_{O_2} < 88%). With pulse pressures between 11 and 20 mmHg, only the Physio-Control 1600 failed significantly more than the other instruments. At < 11 mmHg pulse pressure, the authors were able to rank instruments, reporting that "the Datex Satlite® was found to be more accurate than the average pulse oximeter, and, conversely, the Nellcor N100 and N200 without ECG link were found to be less accurate." They reported that the Nellcor N100, Nellcor N200 without ECG link, and Physio-Control 1600 defaulted to zero significantly more often than expected. The addition of an ECG link to the Nellcor N200 and Criticare 504US significantly increased the frequency of correct function at pulse pressures < 11 mmHg.

Clayton *et al.*[136] evaluated the performance of 20 pulse oximeters with finger probes by comparison of their readings with directly measured arterial blood oxygen saturations in patients who had low peripheral perfusion after cardiac surgery under hypothermic cardiopulmonary bypass. An overall ranking of performance of each pulse oximeter was calculated using five criteria (accuracy, precision, number of readings within 3% of standard, percentage of readings given within 3% of standard, and expected overread limit in 95% of cases). Two pulse oximeter models, the Datex Satlite and the Criticare CSI503, achieved a combination of accuracy and precision such that 95% of measurements would be expected to be within 4% of the laboratory oximeter value; these two also had the lowest dropout rate.

Morris *et al.*[7] compared the response of a group of oximeters to inflation of a brachial arm cuff to raise venous pressure, thereby lowering perfusion pressure. Some but not all appeared to show decreasing Sp_{O_2} as perfusion pressure decreased.

Oximetry during and after open heart surgery was investigated by Pälve and Vuori.[135] In 33 open-heart surgery patients immediately after open-heart surgery and in the intensive care unit after the operation, neither low cardiac index ($\leq$ 2.2 $l \cdot min^{-1} \cdot m^{-2}$) nor low peripheral temperature ($\leq$ 28° C) was found to affect the reliability of three different pulse oximeter models. Kurki *et al.*[143] found that an Ohmeda Biox III continued to function during nonpulsatile bypass, although with somewhat degraded accuracy, while a Nellcor N-100 ceased functioning.

Motion Artifact

This subject has also been explored more systematically, both in investigation and by anecdotal reports since 1988.

When subjects are awake, movement is the most common cause of failure and false alarm.[45] In 63 dental visits, 87–90% of the 235 desaturation episodes were due to patient movement. Similarly, in children with a diagnosis of croup there was poor correlation of clinical status and respiratory rate with low Sp_{O_2}.[144] Frequent dips in Sp_{O_2} were caused by technical problems such as movement artifact.

Probe motion may cause either absent or incorrect readings—the latter particularly if the motion contains frequencies of 0.5–4 Hz (heart rate range). The impression is widespread that shivering interferes. In an effort to simulate recovery shivering and transport, Langton and Hanning[145] vibrated the hand at 4–8 Hz. They noted artifactual decreases of Sp_{O_2} in some instruments (Ohmeda 3700 and Simed S100 but less in Nellcor N-200 with ECG link and Datex Satlite) and extra delay in the response to sudden inhalational hypoxia. Tonic–clonic seizures did not prevent the use of pulse oximeters to document and treat severe desaturation.[146] Vibrational motion during helicopter transport appears not to be a problem.[65,66]

In a study of eight pulse oximeters during moderate exercise on a cycloergometer, Barthelemy *et al.*[108] were able to distinguish two statistically different subgroups in which Datex, Physiocontrol, and Radiometer oximeters were accurate to within ±1.9% of Sa_{O_2} while Nellcor, Ohmeda, Novametrix, Kontron, and Hellige varied by ±2.8–5.0% from Sa_{O_2}.

During cardiopulmonary resuscitation, the body motion induced by rescuers can produce oximeter readings of about 85–90% Sp_{O_2} without any actual circulation,[147] in keeping with earlier observations that Sp_{O_2} displays that are generated by motion artifact often tend toward 85%, the Sp_{O_2} at which the alternating current/direct current (AC/DC) ratio of ratios is 1.0.[148,149]

While monitoring 23 infants with sleep apnea problems (sudden infant death syndrome) at home, Poets *et al.*[150] reported the pulse oximeter to fail in 7 of 69 apneic episodes because of signal loss from movement artifact, whereas they saw no failure of alarm with tcP_{O_2} monitoring, underscoring an the apparent advantage of tcP_{O_2} monitoring in this population. (See "Effect of Pulse Oximetry on Other Monitoring Methods").

To reduce motion artifact, several manufacturers couple the ECG signal to the oximeter to synchronize detection to heart rate (Nellcor N-200, Criticare US). To our knowledge, ECG coupling has not been studied in connection with shivering, although Langton and Hanning[145] found it to be useful when motion was artificially produced *via* an "industrial vibration facility." In a neonatal intensive care unit, Barrington *et al.*[104] reported a nearly 50% reduction (from an incidence of 4.1–2.1%) in motion artifact when ECG coupling was added in the neonatal intensive care unit. They found pulse oximeters to be unreliable for 11.9–25% of events when used in the short averaging mode (display representing average of < 6 s of data), and from 13.8% to 29% in the longer averaging mode. ECG coupling has also been claimed to be of use in experimental hypotension.[136]

Abnormal Pulses

Some oximeters detect a large dicrotic notch as a separate heartbeat, giving about twice the actual rate but (usually) a correct Sp_{O_2}. Venous pulsations due to tricuspid insufficiency[151] or ischemic cardiomyopathy have caused low Sp_{O_2},[152] and venous pulses have been blamed for low or absent readings on the forehead in supine patients.[136]

Ventilator-Induced Pulse Interference

With positive pressure ventilation, cycling venous and arterial pressure may cause continuous searching for an optimal signal in some instruments (*e.g.*, Nellcor).[153] One letter writer[154] makes a virtue of necessity by using ventilator-induced changes in oximeter pulse amplitude as an indicator of developing hypovolemia.

Response Times

Slow finger circulation due to cold vasoconstriction may delay responses by more than 1 min after pulmonary oxygen change at normal blood pressure and by much longer periods during severe hypotension.[77] Similar delays have not been reported when probes are used on the ear, forehead, nose, or lip.

Ambient Light

If ambient light is very strong, or is flickering at frequencies similar to harmonics of the light-emitting diode (LED) pulse rate, it may interfere with the rate and saturation measurements. (Manufacturers either synchronize LED pulse rates with harmonics of line power [Ohmeda] or choose rates with no harmonic overlap.) Some lights (fluorescent and especially xenon operating room lights) have caused both falsely normal and high readings even without a subject connected. In one rare instance,[155] a Nellcor N-100 probe continued to indicate 100% Sp_{O_2} in response to ambient light while the patient became hypoxic because of unrecognized extubation. A 15-W hand-held mercury vapor fluorescent light caused Nellcor readings to decrease dramatically in infants with disposable finger probes.[156] Although anecdotal reports have suggested interference by phototherapy lights and heaters, Zubrow *et al.*[157] were unable to find such effects in a newborn nursery.

Opaque covering of the probe is helpful in minimizing the effects of ambient light.

Electrocautery

Many early pulse oximeters failed in the presence of cautery. With design changes such as careful shielding and filtering, most oximeters are now somewhat better protected. Separation of the probe from the site of surgery and the ground pad may help if problems are seen. In a first-generation Kontron 7840, using an unshielded probe, the memory (random-access memory) was permanently "corrupted," presumably by electrocautery, causing it to read Sp_{O_2} = 95% and heart rate = 139 beats/min at all times.[158]

Interference of Magnetic Resonance Imaging

Ferromagnetic materials within or near the scanner can distort the magnetic field, and monitoring wires act as antennae and may cause granularity in magnetic resonance imaging (MRI).[159] In our own experience, there are remarkable differences between different oximeters, without obvious reason. Unfortunately, no one has reported a comparative study of a variety of pulse oximeters, so the user is left to testing and choosing for his or her own environment. MRI sometimes interferes with pulse oximetry, apparently because of radiofrequency signal detection; an abrupt change in Sp_{O_2} as imaging begins may indicate such interference. Grounding and filtering of radiofrequency have been shown to reduce or eliminate these problems,[160] but this may require special probe extender/couplers, with grounding of the oximeter cable shield to the nuclear magnetic resonance magnet case. In a recently described novel approach, fiberoptics replaced wires between the patient and device, eliminating both MRI interference and possible burns.‡

Alternative Sites

In general, the pulsatile or AC fraction of total light is smaller from the ears than from the fingers because the DC component is greater (thin ear transmits more light), so most pulse oximeters use the finger, except when peripheral vasoconstriction or hypotension limits finger perfusion. Initially, the Biox and Ohmeda ear probes were heated to 37° C to induce local vasodilation, but this practice has been discontinued. In infants, flexible probes work through the palm, foot, penis,[161] or even arm.[162] The bridge of the nose and nasal septum have been used, but for unknown reasons the Nellcor nasal (bridge) probe read 4.7 ± 1.4% higher than Sa_{O_2} in ten postoperative or nonoperated patients with mean Sa_{O_2} of 91% (range about 85–94%)[163,164] and 2.8 ± 3.9% too high in 15 post–cardiac surgery patients. Three other groups reported similar high-reading errors.[138,165,166] Probes have been mounted successfully across the tongue,[167,168] although they are difficult to maintain in place.[169] The cheek may be used by placing either a light source or a detector inside the mouth,[170] to be held in place by the malleable metal from the bridge of an oxygen mask so that the buccal mucosa and skin are transilluminated. The wing of the nostril provides a useful site.

It has often been noted that the Sp_{O_2} reading differs from site to site. The initial comparison of ear and finger sites by Severinghaus and Naifeh[171]—showing both faster response and greater accuracy at very low saturation for the ear—has been supplemented by Clayton *et al.*,[136] who studied the performances of ten pulse oximeters using finger probes and compared them to the same pulse oximeters using alternative probes (eight finger probes, two nose probes, and a forehead probe) in poorly perfused patients. Nose and forehead probes performed poorly. Some ear probes performed well compared to some finger probes, but the overall performance of probes in other sites compared to finger probes was worse (P = 0.05). Two of eight ear probes and no nose or forehead probes were reliable within 4% of the reference value in 95% of readings. Putative causes included 1) low blood flow causing actual desaturation of the pulsing blood due to local tissue oxygen consumption, 2) light leakage around instead of through the tissue, 3) venous pulsation, associated with venous congestion, and 4) variations of tissue thickness.[166] At low saturation, the ear read closer to Sa_{O_2} than the finger in most tested oximeters.[171]

Reflectance Operation

Adults

Cui *et al.*[172] reported the reflectance spectrum of blood in tissue. The peak absorption is in the green region (as with blood *in vitro*), suggesting that the largest pulse signal would be in that region, although that color is not used in present devices. Mendelson *et al.*[173,174] obtained satisfactory monitoring with a forehead reflectance probe of their own design. Cheng *et al.*[175] reported that a Criticare forehead probe performed well in healthy subjects but was less satisfactory in critically ill patients. Although this site might be expected to have some advantages in restless patients, reflectance from skin surfaces seems little used and has not yet been widely tested for accuracy. On the forehead at about 55% Sa_{O_2}, the bias and precision were found to average −0.7 ± 4.0% with Criticare, −0.2 ± 6.5

‡ Shellock FG, Kimble K, Myers S: Monitoring heart rate and oxygen saturation during MRI with a fiber-optic pulse oximeter (abstract). 10th Annual Meeting, Society of Magnetic Resonance Medicine 2: 974, 1991. Device: Nonin Inc. (Plymouth, MN).

with Datex, and −1.6 ± 5.5 with Kontron oximeters,[176] accuracies that matched or surpassed finger data with the same instruments. In each case the probes were experimental. A Simed forehead probe tested by Decker *et al.*[177] was less stable, more subject to motion artifact, and less accurate. Failure to detect signal is more common on the forehead than on the finger. Infrared light penetrates more deeply than red light,[178] so the paths of the two wavelengths traverse different tissue and thus detect different degrees of pulsatility. To obtain accurate tracking at low saturation, it was found that the infrared LED needed to be located slightly closer than the red LED to the detector and that the spacing between the infrared LED and detector should be at least 1 cm.[176]

At least one manufacturer is now actively marketing reflectance oximetry (Ciba-Corning). Barker *et al.*[179] found an unacceptable 59% signal failure rate for this instrument used on the forehead and a 27% rate for the same on the finger, compared to signal failure rates of 1.3–5.8% for various transmission oximetry finger probes.

Mendelson and McGinn[180] found reasonable agreement (within 2–3%) between a standard finger probe and reflectance sensors on the forearm and calf, but it is noteworthy that the reflectance sites required heating of the skin to 40° C to produce a detectable signal.

Fetal

Reflectance oximetry in the fetal presenting part has been investigated with mixed results. Johnson and associates reported reasonable data obtained by placing a reflectance probe on the fetal scalp *via* the vagina.[181] The authors restricted their study to labors involving vertex presentations without palpable caput or meconium staining of amniotic fluid. Continuous fetal monitoring was achieved in all 86 of the labors thus selected. Amniochorionic membranes did not appear to interfere with measurements either *in vitro* (by absorption spectrum analysis) or *in vivo.* The same group also monitored fetuses during caesarean section.[181] Another group[182] attempted application of pulse oximetry to intrapartum monitoring in 105 women. No adequate reading could be obtained in 44 cases. Two major sources of artifact, related to probe apposition and signal processing, were identified and excluded. The average Sp_{O_2} from the fetal scalp was 82% (standard deviation 6%), which is higher than has been inferred from P_{O_2} levels. Major problems were attachment of the probe and stagnant blood when palpable caput was present. Johnson *et al.*[183] focused on this issue by studying 20 neonates with significant caput succedaneum. The scalp average Sp_{O_2} was 69% when Sa_{O_2} was 84%, and in one extreme case at 90% Sa_{O_2} the caput sensor read 40%. These studies suggest the need for a probe designed to slip inside the cervix beyond the caput, when it is present.

Skin Pigments, Dyes, Nail Polish

In black patients, erroneously high readings (about 3–5%) and a higher incidence of signal detection failure have been reported.[61,184–186] In black people, the nail bed and fingertips are usually less pigmented than other areas of the skin. This effect has been simulated using an *in vitro* model.[187] Injected methylene blue and indocyanine green are known to produce transient false desaturation.[188] The effects of dyes, dyshemoglobins, and other pigments were recently reviewed by Ralston *et al.*[12] They pointed out that although nail polish reduces total light and may render the signal too small and cause up to 6% underestimation, probes can be mounted from side to side on a finger. (The effect of nail polish at low Sa_{O_2} has not been studied, but it is predicted to cause overestimation of Sa_{O_2}.)

For a comprehensive statement about the effect of nail polish on pulse oximetry, the work of Coté *et al.*[189] remains definitive. Their analysis, which considers the relative slopes of the nail polish absorbance curve at the two wavelengths of interest, has implications beyond the effects of nail polish; according to their research, pigment may cause error despite its nonpulsatility. Indirect evidence for this is provided by anecdotes about low Sp_{O_2} readings from fingerprinting ink (which can even be transferred from finger to oximeter probe),[190] from henna, a stain used by some Middle Eastern women on the fingers and toes,[191] and from meconium in newborns.[192]

Jaundice appears to have no direct effect on pulse oximetry but may cause confusion because it may be read by multiwavelength laboratory oximeters as increased carboxyhemoglobin (COHb) or methemoglobin (MetHb) or both, reducing the *in vitro* O_2Hb reading.[193] This laboratory error was found greatest with the IL282, less with the Corning Co-2500, and not at all with the Radiometer OSM3.[194] These authors[194] also caution that jaundiced patients often have truly elevated COHb and MetHb as well, which may reduce O_2Hb (but not Sa_{O_2}).

Carboxyhemoglobin and Methemoglobin

With pulse oximeters, COHb is nearly indistinguishable from O_2Hb.[195] In a clinical comparison of pulse oximeter Sp_{O_2} against values obtained from a laboratory blood oximeter in a patient with carbon monoxide poisoning, Sp_{O_2} was equal to the sum of the O_2Hb and COHb values, with COHb as great as 30%.[196] Multiwavelength laboratory blood oximeters read and report O_2Hb as a percentage, which can underestimate Sa_{O_2} by as much as the sum of the concentrations of COHb and MetHb. Consider, for example, a situation with 15% COHb and 10% HHb. The multiwavelength laboratory analyzer will report O_2Hb as 75%. (Some devices may term this "oxygen saturation.") Arterial oxygen saturation will be interpreted as approximately 90% by a pulse oximeter, measured as 90% by gasometric analysis, and computed as about 88% from blood gas analysis, due to the left shift of the dissociation curve caused by COHb. The pulse oximeter Sp_{O_2} of approximately 90% indicates the presence of 10% HHb, desaturated normal Hb, but neither pulse oximetry nor blood gas analysis provides any clue to the presence of COHb.

The effects of MetHb on pulse oximetry has been studied extensively.[197–204] MetHb absorbs both 660- and 940-nm light. Barker *et al.*[198] found that Sp_{O_2} readings decrease with MetHb, but by only about half of the MetHb percent concentration up to 20%, whereas at higher MetHb concentrations, Sp_{O_2} tends toward 85%. MetHb is commonly caused by use of 20% benzocaine sprays and ointments and may be first detected by pulse oximetry.[197,198,203,204]

When clinically significant levels of COHb or MetHb are suspected or known, *in vitro* blood gas analysis and oximetry should supplement pulse oximetry, not only because dyshemoglobins interfere with pulse oximetry but also because they decrease the oxygen-carrying capacity of blood.

Potential Dangers

Instances of second- and even third-degree skin burns have been reported in connection with pulse oximetry during MRI[205,206] due to induced skin current beneath looped pulse oximeter cables acting as antennae. Burns also have been caused by using probes with defects or defective designs[207] and by plugging a Physio-Control probe into an Ohmeda oximeter.[208] There is a possibility of pressure necrosis from some probes left on a single site too long (if a spring compresses the tissue or if tape is applied too tightly[209]). At high FI_{O_2}, changes such as hypoventilation or endobronchial intubation may cause large changes in Pa_{O_2} without altering Sa_{O_2} significantly and thus may go undetected by pulse oximetry. tcP_{O_2} monitoring, on the other hand, is relatively sensitive to such changes at high FI_{O_2}.[54] As Tremper and Barker[1] aptly put it, "the pulse oximeter is effectively a sentry standing at the 'cliff' of *desaturation*" (italics ours)—while tcP_{O_2} monitoring is stationed well up the road.

False Alarms and False Nonalarms

Most false alarms are due to motion. Pan and James[17] demonstrated in a study of 43 post–caesarean section patients monitored on the ward that 88% of false alarms could be avoided by incorporating a 60-s wait-period before sounding the alarm. When the lower Sp_{O_2} alarm limit was set at 90%, with a 60-s wait, the maximum frequency of alarms was reduced from 324 to 4 alarms per 24-h period per patient. It was originally expected[148] that some oximeters without adequate signal might continue to indicate a Sp_{O_2} of 80–90% when saturation is much lower. Direct attempts have failed to confirm this.[77] An instrument that frequently alarms or drops to zero because of motion or weak signals may be ignored by the physician when real desaturation has occurred. A low but nonzero reading should be treated as a danger signal of hypoxemia until proven otherwise, whereas a zero reading usually means no signal. Unfortunately, alarms may be so distracting when problems arise that users may turn them off or even turn the oximeter off if the alarm cannot be silenced, in order to concentrate on the problems.

Accuracy

The indices used to quantify error in connection with accuracy testing of oximeters have been criticized[1,210] and changed as investigators search for a single numerical description of accuracy. Regression analysis was soon found inadequate because in most studies no deliberate wide variations of Sa_{O_2} were introduced and because even a good correlation does not imply an accurate measurement, just as a poor correlation does not imply an inaccurate measurement. Bias, which is defined as the mean error ($Sp_{O_2} - Sa_{O_2}$) and its standard deviation are currently the preferred error indices,[1,2] but a single bias value derived from a large range of Sa_{O_2} (*e.g.*, 40–100%) is less than ideal because bias usually is greater at low Sa_{O_2}.[148,176] Bias and its standard deviation should therefore be presented as a function of Sa_{O_2} range. The standard deviation of the bias has sometimes been called "precision." However, precision has also been defined as mean absolute error. A bias of $10 \pm 1\%$ standard deviation would have a precision of 1% according to the former but 10% according to the latter. An additional possible confusing aspect is that a high numerical "precision" reflects a poor performance.

A table summarizing 39 accuracy studies from 1983 to 1988 was included in a previous review.[2] Subsequent studies of accuracy are likewise numerous.[7,49,101,211–217] In general, the claim of most manufacturers that errors are $< \pm 3\%$ at $Sa_{O_2} > 70\%$ has been confirmed.[10,11,171,176,216,218] Such studies continue to appear, sometimes with special groups of patients. In a subset of 17 patients with chronic obstructive pulmonary disease, Hannhart *et al.*[218] found consistent overestimation of Sa_{O_2} by Sp_{O_2} at low saturation in at least three oximeters (Nellcor, Ohmeda, and Critikon), but the bias was within 4% for all instruments. This group also found overestimation error with the same instruments in steady-state hypoxic tests in normal subjects. Their "gold standard," the two wavelength OSM-2 (Radiometer), is less dependable than the newer multiwavelength oximeters. Most other workers have not found similar high readings at low saturation.

Pulse oximeters may be considered more than sufficiently precise for most clinical purposes (except perhaps for detecting neonatal hyperoxia; see above). The above-described limitations on accuracy appear minor in comparison with requirements for effective patient monitoring. The device's ability to detect an unfavorable *trend* in oxygenation—subject to acknowledged limitations at high $F_{I_{O_2}}$ and in the presence of artifact—can be at least as important as its accuracy. In the clinical setting, pulse oximeters often function appropriately as "desaturation meters," with a low Sp_{O_2} taken to imply a low Sa_{O_2} until proven otherwise by clinical evaluation.

Effect of Anemia on Errors

Retrospective analysis in tests of 43 oximeters of 12 manufacturers[219] disclosed a negative error inversely proportional to Hb concentration when Sa_{O_2} was < 80%. The mean error when Sa_{O_2} = 54.5% appeared to be a nearly linear function of Hb concentration, with no error at 14.5 g/dl. In 45 determinations with 13 oximeters at Hb = 8.2 g/dl, the mean bias at 53% Sa_{O_2} was −15 ± 9%, of which 8% could be attributed to anemia and 7% to oximeter errors at normal Hb concentrations. This was a "fail-safe" error, providing exaggerated warning of hypoxemia in anemia.

Anemia has been studied in dogs by Lee *et al.*[220] The overall Sp_{O_2} bias and precision was 0.2 ± 7.6% for 178 points. Below 10% hematocrit, the bias and precision worsened to −5.4 ± 18.8%.

No errors or problems were detected in the use of pulse oximeters in 27 burned patients.[221]

In Vitro Methods of Testing The Accuracy of Pulse Oximeters

De Kock and Tarassenko[222] attempted to investigate the effect of a number of physiologic parameters on pulse oximetry accuracy in an *in vitro* model but limited their conclusions to the effects on the pulsatile or AC ratio of red to infrared light. At > 50% saturation, pulse oximeters were not affected by variations in hematocrit, blood flow rate, tissue blood content, or pulse amplitude. A variety of *in vitro* models have been tried in an effort to test oximeter response more simply, especially at very low saturation.[223–227] Volgyesi *et al.*, using a mechanical *in vitro* finger model with two oximeters,[225] reported a strongly positive (*i.e.*, dangerous) bias error (Sp_{O_2} − Sa_{O_2}) with normal Hb (16 g/dl) at low (50%) saturation. The error disappeared with 3-fold dilution of blood.[226] In view of the conflict between these *in vitro* results and the *in vivo* tests reported above, the validity of these finger models was inadequate as described. Volgyesi has been able to correct this error by use of a thinner (less opaque) model.§ Aoyagi and Miyasaka[227] devised a model finger with a layer of blood on one side of an elastic membrane and milk on the other side in a rigid opal cuvette. This model yielded a relationship (of Φ *vs.* S_{O_2}) "similar to that of the human finger" down to 60% S_{O_2} (the limit of testing). Φ is the ratio of ratios, $(AC_{red}/DC_{red})/(AC_{infrared}/DC_{infrared})$. However, neither this nor any *in vitro* calibration models have been documented *in vivo* as adequate to represent human responses at low saturation.

Evaluations of Pulse Oximeter Performance and Features

New to the literature on pulse oximetry is the *Consumer Reports*–style comparison of multiple features of several devices. Alexander *et al.*,[16] evaluating nine oximeters, compared 21 aspects of each, gave their ranking of overall performance, and judged four to perform significantly better than the other five (the Ohmeda 3700, In-Vivo 4500, Nellcor N-200, and Datascope Accusat, were better than the Criticare 501+, Physio-Control 1600, SARA, SensorMedics, and Catalyst MiniOx). This ranking differed from that based only on bias and precision data obtained at lower saturations[171,176] because accuracy (which they evaluated only down to $Sa_{O_2} \simeq$ 85%) contributed only a small and undefined part of their determination of performance rank. Morris *et al.*[7] compared 15 oximeters, listing 41 features, and were able to divide them into "two major groupings with considerable variation in each group." The reader is referred to these comparisons for further details.

The papers listed and described above (under "Accuracy") all are partial performance evaluations in that all of the tested instruments worked, providing useful data. The other features evaluated by Alexander *et al.*[16] and Morris *et al.*[7] should be considered in this context. There appears to be relatively little difference in failure at low perfusion and pressure among tested instruments, while some evidence does support differences in motion rejection as described (see "Limitations of Pulse Oximetry: Motion Artifact").

Does Pulse Oximetry Increase Patient Safety?

E. C. Pierce, Jr., President of the Anesthesia Patient Safety Foundation, recently suggested¶ that since 1984,

§ Volgyesi GA: Personal communication to Severinghaus JW. December 19, 1991.

¶ Pierce EC Jr: Anesthesia Patient Safety Movement, 1991. ASA Newsletter 55(11):4–8, 1991.

In my view, it is probable that mortality from anesthesia in the healthy patient has declined from the range of 1 to 2 deaths per 10,000 anesthetics to the range of 1 per 100,000 or more anesthetics, at least a 10-fold decrease.

If it is true, why has this change occurred? While technological advances in anesthesiology are considered a strong factor by many, perhaps more important is the way anesthesiologists view their practice today, given the explosion of anesthesia patient safety and risk management endeavors.

Is it possible to dissect from these improvements the contribution of pulse oximetry? Many of the studies reviewed above, like several earlier studies,[1,2] appear to demonstrate clearly that pulse oximetry is superior to clinical judgment (and to capnography[20]) in providing early warning of hypoxic events. Although this capability is accepted *prima facie* as impressive and valuable by most anesthesiologists, it is equally impressive that *no published investigation has yet demonstrated that pulse oximetry makes a difference in morbidity and mortality.* The task of making such a determination is daunting in view of the relative safety of anesthesia even before pulse oximetry was available; very large numbers of patients may be required.

In general, the myriad studies documenting clinically undetected hypoxemia aim only at description. They do not answer the questions raised by Fairley[228] and others: "What kind of desaturation is *unacceptable*? Under what circumstances? For how long? In whom?" (italics ours). No answers will ever satisfy all conditions for all observers and patients. At the physiologic level, recent pulse oximetry data do provide some surprises about how tolerable severe hypoxemia is in humans. Saturation cycling repeatedly down to 30–40% has been recorded during sleep without detectable brain or other systemic damage both in subjects with chronic mountain polycythemia[229] and in obese patients with chronic obstructive pulmonary disease and sleep apnea.[111,230] In addition, the subtle evidence of permanent brain injury reported by Hornbein *et al.*[231] in Mount Everest climbers was found in those who had the best hypoxic ventilatory drive, and who therefore were presumed to have been least hypoxic but most hypocapnic during exposure. On the other hand, when anesthesiologists find Sp_{O_2} decreasing from normal to 90% without evident cause, they may well judge this sufficiently unacceptable to warrant further investigation and therapy.

The near-uncritical enthusiasm that greeted the introduction of pulse oximetry has become tempered, especially in the past 3 yr, by commentary regarding the paucity of risk/benefit data. As Keats[18] so trenchantly observed, *prima facie* clinical impressions need not bear any relationship to what might be demonstrable *via* that grail of clinical research, the outcome study: "Without [outcome data on pulse oximetry] I can envision a subpopulation of this country walking around without their front teeth because of urgent intubation when an oximeter read less than 90%."[232]

Attempts to examine outcome with pulse oximetry date back to 1987 when Cooper *et al.*[233] showed that significantly fewer patients experienced "recovery room impact events" such as hypotension and dysrhythmia after pulse oximetry was introduced into the operating room. Their study fell short of establishing a cause-and-effect relationship, however, perhaps (as the authors suggest) because of insufficiently sensitive definitions of "impact events."

In 1988 Coté *et al.*[234] showed that "major hypoxic events" (Sp_{O_2} < 85% for ≥ 30 s) were significantly less common when pulse oximetry was available to the anesthesia team, and thereby drew editorial praise[235] for demonstrating the device's early-warning capability. Coté *et al.* also found, however, that "no morbidity was documented in any patient [in either group] who suffered an hypoxic event." The 1991 study by Coté *et al.*[21] makes no mention of differences in morbidity or mortality.

A 20,802-case prospective controlled study in Denmark in which half were monitored by pulse oximetry failed to show an effect of that monitoring on morbidity or mortality, except for a decreased incidence of intraoperative myocardial ischemia.[236,237] Although the final report has not been published, data in the abstracts suggest that there were 113 deaths in the monitored group and 94 in the group not using oximetry (difference not significant). Four deaths in each group (of 10,000) were believed to be related to anesthesia. (Note: this study included all ASA categories, which suggests that anesthesia-related deaths are more common in patients who are more severely ill.)

Another approach to assessing the benefits of pulse oximetry is retrospective. The Closed Claims Project of the Professional Liability Committee of the ASA[238] reported in 1989 a review of 1,175 claims from 17 insurance companies. The reviewers determined that, of 348 "preventable" injuries or deaths, "pulse oximetry . . . would have been efficacious in preventing injury in 138 cases."

The need for comparable routine use during postoperative transport and recovery is supported by evidence of hypoxic injury after discontinuation of operating room oximetry.**

Eichhorn,[239] in a 1989 analysis of the anesthetics of an estimated 1,001,000 ASA I and II patients in the Harvard hospitals between 1976 and mid-1988, found 11 major anesthesia-related accidents, 7 or 8 related to inadequate ventilation or oxygenation, only 1 of which occurred after pulse oximetry began to be used routinely in 1985. A thoughtful editorial by Orkin[240] accompanied the article, pointing out that this was not a statistically significant difference and that neither Eichhorn's nor any other work had yet shown clear evidence of a cost–benefit justification for additional monitoring, including pulse oximetry.

** Cheney FW: The ASA Closed Claims Project after the pulse oximeter: A preliminary look. ASA Newsletter 54:10, 1990.

Caplan *et al.*,[241] using the Closed Claims Project database, described 14 cardiac arrests in healthy patients during spinal anesthesia between 1978 and 1986. All were monitored by blood pressure cuff and 13 by ECG, but apparently none were monitored by pulse oximetry. In 12 of these patients, intravenous sedation or opioids had been given, although never "inappropriately or carelessly" in the reviewers' judgment. Because "half of the patients were verbalizing at the time of arrest," the authors believed that "respiratory changes produced by sedation may have played an important role in approximately one-half of the arrests." They postulated an adverse cascade of physiologic events, involving hypoxia, hypercapnia, vasodilation, and inability to maintain circulatory homeostasis in the face of sympathetic block. On the basis of this information, the authors recommended pulse oximetry when sedatives are given or the patient is otherwise not communicating well, but they refrained from judgments about whether any of the arrests might have been thereby "preventable."

More recent work by Caplan's group,[242] using cases from the Closed Claims Project database, has suggested the possibility that knowledge of the severity of outcome could influence a reviewer's judgment of the appropriateness of care, which may prompt a reinterpretation of the Closed Claims Project's findings about the preventability of injury by monitors. Keats,[243] commenting on ongoing Professional Liability Committee work, notes that "cases that only two years ago would have been classified as inadequate ventilation . . . now . . . have oximeters in place and they show no desaturation." In view of this very recent development, clinical intuitions about the benefits of pulse oximetry continue to await rigorous corroboration.

We conclude that pulse oximetry *probably* did contribute to the increasing safety of anesthesia. In one sense, however, this change may have come through the device's educational role in promoting vigilance and awareness of inadequacies in technique. We suspect that the experience anesthesiologists have had in the last decade with oximetry would ensure safer anesthesia even if a functioning oximeter were unobtainable. However, we may never be able to prove it.

Effect of Pulse Oximetry on Other Monitoring Methods

Pulse oximetry and tcP_{O_2} measurement were invented in the same year (1972). The need to protect premature infants from hyperoxia resulted in rapid application of tcP_{O_2} in nurseries within 5 yr, whereas pulse oximetry development and application required > 10 yr, as it awaited both technological development and realization of its potential benefits in all anesthesia and critical care settings.

tcP_{O_2} closely estimates Pa_{O_2} in hemodynamically stable infants, permitting control of oxygenation to avoid retinal oxygen damage (see "Role in Preventing Retinopathy of Prematurity"). Comparison of tcP_{O_2} with oximetry in hemodynamically stable infants and children showed no difference in the value of Sa_{O_2} computed from tcP_{O_2} *versus* measured Sa_{O_2} or Sp_{O_2}.[244,245] Poets *et al.*[150] compared oximetry and tcP_{O_2} as home monitors in 23 patients (age 0.5–40 months) with recurrent cyanotic episodes. Of 69 episodes in which the arterial oxygen saturation was ≤ 80% for ≥ 20 s and/or central cyanosis was present, the tcP_{O_2} monitor alarm sounded (≤ 20 mmHg or 2.67 kPa) in every episode. The pulse oximeter (Poet®, Criticare) identified hypoxemia in 62 of 69 episodes, failing in seven episodes because of signal loss from movement artifact. In 32 episodes in which Sa_{O_2} decreased to ≤ 60%, the tcP_{O_2} monitor alarm sounded after a median time interval of 16 s (maximum time interval 30 s). Indications for monitoring included apparently life-threatening events or cyanotic episodes (n = 163), prematurity and prematurity related disorders (n = 86), and sudden unexpected death in one or more siblings (n = 122).

In adults and during anesthesia, tcP_{O_2} is variable, usually averaging 60–80% of Pa_{O_2}.[244] However, pulse oximetry has several advantages over tcP_{O_2} monitoring: permanent calibration; speed; simplicity; extremely low incidence of burns; no drift; and no electrode membrane failures. Perhaps most important, oximetry can be used and maintained by personnel involved in direct patient care rather than by specially trained technical support staff. Accordingly, pulse oximetry has both supplemented and partially replaced tcP_{O_2} in the care of premature infants.

Because of pulse oximetry, the use of arterial blood gas analysis has decreased in patient care arenas,[59] but it remains essential for *p*H and P_{CO_2} measurement, for high P_{O_2} analysis in the determination of shunts, for instances when pulse oximetry fails, and for determination of whether a low Sp_{O_2} reading reflects arterial or only finger tissue hypoxia. By 1988, institutional surveys had already suggested that pulse oximetry had reduced the need for arterial blood gas analysis on various hospital services[2]; this was supplemented in 1991 by a study of 20,120 emergency-room visits in which physician orders for arterial blood gas analysis decreased by 37% without adversely affecting the quality of emergency care.[246]

Regulation, Insurance, Standards, and Cost

On January 1, 1990, pulse oximetry became an ASA standard for basic intraoperative monitoring, and after January 1, 1992 the same standard applied to the postanesthesia care unit,†† stated as follows: "During recovery from all anesthetics, a quantitative method of assessing oxygenation such as pulse oximetry shall be employed in the initial phase of recovery." An ASA publication‡‡ described the various state governmental, medical, and insurance regulation agency actions relative to the use of pulse oximetry. These efforts began in 1986 in Massachusetts with the establishment of a risk management unit in the Board of Registration in Medicine, set up by the state legislature "to provide technical assistance and quality assurance programs designed to reduce or stabilize the frequency, amount and cost of claims against physicians." The Board was given the authority to promulgate regulations requiring physicians to participate in risk management programs as a condition of licensure. The Medical Malpractice Joint Underwriting Association of Massachusetts was required, subject to the Insurance Commissioner's approval, "to impose a system of discounts for physicians or other insured who participate in risk management activities." By 1987 the Joint Underwriting Association and the Commissioner had approved the use of standards (243 CMR 3.00) that reduced premiums for "anesthesiologists who participate in risk management activities that would require the use of a pulse oximeter, whenever physically possible. . . . The 20 percent premium discount in 1989 translates into a savings of approximately $4000 per year for each anesthesiologist who holds a policy that provides $1 million/$3 million coverage." An updated review of state efforts has been published.§§

According to Pierce,¶ between 1985 and 1990, the "liability insurance relativity factor," an industry index of relative risk, decreased from 5.0 to 2.5–3.0. In the 1975–1978 period, anesthesia liability claims paid by members of the National Association of Insurance Commissioners were 367% of the average of all specialties' payments, whereas in 1986–1987, the ratio had fallen to equal the mean (103%, St. Paul Insurance Co). It may never be known whether the temporal relationship of reduced insurance costs and payments to the introduction of pulse oximetry was incidental or causal. Concurrent with the introduction of pulse oximetry came far greater emphasis on patient safety, increased use of capnometry, and appreciation, in part due to publication of closed claims analyses, that there were preventable gaps in anesthesia practice in which hypoxia occurred.

The American Society for Testing and Materials Committee has proposed a specification standard for pulse oximeters.¶¶ Similarly, the International Standardization Organization has proposed a draft standard for pulse oximeters.*** Neither document is final; the contents are subject to change; and their impact on manufacturers cannot be accurately foreseen.

Possible Effects of Oximetry on Anesthesiologists

Pulse oximetry is remarkable among monitors in that it involves no calibration, negligible time lag, and infrequent false negative data (*i.e.*, infrequent incorrectly high Sp_{O_2}) and requires no routine maintenance, no disposable components, no training, and little interpretation while it continuously and noninvasively displays a vital variable. Oximetry reduces dependence on blood gas analysis, obviates visual dependence on cyanosis to detect hypoxemia, and may make anesthesia safer (and, by implication, easier). Does it thereby threaten to make the anesthesiologist less vigilant, as suggested by Orkin?[240] What are the potential effects on anesthesiologists as well as on patients of increasing technological perfection? Can technology and vigilance coexist? Is Hein right in this grook?[247]

When technology is master
We shall reach disaster faster.

Monitors and associated computers, robots, and printers might replace three human functions: measuring, recording, and responding. An example is servo-control of administration of vapors depending on the patient's end-tidal concentration. Is a machine with alarms vigilant? Does it add to or subtract from supervision and care and attention? What will be the effect on vigilance of automatic generation of the anesthetic record, with which the vital signs can be precisely recorded without having to pass through the brain of the anesthetist?

Snow deplored the separation of intellectual human life into two cultures, sciences and humanities, unable to communicate with each other.[248] In anesthesia, the two-culture metaphor translates loosely into technology *versus* vigilance. The contemporary writer Robert Pirsig, in *Zen and the Art of Motorcycle Maintenance,*[249] traces Snow's two-

†† Standards for postanesthesia care. (Approved by House of Delegates on October 12, 1988 and last amended on October 23, 1990.) ASA Directory of Members, 56th edition, 1991, p 672.

‡‡ FYI . . . A commitment to patient safety. ASA Office of Government Affairs, 111 14th Street NW, Suite 501, Washington, DC 20005. January 1990, pp 1–12.

§§ Anesthesia Patient Safety Newsletter. Anesthesia Patient Safety Foundation 5(4):40–41, Winter 1990–1991.

¶¶ American Society for Testing and Materials document F29.03.10-005. Contact R. I. Godinez, M.D., Ph.D., Children's Hospital of Philadelphia, 34th Street and Civic Center Boulevard, Philadelphia, Pennsylvania 19104.

*** ISO/DIS 9919.2. Obtainable from ISO, Case postale 56, CH1221 Geneva 20, Switzerland.

culture dichotomy back to the dialogues of Plato. Pirsig maintains that a catastrophic loss of human cultural development over the past 2,500 yr resulted from alienation between the two cultures, a "Socratic" emphasis on discovery of the facts of nature, and a "Sophistic" preoccupation with merit, virtue, and excellence. The maintenance of the metaphoric motorcycle requires of its user both thorough knowledge of its mechanical workings and limitations and a resolute determination to use one's skills. To combine Socratic science—medical intelligence—with Sophist emphasis on quality in the healing art: that is the goal.

References

1. Tremper KK, Barker SJ: Pulse oximetry. ANESTHESIOLOGY 70:98–108, 1989
2. Kelleher JF: Pulse oximetry. J Clin Monit 5:37–62, 1989
3. Brown M, Vender JS: Noninvasive oxygen monitoring. Crit Care Clin 4:493–509, 1988
4. Lin WS, Chan KH: Clinical application of pulse oximeter (translation). Ma Tsui Hsueh Tsa Chi 26:77–90, 1988
5. Bowes WA 3d, Corke BC, Hulka J: Pulse oximetry: A review of the theory, accuracy, and clinical applications. Obstet Gynecol 74:(3 Pt 2)541–546, 1989
6. Striebel HW, Kretz FJ: The functional principle, reliability and limitations of pulse oximetry (Funktionsprinzip, Zuverlassigkeit und Grenzen der Pulsoximetrie). Anaesthesist 38:649–657, 1989
7. Morris RW, Nairn M, Torda TA: A comparison of fifteen pulse oximeters:1. A clinical comparison; II. A test of performance under conditions of poor perfusion. Anaesth Intensive Care 17: 62–73, 1989
8. Schnapp LM, Cohen NH: Pulse oximetry. Uses and abuses. Chest 98:1244–1250, 1990
9. Gravenstein JS: Gas monitoring and pulse oximetry. Boston, Butterworth-Heinemann, 1990, pp 84–148
10. Ralston AC, Webb RK, Runciman WB: Potential errors in pulse oximetry: 1. Pulse oximeter evaluation. Anesthesia 46:202–206, 1991
11. Webb RK, Ralston AC, Runciman WB: Potential errors in pulse oximetry: II. Effects of changes in saturation and signal quality. Anaesthesia 46:207–212, 1991
12. Ralston AC, Webb RK, Runciman WB: Potential errors in pulse oximetry: III. Effects of interferences, dyes, dyshemoglobins and other pigments. Anaesthesia 46:291–295, 1991
13. Severinghaus JW, Astrup P: The history of blood gas analysis: VI. The history of oximetry. J Clin Monit 2:270–288, 1986
14. Severinghaus JW, Astrup P: The history of blood gas analysis. Int Anesthesiology Clin 25:205–214, 1987
15. Blackwell GR: The technology of pulse oximetry. Biomed Instrum Technol 23:188–193, 1989
16. Alexander CM, Teller LE, Gross JB: Principles of pulse oximetry: Theoretical and practical considerations. Anesth Analg 68:368–376, 1989
17. Pan PH, James CF: Effects of default alarm limit settings on alarm distribution in telemetric pulse oximetry network in ward setting (abstract). ANESTHESIOLOGY 75:A405, 1991
18. Keats AS: The Rovenstine Lecture, 1983: Cardiovascular anesthesia: Perceptions and perspectives. ANESTHESIOLOGY 60:467–474, 1984
19. Moller JT, Johannessen NW, Berg H, Espersen K, Larsen LE: Hypoxaemia during anaesthesia: An observer study. Br J Anaesth 66:437–444, 1991
20. McKay WPS, Noble WH: Critical incidents detected by pulse oximetry during anesthesia. Can J Anaesth 35:265–269, 1988
21. Coté CJ, Rolf N, Liu LM, Goudsouzian NG, Ryan JF, Zaslavsky A, Gore R, Todres TD, Vassallo S, Polaner D, Alifimoff JK: A single-blind study of combined pulse oximetry and capnography in children. ANESTHESIOLOGY 74:980–987, 1991
22. Schulz C, Lenz G, Madee S, Schulze M: Frequency of hypoxic episodes during general anesthesia in children (Frequence des episodes hypoxiques au cours de l'anesthesie generale de l'enfant). Cah Anesthesiology 37:403–407, 1989
23. Morris RW, Buschman A, Warren DL, Philip JH, Raemer DB: The prevalence of hypoxemia detected by pulse oximetry during recovery from anesthesia. J Clin Monit 4:16–20, 1988
24. Murray RS, Raemer DB, Morris RW: Supplemental oxygen after ambulatory surgical procedures. Anesth Analg 67:967–970, 1988
25. Laycock GJ, McNicol LR: Hypoxaemia during recovery from anaesthesia: An audit of children after general anaesthesia for routine elective surgery. Anaesthesia 43:985–987, 1988
26. Smith DC, Canning JJ, Crul JF: Pulse oximetry in the recovery room. Anaesthesia 44:345–348, 1989
27. Thomson KD, Inoue T, Payne JP: The use of pulse oximetry in post-operative hypoxaemia in patients after propofol induction of anaesthesia. Int J Clin Monit Comput 6:7–10, 1989
28. McKenzie AJ: Perioperative hypoxaemia detected by intermittent pulse oximetry. Anaesth Intensive Care 17:412–417, 1989
29. Hudson RJ: Apnea and unconsciousness after apparent recovery from alfentanil-supplemented anaesthesia. Can J Anaesth 37: 255–257, 1990
30. Hardeman JH, Sabol SR, Goldwasser MS: Incidence of hypoxemia in the postanesthetic recovery room in patients having undergone intravenous sedation for outpatient oral surgery. J Oral Maxillofac Surg 48:942–944, 1990
31. Lampe GH, Wauk LZ, Whitendale P, Way WL, Kozmary SV, Donegan JH, Eger EI: Postoperative hypoxemia after nonabdominal surgery: A frequent event not caused by nitrous oxide. Anesth Analg 71:597–601, 1990
32. Moller JT, Wittrup M, Johansen SH: Hypoxemia in the postanesthesia care unit: An observer study. ANESTHESIOLOGY 73: 890–895, 1990
33. Rosenberg J, Rasmussen V, von Jesse F, Ullstad T, Kehlet H: Late postoperative episodic and constant hypoxaemia and associated ECG abnormalities. Br J Anaesth 65:684–691, 1990
34. Brown LT, Purcell GJ, Traugott FM: Hypoxaemia during postoperative recovery using continuous pulse oximetry. Anaesth Intensive Care 18:509–516, 1990
35. Croston J, Brown L: Hypoxemia after general anesthesia in healthy adults (Hipoxemia despues de anestesia general en adultos sanos). Rev Med Panama 15:230–234, 1990
36. Canet J, Ricos M, Vidal F: Early postoperative arterial desaturation: Determining factors and response to oxygen therapy. Anesth Analg 69:207–212, 1989
37. Schnapf BM: Oxygen desaturation during fiberoptic bronchoscopy in pediatric patients. Chest 99:591–594, 1991
38. O'Connor KW, Jones S: Oxygen desaturation is common and clinically underappreciated during elective endoscopic procedures. Gastrointest Endosc 36(suppl):S2–S4, 1990
39. Moore FA, Haenel JB, Moore EE, Abernathy CM: Hypoxic events in the surgical intensive care unit. Am J Surg 160:647–651, 1990

40. Bell GD: Monitoring and safety in endoscopy. Baillieres Clin Gastroenterol 5:79–98, 1991
41. Al-Hadeedi S, Leaper DJ: Falls in hemoglobin saturation during ERCP and upper gastrointestinal endoscopy. World J Surg 15: 88–94, 1991
42. Bendig DW: Pulse oximetry and upper intestinal endoscopy in infants and children. J Pediatr Gastroenterol Nutr 12:39–43, 1991
43. Bell GD, McCloy RF, Charlton JE, Campbell D, Dent NA, Gear MWL, Logan RFA, Swan CHJ: Recommendations for standards of sedation and patient monitoring during gastrointestinal endoscopy. Gut 32:823–827, 1991
44. Hempenstall PD, de Plater RM: Oxygen saturation during general anaesthesia and recovery for outpatient oral surgical procedures. Anaesth Intensive Care 18:517–521, 1990
45. Wilson S: Conscious sedation and pulse oximetry: False alarms? Pediatr Dent 12:228–232, 1990
46. Marjot R, Valentine SJ: Arterial oxygen saturation following premedication for cardiac surgery. Br J Anaesth 64:737–740, 1990
47. Minnich ME, Brown M, Clark RB, Miller FC, Thompson DS: Oxygen desaturation in women in labor. J Reprod Med 35: 693–696, 1990
48. Barrington KJ, Finer NN: Periodic breathing and apnea in preterm infants. Pediatr Res 27:118–121, 1990
49. Aughey K, Hess D, Eitel D, Bleecher K, Cooley M, Ogden C, Sabulsky N: An evaluation of pulse oximetry in prehospital care. Ann Emerg Med 20:887–891, 1991
50. Reissmann H, Beck H, Schontag G, Reimitz PE: Performance of a rescue breathing device with glossopalatinal tube (Die Leistungsfahigkeit eines Atemspende-Hilfsmittels mit glossopalatinalem Tubus). Anasth Intensivther Notfallmed 25:287–292, 1990
51. Viallard M, Sok S, Olivera C, Dehghani J, Riou B: Respiratory tract obstruction caused by ballooning of an intubation tube cuff during nitrous oxide inhalation (Obstruction des voies aeriennes par hernie du ballonnet de la sonde d'intubation au cours d'inhalation de protoxyde d'azote). Ann Fr Anesth Reanim 9:460–462, 1990
52. Sosis MB, Sisamis J: Pulse oximetry in confirmation of correct tracheal tube placement. Anesth Analg 71:309–310, 1990
53. Guggenberger H, Lenz G, Federle R: Early detection of inadvertent esophageal intubation: Pulse oximetry vs. capnography. Acta Anaesthesiol Scand 33:112–115, 1989
54. Barker SJ, Tremper KK, Hyatt J, Heitzmann H: Comparison of three oxygen monitors in detecting endobronchial intubation. J Clin Monit 4:240–243, 1988
55. Schrader M, Guggenberger H: Pulse oximetry: An indicator for the closure of a tracheostome after lateral fixation of the vocal cords (cordopexy) (Pulse oxymetrie: indicateur pour la fermeture d'un tracheostome apres fixation laterale des cordes vocales (cordopexie)). Rev Laryngol Otol Rhinol 111:173–175, 1990
56. Morrissey MS, Venn PJ, Chan HY, Whittet H: Detection of extrinsic bronchial compression during foreign body removal by pulse oximetry. J Laryngol Otol 104:50–51, 1990
57. Boorstein JM, Boorstein SM, Humphries GN, Johnston CC: Using helium-oxygen mixtures in the emergency management of acute upper airway obstruction. Ann Emerg Med 18:688–690, 1989
58. Brendle BC, Reus H, Morgan JA: Pulse oximetry monitoring of single lung anesthesia in non-cardiac thoracic surgery (Pulsoximetrische Uberwachung der Eine-Lunge-Anasthesie bei nichtkardialen thoraxchirurgischen Eingriffen). Anasth Intensivther Notfallmed 24:323–326, 1989
59. Withington DE, Ramsay JG, Saoud AT, Bilodeau J: Weaning from ventilation after cardiopulmonary bypass: Evaluation of a non-invasive technique. Can J Anaesth 38:15–19, 1991
60. Hirlinger WK, Friesdorf W, Brandt L, Lichtwark-Aschoff M: Improvement of oxygenation in thoracic surgery with one-lung ventilation using a new intraoperative CPAP device (Untersuchungen zur Verbesserung der Oxigenierung bei thoraxchirurgischen Eingriffen unter Ein-Lungen-Beatmung mit einem neuen intraoperativen CPAP-Gerat). Anaesthesist 38:437–439, 1989
61. Jubran A, Tobin MJ: Reliability of pulse oximetry in titrating supplemental oxygen therapy in ventilatory-dependent patients. Chest 97:1420–1425, 1990
62. Choi HJ, Little MS, Garber SZ, Tremper KK: Pulse oximetry for monitoring during ward analgesia: Epidural morphine versus parenteral narcotics. J Clin Monit 5:87–89, 1989
63. Bowton DL, Scuderi PE, Harris L, Haponik EF: Pulse oximetry monitoring outside the intensive care unit: Progress or problem? Ann Intern Med 115:450–454, 1991
64. Phillips GD, Runciman WB, Ilsley AH: Monitoring in emergency medicine. Resuscitation 18:(Suppl)S21–S35, 1989
65. Talke P, Nichols RJ, Traber DL: Monitoring patients during helicopter flight. J Clin Monit 6:139–140, 1990
66. Short L, Hecker RB, Middaugh RE, Menk EJ: A comparison of pulse oximeters during helicopter flight. J Emerg Med 7:639–643, 1989
67. Tiep BL: Long-term home oxygen therapy. Clin Chest Med 11: 505–521, 1990
68. Rosenberg B, Rosenberg M, Birkhan J: Allen's test performed by the pulse oximeter. Anaesthesia 43:515–516, 1988
69. Holm-Knudsen RJ, Nygard E, Ravn JB, Larsen VH: Cannulation of the radial artery: Risks, effective examination methods and monitoring of the circulation in the hand during the procedure (Kanylering af a. radialis. Risici, relevante undersogelsesmetoder og monitorering af handens kredslob i forbindelse med proceduren). Ugeskr Laeger 152:1278–1281, 1990
70. Levinsohn DG, Gordon L, Sessler DI: The Allen's test: Analysis of four methods. J Hand Surg [Am] 16A:279–282, 1991
71. Pillow K, Herrick IA: Pulse oximetry compared with Doppler ultrasound for assessment of collateral blood flow to the hand. Anaesthesia 46:388–390, 1991
72. Glavin RJ, Jones HM: Assessing collateral circulation in the hand: Four methods compared. Anaesthesia 44:594–595, 1989
73. Talke P, Nichols RJ, Traber DL: Does measurement of systolic blood pressure with a pulse oximeter correlate with conventional methods? J Clin Monit 6:5–9, 1990
74. Talke PO: Measurement of systolic blood pressure using pulse oximetry during helicopter flight. Crit Care Med 19:934–937, 1991
75. Wallace CT, Baker JD 3d, Alpert CC, Tankersley SJ, Conroy JM, Kerns RE: Comparison of blood pressure measurement by Doppler and by pulse oximetry techniques. Anesth Analg 66: 1018–1019, 1987
76. Holm-Knudsen RJ, Nielsen J, Ogstrup J: Measurement of systolic finger blood pressure with a pulse oximeter (Måling af systolisk fingerblodtryk ved hjaelp af pulsoximeter). Ugeskr Laeger 152: 3079–3081, 1990
77. Severinghaus JW, Spellman MJ Jr: Pulse oximeter failure thresholds in hypotension and ischemia. ANESTHESIOLOGY 73:532–537, 1990
78. Vegfors M, Tryggvason B, Sjöberg F: Assessment of peripheral blood flow using a pulse oximeter. J Clin Monit 6:1–4, 1990
79. Broome IJ, Mason RA: Identification of autonomic dysfunction with a pulse oximeter. Anaesthesia 43:833–836, 1988
80. Meier-Stauss P, Bucher HU, Hurlimann R, Konig V, Huch R:

Pulse oximetry used for documenting oxygen saturation and right-to-left shunting immediately after birth. Eur J Pediatr 149: 851–855, 1990
81. Joyce WP, Walsh K, Gough DB, Gorey TF, Fitzpatrick JM: Pulse oximetry: A new non-invasive assessment of peripheral arterial occlusive disease. Br J Surg 77:1115–1117, 1990
82. Lindsey LA, Watson JD, Quaba AA: Pulse oximetry in postoperative monitoring of free muscle flaps. Br J Plast Surg 44:27–29, 1991
83. McCleane G, Carragher AM, Bateson PG: Assessment of bowel viability using pulse oximetry. J R Coll Surg Edinb 35:388–389, 1990
84. DeNobile J, Guzzetta P, Patterson K: Pulse oximetry as a means of assessing bowel viability. J Surg Res 48:21–23, 1990
85. Agel J, Levy IM: The use of a pulse oximeter for the monitoring of digital pulse during shoulder arthroscopy. Arthroscopy 4: 124–125, 1988
86. Ray SA, Ivory JP, Beavis JP: Use of pulse oximetry during manipulation of supracondylar fractures of the humerus. Injury 22:103–104, 1991
87. Clay NR, Dent CM: Limitations of pulse oximetry to assess limb vascularity. J Bone Joint Surg [Br] 73:344, 1991
88. Hovagim AR, Backus WW, Manecke G, Lagasse R, Sidhu U, Poppers PJ: Pulse oximetry and patient positioning: A report of eight cases. ANESTHESIOLOGY 71:454–456, 1989
89. Menick FJ: The pulse oximeter in free muscle flap surgery: "A microvascular surgeon's sleep aid." J Reconstr Microsurg 4: 331–334, 1988
90. Barber RE, Lee J, Hamilton WK: Oxygen toxicity in man: a prospective study in patients with irreversible brain damage. N Engl J Med 283:1478–1484, 1970
91. Zierler S: Causes of retinopathy of prematurity: An epidemiologic perspective. Birth Defects 24:23–33, 1988
92. Bossi E, Koerner F: Patterns of simultaneously-measured P_aO_2 and P_aCO_2 levels in newborns developing retinopathy of prematurity. Pediatr Res 19:1128–1130, 1985
93. Cassady G: Relation between persistent patency of the ductus arteriosus and retinopathy of prematurity. Birth Defects 24: 53–66, 1988
94. Patz A: The role of oxygen in retrolental fibroplasia. Trans Am Ophthalmol Soc 66:940–985, 1968
95. Glass P: Role of light toxicity in the developing retinal vasculature. Birth Defects 24:103–117, 1988
96. Johns KS, Johns JA, Feman SS, Dodd DA: Retinopathy of prematurity in infants with cyanotic congenital heart disease. Am J Dis Child 145:200–203, 1990
97. Dziedzic K, Vidyasagar D: Pulse oximetry in neonatal intensive care. Clin Perinatol 16:177–197, 1989
98. Hay WW Jr: The uses, benefits and limitations of pulse oximetry in neonatal medicine: Consensus on key issues. J Perinatol 7: 347–349, 1987
99. Reynolds GJ, Yu VY: Guidelines for the use of pulse oximetry in the non-invasive estimation of oxygen saturation in oxygen-dependent newborn infants. Aust Paediatr J 24:346–350, 1988
100. Bucher HU, Fanconi S, Baeckert P, Duc G: Hyperoxia in newborn infants: detection by pulse oximetry. Pediatrics 84:226–230, 1989
101. Hay WW, Brockway JM, Eyzaguirre M: Neonatal pulse oximetry: Accuracy and reliability. Pediatrics 83:717–722, 1989
102. Mendelson Y, Kent JC: Variations in optical absorption spectra of adult and fetal hemoglobins and its effect on pulse oximetry. IEEE Trans Biomed Eng 36:844–848, 1989
103. Southall DP, Bignall S, Stebbens VA, Alexander JR, Rivers RP, Lissauer T: Pulse oximeter and transcutaneous arterial oxygen measurements in neonatal and paediatric intensive care. Arch Dis Child 62:882–888, 1987
104. Barrington KJ, Finer NN, Ryan CA: Evaluation of pulse oximetry as a continuous monitoring technique in the neonatal intensive care unit. Crit Care Med 16:1147–1153, 1988
105. Tremper KK: Monitoring with transcutaneous PO_2 and pulse oximetry devices, A panel summary: Monitoring of oxygen. Can J Anaesth 34:56–63, 1987
106. Dear PRF: Monitoring oxygen in the newborn: Saturation or partial pressure. Arch Dis Child 62:879–881, 1987
107. Wiswell TE: Pulse oximetry versus transcutaneous oxygen monitoring in perinatology applications. J Perinatol 7:331–332, 1987
108. Barthelemy JC, Geyssant A, Riffat J, Antoniadis A, Berruyer J, Lacour JR: Accuracy of pulse oximetry during moderate exercise: A comparative study. Scand J Clin Lab Invest 50:533–539, 1990
109. Breuer HW, Groeben H, Schondeling H, Worth H: Comparative analysis of arterial oxygen saturations during exercise by pulse oximetry, photometric measurements, and calculation procedures. Int J Sports Med 11:22–25, 1990
110. Dahan A, DeGoede J, Berkenbosch A, Olievier ICW: The influence of oxygen on the ventilatory response to carbon dioxide in man. J Physiol [Lond] 428:485–499, 1990
111. Brzecka A: The influence of obesity on disordered breathing in patients with obstructive sleep apnea syndrome, Control of breathing during sleep and anesthesia. Edited by Karczewski WA, Grieb P, Kulesza J, Bonsignore G. New York, Plenum, 1988, pp 43–46
112. Montgomery M, Wiebicke W, Bibi H, Pagtakhan RD, Pasterkamp H: Home measurement of oxygen saturation during sleep in patients with cystic fibrosis. Pediatr Pulmonol 7:29–34, 1989
113. Stark R, Kohler D: The value and consequences of nocturnal pulse oximetry in severe heart failure, suspected myocardial infarct and acute cerebral ischemia (Wertigkeit und Konsequenzen der nachtlichen Pulsoxymetrie bei schwergradiger Herzinsuffizienz, Verdacht auf Myokardinfarkt und bei akuter zerebraler Ischamie). Pneumologie 43(Suppl 1):596–599, 1989
114. Jackowski M, Fischer J, Korner K, Dahmen K: Study of the prevalence of sleep apnea syndrome in patients with chronic diseases of the respiratory organs using pulse oximetry and polysomnography (Untersuchungen zur Pravalenz des Schlafapnoe-Syndroms bei Patienten mit chronischen Erkrankungen der Atmungsorgane mittels Pulsoxymetrie und Polysomnographie). Pneumologie 43(suppl 1):600–602, 1989
115. Golding-Wood DG, Brockbank MJ, Swanston AR, Croft CB: Assessment of chronic snorers. J R Soc Med 83:363–367, 1990
116. Hoffarth HP, Rasche K, Marek W: Assessment of cyclic and phasic oxygen saturation using pulse oximetry in the diagnosis of nocturnal respiratory disorders (Beurteilung pulsoximetrisch erfasster zyklischer und phasenhafter Sauerstoffsattigungen der Diagnostik nachtlicher Atemregulationsstorungen). Pneumologie 45(suppl 1):229–232, 1991
117. Jense HG, Dubin SA, Silverstein PI, O'Leary-Escolas U: Effect of obesity on safe duration of apnea in anesthetized humans. Anesth Analg 72:89–93, 1991
118. Brodsky JB, McKlveen RE, Zelcer J, Margary JJ: Diffusion hypoxia: A reappraisal using pulse oximetry. J Clin Monit 4:244–246, 1988
119. Glanfield M: High altitude testing of pulse oximeter. Br Med J 297:1516, 1988
120. Schneck HJ, Gurtler R, Schneider N, Stock W: Air transportation of patients: A danger of hypoxic organ lesions? (Lufttransport von Patienten: Gefahr hypoxischer Organschaden?). Dtsch Med Wochenschr 114:123–127, 1989

121. Mehm WJ, Dillard TA, Berg BW, Dooley JW, Rajagopal KR: Accuracy of oxyhemoglobin saturation monitors during simulated altitude exposure of men with chronic obstructive pulmonary disease. Aviat Space Environ Med 62:418–421, 1991
122. Matheson GO, Allen PS, Ellinger DC, Hanstock CC, Gheorghiu D, McKenzie DC, Stanley C, Parkhouse WS, Hochachka PW. Skeletal muscle metabolism and work capacity: A ^{31}P-NMR study of Andean natives and lowlanders. J Appl Physiol 70:1963–1976, 1991
123. McKenzie DC, Goodman LS, Nath C, Davidson B, Matheson GO, Parkhouse WS, Hochachka PW, Allen PS, Stanley C, Ammann W: Cardiovascular adaptations in Andean natives after 6 wk of exposure to sea level. J Appl Physiol 70:2650–2655, 1991
124. Stanek KS, Guyton GP, Hurford WE, Park YS, Ahn DW, Qvist J, Falke KJ, Hong SK, Kobayashi H, Kobayashi K, Zapol WM: Continuous pulse oximetry in the breath-hold diving women of Korea and Japan (abstract). FASEB J 5:4385, 1991
125. Sendak MJ, Harris AP, Donham RT: Accuracy of pulse oximetry during arterial oxyhemoglobin desaturation in dogs. ANESTHESIOLOGY 68:111–114, 1988
126. Pfitzner J, Petito SP, McLean AG: Hypoxaemia following sustained low-volume venous air embolism in sheep. Anaesth Intensive Care 16:164–170, 1988
127. Erhardt W, Lendl C, Hipp R, Schindele M, Blumel G: Pulse oximetry: A non-invasive method for direct and continuous monitoring of oxygen saturation and pulse rate—comparative studies with blood gas analysis and hemoreflectometry in the dog, swine and sheep (Die Pulsoximetrie—ein nicht invasives Verfahren zur unmittelbaren und kontinuierlichen Uberwachung von Sauerstoffsattigung und Pulsfrequenz—Vergleichsstudien zur Blutgasanalyse und zum Hamoreflektometer an Hund, Schwein und Schaf). Berl Munch Tierarztl Wochenschr 102:289–292, 1989
128. Kurki TS, Harjula AL, Heikkila LJ, Lehtola AL, Hammainen P, Taskinen E, Mattila SP: Single-lung allotransplantation in pigs: Effects of two preservation methods on pulmonary gas exchange. J Heart Transplant 9:424–428, 1990
129. Whitehair KJ, Watney GC, Leith DE, Debowes RM: Pulse oximetry in horses. Vet Surg 19:243–248, 1990
130. Ahn ST, Mustoe TA: Effects of ischemia on ulcer wound healing: A new model in the rabbit ear. Ann Plast Surg 24:17–23, 1990
131. Decker MJ, Conrad KP, Strohl KP: Noninvasive oximetry in the rat. Biomed Instrum Technol 23:222–228, 1989
132. Freund PR, Overand PT, Cooper J, Jacobson L, Bosse S, Walker B, Posner KL, Cheney FW: A prospective study of intraoperative pulse oximetry failure. J Clin Monit 7:253–258, 1991
133. Gillies BSA, Overand PT, Bosse S, Walker B, Posner KL, Freund PR, Cheney FW: Failure rate of pulse oximetry in the post anesthesia care unit (abstract). ANESTHESIOLOGY 73:A1009, 1990
134. Falconer RJ, Robinson BJ: Comparison of pulse oximeters: Accuracy at low arterial pressure in volunteers. Br J Anaesth 65: 552–557, 1990
135. Pälve H, Vuori A: Accuracy of three pulse oximeters at low cardiac index and peripheral temperature. Crit Care Med 19:560–562, 1990
136. Clayton DG, Webb RK, Ralston AC, Duthie D, Runciman WB: A comparison of the performance of 20 pulse oximeters under conditions of poor perfusion. Anaesthesia 46:3–10, 1991
137. Kelleher JF, Ruff RH: The penumbra effect: Vasomotion-dependent pulse oximeter artifact due to probe malposition. ANESTHESIOLOGY 71:787–791, 1989
138. Langton JA, Lassey D, Hanning CD: Comparison of four pulse oximeters: effects of venous occlusion and cold-induced peripheral vasoconstriction. Br J Anaesth 65:245–247, 1990
139. Al Khudhairi D, Prabhu R, el Sharkawy M, Burtles R: Evaluation of a pulse oximeter during profound hypothermia: An assessment of the Biox 3700 during induction of hypothermia before cardiac surgery in paediatric patients. Int J Clin Monit Comput 7:217–222, 1990
140. Wilkins CJ, Moores M, Hanning CD: Comparison of pulse oximeters: Effects of vasoconstriction and venous engorgement. Br J Anaesth 62:439–444, 1989
141. Grayson RF, Bourke DL: Digital block for pulse oximetry failure (abstract). ANESTHESIOLOGY 75:3A407, 1991
142. Greenblott GB, Gerschultz S. Tremper KK: Blood flow limits and signal detection comparing five different models of pulse oximeters (correspondence). ANESTHESIOLOGY 70:367–368, 1989
143. Kurki TS, Smith NT, Sanford TJ, Head N: Pulse oximetry and finger blood pressure measurement during open heart surgery. J Clin Monit 5:221–228, 1989
144. Stoney PJ, Chakrabarti MK: Experience of pulse oximetry in children with croup. J Laryngol Otol 105:295–298, 1991
145. Langton JA, Hanning CD: Effect of motion artifact on pulse oximeters: Evaluation of four instruments and finger probes. Br J Anaesth 65:564–570, 1990
146. James MR, Marshall H, Carew-McColl M: Pulse oximetry during apparent tonic-clonic seizures. Lancet 337:394–395, 1991
147. Moorthy SS, Dierdorf SF, Schmidt SI: Erroneous pulse oximeter data during CPR (letter). Anesth Analg 70:339, 1990
148. Pologe JA: Pulse oximetry: Technical aspects of machine design, Advances in Oxygen Monitoring. Edited by Tremper K, Barker S. Int Anesthesiol Clin 25:137–176, 1987
149. Wukitsch MW, Petterson MT, Tobler DR, Pologe JA: Pulse oximetry: Analysis of theory, technology and practice. J Clin Monit 4:290–301, 1988
150. Poets CF, Samuels MP, Noyes JP, Jones KA, Southall DP: Home monitoring of transcutaneous oxygen tension in the early detection of hypoxaemia in infants and young children. Arch Dis Child 66:676–682, 1991
151. Skacel M, O'Hare E, Harrison D: Invalid information from the ear probe of a pulse oximeter in tricuspid incompetence (letter). Anaesth Intensive Care 18:270, 1990
152. Sami HM, Kleinman BS, Lonchyna VA: Central venous pulsations associated with a falsely low oxygen saturation measured by pulse oximetry. J Clin Monit 7:309–312, 1991
153. Scheller J, Loeb R: Respiratory artifact during pulse oximetry in critically ill patients. ANESTHESIOLOGY 69:602–603, 1988
154. James DJ, Brown RE Jr: Vascular volume monitoring with pulse oximetry during pediatric anaesthesia (letter). Can J Anaesth 37:266–267, 1990
155. Costarino AT, Davis DA, Keon TP: Falsely normal saturation reading with the pulse oximeter. ANESTHESIOLOGY 67:830–831, 1987
156. Amar D, Neidzwski J, Wald A, Finck AD: Fluorescent light interferes with pulse oximetry. J Clin Monit 5:135–136, 1989
157. Zubrow AB, Henderson GW, Imaizumi SO, Pleasure JR: Pulse oximetry in sick premature infants and the effects of phototherapy and radiant warmers on the oxygen saturation readout. Am J Perinatol 7:75–78, 1990
158. Broome IJ, Reynolds MI: A dangerous failure of a pulse oximeter (letter). Anaesthesia 45:166, 1990
159. Tommasino C, Beretta L, Cozzi S, Paolillo G, Torri G: Monitoring of pediatric patients undergoing magnetic resonance diagnosis with a superconducting magnet (Il monitoraggio del paziente pediatrico in corso di risonanza magnetica con un magnete superconduttore). Minerva Anestesiol 57:7–11, 1991

160. Wagle WA: Technique for RF isolation of a pulse oximeter in a 1.5-T MR unit (letter). AJNR 10:208–209, 1989
161. Robertson RE, Kaplan RF: Another site for the pulse oximeter probe. ANESTHESIOLOGY 74:198–198, 1991
162. Miyasaka K, Katayama M, Kusakawa I, Ohata J, Kawano T, Honma Y: Use of pulse oximetry in neonatal anesthesia. J Perinatol 7:343–345, 1987
163. Rosenberg J, Pedersen MH: Nasal pulse oximetry overestimates oxygen saturation. Anaesthesia 45:1070–1071, 1990
164. Rosenberg J, Pedersen MH, Dahl JB: Discrepancy between finger and nasal pulse oximetry (letter). Crit Care Med 18:582–583, 1990
165. Pälve H, Vuori A: Pulse oximetry during low cardiac output and hypothermia states immediately after open heart surgery. Crit Care Med 17:66–69, 1989
166. Broome IJ, Reilly CS: Explanation for the overestimation of oxygen saturation seen using nasal pulse oximetry (letter). Anaesthesia 46:424, 1991
167. Jobes DR, Nicolson SC: Monitoring of arterial hemoglobin oxygen saturation using a tongue sensor. Anesth Analg 67:186–188, 1988
168. Hickerson W, Morrell M, Cicala RS: Glossal pulse oximetry (letter). Anesth Analg 68:73–74, 1989
169. Lema GE: Oral pulse oximetry in small children (letter). Anesth Analg 72:414, 1991
170. Gunter JB: A buccal sensor for measuring arterial oxygen saturation. Anesth Analg 69:417–418, 1989
171. Severinghaus JW, Naifeh KH: Accuracy of response of six pulse oximeters to profound hypoxia. ANESTHESIOLOGY 67:551–558, 1987
172. Cui WJ, Ostrander LE, Lee BY: In vivo reflectance of blood and tissue as a function of light wavelength. IEEE Trans Biomed Eng 37:632–639, 1990
173. Mendelson Y, Kent JC, Yocum BL, Birle MJ: Design and evaluation of a new reflectance pulse oximeter sensor. Med Instrum 22:167–173, 1988
174. Mendelson Y, Ochs BD: Noninvasive pulse oximetry utilizing skin reflectance photoplethysmography. IEEE Trans Biomed Eng 35:798–805, 1988
175. Cheng EY, Hopwood MB, Kay J: Forehead pulse oximetry compared with finger pulse oximetry and arterial blood gas measurement. J Clin Monit 4:223–226, 1988
176. Severinghaus JW, Naifeh KH, Koh SO: Errors during profound hypoxia in 14 pulse oximeters. J Clin Monit 5:72–81, 1989
177. Decker MJ, Dickensheets D, Arnold JL, Cheung PW, Strohl KP: A comparison of a new reflectance oximeter with the Hewlett-Packard ear oximeter. Biomed Instrum Technol 24:122–126, 1990
178. Jöbsis-Vander Vliet FF, Piantadosi CA, Sylvia AL, Lucas SK, Keizer HH: Near-infrared monitoring of cerebral oxygen sufficiency. Neurol Res 10:7–17, 1988
179. Barker SJ, Le N, Hyatt J: Failure rates of transmission and reflectance pulse oximetry for various sensor sites (abstract). J Clin Monit 7:102, 1991
180. Mendelson Y, McGinn MJ: Skin reflectance pulse oximetry: In vivo measurements from the forearm and calf. J Clin Monit 7: 7–12, 1991
181. Johnson N, Johnson VA, Fisher J, Jobbings B, Bannister J, Lilford RJ: Fetal monitoring with pulse oximetry. Br J Obstet Gynaecol 98:36–41, 1991
182. Gardosi JO, Schram CM, Symonds EM: Adaptation of pulse oximetry for fetal monitoring during labour. Lancet 337:1265–1267, 1991
183. Johnson N, Johnson VA, Bannister J, Lilford RJ: The effect of caput succedaneum on oxygen saturation measurements. Br J Obstet Gynaecol 97:493–498, 1990
184. Cahan C, Decker MJ, Hoekje PL, Strohl KP: Agreement between noninvasive oximetric values for oxygen saturation. Chest 97: 814–819, 1990
185. Ries AL, Prewitt LM, Johnson JJ: Skin color and ear oximetry. Chest 96:287–290, 1989
186. Emery JR: Skin pigmentation as an influence on the accuracy of pulse oximetry. J Perinatol 7:329–330, 1987
187. Volgyesi GA, Spahr-Schopfer I: Does skin pigmentation affect the accuracy of pulse oximetry? (abstract). ANESTHESIOLOGY 75:3A406, 1991
188. Scheller MS, Unger RJ, Kelner MJ: Effects of intravenously administered dyes on pulse oximetry readings. ANESTHESIOLOGY 65:550–552, 1986
189. Coté CJ, Goldstein EA, Fuchsman WH, Hoaglin DC: The effect of nail polish on pulse oximetry. Anesth Analg 67:683–686, 1988
190. Battito MF: The effect of fingerprinting ink on pulse oximetry (letter). Anesth Analg 69:260–269, 1989
191. Goucke R: Hazards of henna (letter). Anesth Analg 69:416–416, 1989
192. Johnson N, Johnson VA, Bannister J, McNamara H: The effect of meconium on neonatal and fetal reflectance pulse oximetry. J Perinat Med 18:351–355, 1990
193. Beale SN, Moorthy SS: Jaundice, oximetry, and spurious hemoglobin desaturation (letter). Anesth Analg 68:806–807, 1989
194. Veyckemans F, Baele PL: More about jaundice and oximetry (letter). Anesth Analg 70:335–336, 1990
195. Barker SJ, Tremper KK: The effect of carbon monoxide inhalation on pulse oximetry and transcutaneous P_{O_2}. ANESTHESIOLOGY 66:677–679, 1987
196. Vegfors M, Lennmarken C: Carboxyhemoglobinemia and pulse oximetry. Br J Anaesth 66:625–626, 1991
197. Anderson ST, Hajduczek J, Barker SJ: Benzocaine-induced methemoglobinemia in an adult: Accuracy of pulse oximetry with methemoglobinemia. Anesth Analg 67:1099–1101, 1988
198. Barker SJ, Tremper KK, Hyatt J, Zaccari J: Effects of methemoglobinemia on pulse oximetry and mixed venous oximetry. ANESTHESIOLOGY 70:112–117, 1989
199. Watcha MF, Connor MT, Hing AV: Pulse oximetry in methemoglobinemia. Am J Dis Child 143:845–847, 1989
200. Rieder HU, Frei FJ, Zbinden AM, Thomson DA: Pulse oximetry in methaemoglobinaemia: Failure to detect low oxygen saturation. Anaesthesia 44:326–327, 1989
201. Bardoczky GI, Wathieu M, D'Hollander A: Prilocaine-induced methemoglobinemia evidenced by pulse oximetry. Acta Anaesthesiol Scand 34:162–164, 1990
202. Schweitzer SA: Spurious pulse oximeter desaturation due to methaemoglobinaemia. Anaesth Intensive Care 19:269–271, 1991
203. Delwood L, O'Flaherty D, Prejean EJ 3d, Giesecke AH: Methemoglobinemia and its effect on pulse oximetry (letter). Crit Care Med 19:988, 1991
204. Severinghaus JW, Xu F, Spellman MJ Jr: Benzocaine and methemoglobin: Recommended FDA action (letter). ANESTHESIOLOGY 74:385–386, 1991
205. Shellock FG, Slimp GL: Severe burn of the finger caused by using a pulse oximeter during MR imaging. Am J Roentgenol 153:1105–1106, 1989
206. Bashein G, Syrory G: Burns associated with pulse oximetry during magnetic resonance imaging. ANESTHESIOLOGY 75:382–383, 1991

207. Sloan TB: Finger injury by an oxygen saturation probe. ANESTHESIOLOGY 68:936–938, 1988
208. Murphy KG, Secunda JA, Rockoff MA: Severe burns from a pulse oximeter. ANESTHESIOLOGY 73:350–352, 1990
209. Rubin MM, Ford HC, Sadoff RS: Digital injury from a pulse oximeter probe. J Oral Maxillofac Surg 49:301–302, 1991
210. Gorback MS: Errors in 14 pulse oximeters during profound hypoxia (letter). J Clin Monit 6:158–159, 1990
211. Praud JP, Carofilis A, Bridey F, Lacaille F, Dehan M, Gaultier CL: Accuracy of two-wavelength pulse oximetry in neonates and infants. Pediatr Pulmonol 6:180–182, 1989
212. Martinez P, Haberer JP, Hannhart B, Saunier C, Laxenaire MC: Comparative evaluation of 13 pulse oximeters (Evaluation comparative de 13 oxymetres de pouls). Ann Fr Anesth Reanim 8: R225, 1989
213. Norreslet J, Ahlburg P, Knage K, Rasmussen JB: Testing and comparison of the accuracy and precision of 5 pulse oximeters (En afprovning og sammenligning af 5 pulsoxymetres nojagtighed og precision). Ugeskr Laeger 152:1906–1909, 1990
214. Hannhart B, Haberer JP, Saunier C, Laxennaire MC: Accuracy and precision of fourteen pulse oximeters. Eur Respir J 4:115–119, 1991
215. Lebecque P, Shango P, Stijns M, Vliers A, Coates AL: Pulse oximetry versus measured arterial oxygen saturation: A comparison of the Nellcor N100 and the Biox III. Pediatr Pulmonol 10:132–135, 1991
216. Taylor MB, Whitwam JG: The accuracy of pulse oximeters. A comparative clinical evaluation of five pulse oximeters. Anaesthesia 43:229–232, 1988
217. DePauw C, Poelaert J, Rolly G, Colardyn F: Clinical evaluation of pulse oximetry monitors on critically ill patients. Acta Anaesthesiol Belg 41:33–39, 1990
218. Hannhart B, Michalski H, Delorme N, Chapparo G, Polu JM: Reliability of six pulse oximeters in chronic obstructive pulmonary disease. Chest 99:842–846, 1991
219. Severinghaus JW, Koh SO: Effect of anemia on pulse oximeter accuracy at low saturation. J Clin Monit 6:85–88, 1990
220. Lee S, Tremper KK, Barker SJ: Effects of anemia on pulse oximetry and continuous mixed venous hemoglobin saturation monitoring in dogs. ANESTHESIOLOGY 75:118–122, 1991
221. Barillo DJ, Mastropieri CJ, Cohen MB, Okunski W: How accurate is pulse oximetry in patients with burn injuries? J Burn Care Rehabil 11:162–166, 1990
222. De Kock JP, Tarassenko L: In-vitro investigation of the factors affecting pulse oximetry. J Biomed Eng 13:61–66, 1991
223. Mendelson Y, Kent JC: An in-vitro tissue model for evaluating the effect of carboxyhemoglobin concentration on pulse oximetry. IEEE Trans Biomed Eng 36:625–627, 1989
224. Munley AJ, Sik MJ, Shaw A: A test object for assessing pulse oximeters. Lancet 1:1048–1049, 1989
225. Volgyesi GA, Kolesar R, Lerman J: An in vitro model for evaluating the accuracy of pulse oximeters (abstract). Can J Anaesth 37:S67, 1990
226. Kolesar R, Volgyesi G, Lerman J: Effect of haemoglobin concentration on the accuracy of pulse oximetry (abstract). Can J Anaes 37:S88, 1990
227. Aoyagi T, Miyasaka K: Pulse oximetry and its simulation. IEEE Tokyo Section Denshi Tokyo 29:184–187, 1990
228. Fairley HB: Changing perspectives in monitoring oxygenation (editorial). ANESTHESIOLOGY 70:2–4, 1989
229. Kryger M, Glas R, Jackson D, McCullough RE, Scoggin C, Grover RF, Weil JV: Impaired oxygenation during sleep in excessive polycythemia of high altitude: Improvement with respiratory stimulation. Sleep 1:3–17, 1978
230. Bradley TD, Phillipson EA: Pathogenesis and pathophysiology of the obstructive sleep apnea syndrome. Med Clin North Am 69:1169–1185, 1985
231. Hornbein TF, Townes BD, Schoene RB, Sutton JR, Houston CS: The cost to the central nervous system of climbing to extremely high altitude. N Engl J Med 321:1714–1719, 1989
232. Keats AS: Anesthesia mortality in perspective (editorial). Anesth Analg 71:113–119, 1990
233. Cooper JB, Cullen DJ, Nemeskal R, Hoaglin DC, Gevirtz CC, Csete M, Venable C: Effects of information feedback and pulse oximetry on the incidence of anesthesia complications. ANESTHESIOLOGY 67:686–694, 1987
234. Coté CJ, Goldstein EA, Coté MA, Hoaglin DC, Ryan JF: A single-blind study of pulse oximetry in children. ANESTHESIOLOGY 68:184–188, 1988
235. Cohen DE, Downes JJ, Raphaely RC: What difference does pulse oximetry make? (editorial). ANESTHESIOLOGY 68:181–183, 1988
236. Moller JT, Pedersen T, Johannessen NW, Rasmussen L, Espersen K, Dyrlung B, Jensen PF, Rasmussen NH, Ravlo O, Chraemmer-Jorgensen B, Djernes M, Wiberg-Jorgensen F, Cooper JB, Gravenstein JS, Johansen SH: Pulse oximetry does not reduce post-operative complications. A prospective study of 20,802 patients (abstract). ANESTHESIOLOGY 75:3A867, 1991
237. Moller JT, Ravlo O, Jensen PF, Rasmussen L, Dyrlund B, Espersen K, Pedersen T, Rasmussen NJ, Johannesen NW, Chraemmer-Jorgensen B, Djernes M, Wiberg-Johansen F, Cooper JB, Gravenstein JS, Johansen SH: Pulse oximetry uncovers hypoxemia and decreases the incidence of evidence for myocardial ischemia during anesthesia. A prospective study of 20,802 patients (abstract). ANESTHESIOLOGY 75:A1057, 1991
238. Tinker JH, Dull DL, Caplan RA, Ward RJ, Cheney FW: Role of monitoring devices in prevention of anesthetic mishaps. ANESTHESIOLOGY 71:541–546, 1989
239. Eichhorn J: Prevention of intraoperative anesthesia accidents and related severe injury through safety monitoring. ANESTHESIOLOGY 70:572–577, 1989
240. Orkin F: Practice standards: The Midas touch or the emperor's new clothes? (editorial). ANESTHESIOLOGY 70:567–571, 1989
241. Caplan RA, Ward RJ, Posner K, Cheney FW: Unexpected cardiac arrest during spinal anesthesia: A closed claims analysis of predisposing factors. ANESTHESIOLOGY 68:5–11, 1988
242. Caplan RA, Posner KL, Cheney FW: Effect of outcome on physician judgments of appropriateness of care. JAMA 265:1957–1960.
243. Keats AS: The closed claims study (editorial). ANESTHESIOLOGY 73:199–201, 1990
244. Tremper KK, Barker SJ: Transcutaneous oxygen measurement: Experimental studies and adult applications. Int Anesthesiol Clin 25:67–96, 1987
245. Ross RRI, Helms PJ: Comparative accuracy of pulse oximetry and transcutaneous oxygen in assessing arterial saturation in pediatric intensive care. Crit Care Med 18:725–727, 1990
246. Kellerman AL, Cofer CA, Joseph S, Hackman BB: Impact of portable pulse oximetry on arterial blood gas test ordering in an urban emergency department. Ann Emerg Med 20:130–134, 1991
247. Hein P: Grooks VI, Borgen's Pocketbooks 154. New York, Doubleday, 1978, pp 30–31
248. Snow CP: The Two Cultures and the Scientific Revolution. New York, Cambridge University Press, 1961
249. Pirsig RM: Zen and the Art of Motorcycle Maintenance. New York, William Morrow, 1974

APPENDIX I

MIO Alpha BLE Review

By Jill Duffy January 28, 2013

4.0 Excellent

THE BOTTOM LINE

For running, cycling, and plenty of other endurance sports, the MIO Alpha BLE represents a major upgrade in comfort and ease-of-use in heart rate monitors, but it's also quite expensive in comparison.

MSRP $199.99

Amazon Check Stock

PROS

- Reads heart rate without the need for a chest strap.
- Accurate.
- Comfortable.
- Rechargable battery.
- Waterproof.

CONS

- Somewhat expensive.
- Chunky.
- Heart rate is the only personal data measured.

Heart rate, as athletes know, indicates fitness and exercise intensity better than most other metrics. Until very recently, the only reliable way to measure heart rate was to wear a chest strap, as I did while testing the Digifit iCardio Multi-Sport Heart Rate Monitor. I can say from personal experience that they're not only uncomfortable, but also require another device to read their output, and try doing that while maintaining speed and watching where you're going. A new wristwatch, the MIO Alpha BLE ($199 direct) (at Amazon) reads heart rate through an optical sensor on its back and displays it in real time. Simple as that.

For running, cycling, and plenty of other endurance sports, the Alpha represents a huge upgrade in comfort and ease-of-use in heart rate monitors. It includes a number of useful features and settings, too, such as stopwatch functionality during which you can record your heart rate and keep track of your time spent in the zone (between the low and "up" heart rate you set for yourself). Considering the $200 price, though, the MIO Alpha BLE is somewhat expensive. Because I follow the rapidly growing field of activity trackers and other personal fitness gadgets, I wanted the Alpha to do a little more, such as measure distance traveled or steps taken, which it does not. You can get some of these stats by pairing the MIO with a compatible app, such as MapMyRun or RunKeeper, but I'd ideally like to see a pedometer-like reading right on the device itself.

Design

Much more comfortable than a chest strap, the MIO Alpha looks like a chunky sports watch, with a pliant, durable silicone band. The watch face, available in two accent colors, "shadow" (black) and "arctic" (white), displays data in large format using a negative dot matrix LCD, which makes it easy to read even in strong sunlight. On both the left and right of the watch is a single button that's flush against the watch face, for navigating the features and changing the settings.

SIMILAR PRODUCTS

3.5 Good

Motorola MotoActv

Read Our Motorola MotoActv Review

It also comes with a USB charging station for the rechargable lithium polymer battery, which attaches magnetically to the back of the watch.

I find the device rather attractive, and especially like the row of three holes in the band, for securing with a three-pronged clasp, that travel its entire length. The MIO Alpha should be worn a little higher on the arm and more snugly than a typical watch, as it needs to be in close contact with your skin to accurately read your heart rate. Of course, when you're not taking your heart rate, you can readjust it to wherever it's most comfortable.

How it Works

The MIO Alpha BLE works by using an optical sensor, located on the back of the watch, to read the volume of blood under your skin, and therefore take your pulse. The heart rate function does not run constantly. You have to turn it on and off. Press and hold the right side button, and it will read your current heart rate, displaying it on the watch face in real time. When you're not taking your heart rate,the MIO Alpha displays only the time.

Accuracy

In testing the MIO Alpha BLE, I took several readings of my resting heart rate just to get a sense of how the device worked and found it to always be within two beats per minute of my own reading (using the rudimentary two-fingers-to-the-neck method).

Then, I wore the watch to the gym and took a few more readings that I compared with the readings from the hand-grip sensors on some cardio equipment, which are sometimes accurate and sometimes ghastly off. I jumped on an elliptical trainer, took a few readings using the hand sensors to make sure they were at least within the range of my expectations (they were), and worked up a sweat. I turned on the Alpha MIO and started comparing. Every reading was once again within two beats per minute. Impressive.

Additional Features

The button to the left of the watch face activates additional features that make the MIO Alpha BLE a true athletic gadget. You can adjust your minimum and maximum desired heart rate (it defaults to 110 to 130 beats per minute), and while you're working out, the Alpha will beep if you're not in the desired zone. It also flashes a colored light to indicate whether you're over (red), under (blue), or within (green) the zone you set.

You can also turn on a stopwatch feature that lets you time an activity while reading your heart rate in the background, which is where the colored lights and audio cues really help, as you can hear them and see them from the corner of your eye without slowing down to focus on the precise reading.

To integrate your heart rate stats into other data from health and fitness apps, you'll need a mobile device with Bluetooth 4.0, and one of the following compatible apps: Adidas MiCoach, Endomo, MapMyRide, MapMyRun, RunKeeper, Strava, or Wahoo Fitness.

While the watch is waterproof and you can even swim while wearing it, the instructions warn against pressing the watch's buttons while underwater. You'll need to turn on the heart rate function and set up the timer before hopping into the pool.

Pricey, but Among the Best

I highly recommend the MIO Alpha BLE over a chest strap for any athlete or fitness buff looking to add heart rate to their personal data measurements. For the price, however, I do wish it had at least one or two more features for tracking activity directly, although for the time being, at least you can pair it with an app.

If in its second or third iteration the MIO Alpha can add a few key personal fitness tracking features, such steps taken and total distance traveled, it might be a five-star product. The question is whether it will get there first, as the competition is fierce—which is a good thing for consumers.

MIO Alpha BLE

4.0

PROS

- Reads heart rate without the need for a chest strap.
- Accurate.
- Comfortable.

View More

CONS

- Somewhat expensive.
- Chunky.
- Heart rate is the only personal data measured.

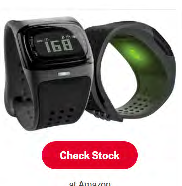

Check Stock

at Amazon

MSRP $199.99

THE BOTTOM LINE

For running, cycling, and plenty of other endurance sports, the MIO Alpha BLE represents a major upgrade in comfort and ease-of-use in heart rate monitors, but it's also quite expensive in comparison.

Comment or Add Your Own Review

0 0 Ratings

Log in | Sign up

Be the first to Review...

No one seems to have shared their thoughts on this topic yet

Leave a comment so your voice will be heard first.

Popular in the Community

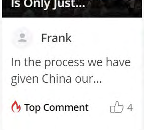

Frank

In the process we have given China our...

Top Comment 4

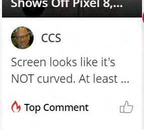

CCS

Screen looks like it's NOT curved. At least ...

Top Comment

FURTHER READING

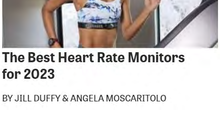

The Best Heart Rate Monitors for 2023

BY JILL DUFFY & ANGELA MOSCARITOLO

Give Your Eyes a Break: How to Choose the Right Blue Light Glasses

BY WILL GREENWALD

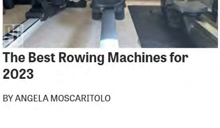

The Best Rowing Machines for 2023

BY ANGELA MOSCARITOLO

The Doctor Is In (Your Pho Online Therapy Services t

BY CHANDRA STEELE

TRENDING

The Best Internet Service Providers Methodology: How We Rate Broadband Providers

BY ERIC GRIFFITH

Apple's Impressive Emulation Tech Brings Popular Windows Games to Mac

BY GABRIEL ZAMORA

Twitter Deletes Photos Posted Between 2011-2014

BY EMILY PRICE

Roccat Vulcan II Mini Air

3.0

About Jill Duffy

Columnist and Deputy Managing Editor, Software

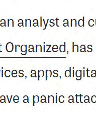

I've been contributing to PCMag since 2011, at times as an analyst and currently as deputy managing editor for the software team. My column, Get Organized, has been running on PCMag since 2012. It gives advice on how to manage all the devices, apps, digital photos, email, and other technology that can make you feel like you're going to have a panic attack.

My latest book is *The Everything Guide to Remote Work*, which goes into great detail about a subject that I've been covering as a writer and participating in personally since well before the COVID-19 pandemic.

I specialize in apps for productivity and collaboration, including project management software. I

APPENDIX J

Received October 29, 2014, accepted November 14, 2014, date of publication December 18, 2014, date of current version January 12, 2015.

Digital Object Identifier 10.1109/ACCESS.2014.2382179

A Neo-Reflective Wrist Pulse Oximeter

GRANTHAM PANG, (Senior Member, IEEE), and CHAO MA
Department of Electrical and Electronic Engineering, the University of Hong Kong, Hong Kong

Corresponding author: G. Pang (gpang@eee.hku.hk)

This work was supported by the CRGC through The University of Hong Kong, Hong Kong, under Grant 104002477.

ABSTRACT This paper relates to a genuine wrist pulse oximeter, which is a noninvasive medical device that can measure the pulse rate and oxygen saturation level in a person's blood. The device is novel due to its innovative design. It is a new type of reflective oximeter, which has a concave structure for housing the optical source and sensor. The neo-reflective sensor module of the device is designed to send the sensor data to a nearby intelligent mobile phone using wireless data transmission. The pulse oximeter has been developed and calibrated, and the calibration curve was analyzed. The innovative design of this pulse oximeter would enable the user to wear the low-cost device on one wrist continuously throughout the day, without the inconvenience of a conventional finger pulse oximeter.

INDEX TERMS Biomedical sensor, pulse oximetry, blood oxygen saturation, wrist oximeter, reflective oximetry.

I. INTRODUCTION

A pulse oximeter is a non-invasive medical device that can measure the pulse rate and oxygen saturation level in a person's blood. People with cardiac or pulmonary disease may check on their blood oxygenation continuously, especially while jogging or exercising. Pilots use them to determine if they need supplemental oxygen, especially when they fly a non-pressurized airplane. When climbing on high altitudes, alpinists may use pulse oximeters as well.

In the blood vessels, the hemoglobin with oxygen are called oxygenated hemoglobin (oxy Hb), whereas the hemoglobin without oxygen are called deoxygenated hemoglobin (deoxy Hb). The basic principle of operation of a pulse oximeter depends on the use of LED light, which is used to determine the oxygen saturation. In particular, red LED light of around 630nm wavelength and infrared LED light of around 880nm wavelength are utilized. (Some pulse oximeters use LEDs of around 660nm and 940 nm wavelengths.) It must be noted that oxy Hb absorbs red and infrared light differently. One fundamental property is that oxy Hb absorbs more infrared light than red light, whereas deoxy Hb absorbs more red light than infrared light. A pulse oximeter calculates the oxygen saturation by comparing how much red light and infrared light are absorbed by the blood.

Currently, there are many different models of pulse oximeters in the market. They differ in size, quality and cost. The complex ones used in hospitals are typically large and not portable. However, there are many hand held pulse oximeters for home use which are very compact and easy to use. The most common model is the finger model, which displays the blood oxygenation level (SpO_2) and pulse rate.

A wrist-finger model is very common in the market [1]. The device is actually a finger model as the sensor is placed on a finger which is then connected to a wrist display. Yet, the pulse oximeter on the finger is quite noticeable and the finger may not be too comfortable for long period and continuous monitoring. Early work on reflectance type of pulse oximeter have been carried out by Mendelson et al. [2], [3]. Design to lower the power consumption has also been studied in [4] and [5].

The development of a small-sized reflectance pulse oximeter was investigated by Santha et al. [6]. The distance between the light sources and the detector was examined, as well as the pressure of the reflective pulse oximeter sensor head onto the skin. In [7], a reflectance pulse oximeter with circuitry and method for obtaining the percentage of oxygen saturation is given. A microcomputer is used for the signal processing, as well as the calculation of the oxygen saturation based on the input light intensity signals.

A wrist-worn pulse oximeter is described in [8] which has illustrated the feasibility of reflectance oximetry based on a sensor mounted onto a wrist band. The motivation is that the typical finger-tip model is a transmittance pulse oximeter, and is practical only when the patient is hospitalized or lying steadily. Usually, the sensor would press on a finger or the ear lobe which would sometimes cause discomfort or pain as the sensor would block the blood flow. In their prototype model, the reflectance sensor and LED light source are mounted onto a wrist band of width 30mm. The wristband sensor design is novel and a wireless data transmission module would further enable the data to be sent to a remote receiver for processing and display. Yet, the calibration of the oximeter and further details on the implementation are not shown.

In [9], a ring-shaped photodiode designed for use in a reflectance pulse oximetry sensor is shown. Li and Warren [10] have also developed a small and low-cost wireless reflectance oximeter suitable for wearable and surface-based applications including at the wrist location. High quality photoplethysmographic (PPG) data can be collected. Further signal processing is needed to obtain the actual value of oxygen saturation. In [11], another reflectance type PPG device is developed for the continuous monitoring of arterial oxygen saturation. The result obtained was in good agreement with the finger PPG.

II. THE INNOVATIVE FEATURES OF A NEO-REFLECTIVE WRIST PULSE OXIMETER

In this paper, we present another novel reflective wrist pulse oximeter that has been developed in our laboratory. As mentioned in the previous section, recent mature technology and products of oximeter are mostly based on the principle of transmittance of light through a finger. However, oximetry based on the principle of light reflectance from human tissue has a great potential for wide acceptance. In our design, the light source and sensor are placed in a concave structure using the principle of reflective oximetry. In addition, the design is for wrist wearing as it is a more convenient and comfortable location than the finger for long duration measurement and continuous monitoring. It must be noted that for pulse and blood pressure monitoring, some products located at the wrist already exist in the market (e.g. Casio BP-100 and Omron HEM-608).

To summarize, our design has a novel sensor module design. A concave structure is designed to house the sensor module components so as to obtain improved operational efficiency when collecting the wrist pulse signals. In order to obtain desirable wrist pulse signals, the sensor module is designed to be placed at an inner part of the wrist. The special design of its concave shape helps the sensor module to stay in the chosen location of the wrist. The device has a very simple hardware structure without even a display because all data further processing, calculations and display will not be carried out on the wearable wrist device. A wireless transmission module will transmit all sensor data to an application of a nearby smart phone, which would perform all those tasks. Hence, the device can communicate in a cordless manner with a remote monitoring system. The radio interface can use the Bluetooth protocol.

III. PRINCIPLE OF OPERATION OF REFLECTIVE OXIMETRY

The scattering coefficient is much bigger than the absorption coefficient for most human tissue. Therefore, it is possible to build a model where the photon movement in the body tissue can be considered as a diffusion process, when the geometric dimension is bigger than the scattering length, and then the photon will mainly scatter before it get sized by the photo-transistor. Therefore, light through wrist tissue can be described by photon diffusion equation [8]:

$$\frac{1}{c}\frac{\partial}{\partial t}\emptyset(r,t) - D\nabla^2\emptyset(r,t) + \mu_a\emptyset(r,t) = S(r,t) \tag{1}$$

where $\emptyset(r, t)$ is the fluence rate, which represents the effective photon density at the position r and at time t. D denotes a diffusion coefficient, μ_a represents absorption coefficient of the tissue and S(r, t) represents the light source.

Hence, the density of the photon reflecting from the body tissue is determined by the flux of the illumination and the detected light intensity. The equation of the density of the photon reflected is [8]:

$$R(\rho, r, t) = (4\pi Dc)^{-3/2} Z_0 t^{-5/2} \exp(-\mu_a ct)\exp(-\frac{\rho^2 + z_0^2}{4Dct}) \tag{2}$$

When time is long enough, the change ratio of reflected light intensity will be close to $-\mu_a ct$, as below:

$$\lim_{t\to\infty} \frac{\partial}{\partial t} \ln R(\rho, r, t) = -\mu_a ct \tag{3}$$

As a result, the change ratio of reflected light intensity $W = I_{AC}/I_{DC}$ is proportional to the absorption coefficient of the tissue. The AC part of the signal represents absorption of fluctuating wave of pulsing blood, while the DC part represents absorption of human tissue and vessel.

The absorption of red and infrared light by oxygenated hemoglobin (HbO2) and reduced hemoglobin (Hb) is much bigger than that by other human tissue or water. Besides at different wavelengths, the light absorbance of HbO2 and Hb are different. By this principle, we can deduce the oxygen saturation from the different ratio of reflective light intensity rate when two light with different wavelengths go through vessel blood inside human tissue [7], [8].

$$\begin{aligned} SpO_2 &= \alpha - \beta\frac{W_{\lambda 1}}{W_{\lambda 2}} = \alpha - \beta\frac{I_{AC}^{\lambda 1}/I_{DC}^{\lambda 1}}{I_{AC}^{\lambda 2}/I_{DC}^{\lambda 2}} \\ SpO_2 &= \alpha - \beta R \end{aligned} \tag{4}$$

where R is defined as follows:

$$R = \frac{I_{AC}^{\lambda 1}/I_{DC}^{\lambda 1}}{I_{AC}^{\lambda 2}/I_{DC}^{\lambda 2}}$$

and α, β are parameters that need to be determined experimentally. Hence, when the values of the DC and AC component of the red and infrared light intensity are obtained, the blood oxygen saturation can be calculated.

Equation (4) has assumed a linear relationship between oxygen saturation and the R value, which is commonly used in the field and in the market products. Yet, considering the differences in light intensities between red and infrared light, it is also reasonable to state a second-order relationship between R and the oxygen saturation:

$$SpO_2 = \alpha - \beta R - \gamma R^2 \tag{5}$$

The parameters α, β and γ can be determined in an experimental study. It can be shown that the second order equation can potentially provide a more accurate calculation for the value of oxygen saturation.

IV. SYSTEM DESIGN

Fig. 1 gives the overall system design of the reflective oximeter, which consists of Concave Sensor Module, Signal Processing Module, A/D Converter Module, Wireless Transmission Module and Smart Phone.

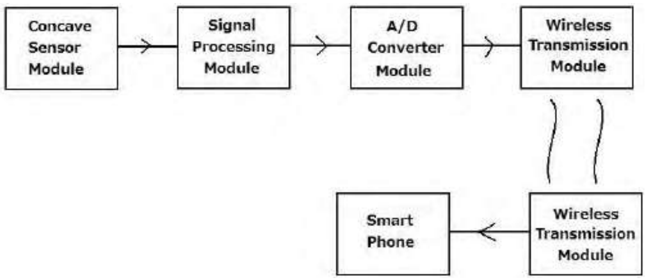

FIGURE 1. System design diagram.

The Concave Sensor Module is used to acquire the original light signal reflected from fluctuating blood and tissue. In the Signal Processing Module, the original signal is separated into a DC and AC component.

In the A/D converter Module, the analog signal is transferred to the digital signal by sampling and regulating. This is because the digital signal is easier to be transferred by wireless transmission module and more suitable for further processing and application.

The Wireless Transmission Module is made of a transmitter and a receiver, which would establish a communication link between the wrist band and the smart phone. Fig. 2 shows the wireless transmission of sensor data from the wrist worn pulse oximeter to the smart phone.

FIGURE 2. Wireless transmission of sensor data from the wrist pulse oximeter.

Further signal processing and computing are done in the application in the smart phone for saving hardware. The result can also be displayed by the smart phone and the data can be stored inside the smart phone. As a result of using minimal hardware for the device and the use of a flexible software solution for handling the sensor data, the cost of device will be very low. In this paper, we focus on the description of the wrist concave sensor and the signal processing module.

V. CONCAVE SENSOR MODULE

As shown in Fig. 3 and Fig. 4, the concave oximeter sensor consists of a concave support structure, one red LED and one infrared LED and two photo-transistors.

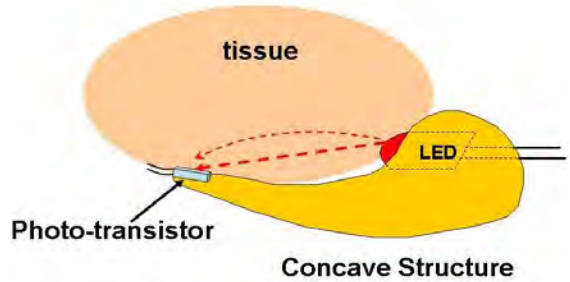

FIGURE 3. Section plan of Concave Sensor Module

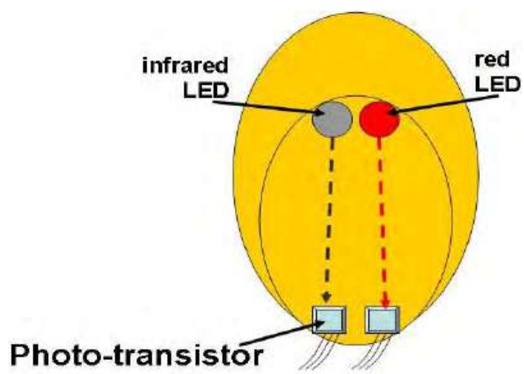

FIGURE 4. Top view of Concave Sensor Module.

The soft concave support structure matches with the convexity of the human wrist, with the two LEDs inside the pinhole. The two photo-transistors are placed on the other end of the structure at a suitable distance from the LEDs. The separation distance has been verified after many experiments.

The peak wavelengths of the red LED and infrared LED are 630nm and 880nm respectively, which are sensitive to the changes in oxygen saturation.

The photo-transistors are placed directly in contact with the skin and their flat surfaces would not cause any discomfort to the wrist. The photo-transistors have nearly the same spectral responsivity at wavelength of 630nm and 880nm, which would have the same the sensitivity for better accuracy.

The black cover wrist band attaches the structure to the wrist tightly to make it wearable, stable and comfortable, and also to reduce noise effect.

The implemented sensor after many testing experiments is shown in Fig. 5, and the sensor with further plan is shown in Fig. 6. At the moment, the wireless data transmission module has not been implemented yet.

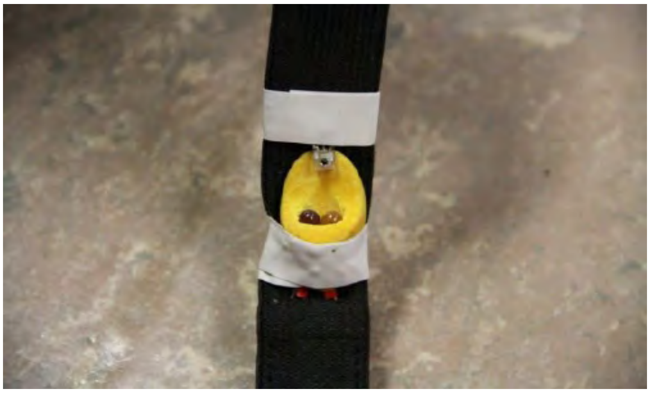

FIGURE 5. Photo of the implemented sensor.

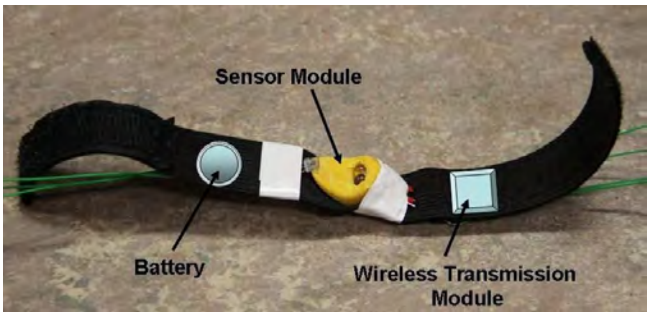

FIGURE 6. Photo of the sensor with further plan.

VI. SIGNAL PROCESSING MODULE

The Fig. 7 shows the diagram of the signal processing module consisting of pass filters and amplifiers, providing signal processing of wave filtering and amplifying. The received signal reflected from blood contains AC signal and DC signal, which are separated by the pass filters and then amplified respectively.

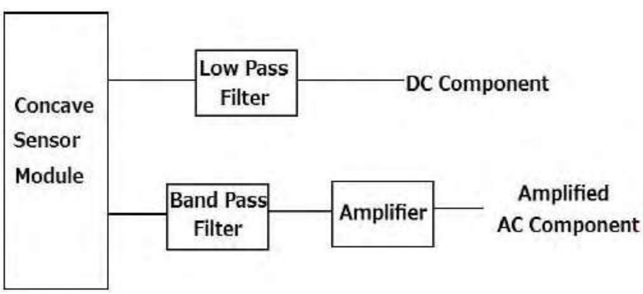

FIGURE 7. Diagram of signal processing module.

The DC Component is filtered by low pass filter (LPF). Circuit Diagram of low pass filter is shown in Fig. 8. The Corner Frequency of low pass filter is 0.16 Hz. As a result, the LPF can filter fluctuating pulse wave (AC Component) and high frequency noise such as interference from daylight lamp and electromagnetic interference from power source.

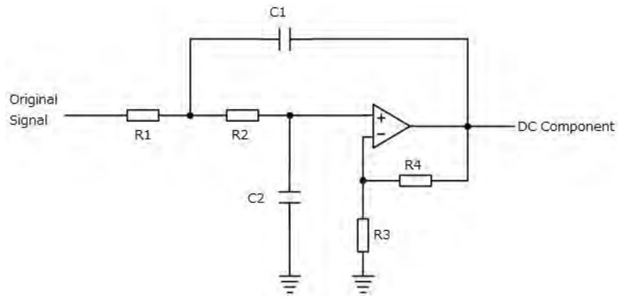

FIGURE 8. Circuit diagram of low pass filter.

The AC Component is through a band pass filter and an amplifier. Circuit diagram of Band Pass filter (BPF) and amplifier (shown with LED and Photo-transistor) is given in Fig. 9. The Center Frequency of the BPF is 1 Hz, which is close to the normal pulse frequency of a person. As a result, the BPF can filter the signal that is caused by light going through the body tissue and vein (DC Component) as well as high frequency noise such as interference from electromagnetic interference from power source and daylight lamp. As the AC component of the signal is too small (about 1 mV), an amplifier is used to amplify it for further processing.

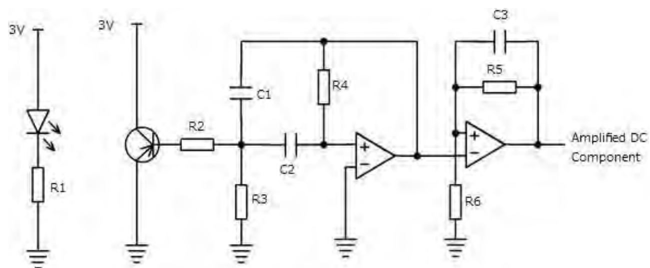

FIGURE 9. Circuit diagram of band pass filter and amplifier (shown with LED and photo-transistor).

The AC and DC signals of red and infrared light are used together to compute the oxygen saturation by equation (4). The computation can be carried out by the application inside a smart phone.

The AC signal is also used to obtain the pulse waveform. By calculating the cycle of pulse waves, we can get the heart rate. The AC signal presenting the pulse wave has other values of further medical research, which can be developed by other applications in the smart phone.

VII. SYSTEM IMPLEMENTATION AND EXPERIMENTAL RESUALTS

In Fig. 10, the overall system implementation is shown. The supply voltage to the prototype is 3V.

The experimental results of the AC pulse signals obtained by red LED and infrared LED are shown

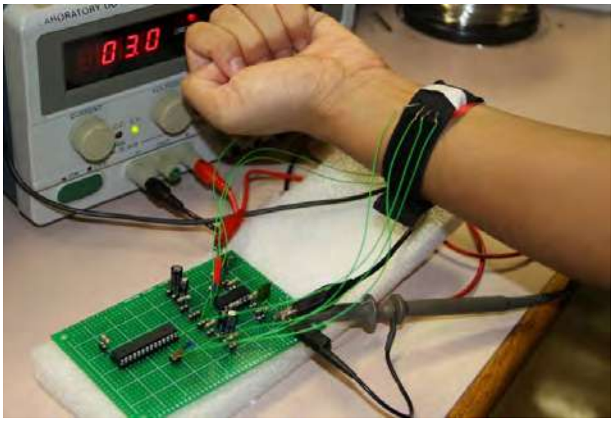

FIGURE 10. The photo of the overall implementation.

in Fig. 11 and Fig. 12 respectively. A section of the recorded data verses time are shown. The two recorded photoplethysmograms both display the cardiovascular cycle clearly.

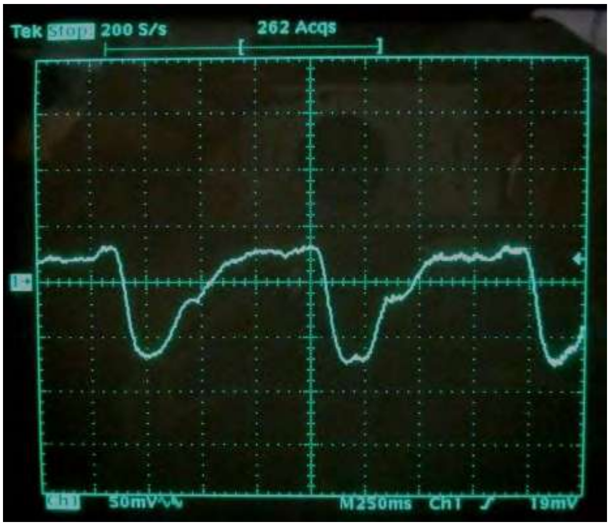

FIGURE 11. The pulse signal obtained by the red LED.

Figure 11 shows the initial pulse wave signal after filtering. The system has detected the pulse wave signal efficiently, which indicates that the incident light can indeed visit the arterial vessel. The DC components and the AC components of the red and infrared light intensity can be obtained with proper processing of the signals. The oxygen saturation can then be calculated by the ratio of the light intensity change rates under the two different wavelengths.

The calibration of an oxygen oximeter can be a complicated task. Experimental procedures are used to obtain the parameters required in equations (4) and (5). An oxygen saturation simulator is used and by doing some experiments, data relating the oxygen saturation and the R values are obtained. The Index 2XL SpO2 simulator by Fluke Biomedical [12] has been used. Figure 13 shows the empirical R to oxygen saturation curve under the linear and quadratic relationships.

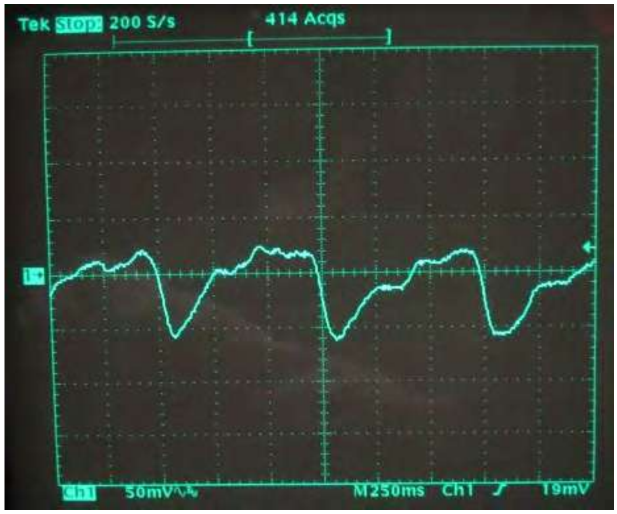

FIGURE 12. The pulse signal obtained by the infrared LED.

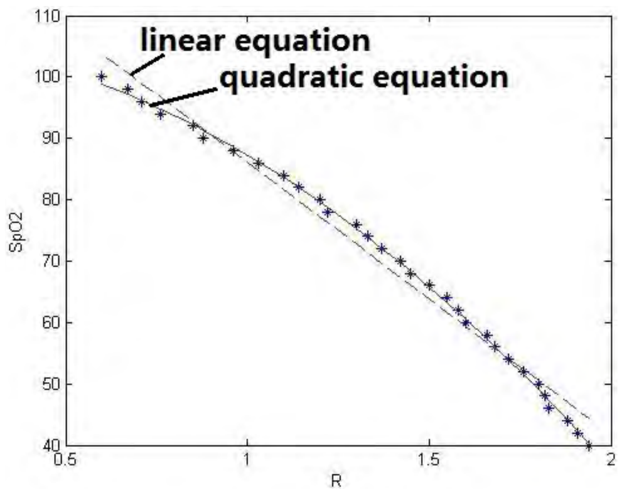

FIGURE 13. The R curve modeled by two relationships.

In the calibration process, the linear equation becomes

$$SpO_2 = 130.4 - 44.4\,R$$

If modeled by second-order, the quadratic equation is

$$SpO_2 = 106.9 - 3.9\,R - 15.6\,R^2$$

It can be seen that the quadratic (second-order), nonlinear relationship can provide a better fit with the data.

VIII. CONCLUSIONS

This paper describes the development of a new kind of wrist pulse oximeter. It is different from the conventional finger pulse oximeter due to the following reasons:

1. The device has a novel design of the sensor module. The optical source has two LEDs (red and infrared). The receiver is consisted of two photodiodes. A new optical structure is designed to house the sensor module components so as to

obtain improved operational efficiency when collecting the wrist pulse signals.

2. The location in the wrist for placing the sensor module of the pulse oximeter is also unique. In order to obtain desirable wrist pulse signals, the sensor module is designed to be placed in an inner part of the wrist. The special design of its concave shape helps the sensor module to stay in the chosen location of the wrist.

3. The device is a genuine wrist pulse oximeter as opposed to the usual finger pulse oximeter. It has a very simple hardware structure without even a display because all data processing, calculations and display will not be carried out on the wearable wrist device.

4. During the calibration process, it is found that a second-order relationship between the R value and the oxygen saturation can provide a better fit with the data.

In the future, a Bluetooth module can be developed to transmit all sensor data to an application of a nearby smartphone, which would perform all those tasks. As a result of using minimal hardware for the device and the use of a flexible software solution for handling the sensor data, the cost of device will be very low. It is expected that the final cost can be only around a fraction of the cost of a typical finger oximeter in the market.

REFERENCES

[1] I. Sarussi, "Device for use with reflective pulse oximetry," U.S. Patent 20 070 038 050, Feb. 15, 2007.

[2] Y. Mendelson and B. D. Ochs, "Noninvasive pulse oximetry utilizing skin reflectance photoplethysmography," *IEEE Trans. Biomed. Eng.*, vol. 35, no. 10, pp. 798–805, Oct. 1988.

[3] Y. Mendelson, J. C. Kent, B. L. Yocum, and M. J. Birle, "Design and evaluation of a new reflectance pulse oximeter sensor," *Med. Instrum.*, vol. 22, no. 4, pp. 167–173, Aug. 1988.

[4] Y. Mendelson and C. Pujary, "Measurement site and photodetector size considerations in optimizing power consumption of a wearable reflectance pulse oximeter," in *Proc. 25th Annu. Int. Conf. IEEE Eng. Med. Biol. Soc.*, Sep. 2003, pp. 3016–3019.

[5] Y. Mendelson, C. Pujary, and M. Savage, "Minimization of LED power consumption in the design of a wearable pulse oximeter," in *Proc. IASTED Conf. Biomed. Eng.*, 2003, pp. 249–254.

[6] H. Santha, N. Stuban, and G. Harsanyi, "Design considerations of small size reflective type pulse oximeter heads in special applications," in *Proc. 1st Conf. Electron. Syst. Integr. Technol.*, Sep. 2006, pp. 404–408.

[7] G. Di, X. Tang, and W. Liu, "A reflectance pulse oximeter design using the MSP430F149," in *Proc. IEEE/ICME Int. Conf. Complex Med. Eng.*, May 2007, pp. 1081–1084.

[8] Q. Cai, J. Sun, L. Xia, and X. Zhao, "Implementation of a wireless pulse oximeter based on wrist band sensor," in *Proc. 3rd Int. Biomed. Eng. Inform. (BMEI)*, Oct. 2010, pp. 1897–1900.

[9] S. B. Duun, R. G. Haahr, K. Birkelund, and E. V. Thomsen, "A ring-shaped photodiode designed for use in a reflectance pulse oximetry sensor in wireless health monitoring applications," *IEEE Sensors J.*, vol. 10, no. 2, pp. 261–268, Feb. 2010.

[10] K. Li and S. Warren, "A wireless reflectance pulse oximeter with digital baseline control for unfiltered photoplethysmograms," *IEEE Trans. Biomed. Circuits Syst.*, vol. 6, no. 3, pp. 269–278, Jun. 2012.

[11] T. Zaman, P. A. Kyriacou, and S. K. Pal, "Free flap pulse oximetry utilizing reflectance photoplethysmography," in *Proc. 35th Annu. Int. Conf. IEEE Eng. Med. Biol. Soc. (EMBC)*, Jul. 2013, pp. 4046–4049.

[12] (2007). *Fluke Biomedical*, Cleveland Calibration Lab., Cleveland, OH, USA. [Online]. Available: http://assets.fluke.com/manuals/index2xlumeng0000.pdf, accessed Dec. 12, 2014.

GRANTHAM PANG received the Ph.D. degree from the University of Cambridge, Cambridge, U.K., in 1986. He was with the Department of Electrical and Computer Engineering, University of Waterloo, Waterloo, ON, Canada, from 1986 to 1996, and then joined the University of Hong Kong, Hong Kong. Since 1988, he has authored over 70 journal papers and 120 international conference papers. He holds five U.S. patents, one European patent, and one Chinese patent. His research interests include biomedical informatics, visual surveillance, machine vision for surface defect detection, optical communications, logistics, intelligent control, and expert systems.

CHAO MA received the M.Sc. degree in electrical engineering from the University of Hong Kong, Hong Kong, in 2014. He is currently with Valeo Inc., Troy, MI, USA. He was with Dr. Pang in the design of the neo-reflective wrist pulse oximeter in 2011, and then with Dr. Hofmann in the design of maximum power point tracking circuit for solar panels and energy harvesting backpacks in 2013 and 2014. His current research interests are in lidar, active safety, auto-parking, and auto-driving.

APPENDIX K

A Wireless Reflectance Pulse Oximeter With Digital Baseline Control for Unfiltered Photoplethysmograms

Kejia Li, *Student Member, IEEE*, and Steve Warren, *Member, IEEE*

***Abstract*—Pulse oximeters are central to the move toward wearable health monitoring devices and medical electronics either hosted by, e.g., smart phones or physically embedded in their design. This paper presents a small, low-cost pulse oximeter design appropriate for wearable and surface-based applications that also produces quality, unfiltered photo-plethysmograms (PPGs) ideal for emerging diagnostic algorithms. The design's "filter-free" embodiment, which employs only digital baseline subtraction as a signal compensation mechanism, distinguishes it from conventional pulse oximeters that incorporate filters for signal extraction and noise reduction. This results in high-fidelity PPGs with thousands of peak-to-peak digitization levels that are sampled at 240 Hz to avoid noise aliasing. Electronic feedback controls make these PPGs more resilient in the face of environmental changes (e.g., the device can operate in full room light), and data stream in real time across either a ZigBee wireless link or a wired USB connection to a host. On-board flash memory is available for store-and-forward applications. This sensor has demonstrated an ability to gather high-integrity data at fingertip, wrist, earlobe, palm, and temple locations from a group of 48 subjects (20 to 64 years old).**

***Index Terms*—Filter-free, high-fidelity photoplethysmogram, low cost, pulse oximeter, reflectance sensor, surface biosensor, wearable, wireless.**

I. Introduction

HEALTH problems such as cardiovascular disease, hypertension, diabetes, and congestive heart failure continue to plague society [1]. These conditions are primary drivers for the development of wearable and mobile health monitoring technologies that offer the potential to (a) increase the quality of life for individuals that already suffer from these health conditions and (b) prevent or mitigate the onset of disease in those that are at risk to acquire these health issues [2]. Of the array of medical devices that can be brought to bear for wearable/mobile applications that address these diseases, pulse oximeters offer significant relative promise because they provide two clinically relevant health parameters [heart rate (HR) and blood oxygen saturation (SpO_2)], they do not require electrical contact to tissue, and they can operate at very low power [3], [4]. Additionally, the pulsatile plethysmographic data offered by this light-based sensing technique (which are usually discarded by commercial pulse oximeters after being used to calculate the parameters for the front panel display) can help to ascertain hemodynamic information that is well-suited for the assessment of the disease states listed above [5]–[8]. This information includes blood pressure [9], [10], arterial compliance [6], [11], [12], pulse wave velocity (PWV) [2], [13], stroke volume (and therefore cardiac output) [14], and other vascular parameters [7], [8], [15], [16]. Other relevant quantities include respiration rate [17], [18], patient motion [16], and even patient authentication [19]–[21].

However, low-cost pulse oximeter designs are unavailable that provide (a) quality, unfiltered PPGs ideally suitable for research and education toward the realization of new PPG diagnostics and (b) positional flexibility suitable for mobile and surface-based applications. While PPGs are often accessible from commercial desktop units via serial ports, these data have been filtered in proprietary ways to stabilize HR and SpO_2 calculations. Further, due to their clinical prevalence, pulse oximetry and PPG analysis deserve coverage in biomedical instrumentation laboratories offered in secondary education curricula, yet low-cost pulse oximeters that provide reasonable-quality PPGs are not a staple in off-the-shelf educational kits.

Regarding ambulatory pulse oximeters, several types of wearable designs exist. Some of these use ring form factors, and others use finger clips. These designs use predominantly transmission-mode sensors. For broader use with wrist watches, head bands, socks, sensor 'Band Aids', and other wearable platforms that are unobtrusive and well suited for mobility, it makes sense to consider reflectance-mode layouts. This is especially true when one contemplates the immense potential of 'surface biosensors' (SBs): medical sensors embedded in the surface of everyday consumer electronics such as hand-held personal device assistants (PDAs), cell phones, smart phones, tablet PCs, head-mounted displays, etc. In this paradigm, physiological sensors will be accessible and signals will be easy to obtain, as human factors considerations for the overall product design will drive ease of use for the integrated biosensors. Additionally, each SB will utilize its host device's processor, memory, display, and wireless communication resources to provide user services typically unavailable in wearable platforms [22]. E.g., consider a reflectance pulse oximeter embedded on the back side of a cell phone alongside a built-in camera. As the user holds their finger against the reflectance sensor, these data will be processed by the microprocessor in the cell phone, and the LCD screen will display the signals and parameters.

In this domain, a reflectance sensor can employ a single small photodiode [23] as in most transmittance sensors. However,

Manuscript received December 03, 2010; revised April 24, 2011 and July 18, 2011; accepted August 15, 2011. Date of publication November 04, 2011; date of current version May 22, 2012. This work was supported in part by the National Science Foundation under Grants BES-0093916, BES-0440183, and CNS-0551626, and by the Kansas State University Targeted Excellence Program. Opinions, findings, conclusions, or recommendations expressed in this material are those of the author(s) and do not necessarily reflect the views of the NSF. This paper was recommended by Associate Editor E. Jovanov.

The authors are with the Department of Electrical and Computer Engineering, Kansas State University, Manhattan, KS 66506 USA (e-mail: kejiali@ksu.edu; swarren@ksu.edu).

Color versions of one or more of the figures in this paper are available online at http://ieeexplore.ieee.org.

Digital Object Identifier 10.1109/TBCAS.2011.2167717

tissue is highly forward scattering, so the relative number of remitted photons detected in reflectance mode is low, yielding lower quality PPGs [5]. Improved sensor configurations are therefore often adopted to better acquire the radial reflectance profile, including a ring-shaped photodiode design [24], [25], a photodiode array around the central LEDs [26], and conversely an LED array around a central photodiode [27]. These designs generally employ cascaded high pass and low pass filters to extract the PPGs [28]. Such analog filters inevitably alter and even distort the signals of interest. These alterations are visibly obvious in some papers, and cycle-to-cycle inconsistencies can be significant. For this reason, a filter-free design is desirable. Finally, in a low-cost wearable sensor with a limited voltage range (e.g., [0, 3.3] V if battery powered) and a low-precision analog-to-digital converter (e.g., 8 to 12 bits), maintaining a sensible vertical resolution, number of digitization levels, and sampling frequency for a PPG can be difficult without flexible baseline subtraction and PPG amplification strategies.

In summary, the desire to extract additional physiological information from PPGs acquired with reflectance-mode sensors imposes design constraints with respect to signal quality. This paper presents the design of a low-cost, wireless, reflectance-mode pulse oximeter suitable for these needs. It is initially housed on the surface of a printed circuit board but can be easily migrated to other surface-based applications. Here, a unique filter-free circuit (that digitally extracts the PPG waveform) and a two-stage, feedback-loop-driven control system enable the acquisition of unfiltered PPGs with $2^{12} = 4096$ levels of precision from varied body locations. An optimized LED/detector configuration promotes surface use, and the device signal quality and cost enhance its potential for integration into SB-based consumer devices.

II. Methods

This section presents a design for a filter-free, reflectance pulse oximeter that combines many desirable features into a single platform. Implementation hardware is unspecified here; board-level components are detailed in Section III. Device Prototype.

A. Requirements and Device Layout

The design requirements are outlined in Table I. Signal requirements include quality, unfiltered PPGs whose baselines are digitally removed, consistent with the discussion in Section I. Introduction. The high sampling rate ensures that (a) primary signal and noise components are adequately sampled without aliasing and (b) secondary noise harmonics, e.g., 120 Hz up to several kHz from fluorescent lighting, are not aliased on top of the signal components of interest.

Regarding sensor requirements, the photodetectors are ideally distributed radially around the central excitation LEDs to maximize the number of photons collected. Further, an LED/detector separation of 3 to 5 mm is appropriate at these wavelengths, as it maximizes the AC/DC ratio for each sensor channel, as verified experimentally [26], [29] and with Monte Carlo simulations [21]. In other words, reflectance photons that contain DC information from shallow, poorly perfused epidermal layers reflect near the central excitation LEDs and are undetected. Photons collected at greater radial distances are more likely to have traveled deeper into blood-perfused tissue and contain a greater percentage of AC data. Given the increased sensing area in a large-area detector, the control circuitry must easily compensate for baseline changes due to ambient light, tissue perfusion, respiration depth, etc.

TABLE I
Wireless Reflectance Pulse Oximeter Design Requirements

Category	*Requirements*
Signal	
Integrity	Unfiltered data with an optimal SNR
Precision	Thousands of peak-to-peak digitization levels
Sampling frequency	≥ 240 Hz to minimize PPG/noise aliasing
Baseline subtraction	Digital and filter-free
Data availability	Full access to all pulsatile/baseline data
Sensor	
LED/detector geometry	Radial arrangement, large area, and 3-5 mm source/detector separation
Ambient light operation	Adjustable gain and reference baseline
Functionality	
Communication	Wireless (10 m range) and USB
Local storage	Onboard flash memory
Battery	USB-rechargeable; Multi-day lifetime
Client Software	Visualization and control panel
Application	
Measurement sites	Multiple body locations; Various vascular profiles and perfusion levels
Wearability	Low-profile reflectance layout adaptable for wearable and SB applications
Cost	Low (<$100)

Fig. 1 shows the block diagram for the pulse oximeter circuitry; a brief description was also included in [30]. The LED, sensor array, and operational amplifier (OPA) circuitry are coordinated by a Jennic JN5139 microcontroller. The intensity and timing of the bi-color LED are controlled by a digital-to-analog converter (DAC) and digital input/output ports (DIOs), respectively. A signal from the sensor array (four photodiodes surrounding the central bi-color LED) is first buffered and then fed to a differential OPA circuit. The buffered signal, designated here as the first-stage PPG signal (entire AC + DC contribution), is sampled by an analog-to-digital converter (ADC). Another ADC collects the second-stage PPG signal (the AC portion only) from the output of the differential OPA circuit that has a positive input from another microcontroller DAC.

No filters are used in the signal acquisition process, whose elements will be introduced in *Part C. Closed-Loop System*. The battery (unstable power source) is isolated from the PPG excitation and collection circuitry, since it is powered by the microcontroller's analog peripheral regulator (APR). Normally, the pulse oximeter uses a wireless link to communicate with a receiver on a PC, and data are stored on the PC through a MATLAB graphical user interface (GUI). A mini-USB connection can provide a wired interface to the PC while the battery is recharged. If neither the wireless link nor the USB connection is available, sampled data will be temporarily stored on the flash memory module (e.g., for store-and-forward applications).

B. AC Extraction and Drift Resistance

The first-stage PPG is characterized by a large DC portion and a small AC portion, as in Fig. 2. The goal is to extract the

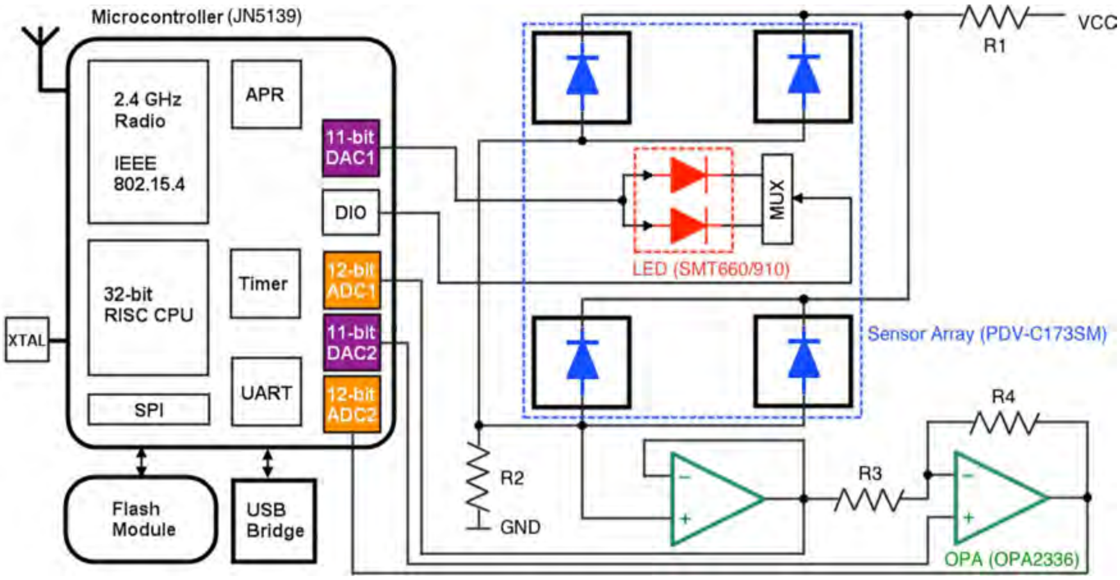

Fig. 1. Circuit-level system layout. Coordinated by the microcontroller, signal baselines are digitally extracted as an alternative to conventional filtering.

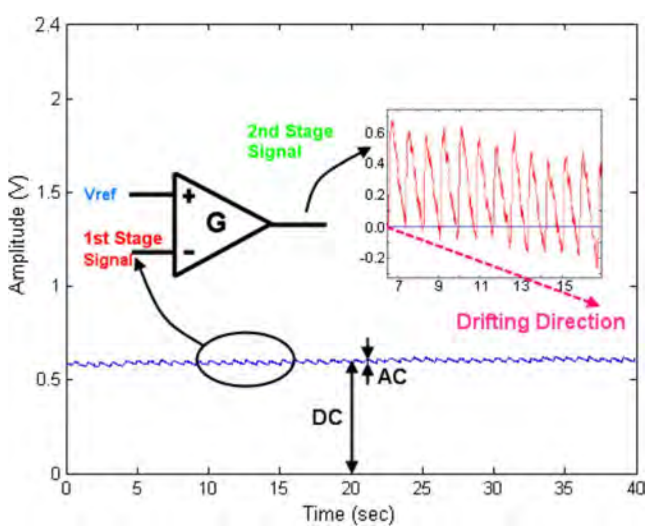

Fig. 2. A differential amplifier with gain G compares the first-stage PPG (S_1) to a DC reference voltage to obtain the second-stage PPG (S_2).

second-stage AC signal by eliminating the DC component. (In many systems, a high pass filter extracts the AC signal.) If the DC portion instead remains, then obtaining hundreds to thousands of digitization levels in the AC portion over its small voltage range requires an ADC of very high precision (e.g., 16-bit), which is inappropriate for a low-cost, low-power-consumption device. This extraction, or DC removal, process is executed by the OPA unit. Its role is expressed as

$$S_2 = G \times (V_{ref} - S_1) \quad (1)$$

where S_1 and S_2 are the first-stage and second-stage signals, respectively, G is the gain of the OPA, and V_{ref} is a user-defined reference voltage that functionally equates to the DC signal level. To show an upward-oriented PPG peak during systole as with a blood pressure curve, V_{ref} is connected to the positive pin of the OPA, effectively inverting the AC signal amplitude prior to digitization.

S_1 is naturally unstable, as both its AC and DC levels are influenced by changes in intrinsic blood flow, extrinsic motion, respiration, background light, etc. These factors cause drifting in S_2. The input voltage range, or digitization range, of the 12-bit ADC is set to [0, 2.4] V, so one digitization level is $2.4\ \mathrm{V}/4095\ \mathrm{levels} = 0.586\ \mathrm{mV}$. For example, given a gain $G = 30$ and a constant V_{ref}, one digitization-level increment in the DC signal results in a decrement of 30 digitization levels in S_2 according to (1). As in Fig. 2, S_2 may drift 0.3 V (512 digital levels) in 10 seconds, which is unacceptable because the signal will eventually clip at the lower bound of the sampling range, and clipped data mean signal corruption. To address this issue, (1) implies that one can adjust one or more elements on the right side to adjust the value of S_2 on the left. In this effort, a V_{ref} adjustment is employed to resist S_2 drifting, since V_{ref} is an output of the DAC and can be easily updated. V_{ref} is defined as

$$V_{ref} = MA(t) + V_+ \quad (2)$$

where $MA(t)$, the estimator of the DC component, V_{DC}, is a W-point (e.g., $W = 256$) moving average of the first-stage signal over the time interval that ends at t. V_+ (the adjustable term) is added to $MA(t)$ to ensure that V_{ref} makes S_2 in (1) positive.

V_{ref} usually varies slowly (several seconds per digitization level change, in an environment with minimal motion and ambient noise), and the V_{ref} adjustment leads to a discontinuity in S_2. Hence, the V_{ref} data must also be transmitted or stored along with the digitized second-stage data in order to restore the original PPGs, a process called "compensation."

Fig. 3 shows a data set from the palm. Collected data are compensated to remove discontinuities caused by V_{ref} jumps, or immediate value changes, in the pulsatile waveform using

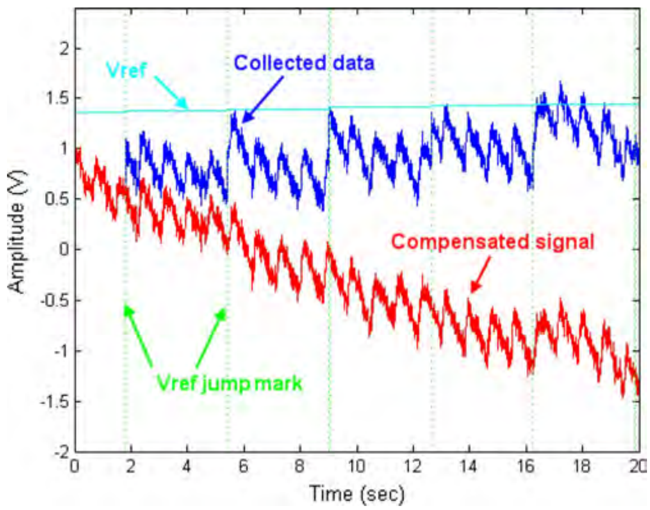

Fig. 3. Palm PPG data before (blue) and after (red) compensation.

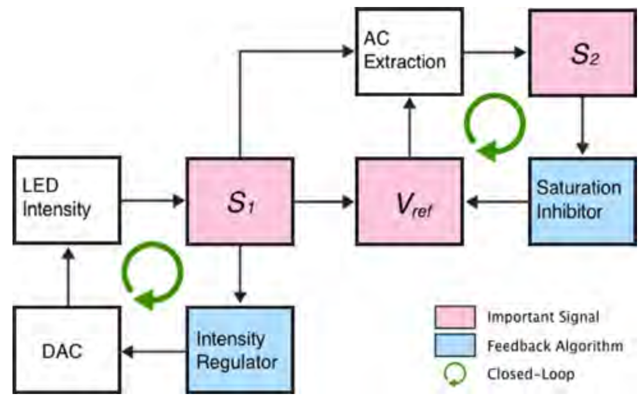

Fig. 4. Pulse oximeter control flow that illustrates how the first-stage PPG (S_1) can be used to create the second-stage PPG (S_2), where both signals provide feedback to stabilize the acquisition process.

the following method. Inserting V_{ref} from (2) into (1) and then rearranging the result isolates the first-stage signal, S_1

$$S_1 = MA(t) + V_+ - \frac{S_2}{G}. \tag{3}$$

The compensated second-stage signal, $\hat{S}_2$, can be represented as

$$\hat{S}_2 = G \times (V_{DC} + V_+ - S_1) \tag{4}$$

where V_+ is added to V_{DC} to ensure a positive $\hat{S}_2$. Substituting (3) into (4) yields

$$\hat{S}_2 = S_2 - G \times (MA(t) - V_{DC}). \tag{5}$$

Typically, V_{DC} is an unknown constant, but it is sensible to initially set $V_{DC} = MA(t_0)$ at time t_0 and define $V_{jump} = MA(t) - MA(t_0)$ at time t $(t > t_0)$ so that (5) becomes

$$\hat{S}_2 = S_2 - G \times V_{jump}. \tag{6}$$

With this method, each PPG can be restored as long as the second-stage signal is unsaturated. The V_{ref} adjustment effectively resists first-stage-signal drifting. For example, in Fig. 3, the compensated signal drifts below 0 V after 6 seconds. If no V_{ref} adjustment occurs, the subsequent signal is sampled as 0 V. To calculate blood oxygen saturation, V_{ref} is usually considered equal to V_{DC}.

C. Closed-Loop System

The V_{ref} adjustment mechanism not only helps to realize the AC extraction task; it also results in resilience in the PPG signal. In the control system, as illustrated in Fig. 4, two closed loops provide stability for the whole data acquisition process. The closed loop in the lower left maintains the S_1 value in a predetermined range, which is set by the Intensity Regulator that controls the led intensity via a DAC. The physical function of this control loop is to maintain the number of reflected photons at an optimal level within the active range of the photodiode, independent of a subject's vascular and perfusion profiles [30]. The closed loop in the upper right prevents S_2 from saturation, since the compensation method described in (6) requires an unsaturated second-stage signal. Upon detecting saturation onset, the Saturation Inhibitor adjusts the V_+ component of V_{ref}, which leads to a corresponding change in S_2 according to (1).

To maintain signal quality, the Intensity Regulator sensitivity should be minimized. When the regulator affects changes in LED excitation level, the influence on the first-stage signal converted by the photodiode sensor array will be hard to predict because the blood-perfused tissue between the LED and the sensor is an unknown system. Conversely, the sensitivity of the Saturation Inhibitor should be set high to ensure a rapid response to signal drift. Since this adjustment only influences V_{ref}, the native PPG is uncontaminated, and the second-stage signal can be adjusted using (6).

In a controlled scenario, ambient noise variations can be ignored. If the desired signal intensity increases as the LED intensity increases, the signal-to-noise ratio (SNR) will improve. However, this implies a saturation risk due to a second-stage signal with too large of a magnitude within a fixed digitization range, in spite of the aforementioned drift-resistant method. Additionally, a more intense LED consumes more power. So, an optimized intensity level should be empirically predetermined as an Intensity Regulator reference.

D. Removable Noise

In the U.S.A, ambient light often includes a 60 Hz component and the associated harmonic noise, e.g., 120 Hz flicker from full-wave-rectified fluorescent room lights plus higher-frequency harmonics. Most physiological information in a PPG resides in the range of 0–20 Hz. From the Nyquist-Shannon sampling theorem, the lowest sampling frequency, f_s, should then be 40 Hz, but to prevent ambient noise aliasing, sampling frequencies of at least 240 Hz are needed.

Fig. 5 depicts the magnitude spectrum of a PPG containing ambient noise. The heart rate component is 1.329 Hz, and its harmonics dominate in the frequency band below 20 Hz. At greater frequencies, noise is apparent at 60.02 Hz, 84.43 Hz (unclear source), and 119.9 Hz. Most of this noise is removable

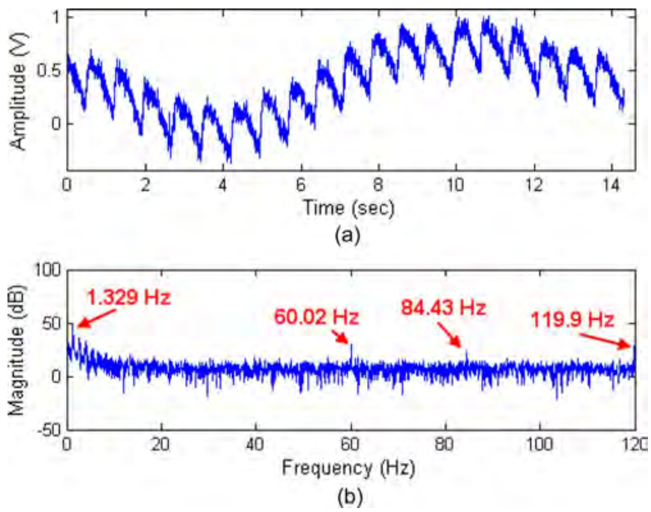

Fig. 5. An example of removable noise. (a) Compensated PPG corrupted by ambient noise. (b) Frequency spectrum of these data sampled at 240 Hz.

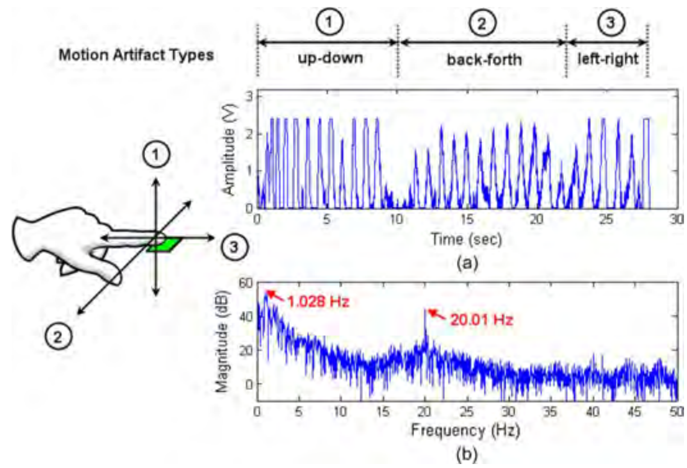

Fig. 6. (a) PPG severely corrupted by hand motion along three axes. (b) Frequency spectrum of the 28 seconds of data sampled at 100 Hz.

by post-processing as long as the sampling frequency is high enough that these noise components do not alias into the frequency range of the signal components of interest. Note that the raw signal exhibits a low SNR compared to PPGs from pulse oximeters that employ filters, but all signal components are intact and many can be removed to create a high SNR (see Fig. 12).

E. Motion Artifact

Motion artifact is an issue for a pulse oximeter, especially in reflectance mode [5]. Existing literature focuses on signal processing to reduce motion artifact and restore PPGs [31]. Most methods assume that enough information exists in the corrupted signal for PPG recovery. However, if motion is severe, saturation occurs frequently and lasts for some time, leading to data loss. With this in mind, this development considered motion artifact to be a type of signal drift that can be partially addressed with a drift-resistant method (V_{ref} adjustment); the design does not address motion extraction.

Motion artifact can be classified into two categories: slight and severe. Fig. 6 demonstrates the severe condition characterized by three axes of hand motion, where the sensor is taped to the finger. Movements are within a 10 cm range and occur at a rate of ~1 Hz. The PPG is severely corrupted (the fundamental frequency is 1.028 Hz), and it is clipped at the upper and lower bounds of the digitization range; many AC segments are lost and unrecoverable.

The slight condition refers to, e.g., slow body movements, where a PPG retains its general shape but contains spurious components relative to a still condition. To counteract this type of artifact, the shift-resistant method is promising and relies on the setting of an optimal assignment rate and window width for V_{ref} adjustment. The DAC assigns the V_{ref} value to the positive amplifier pin, and that voltage remains constant until the next V_{ref} assignment to the DAC. The window size of the moving average filter (the DC estimation time delay, or count) and the rate of assigning V_{ref} to the DAC (not the rate of V_{ref} variation) influence the second-stage signal. An extreme case occurs when the window size $W = 1$ data point and the rate of assigning V_{ref} to the DAC is $A = f_s$: motion will never influence

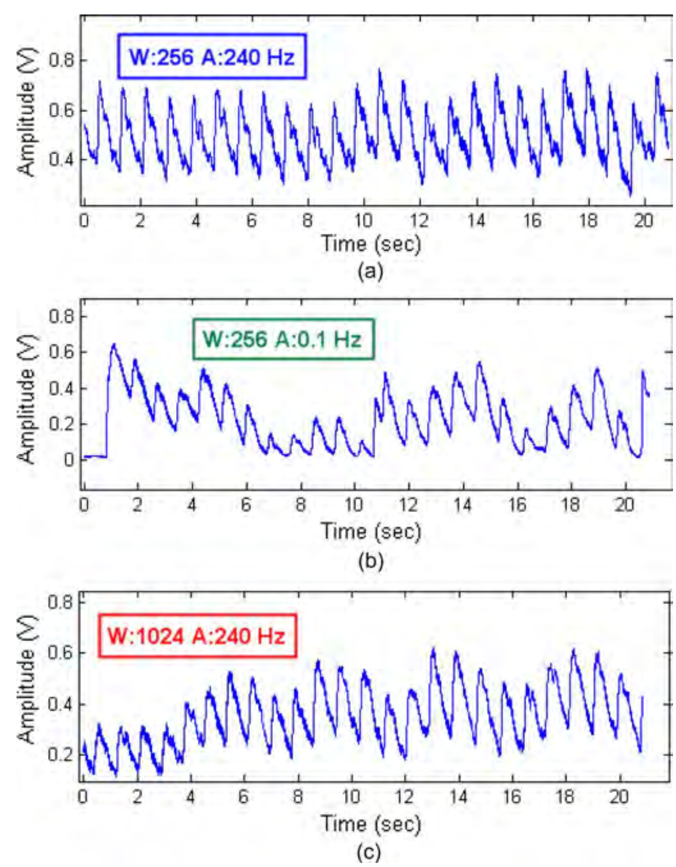

Fig. 7. Three uncompensated PPGs acquired at $f_s = 240$ Hz under similar slight-motion conditions but with different parameter pairs (W, A).

the signal since $MA(t) \equiv S_1$ and consequently $S_2 = G \times V_+$ according to (1) and (2).

As an illustration of slight motion response, Fig. 7 shows three experimental records acquired under similar conditions (exaggerated deep respiration activity), where a different moving-average window width, W, and V_{ref} assignment rate, A, are employed in each case. Only subplot (a) offers a reasonable representation of the PPG. A lower assignment rate (b) or wider window (c) causes the signal to drift severely, and some

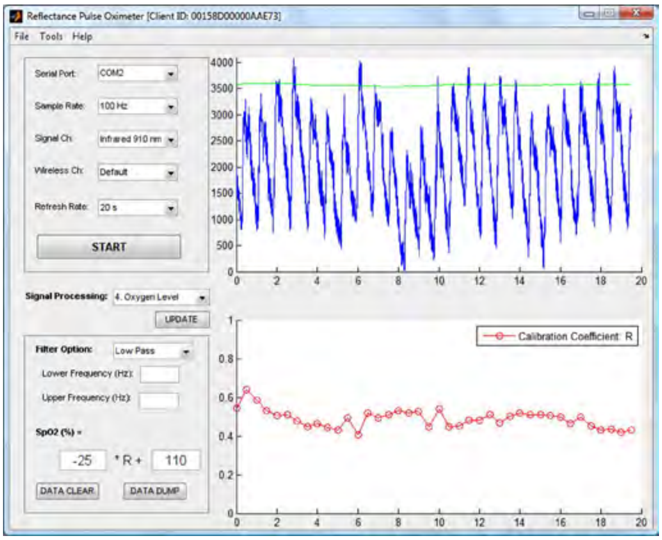

Fig. 8. Pulse oximeter MATLAB GUI. In this example, a series of calibration coefficients (lower right) is extracted from the current data (upper right).

segments are nearly saturated. The empirical parameter pair ($W = 256$, $A = f_s$) was adopted for V_{ref} adjustment.

F. MATLAB Interface

A MATLAB GUI allows a user to set/view communication parameters, visualize PPGs, process these data in real time (e.g., digitally filter a signal with a linear-phase filter), and store raw data to files, making it a helpful development tool (see [16] for a full description). Fig. 8 illustrates an example data set obtained by this GUI, where acquisition options (e.g., Serial Port, Sampling Rate, Signal Channel, and Signal Processing Type) are specified on the left control panel. The upper axes display the raw PPG and baseline for the near-infrared channel, whereas the lower axes show the real-time calibration coefficient, R, calculated from the magnitudes of the fundamental red/infrared frequency components using a Fourier transform method [21]. R is updated every 0.5 seconds using the previous 4 seconds of PPG data. An overall $\mathrm{SpO_2}$ value is achieved by calculating the median or mean of 40 consecutive R values (in a 20-second segment) and inserting the result into a pre-determined linear calibration equation.

III. Device Prototype

Figs. 9 and 10 contain top and bottom views of the pulse oximeter prototype, which consists of four main modules: microcontroller module, excitation LED module, signal sampling module, and power management module. The main printed circuit board is 41 mm by 36 mm, excluding the antenna board. This hardware combines functionality from the Jennic JN5139-EK020 development kit with lessons learned from an earlier reflectance pulse oximeter design [29].

A *microcontroller module* is the prototype kernel. The JN5139 wireless module, designed for robust and secure low-power wireless applications, integrates a 32-bit RISC processor with a 2.4 GHz IEEE 802.15.4 (ZigBee) transceiver, 192 kB of ROM, 96 kB of RAM, a mix of analog and digital

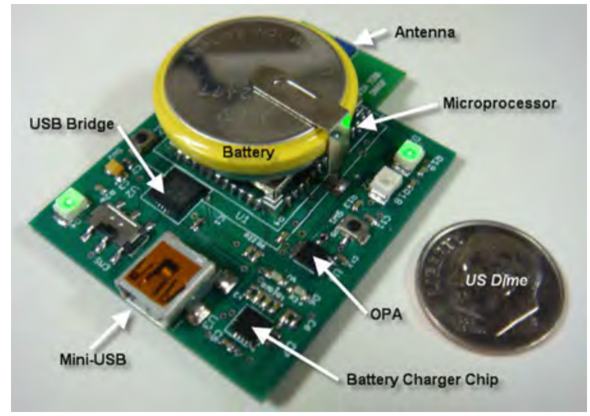

Fig. 9. Top view of the wireless reflectance pulse oximeter.

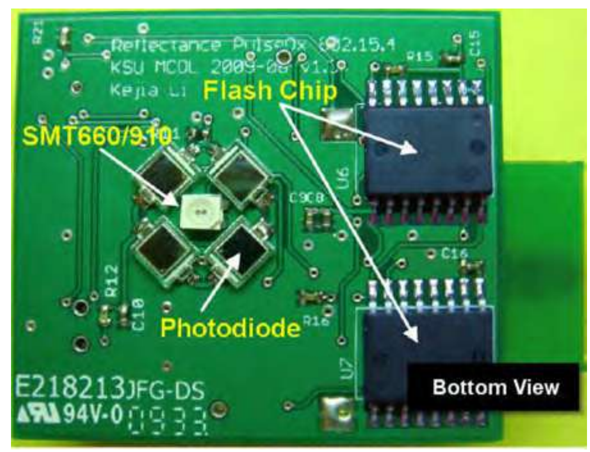

Fig. 10. Bottom view of the wireless reflectance pulse oximeter.

peripherals (including four 12-bit ADCs and two 11-bit DACs), and up to 21 DIO ports. The wireless link requires the most current, with a TX (transmitter) current draw of 38 mA and an RX (receiver) current draw of 37 mA. The CPU consumes 7.75 mA at full speed, and the current required by the peripherals (ADC, DAC, UART, Timer, etc.) is less than 1 mA in aggregate. The JN5139 sleep current (with an active sleep timer) is only 2.6 μA.

The *excitation LED module* uses a low-cost Marubeni SMT660/910 bi-color LED with a typical forward current of 20 mA and forward voltages of 1.9 V and 1.3 V for the 660 nm and 910 nm sources, respectively. The 11-bit DAC output (0–2.4 V) provides excitation signal modulation by managing the power supply for the excitation LED module.

The *signal sampling module* consists of OPA circuitry connected to the sensor array. Four API PDV-C173SM high-speed photodiodes are connected in parallel; their responsivity to wavelengths above 650 nm is more than 0.3 A/W. The photodiodes are arranged radially around the central LEDs and maintain a source/detector separation of 3–5 mm. The OPA chip contains two amplifier units. The sensor array signal is buffered at the first unit and amplified by the second unit.

The *power management module* includes two chips: (a) a Silicon Labs CP2102 USB-to-UART bridge that powers the pulse oximeter when the USB connection is detected and bridges

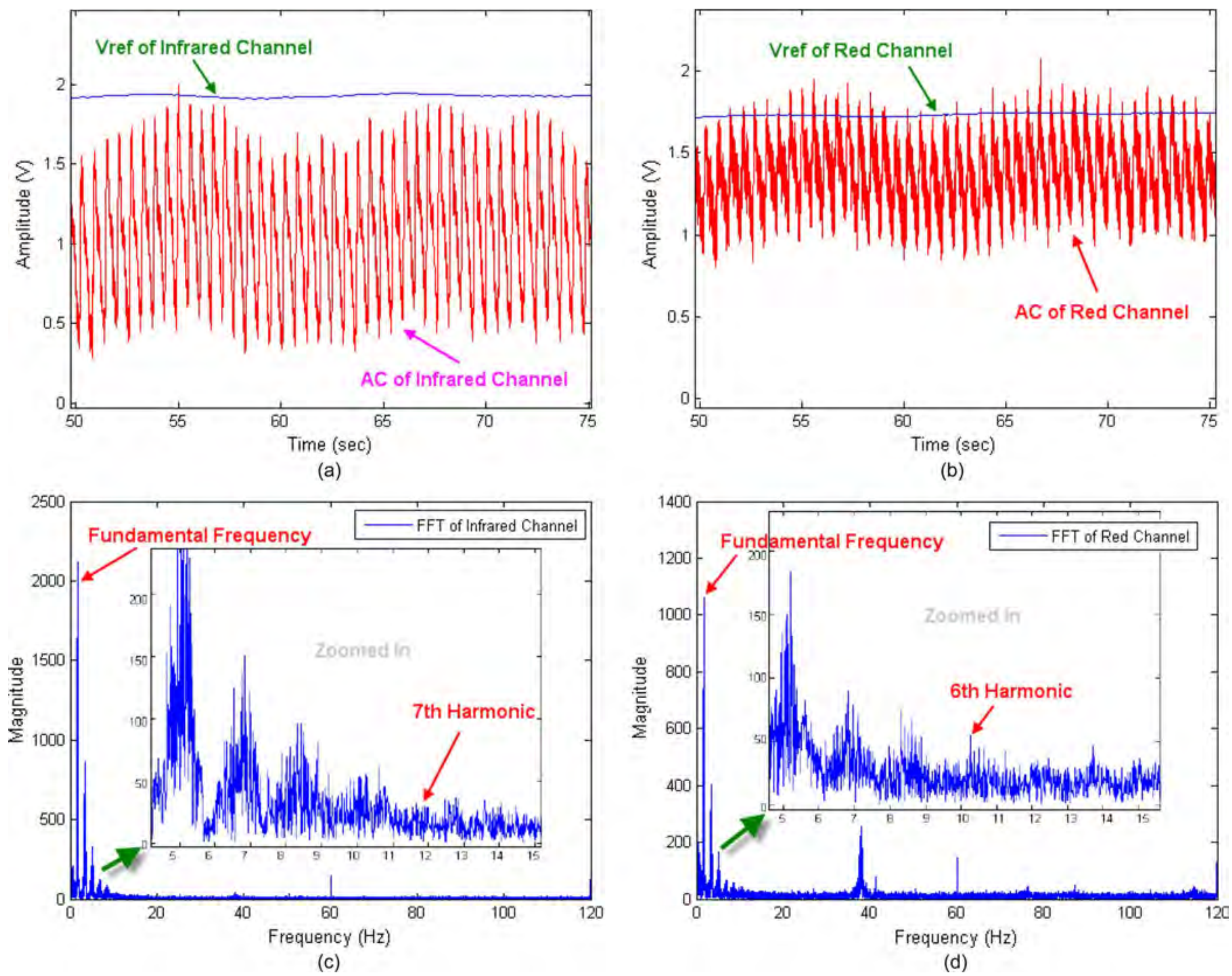

Fig. 11. Fingertip results: 25 seconds of (a) near-infrared and (b) red PPG data, accompanied by their (c) near-infrared and (d) red magnitude spectra.

data communication to the host and (b) an STMicroelectronics L6924D battery charger system with an integrated power switch for lithium-ion batteries which charges the battery when the USB connection is detected. An LIR2477 3.6 V lithium-ion rechargeable button cell with a capacity of 180–200 mAh serves as the power source when the USB connection is absent.

Memory chips, indicators, and buttons are also housed on the board. Two Numonyx M25PX64 64-Mbit flash memory chips with SPI bus interfaces provide storage space when the pulse oximeter works in offline mode; each consumes 20 mA of current while being accessed.

IV. Results and Discussion

The pulse oximeter prototypes were used to acquire hundreds of PPG records from 48 different subjects that are 20 to 64 years old. Experimental results in this section were acquired in an indoor environment. The results are categorized according to conventional location (fingertip) versus other locations (wrist, earlobe, temple, etc.).

A. *Fingertip Data*

Fig. 11 illustrates 25 seconds of representative fingertip data from a 24-year-old subject. Both channels of PPG data, red and near-infrared, are uncompensated. The AC values of the near-infrared channel [Fig. 11(a)] offer 1.2 V peak-to-peak (i.e., 2048 digitization levels), and the AC values of the red channel [Fig. 11(b)] offer fewer digitization levels: about half compared to the near-infrared channel. Even without the use of analog or digital filters, the signal demonstrates distinguishable period and amplitude information useful for HR and $\mathrm{SpO_2}$ determination. The SNRs of the raw near-infrared and red PPGs are 8.0, and 3.0, respectively. As shown in Fig. 11(c) and (d), up to seven harmonics reside in the spectrum of the near-infrared data (the inset shows frequency components above 5 Hz), and six distinguishable harmonics reside in the spectrum of the red data. Additionally, the PPG information and noise components (e.g., 60 Hz and 120 Hz grid noise) are clearly separated in the frequency domain. To further refine the signal, a properly designed digital band pass filter can be applied.

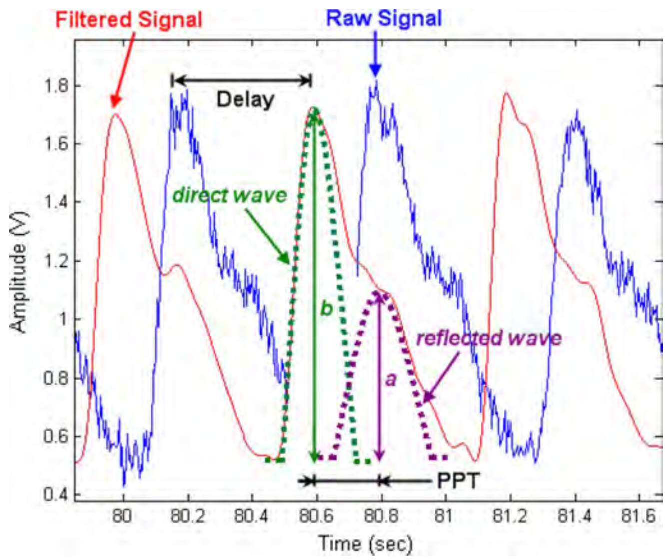

Fig. 12. Fingertip signal processing and digital volume pulse (DVP) analysis.

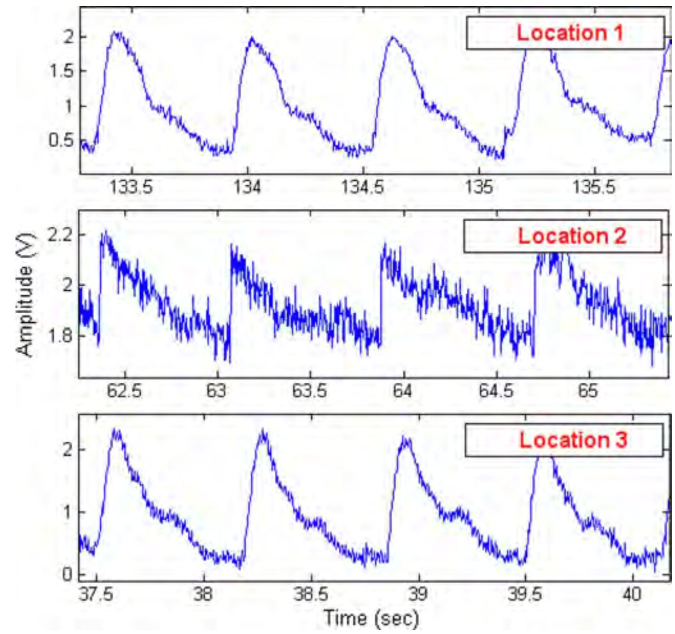

Fig. 13. Wrist PPGs corresponding to the placement locations in Fig. 14.

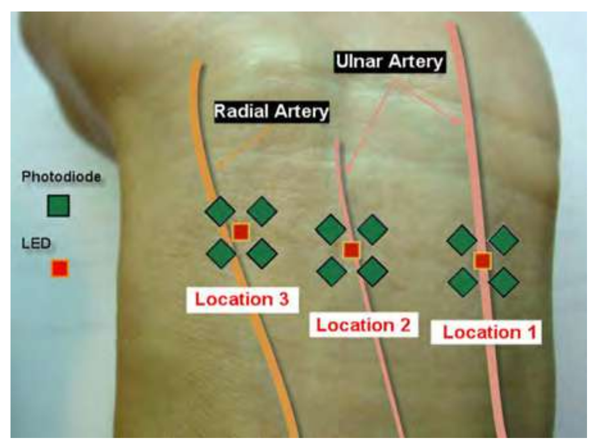

Fig. 14. Pulse oximeter measurement locations on the left wrist.

Fig. 12 displays another short segment of an experimental fingertip data set, where the raw near-infrared PPG is accompanied by its real-time filtered form within a MATLAB GUI. The filter is a 200^{th}-order low pass filter with a 10 Hz cut-off frequency realized by the MATLAB function `firls()`: a linear-phase FIR filter that uses least-squares error minimization. This high-order filter causes a time delay of $t_d = (n-1)/(2f_s) = 0.414$ seconds, where $n = 200$ and $f_s = 240$ Hz; the time delay helps to visually separate the original and filtered waveforms. Since the peak-to-peak noise of the filtered signal is too small to be recognizable (<1 digitization level) the SNR is assumed to be $>2048/1$ if the signal amplitude is 1.2 V.

Digital Volume Pulse (DVP) Analysis: Cardiovascular parameters other than HR and SpO_2 can be accurately extracted [2], [13], [15] given the quality of this DVP waveform. For example, the peak-to-peak time (PPT), as marked in Fig. 12, can be used to calculate pulse wave velocity, which correlates to arterial stiffness, and "a" and "b" are used to calculate the reflectance index, which correlates to endothelial function. Additionally, as noted in the Introduction, these unfiltered PPG waveforms could potentially lead to improved assessments of blood pressure and stroke volume via light.

B. Multi-Location Data

Fig. 13 displays experimental data from the wrist at the three placement locations depicted in Fig. 14. The signal quality in location 2 is obviously lower relative to the SNR in locations 1 and 3, but all three are suitable PPGs. At present, it is difficult to consistently obtain high quality PPG data from the wrist; that often requires the application of pressure to bring the optical sensor closer to the major arteries [21]. An operation to achieve the same effect (i.e., bending the wrist at about a 45° angle), was usually employed if the PPG had a low SNR. Since subjects demonstrate a variety of different arterial locations and depths at the wrist, sensor placement flexibility is essential to acquire commendable data sets at this body location, which was also noted in [32].

New Pulse Wave Velocity (PWV) Estimation Approach: Given the capability to acquire quality PPG data from the wrist (where the SNR dramatically improves with post-filtering), a new approach to estimate PWV has been evaluated by the authors [33]. This approach compares near-infrared PPGs from two synchronized pulse oximeters placed at the fingertip and wrist of the same hand. PWVs can be estimated from several time differences/delays extracted from corresponding features on the two PPGs.

Fig. 15 displays two channels of data acquired from the earlobe. The near-infrared channel has an SNR of 5.7 and a peak-to-peak range of 1.0 V (1706 digital levels); the red channel has a much lower SNR of 1.8 and a peak-to-peak range of 0.6 V (1024 digital levels).

Respiration Activity Analysis: Fig. 16(a) displays 120 seconds of experimental data from the temple that include respiration activity and a swallowing motion. There are 33 respiration cycles present during the 120-second recording time (i.e., the respiration rate is 0.275 Hz). An FFT was applied to ascertain

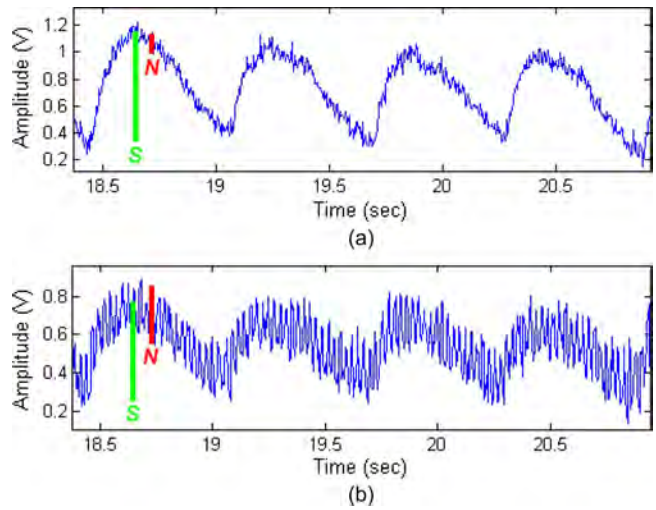

Fig. 15. Earlobe results. (a) Near-infrared channel. (b) Red channel.

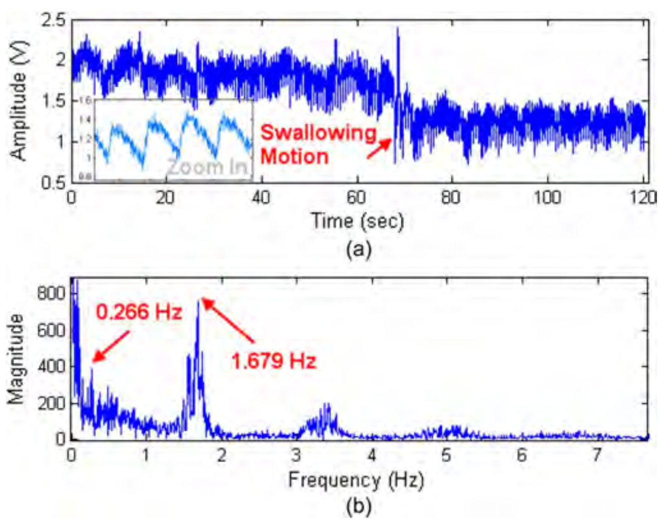

Fig. 16. Temple results. (a) Time-domain PPG with respiration and swallowing motion. (b) Corresponding frequency-domain spectrum.

the visibility of these events in the magnitude spectrum, as noted in Fig. 16(b). The peak at 1.679 Hz corresponds to the subject's heart rate (100.7 bpm) and the 0.266 Hz frequency component is likely the respiration rate.

V. Conclusion

A high-performance wireless reflectance pulse oximeter was designed that includes functional features desired for research and education that are either unavailable or hard to find on commercial units and design optimizations based on lessons learned from previous work or published in the pulse oximetry literature. These primary features include (a) a unique filter-free circuit design, (b) full access to unfiltered PPG data, (c) many digitization levels in the pulsatile PPG signals that demonstrate a sampling frequency up to 240 Hz, (c) a feedback mechanism to allow sensor operation in normal ambient room light, and (d) a large-area reflectance sensor that speaks to the promise of surface-infused biosensors and enables sensor placement at many body locations while optimizing the resistance of the sensor to stray photons and motion artifact. Onboard flash memory, ZigBee wireless support, and mini-USB connectivity for data transfers and battery recharging are additional highlights. The associated MATLAB GUI makes signal acquisition, visualization, restoration, and post-processing convenient.

High-integrity PPGs acquired from 48 human subjects over a wide range of ages (20 to 64 years old) indicate the device's potential as a research and teaching platform in support of the extraction of new physiological parameters from time-domain PPGs. Finally, the size, cost, layout, and design of the sensing platform speak to its suitability for wearable applications and scenarios where medical sensors are connected to or embedded in consumer electronics such as smart phones and tablet PCs.

Acknowledgment

The authors would like to thank D. Huddleston, KSU Electronics Design Laboratory, for his assistance with the reflow soldering on the surface-mounted devices. Measurements from human subjects were acquired with the oversight of the Kansas State University Human Subjects Board under protocol #5448.

References

[1] American Heart Association, Heart Disease and Stroke Statistics—2009 Update At-a-Glance [Online]. Available: http://www.americanheart.org
[2] S. R. Alty, N. Angarita-Jaimes, S. C. Millasseau, and P. J. Chowienczyk, "Predicting arterial stiffness from the digital volume pulse waveform," *IEEE Trans. Biomed. Eng.*, vol. 54, pp. 2268–2275, Dec. 2007.
[3] K. N. Glaros and E. M. Drakakis, "Trade-offs for low power integrated pulse oximeters," in *Proc. IEEE Biomedical Circuits and Systems Conf.*, Nov. 26–28, 2009, pp. 245–248.
[4] M. Tavakoli, L. Turicchia, and R. Sarpeshkar, "An ultra-low-power pulse oximeter implemented with an energy-efficient transimpedance amplifier," *IEEE Trans. Biomed. Circuits Syst.*, vol. 4, pp. 27–38, 2010.
[5] H. Asada, P. Shaltis, A. Reisner, S. Rhee, and R. Hutchinson, "Mobile monitoring with wearable photoplethysmographic biosensors," *IEEE Eng. Med. Biol. Mag.*, vol. 22, pp. 28–40, 2003.
[6] A. Reisner, P. A. Shaltis, D. McCombie, and H. H. Asada, "Utility of the photoplethysmogram in circulatory monitoring," *Anesthesiology*, vol. 108, pp. 950–958, May 2008.
[7] W. B. Murray and P. A. Foster, "The peripheral pulse wave: Information overlooked," *J. Clin. Monit.*, vol. 12, pp. 365–377, Sept. 1996.
[8] K. H. Shelley, "Photoplethysmography: Beyond the calculation of arterial oxygen saturation and heart rate," *Anesthesia Analges.*, vol. 105, pp. S31–S36, Dec. 2007.
[9] S. C. Millasseau, F. G. Guigui, R. P. Kelly, K. Prasad, J. R. Cockcroft, J. M. Ritter, and P. J. Chowienczyk, "Noninvasive assessment of the digital volume pulse: Comparison with the peripheral pressure pulse," *Hyperten.*, vol. 36, pp. 952–956, 2000.
[10] J. Allen and A. Murray, "Modelling the relationship between peripheral blood pressure and blood volume pulses using linear and neural network system identification techniques," *Physiol. Meas.*, vol. 20, pp. 287–301, 1999.
[11] K. H. Shelley, W. B. Murray, and D. Chang, "Arterial-pulse oximetry loops: A new method of monitoring vascular tone," *J. Clin. Monit.*, vol. 13, pp. 223–228, 1997.
[12] N. Westerhof, N. Stergiopulos, and M. I. M. Noble, *Snapshots of Hemodynamics*, 1st ed. Boston, MA: Springer, 2004.
[13] S. C. Millasseau, R. P. Kelly, J. M. Ritter, and P. J. Chowienczyk, "Determination of age-related increases in large artery stiffness by digital pulse contour analysis," *Clin. Sci.*, vol. 103, pp. 371–377, Oct. 2002.
[14] J. Li, L. Yang, S. Zhang, and Y. Yang, "Computation of cardiac output by pulse wave contour," in *Proc. 1st Int. Conf. Bioinformatics and Biomedical Engineering*, Wuhan, China, 2007, pp. 1088–1090.
[15] P. J. Chowienczyk, R. P. Kelly, H. MacCallum, S. C. Millasseau, T. L. G. Andersson, R. G. Gosling, J. M. Ritter, and E. E. Änggârd, "Photoplethysmographic assessment of pulse wave reflection: Blunted response to endothelium-dependent beta2-adrenergic vasodilation in type II diabetes mellitus," *J. Amer. College Cardiol.*, vol. 34, pp. 2007–2014, 1999.

[16] K. Li, "Wireless reflectance pulse oximeter design and photoplethysmographic signal processing," M.S. thesis, Kansas State Univ., Manhattan, 2010.

[17] K. Nakajima, T. Tamura, and H. Miike, "Monitoring of heart and respiratory rates by photoplethysmography using a digital filtering technique," *Med. Eng. Phys.*, vol. 18, pp. 365–372, Jul. 1996.

[18] P. A. Leonard, J. G. Douglas, N. R. Grubb, D. Clifton, P. S. Addison, and J. N. Watson, "A fully automated algorithm for the determination of respiratory rate from the photoplethysmogram," *J. Clin. Monit. Comput.*, vol. 20, pp. 33–36, 2006.

[19] L. C. Ludeman and M. I. Chacon, "Use of blood pulse signature for identity verification," in *Proc. 7th Int. Conf. Signal Processing Applications and Technology*, Boston, MA, Oct. 7–10, 1996, pp. 1608–1612.

[20] L. C. Ludeman and M. I. Chacon, Evaluation of Blood Pulse Signature for Potential Application in a Multisensor Biometric Identity Verification System, New Mexico State Univ., Sep. 1995, Final rep. to Sandia National Laboratories under Contract AM-5506.

[21] J. T. Love, S. Warren, G. R. Laguna, and T. J. Miller, "Personal status monitor," Sandia National Laboratories SAND97-0418, UC-706, unlimited release, Feb. 1997.

[22] M. Locke, "Android and RTOS together: The dynamic duo for today's medical devices," *Embed. Comput. Des.*, pp. 36–38, Apr. 2010.

[23] S. Rhee, B. H. Yang, and H. Asada, "Artifact-resistant, power-efficient design of finger-ring plethysmographic sensors," *IEEE Trans. Biomed. Eng.*, vol. 48, pp. 795–805, Jul. 2001.

[24] S. B. Duun, R. G. Haahr, K. Birkelund, and E. V. Thomsen, "A ring-shaped photodiode designed for use in a reflectance pulse oximetry sensor in wireless health monitoring applications," *IEEE Sensors J.*, vol. 10, pp. 261–268, 2010.

[25] P. Branche and Y. Mendelson, "Signal quality and power consumption of a new prototype reflectance pulse oximeter sensor," in *Proc. 31st Annu. Northeast Conf. IEEE Bioengineering*, Apr. 2–3, 2005, pp. 42–43.

[26] Y. Mendelson and C. Pujary, "Measurement site and photodetector size considerations in optimizing power consumption of a wearable reflectance pulse oximeter," in *Proc. 25th Annu. Conf. IEEE Engineering in Medicine and Biology Society*, 2003, pp. 3016–3019.

[27] M. Nogawa, T. Kaiwa, and S. Takatani, "A novel hybrid reflectance pulse oximeter sensor with improved linearity and general applicability to various portions of the body," in *Proc. 20th Annu. Int. Conf. IEEE Engineering in Medicine and Biology Society*, Oct. 29–Nov. 1 1998, pp. 1858–1861.

[28] D. Guowei, T. Xiaoying, and L. Weifeng, "A reflectance pulse oximeter design using the MSP430F149," in *Proc. IEEE Int. Conf. Complex Medical Engineering*, May 23–27, 2007, pp. 1081–1084.

[29] D. Thompson and S. Warren, "A small, high-fidelity reflectance pulse oximeter," in *Proc. 2007 Annu. Conf. and Expo. Amer. Society for Engineering Education*, Honolulu, HI, Jun. 24–27, 2007.

[30] K. Li, S. Warren, and B. Natarajan, "Onboard tagging for real-time quality assessment of photoplethysmograms acquired by a wireless reflectance pulse oximeter," *IEEE Trans. Biomed. Circuits Syst.*, to be published.

[31] R. Krishnan, B. Natarajan, and S. Warren, "Two-stage approach for detection and reduction of motion artifacts in photoplethysmographic data," *IEEE Trans. Biomed. Eng.*, vol. 57, pp. 1867–1876, 2010.

[32] E. Geun, H. Heo, K. C. Nam, and Y. Huh, "Measurement site and applied pressure consideration in wrist photoplethysmography," in *Proc. 23rd Int. Technical Conf. Circuits/Systems, Computers and Communications*, 2008, pp. 1129–1132.

[33] K. Li and S. Warren, "Initial study on pulse wave velocity acquired from one hand using two synchronized wireless reflectance pulse oximeters," in *Proc. 33rd Annu. Int. Conf. IEEE Engineering in Medicine and Biology Society*, Boston, MA, Aug. 30–Sep. 3 2011, pp. 6907–6910.

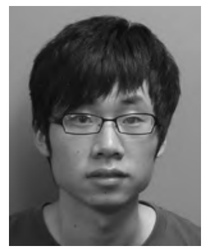

Kejia Li (S'11) received the B.S. degree in electronic and information technology and instrumentation from Zhejiang University, Hangzhou, China, and the M.S. degree in electrical and computer engineering from Kansas State University (KSU), Manhattan, in 2008 and 2010, respectively.

Currently, he is working toward the Ph.D. degree at KSU. He is a Research Assistant in the Medical Component Design Laboratory, Department of Electrical and Computer Engineering, KSU. His research interests involve wearable medical device design, mobile health, and statistical signal processing.

Steve Warren (M'02) received the B.S. and M.S. degrees in electrical engineering from Kansas State University (KSU), Manhattan, and the Ph.D. degree in electrical engineering from The University of Texas at Austin, Austin, in 1989, 1991, and 1994, respectively.

Currently, he is an Associate Professor in the Department of Electrical and Computer Engineering at KSU. Prior to joining KSU in 1999, he was a Principal Member of the technical staff at Sandia National Laboratories, Albuquerque, NM. He directs the KSU Medical Component Design Laboratory, a facility supported by the National Science Foundation that provides resources for the research and development of distributed medical monitoring technologies and learning tools that utilize biomedical contexts. His research focuses on plug-and-play, point-of-care medical monitoring systems that utilize interoperability standards; wearable sensors and signal processing techniques for the determination of human and animal physiological status; and particle transport simulation applied to radiation hardness analysis of complex assemblies and the determination of photon dose distributions in tissue.

Dr. Warren is a member of the American Society for Engineering Education.

APPENDIX L

US 20060253010A1

(19) United States
(12) Patent Application Publication
(10) Pub. No.: US 2006/0253010 A1
Brady et al.
(43) Pub. Date: Nov. 9, 2006

(54) MONITORING DEVICE, METHOD AND SYSTEM

(76) Inventors: **Donald Brady**, Las Vegas, NV (US); **Sammy I. Elhag**, San Diego, CA (US); **Steve Lui**, San Diego, CA (US)

Correspondence Address:
Impact Sports Technologies, Inc.
2101 Plaza Del Dios
Las Vegas, NV 89102 (US)

(21) Appl. No.: **11/398,821**

(22) Filed: **Apr. 6, 2006**

Related U.S. Application Data

(63) Continuation-in-part of application No. 11/085,778, filed on Mar. 21, 2005.

(60) Provisional application No. 60/669,325, filed on Apr. 7, 2005. Provisional application No. 60/613,785, filed on Sep. 28, 2004.

Publication Classification

(51) **Int. Cl.**
A61B 5/00 (2006.01)

(52) **U.S. Cl.** **600/324**; 600/344; 128/921

(57) **ABSTRACT**

A monitoring device (**20**) and method (**200**) for monitoring the health of a user is disclosed herein. The monitoring device (**20**) is preferably a watch (**25**), an optical sensor (**30**) disposed on a band of the watch (**25**), a circuitry assembly (**35**) embedded within a main body of the watch (**25**), a display member (**40**) disposed on an exterior surface of the main of the watch, and a control component (**43**). The monitoring device (**20**) preferably displays the following information about the user: pulse rate; blood oxygenation levels; calories expended by the user of a pre-set time period; target zones of activity; time; distance traveled; and dynamic blood pressure. The watch (**25**) also displays the time of day on the display member (**40**).

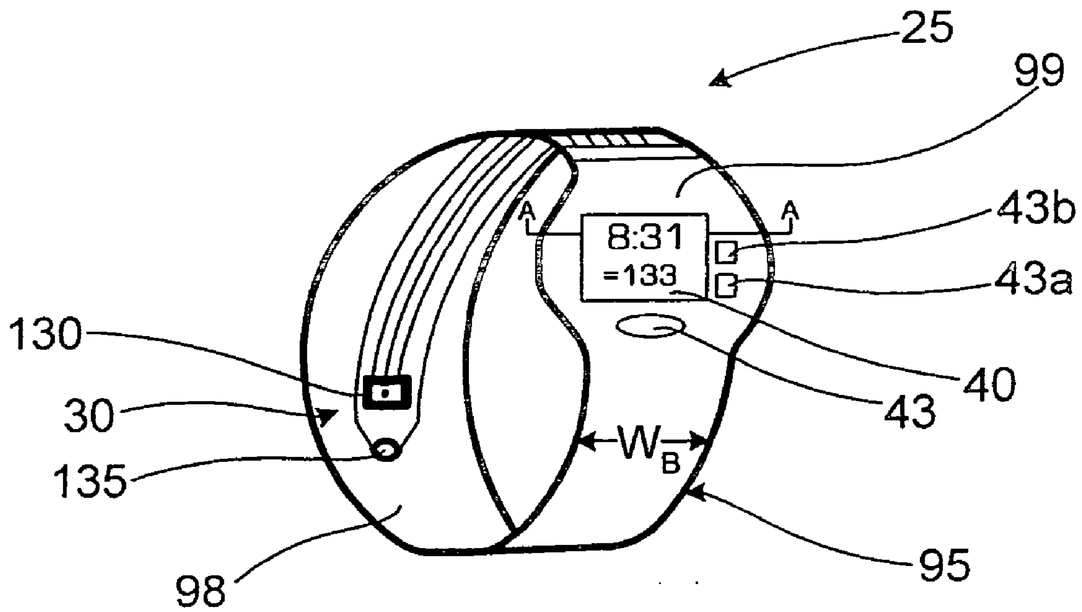

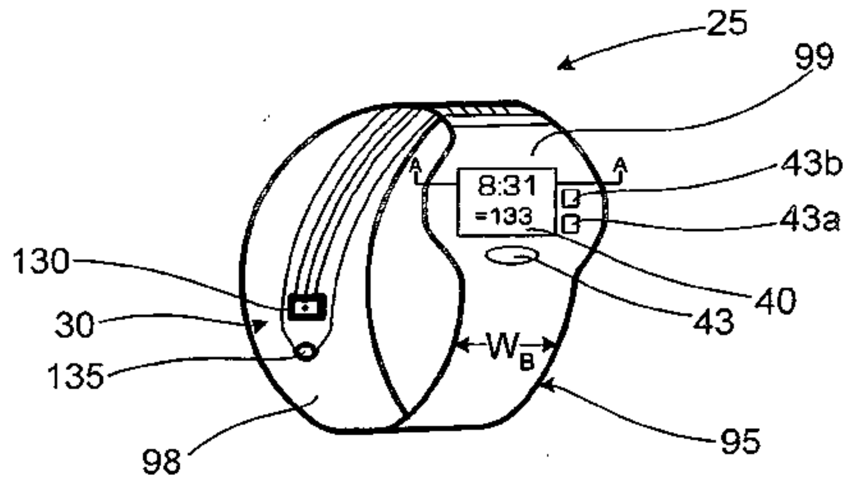

FIGURE 1

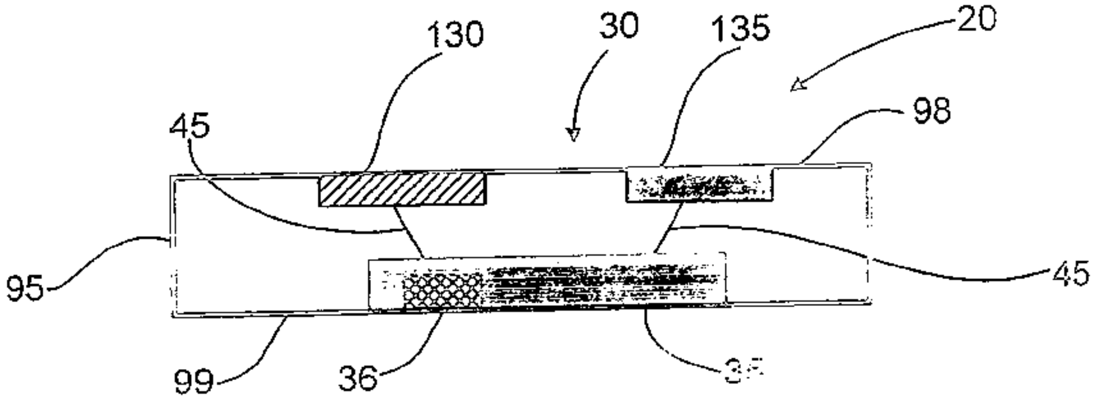

FIGURE 1A

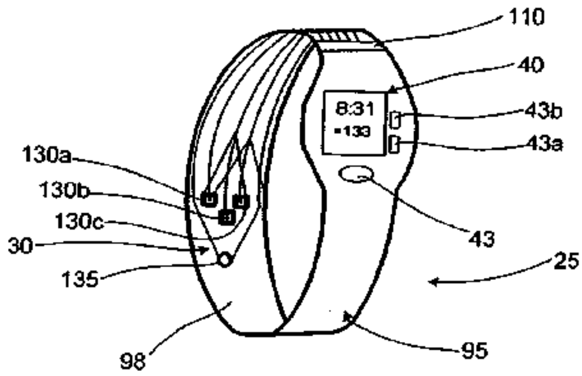

FIGURE 2

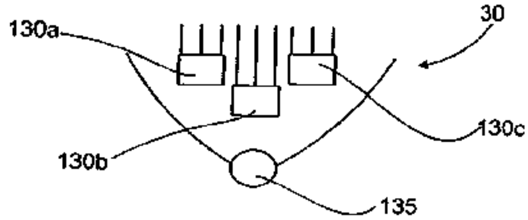

FIGURE 2A

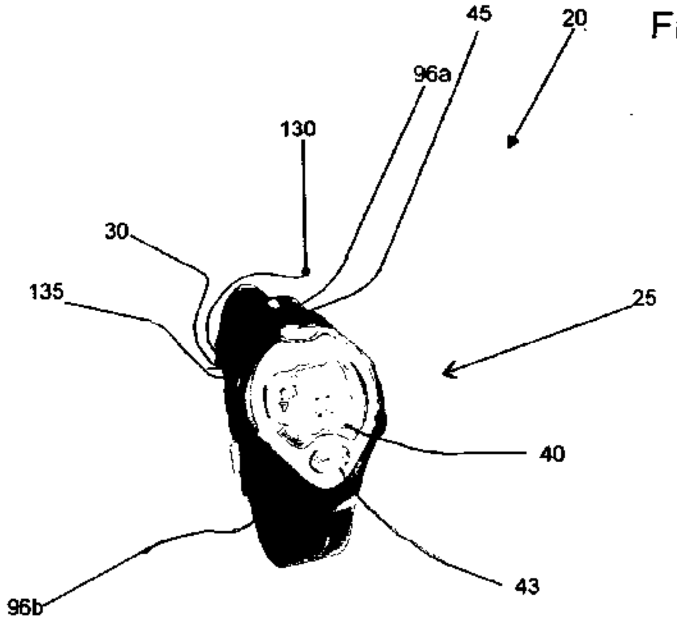

FIGURE 3

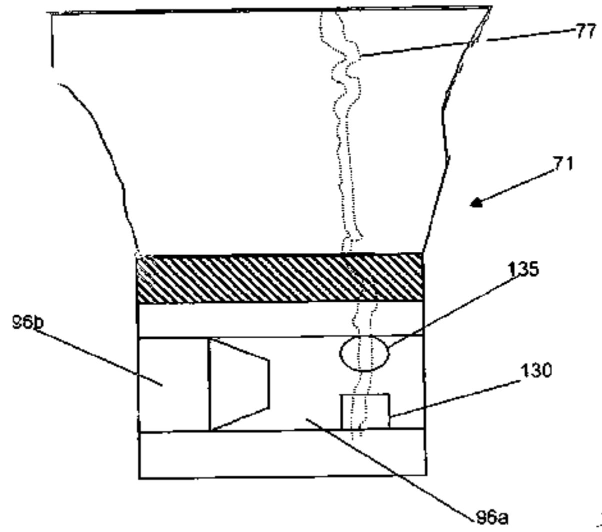

FIGURE 4

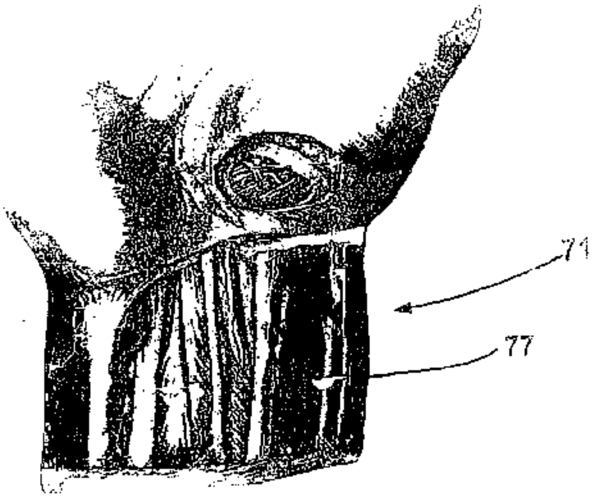

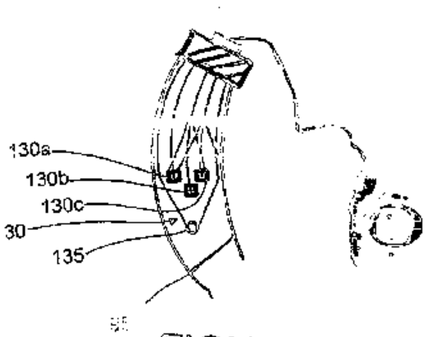

FIGURE 3A

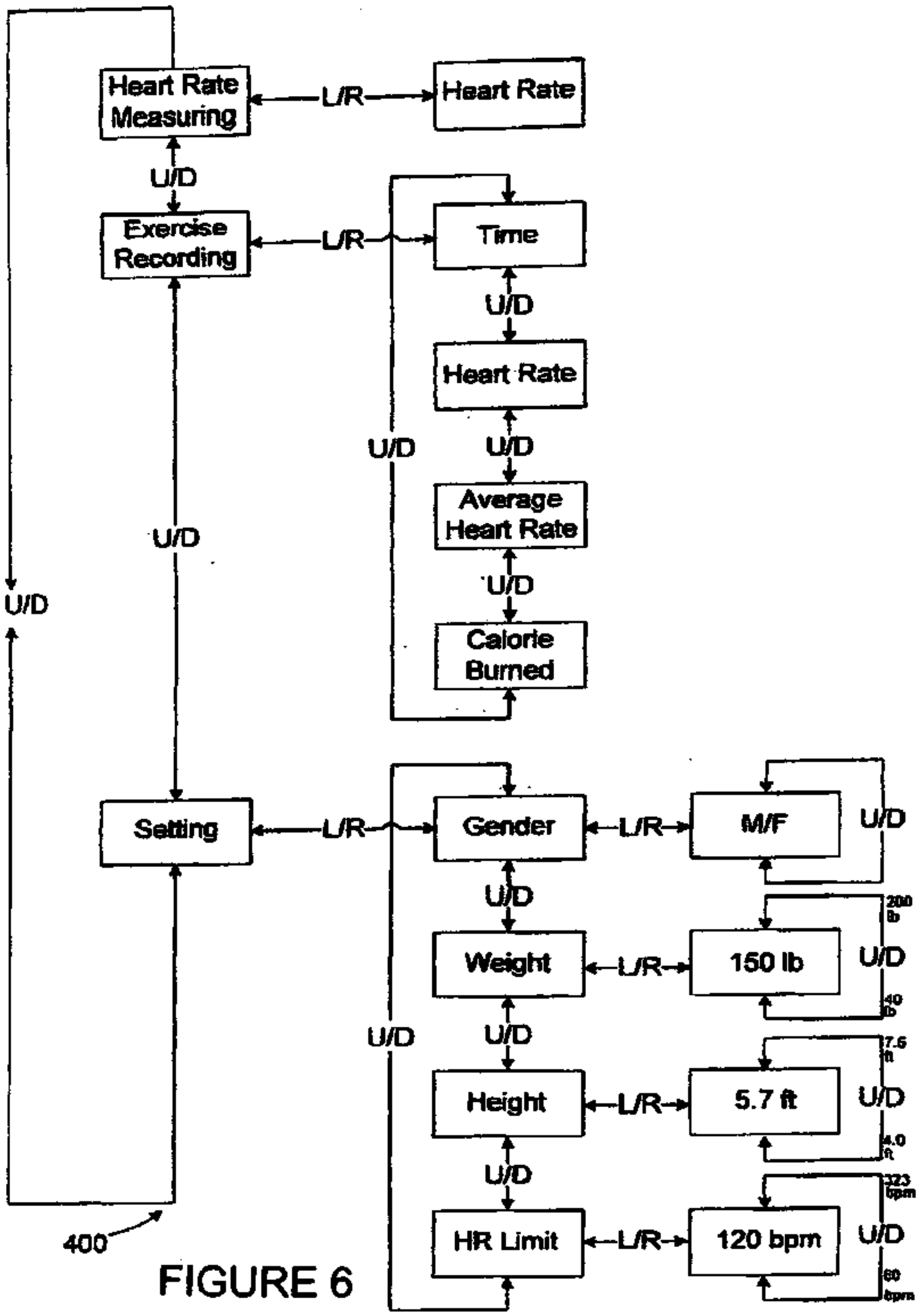
Heart Rate Measuring
L/R
Heart Rate
U/D
Exercise Recording
L/R
Time
U/D
Heart Rate
U/D
U/D
Average Heart Rate
U/D
U/D
U/D
Calorie Burned
Setting
L/R
Gender
L/R
M/F
U/D
U/D
200 lb
Weight
L/R
150 lb
U/D
40 lb
U/D
U/D
7.6 ft
Height
L/R
5.7 ft
U/D
4.0 ft
U/D
323 bpm
HR Limit
L/R
120 bpm
U/D
60 bpm
400

FIGURE 6

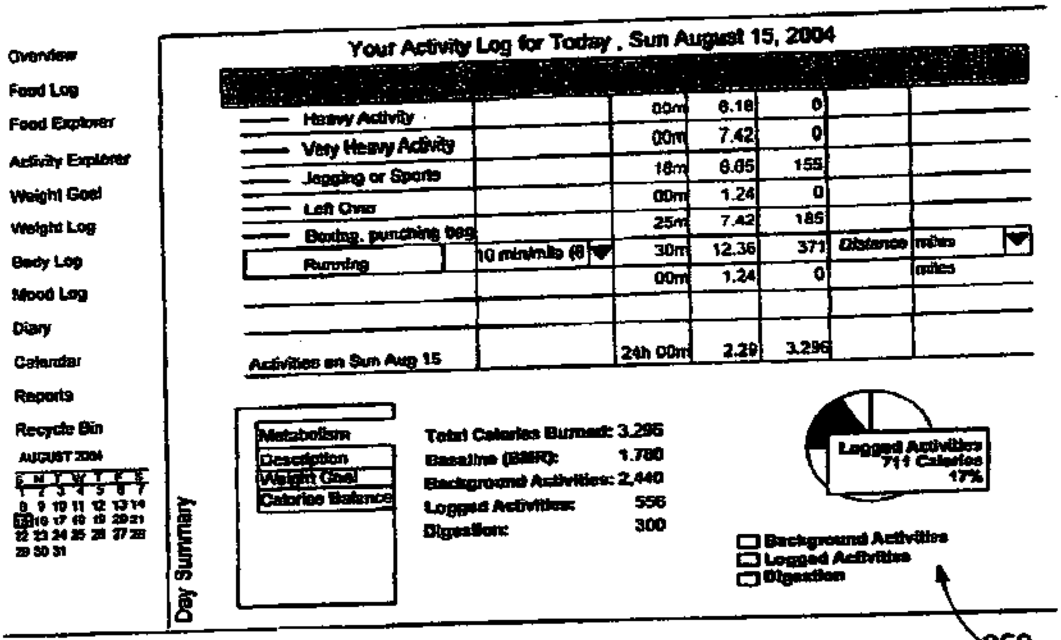

FIGURE 7

250

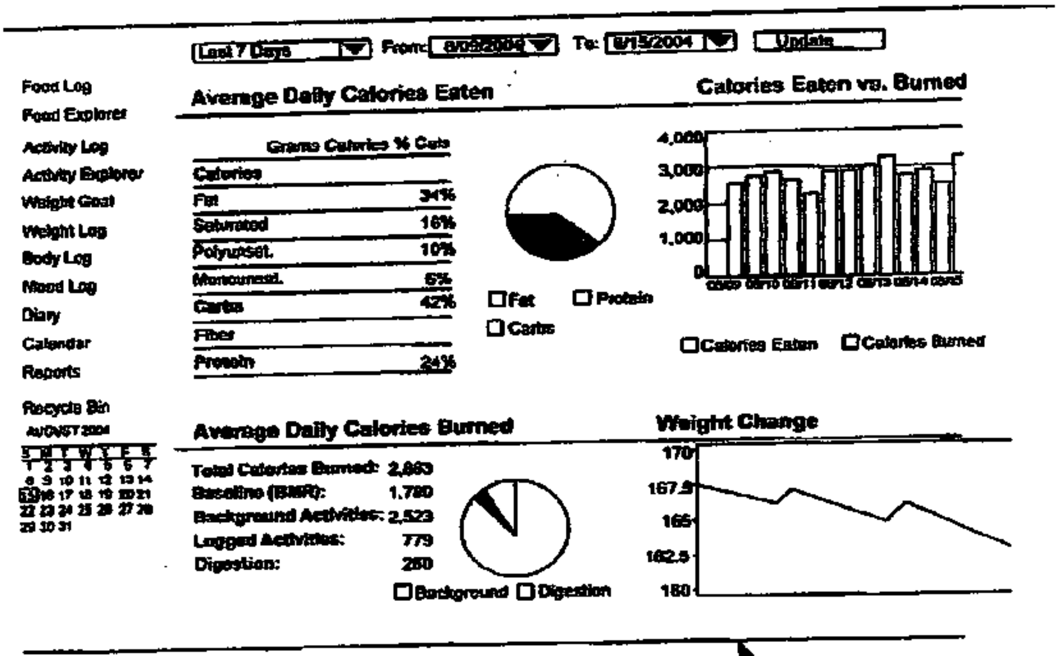

FIGURE 8

255

MONITORING DEVICE, METHOD AND SYSTEM

CROSS REFERENCES TO RELATED APPLICATION

[0001] The Present application claims priority to U.S. Provisional Patent Application No. 60/669,325, filed on Apr. 7, 2005. The Present application is also a continuation-in-part application of U.S. patent application Ser. No. 11/085,778, filed on Mar. 21, 2005, which is a continuation-in-part application of U.S. Provisional Application No. 60/613,785, filed on Sep. 28, 2004, now abandoned.

STATEMENT REGARDING FEDERALLY SPONSORED RESEARCH OR DEVELOPMENT

[0002] Not Applicable

BACKGROUND OF THE INVENTION

[0003] 1. Field of the Invention

[0004] The present invention is related to health monitoring devices. More specifically, the present invention relates to a wrist worn article for monitoring a user's vital signs.

[0005] 2. Description of the Related Art

[0006] There is a need to know how one is doing from a health perspective. In some individuals, there is a daily, even hourly, need to know one's health. The prior art has provided some devices to meet this need.

[0007] One such device is a pulse oximetry device. Pulse oximetry is used to determine the oxygen saturation of arterial blood. Pulse oximeter devices typically contain two light emitting diodes: one in the red band of light (660 nanometers) and one in the infrared band of light (940 nanometers). Oxyhemoglobin absorbs infrared light while deoxyhemoglobin absorbs visible red light. Pulse oximeter devices also contain sensors that detect the ratio of red/infrared absorption several hundred times per second. A preferred algorithm for calculating the absorption is derived from the Beer-Lambert Law, which determines the transmitted light from the incident light multiplied by the exponential of the negative of the product of the distance through the medium, the concentration of the solute and the extinction coefficient of the solute.

[0008] The major advantages of pulse oximetry devices include the fact that the devices are non-invasive, easy to use, allows for continuous monitoring, permits early detection of desaturation and is relatively inexpensive. The disadvantages of pulse oximetry devices are that it is prone to artifact, it is inaccurate at saturation levels below 70%, and there is a minimal risk of burns in poor perfusion states. Several factors can cause inaccurate readings using pulse oximetry including ambient light, deep skin pigment, excessive motion, fingernail polish, low flow caused by cardiac bypass, hypotension, vasoconstriction, and the like.

[0009] Chin et al., U.S. Pat. No. 6,018,673 discloses a pulse oximetry device that is positioned entirely on a user's nail to reduce out of phase motion signals for red and infrared wavelengths for use in a least squares or ratio-of-ratios technique to determine a patient's arterial oxygen saturation.

[0010] Smith, U.S. Pat. No. 4,800,495 discloses an apparatus for processing signals containing information concerning the pulse rate and the arterial oxygen saturation of a patient. Smith also discloses maintaining the position of the LEDs and detectors to prevent motion-artifacts from being produced in the signal.

[0011] Another method for using a pulse oximeter to measure blood pressure is disclosed in U.S. Pat. No. 6,616,613 to Goodman for a 'Physiological Signal Monitoring System'. The '613 patent discloses processing a pulse oximetry signal in combination with information from a calibrating device to determine a patient's blood pressure.

[0012] Chen et al, U.S. Pat. No. 6,599,251 discloses a system and method for monitoring blood pressure by detecting pulse signals at two different locations on a subjects body, preferably on the subject's finger and earlobe. The pulse signals are preferably detected using pulse oximetry devices.

[0013] Schulze et al., U.S. Pat. No. 6,556,852, discloses the use of an earpiece having a pulse oximetry device and thermopile to monitor and measure physiological variables of a user.

[0014] Malinouskas, U.S. Pat. No. 4,807,630, discloses a method for exposing a patient's extremity, such as a finger, to light of two wavelengths and detecting the absorbance of the extremity at each of the wavelengths.

[0015] Jobsis et al., U.S. Pat. No. 4,380,240 discloses an optical probe with a light source and a light detector incorporated into channels within a deformable mounting structure which is adhered to a strap. The light source and the light detector are secured to the patient's body by adhesive tapes and pressure induced by closing the strap around a portion of the body.

[0016] Tan et al., U.S. Pat. No. 4,825,879 discloses an optical probe with a T-shaped wrap having a vertical stem and a horizontal cross bar, which is utilized to secure a light source and an optical sensor in optical contact with a finger. A metallic material is utilized to reflect heat back to the patient's body and to provide opacity to interfering, ambient light. The sensor is secured to the patient's body using an adhesive or hook and loop material.

[0017] Modgil et al., U.S. Pat. No. 6,681,454 discloses a strap that is composed of an elastic material that wraps around the outside of an oximeter probe and is secured to the oximeter probe by attachment mechanisms such as Velcro, which allows for adjustment after initial application without producing excessive stress on the spring hinge of the oximeter probe.

[0018] Diab et al., U.S. Pat. No. 6,813,511 discloses a disposable optical probe suited to reduce noise in measurements, which is adhesively secured to a patient's finger, toe, forehead, earlobe or lip.

[0019] Diab et al., U.S. Pat. No. 6,678,543 discloses an oximeter sensor system that has a reusable portion and a disposable portion. A method for precalibrating a light sensor of the oximeter sensor system is also disclosed.

[0020] Tripp, Jr. et al., U.S. Statutory Invention Registration Number H1039 discloses an intrusion free physiological condition monitor that utilizes pulse oximetry devices.

[0021] Hisano et al., U.S. Pat. No. 6,808,473, discloses a headphone-type exercise aid which detects a pulse wave using an optical sensor to provide a user with an optimal exercise intensity.

[0022] In monitoring one's health there is a constant need to know how many calories have been expended whether exercising or going about one's daily routine. A calorie is a measure of heat, generated when energy is produced in our bodies. The amount of calories burned during exercise is a measure of the total amount of energy used during a workout. This can be important, since increased energy usage through exercise helps reduce body fat. There are several means to measure this expenditure of energy. To calculate the calories burned during exercise one multiplies the intensity level of the exercise by one's body weight (in kilograms). This provides the amount of calories burned in an hour. A unit of measurement called a MET is used to rate the intensity of an exercise. One MET is equal to the amount of energy expended at rest.

[0023] For example, the intensity of walking 3 miles per hour ("mph") is about 3.3 METS. At this speed, a person who weighs 132 pounds (60 kilograms) will burn about 200 calories per hour ($60\times3.3=198$).

[0024] The computer controls in higher-quality exercise equipment can provide a calculation of how many calories are burned by an individual using the equipment. Based on the workload, the computer controls of the equipment calculate exercise intensity and calories burned according to established formulae.

[0025] The readings provided by equipment are only accurate if one is able to input one's body weight. If the machine does not allow this, then the "calories per hour" or "calories used" displays are only approximations. The machines have built-in standard weights (usually 174 pounds) that are used when there is no specific user weight.

[0026] There are devices that utilize a watch-type monitor to provide the wearer with heart rate as measured by a heartbeat sensor in a chest belt.

[0027] The prior art has failed to provide a means for monitoring one's health that is accurate, easy to wear on one's body for extended time periods, allows the user to input information and control the output, and provides sufficient information to the user about the user's health. Thus, there is a need for a monitoring device that can be worn for an extended period and provide health information to a user. Further, there is a need for an add-on product to enhance the communication of information provided by a sports watch to an individual wearing the sports watch.

BRIEF SUMMARY OF THE INVENTION

[0028] The present invention provides a solution to the shortcomings of the prior art. The present invention is accurate, comfortable to wear by a user for extended time periods, is light weight, and provides sufficient real-time information to the user about the user's health. Further, the present invention may be added to a sports watch to enhance the amount of information provided to the user.

[0029] One aspect of the present invention is a monitoring device comprising a digital watch and at least one band of the watch having an optical sensor connected to a circuitry assembly. The circuitry assembly is in communication with the digital watch to provide health-related information for display on the display unit of the watch. In particular, the band with the optical sensor and circuitry assembly may be utilized with the BODYLINK system used on or with TIMEX digital watches.

[0030] Another aspect of the present invention is a monitoring device comprising a digital watch and at least one band of the watch having an optical sensor in communication with the digital watch to provide health-related information for display on the display unit of the watch. The location of the optical sensor on the band allows for integration with a conventional digital watch such as a TIMEX digital watch, several of which are disclosed at www.timex.com. In particular, the band with the optical sensor may be utilized with the BODYLINK system used on or with TIMEX digital watches.

[0031] Another aspect of the present invention is a monitoring device for monitoring the health of a user. The monitoring device includes an article, an optical device for generating a pulse waveform, a circuitry assembly embedded within the article, a display member positioned on an exterior surface of the article, and a control means attached to the article.

[0032] The article is preferably a watch having a main body and bands connectable to each other. The article preferably has a minimal mass, one to five ounces, and each band is preferably flexible so that the user can wear the watch the entire day if necessary. The monitoring device allows the user to track calories burnt during a set time period, monitor heart rate, blood oxygenation levels, distance traveled, target zones and optionally dynamic blood pressure.

[0033] Another aspect of the present invention is a method for monitoring a user's vital signs. The method includes generating a signal corresponding to the flow of blood through an artery of the user. The signal is generated from an optical device. Next, the heart rate data of the user and an oxygen saturation level data of the user is generated from the signal. Next, the heart rate data of the user and the oxygen saturation level data of the user are processed for analysis of calories expended by the user and for display of the user's heart rate and blood oxygen saturation level. Next, the calories expended by the user, the user's heart rate or the user's blood oxygen saturation level are displayed on a display member disposed on an exterior surface of an article, which is controlled by the user using a control component extending from the article.

[0034] Having briefly described the present invention, the above and further objects, features and advantages thereof will be recognized by those skilled in the pertinent art from the following detailed description of the invention when taken in conjunction with the accompanying drawings.

BRIEF DESCRIPTION OF THE SEVERAL VIEWS OF THE DRAWINGS

[0035] **FIG. 1** is a perspective view of a preferred embodiment of a monitoring device worn by a user.

[0036] **FIG. 1A** is a cross-sectional view of a band of a watch of the present invention.

[0037] **FIG. 2** is a perspective view of an alternative embodiment of a monitoring device worn by a user.

[0038] **FIG. 2A** is an isolated view of a light source and plurality of photodetectors of the monitoring device of **FIG. 2**.

[0039] **FIG. 3** is a perspective view of a watch of the present invention.

[0040] **FIG. 3A** is an enlarged view of a band of a watch, and the watch.

[0041] **FIG. 4** is a view of a user's wrist with the user's radial artery shown in phantom lines with an optical sensor of an article of the present invention placed over the radial artery.

[0042] **FIG. 5** is a cut-away of a user's wrist to illustrate the user's radial artery.

[0043] **FIG. 6** is a flow chart for using the control component to input information and output information on a display of the monitoring device.

[0044] **FIG. 7** is an image of an activity log of information obtained from a monitoring device.

[0045] **FIG. 8** is an image of calorie information obtained from a monitoring device.

DETAILED DESCRIPTION OF THE INVENTION

[0046] As shown in **FIGS. 1-4**, a monitoring device is generally designated **20**. The monitoring device **20** preferably includes an article **25**, an optical sensor **30**, a circuitry assembly **35**, a control component **43**, connection wires **45**, and optionally a display member **40**. The monitoring device **20** is preferably worn on a user's wrist **71**.

[0047] The article **25**, which is preferably a watch, preferably has a main body portion **95**, a first band **96*a*** and a second band **96*b***. The watch **25** is sized to securely attach to a user's wrist **71**. The watch **25** is adopted to act as a monitoring device or a monitoring device is integrated into a watch. The term article and watch are used interchangeably and those skilled in the pertinent art will recognize that a watch is a preferred embodiment of the article **25**.

[0048] It is desirous to adapt the article **25** to the anatomy of the user's wrist. Each of the first band **96*a*** and the second **96*b*** is preferably composed of neoprene, leather, synthetic leather, or other similar material, or a combination thereof. The article **25** preferably has a mass ranging from 5 grams to 50 grams. Preferably, the lower the mass of the article **25**, the more comfort to the user. The optical sensor **30** and optional circuitry assembly **35** are preferably disposed on one of the first band **96*a*** or second band **96*b***.

[0049] The optical sensor **30** is preferably positioned on an interior surface **98** of one of the first band **96*a*** or second band **96*b*** of the watch **25**. The optical sensor **30** is preferably connected to the circuitry assembly **35** by the connection wires **45**. The connection wires **45** are preferably embedded within one of the first band **96*a*** or second band **96*b*** of the watch **25**, and also connected to the main body portion **95**.

[0050] The optical sensor **30** of the monitoring device **20** is preferably positioned over the radial artery **77** of a user. However, those skilled in the pertinent art will recognize that the optical sensor may be placed over other arteries of the user without departing from the scope and spirit of the present invention. Further, the optical sensor **30** need only be in proximity to an artery of the user in order to obtain a reading or signal.

[0051] In a preferred embodiment, the optical sensor **30** is a photodetector **130** and a single light emitting diode ("LED") **135** transmitting light at a wavelength of approximately 660 nanometers. As the heart pumps blood through the arteries in the user's ankle or wrist, blood cells absorb and transmit varying amounts of the light depending on how much oxygen binds to the cells' hemoglobin. The photodetector **30**, which is typically a photodiode, detects transmission at the red wavelengths, and in response generates a radiation-induced signal. Yet in an alternative embodiment, the optical device **30** is based on green light wherein a LED generates green light (λ~500-600 nm), and the phtotodetector detects the green light.

[0052] Alternatively, the optical sensor **30** is a pulse oximetry device with a light source **135** that typically includes LEDs that generate both red (λ~660 nm) and infrared (λ~900 nm) radiation. As the heart pumps blood through the arteries in the wrist of the user, blood cells absorb and transmit varying amounts of the red and infrared radiation depending on how much oxygen binds to the cells' hemoglobin. The photodetector **130**, which is typically a photodiode, detects transmission at the red and infrared wavelengths, and in response generates a radiation-induced signal.

[0053] Alternatively, the optical sensor **30** is pulse oximetry device comprising the photodetector **130**, a first light source **135** and a second light source **135*a***, not shown. In this embodiment, the first light source **135** emits light in an infrared range (λ~900 nm) and the second light source **135*a*** emits light in a red range (λ~630 nm).

[0054] The light source **135** typically is a light-emitting diode that emits light in a range from 570 nanometers to 1100 nanometers. As the heart pumps blood through the patient's wrist, blood cells absorb and transmit varying amounts of the red and infrared radiation depending on how much oxygen binds to the cells' hemoglobin. The photodetector **130**, which is typically a photodiode, detects transmission at the red and infrared wavelengths, and in response generates a radiation-induced current that travels through the connection wires **45** to the circuitry assembly **35** on the article **25**.

[0055] Alternatively, as shown in **FIGS. 2 and** 2A, the optical sensor includes a plurality of photodetectors **130** and a single LED **135**.

[0056] A preferred photodetector **130** is a light-to-voltage photodetector such as the TSL260R and TSL261, TSL261R photodetectors available from TAOS, Inc of Plano Tex. Alternatively, the photodetector **130** is a light-to-frequency photodetector such as the TSL245R, which is also available from TAOS, Inc. The light-to-voltage photodetectors have an integrated transimpedance amplifier on a single monolithic integrated circuit, which reduces the need for ambient light filtering. The TSL261 photodetector preferably operates at a wavelength greater than 750 nanometers, and optimally at 940 nanometers, which would preferably have a LED that radiates light at those wavelengths. A preferred optical sensor **30** utilizing green light is a TRS1755 sensor from TAOS, Inc of Plano Tex. The TRS1755 comprises a green LED light source (567 nm wavelength) and a light-to-voltage converter. The output voltage is directly proportional to the reflected light intensity.

[0057] In a preferred embodiment, the circuit assembly **35** is flexible to allow for the contour of the user's wrist, and the movement thereof. Preferably the dimensions of a board of the circuit assembly **35** are approximately 39 millimeters (length) by approximately 21 millimeters (width) by 0.5 millimeters (thickness). The circuit assembly **35** is preferably embedded within a band **96***a* of the watch **25**. The circuit assembly **35** is preferably shaped to fit within the first band **96***a*.

[0058] Alternatively, the circuitry assembly **35** includes a flexible microprocessor board and a flexible pulse oximetry board. An alternative pulse oximetry board is a BCI MICRO POWER oximetry board, which is a low power, micro-size easily integrated board which provides blood oxygenation level, pulse rate (heart rate), signal strength bargraph, plethysmogram and status bits data. The size of the board is preferably 25.4 millimeters (length)×12.7 millimeters (width)×5 millimeters (thickness). The microprocessor board receives data from the pulse oximetry board and processes the data to display on the display member **40**. The microprocessor can also store data. The microprocessor can process the data to display pulse rate, blood oxygenation levels, calories expended by the user of a pre-set time period, target zone activity, time and dynamic blood pressure. Alternatively, the circuitry assembly **35** is a single board with a pulse oximetry circuit and a microprocessor.

[0059] The display member **40** is preferably a light emitting diode ("LED"). Alternatively, the display member **40** is a liquid crystal display ("LCD") or other similar display device.

[0060] On the circuitry assembly **35**, a microcontroller processes the signal generated from the optical sensor **30** to generate the plurality of vital sign information for the user which is displayed on the display member **40**. The control component **43** is connected to the circuit assembly **35** to control the input of information and the output of information displayed on the display member **40**.

[0061] The monitoring device **20** is preferably powered by a power source positioned on the watch **25**. Preferably the power source is a battery accessible at an interior surface of the main body portion **95**. The power source is preferably connected to the circuit assembly **35** by positive wire and ground wire, and the ground wire and positive wire are embedded within the article **25**.

[0062] In an alternative embodiment, a short range wireless transceiver **36** is included in the circuitry assembly **35** for transmitting information processed from the optical sensor **30** to a receiver on the watch **25**. Alternatively, the information is transmitted to a handheld device or a computer, not shown, to form a system. The display member **40** is optional in this embodiment.

[0063] The short-range wireless transceiver is preferably a transmitter operating on a wireless protocol, e.g. Bluetooth™, part-15, or 802.11. "Part-15" refers to a conventional low-power, short-range wireless protocol, such as that used in cordless telephones. The short-range wireless transmitter (e.g., a Bluetooth™ transmitter) receives information from the microprocessor and transmits this information in the form of a packet through an antenna. The external laptop computer or hand-held device features a similar antenna coupled to a matched wireless, short-range receiver that receives the packet. In certain embodiments, the hand-held device is a cellular telephone with a Bluetooth circuit integrated directly into a chipset used in the cellular telephone. In this case, the cellular telephone may include a software application that receives, processes, and displays the information. The secondary wireless component may also include a long-range wireless transmitter that transmits information over a terrestrial, satellite, or 802.11-based wireless network. Suitable networks include those operating at least one of the following protocols: CDMA, GSM, GPRS, Mobitex, DataTac, iDEN, and analogs and derivatives thereof. Alternatively, the handheld device is a pager or PDA.

[0064] A flow chart diagram **400** for using the control component **43** with the display member **40** is shown in **FIG. 6**. As mentioned above, the control component **43** allows a user to scroll and select from terms displayed on the display member **40**. User inputs preferably include age, gender, weight, height and resting heart rate which can be inputted and stored in a memory of the circuit assembly **35**. The real time heart rate of the user is preferably displayed as a default display, and the user's real time heart rate is preferably updated every ten seconds based on measurements from the optical sensor **30**. Based on the user inputs, the calories expended by the user for a set time period are calculated and displayed on the display member **40** as desired by the user using the control component **43**. The monitoring device **20** will also preferably include a conventional stop watch function, which is displayed on the display member **40** as desired by the user. The display member **40** preferably displays a visual alert when a user enters or exits a target zone such as a cardio zone or fat burning zone. The monitoring device **20** optionally includes an audio alert for entering or exiting such target zones.

[0065] The user can use the control component **43** to maneuver between the user's real-time heart rate and real time calories expended by the user during a set time period. The user can also scroll through a menu-like display on the display member **40** and enter options by pushing downward on the control component **43**. The options can preferably include a "My Data" section which the user inputs by scrolling and selection an option by pushing downward, such as selecting between male and female for gender. The user can also select target zones by scrolling through a different section of the menu. As discussed below, each target zone is calculated using a formula based upon the user's personal data. In operation, when a specific target zone is selected, a visual alert in the form of a specific display such as an icon-like picture is displayed on the display member **40** to demonstrate that the user is now in the specified target zone. The icon preferably blinks for a set period of time such as ten seconds. Those skilled in the pertinent art will recognize that other options may be included on the menu-like display without departing from the spirit and scope of the present invention.

[0066] In yet an alternative embodiment, an accelerometer, not shown, is embedded within the main body portion **95** of the watch **25** and connected to the circuitry assembly

35 in order to provide information on the distance traveled by the user. In a preferred embodiment, the accelerometer is a multiple-axis accelerometer, such as the ADXL202 made by Analog Devices of Norwood, Mass. This device is a standard micro-electronic-machine ("MEMs") module that measures acceleration and deceleration using an array of silicon-based structures.

[0067] In yet another embodiment, the monitoring device **20** comprises a first thermistor, not shown, for measuring the temperature of the user's skin and a second thermistor, not shown, for measuring the temperate of the air. The temperature readings are displayed on the display member **40** and the skin temperature is preferably utilized in further determining the calories expended by the user during a set time period. One such commercially available thermistor is sold under the brand LM34 from National Semiconductor of Santa Clara, Calif. A microcontroller that is utilized with the thermistor is sold under the brand name ATMega 8535 by Atmel of San Jose, Calif.

[0068] The monitoring device **20** may also be able to download the information to a computer for further processing and storage of information. The download may be wireless or through cable connection. The information can generate an activity log **250** such as shown in **FIG. 7**, or a calorie chart **255** such as shown in **FIG. 8**.

[0069] The microprocessor can use various methods to calculate calories burned by a user. One such method uses the Harris-Benedict formula Other methods are set forth at www.unu.edu/unupress/food2/which relevant parts are hereby incorporated by reference. The Harris-Benedict formula uses the factors of height, weight, age, and sex to determine basal metabolic rate (BMR). This equation is very accurate in all but the extremely muscular (will underestimate calorie needs) and the extremely overweight (will overestimate caloric needs) user.

[0070] The equations for men and women are set forth below:

$$\text{Men: BMR}=66+(13.7\times\text{mass (kg)})+(5\times\text{height (cm)})-(6.8\times\text{age (years)})$$

$$\text{Women: BMR}=655+(9.6\times\text{mass})+(1.8\times\text{height})-(4.7\times\text{age})$$

[0071] The calories burned are calculated by multiplying the BMR by the following appropriate activity factor: sedentary; lightly active; moderately active; very active; and extra active.

Sedentary=BMR multiplied by 1.2 (little or no exercise, desk job)

Lightly active=BMR multiplied by 1.375 (light exercise/sports 1-3 days/wk)

Moderately Active=BMR multiplied by 1.55 (moderate exercise/sports 3-5 days/wk)

Very active=BMR multiplied by 1.725 (hard exercise/sports 6-7 days/wk)

Extra Active=BMR multiplied by 1.9 (hard daily exercise/sports & physical job or 2×day training, marathon, football camp, contest, etc.)

[0072] Various target zones may also be calculated by the microprocessor. These target zones include: fat burn zone; cardio zone; moderate activity zone; weight management zone; aerobic zone; anaerobic threshold zone; and red-line zone.

Fat Burn Zone=(220−age)×60%&70%

An example for a thirty-eight year old female:

$$(220-38)\times0.6=109$$

$$(220-38)\times0.7=127$$

[0073] Fat Burn Zone between 109 to 127 heart beats per minute.

Cardio Zone=(220−your age)×70%&80%

An example for a thirty-eight year old female:

$$(220-38)\times0.7=127$$

$$(220-38)\times0.8=146$$

[0074] Cardio zone is between 127 & 146 heart beats per minute.

[0075] Moderate Activity Zone, at 50 to 60 percent of your maximum heart rate, burns fat more readily than carbohydrates. That is the zone one should exercise at if one wants slow, even conditioning with little pain or strain.

[0076] Weight Management Zone, at 60 to 70 percent of maximum, strengthens ones heart and burns sufficient calories to lower one's body weight.

[0077] Aerobic Zone, at 70 to 80 percent of maximum, not only strengthens one's heart but also trains one's body to process oxygen more efficiently, improving endurance.

[0078] Anaerobic Threshold Zone, at 80 to 90 percent of maximum, improves one's ability to rid one's body of the lactic-acid buildup that leads to muscles ache near one's performance limit. Over time, training in this zone will raise one's limit.

[0079] Red-Line Zone, at 90 to 100 percent of maximum, is where serious athletes train when they are striving for speed instead of endurance.

EXAMPLE ONE

Female, 30 yrs old, height 167.6 centimeters, weight 54.5 kilograms.

The BMR=655+523+302−141=1339 calories/day.

[0080] The BMR is 1339 calories per day. The activity level is moderately active (work out 34 times per week). The activity factor is 1.55. The TDEE=1.55×1339=2075 calories/day. TDEE is calculated by multiplying the BMR of the user by the activity multiplier of the user.

[0081] A system may use the heart rate to dynamically determine an activity level and periodically recalculate the calories burned based upon that factor. An example of such an activity level look up table might be as follows:

Activity/Intensity Multiplier Based on Heart Rate

Sedentary=BMR×1.2 (little or no exercise, average heart rate 65-75 bpm or lower)

Lightly active=BMR×3.5 (light exercise, 75 bpm-115 bpm)

Mod. active=BMR×5.75 (moderate exercise, 115-140 pm)

Very active=BMR×9.25 (hard exercise, 140-175 bpm)

Extra active=BMR×13 (175 bpm-maximum heart rate as calculated with MHR formula)

[0082] For example, while sitting at a desk, a man in the above example might have a heart rate of between 65 and 75 beats per minute (BPM). (The average heart rate for an adult is between 65 and 75 beats per minute.) Based on this dynamically updated heart rate his activity level might be considered sedentary. If the heart rate remained in this range for 30 minutes, based on the Harris-Benedict formula he would have expended 1.34 calories a minute×1.2 (activity level)×30 minutes, which is equal to 48.24 calories burned.

[0083] If the man were to run a mile for 30 minutes, with a heart rate ranging between 120 and 130 bpm, his activity level might be considered very active. His caloric expenditure would be 1.34 calories a minute×9.25 (activity level)×30 minutes, which is equal to 371.85.

[0084] Another equation is weight multiplied by time multiplied by an activity factor multiplied by 0.000119.

[0085] From the foregoing it is believed that those skilled in the pertinent art will recognize the meritorious advancement of this invention and will readily understand that while the present invention has been described in association with a preferred embodiment thereof, and other embodiments illustrated in the accompanying drawings, numerous changes modification and substitutions of equivalents may be made therein without departing from the spirit and scope of this invention which is intended to be unlimited by the foregoing except as may appear in the following appended claim. Therefore, the embodiments of the invention in which an exclusive property or privilege is claimed are defined in the following appended claims.

We claim as our invention:

1. A monitoring device for monitoring the health of a user, the monitoring device comprising:

an article having a main body, a first band attached to one end of the main body and a second band attached to a second end of the body, the first band and the second band having a connection mechanism for connecting to each other;

means for measuring blood flow through an artery of the wrist of the user, the measuring means disposed on the first band of the article;

means for calculating calories expended by the user during a time period, the calculating means disposed on the main body of the article;

means for visually displaying the calories expended by the user, the visually displaying means disposed on an exterior surface of the main body of the article; and

means for controlling the input information and the output of information displayed on the visually displaying means, the controlling means disposed on the exterior surface of the main body of the article.

2. The monitoring device according to claim 1 further comprising means for determining the pulse rate of the user.

3. The monitoring device according to claim 1 further comprising a time function mechanism disposed on the main body of the article to provide a time of day.

4. The monitoring device according to claim 1 wherein each of the first band and the second band of the article is composed of a neoprene material.

5. The monitoring device according to claim 1 wherein the measuring means is an optical sensor comprising a light-to-voltage photodetector capable of transmitting a digital signal, and at least one light emitting diode capable of radiating light ranging from 600 nanometers to 1100 nanometers.

6. The monitoring device according to claim 1 wherein the measuring means is a pulse oximetry sensor comprising a light-to-voltage photodetector capable of transmitting a digital signal, first light emitting diode capable of radiating red light and a second light emitting diode capable of emitting infrared light.

7. The monitoring device according to claim 1 wherein the measuring means is an optical sensor comprising a light-to-frequency photodetector capable of transmitting a digital signal, and at least one light emitting diode capable of radiating light ranging from 570 nanometers to 1100 nanometers.

8. The monitoring device according to claim 1 wherein the measuring means is an optical sensor comprising a plurality of light-to-voltage photodetectors capable of transmitting a digital signal, and at least one light emitting diode capable of radiating light ranging from 600 nanometers to 1100 nanometers.

9. The monitoring device according to claim 1 wherein the measuring means is an optical sensor comprising a plurality of light-to-frequency photodetectors capable of transmitting a digital signal, and at least one light emitting diode capable of radiating light ranging from 570 nanometers to 1100 nanometers.

10. A monitoring device for monitoring the health of a user, the monitoring device comprising:

an article to be worn on the user's wrist, the article comprising a main body having an interior surface and an exterior surface, a first band attached to one end of the main body and a second band attached to a second end of the body, the first band and the second band having a connection mechanism for connecting to each other;

an optical sensor disposed on an interior surface of the first band of the article;

a circuitry assembly embedded within the main body of the article;

a display member disposed on an exterior surface of the main body of the article; and

a control component disposed on the exterior surface of the main body of the article, the control component controlling the input of information and the output of information displayed on the display member.

11. The monitoring device according to claim 10 wherein the optical sensor comprises a light-to-voltage photodetector capable of transmitting a digital signal, and at least one light emitting diode capable of radiating light ranging from 600 nanometers to 1100 nanometers.

12. The monitoring device according to claim 10 wherein the optical sensor comprises a light-to-frequency photodetector capable of transmitting a digital signal, and at least one light emitting diode capable of radiating light ranging from 570 nanometers to 1100 nanometers.

13. The monitoring device according to claim 10 wherein the optical sensor comprises a plurality of light-to-voltage photodetectors capable of transmitting a digital signal, and at least one light emitting diode capable of radiating light ranging from 600 nanometers to 1100 nanometers.

14. The monitoring device according to claim 10 wherein the optical sensor comprises a plurality of light-to-frequency photodetectors capable of transmitting a digital signal, and at least one light emitting diode capable of radiating light ranging from 570 nanometers to 1100 nanometers.

15. A watch with a monitoring device for monitoring the health of a user, the watch comprising:

a main body having an interior surface and an exterior surface, the main body comprising a timepiece mechanism;

a first band connected to a first end of the main body;

a second band connected to a second end of the main body, the first band and the second connectable to each other;

an optical sensor disposed on the interior surface of the first band;

a circuitry assembly embedded within the first band, the circuitry assembly comprising a microprocessor and connected to the optical sensor;

a display member disposed on an exterior surface of the main body; and

a control component disposed on the exterior surface of the main body, the control component controlling the input of information and the output of information displayed on the display member.

16. The watch according to claim 15 wherein the optical sensor comprises a light-to-voltage photodetector capable of transmitting a digital signal, and at least one light emitting diode capable of radiating light ranging from 600 nanometers to 1100 nanometers.

17. The monitoring device according to claim 15 wherein the optical sensor comprises a light-to-frequency photodetector capable of transmitting a digital signal, and at least one light emitting diode capable of radiating light ranging from 570 nanometers to 1100 nanometers.

18. The monitoring device according to claim 15 wherein the optical sensor comprises a plurality of light-to-voltage photodetectors capable of transmitting a digital signal, and at least one light emitting diode capable of radiating light ranging from 600 nanometers to 1100 nanometers.

19. The monitoring device according to claim 15 wherein the optical sensor comprises a plurality of light-to-frequency photodetectors capable of transmitting a digital signal, and at least one light emitting diode capable of radiating light ranging from 570 nanometers to 1100 nanometers.

20. The monitoring device according to claim 15 wherein the circuitry assembly is in wireless communication with a receiver on the main body.

* * * * *

APPENDIX M

Implementation of a Wireless Pulse Oximeter Based on Wrist Band Sensor

Qing Cai, Jinming Sun, Ling Xia, Xingqun Zhao*
Collage of Biological Science and Medical Engineering
Southeast University, Nanjing, China
*Corresponding author E-mail address: ndt@seu.edu.cn

***Abstract*—In order to develop a wrist band pulse oximeter, the detected light intensities and effective transmission depth of reflectance oximetry are investigated by analyzing the light propagation through tissue. A reflectance probe is fabricated based on the analytical results. An oxygen saturation measurement system is also implemented and some preliminary experiments are conducted. The experimental results have confirmed the feasibility of this wrist-band oximeter. Home healthcare can be ensured by transmitting the realtime measurements through wireless technology to the community monitoring system.**

Keywords- Wrist-band sensor; Oxygen saturation; Remote healthcare

I. INTRODUCTION

Non-invasive pulse oximetry has been widely used in clinical care for critical ill patient, monitor of patient during the anesthesia in operations, research of breath state while sleeping, etc. It's a safe, reliable, real time and continuous measurement method. Nowadays transmittance oximetry has been fully developed and there're many mature products which are widely and frequently used in hospitals. However, a transmittance pulse oximeter is reliable and practical only in case the patient is hospitalized or lying steadily. Besides, transmittance measurements sometimes cause discomfort, pain or injury because its sensor lightly presses a finger or ear lobe and occasionally blocks the blood flow. A reflectance oximeter which increases the flexibility of installation can avoid such problems and meet the needs of modern home healthcare, whereas the research of reflectance oximeters is still in a shortage relative to the transmittance type and there are few complete solutions for reflectance oximetry[1][2].

In this study, the detected light intensities and effective transmission depth of reflectance oximetry are investigated by analyzing light propagation through tissue using the photon diffusion equation. We fabricated a reflectance probe based on the analytical results, implemented an oxygen saturation measurement system and conducted some preliminary experiments, whose results have comfirmed the feasibility of our oximeter. We also implemented a RF transmitting module to found a communication between the measurement system and community care center to ensure home monitor of oxygen saturation, which is mainly used in night care of patients with sleep apnea syndrome [3].

II. THE PRINCIPLE OF RELECTANCE OXIMETRY BASED ON DIFFUSION PROPAGATION THEORY

Human tissue is a strongly scattering media, in which the movement of light is random. In transmittance oximetry, the light detector mainly receives the forward scattered light; while in reflectance oximetry, the light source and the detector are both placed on the same side of the measurement site, the detector mainly receives scattered light after a parabolic path in tissue, as shown in figure 1.

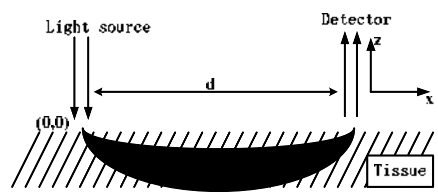

Figure 1. Boundary of the parabolic region for photon path distribution

A. Detected light intensity

For most human tissue, the scattering coefficient is much greater than the absorption coefficient. Therefore, when the scattering length of tissue is much smaller than its geometric dimensions, the photon will experience repeatedly scattering before it's absorbed or escaping outside the tissue boundary. In this case, the photon migration in biological tissue can be considered as a diffusion process. Light propagation in homogeneous biological tissue can be described by photon diffusion equation [4]:

$$\frac{1}{c}\frac{\partial}{\partial t}\phi(r,t) - D\nabla^2\phi(r,t) + \mu_a\phi(r,t) = S(r,t) \tag{1}$$

Where $\phi(r,t)$ is the fluence rate at the position r in the tissue, which means the effective photon density at the position r at time t. D represents diffusion coefficient, μ_a is absorption coefficient and $S(r,t)$ represents the light source.

The diffusion coefficient D for photon migration is:

$$D = \frac{1}{3\{\mu_a + (1-g)\mu_s\}} \tag{2}$$

Thus the density of the photon leaving the tissue is given by the flux of the fluence and the detected light intensity is:

$$\phi(\rho,t) = (4\pi Dc)^{-3/2} z_0 t^{-5/2} \exp(-\mu_a ct)\exp(-\frac{d^2+z_0^2}{4Dct}) \tag{3}$$

Where z_0 is $[(1-g)\mu_s]^{-1}$, d is the source-detector separation.

When time is long enough, the change rate of reflected light intensity is as below:

$$\lim_{t\to\infty} \frac{\partial}{\partial t} \ln \phi(\rho,t) = -\mu_a c \tag{4}$$

Therefore the change rate of reflected light intensity is proportional to tissue's absorption coefficient [4].

In the near infrared region, the absorption caused by such substance as water, cytopigment, etc. is much smaller than that caused by oxygenated hemoglobin (HbO2) and reduced hemoglobin (Hb), and the light absorbance of HbO2 is different from that of Hb at two different wavelengths. Therefore when illuminating the tissue containing an arterial bed with light of different wavelengths, we can deduce the oxygen saturation from the ratio of change rates of reflected light intensity in these two wavelengths.

Note the change rate of reflectance light intensity W, the blood oxygen saturation can be expressed as:

$$SpO_2 = A - B \cdot \frac{W_{\lambda 1}}{W_{\lambda 2}} \tag{5}$$

The light attenuated by body tissue consists of a direct current (DC) component and an alternating current (AC) component. The DC component is the result of the absorption by the body tissue and veins, while the AC component is the result of the absorption by the fluctuating volume of arterial blood. The change rate of reflectance light intensity can be expressed as: $W = I_{AC} / I_{DC}$, accordingly the formula for determining oxygen saturation can be obtained :

$$SpO_2 = A - B \cdot \frac{I_{AC}^{\lambda 1} / I_{DC}^{\lambda 1}}{I_{AC}^{\lambda 2} / I_{DC}^{\lambda 2}} \tag{6}$$

B. *Effective transmission depth*

In order to measure oxygen saturation, it is important to know whether or not the light reaches the arteries and the pulse wave is detected. The distribution function of photon path in tissue is [5]:

$$P(x,y,z) = \frac{z^2 \exp(-k\{(x^2+y^2+z^2)^{1/2} + [(d-x)^2+y^2+z^2]^{1/2}\})}{(x^2+y^2+z^2)^{3/2}[(d-x)^2+y^2+z^2]^{3/2}} * [k(x^2+y^2+z^2)^{1/2}+1]\{[(d-x)^2+y^2+z^2]^{1/2}+1\} \tag{7}$$

As is shown in figure 1, the photon path in tissue is parabolic in the x-z cross section. Under conditions of weak absorption (kd<<1), when coordinate is (x,0,0) the z position z0 (x) of the cambered region is:

$$z_0(x) \approx \sqrt{\frac{1}{8}\left[\sqrt{\left[x^2+(d-x)^2\right]^2 + 32x^2(d-x)^2} - x^2 - (d-x)^2\right]} \tag{8}$$

The maximum depth the incident light reaches is called effective transmission depth. z_0 reaches the maximum when x=d/2;

$$z_0^{\max} \approx \sqrt{2}d/4 \tag{9}$$

This shows that the effective transmission depth depends on the source-detector separation d. So choose a suitable distance between the light source and detector can ensure the effective detection of blood oxygen saturation.

III. System Design and Implementation

A. *System design*

The system consists of wristband sensor, signal acquisition and processing module, wireless transmission module, power module, display module, etc. Figure 2 shows the system block diagram.

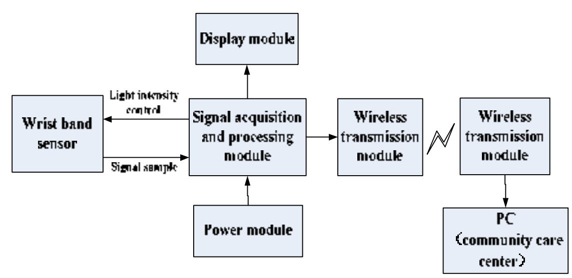

Figure 2. System block diagram

B. *Sensor*

A wrist located reflectance sensor is used to sample the pulse wave signal. It has functions of optical source control, signal conversion and signal amplification. It's composed of light source, light detector, and a wrist band which is used for mounting the sensor.

For reflectance oximetry, the ratio of absorption coefficient in the wavelength of 660nm and 900nm is the most sensitive to the change in oxygen saturation. To avoid the difference of transmission path caused by the distance between two separated light sources, the system employs dual-wavelength light-emitting diode as the light source, with the peak emission wavelength of 940nm and 660nm.

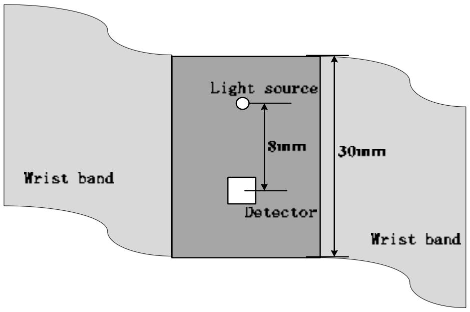

Figure 3. Wristband sensor

By the formula (3) and (9), both the detected light intensity and effective transmission depth are affected by the source-detector separation. To ensure sufficient detected light intensity and transmission depth, the optimum source-detector separation was chose as 8mm based on several experiments. The wristband sensor design is shown in Figure 3. To get the best measurement effect, the wrist band mounts the sensor on the inner wrist right above the arterial vessel.

C. Signal sampling and processing

To meet the design requirements of miniaturization, portable and low power consumption, the system employs MSP430 microcontroller as the core of hardware control, data processing and transmission.

The internal 12-bit DAC0 in the MCU periodically send two pulses to light source drive module, making light emitting diode emit red and infrared light alternatively to obtain optical modulation. When the pulse beats, the volume of blood flow through the wrist artery changes, the detected red and infrared light intensity changed consequently. The ADC sampled the output signal of the light detector so as to get the modulated photoplethysmography signal.

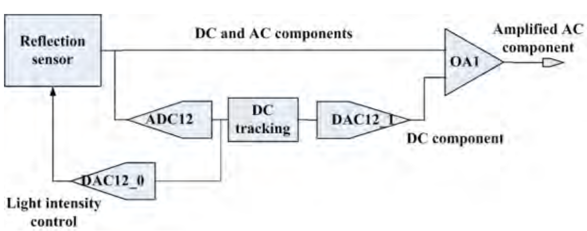

Figure 4. Signal procesing diagram

The AC component of this signal is effectively extracted and amplified through differential amplification performed by the built-in operational amplifier OA1 of the microcontroller. Figure 4 shows the processing procedure of pulse signal.

The initial pulse wave signal extracted at this stage comprises electromagnetic interference and power supply noise; therefore, it's necessary to eliminate ambient noises in 50Hz and above, considering the fundamental frequency of the pulse wave is about 1Hz[6]. A symmetric FIR filter as is shown in formula (10) is implemented for removing the noise, with cutoff frequency of 6Hz and -50dB attenuation in 50 Hz and above. Where x[n] and y[n] represents the input and output signal respectively, while N represents the length of the FIR filter. h[n] is the FIR filter coefficients.

$$y[n]=\sum_{k=0}^{N}h[k]x[n-k]$$
$$h[n]=h[N-n] \qquad (10)$$

Figure 5 shows the initial pulse wave signal extracted by the built-in amplifier and effective pulse wave signal after filtering. As can be seen from the figure, the system efficiently detected the human pulse wave signal， indicating that the incident light can visit the arterial vessel.

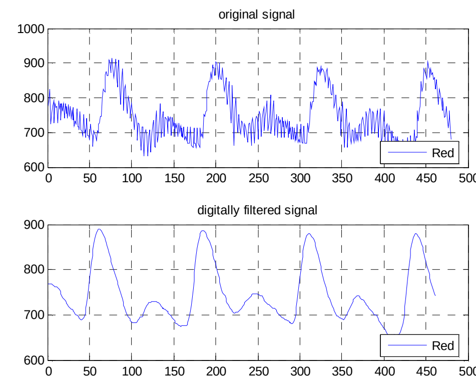

Figure 5. Original signal(upper) and filtered signal(lower) of pulse wave

The heart rate is measured by calculating the cycle of pulse wave signal, and the oxygen saturation is deduced by computing the ratio of the light intensity change rates under two different wavelengths. The real time measurement results and pulse wave are displayed on an OLED continuously

D. Wireless data transmission

The wireless transmission module founds a communication between measurement system and community care system, transfers the measurement results to a PC. Therefore, a number of users can be centralized monitored by creating a small wireless network.

The wireless transmitting module consists of a transceiver CC2500, a chip antenna, etc. CC2500 is a single chip transceiver designed for very low power wireless applications and intended for the ISM frequency band at 2.4 GHz. Wireless receiving module integrates a MSP430 MCU, CC2500 RF transceiver and a USB interface. It can be directly connected to the PC of community care center.

Wireless transmitting module communicates data with measurement system through the SPI interface and sends measurement results to the receiving module. Wireless receiving module transfers the received data to the PC of community care system via USB interface. RF chip CC2500 keeps control of RF module and IEEE 802.15.4 protocol to regulate the wireless transmission of measurement data.

Several oximeters can easily set up a star wireless network [7]. Transmission distance can reach 100m in an open space, relay stations are needed while transferring data for farther distance or through walls.

IV. EXPERIMENTAL RESULTS

To test the reliability of this system, an apnea experiments is conducted; five healthy people took part in this experiment. We recorded the values of R at time intervals during the slowly recovery process after several seconds of breath holding, and drew the value changes in line graphs as shown in Figure 6.

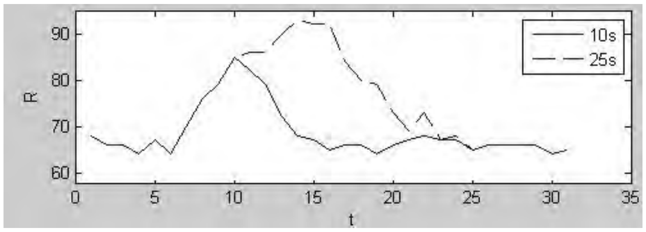

Figure 6. Change map of the value of R after breath holding for 10s and 25s

About 6s after the apnea, R values began to rise to a peak, which means oxygen saturation began to decrease. It can be seen from the comparison of these two graph that for the longer time of breath holding, the increasing amplitude of R is larger, that is the decreasing extend of oxygen saturation is larger, and the recovery time is longer as well.

The experimental results indicate that this system can effectively detect the change of oxygen saturation

V. CONCLUSION

This paper describes the system design of a wristband pulse oximer and completes the prototype fabrication. This oximeter can obtain oxygen saturation and heart rate information continuously and non-invasively through a wearable reflection sensor placed on the inner wrist; its facility makes it quite suitable for daily home care. From the waveform and measurement results it can be seen that the system can achieve the wrist pulse signal acquisition and noise filtering. The preliminary experiments have confirmed the reliability of the measurement results. The wireless transmission module transfers real time measurement data to community care center, providing the basis for community centralized care and remote monitoring. This wrist band pulse oximeter offers an effective means of home monitoring oxygen saturation, which has a broad application scope and aspects

REFERENCES

[1] Miia M, Antti K, Esko A, YoungChung W. Optimum Place for Measuring Pulse Oximeter Signal in Wireless Sensor-Belt or Wrist-Band. International Conference on Convergence Information Technology, 2007 .

[2] O. Abdallah, A. Bolz. Signal Processing by Reflectance Pulse Oximetry for Monitoring the fractional Oxygen Saturation and the Detektion of Anemia. IFMBE Proceedings, 2(7): 1152-1155.

[3] Chaudhary B, Dasti S, Park Y, et a1. Hour-to-hour variability of oxygen saturation in sleep apnea. Chest,1998,113(3):719-722.

[4] Y. Wei, G. Qingen, Y. Xiang, L. Feixue, D. QinKai. ExperimentaI study on non-invasive detection of reflectance oxygen saturation. Chinese Medical Equipment Journal, 2007;28(10): 4-7.

[5] ShechaoFeng, Fan-AnZeng and Britton Chance. Photon migration in the presence of a single defect: a pertubation analysis. Appl.Opt.,1995, 34(19): 3826-3837.

[6] Frans M .Coetzee and Ziad Elghazzawi. Noise-Resistant Pulse Oximetry Using a Synthetic Reference Signal, IEEE Transaction on Biomedical Engineering,2000;47(8): 1018-1026.

[7] M. Site, L. Jun. Design of Wireless Network for Multi- par ameter Patient Monitor Based on ZigBee Technology. Chinese Medical Equipment Journal, 2008;29(9): 53-56.

APPENDIX N

(12) INTERNATIONAL APPLICATION PUBLISHED UNDER THE PATENT COOPERATION TREATY (PCT)

(19) World Intellectual Property Organization
International Bureau

(43) International Publication Date
15 March 2001 (15.03.2001)

PCT

(10) International Publication Number
WO 01/17421 A1

(51) International Patent Classification[7]: A61B 5/00, G01N 33/49, 21/55

(21) International Application Number: PCT/SE00/01740

(22) International Filing Date: 7 September 2000 (07.09.2000)

(25) Filing Language: English

(26) Publication Language: English

(30) Priority Data:
9903182-5 8 September 1999 (08.09.1999) SE
0001711-1 9 May 2000 (09.05.2000) SE

(71) Applicant: OPTOQ AB [SE/SE]; Box 20030, S-161 02 Bromma (SE).

(72) Inventors: LINDBERG, Lars-Göran; Bankekind Haga, S-585 93 Linköping (SE). ENLUND, Gunnar; Bergslagsgatan 49, S-602 18 Norrköping (SE). VEGFORS, Magnus; Högalidsgatan 15, S-582 45 Linköping (SE).

(74) Agents: LINDBERG, Åke et al.; Bergenstråhle & Lindvall AB, P.O. Box 17704, S-118 93 Stockholm (SE).

(81) Designated States (*national*): AE, AG, AL, AM, AT, AU, AZ, BA, BB, BG, BR, BY, BZ, CA, CH, CN, CR, CU, CZ, DE, DK, DM, DZ, EE, ES, FI, GB, GD, GE, GH, GM, HR, HU, ID, IL, IN, IS, JP, KE, KG, KP, KR, KZ, LC, LK, LR, LS, LT, LU, LV, MA, MD, MG, MK, MN, MW, MX, MZ, NO, NZ, PL, PT, RO, RU, SD, SE, SG, SI, SK, SL, TJ, TM, TR, TT, TZ, UA, UG, UZ, VN, YU, ZA, ZW.

(84) Designated States (*regional*): ARIPO patent (GH, GM, KE, LS, MW, MZ, SD, SL, SZ, TZ, UG, ZW), Eurasian patent (AM, AZ, BY, KG, KZ, MD, RU, TJ, TM), European patent (AT, BE, CH, CY, DE, DK, ES, FI, FR, GB, GR, IE, IT, LU, MC, NL, PT, SE), OAPI patent (BF, BJ, CF, CG, CI, CM, GA, GN, GW, ML, MR, NE, SN, TD, TG).

Published:
— *With international search report.*
— *Before the expiration of the time limit for amending the claims and to be republished in the event of receipt of amendments.*

WO 01/17421 A1

(54) Title: METHOD AND APPARATUS FOR COMBINED MEASUREMENT OF HEMOGLOBIN AND OXYGEN SATURATION

(57) Abstract: The present invention relates to a method for accurately detecting SpO_2, partly by using determination of blood characteristics including hemoglobin, in a fluid medium using the reflection of at least one light beam.

Method and apparatus for combined measurement of hemoglobin and oxygen saturation.

The present invention relates to a non-invasive method for determination of SpO_2, including a first determination of blood characteristics including hemoglobin (EVF/hematocrit), in a vessel containing a mixture of liquid and blood cells using the orientation effects of the red blood cells. The present invention also relates to an apparatus for performing the method.

Background to the invention

There are different non-invasive methods known for measurement of hemoglobin. These methods make use of absorption of energy at a certain light wavelength, of the red blood cells (RBCs). Carim et al disclose in US 5755226 a non-invasive method and apparatus for the direct non-invasive prediction of hematocrit in mammalian blood using photopletysmography (PPG) techniques and data processing. However, this method only makes use of the ability of the RBCs to absorb energy. This method is also quite complicated regarding the formulas which are to be used when calculating the predicted hematocrit. Thus the method is time consuming. This method has not taken into account the red blood cell orientation and distribution in blood vessels.

Further, a method and an apparatus, are disclosed in WO 97/15229 for determining hemoglobin concentration in blood. The method is used for detecting hemoglobin in the microvascular system beneath the mucosal membranes on the inside of the lip of a human subject by introducing a measuring tip into the mouth of a subject. This means that the measuring tip of the apparatus must have some kind of sterile shell before it may be placed in the mouth. This sterility of the measuring tip means that either the apparatus must be autoclaved before measuring or that a disposable plastic tip has to be used when performing the method. This method further uses the reflection of light for determining the concentration of hemoglobin.

Photopletmysmography and pulse oximetry has been thoroughly investigated by two of the present inventors ("Photopletmysmography, methodological studies and applications", Lars-Göran Lindberg, Linköping Studies in Science and Technology Dissertations, No 262, 1991 and "Pulse oximetry - methodological considerations", Magnus Vegfors, Linköping University Medical Dissertations, No 347 1992, both hereby incorporated by reference thereto).
They found e.g. that when pulse oximeter was tested on an artificial bed different flow conditions greatly affected the accuracy of the pulse oximeter. Different states of the blood, diluted and haemolysed blood changed the pulse oximeter accuracy indicating that orientation of red blood cells and the viscosity of blood as a whole may play important role for the generation of the two PPG signals utilised in pulse oximetry. (in Lindberg above)

Further there was mentioned in Vegfors' paper above about some previous studies which have indicated that pulse oximeter accuracy may be dependent on blood haematocrit. For ethical reasons, it is impossible to study the accuracy of pulse oximetry on humans at very low haematocrit levels. Therefore, little human data is available during anaemia. Some investigations document an increasing negative bias in mildly anaemic subjects.

The majority of pulse oximeters uses transmitted light to calculate the oxygen saturation. This limits the probe application to for example finger tips, toes or ear lobes.

There is therefore an increasing interest in reflection pulse oximetry. (Vegfors above) Further examples of pulse oximeters are described in the historical review "History of Blood Gas Analysis. VI. Oximetry", J. W. Severinghaus and P.B. Astrup, Journal of Clinical Monitoring, Vol 2, No. 4, October 1986, pp 270-287 (hereby incorporated by reference thereto).

Since haematocrit values outside normal ranges are known to effect the accuracy of pulse oximetry a combined measurement of haemoglobin and oxygen saturation it would be desirable with a method and apparatus which makes it possible to alert for false pulse oximetry readings and perform on-line corrections.

Accordingly, there is a need for new methods for detecting SpO_2 which takes into account blood characteristics including Hb, and accordingly also the blood cell orientation and thus give a more accurate detection value. Further, methods which do not involve an extra step of making the apparatus sterile before measuring or disposable tips are desirable. The new methods should also be less sensitive to variations in the blood pressure, e.g. the pulsative, (systolic) pressure.

Summary of the invention

The present invention solves the above problems by increasing the accuracy of pulse oximetry measurements by reflection and transmittance measurements:

- on central arterial blood vessels better reflecting the oxygenation than peripheral vascular beds,

- on-line correction for haematocrit values affecting the accuracy,

- simultaneous results of oxygen saturation and blood values (such as haematocrit) improving the quality and safety in patient monitoring.

In accordance with a first aspect of the present invention there is provided a new non-invasive method for accurate determination of SpO_2 from a mixture of liquid and blood cells contained in a light pervious vessel comprising:

a) directing light beams against the mixture;

b) determining at least one blood characteristic other than SpO_2 including hemoglobin of the mixture by analyzing the intensity of the light reflected from the mixture, or the intensity of the light reflected from the mixture in combination with the intensity of the light transmitted through the mixture; and

c) determining oxygen saturation, SpO_2, of the mixture by analyzing the intensity of the light transmitted through the mixture.

In the new method, (b) and (c) may be performed in the reverse order or even simultaneously.

In accordance with the invention, the new method further comprises establishing whether the result of c) is relevant with respect to the result of b).

Advantageously, (c) is performed by pulse-oximetrically determining oxygen saturation.

With regard to the determination of oxygen saturation, first, (a) is performed by directing at least one light beam with a wavelength in the red light range against the vessel, and directing at least one light beam with a wavelength in the infrared light range against the vessel. Then, (c) is performed by detecting the intensities of the red light and infrared light transmitted through the mixture, calculating a quotient of the detected intensities, red/infrared, of the transmitted light, and determining SpO_2 by analyzing the quotient.

By analyzing the quotient of the detected intensities of transmitted light the advantage is achieved that influences from pressure and flow, in particular pulsating flow, of the liquid mixture is compensated for, whereby the determined SpO_2 will be accurate. The quotient is analyzed by comparing it with previously obtained quotients for known values of SpO_2.

With regard to the determination of the blood characteristic (i.e. at least hemoglobin), (b) is performed by:
i) detecting the intensity of the light of the light beams reflected from the mixture and the intensity of the light of the light beams transmitted through the mixture;
ii) calculating a quotient of the detected intensity of the transmitted light and detected intensity of the reflected light or a quotient of the detected intensity of the reflected light and detected intensity of the transmitted light; and
iii) analyzing the quotient to determine the blood characteristic.

By analyzing the quotient of the detected intensities of transmitted and reflected lights the advantage is achieved that influences from pressure and flow, in particular pulsating flow, of the liquid mixture is compensated for, whereby the determined blood characteristic (hemoglobin) will be accurate. The quotient is analyzed by comparing it with previously obtained quotients for known values of the blood characteristic in question.

Alternatively, first, (a) is performed by directing at least two light beams with different wavelengths against the vessel, then, (b) is performed by:
i) detecting the intensities of the light of the light beams reflected from the vessel;
ii) calculating a quotient of the detected intensities of the

reflected lights; and

iii) analyzing the quotient to determine the blood characteristic.

In accordance with a second aspect of the present invention there is provided an apparatus for accurate determination of SpO_2 from a mixture of liquid and blood cells contained in a light pervious vessel comprising:

- light sources for directing light beams against the vessel,

- means for determining a blood characteristic other than oxygen saturation, SpO_2, including hemoglobin and capable of analyzing the intensity of the light reflected from the vessel, or the intensity of the light reflected from the vessel in combination with the intensity of the light transmitted through the mixture, and

- means for determining oxygen saturation, SpO_2, of the mixture, preferably pulse-oximetrically, and of analyzing the intensity of the light transmitted through the mixture.

In accordance with the invention, the apparatus further comprises means for establishing whether the determined value of SpO_2 is relevant with respect to the determined value of the blood characteristic.

The light sources comprise a first light source for emitting a first light beam with a wavelength in the red light range against the vessel, and a second light source for emitting a second light beam with a wavelength in the infrared light range against the vessel.

The apparatus may further comprise a first detector for detecting the intensity of the light of the red first light beam transmitted through the vessel, and a second detector for detecting the light of the infrared second light beam transmitted through the vessel. The oxygen saturation determining means may comprise a processor adapted to calculate a quotient of the detected intensities of the transmitted red and infrared lights and to determine the value of the oxygen saturation by analyzing the quotient.

The light sources suitably comprise a third light source for emitting a third light beam against the vessel, and the apparatus may further comprise a third detector for detecting the intensity of the light of the third light beam reflected from the vessel and a fourth detector for detecting the intensity of the light of the third light beam transmitted through the vessel. The blood characteristic determining means may comprise a processor adapted to calculate a quotient of the detected intensities of the reflected and transmitted lights of the third light beam and to determine the value of the blood characteristic by analyzing the quotient.

The apparatus may further comprise registration means for storing the determined blood characteristic and SpO_2, and optionally means for visualization of the determined blood characteristic and SpO_2.

In accordance with a third aspect of the present invention there is provided use of an apparatus according to the second aspect of the present invention in a dialysis device.

Detailed description of the invention

The term "light source" is to be understood to encompass one or more light emitting elements, such as light diodes.

With the expression "blood characteristics" is meant in the present application characteristics of blood such as concentration of blood components, e.g. hemoglobin, total hemoglobin, red blood cells, white blood cells, platelets, cholesterol, albumin, thrombocytes, lymphocytes, drugs and other substances, viscosity, blood pressure, blood flow, blood volume, blood cell illnesses, abnormal blood cell appearances, anemia, leukemia, lymphoma.

With the expression "hemoglobin" is meant in the present application oxyhemoglobin, reduced hemoglobin, carboxy hemoglobin, methemoglobin and sulphhemoglobin.

With the expression "red blood cells", also known as erythrocytes, is meant in the present application whole or partly lysed red blood cells which contain hemoglobin.

With the expression "light pervious vessel" is meant in the present application a blood vessel in an animal, a pipe, a tube or a tubing which is light pervious. The pipe, tube or tubing may be manufactured from acrylonitrile butadiene styrene (ABS), polycarbonate or acrylic glass (polymethylmethacrylate; PMMA) which gives a non-flexible material or from polyvinyl chloride (PVC) or silicon rubber, plasticized PVC, e.g. PVC plasticized with dioctylphtalate, diethylhexylphtalate or trioctyltrimellitate, which gives a flexible material. PMMA is the most preferred non-flexible material. The light pervious vessel may further be used when performing liquid transfusions or blood transfusions. The elasticity of the material may be varied in a wide range. The animal containing a blood vessel is preferably a mammal, most preferred a human being.

As used herein, "light" refers generally to electromagnetic radiation at any wavelength, which includes the infrared, visible and ultraviolet portions of the spectrum. A particularly preferred portion of the spectrum is that portion where there is relative transparency of the tissue, such as in the visible and near-infrared wavelengths. It is to be understood that for the present invention, light may be nonpolarized or polarized light, coherent light or incoherent light and illumination may be steady pulses of light, amplitude modulated light or continuos light.

Light sources which may be used in the method and the apparatus according to the invention are e.g. light emitting diodes (LEDs) or laser diodes or combinations thereof such as VCSEL (vertical cavity surface emitting laser) . Preferably less expensive LEDs are used. Today there are also new strong light emitting diodes which may be used in the method and the apparatus according to the invention. Flash lamp light sources are also conceivable for use in the present invention. The light source may further be capable of emitting monochromatic light, i.e. a monochromator. Quartz halogen lamps or tungsten lamps may also be used as light sources. Optical light fibres, for guiding the light to and from the measured spot, and or direct illumination on the measured spot may also be used.

Detectors which may be suitable for use when performing the method according to the present invention, are phototransistors, photodiodes, photomultipliers, photocells, photodetectors, optical power meters, amplifiers, CCD arrays and so on.

In the present application the expression "means for determining blood characteristics including hemoglobin" refers to any non-invasive apparatus for determining blood characteristics including hemoglobin in a liquid comprising blood cells. Preferred examples of such non-invasive apparatuses are given below and in the appended claims.

In the present application the expression "means for determination of SpO_2" refers to any apparatus for measuring oxygen saturation non-invasively in a liquid comprising blood cells. Preferably pulse-oximetrically measuring apparatuses are preferred as e.g. are dislosed in Vegfors above and in Severinghaus et al above, disclosing e.g. the Minolta pulse oximeter. The Minolta pulse oximeter uses 650 nm and 805 nm. The apparatus in Vegfors above is the most preferred, as is diclosed below.

The mixture of liquid and blood cells in the method of the present application is preferably flowing, but it may as well be standing such as is the case for a fluid medium in a blood bag. The mixture of liquid and blood cells may comprise plasma or any other liquid as e.g. water or dialysis liquids. The plasma is preferably in or from a mammal. The liquid may as well be any other fluid comprising blood cells which may be obtained during or after the processing of blood.

Further, the method according to the present application is also characterized by that it may be performed on a mammal such as domestic animals or human beings, preferably on a human being.

The method according to the invention may be performed on any part of the human body or the body as a whole comprising a greater blood vessel, preferably a vein, an arteriole or artery, most preferred a blood vessel with a diameter >0.1 mm. The detection is, according to a preferred embodiment of the present invention, performed on an arm, a toe or a finger. The detection is most preferably performed on a wrist or on a finger on the third phalanx.

The present invention, especially the SpO_2 measuring part thereof, is based upon the principle that individual wavelengths of light are absorbed differently by various components of arterial blood. One application of this principle is used to measure oxygen saturation of arterial blood. In pulse oximetry two wavelengths of light emitted from suitable light sources are used, one with a wavelength within the red light range and one within the infrared range. The oximeter passes light through a monitoring site and measures the relative absorption of red light preferably at 660 nanometers (by reduced haemoglobin, Hb) and infrared light preferably at 940 nanometers (by oxyhaemoglobin, HbO_2). Because HbO_2 and Hb absorb different amounts of light at each of these two wavelengths, the oximeter can compare the ratio of each absorbance and convert it into an SpO_2 value. More specific it may preferably be expressed $(AC_{660}/DC_{660})/(AC_{940}/DC_{940})$ or AC_{660}/AC_{940} at constant DC levels. Pulse oximetry reduces the effect of other absorbers by looking only on the pulsative absorbances. The oximeter considers only the absorbers in the arterial blood. This is thus in analogy with the measuring global principle of the present innovation for haemoglobin especially, and can thus be attained by including preferably 940 nanometers and preferably 660 nanometers light sources and suitable detectors.

In one preferred embodiment of the method according to the present invention, one or more of the detected intensity of the light of said light beam(s) reflected from the vessel and the detected intensity of the light of said light beam(s) transmitted through the vessel, is transmitted over a wireless connection to a unit for performing step a), e) and/or f), preferably using a module for wireless communication. The wireless communication is preferably performed using a Bluetooth™ standard based communication path.

In the method according to the invention preferably light beam(s) are directed essentially perpendicular to a measuring area of the vessel.

In the method according to the invention preferably the wavelength of the light in (a), when transmitted light also is detected, is from 200 nm to 2000 nm, preferably from 770 nm to 950 nm, most preferred approximately 770, 800, 850, 940 or 950 nm.

In one preferred embodiment of the method according to the invention preferably at least two light beams with different wavelengths in (a) are directed against the mixture and selected such that the light absorbance of the red blood cells, as the first light beam passes theerethrough, is relatively insignificant, whereas the wavelength in the second light beam is selected such that the light absorbance of the red blood cells, as the second light beam passes therethrough, is relatively significant.

In one preferred embodiment of the method according to the invention preferably at least two light beams with different wavelengths in (a) are directed against the vessel, preferably essentially in parallel with each other, wherein one with a wavelength of from 770 to 950 nm and the other with a wavelength of from 480 to 590 nm.

In one preferred embodiment of the method according to the invention, in (a) light is emitted from at least four light sources, preferably six light sources, wherein the light sources being adapted to appear on either side of the detector(s), preferably the light sources are arranged in groups of two, most preferred in groups of three when six light sources are present, most preferred the light sources form an "H" with one detector in the centre. Preferably the "H" above is tilted approximately 90° during the measurement on preferably a wrist when looking from the direction of the arm or the blood vessel. The measurement is further preferably performed on the inside of the wrist.

In one preferred embodiment of the method according to the invention, in (a) light is emitted from two light sources, which are positioned and thus appearing on two different opposite sides of a vessel containing the mixture, and detection of reflected light from and transmitted light through the vessel is performed by at least two detectors, preferably by only two detectors.

In one preferred embodiment of the method according to the invention (b) comprises the following steps:

I) sweeping a window over a curve with detected values from transmission and/or reflection, wherein the size of said window preferably is approximately 60 % of the period time, divided equally to the right and to the left;

II) if no value within said window is higher than the middle value, designating the value a maximum point whereupon moving the window by leap half of the window length, or if a value exceeds the middle value moving the window only one step;

III) designating the minimum points in the same manner as in II) but with regards to minimum values instead of maximum values;

IV) obtaining the height of the AC-signal by subtracting from a value on a connection line involving two maximum points, the vertically laying value of an in between laying minimum point;

V) repeating step IV) at least 8 times, and summarizing the values from IV) and dividing the sum with the number of observations, thus obtaining a median AC-value; and

VI) optionally obtaining the DC-signal by adding the total height of the minimum point in IV) to the median AC-signal of step V);

whereby preferably using a computer program for obtaining said

AC-signal and optionally said DC-signal.

In one preferred embodiment of the method according to the present invention the wavelength of the red light is approximately 660 nm and the wavelength of the infrared light is approximately 940 nm.

In the method according to the invention, preferably the determined SpO_2 and determined blood characteristics including hemoglobin are presented simultaneously.

In the method according to the invention, preferably the determined SpO_2 is corrected by using the determined blood characteristics including hemoglobin.

The method according to the present invention may, according to a preferred embodiment, be used for determination of blood characteristics including hemoglobin in extracorporeal equipments including e.g. dialysis apparatuses (dialysers), cell savers, dialysis monitors, or on a blood bag device (which includes assemblies), or on a slaughter house device, or on a blood fractionation device. The light pervious vessel, preferably a tube or pipe, may in this embodiment of the present invention have a diameter >0.1 mm. In dialysis apparatuses it may be desirable to see how much hemoglobin and the SpO_2 value which is present in a fluid which is subjected to any form of dialysis, preferably hemodialysis. During dialysis it may further be desirable to measure the hemoglobin concentration in order to follow changes in blood volume of the patient and SpO_2 in said patient. Regarding blood bag constructions and blood bag assemblies, the method according to the invention may be applied to tubings, bags, filters or any other component that may be used in association with blood bags which may contain whole blood or buffy coat i.e. concentrate of white blood cells (leukocytes). The method may also be used during blood transfusions on tubings, or during blood donations as well. In slaughter houses, the method according to the present application may be useful when recovering blood from slaughter animals and when further processing that blood to give whole blood for use directly in food or fractionate it to obtain the blood components albumin, immunoglobulins and so on. The method according to the present application may also be used when counting blood cells i.e. a process when you count red and white blood cells. This may be done in an apparatus such as a blood cell counter e.g. a Coulter counter manufactured by Coulter Diagnostics of Miami Florida. The method according to the invention may also be used in association with blood analysing, blood typing and other blood gas analyses, in addition to SpO_2. The method according to the invention may also be used when fractionating human blood in a blood fractionating unit. It may be desirable to use the method according to the present application when plasma is obtained from donors. The method may also be useful when obtaining buffy coats from a donor or when these buffy coats are further processed for producing e.g. cytokines such as interferon alpha. The method may be useful to determine how the lysis of the RBC:s are performing during the purification of white blood cells which subsequently after one or more steps involving RBC lysis with e.g. ammonium chloride, are exposed to virus e.g. Sendai virus during incubation in a suitable medium e.g. Eagles Minimal Essential Medium, EMEM.

The method, according to the present application, is preferably performed on a blood vessel, tube or pipe.

According to a preferred embodiment of the present invention the light beams are preferably directed essentially perpendicular to a measuring area of a vessel containing the mixture.

According to a preferred embodiment of the present invention, at least two light beams are directed against the vessel from two light sources and detection of the intensity of the reflected light from the vessel is performed by at least one detector, preferably by only one detector.

According to yet another preferred embodiment of the method according to the present invention, in step a) at least two light beams, preferably with two different wavelengths, are directed against the vessel, from two light sources, (which may be incorporated in the same shell, e.g. a chip), which are positioned and thus appearing on one common side of the measuring object. These light sources may when used together in a chip be lightened alternately. One of the light beams may have a wavelength of from 770 nm to 950 nm, preferably 770, 800, 850, 940 or 950 nm, and the other may have a wavelength of from 480 nm to 590 nm, preferably 500 nm.

An apparatus according to one preferred embodiment of the present invention may comprise at least four light sources and at least two detectors for reflected light, wherein two light sources have different wavelengths for directing two light beams appearing on the same side of the vessel, wherein preferably one light source is having a wavelength of from 770 to 950 nm and the other a wavelength of from 480 to 590 nm.

In an apparatus according to one preferred embodiment of the present invention at least two components of the apparatus may communicate with each other over a wireless connection, preferably over a module for wireless communication. The module for wireless communication may comprise at least one transmitter and one receiver.

In an apparatus according to a preferred embodiment of the present invention there may be one module for wireless communication between at least three components, i.e. light sources, light detectors, and the processor and/or one module for wireless communication between the processor and the registration means.

In an apparatus according to a preferred embodiment of the present invention the wireless communication may be performed using a Bluetooth™ standard based communication path.

In an apparatus according to a preferred embodiment of the present invention the light sources may be positioned essentially perpendicular to a measuring area of the vessel.

In an apparatus according to a preferred embodiment of the present invention the wavelength of at least one of the light is from 200 nm to 2000 nm, preferably from 770 nm to 950 nm, most preferred approximately 770, 800, 850, 940 or 950 nm.

An apparatus according to a preferred embodiment of the present invention may have two light sources for directing two light beams with different wavelengths on the same side of the vessel, whereby one of the light beams having a wavelength of from 770 nm to 950 nm, preferably 770, 800, 850, 940 or 950 nm, and the other light beam having a wavelength of from 480 to 590 nm, preferably 500 nm.

An apparatus according to a preferred embodiment of the present invention may comprise at least four light sources on one common side, preferably at least six light sources, wherein the light sources being adapted to appear on either side of the detector(s), preferably the light sources are arranged in groups of two , preferably groups of three, wherein the light sources preferably form an "H" with one detector in the centre.

An apparatus according to a preferred embodiment of the present invention may have the form of a wrist, finger or toe fitting test device equipped with the light sources and the detectors.

In an apparatus according to a preferred embodiment of the present invention the test device comprises a thimble-like shell to be applied on a finger or toe, the light sources and the detectors being arranged to direct the light beams and detect the light intensities within the shell.

In an apparatus according to a preferred embodiment of the present invention at least three sources and the detectors are positioned in the shell comprising a constriction whereby said light sources and detectors are positioned and thus appearing in said constriction, whereby said shell preferably is a part of a thimble design for covering a finger or a toe.

An apparatus according to a preferred embodiment of the present invention may have at least four light emitting diodes on one common side, preferably at least six light emitting diodes and one detector which together form an "H" with the detector in the centre, fixed on a patch which in turn is making part of a handcuff construction suitable for wrist measurements, wherein the distance between the light sources and the detector preferably is, for determining blood characteristics including Hb and also SpO_2, from 4 to 12 mm when referring from the centres of respective component, most preferred said distance is approximately from 8 to 9 mm.
If wrists (containing Radialis) or thicker parts of the body, like upper parts of the arms, are to be measured, when regarding blood characteristics including Hb and also SpO_2, the above distances between the fibres (light source and detector) may be from 6 to 12 mm. For thicker parts (like arms containing Brachialis) of the body the distance may be from 12 to 30 mm. When measuring on wrists or thicker parts of the body a

pressure may preferably be put on the measurement locus. The method according to the present invention may further be used when measuring on vessels situated below the ankles (containing Dorsalis pedis). Thus the present invention may have, for especially the determination of blood characteristics including Hb, light source(s) and detector(s) on different distances as set out above depending on which measuring area is to be monitored, which enables reaching the aimed vessel and thus the detection of the blood characteristics including Hb. The distance between detector(s) and light source(s) may, as set out above, thus be from 1 to 20 mm depending on the measuring area.

In an apparatus according to one preferred embodiment of the present invention the light sources and the detectors for reflection may be fixed at the edge of the patch, which may house a finger, a toe or wrist, preferably a wrist, wherein preferably the patch is a flexible plastic patch anchored to a strap for fastening to the wrist wherein the strap preferaby has a locking device.

In an apparatus according to one preferred embodiment of the present invention the light sources and detectors for reflection may be incorporated in the above patch whereby the electric components are fixed on one side of a printed circuit card covered with black-coloured silicone and the optical components are fixed on the other side covered with transparent silicone.

In an apparatus according to one preferred embodiment of the present invention the patch is rectangular with a size of 51 x 35 mm, and the light sources and detector arranged as an "H" are fixed in a corner of said patch.

In an apparatus according to one preferred embodiment of the present invention the processor is adapted to convert the reflection values to a concentration value of the determined blood characteristics, preferably by making a quotient of the detected reflected intensities.

In an apparatus according to one preferred embodiment of the present invention the processor may comprise a computer program for performing the method according to the present invention.

In an apparatus according to one preferred embodiment of the present invention the wavelength in the red light range of I) is approximately 660 nm and the wavelength in the infrared light is approximately 940 nm.

According to one embodiment there is provided a computer program stored on a data carrier for performing the method according to the present invention.

By combining the method and the apparatus of the present invention with cable-free communication this allow for broadening the use of said method and apparatus by making it more user-friendly. The cable free communication may allow for internet-billing, patient information follow up and statistics, software package updates and service. The user may by ordering via a modem get the necessary codes to perform a certain number of tests much in the same way as with cellular phones.

The radio communication standard Bluetooth™ has opened the opportunity for cable-free equipment in the hospital environment. Bluetooth™ technology enables electronic devices to communicate with one another without cables. Bluetooth™ modules comprising a transmitter and a receiver may replace cables in many applications. Figure 18 shows a system including a computer and a SpO_2 (including determination of blood characteristics) detector where there is no need for cables between them when using the Bluetooth™ technology.

Bluetooth™ technology, developed by L M Ericsson, may use the ISM band 2.45 Ghz and may ensure interruption-free communication. The system may work with quick frequency hopping of 1,600 hops per second. The output power from the transmittor may be low and may be adapted to work at a maximum distance of 10 meters. The distance between the wireless communicable components in the apparatus of the present invention may however be variable from 1 cm up to 10000000 miles.

In the apparatus according to the present application at least one of the detectors may be capable of receiving reflected light and be positioned alongside the light source.

According to a preferred embodiment of the apparatus according to the present application the detector, capable of receiving reflected light, is positioned alongside the light source.

According to a preferred embodiment of the apparatus according to the present application the apparatus may have the form of a finger or toe fitting test device or a handcuff equipped with the light source(s) and the detector(s).

The above test device according to the present application may according to a preferred embodiment comprise a thimblelike shell, in short thimble, which is preferably used for detection of SpO_2 (including blood characteristics including hemoglobin) in fingers or toes, where at least three light sources and the detectors are positioned as part of the thimble construction. The thimble embodiment may also be useful for detection of hemoglobin in paws on domestic animals.

The above test device according to the present application may according to a preferred embodiment comprise a handcufflike shell, in short handcuff, which is preferably used for detection of SpO_2 (including blood characteristics including hemoglobin) in fingers, toes or arms, preferably wrists or fingers, where at least three light sources and the detectors are positioned as part of the handcuff construction. The handcuff embodiment may also be useful for detection of SpO_2 (including hemoglobin) in paws and legs on domestic animals.

The apparatus (especially the test device thereof) according to a preferred embodiment of the present invention may comprise a thimble-like shell to be applied on a finger or toe, the light source and the detectors being arranged to direct the light beam and detect the light intensity within the shell. This embodiment may have at least three light sources and the detectors positioned in the same shell, optionally comprising a bend (constriction), whereby said light sources and detectors are positioned and thus appearing in said bend (constriction), whereby said shell preferably is a part of a thimble or handcuff construction for covering a finger, a toe or a wrist. The above test device may thus be shaped to fit a wrist, toe or a finger.

The thimble and handcuff embodiments are essentially characterized by that they comprises at least three light emitting diodes (LED) positioned on one side together with at least one detector (and two detectors for detecting transmitted light). The above components may be housed in a shell comprising:

a) a first part in close proximity to said components i.e. diode and detectors, which preferably houses the components in a flexible way comprising a flexible material preferably a polymeric material, most preferred silicon rubber.

b) an optional second part also comprising a flexible material, preferably a polymeric material, most preferred silicon rubber.

The first part may also comprise a black plastic material, most preferred epoxy plastic or PMMA. The shell may be cast in industrial scale or may be hand made according to methods known to a person skilled in the art. When silicon rubber is cast to make first and optionally the second part, preferably a colour powder (dye) is added to the rubber. The shorter the wavelength, the larger are the problems with external light, which thus may be minimized by adding dye to the material. Preferably the dye is black to minimize disturbances from other light sources. The shell may be fixed in a position on e.g. a finger, toe or wrist through that the first and, if present, the second part are held together, preferably linked together by gluing the parts together or make the parts stick together in any other way. Further the shell preferably forms an inward bend, an internal constriction, preferably the first part of the shell, where the finger, toe or wrist may be positioned during the measuring. The shell may have an arbitrary shape which surrounds said inward bend or constriction. In this way the finger, toe or wrist may be "squeezed" so that a blood vessel is easily accessible for the measuring method according to the present invention. This squeezing may be acheived by mechanical means or by just pressing by hand. By using a clamping device, which may comprise e.g. a rubber band together with a clamping ring , or a strap device, it may also be possible to fix the thimble or handcuff and squeeze the measuring object.

The flexible material in the first part may also be made out of natural rubber or any pure flexible polymer or any co-polymer. The flexible material may also comprise one or more polymers. The materials in both parts do preferably not contain allergenic substances and thus the thimble is preferably well tolerable to the skin of a mammal. The shell allows for a finger, toe or wrist of a subject to be "sqeezed" so that preferably a blood vessel is easily accessible for the measuring method according to the present invention. The blood vessel is preferably an artery, vein or arteriol. The detection is preferably performed on a wrist or finger on the third phalanx.

The test device according a preferred embodiment of the present invention may comprise a thimble-like shell to be applied on a finger or toe, the light source and the detectors being arranged to direct the light beam and detect the light intensity within the shell.

Another preferred embodiment of the present invention is an apparatus having additional light sources, the light sources being adapted to appear on either side of the detector(s) for detecting reflected light on a common side.

Another preferred embodiment of the present invention is an apparatus having at least three additional light sources, preferably at least five additional light sources, thus totalling at least four light sources (preferably six light sources), wherein the light sources being adapted to appear on either side of the detector(s) on a common side, preferably in groups of two, most preferred groups of three, whereby the components preferably form an "H" with the detector in the centre. The preferred embodiment with six light sources, preferably six light emitting diodes, and one detector may preferably form an "H" with the detector in the centre.

This further embodiment, the handcuff, which is one preferred embodiment of the invention according to the present application is exemplified by a design which is described in example 3 in detail and also in figure 16. In the handcuff embodiment of the present invention, the distance between the light source(s) and the detector may be from 4 to 12 mm when referring from the centres of respective component, preferably it is approximately 8 mm. In figure 16 this is the distance between the LEDs and the photodetector in the middle. Preferable the components are fixed to the edge of the bend, which may house a finger, a toe or wrist, preferably a wrist.

The handcuff according to one embodiment of the present invention may preferably be present as a flexible plastic patch anchored to a strap for fastening to the wrist, wherein the strap in turn may be locked, using a locking device, during the measurement, thus squeezing the wrist. This embodiment can be seen in figure 15 and 16. As can be seen in figure 16, the components may preferably be arranged, as an "H", in the corner of a flexible essentially rectangular patch. The patch may preferably have rounded corners and a size of 51 x 35 mm. The patch may additionally preferably have an elevated side, to be in touch with the measuring area e.g. skin of a human, where the light sources and the detector appear. The patch may preferably have a size of 51 x 35 mm and the elevation 31 x 47 mm, leaving a margin of 2 mm to the outer size. The components, when arranged as an "H", may preferably be fixed in a corner of the smaller of the smaller rectangle, i.e. 31 x 47 mm, as can be seen in the figure 16. The "H" is preferably tilted approximately 90° during the measurement on e.g. a wrist when looking from the direction of the arm or the blood vessel. Preferably the measurement may performed on the inside and outside of the wrist, whereby the detectors for the detecting of transmitted light (red and infrared) are present on the outside of the wrist.

The light sources and the detectors may further preferably be fixed at the edge of the patch, which may house a finger, a toe or wrist, preferably a wrist, most preferred the patch is a flexible plastic patch anchored to a strap for fastening to the wrist wherein the strap preferaby has a locking device. Additionally the apparatus may have the light sources and detector incorporated in the patch whereby the electric components are fixed on one side of a printed circuit card covered with black-coloured silicone and the optical components are fixed on the other side covered with transparent silicone, which ensures electrical isolation, reduction of stray light and the possibility for sterilization. The patch may preferably be rectangular with a size of 51 x 35 mm, and the light sources and detector may be arranged as an "H" fixed in a corner of said patch.

The vessel in which the blood characteristics is to be monitored may be identified by proper choice of the separation between the light source(s) and the detector(s). The theoretical analysis and experimental verification of this optical technique has been presented by I. Fridolin, K. Hansson and L.-G. Lindberg in two papers which have been accepted and are to be published in Physics in Medicine and Biology (Optical non-invasive technique for vessel imaging I and II, Department of Biomedical Engineering, Linköping University, Sweden). The following is a summary of their analysis and experimental verifications.

Light reflection from human tissue depends on many parameters, such as optical wavelength, source-detector separation, size and aperture of the light source and detector and optical properties of the blood and tissues. The separation between the light source and the detector fibre was varied between five centre-to-centre distances: 2, 3 ,4, 5 and 6 mm.

The analysis agreed with the earlier conclusion that to increase the influence from deeper tissue on the measured signal, a larger light source-detector separation should be selected.

The resultant mathematical analysis and verified experimental results can be summarized as:
At larger separation values the photons forming maximum photon paths and detected by the photodetector originate from deeper layer than for short separation values. This is illustrated in figure 14. Figure 14 is a schematic diagram of photon migration at two different source-detector separations and for different FL (α) (FL(0) and FL($\pi/2$)). FL = fibre pair position relative the Lining of the vein. Two positions of the light source and the photodetector fibres relative to the lining of the vein were considered. An angle α is defined to characterize different positions. The abbreviation FL(0) means that the light source and the photodetector are positioned in parallel and FL($\pi/2$) that the light source and the photodetector are positioned perpendicular to the vessel. Monte Carlo simulations have shown that for human tissues in the near infrared region photons penetrate approximately 2 mm before being detected if the separation is about 2 mm between the source and the detector.

The blood vessels in terms of veins may be determined at three vascular levels in combination with a fixed fibre diameter (1 mm) using the probe and technique above summarized and according to;
* a superficial vascular level (approximately 1 mm). This may be sufficient to set the minimal distance between the illuminating and detecting fibre (2 mm during the above experiments.

* an intermediate vascular level (approximately 2 mm). The minimal distance between the illuminating and detecting fibre may preferably be 2 - 3 mm
* a deep vascular level (approximately 3 mm). The distance between the illuminating and detecting fibre may preferably be greater than 3 mm.
The result of this above summarized research makes it possible to determine blood characteristics and monitor physiological parameters on a selected vascular bed, vein or artery, such as blood flow, blood constants and oxygen saturation e.g. on a selected vascular bed in veins or arteries.

If wrists (containing Radialis) or thicker parts of the body, like upper parts of the arms, are to be measured, when regarding SpO_2 (and blood characteristics including Hb), the above distances between the fibres (light source and detector) may be from 6 to 12 mm. For thicker parts (like arms containing Brachialis) of the body the distance may be from 12 to 30 mm. When measuring on wrists or thicker parts of the body a pressure may preferably be put on the measurement locus. The method according to the present invention may further be when measuring on vessels situated below the ankles (containing Dorsalis pedis).

The theoretical solution for light distribution in tissue, described in paper II above, may be the base for describing how hemoglobin can be measured in reflection mode. Equation 32 provides a general solution in which equation μ_a and μ_s describes the influence of the optical coefficients and H and B (or Z) the influence on pulsative variations in vessel diameter during the cardiac pulse.

The light sources is are connected by cords to any power source, which may be an oscillator or a battery. The oscillator may be connected to amplifiers and LED-Drivers. These drivers may be connected to one or more LEDs. Detectors, e.g. photodiodes for reflection may be connected to at least one current/voltage converter, which in turn may be connected to the amplifiers. The signals may then pass to Band pass Filters and subsequently to analog outputs or to a μ-controller which is connected to a Read out unit.

For the performance of the method according to the invention one or more calibration curves may be used. One calibration curve stored in a memory of a processor, which preferably is part of a computer, may allow the readily conversion from the quotient reflection/transmission %, which may be stated: AC_R/AC_T or DC_R/DC_T, or reflection/reflection % which may be stated: AC_R/AC_R or DC_R/DC_R, obtained when directing light beam(s) against the vessel and subsequently detecting the reflection and transmission or only reflection, to a hemoglobin value in mmol/l. By analyzing the quotient of the detected intensities of reflected or, reflected and transmitted light, the advantage is achieved that influences from pressure and flow, in particular pulsating flow, of the liquid mixture is compensated for, whereby the determined blood characteristics including will be accurate, and accordingly also SpO_2. The quotient is analyzed by comparing it with previously obtained quotients for known values of the blood characteristic in question. The calibration curve may preferably be obtained by analysing in parallel with the method according to the present invention, drawn blood samples from volontary healthy persons and patients on a Hemocue apparatus or blood gas analyser. A spectrophotometric absorption curve in reflection mode or recording curve in reflection mode may also be used in conjunction with the method above. The obtained values for measuring SpO_2, preferably in form of a quotient described above, may be compared to an already existing calibration curve, thus enabling an easy conversion to a SpO_2 value.

Apparatuses according to the present invention may further big matrix probes comprising several light sources (more than six) and detectors (more than one) which may have the form of a ring, plate, cube, sphere..

The apparatus according to the present application may according to an additionally preferred embodiment be comprised in a dialysis apparatus, preferably for performing hemodialysis.

The apparatus according to the present invention may be divided geographically on the body, thus e.g. further having a SpO_2 measuring part to be used in an ear and connected thereto, optionally wireless, the Hb measuring part in a finger, wrist or a toe.

The apparatus according to the present application may according to an additionally preferred embodiment have at least two, preferably at least four , most preferred six, light sources which are positioned and thus appearing on a common side of the measuring object during detection. When two or more LEDs are used they are preferably interchangable with each other. They may further preferably emit light with different wavelengths. Measuring the intensity of the reflected light at one or more wavelengths with light sources of suitable wavelengths may also attain the independence of blood characteristics on blood flow and blood pressure. Similar measuring technique may be used to compensate for differences in tissue absorbencies over the artery between individuals. The LEDs may be present in the same handcuff (a patch thereof) or thimble.

The apparatus according to the present application may according to an additionally preferred embodiment have at least two light sources, wherein the first light source emits light of a wavelength which is relatively not absorbable by red blood cells, and the second light source emits light of a wavelength which is relatively absorbable by red blood cells. The above first and second light sources may preferably be directed substantially in parallel with each other.

The apparatus according to the present application may according to an additionally preferred embodiment have at least two light sources, preferably at least four light sources, most preferred at least six light sources, which are positioned and thus appearing on the same common side of the measuring object during detection, where at least one light source (preferably a LED) emits green light and at least another light source (preferably a LED) emits NIR light of from 770 nm to 950 nm. The at least two light sources direct two light beams against the same side of the vessel, one of the light beams having from 770 nm to 950 nm and the other light beam having a wavelength of from 480 to 590 nm. Preferably the green light is emitted in the green wavelength range i.e. 480-590 nm, most preferred at 500 nm.

By directing two light beams with a wavelength <1500 nm a better sensitivity of the method may be obtained. In this above preferred embodiment of the present invention one light beam has a longer wavelength, preferably NIR (Near InfraRed) light, and the other has a shorter wavelength preferably in the range of 200-580 nm, most preferred green light, 400 or 500 nm. Using green light in the other light source is advantageous because green light is heavily absorbed by red blood cells.

The processor for analyzing said intensity of said reflected (and tranmitted) light detected by the detector(s) and for determining SpO_2, including the blood characteristics including hemoglobin, may be included in a computer (CPU). Further, the registration means may also be included in a computer. The visualization may be accomplished by any visualization means, but is preferably accomplished by using a computer display and/or a printer device. The processing of the data obtained during the measurement may also include quotient forming of reflection/transmission, transmission/reflection (for SpO_2, transmission/transmission) with or without AC and/or DC with or without multiplying of one or more of the obtained data in order to compensate for variations in volume or flow. If any additional light sources and detectors are used in the invention (especially in the determination of blood characteristics including Hb) according to the present invention, there may be several quotients formed with basis from the detected intensities depending on the number of detected intensities available. There may also be included a computer program in the processor for search for the optimal measuring spot, especially when using a matrix comprising several light sources and detectors, for controlling/verifying reliable strength of the signal, for performing algorithm calculations, for evaluating data against stored standard curves, for displaying (and storing) the results together with patient data and relevant quality criteria. The output of the results from measuring using the present invention may be accomplished on a connected printer device, optionally connected via the visualization means.

Of course, it may be possible to process the reflection signals in a manual way and hereby determine SpO_2, including the blood characteristics including hemoglobin. The results may also be visualized in a manual way by e.g. plotting the results in a diagram. The signal(s) detected by the detector(s) may further preferably be analysed using the following procedure: As the PPG-signal is consisting of two parts, a constant signal and a pulsating signal superposed on the constant signal, first maximum and minimum points are calculated. The maximum points are calculated through sweeping a window over a curve plotted by values of detected light intensities. The size of the window is adjusted according to the frequency of the AC-signal (the pulse) to approximately 60% of the period time, divided equally to the right and to the left. If no value within the window is higher than the value in the middle, this value is designated a maximum point, whereafter the window is moved by leaps half of the window length in order to avoid that a plateau formed curve is registrated as many maximum points. If any value within the window exceeds the value in the middle, the window is moved only one step. In a corresponding way the minimum points are calculated.

For each minimum point an AC-height is calculated as the height to the connection line between the maximum points closest to the left and to the right of the middle (mean) point, respectively, taken from the in between lying minimum point. Of nine subsequetly following AC-heights, the median height is selected as the representative of the AC-signal, in order to filter away artefacts that may give rise to erroneously detected minimum or maximum points. The DC-signal is then calculated as the total height to the minimum point that laid basis for the AC-signal, plus the AC-signal. Figure 19 shows an example of the above procedure. Step d) in the summary of the invention above may preferably comprise the following steps:

I) sweeping a window over a curve with detected values from transmission and/or reflection, wherein the size of said window preferably is approximately 60 % of the period time, divided equally to the right and to the left;
II) if no value within said window is higher than the mean (middle) value, the value is designated a maximum point whereupon the window is moved by leap half of the window length, or if a value exceeds the middle value the window is moved only one step;
III) the minimum points are designated accordingly in the same manner as in II) but with regards to minimum values instead of maximum values;
IV) the height of the AC-signal is obtained by subtracting from a value on a connection line involving two maximum points, the vertically lying value of an in between lying minimum point;
V) repeating step IV) at least 8 times, and summarize the values from IV) and dividing the sum with number of observations, thus obtaining a median AC-value
VI) optionally obtaining the DC-signal by adding the total height of the minimum point in IV) to the median AC-signal of step V). Preferably these above steps are accomplished by using a computer program for obtaining said AC-signal and optionally said DC-signal. Preferably the computer program is stored on a data carrier for performing the above steps I) to VI). Preferably the data carrier is part of the processor (or central processing unit, CPU) designated iv) above, in one preferred embodiment of the present invention, or a separate floppy disc to be inserted and used by the processor. The processor may preferably comprise a computer program for performing the method according to the present invention, as e.g. set forth in the summary of the invention and in the

preferred embodiments of the present invention, and/or the above steps I to VI.

Another embodiment of the present invention is also a computer program stored on a data carrier for performing the method according to the present invention, as e.g. set forth in the summary of the invention and preferred embodiments of the present invention, and/or the above steps I to VI.

When measuring on the skin the equation may look similar except that the light may be reduced depending on the absorption of light and the light scattering in the tissue. The intensity may be compensated at different blood flows when performing the current invention, the method and using the apparatus. When performing skin measurement, this is preferably performed over a large blood vessel, e.g. on the wrist or on the finger of the third phalanx. The blood vessel preferably contains a blood volume which markedly differs from the blood volume in the surroundings (which may comprise capillaries). It should be noted that the method and apparatus according to the present invention may preferably be used for measuring SpO_2 (including the central blood characteristics) as represented in larger vessels such as arteries. This may be achieved by compensating for the influence of blood pressure and blood flow on the measured intensities of the reflected and transmitted light, by taking the quotient between the reflected and transmitted light. The effect used in the present method and apparatus according to the present invention may also be used for measuring the change in SpO_2 (and blood characteristics) in one individual or in an extracorporeal system when the blood haemoglobin value is constant. This is further illustrated in example 4 where this was performed by using an apparatus according to the present invention. Using the method it is thus possible to follow changes in SpO_2 (and in blood volume and pathological changes in the body).

The present invention with its method and its apparatus may also be adapted to detect oxygen together with SpO_2, as 97-98 % of all oxygen in the blood of a human being is transported by hemoglobin molecules in the blood. Of course the method may also be used for detecting SpO_2 (and red cells themselves) as hemoglobin is normally incorporated in the red blood cells, unless they are lysed. As the viscosity of blood corresponds to the amount of red blood cells in the blood, the method may also be used for detection of viscosity as well. The method and apparatus according to the present invention may also be used to determine the hematocrit (Hct). The difference between hemoglobin (which is the grams of hemoglobin per volume of blood) and hematocrit (which is the volume of blood cells per volume of blood) is determined by the concentration of hemoglobin within the cells which determines the index of refraction of the cells.

Several different blood constants are used in diagnostics. Some are interchangeable and there are generally accepted relationships between these. The generally accepted relationships are:

Constant	Measures	Calculation
RBC EPC	number of red blood cells per unit volume of blood *or* erythrocyte particle concentration	
Hb	concentration of haemoglobin in blood	

Hct	hematocrit or erythrocyte	Hct=RBCxMCV
EVF	erythrocyte volume fraction. Fraction of red blood cell volume of total volume.	
MCV	erythrocyte volume, *abr.* mean corpuscular volume	MCV=EVF/RBC
MCH	weight of haemoglobin in erythrocytes, *abr.* mean corpuscular haemolglobin	MCH=Hb/RBC
MCHC	concentration of haemoglobin in erythrocytes, abr. mean corpuscular haemoglobin concentration	MCHC=Hb/EVF

Further, human blood is made up of formed elements and plasma. There are three basic types of formed blood cell components: red blood cells, white blood cells (leukocytes) and platelets. The red blood cells contain hemoglobin that carries oxygen from the lungs to the tissues of the body. Normally the hemoglobin concentration varies between 132 - 163 gram/litre in men, and 116 - 148 gram/litre in women. The hematocrit (Hct) normally varies between 39 - 49 % (EVF 0.39 - 0.49) in men, and 37 - 44 % (EVF 0.37 - 0.44) in women. White blood cells are of approximately the same size as red blood cells, but they do not contain hemoglobin. A normal healthy individual has approximately 5,000,000 red blood cells per cubic millimeter of blood (the human body contains approximately 5 litres of blood), and approximately 7,500 white blood cells per cubic millimeter of blood. Therefore, a normal healthy individual will have approximately one white blood cell (leukocyte) for every 670 red blood cells circulating in the vascular system. The white blood cells (WBCs) are responsible for the immune system in a mammal, preferably a human being. E.g. certain WBCs engulf intruder agents.

Concerning platelets, they are the smallest of the formed blood cell components, being typically less than 1 μm in diameter. Platelets are less abundant than red cells, but more abundant than white blood cells. A normal healthy individual has approximately one platelet for every 17 red blood cells circulating in the vascular system for a total of about two trillion.

In summary, the method and apparatus according to the present invention may be used to determine SpO_2 (and various characteristics of the vascular system) through the use of known relationships between parameters, as for the cases when determining indirectly the amount of white blood cells and/or platelets. (For WBCs the factor is 1/670 of the red blood cells and for platelets it is 1/17). Thus the blood characteristics in steps a) in the method according to the invention may also include white blood cells and/or platelets. Cholesterol and albumin concentration may also be determined when using the known hemoglobin concentration in connection with the method described in GB 2 329 015, hereby incorporated by reference thereto. The above method refers to non-invasive measurement of blood component concentrations.

The method and apparatus according to the invention also enables SpO_2 determination and diagnosing of irregularites or diseases in a mammal e.g. anemia where there is a shortage of red blood cells. Bulimia patients often suffer from anemia in which accurately determination of SpO_2 may be accomplish using the method and apparatus according to the present invention. Further, also congestive heart failure and cardiac arythmies may be detected using the method and apparatus according to the invention. Further, the method and the apparatus gives an indirect possibility of measuring platelet diseases such as thrombocytopenia. This could be indicative for problems of menostasis and coagulation. An elevated level of certain white blood cells is further indicative of a viral infection. Leukocytosis and leukopenia are also thinkable indications which may be possible to detect indirectly. Other diseases of the phagocytic and Immune Systems may also be detectable. Neonatal monitoring is another application area for the present invention. Operative monitoring is also a conceivable application. The apparatus may be set to a "zero-level" at the start of an operation, in order to compensate for stable interactive effects (skin colour, lipids and so on) and thus a readily monitoring of SpO_2 (and blood characteristics including hemoglobin) may be acheived.

The current invention, the method and apparatus, also enables an accurate measurement of SpO_2 in patients blood, without any risks associated with drawing blood (e.g. AIDS, hepatitis A, B and C etc). Drawing blood by using injection needles is also a painful method, especially for individuals requiring many blood samples to be drawn. These drawbacks may be eliminated by using the method and apparatus according to the present invention. Further the method and apparatus according to the present invention is especially suitable for measurements on children.

The present invention also refers to use of an apparatus according the present application in a dialysis apparatus (or dialysis device).

The examples which follow illustrate embodiments of the present invention, but are not intended to limit the scope in any way.

Description of the figures

Figure 1 shows schematically a flow model for detection of light reflection.

Figure 2 shows the orientation of red blood cells at an intermediate or high level of shear rate or blood flow.

Figure 3 shows light absorption in blood due to different absorbing matter.

Figure 4 shows light scattering due to red blood cells.

Figure 5 shows the relative change in transmitted light *versus* blood flow for two different types of red blood cells.

Figure 6 shows the relative change in transmitted light intensity *versus* blood flow for two types of blood cells.

Figure 7 shows essentially the experimental setup of an example (example 2).

Figure 8 shows a diagram with the relative change of the quotient reflection/transmission (%) i.e. AC_R/AC_T, on the y-axis and the hemoglobin concentration in mmol/l on the x-axis.

Figure 9 shows reflection and transmission vs. hemoglobin concentration.

Figure 10 shows the thimble-like shell construction according the apparatus of the present invention comprising two light sources, from four different views, without cords.

The numbers in the figures have the following explanations:

1. Green Light Emitting Diode (LED) and NIR LED;

they are interchangable

2. Detector
3. Detector
4. Second part comprising a stiffer material
5 First part comprising a flexible material

The A-A, B-B, C-C are sections of the thimble.

Figure 11 shows a block diagram illustrating schematically how the thimble (the shell is not shown; only light sources and detectors is shown) is connected. The numbers in the figure has the following explanations:

1. oscillator
2. LED-Driver λ 1
3. LED-Driver λ 2
4. LED λ 1 or 2
5. Photodiode reflection
6. Subject
7. Photodiode transmission
9. Current/Voltage converter
10. Current/Voltage converter
11. Lowpass Filter
12. Lowpass Filter
13. Sample and Hold amplifier
14. Sample and Hold amplifier
15. Band pass Filter
16. Band pass Filter
17. Analog output
18. Analog output
19. μ-controller
20. Read out unit

Figure 12 shows a block diagram illustrating schematically how the thimble (the shell is not shown; only light sources and detectors is shown) is connected in another embodiment of the thimble. The numbers in the figure has the following explanations:

1. oscillator
2. LED-Drivers
3. LED
4. Photodiode reflection.
5. Photodiode transmission
6. Subject
7. Current/Voltage converter
8. Current/Voltage converter
9. Lowpass Filter
10. Lowpass Filter
11. Sample and Hold amplifier
12. Sample and Hold amplifier
13. Band pass Filter
14. Band pass Filter
15. Analog output
16. Analog output
17. μ-controller
18. Read out unit

Figure 13 shows the intensity of the reflected pulsative light versus increasing systolic pressure.

Figure 14 shows at larger separation values the photons forming maximum photon paths and detected by the photodetector originate from deeper layer than for short separation values.

Figure 15 shows a probe of one preferred embodiment of the apparatus according to the present invention, where only reflected light was detected, fastened on the wrist of a subject. The probe was placed on the wrist over the radial artery.

Figure 16 shows the probe comprising a patch made of flexible material. The probe was placed on the wrist, on the inside of the arm, over the radial artery.

Figure 17 shows three diagrams illustrating when saline was injected in the flow direction close to the probe in figure 15 and 16. Only the intensity of the reflected light was recorded and the change in signal corresponded to the dilution effect in the blood. The two diagrams in the bottom of figure 17 shows a recording on a patient with atrial fibrillation, i.e. the PPG and ECG signals.

Figure 18 shows an apparatus according to the present invention, including a computer and a SpO_2 (including blood characteristics) measuring apparatus, including cable-free Bluetooth™ equipment for wireless communication of data between seperate elements of the apparatus.

Figure 19 shows the PPG-signal with DC-signal, AC-signal, minimum points and maximum points.

Experimental details

Example 1

Detection was performed using the following equipment:
-A tube of acrylic glass (PMMA) with an inside diameter of 3 mm
-Two optical fibres with a diameter of 0.094 mm. One fibre was for transmission of light (light source) and the other for receiving reflection of light (photo detector).
-A glass tube with an outside diameter of 0.210 mm for housing the optical fibres placed in parallel with each other.
-Whole blood from volonteers, which was pumped through the tube made up of PMMA.

Figure 1 shows schematically the flow model for detection of light reflection. Figure 2 shows the orientation of red blood cells at an intermediate level of shear rate. Figure 3 shows light absorption in blood due to different absorbing matter. Figure 4 shows light scattering due to red blood cells.

The results from this experiment suggest that the light is spread in a special way when hitting the red blood cells in the tube. This probably depends on the shape of the blood cells, bi-concave disc, which forces the cells to orientate in different way as they move in the circular tube. This is demonstrated with optical technique through placing two optical fibres in a small catheter, where one of the fibres works as a light source and the other as photodetector as set out above. The fibre pair is moved from one periphery to the other in a cross-section of a circular tube.

Figures 5 and 6 are summaries of experimental results. The intensity of the light transmitted from the red blood cells flowing through a tube of acrylic glass. The experimental setup was the same as in the above mentioned experiments.

Figure 5 shows the relative change in transmitted light *versus* blood flow for two different types of red blood cells. The "stiff cells" are red blood cells, which were treated with glutaraldehyde in order to make them stiff i.e. they had lost their ability to change shape with the stress created by the flow.

The results show that one important characteristic of the red blood cells is their flexibility. This results in a change of shape - elongation - and orientation with increasing flow as demonstrated by the reduced transmission intensity with increasing flow. Red blood cells without this flexibility (stiff) show little or no orientation effect with flow as measured with light transmission change.

Figure 6 shows the relative change in transmitted light intensity *versus* blood flow for two types of blood cells. The "spherical cells" are red blood cells treated with non-isotonic buffer solution. This makes the cells loose their bi-concave disc shape. This results in a close contact and orientation with increasing flow as demonstrated by the reduced transmission intensity with increasing flow. Red blood cells with spherical shape exhibit less shear stress with increasing flow and show little or no orientation effect with flow as measured light transmission changes.

We can thus conclude that the cell orientation of the red blood cells as a function of flow e.g. flexible or inflexible tubes or arteries in humans and mammals is mainly due to their unique bi-concave disc shape and flexibility.

Example 2

A second experimental setup consisted essentially of the following. There were essentially three main parts:

* a cylindrical disc oxygenator which also served as a blood reservoir.
* a flow controlled roller pump (peristaltic pump)
* a rigid flow-through model connected to a light source and photodetectors via optical fibres

The setup is essentially shown in figure 7, but it lacks one photodetector, as both transmission and reflection was measured. A waveform generator regulated the roller pump, which produced a continuous blood flow. A pressure transducer was also part of the circuit for the blood flow. The blood temperature was maintained constant at 37.0° ± 0.1°C, by circulating warm air around the setup.

A gas mixture was lead into the reservoir and mixed with the blood. The gas exchange was simulated by a disc oxygenator and the gas mixture consisted of 19% oxygen and 5.6 % carbon dioxide in nitrogen. The oxygen saturation was maintained at 98-99%, and the blood gas parameters (pO_2, pCO_2 and pH) were assumed not to deviate from normal physiological values.

Laminar flow-through model was used in order to minimize hemolysis of the red blood cells. The wavelength that was used was 800 nm, an isobestic point where a minimal absorbance of light take place on the red blood cells. The measurements were performed on a tube made of acrylic glass with an inner diameter of 3.0 mm.

Figure 8 shows a diagram with the relative change of the quotient reflection/transmission (%) i.e. AC_R/AC_T, on the y-axis and the hemoglobin concentration in mmol/l on the x-axis. The quotient between reflection/transmission appears to be independent of the blood flow, but appears to vary according to the concentration of hemoglobin. The optically registered hemoglobin (Hb) signal may thus be stated;

$Hb=AC_R/AC_T$

and this has been confirmed by analysing in parallel with the method according to the present invention, drawn blood samples from volontary healthy persons and patients on a Hemocue apparatus (Ängelholm, Sweden) in a Clinical Chemistry Laboratory. Thus a calibration curve was obtained. This calibration curve may be stored in a memory of the processor, which preferably is part of a computer, which allows readily the conversion from AC_R/AC_T, obtained when directing light beam and subsequently detecting the reflection and transmission in accordance with the method of the invention, to a hemoglobin value in mmol/l. This curve may be linear at certain conditions.

Figure 9 shows light reflection and transmission vs. hemoglobin concentration. When illuminating intact blood cells in a circular pipe, the light transmission and reflection will follow the concentration of red blood cells. The transmission of light decreases with increased hemoglobin and the reflection of light increases with increased hemoglobin.

Example 3

A thimble-like test device comprising a shell which is one preferred embodiment of the present invention shown in Figure 10 was used. This thimble comprises:

i) two light sources: One Green Light Emitting Diode (LED), essentially of type 110104, 540, diameter ⌀ 5 mm, and one NIR LED , essentially of type SFH 585, 880, diameter ⌀ 4.85 which are interchangable,

ii) two detectors, essentially of type SD 1420-002 and CFD 10 respectively.

For SpO_2 measurements there may preferably be incorporated two additional light sources (red and infrared light) and corresponding detectors for detecting transmitted light, in said thimble construction.

The thimble has one rigid part comprising a stiffer material and one flexible part comprising a flexible material. The rigid part comprises PMMA or any other similar plastic material. The flexible part comprises silicon rubber with black dye (ceramic pigment which is non-conducting). The rigid and flexible parts form a circular ring forming a keyhole-like hole in the middle, with a bend for e.g. a finger or a toe. The rigid and flexible parts may be glued together or held together by other means.

How the thimble is connected to a power source and so on, is shown in Figure 11 through a block diagram illustrating this schematically. The numbers in the figure has the following explanations:

1. oscillator
2. LED-Driver λ 1
3. LED-Driver λ 2
4. LED λ 1 or 2
5. Photodiode reflection
6. Subject
7. Photodiode transmission
9. Current/Voltage converter
10. Current/Voltage converter
11. Lowpass Filter
12. Lowpass Filter
13. Sample and Hold amplifier
14. Sample and Hold amplifier
15. Band pass Filter
16. Band pass Filter
17. Analog output
18. Analog output
19. μ-controller
20. Read out unit

The oscillator is connected to the Sample and Hold amplifiers and the LED-Driver λ 1 and LED-Driver λ 2. These drivers are connected to one or in this case two LEDs and one photodiode for detecting the reflected light. The photodiode for detecting transmitted light is connected to at least one current/voltage converter in this case two, which in turn are connected to the Sample and Hold amplifiers . The signals then pass to the Band pass Filters and subsequently to the analog outputs or to a μ-controller which is connected to a Read out unit.

Example 4

A handcuff-like test device comprising a shell which is one preferred embodiment of the present invention shown in Figure 16 was used. This handcuff comprises:

i) six light sources: LEDs, λ=875 nm;
ii) one detector.

At least one of the light sources may preferably have a wavelength different from the other ones.

The handcuff comprises a patch of flexible material and a strap. The flexible material comprises silicon rubber with black dye (ceramic pigment which is non-conducting). The flexible material may form a bend for e.g. a wrist, a finger or a toe. The PPG sensor was especially designed to be used on the wrist. The optical geometry of the sensor was optimized in order to make it possible to monitor blood characteristics, preferably blood flow, deep in the tissue from the radial artery where it passes over the flat portion of the radius bone. The center to center distance between the LEDs and the photodetector is approximately 8-9 mm.

All components are incorporated in the sensor with the electronics on one side of the printed circuit card covered with black-coloured silicone and the optical components on the other side covered with transparent silicone. This ensures electrical isolation, reduction of stray light and the possibility for sterilization.

For SpO_2 determination, the above handcuff construction may preferably comprise two LEDs with wavelengths within the red and infrared range, respectively. The handcuff preferably also comprises two detectors for appearing on the opposite side of the wrist and detecting the transmitted SpO_2 light intensities, red/infrared.

How the handcuff is connected to a power source, a battery eliminator, is shown in Figure 16 through a block diagram illustrating this schematically. The handcuff is further connected to a laptop computer where all measured signals were stored.

Measurement was performed by using the above probe fastened on the wrist (see figure 16) of a subject. The probe was placed on the wrist over the radial artery. Saline was injected in the flow direction close to the probe. The artery needle was inserted 10 cm from the hand into the radial artery with the needle in the flow direction. The distance between the sensor and the tip of the needle was approximately 5 cm. Physiological saline was injected during 1-5 seconds at different volumes. The PPG signal was recorded in order to confirm the monitoring depth.

In clinical measurements the PPG signal was recorded in heart failure patients simultaneously with ECG recording. Only the intensity of the reflected light was recorded and the change in signal corresponded to the dilution effect in the blood. The result, i.e. the PPG signal which consists of two components namely a pulsatile component (AC) synchronous with the heart rate and a slowly varying component (DC), can be seen in figure 17, where the light reflection showed in change in both AC and DC signals corresponding to dilution effect in the blood after a delay of approximately 0.5 seconds. This proves the ability to extract information from the radial artery itself using the apparatus according to the present invention. The two diagrams in the bottom of figure 17 shows a recording on a patient with atrial fibrillation. The AC PPG signal (upper curve) is in accordance with the irregular appearance of the QRS complex in the electrocardiogram. The DC component reflects total blood volume changes of different physiological features in the circulation, e.g. vasomotion, temperature regulation and respiration.

The apparatus according to the present invention thus is useful for e.g. central related blood flow monitoring together with SpO_2 on the wrist. Signal variations in amplitude, curve form and frequency content may further reflect different pathological events in the body corresponding to congestive heart failure and cardiac arythmies. Other telemetrical applications in telemedicine are thinkable for the apparatus and the method according to the present invention.

As with other blood flow monitoring system, the apparatus according to the present invention is susceptible to patient arm movement. An artefact reducing loop may further be incorporated in the apparatus. Besides the blood flow parameter described above there may be incorporated in the apparatus means for monitoring blood pressure, heart rate and respiratory rate together with the oxygen saturation, SpO_2.

Another measurement was performed by using an apparatus according to present invention. The relative pressure was monitored and the results can be seen in figure 13. The diagram in figure 13 shows the intensity of the reflected pulsative light versus increasing systolic pressure. The diastolic pressure was kept constant. This exemplifies the central measurement of blood characteristics including Hb, as represented in larger vessels such as arteries. This is acheived by compensating for the influence of blood pressure and blood flow, by using a quotient of the transmitted/reflected, reflected/transmitted or reflected/reflected values for light intensities, on the measured intensities of the reflected and transmitted light. The effect may be used to measure the change in blood characteristics including Hb together with SpO_2 in one individual or in an extracorporeal system when the blood hemoglobin value is constant.

Another measurement was performed by using a probe, where only reflected light was detected, fastened on the wrist (see figure 16) of a subject. The probe was placed on the wrist over the radial artery. Saline was injected in the flow direction close to the probe. The artery needle was inserted 10 cm from the hand into the radial artery with the needle in the flow direction. The distance between the sensor and the tip of the needle was approximately 5 cm. Physiological saline was injected during 1-5 seconds at different volumes. The PPG signal was recorded in order to confirm the monitoring depth. Only the intensity of the reflected light was recorded and the change in signal corresponded to the dilution effect in the blood. The result, i.e. the PPG signal which consists of two components namely a pulsatile component (AC) synchronous with the heart rate and a slowly varying component (DC), can be seen in figure 17, where the light reflection showed in change in both AC and DC signals corresponding to dilution effect in the blood after a delay of approximately 0.5 seconds. The DC component reflects total blood volume changes of different physiological features in the circulation, e.g. vasomotion, temperature regulation and respiration.

Various embodiments of the present invention have been described above but a person skilled in the art realizes further minor alterations which would fall into the scope of the present invention. The breadth and scope of the present invention should not be limited by any of the above-described exemplary embodiments, but should be defined only in accordance with the following appended claims and their equivalents.

Claims

1. A non-invasive method of determining SpO_2 of a mixture of liquid and blood cells, comprising:
a) directing light beams against the mixture;
b) determining at least one blood characteristic other than SpO_2 including hemoglobin of the mixture by analyzing the intensity of the light reflected from the mixture, or the intensity of the light reflected from the mixture in combination with the intensity of the light transmitted through the mixture;
c) determining oxygen saturation, SpO_2, of the mixture by analyzing the intensity of the light transmitted through the mixture; and optionally
d) based on the result of step b), establishing whether the result of step c) is relevant.

2. A method according to claim 1, wherein (c) is performed by pulse-oximetrically determining oxygen saturation.

3. A method according to claim 1, wherein (a) is performed by directing at least one light beam with a wavelength in the red light range against the mixture, and directing at least one light beam with a wavelength in the infrared light range against the mixture.

4. A method according to claim 3, wherein (c) is performed by detecting the intensities of the red light and infrared light transmitted through the mixture, calculating a quotient of the detected intensities, red/infrared, of the transmitted light,

and determining SpO_2 by analyzing the quotient.

5. A method according to claim 1; wherein (b) is performed by:
i) detecting the intensity of the light of the light beams reflected from the mixture and the intensity of the light of the light beams transmitted through the mixture;
ii) calculating a quotient of the detected intensity of the transmitted light and detected intensity of the reflected light or a quotient of the detected intensity of the reflected light and detected intensity of the transmitted light; and
iii) analyzing the quotient to determine the blood characteristic.

6. A method according to claim 1, wherein (a) is performed by directing at least two light beams with different wavelengths against the mixture.

7. A method according to claim 6, wherein (b) is performed by:
i) detecting the intensities of the light of the light beams reflected from the mixture;
ii) calculating a quotient of the detected intensities of the reflected lights; and
iii) analyzing the quotient to determine the blood characteristic.

8. The method according to claim 1 wherein one or more of the values of the detected intensity of the light of the light beam(s) reflected from the mixture and the detected intensity of the light of the light beam(s) transmitted through the mixture, is transmitted over a wireless connection to a unit for performing (b), (c) and (d), preferably using a module for

wireless communication.

9. The method according to claim 8, wherein the wireless communication is performed using a Bluetooth™ standard based communication path.

10. The method according to claim 1, wherein the light beam(s) are directed essentially perpendicular to a measuring area of a vessel containing the mixture.

11. A method according to claim 1, wherein the wavelength of the light beams, when transmitted light also is detected, is from 200 nm to 2000 nm, preferably from 770 nm to 950 nm, most preferred approximately 770, 800, 850, 940 or 950 nm.

12. A method according to claim 1, wherein at least two light beams with different wavelengths are directed against the mixture, wherein one with a wavelength of from 770 to 950 nm and the other with a wavelength of from 480 to 590 nm.

13. A method according to claim 1, wherein the mixture of liquid and blood cells is flowing.

14. A method according to claim 1, wherein the mixture of liquid and blood cells comprises plasma.

15. A method according to claim 1, wherein it is performed on a mammal, preferably on a human being.

16. A method according to claim 15, wherein it is performed on a blood mixture with a diameter greater than 0,1 mm, preferably

a vein, an artery or an arteriol.

17. A method according to claim 15, wherein it is performed on an arm, a toe or a finger, preferably on a wrist or a finger on the third phalanx.

18. A method according to claims 1, wherein it is performed in a dialysis apparatus, or on a blood bag assembly, or on a slaughter house device, or on a blood fractionation device, preferably it is performed on a tube or pipe.

19. A method according to claim 1, wherein in step (b) light is emitted from at least four light sources, preferably six light sources, wherein the light sources being adapted to appear on either side of the detector(s), preferably the light sources are arranged in groups of two, most preferred in groups of three when six light sources are present, most preferred the light sources form an "H" with one detector in the centre.

20. A method according to claim 19, wherein the "H" is tilted approximately 90° during the measurement on preferably a wrist when looking from the direction of the arm.

21. A method according to claim 1, wherein in (b) light is emitted from two light sources, which are positioned and thus appearing on two different opposite sides of a vessel containing the mixture, and detection of reflected light from and transmitted light through the vessel is performed by at least two detectors, preferably by only two detectors.

22. A method according to claim 1, wherein (b) comprises the following steps:

I) sweeping a window over a curve with detected values from transmission and/or reflection, wherein the size of the window preferably is approximately 60 % of the period time, divided equally to the right and to the left;
II) if no value within the window is higher than the middle value, designating the value a maximum point whereupon moving the window by leap half of the window length, or if a value exceeds the middle value moving the window only one step;
III) designating the minimum points in the same manner as in II) but with regards to minimum values instead of maximum values;
IV) obtaining the height of the AC-signal by subtracting from a value on a connection line involving two maximum points, the vertically lying value of an in between lying minimum point;
V) repeating step IV) at least 8 times, and summarizing the values from IV) and dividing the sum with the number of observations, thus obtaining a median AC-value; and
VI) optionally obtaining the DC-signal by adding the total height of the minimum point in IV) to the median AC-signal of step V);
whereby preferably using a computer program for obtaining the AC-signal and optionally the DC-signal.

23. A method according to claim 3, wherein the wavelength in the red light range is approximately 660 nm and the wavelength in the infrared light is approximately 940 nm.

24. A method according to claim 1, wherein the determined SpO_2 and determined blood characteristic including hemoglobin is presented simultaneously.

25. A method according to claim 1, wherein the determined SpO_2 is corrected by using the determined blood characteristic including hemoglobin.

26. An apparatus for accurate determination of SpO_2 from a mixture of liquid and blood cells contained in a light pervious vessel comprising:
- light sources for directing light beams against the vessel,
- means for determining a blood characteristic other than oxygen saturation, SpO_2, including hemoglobin and capable of analyzing the intensity of the light reflected from the vessel, or the intensity of the light reflected from the vessel in combination with the intensity of the light transmitted through the mixture,
- means for determining oxygen saturation, SpO_2, of the mixture, preferably pulse-oximetrically, and of analyzing the intensity of the light transmitted through the mixture; and optionally means for establishing whether the determined value of SpO_2 is relevant with respect to the determined value of the blood characteristic.

27. An apparatus according to claim 26, wherein the light sources comprise a first light source for emitting a first light beam with a wavelength in the red light range against the vessel, and a second light source for emitting a second light beam with a wavelength in the infrared light range against the vessel.

28. An apparatus according to claim 27, further comprising a first detector for detecting the intensity of the light of the red first light beam transmitted through the vessel, and a

second detector for detecting the light of the infrared second light beam transmitted through the vessel.

29. An apparatus according to claim 28, wherein the oxygen saturation determining means comprises a processor adapted to calculate a quotient of the detected intensities of the transmitted red and infrared lights and to determine the value of the oxygen saturation by analyzing the quotient.

30. An apparatus according to claim 26, wherein the light sources comprise a third light source for emitting a third light beam against the vessel, and further comprising a third detector for detecting the intensity of the light of the third light beam reflected from the vessel and a fourth detector for detecting the intensity of the light of the third light beam transmitted through the vessel.

31. An apparatus according to claim 30, wherein the blood characteristic determining means comprises a processor adapted to calculate a quotient of the detected intensities of the reflected and transmitted lights of the third light beam and to determine the value of the blood characteristic by analyzing the quotient.

32. An apparatus according to claim 26, further comprising registration means for storing the determined blood characteristics and SpO_2.

33. An apparatus according to claim 26, further comprising means for visualization of the determined blood characteristic and SpO_2.

34. An apparatus according to claim 26, wherein the light sources direct at least two light beams on the same side of the vessel, preferably one of the light sources emits a light of a wavelength in the range of 770 to 950 nm and the other a wavelength in the range of 480 to 590 nm.

35. An apparatus according to claim 26, wherein at least two of the components of the apparatus communicate with each other over a wireless connection, preferably over a module for wireless communication.

36. An apparatus according to claim 35, wherein the module for wireless communication comprises at least one transmitter and one receiver.

37. An apparatus according to claim 31, wherein there is one module for wireless communication between at least three components of the apparatus, i.e. light sources, detectors, and the processor.

38. An apparatus according to claim 35, wherein the wireless communication is performed using a Bluetooth™ standard based communication path.

39. An apparatus according to claim 26 wherein the light sources are positioned essentially perpendicular to a measuring area of the vessel.

40. An apparatus according to claim 26, wherein the wavelength of at least one of the light beams is from 200 nm to 2000 nm,

preferably from 770 nm to 950 nm, most preferred approximately 770, 800, 850, 940 or 950 nm.

41. An apparatus according to claim 26, wherein two of the light sources direct two light beams on the same side of the vessel, one of the light beams having a wavelength of from 800 nm to 940 nm and the other light beam having a wavelength of from 480 to 590 nm.

42. An apparatus according to claim 30, wherein the light sources are at least four, preferably at least six, the light sources being adapted to appear on either side of the detector(s), preferably the light sources are arranged in groups of two , preferably groups of three, wherein the light sources preferably form an "H" with one detector in the centre.

43. An apparatus according to claim 26, further comprising a test device having the shape of a wrist, finger or toe fitting device equipped with the light source(s) and at least one light detector.

44. An apparatus according to claim 43, wherein the test device comprises a thimble-like shell to be applied on a finger or toe, the light source and detector being arranged to direct the light beam and detect the light intensity within the shell.

45. An apparatus according to claim 44, wherein at least one light source and the detector are positioned in the shell comprising a constriction whereby the light source and detector are positioned and thus appearing in the constriction, whereby the shell preferably is a part of a thimble design for covering

a finger or a toe.

46. An apparatus according to claim 26, wherein the light sources comprise at least four light emitting diodes, preferably at least six light emitting diodes, and further comprising one light detector which together form an "H" with the detector in the centre, fixed on a patch which in turn is making part of a handcuff construction suitable for wrist measurements, wherein the distance between the light sources and the detector preferably is for determining blood characteristics including Hb from 4 to 12 mm when referring from the centres of respective component, most preferred the distance is approximately from 8 to 9 mm.

47. An apparatus according to claim 46, wherein the light sources and the detectors, which are arranged for detecting reflected light, are fixed at the edge of the patch, which may house a finger, a toe or wrist, preferably a wrist, wherein preferably the patch is a flexible plastic patch anchored to a strap for fastening to the wrist wherein the strap preferaby has a locking device.

48. An apparatus according to claim 47, wherein the light sources and detectors are incorporated in the patch whereby the electric components are fixed on one side of a printed circuit card covered with black-coloured silicone and the optical components are fixed on the other side covered with transparent silicone.

49. An apparatus according to claim 47, wherein the patch is rectangular with a size of 51 x 35 mm, and the

light sources and detector arranged as an "H" are fixed in a corner of the patch.

50. An apparatus according to claim 31, wherein the processor is adapted to convert the reflection values to a concentration value of the determined blood characteristic.

51. An apparatus according to claim 26, further comprising a processor having a computer program for performing the method according to any of claims 1 to 20.

52. An apparatus according to claim 27, wherein the wavelength of the red light is approximately 660 nm and the wavelength of the infrared light is approximately 940 nm.

53. A computer program stored on a data carrier for performing the method according to any one of claims 1 to 25.

54. Use of an apparatus according to any of claims 26 to 52 in a dialysis apparatus.

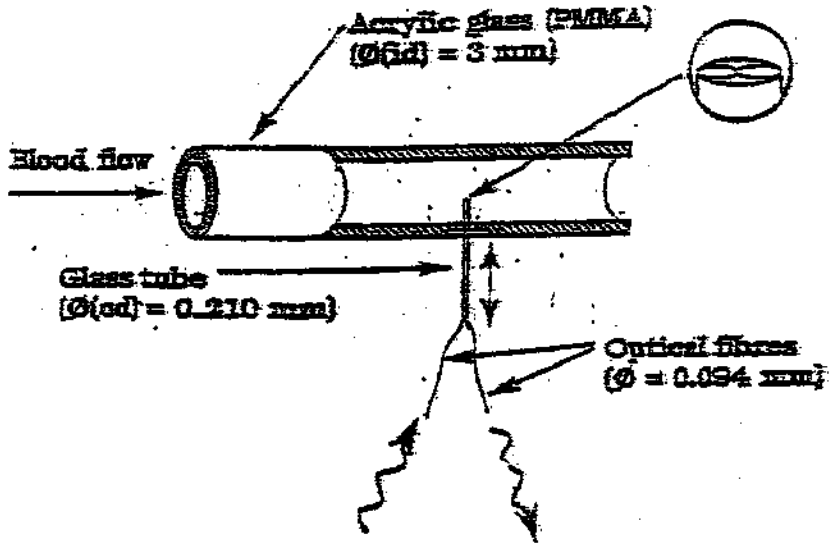
Acrylic glass (PMMA)
(Ø(id) = 3 mm)
Blood flow
Glass tube
(Ø(od) = 0.210 mm)
Optical fibres
(Ø = 0.094 mm)

1/19

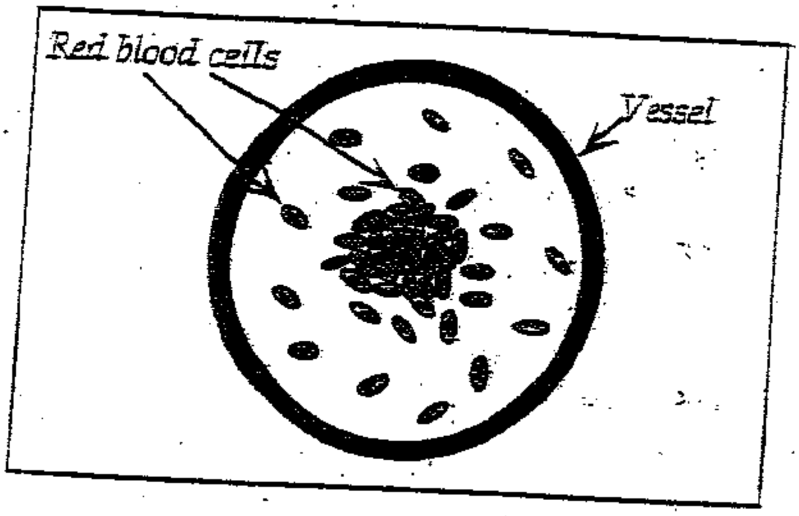
Red blood cells
Vessel

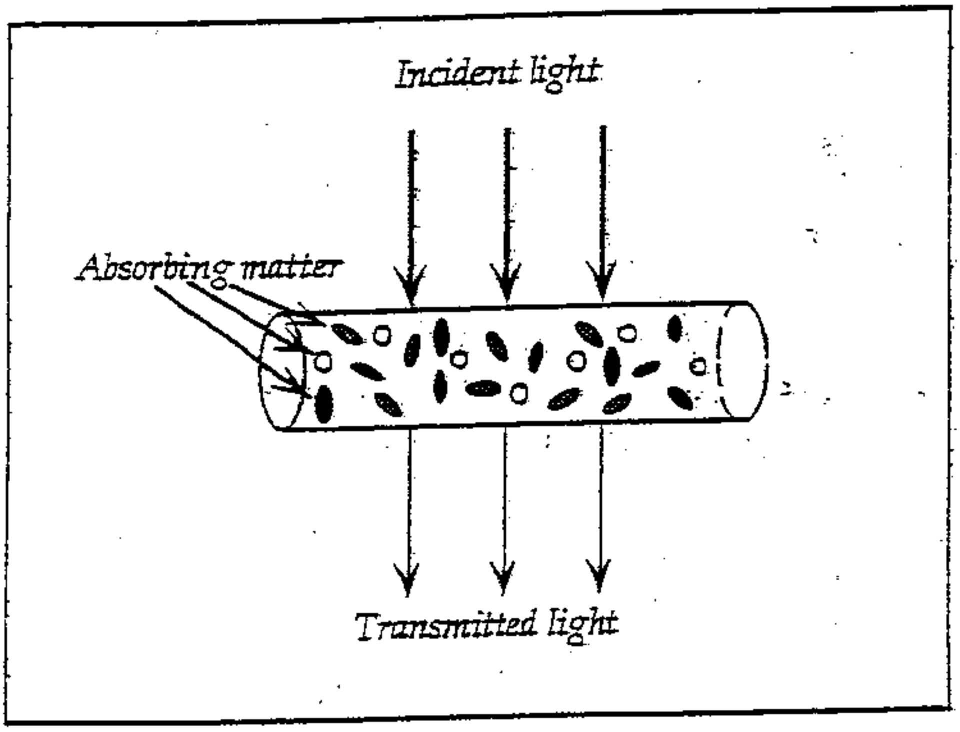
Incident light
Absorbing matter
Transmitted light

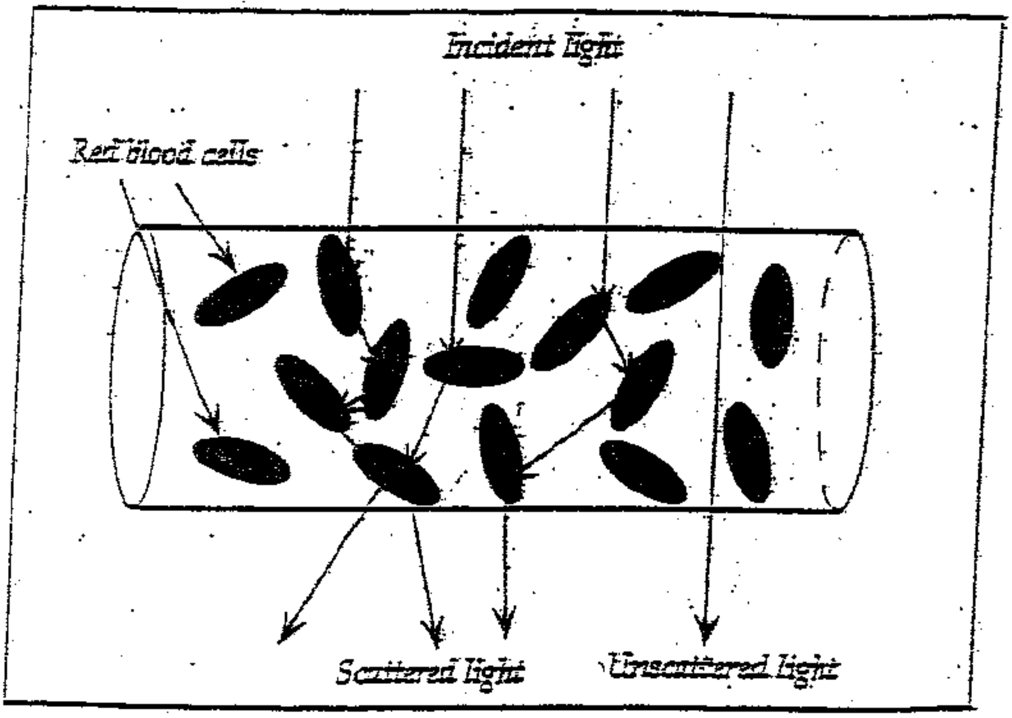
Incident light
Red blood cells
Scattered light
Unscattered light

Light transmission - stiff RBCs

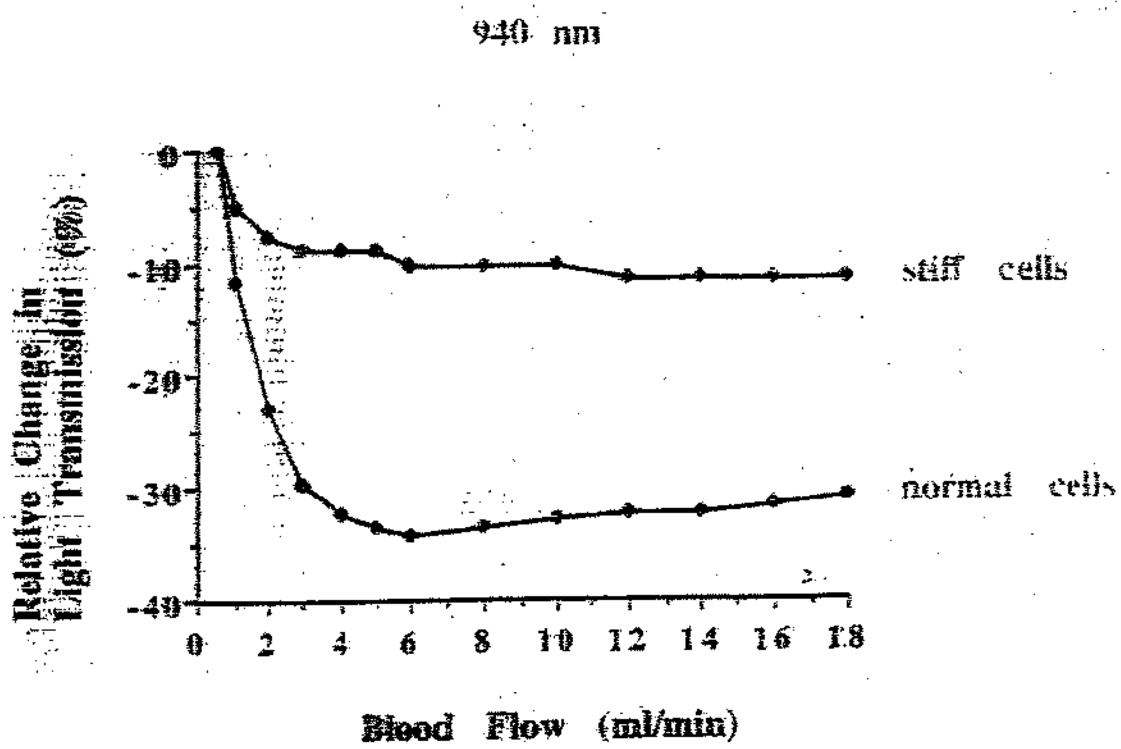

Light transmission - spherical RBCs

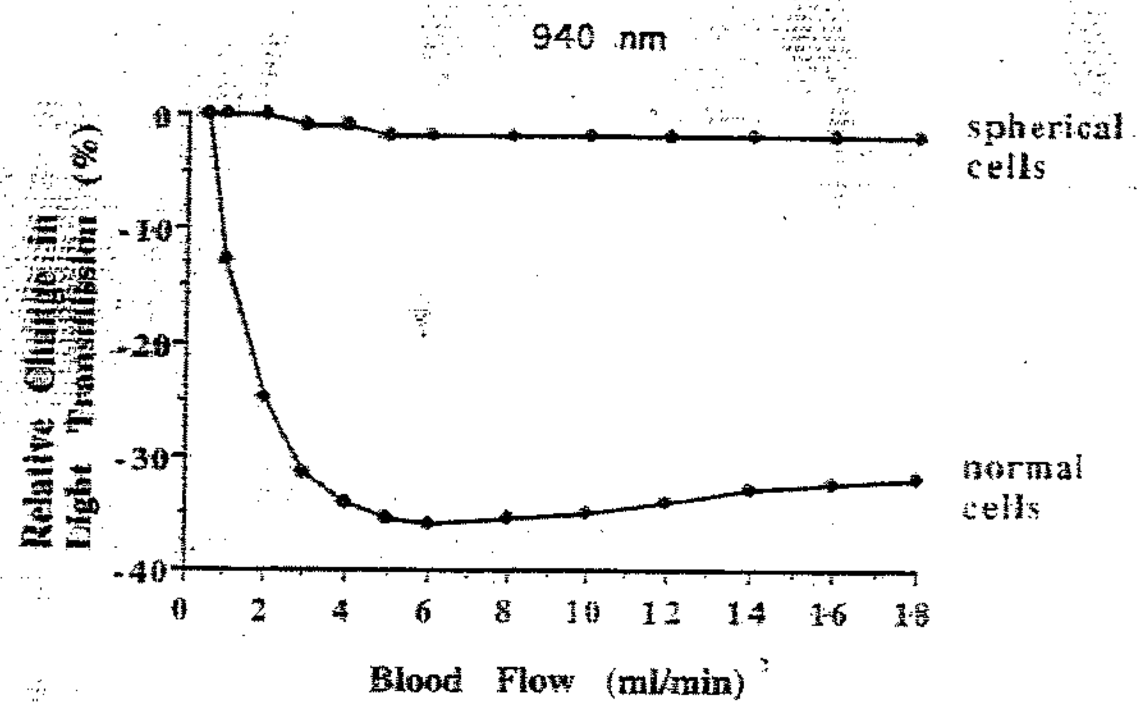

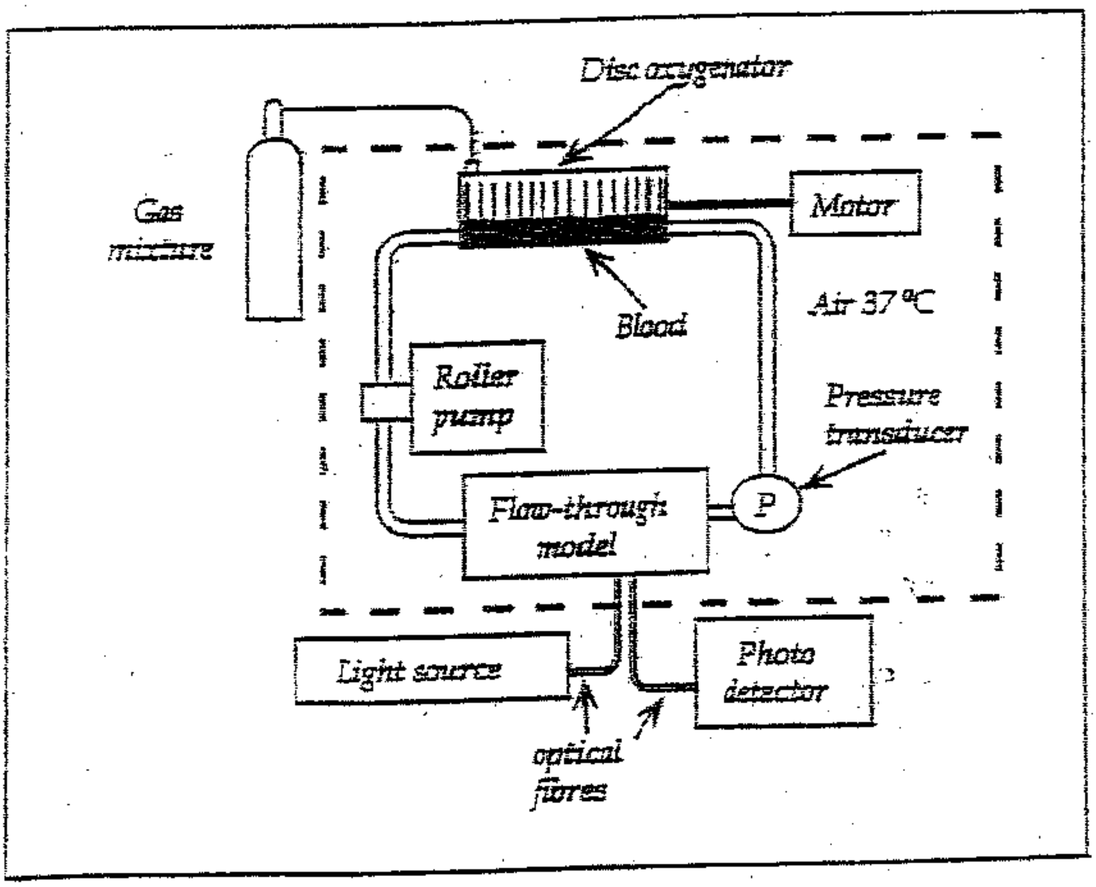
Disc oxygenator
Gas mixture
Motor
Blood
Air 37 °C
Roller pump
Pressure transducer
Flow-through model
P
Light source
Photo detector
optical fibres

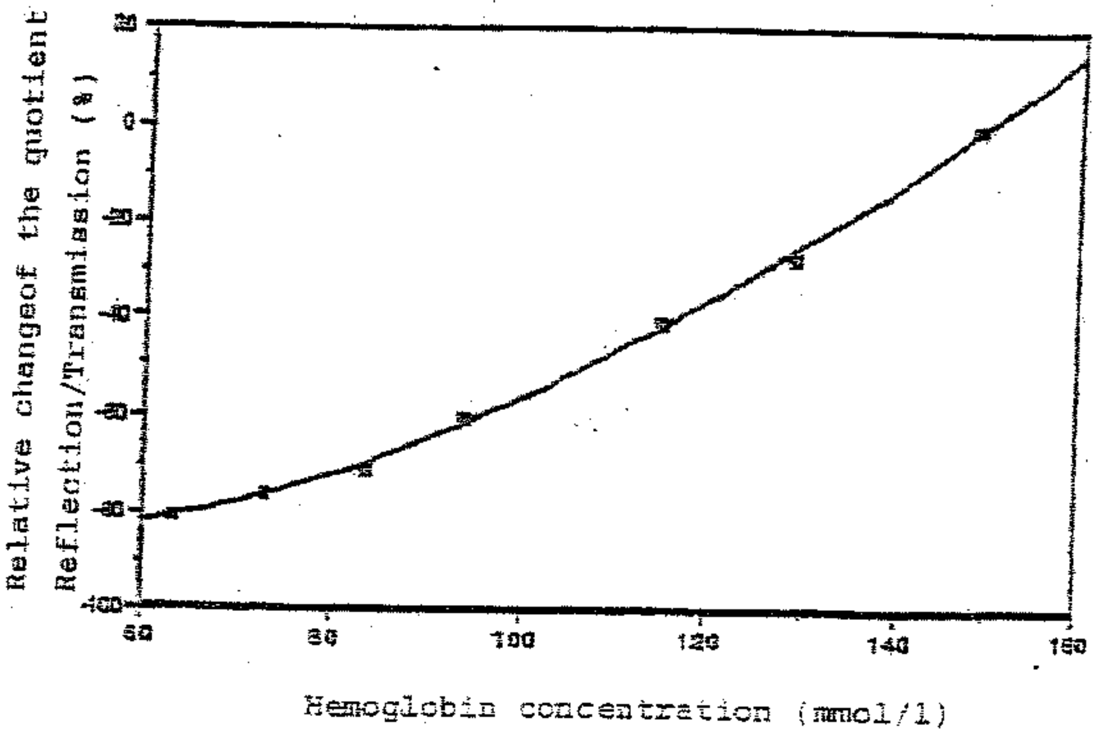

SUBSTITUTE SHEET (RULE 26)

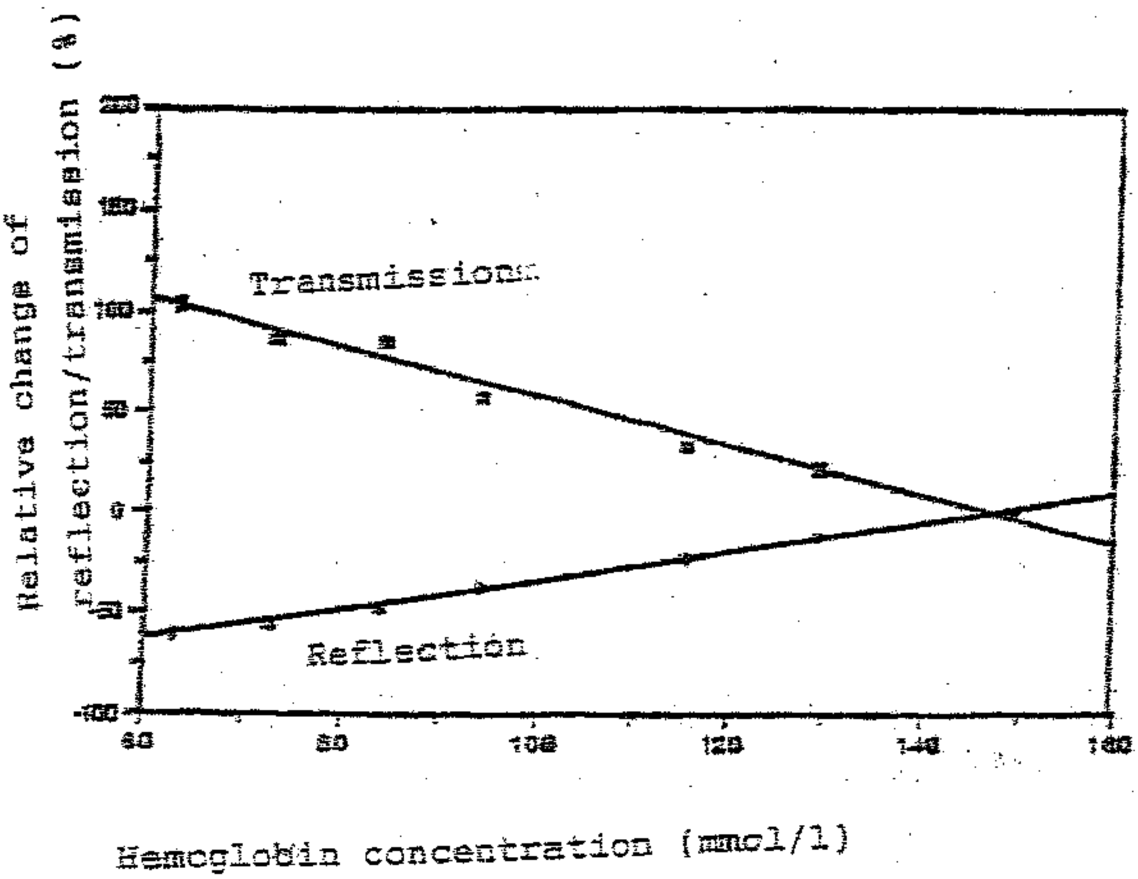
Relative change of reflection/transmission (%)
Transmission
Reflection
Hemoglobin concentration (mmol/1)

9/19

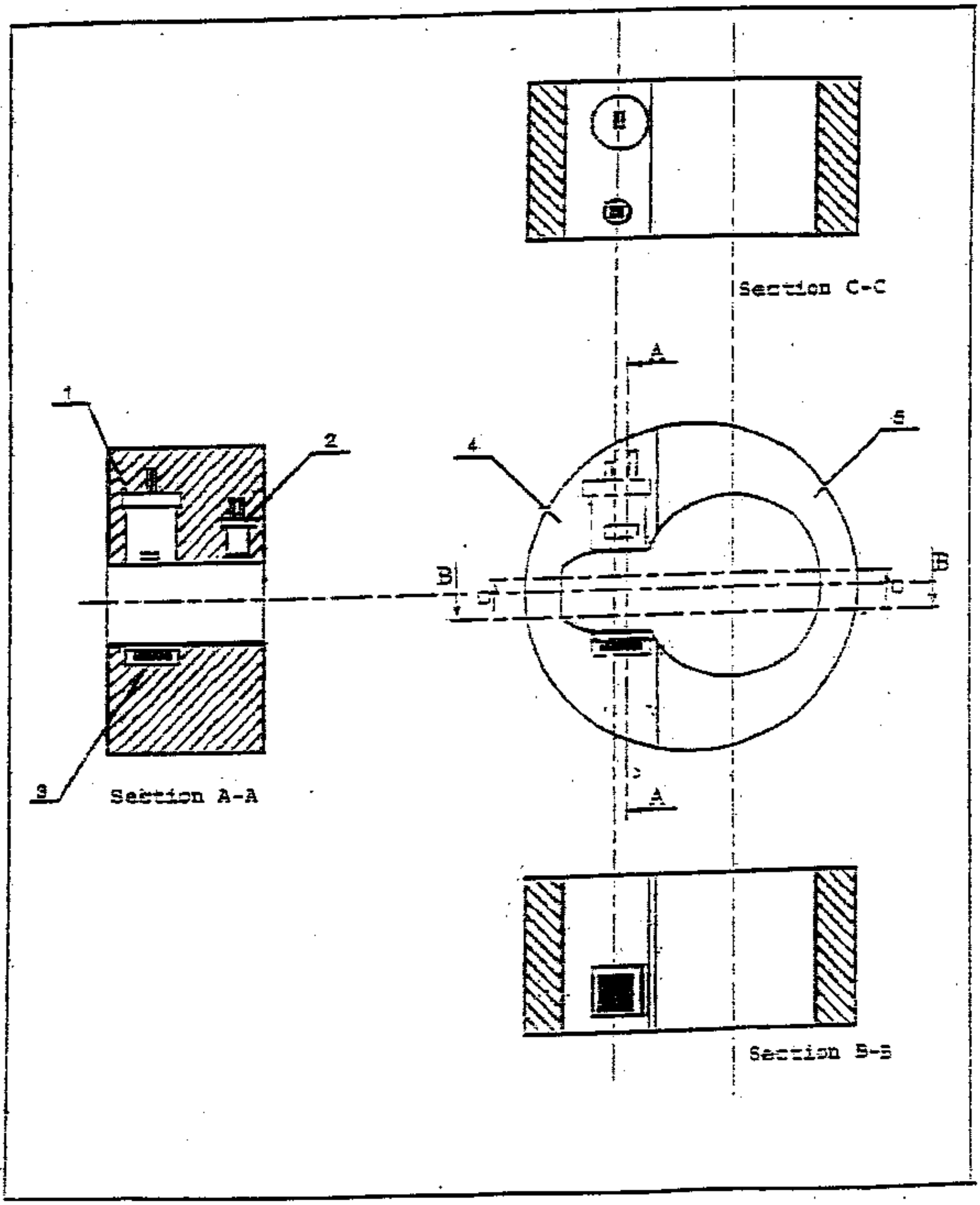
Section C-C
A
1
2
4
5
B
C
B
C
3
Section A-A
A
Section B-B

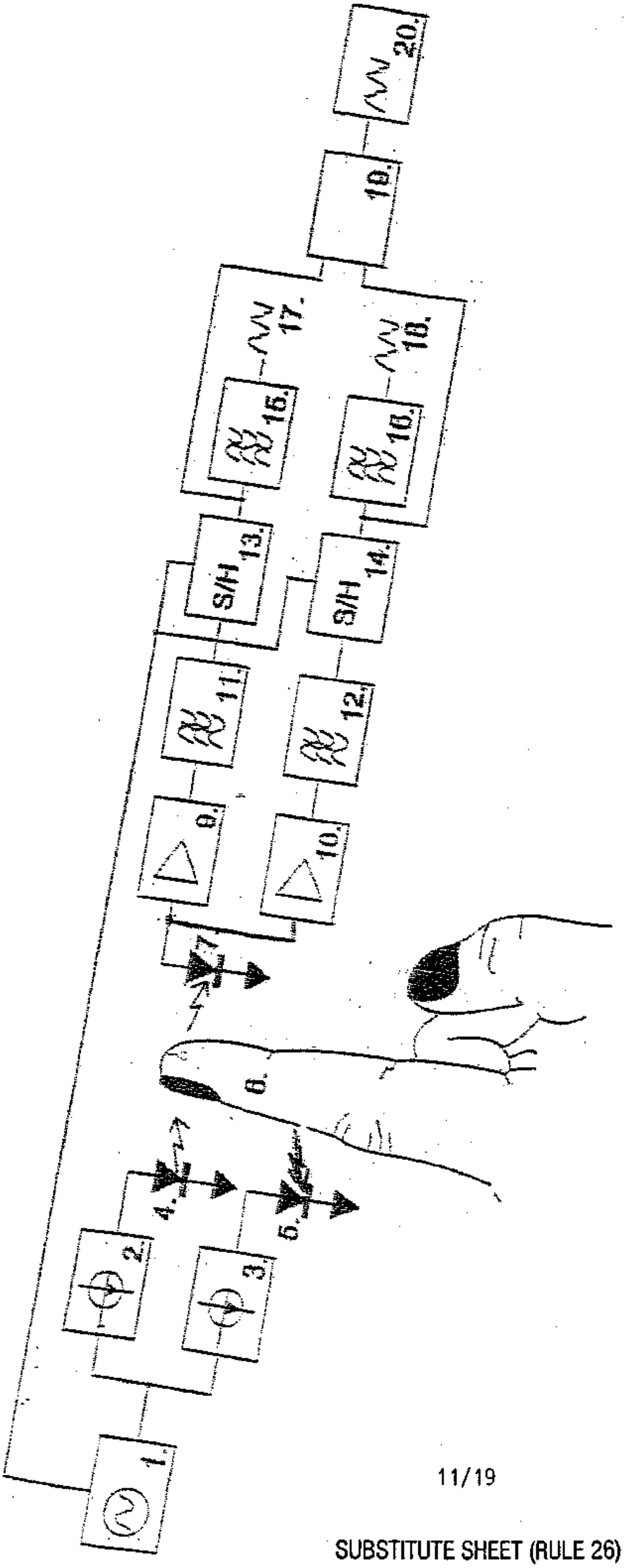

SUBSTITUTE SHEET (RULE 26)

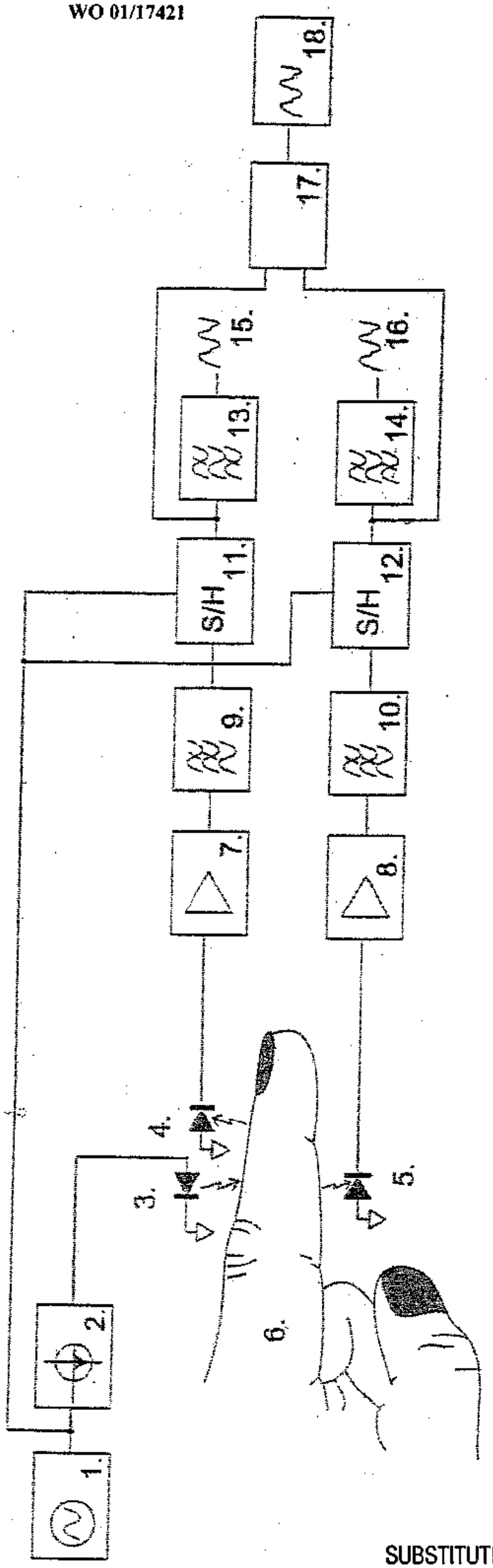
1.
2.
3.
4.
5.
6.
7.
8.
9.
10.
S/H 11.
S/H 12.
13.
14.
15.
16.
17.
18.

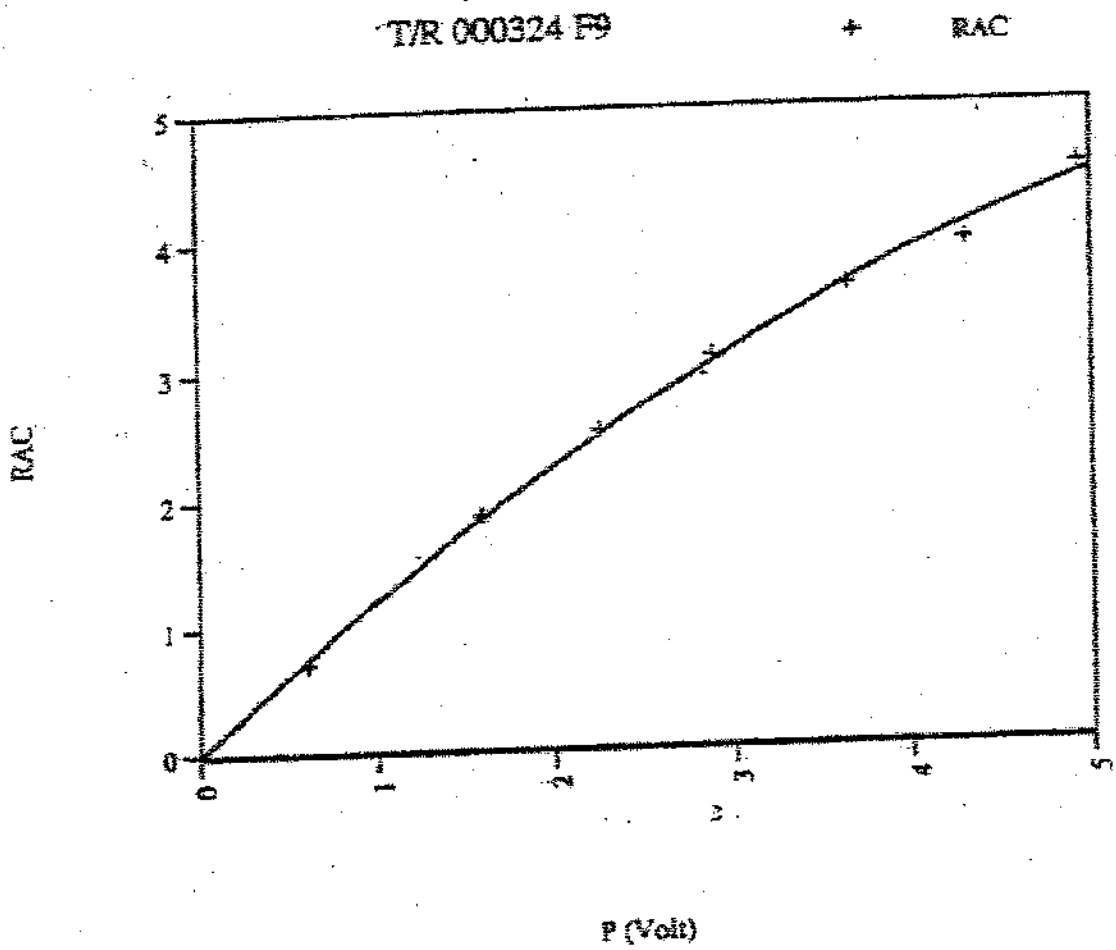
T/R 000324 F9
+ RAC
RAC
P (Volt)
0
1
2
3
4
5

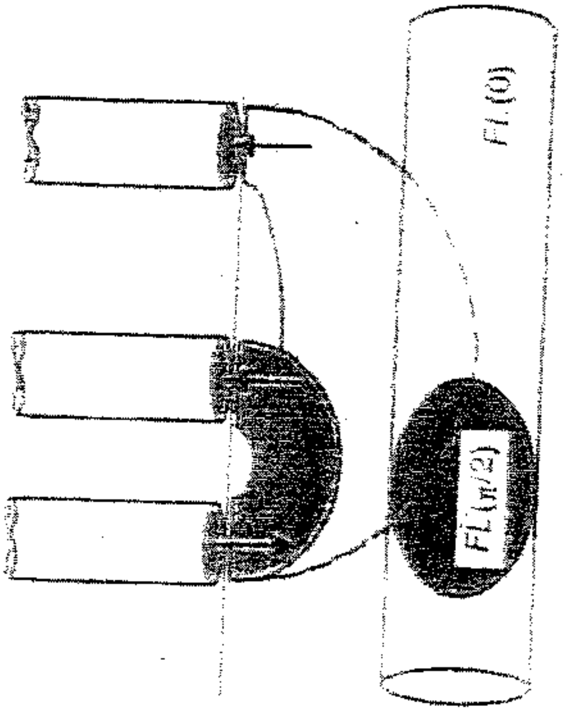
FL(0)
FL(π/2)

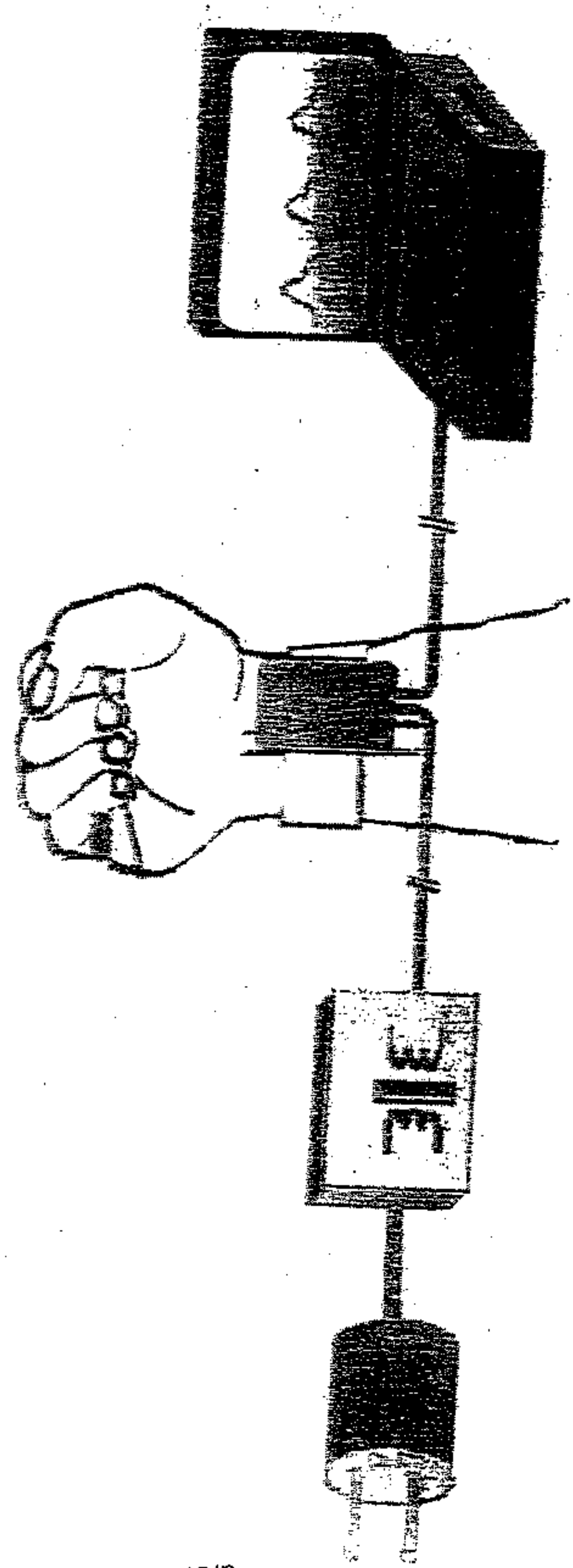

Experimental set-up.

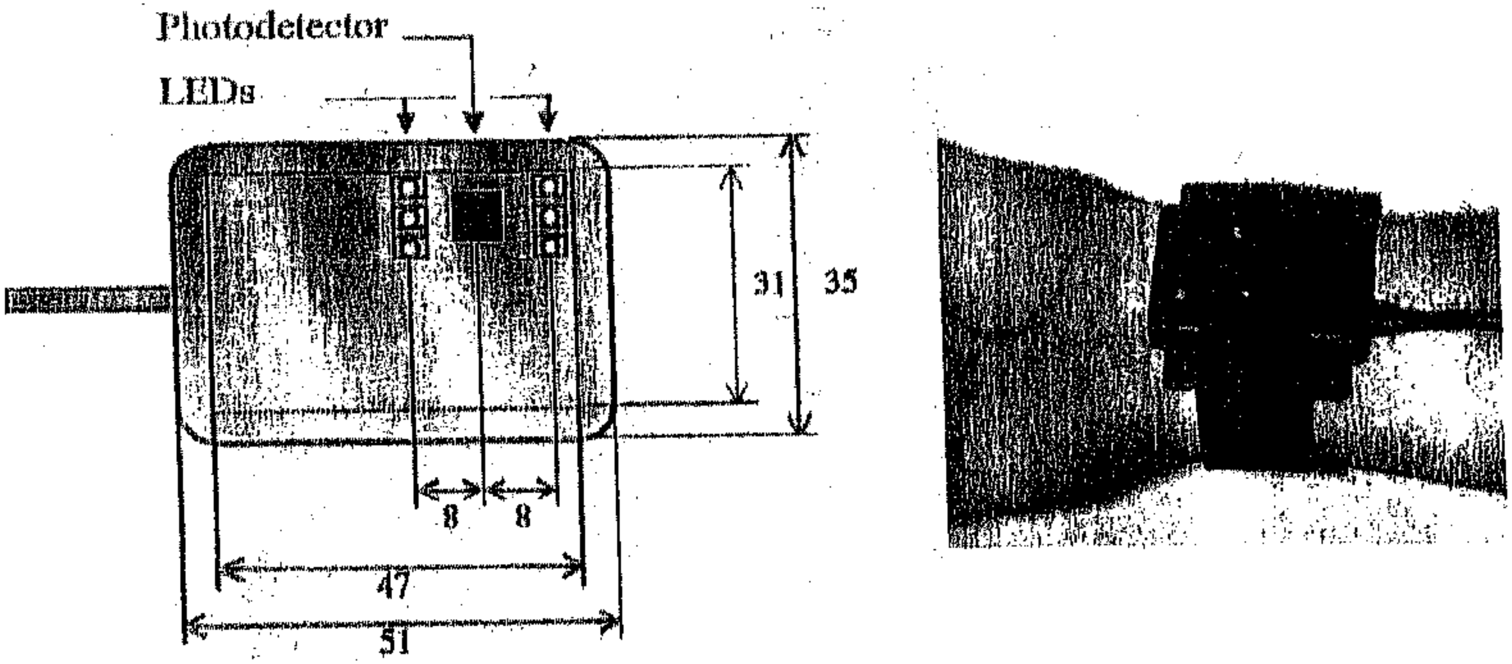

The optical sensor (all numbers are in mm).

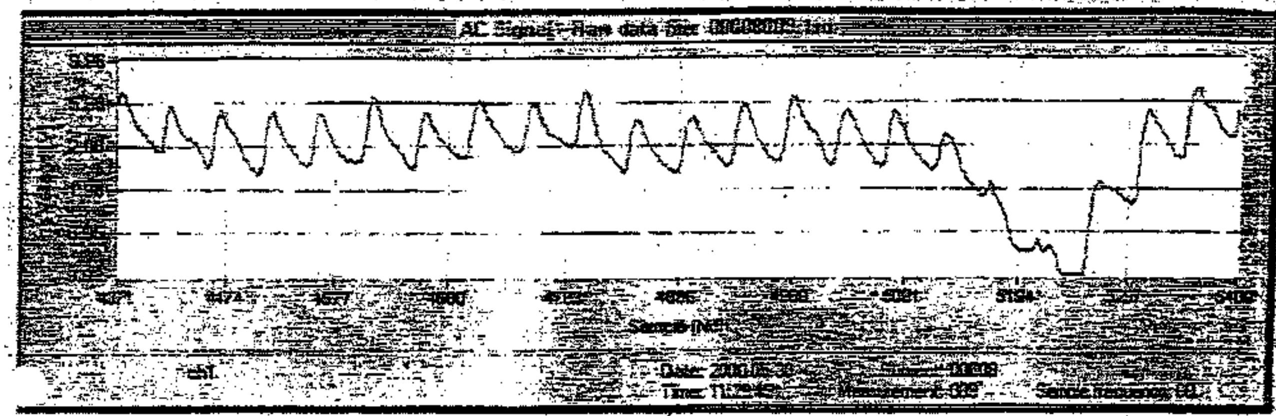

. The PPG signal during blood dilution in the radial artery.

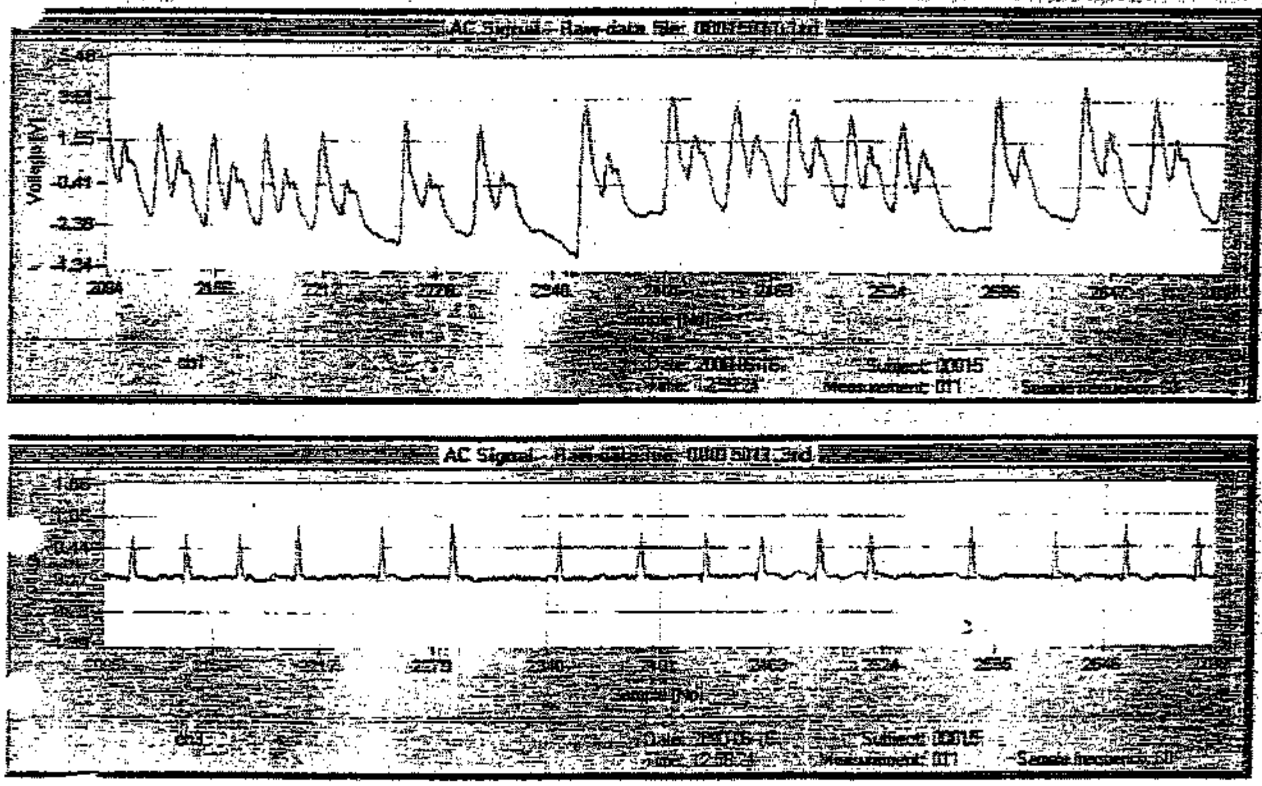

The PPG and ECG signals in a patient with arterial fibrillation.

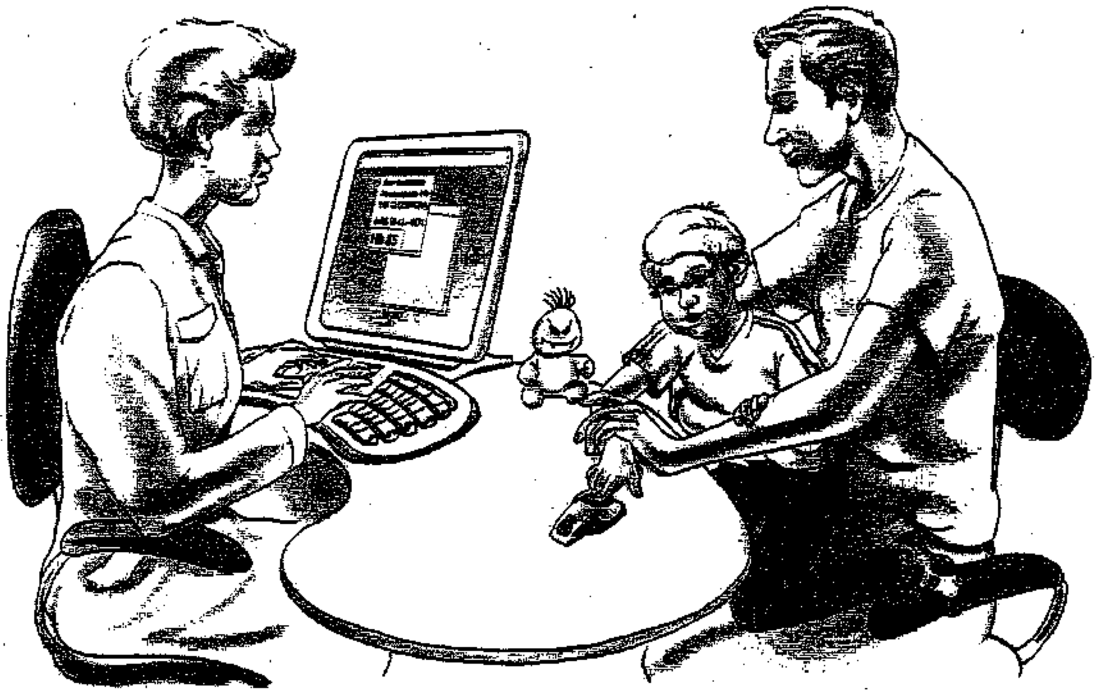

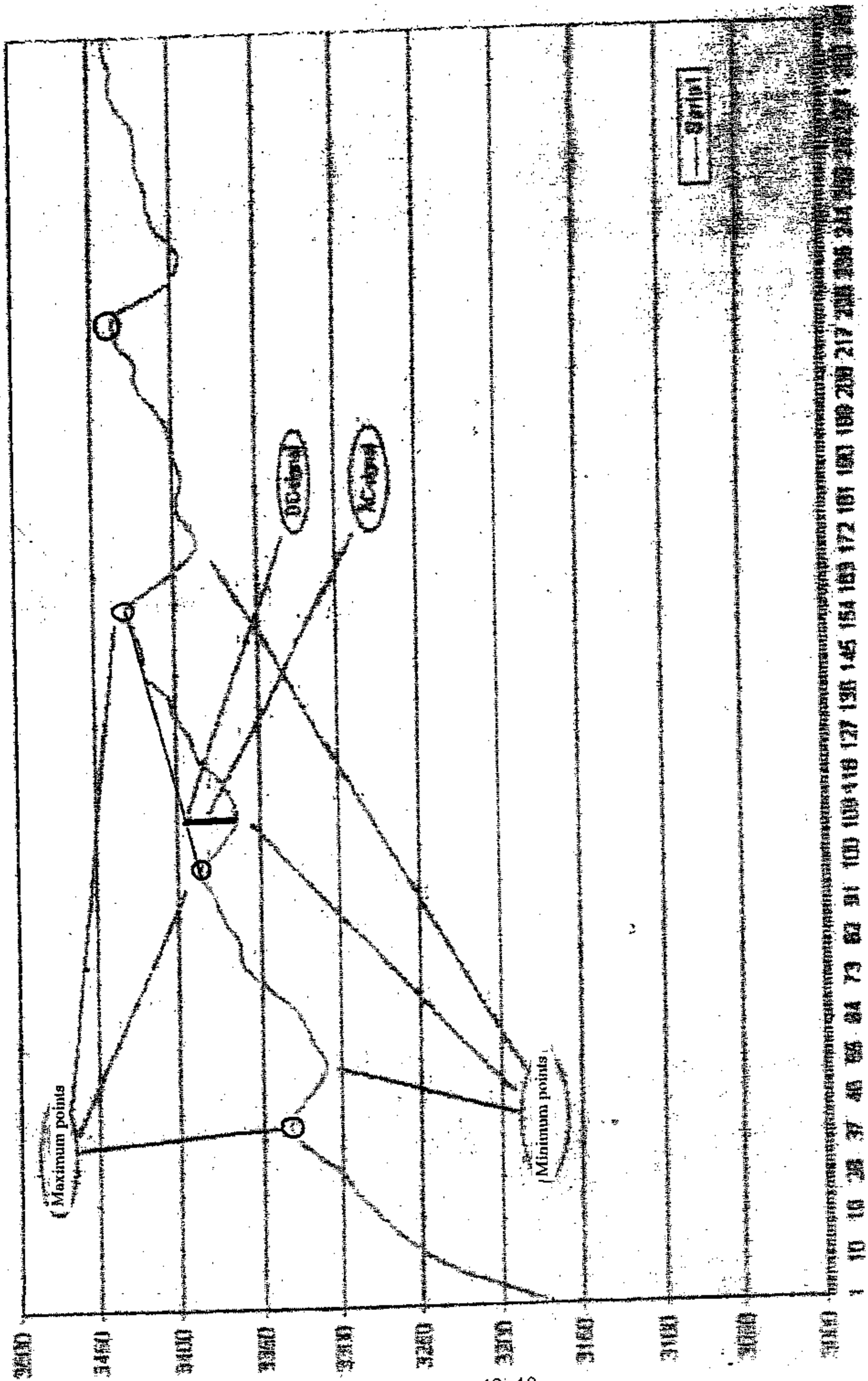
Maximum points
Minimum points

INTERNATIONAL SEARCH REPORT

International application No.
PCT/SE 00/01740

A. CLASSIFICATION OF SUBJECT MATTER

IPC7: A61B 5/00, G01N 33/49, G01N 21/55
According to International Patent Classification (IPC) or to both national classification and IPC

B. FIELDS SEARCHED

Minimum documentation searched (classification system followed by classification symbols)

IPC7: A61B, G01N

Documentation searched other than minimum documentation to the extent that such documents are included in the fields searched

SE,DK,FI,NO classes as above

Electronic data base consulted during the international search (name of data base and, where practicable, search terms used)

C. DOCUMENTS CONSIDERED TO BE RELEVANT

Category*	Citation of document, with indication, where appropriate, of the relevant passages	Relevant to claim No.
X	US 5499627 A (ROBERT R. STEUER ET AL), 19 March 1996 (19.03.96) --	1-4,6-54
A	WO 9111136 A1 (BOSTON ADVANCED TECHNOLOGIES, INC.), 8 August 1991 (08.08.91) --	6-7
A	WO 8901758 A1 (VANDER CORPORATION), 9 March 1989 (09.03.89) --	1-5
A	US 5720284 A (TAKUO AOYAGI ET AL), 24 February 1998 (24.02.98) --	1-5

[X] Further documents are listed in the continuation of Box C. [X] See patent family annex.

* Special categories of cited documents:
"A" document defining the general state of the art which is not considered to be of particular relevance
"E" earlier application or patent but published on or after the international filing date
"L" document which may throw doubts on priority claim(s) or which is cited to establish the publication date of another citation or other special reason (as specified)
"O" document referring to an oral disclosure, use, exhibition or other means
"P" document published prior to the international filing date but later than the priority date claimed
"T" later document published after the international filing date or priority date and not in conflict with the application but cited to understand the principle or theory underlying the invention
"X" document of particular relevance: the claimed invention cannot be considered novel or cannot be considered to involve an inventive step when the document is taken alone
"Y" document of particular relevance: the claimed invention cannot be considered to involve an inventive step when the document is combined with one or more other such documents, such combination being obvious to a person skilled in the art
"&" document member of the same patent family

Date of the actual completion of the international search	Date of mailing of the international search report
22 January 2001	29 -01- 2001
Name and mailing address of the ISA/ Swedish Patent Office Box 5055, S-102 42 STOCKHOLM Facsimile No. +46 8 666 02 86	Authorized officer Carolina Palmcrantz/ELY Telephone No. +46 8 782 25 00

Form PCT/ISA/210 (second sheet) (July 1998)

INTERNATIONAL SEARCH REPORT

International application No.
PCT/SE 00/01740

C (Continuation). DOCUMENTS CONSIDERED TO BE RELEVANT

Category*	Citation of document, with indication, where appropriate, of the relevant passages	Relevant to claim No.
A	WO 9637259 A1 (DOMJÁN, GYULA ET AL), 28 November 1996 (28.11.96) --	1-5
A	EP 0762108 A2 (KYOTO DAI-ICHI KAGAKU CO., LTD.), 12 March 1997 (12.03.97) -- --------	1-5

Patent document cited in search report			Publication date	Patent family member(s)			Publication date
US	5499627	A	19/03/96	US	5351686	A	04/10/94
				US	5372136	A	13/12/94
				US	5456253	A	10/10/95
				US	5803908	A	08/09/98
WO	9111136	A1	08/08/91	AU	7302991	A	21/08/91
				US	5239180	A	24/08/93
				US	5054487	A	08/10/91
				US	5222495	A	29/06/93
				US	5222496	A	29/06/93
				US	5246004	A	21/09/93
WO	8901758	A1	09/03/89	AU	630594	B	05/11/92
				AU	2538488	A	31/03/89
				DE	3855749	D,T	24/04/97
				DK	54690	A	03/05/90
				EP	0374190	A,B	27/06/90
				JP	3500207	T	17/01/91
				US	4805623	A	21/02/89
US	5720284	A	24/02/98	DE	19612425	A,C	02/10/96
				JP	8322822	A	10/12/96
WO	9637259	A1	28/11/96	AU	5842596	A	11/12/96
				EP	0828533	A	18/03/98
				HU	216847	B	28/12/99
				HU	9501512	D	00/00/00
				US	5974337	A	26/10/99
EP	0762108	A2	12/03/97	JP	9126996	A	16/05/97

APPENDIX O

Optimum Place for Measuring Pulse Oximeter Signal in Wireless Sensor-Belt or Wrist-Band

Miia Määttälä, Antti Konttila and Esko Alasaarela
Optoelectronics and Measurement Techniques Laboratory, University of Oulu, Oulu, Finland
miia.maattala@ee.oulu.fi
Wan-Young Chung
Division of Computer & Information Engineering, Dongseo University, Busan, South-Korea

Abstract

This study was done in order to solve the optimum place for integrated pulse oximeter in case of a belt around human chest or wrist so that it would provide reliable oxygen saturation (SpO_2) readings for non-invasive constant health monitoring in modern wireless applications. In the study four spots on the wrist and on the chest were chosen and measurements from these spots were done by using a special device with an adjustable angle between light detector and the light sources. Then resulted signals were analyzed by calculating the average amplitude, normalized amplitude and signal-to-noise –ratio (SNR). Considerably clear signals were achieved both from wrist and chest and best resulted SNR was 27dB from the chest. The highest normalized signal amplitude was detected from the wrist appearing as big as 5.9% of the total measured signal, which was relatively high compared to other values. Results were promising and showed that an easy portable monitoring device is possible but also many problems, that should be overcome, were detected.

1. Introduction

Pulse oximetry is used universally in the supervision of critically ill patients in intensive care units and operating theatres to provide a reliable oxygen saturation reading [1]**.** Signs and symptoms of decreased ability to ventilate are, for example, cyanosis, dyspnea, tachypnea, decreased level of consciousness, increased work of breathing and loss of protective airway reflexes [2]. If some of these symptoms occur, patient assesment will determine the need for continuous oxygen saturation monitoring. Nowadays measurements are normally done by using a finger probe which can be considered reliable and practical in case the patient is hospitalized or lying steadily. Though, technologies and needs for different kind of healthcare are constantly changing. That is why it is extremely important to be able to offer solutions which can be used also when supervising moving patients in different kinds of environments. Especially, different modern home healthcare and sport applications recall for wireless, reliable and easy-to-use –methods so that testing could be done continuously also in real-life situations and not only in hospitals. In addition, elderly people healthcare is changing markedly because of internet and high technology telemedicine. It is already possible to see patient's physiological state or some parts of it by transferring information through sensor networks and servers straight to doctor's mobile phone or work station. That would make it easy for old people to stay home alone even though they have some disease which requires continuous supervision.

In this study, pulse oximeter device, which was built in the University of Oulu (see Fig 5), was used in order to find the best place on human's chest or wrist to provide the highest accuracy for pulse oximeter signal with lowest noise and disturbances. This study aims to optimize integration of pulse oximetry to wireless sensor belt and wrist band development.

2. Principle and instrumentation

2.1. Pulse oximeter principle

Haemoglobin consists of four subunits joined together. When an oxygen molecule binds to one subunit, the other subunits become more likely also to bind oxygen. Haemoglobin saturation curve is characterized in to its S-form by this feature of haemoglobin. Shift to the right in the curve indicates that oxygen is bound less tightly – less is taken up in the lungs but is more easily released in tissues. The

0-7695-3038-9/07 $25.00 © 2007 IEEE
DOI 10.1109/ICCIT.2007.63

oxyhaemoglobin dissociation curve is the relationship between the partial pressure of oxygen in the blood and the percentage of oxygen bound to haemoglobin compared to the maximum. Factors such as decreasing carbon dioxide concentration, increasing pH and decreasing temperature will shift the curve toward the left. A left-shifted curve implies that the haemoglobin molecules will be more saturated at lower partial pressure of oxygen. Figure 1 shows the oxyhaemoglobin dissociation curve in three different cases [3].

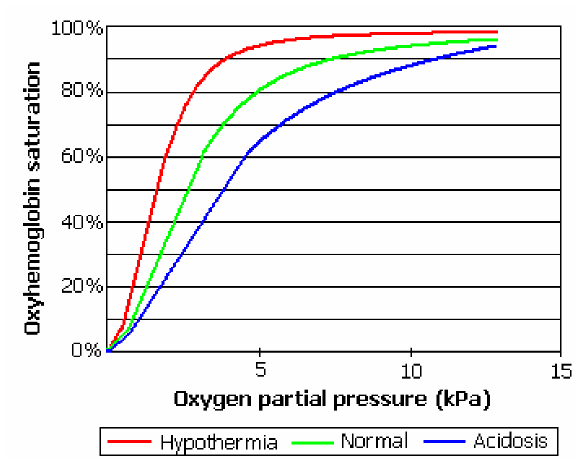

Figure 1. Oxyhaemoglobin dissociation curve.

Clinical measurement of the arterial oxygen saturation of haemoglobin has been dominated lately by pulse oximetry – a non-invasive technology that is common practice under anaesthesia in operating theatres worldwide [4]. Dual-wavelength illumination of arterial blood results in an absorption contrast that depends upon the proportion of haemoglobin that is chemically combined with oxygen. Pulse oximeters differentiate between optical absorption by blood and other anatomical constituents by observation that pulsating arterial blood induces dynamics into the absorption characteristics of well-perfused peripheral sites [5]. The sensor is based on the fact that the colour of blood varies depending on the oxygen it contains. In particular the haemoglobin molecules reflect more red light when they are oxygenated than when reduced while its behaviour is the opposite when the light is infra-red. The oximeter shines two beams of light through a finger or earlobe or etc and those beams are finally received in the photodetector. By comparing the light intensity that is received for each wavelength, the oximeter is able to derive the light that is being absorbed by the blood and, consequently, the oxygen saturation. Moreover, the heart rate can be estimated from the slight change in the colour provoked by a beat of the heart pushing arterial blood into the finger [6].

Pulse oximetry utilizes the plethysmographic principle in combination with the optical absorption characteristics of haemoglobin [7]. Photoplethysmoraphy (PPG) is an electro-optic technique to measure the pulse wave of blood vessels. In pulse oximeter, which is the measuring apparatus for PPG, motion artefacts can limit the accuracy of the measured PPG signal during movement [8]. The typical pulse oximetry sensor contains two LEDs that emit red and infrared light into a pulsatile tissue bed. The scattered light is collected with a photodiode positioned on an opposite surface (forward scattering method) or an adjacent surface (reflection method). The “pulse” comes from the time-varying amount of arterial blood in the tissue during the cardiac cycle. Then the signals which are collected by the photodetector, crate a plethysmographic waveform due to the resulting cycling light attenuation. The relative modulation of the collected red and infrared light signals, referred to as the modulation ratio R, is used to estimate arterial oxygen saturation, SpO_2, based on an empirical calibration relationship expressed within the oximeter [9]. Figure 2 shows a model of a pulse oximetric assumption in which pulsatile signal change is due to arterial blood volume change. In the figure alternative current and direct current can be calculated by using two equations given below [7].

$$AC = Rd - Rs \quad \text{and} \quad DC = \frac{Rd + Rs}{2}.$$

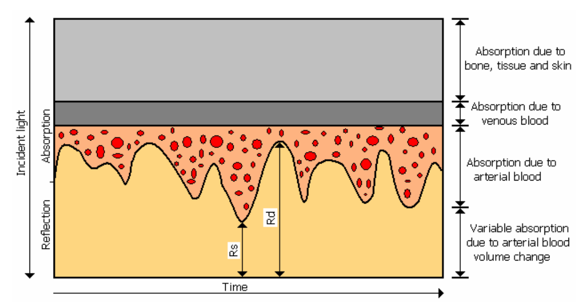

Figure 2. Conceptual tissue model for pulse oximetry.

2.2. Measurement device introduction

When designing our device, we aimed to an easily and diversifiedly adjustable prototype. To reach this goal, programmable electronics was used to get the system adjustable straight from the computer. In addition, separate transmitter and receiver units were used to make different kinds of measurement geometries possible. The instrumentation which is used to form the pulse oximeter is built by PC, LabView 8.2 –program, National Instrument Data Acquisition Card 6211, voltage supply and the sensor part which was built in our university.

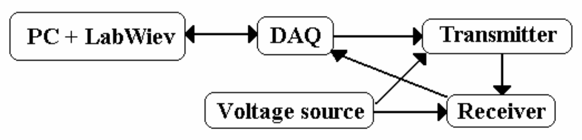

Figure 3. Instrumentation

In executing pulse oximetry, the controlling signals for the photo diodes are generated by the Data Acquisition Card. The photo diodes are time multiplexed by a frequency of 312.5 Hz by turns and when one is emitting light, it simultaneously transmits carrier wave whose frequency is 20 kHz. If the volume of blood in the measurement spot is changed, an amplitude modulation to the carrier wave is triggered and this modulation is demodulated by using coherent expression. The signal which reaches the receiver is high-pass filtered, rectified synchronously by using a demodulator.

The phase shift of the carrier waves at the photo diodes is 180°. After low-pass filtering the voltage at the red photo diode is negative and for the infrared light diode positive. Because of this, no multiplexing is needed because differentiating these two different signals is based on the fact that one is negative and the other one positive.

Now we have a curve which has minimum and maximum peaks which change their values by the change of the blood volume at the measurement spot. The peaks which are obtained at the frequency of 312.5 Hz are identified by using the LabWiev-program created for this task. Minimum and maximum peaks are collected both to their own curves and from these two curves the amplitude modulation, caused by the blood volume change, can easily be seen. After this the program finds AC and DC components of red and infrared lights and calculates the ratio R which is used to determine the actual oxygen saturation value.

The pulse oximeter execution principle is presented in figure 4.

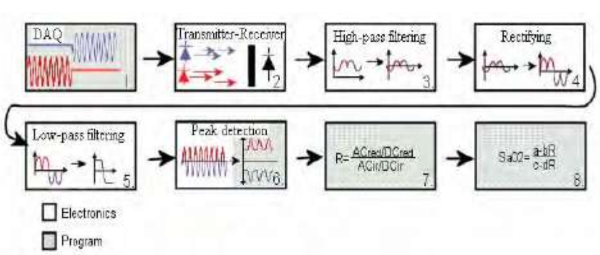

Figure 4. Pulse oximeter execution principle

In our measurements we concentrated on studying SNRs and signal amplitudes instead of finding out actual SpO_2-readings. That was done because of looking for an optimum spot that would provide strong noiseless signal from which actual SpO_2 reading could later be calculated in our sensor belt or wrist band development.

All measurements were done by using a special pulse oximeter device which was built in the University of Oulu. Device was built so that the adjusting angle, α, can be changed as big or as small as needed due to the location of the sensor on patient's skin. By using this adjustable probe, it was possible to obtain visible pulse oximeter signal from almost every spot on patient's skin by adjusting the angle and simultaneously checking the signal on computer screen. For each patient this angle in all measurement spots was a little bit different so it had to be specified separately every time.

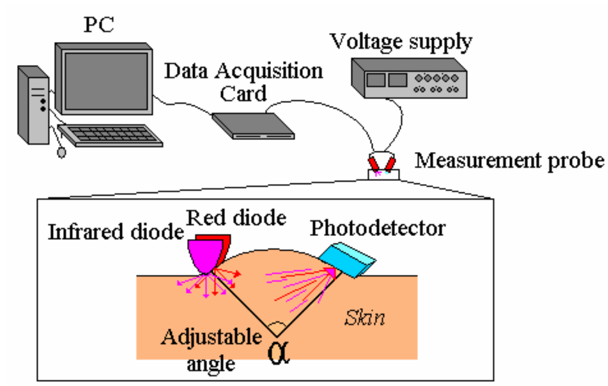

Figure 5. Measurement setup and principle from patient's skin by using a special device with an adjustable angle between light sources and a detector

3. Experiments

In the experimental part of the study we only concentrated on measuring spots around human chest and wrist in order to find the most optimal places for the integrated SpO_2 sensor. Before real measurements, some preliminary tests were accomplished in order to find the spots which would give the most clear saturation curves. Four spots from both wrist and chest were chosen (figures 6-9) and measurements from those areas were done. Measurement setup was built in a dark room to avoid external light interference. Also target vibration was tried to eliminate as well as possible. The age distribution of the measured patients was 23-29 and their body structures were normal. 20% of the patients were Asian and 80% were Finnish but skin colour did not seem to make any affect on the results. More problems occurred if the thickness of the fat tissue in the measurement spots was bigger than others and that is why the spots were chosen locating near bones so that the distance between the sensor and the bone was small enough to provide good returning signal for the photo detector if the probe without too many reflections and refractions.

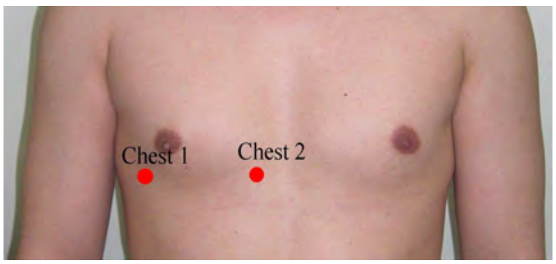

Figure 6. Measurement spots on the chest

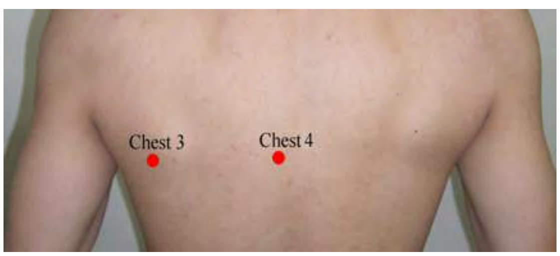

Figure 7. Measurement spots on the back

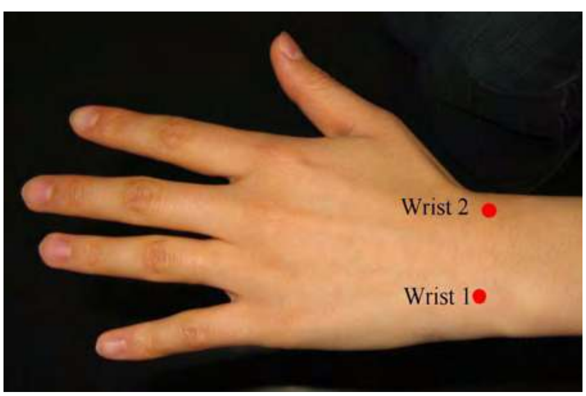

Figure 8. Measurement spots on the outer wrist

Figure 9. Measurement spots on the inner wrist

Figures 10 and 11 are demonstrating how normalized amplitudes and SNRs were resulted in the measurements. Measurements from the wrist area were easier to accomplish because unfortunately chest area is extremely sensitive for disturbances because of a constant movement caused by breathing. Still all 8 measurement areas were resulting close to each others and gave similar results. The basic rule was that big amplitudes were achieved by using wrist spots and higher SNR by using chest spots.

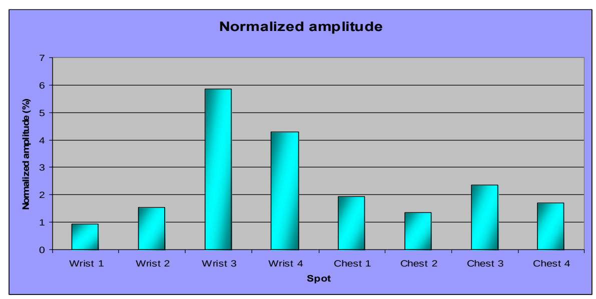

Figure 10. Normalized amplitude of the pulse oximeter signal in all eight measurement spots

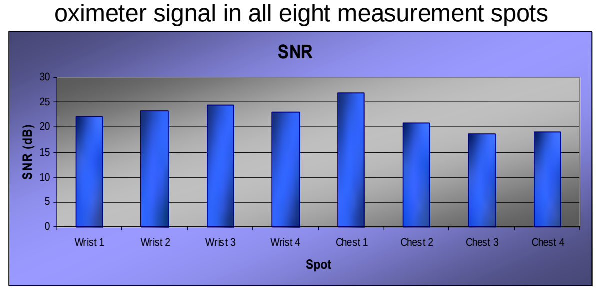

Figure 11. The signal-to-noise –ratio of the pulse oximeter signal in all eight measurement spots

The signal analysis showed that if the device is wanted to be integrated in a chest belt, the optimum place for integration would be chest 1 -spot. It provided SNR almost as great as 27dB, which tells that signal recorded from this spot is really clear. Promising SNR, 26dB, was also recorded from the wrist 3 –spot which offered also relatively big amplitude, 0.8V, and normalized amplitude, 5.9% of the total measured signal. In case of chest 1 –spot normalized amplitude was only 1.9% of the total.

4. Errors

Few of many possible facts that may have caused errors in the measurement results given above are perfusion problems, target movement and wrong target, detecting errors, optical interference and broken fibers. Perfusion problems are caused usually by a significant decrease in peripheral vascular pulsation, such as in hypothermia, vasoconstriction, hypotension, during cardiopulmonary bypass or cardiac arrest and they may result in a plethysmographic signal which is insufficient to be processed reliably by the oximeter [3]. Patient movement reduces the reliability of a pulse oximeter severely. Even small patient movements, such as shivering, can cause powerful artifacts that swamp the pulsatile absorption signal [10]. Also any dislocation of the nail bed for example can affect the transmission of light through the digit in case the measurement is done through a finger. Dark nail polish and bruising under the nail can also severely limit the transmission of light and result in an artificially decreased SpO_2-value [11]. Detecting errors happen because pulse oximeters are unable to differentiate between oxygen and carbon monoxide bound to haemoglobin. Readings in the presence of carbon monoxide will be falsely elevated. Pulse oximetry should never be used in suspected cases of carbon monoxide exposure and an arterial blood gas reading would also be good to obtain. In addition they should never been used in a cardiac arrest situation because of the extreme limitations of blood flow [11]. Bright external light sources are known to affect pulse oximeters and all pulse oximeters share this sensitivity. This occurs because these instruments use optical means to make their measurements. Consequently, to obtain accurate measurements, potential sources of optical interference must be controlled. Because pulse oximeters' optical components are located in the probe, proper probe application and use are key factors in reducing optical interference. Optical interference occurs when bright light from an external source reaches the photodiode or when light reaches the photodiode without passing through a pulsatile arteriolar bed [3]. In case of intra-vascular fibre optic oximetry sensors, optical fibres which are used to guide the light into the target may suffer several damages before reaching the target. This may cause severe measurement errors [7].

5. Discussion

This study concentrated on finding out the most suitable spot for the integrated pulse oximetry sensor which would make measurements not only when the patient is lying down but also while he or she is moving. That forces us to take into account the principal factor which limits both the practical accuracy and general applicability of pulse oxymetry – poor photoplethysmographic signal [12]. It is caused usually by low perfusion states or artifact corruptions arising from ambient light or subject movement [13], which lead usually to interpretation errors and false alarms [14].

These days especially motion artifacts are tried to minimize because many applications are wanted to design for moving patients. Also measurements which were done in this study were affected by these artefacts for example by moving chest or shivering wrist. In case the interface between the measurement probe and the skin was moving, the signal immediately showed the movement by temporarily fading or peaks. That is why all measurements from all spots had to be taken many times from each patient so that reliable results could be recorded. Also the person executing the measurements was affecting the results by giving some small vibrations to the probe.

Before the sensor can be reliably integrated to a chestbelt or wrist device, more experiments with moving patients should be done in order to see how movement in these spots affects the signal and can results be trusted. Also many signal processing steps still have to be completed in order to eliminate motion artifacts Many problems still have to be overcome but this study proves that wireless integrated pulse oximeter implanted in a chest belt or wrist band is possible to achieve with many benefits and practical applications.

6. References

[1] A. Jubran, "Advances in respiratory monitoring during mechanical ventilation", *Chest*, vol. 116,1999, pp 1416-1425.

[2] S.L. Schutz, "Oxygen Saturation Monitoring by Pulse Oximetry", *AACN Procedure manual for Critical Care*, Fourth Edition, W.B.Saunders.

[3] J. G. Webster, "Design of Pulse Oximeters", *Taylor & Francis Group*, LLC, 1997.

[4] I.Yoshiya, Y. Shimada and K. Tanaka, "Spectrophotometric monitoring of arterial oxygen saturation in the finger tip", *Med. Biol. Eng. Comput.*, vol. 18, no. 1, 1980, pp 27-32.

[5] A. B. Herzman, "Photoelectronic plethysmoraphy of the fingers and toes in man", *Proc. Soc. Exp. Biol. Med.*, vol. 37, 1937, pp 529.

[6] M. J. Moron, E. Casilari, R. Luque and J. A. Gazguez, "A Wireless Monitoring System for Pulse-oximetry Sensors", *IEEE Proceedings of the 2005 Systems Communications* (ICW´05), 2005.

[7] S. Takatani, and J. Ling, "Optical Oximetry Sensors for Whole Blood and Tissue", *IEEE Engineering in medicine and biology*, no. 6, 1994, pp 347-357.

[8] B. S. Kim and S. K. Yoo, "Motion Artifact Reduction in Photoplethysmography Using Independent Component Analysis", *IEEE Trans Biomed Eng*, vol. 53, no.3, 2006, pp 566-568.

[9] M. Yelderman and J. Corenman, "Real time oximetry in Computing in Anesthesia and Intensive Care", O. Prakash, Ed. Boston, MA: Martinus Nijhoff, 1983.

[10] M. J. Hayes and P. R. Smith, "A New Method for Pulse Oximetry Possessing Inherent Insensivity to Artifact", *IEEE Transactions on biomedical engineering*, vol. 48, no. 4, 2001 pp 452-461.

[11] S. L. Schutz, "Oxygen Saturation Monitoring by Pulse Oximetry", *AACN Procedure manual for Critical Care*, Fourth Edition, W.B.Saunders, 2001.

[12] M.J. Hayes, P.R. Smith, D.M. Barnett, M.D.L. Morgan, S. Singh and D.D. Vara, "Quantitative investigation of artefact in photoplethysmography and pulse oximetry for respiratory exercise testing", *Frontiers Computer-Aided Visual.* Vascular Functions, vol. 263, 1997, pp 117-124.

[13] N.S. Trivedi, A.F. Ghouri, N.K. Shah, E. Lai and S.J. Barker, "Effects of motion, ambient light, and hypoperfusion on pulse oximeter function", *J. Clin. Anesth.*, vol. 9, no. 3, 1997, pp 179-183.

[14] L. Wiklund, B. Hok, K. Stahl and A.Jordeby-Jonsson, " Postanaesthesia monitoring revisited: Frequency of true and false alarms for different monitoring devices", *J. Clin. Anesth.*, vol. 6, no. 6, 1994, pp 182-188.

APPENDIX P

REFLECTANCE-BASED PULSE OXIMETER FOR THE CHEST AND WRIST

A Major Qualifying Project Report:

Submitted to the Faculty

Of the

WORCESTER POLYTECHNIC INSTITUTE

In partial fulfillment of the requirements for the

Degree of Bachelor of Science

By

Alexandra Fontaine

Arben Koshi

Danielle Morabito

Nicolas Rodriguez

Submitted on:

Approved by:

Professor Yitzhak Mendelson, Advisor, Dept. of Biomedical Engineering

Authorship

Section	Author
Introduction	Nicolas Rodriguez, Danielle Morabito, Alex Fontaine, Arben Koshi
Literature Review	Nicolas Rodriguez, Danielle Morabito, Alex Fontaine, Arben Koshi
Design Approach	Alex Fontaine, Danielle Morabito
Device Development	Nicolas Rodriguez, Danielle Morabito
Methods	Nicolas Rodriguez, Danielle Morabito
Final Design	Arben Koshi, Nicolas Rodriguez, Danielle Morabito
Results	Alex Fontaine, Arben Koshi
Discussion	Arben Koshi, Alex Fontaine
Summary	Arben Koshi
Conclusion	Arben Koshi
Future Improvements	Arben Koshi, Nicolas Rodriguez
Appendix A	Danielle Morabito
Appendix B	Arben Koshi
Appendix C	Alex Fontaine
Appendix D	Arben Koshi

Abstract

Reflectance-based pulse oximetry is a technique used for noninvasively monitoring the oxygen saturation (SpO_2) and pulse rate (PR). However, there is little supporting evidence that it can accurately collect measurements from the chest and wrist. In this project, a reflectance-based pulse oximeter was built and used to collect measurements while sitting, standing, during self-induced hypoxia, and during self-induced hyperventilation then compared to the measurements taken by a HOMEDIC Deluxe Pulse Oximeter. The prototype was able to accurately measure within an error of $\pm$ 1% and ±3% for SpO_2 and PR respectively from the wrist while an error of ±1% and $\pm$4% for SpO_2 and PR respectively from the chest.

Acknowledgements

We would like to thank Professor Mendelson for advising this project. We would also like to acknowledge Dr. Adriana Hera and Lisa Wall for their support.

Executive Summary

Oxygen saturation (SpO_2) is the measurement of oxyhemoglobin (HbO_2) in arterial blood. SpO_2 is an important vital measurement because it shows the levels of blood oxygenation. Traditionally, SpO_2 is measured by invasively drawing blood samples. This method, however, is not ideal and it is unable to provide clinicians with real-time measurements. With the need for a noninvasive way to measure SpO_2, pulse oximetry was developed. The use of this technology allows clinicians to determine SpO_2 in patients that are sedated, anesthetized, unconscious, or unable to regulate their own oxygen supply.

Reflectance-based pulse oximetry allows measurements to be taken from areas of the body in which transmittance based pulse oximetry cannot be applied. In reflectance-based pulse oximetry, the incident light is passed through the skin and is reflected off the subcutaneous tissue and bone. To this day, being able to measure signals from the chest and wrist with one single device has not been successfully achieved. Such a device would allow patients to measure SpO_2 and pulse rate (PR) without hindering their normal day-to-day activities.

The prototype pulse oximeter constructed during this project consists of two hardware components and a programmed LabVIEW Virtual Instrument (VI). The hardware components consist of the sensor and a circuit which produces, collects, and processes photoplethysmographic (PPG) signals. The VI collects the PPG signals produced by the hardware and process them in order to produce numerical results for PR and SpO_2 . The optical sensor is made up of two Light Emitting Diodes (LEDs), a red LED, with a peak emission wavelength of 660 nm, and an infrared emitter with a peak emission wavelength of 940 nm. These LEDs are positioned next to each other in the center of a circular Printed Circuit Board (PCB) and surrounded by 8 photodiodes (PD). The circuitry for the sensor consists of an Arduino Duo Microprocessor which is programmed to light up the red and infrared LEDs intermittently at a frequency of 100Hz. The PDs are connected in photovoltaic mode in order to produce a voltage output. Operational amplifiers are utilized to amplify the photodiode output. Once amplified, the red and infrared PPG signals obtained from the photodetectors are sent through two Sample-and-Hold circuits to separate the signals into their respective alternating current (AC) and direct current (DC) components for further filtering and amplification.

The four input signals sent to the LabVIEW software : AC red, AC infrared, DC red and DC infrared access the VI via a National Instruments (NI) Data Acquisition (DAQ) system. The AC components of the red and infrared PPGs are measured using a peak-to-peak detection algorithm, while the DC components are measured by finding their respective averages. Once the signals are processed, SpO_2 is calculated by obtaining the ratio of the AC and DC components of the red PPG and dividing that by the ratio of the AC and DC components of the infrared PPG. To calculate PR, the frequency of the infrared AC signal is measured using frequency measurement parameters in LabVIEW and then multiplied by 60 to display PR in beats per minute (bpm). To compare the measurants taken from the pulse oximeter prototype, a transmission-type finger HOMEDICS Deluxe Pulse Oximeter was utilized as reference. The reliability of the Deluxe Pulse Oximeter was tested against a Biopac ECG model 100C module and was concluded that the HOMEDICS Deluxe Pulse Oximeter was provided accurate enough measurements for pulse rate.

For testing, the sensor was strapped to the wrist and chest of each subject using a Velcro strap while the HOMEDICS Deluxe Pulse Oximeter was placed on the subject's index finger. The VI was set up to collect, average and display SpO_2 and PR data every 10 seconds throughout a 6 minute timespan accounting for 36 measurements. At this point, a second individual that was monitoring the reference device recorded the corresponding SpO_2 and PR values displayed by the HOMEDICS pulse oximeter. Subjects were tested on the chest and wrist while sitting, standing, during self-induced hyperventilation, and during self-induced hypoxia.

While collecting data, it was noticed that the PR measurements collected from the chest had significantly larger margins of error compared to those from the wrist. One possible explanation for this discrepancy deals with the LabVIEW algorithm for PR calculation. Instead of doing peak-peak analysis, we opted to use a search tool which graphs a power spectrum of the data and searches for the highest amplitude frequency between 0.75Hz and 2.25Hz. This method is very effective at PR values ranging between 45 and 135 bpm, but loses its accuracy at higher PR values. Measurements above 135 bpm were detected by the reference, but not accurately detected by the prototype.

Margins of error obtained from the standing and sitting measurement tests on the wrist included 0.6%, and 0.2% for SpO_2 and 0.2%, 1.1% for PR respectively. Measurements from the chest displayed errors of 0.4% and 0.3% for SpO_2 and 0.1%, and 0.7% for PR while standing and sitting respectively. Based on this data, our prototype for a reflectance-based pulse oximeter for the chest and wrist was successful in measuring PR and SpO_2.

Table of Contents

Table of Figures

Table of Tables

Abbreviations

O_2: Oxygen
Hb: Hemoglobin
HbO_2: Oxyhemoglobin
SpO_2: Oxygen saturation
SaO_2: Oxygen saturation measured invasively
PR: Pulse rate
COHb: Carboxyhemoglobin
MetHb: Methyl hemoglobin
PPG: Photoplethysmogram
VI: Virtual Instrument

1 Introduction

One of the most important elements needed to sustain life is oxygen (O_2) because it is used by cells to turn sugars into useable energy. Oxyhemoglobin (HbO_2) is the protein hemoglobin, found in red blood cells, bounded to O_2 that delivers 98% of oxygen to cells. The measurement and calculation of the percentage of HbO_2 in arterial blood is known as oxygen saturation (SpO_2). [1]

Originally, SpO_2 was measured by taking samples of blood and measuring O_2 levels directly. This method was invasive and was unable to provide real-time measurements. This measuring technique made it impossible for SpO_2 to be recognized as an important measure of wellness until a non-invasive method of measuring SpO_2 in real-time was established. [2]

The need for a non-invasive method of measuring SpO_2 in real-time led to the development of pulse oximetry. Pulse oximetry derives SpO_2 and pulse rate (PR) from a photoplethysmogram (PPG). The PPG is obtained by measuring changes in light absorbed by the blood. Red and infrared wavelengths are used to obtain the PPG because these wavelengths are easily transmitted through tissues, allowing SpO_2 to be calculated from the ratio of the absorption of the red and infrared light.

The first device used to continuously measure blood oxygen saturation of human blood in vivo (SaO_2) was built by Karl Matthes in 1935. [2] However, it was not until 1983 that William New and Mark Yelderman, after recognizing the need of an accurate oximeter in the operating room evaluated and produced the pulse oximeter with aims to make it an intraoperative monitoring device. [2] Pulse oximetry allows for an accurate determination of O_2 levels in patients that are sedated, anesthetized, unconscious, and unable to regulate their own oxygen supply as well as provides information needed to avoid irreversible tissue damage. [2]

Since the invention of pulse oximetry, the measurement of SpO_2 has become an important part of the medical world. Nevertheless, improvements such as the application of the reflectance-based technique to measure SpO_2 from multiple locations on the body are still to be developed. This project demonstrates the use of reflectance-based pulse oximetry to obtain measurements for PR and SpO_2 from the chest and wrist. This development in pulse oximetry technology will pave the way for the development of new and novel pulse oximeters that can be worn as accessories, are easily concealed under clothing, and more acclimated to use outside of hospital settings.

2 Literature Review

This is a thorough literature review covering the necessary background needed to fully understand this project.

2.1 Oxygen Saturation

SpO_2 is the amount of O_2 that is carried in the blood. In the human body, SpO_2 is defined as the ratio of HbO_2 to the total concentration of Hb (reduced Hb + HbO_2) present in the blood [1].

$$Oxyhemoglobin\ Saturation\ (\%) = \frac{[HbO_2]}{[Hb]+[HbO_2]} * 100 \quad (1)$$

Hb is the iron-containing protein in red blood cells that transports O_2 to the tissues. This protein forms an unstable and reversible bond with O_2. Thus, Hb in its oxygenated state is called HbO_2 and exhibits a bright red color. Conversely, in its reduced state, it exhibits a purplish blue color [3]. Hb can carry up to four O_2 molecules.

In calculating the absorption of light at a specific wavelength by a homogeneous substance, the Beer-Lambert law can be used to show the basic relationship between the transmitted light intensity and the incident light:

$$I_t = I_o * 10^{-\varepsilon c d} \quad (2)$$

where 'I_t' is the intensity of transmitted light, 'I_o' is incident light intensity, 'ε' is the extinction coefficient (fraction of light absorbed at a specific wavelength), 'c' is the concentration of the sample, and 'd' is the length of the light path through the sample. However, this is difficult to use in pulse oximetry because the light scattering through the tissue cannot be distinguished from that of blood [1].

Two independent equations can be derived to describe the absorption of light by both Hb and HbO_2 at two distinct wavelengths. These equations can then be solved to find the concentration of Hb and HbO_2 in blood and establish the relationship,

$$SO_2 = A - B\frac{OD(\lambda_1)}{OD(\lambda_2)} \quad (3)$$

where A and B are functions of the extinction coefficients of Hb and HbO_2 while 'OD' is the optical density or the $\log(I_o/I_t)$. The relationship above is the underlying principle used by commercial pulse oximeters to measure SpO_2. [1]

2.2 Pulse Oximetry

Pulse oximetry was initially intended for monitoring hospitalized patients after surgery. However, after recognizing the importance of an accurate oximetry device during surgery in operating rooms, non-invasive pulse oximetry became a standard for anesthesiologists for intraoperative monitoring since 1990. By the use of this technique, physicians can determine the SpO_2 in patients that are sedated, anesthetized, unconscious, and unable to regulate their own oxygen supply avoiding irreversible tissue damage [2].

It is not until 1935 that Karl Matthes used red and infrared wavelengths to build a device that continuously measured SaO_2 in vivo. Matthes stated that "the red light can pass through HbO_2, but reduced Hb absorbs it" [2]. Non-invasive oximetry evolved even further when Robert Brinkman and William Ziilstra began measuring SpO_2 from the forehead with the use of reflected light. Brinkman and Zijlstra made an additional modification when they divided the red signal by the infrared signal to show continuous measurements of SpO_2 [2,4]. However, differentiating various types of Hb was still a problem. This is when Robert Shaw invented an absolute reading ear oximeter in 1964. This device used eight different wavelengths to identify the separate Hb species present in the blood. Although expensive, this instrument was accurate down to 70% of SpO_2 and it was commercialized for use in physiology laboratories for pulmonary and cardiac applications. [2] In 1970, research performed by Takuo Aoyagi and his associates on dye-dylution techniques for measuring cardiac output led to the development of photoplethysmogram (PPG) ,which optically generates time dependent volumetric changes in living tissues leading to the development of pulse oximeter [1, 2]. Here, the time dependent changes are associated with arterial blood allowing for the measurement of SpO_2. Figure 2.1 shows the amount of light absorbed by tissue over time.

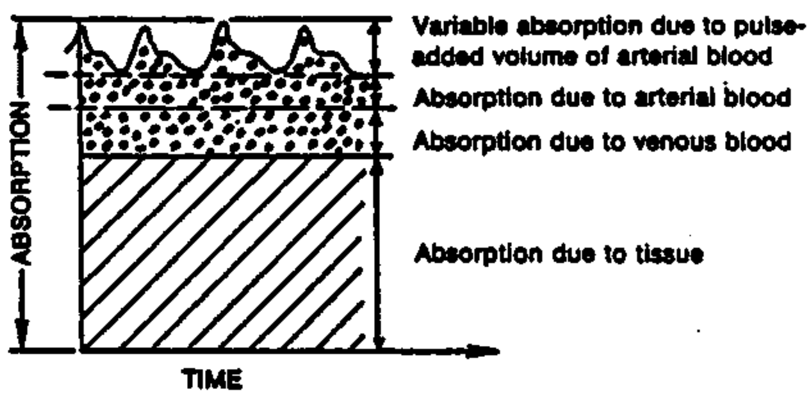

Figure 2.1: Arterial blood changing over time, PPG [11]

Aoyagi and his associates researched this technique even further and applied it to the already existent ear-piece oximeter [2]. Next, in 1977 Minolta Camera developed an oximeter using the same method with a fingertip probe and fiberoptic cables from the instrument. Finally, New and Yederman produced the Nellcor Pulse Oximeter in 1983 for patients admitted in clinic and hospitals sites [2]. Improvements on the idea of pulse oximetry led to its reliability to the extent that in 1990 the American Society of Anesthesiologists recognized the pulse oximeter as their standard for intraoperative monitoring [2].

2.2.1 Principle of a Pulse Oximeter

A noninvasive pulse oximeter relies on an optical sensor to detect SpO_2 and PR. This optical sensor is made up of a red and an infrared LED as well as silicone photodiodes (PD) [5]. In order to obtain SpO_2, the red wavelength must range within a region where the absorption of Hb and HbO_2 are markedly different. This is why a red light with a wavelength close to 660nm is chosen as shown in Figure 2. On the other hand, the region for the infrared light must revolve around a wavelength where the absorption coefficients of Hb and HbO_2 are practically the same. This happens between 940nm and 960nm as also shown in Figure 2.2 [1].

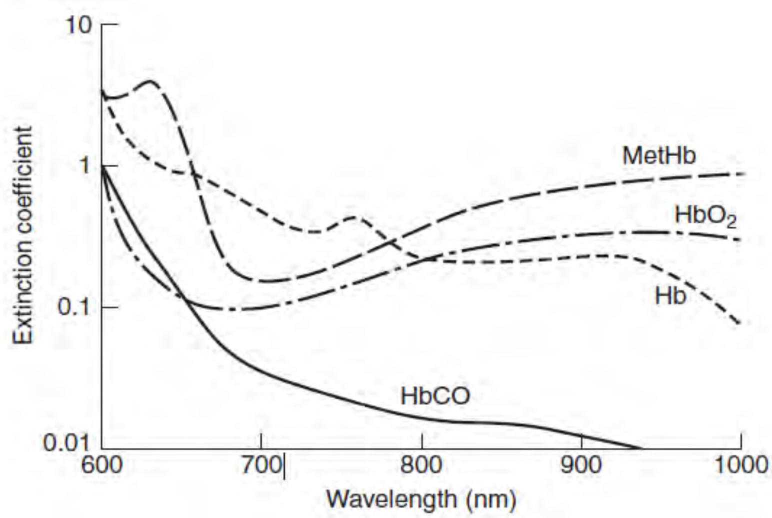

Figure 2.2: Optical absorption spectra of Hb, HbO_2, MetHb, and BbCO [11]

The sensor containing the red and infrared LED is applied over the radial artery on the wrist so arterial pulsation can be readily sensed. The PDs concentrically located around the LEDs will absorb the emission spectra of the red and infrared wavelengths when bounced back from the skin [5]. However, there are certain variables that could cause a barrier to the photodiodes from detecting light intensity. These include: the opacity of the skin, reflection of light by the bones, light scattered away through the tissues and the amount of blood in the vascular bed [5]. Furthermore, when blood flows into the vascular bed onto which the sensor is applied, the light emitted by the diodes will have a greater rate of absorption by the blood. The light absorbed when the tissue is either full or lacking blood with every heart beat will create an alternating light intensity signal. This difference in light intensity created by every heart beat accounts to approximately 0.05-1 percent of the whole light intensity that is either transmitted into the skin or backscattered into the photodetectors [5].

A pulse oximeter consists of a circuit that features a microprocessor used to light up the red and infrared LEDs one at a time in a synchronous manner, so that when the red light is turned on the infrared LED is turned off and vice versa [1]. With the use of sample-and-hold circuits, the overlapped signal acquired by the photodetector can be split into two different analog channels that correspond to the red and infrared PPGs [1]. The red and infrared PPG signals can be further amplified through the implementation of high and a low pass filters so that the AC and DC components for each PPG signal can be obtained [1]. The new four signals can be processed through a virtual instrument (VI) designed in a software program or a virtual instrument that calculates the ratio of AC red and DC red components and divides it by the ratio of AC infrared and DC infrared to produce SPO_2.

2.2.2 Methods of Light Detection

As previously discussed, pulse oximetry relies on the PPG signals produced by the difference in the amount of arterial blood, which in turn depends on the systolic and diastolic movements of the heart. Measurement of light by the photodetectors can be performed either in transmission or reflection modes. When the PPG is measured through transmission, the light source and the photodetectors are placed on opposite sides of the vascular bed so that the light travels across the pulsating blood. Thus, this method is limited to earlobes, feet, and fingertips. On the other side, reflectance pulse oximetry measures PPG signals with LEDs and photodetectors placed on the same side of the sensor surface. This method allows measurements to be taken from body parts where the transmission method cannot be used, for example on the chest, wrist, and forehead. [6]

2.2.2.1 Distance Between LED and Photodiode

In 1988, the effects of separation between the source and detector were studied [5]. Although it is understood that the farther away the photodiode and LED are from each other that the readings will degrade, it was demonstrated that larger PPGs can be detected by mounting the photodiode further from the LED. However, the tradeoff is that higher LED driving currents are required in order to overcome the absorption of incident light due to a longer optical path length. Mendelson also shows that by mounting more than one photodiode, a greater fraction of backscattered light can be collected and larger PPGs can be recorded. [5]

Furthermore, in 2010, there was a similar conclusion regarding the gap sizes between the LEDs and the photodiodes [7]. It was found that the amount of light backscattered from the skin on the optical module and that was absorbed by the PDs was directly proportional to the number of PDs surrounding the LEDs. Thus, the more PDs, the more light would be absorbed.[8] This research showed that 7mm was the optimal distance between the LED and PD and produced the highest AC signal. Similar to Mendelson's research above, a higher current output obtained from a larger number of PDs was required in order to obtain a stronger AC components.

2.2.3 Photoplethysmogram

PPG is an optical measurement used to represent the volume of blood in vessels used to compute SpO_2 and PR based on the light absorbance of blood. During the cardiac cycle, the amount of blood in tissue varies in relation to each heartbeat, so a PPG signal is an optical representation of the cardiac cycle wave. This results in a distinguishable AC component. The PPG is usually taken at peripheral sites such as the finger, ear, or forehead. Since skin is perfused by blood, conventional pulse oximeters monitor the perfusion of blood in the dermis and subcutaneous tissue of the skin. The AC component of the oximeter signal is attributed to variation in blood volume and the DC component of the oximeter signal is generally attributed to skin tissue absorption. [9;10;11]

2.2.4 Wavelength Optimization

Although wavelengths at which the SpO_2 are typically measured are 660nm for red and 910 nm or 940 nm for infrared, it is possible to measure SpO_2 at different wavelengths and also with more than 2 wavelengths. In fact, the Hewlett-Packard model 47201 Ear Oximeter which debuted in the 1960s utilized 8 wavelengths. The advantage to using more than two wavelengths is that it makes it possible to measure saturation of more than just oxygen in the hemoglobin chains. However, for the purposes of measuring only SpO_2, two wavelengths are sufficient.

Nogawa, in 1998, also showed that by changing the two selected wavelengths from 665/910 nm to 730/880nm, a linear relationship could be established for oxygen saturation rates over the 100-30% range. In the 70-30% range, the improvement was significant with a standard error of 2.69% as compared to 9.49% for a sensor utilizing 665/910nm wavelengths. Results also showed that in the 100-70% range, the 730/880 nm sensor showed a slight improvement in the standard error, lowering it from 3.50 to 2.11%. [12]

2.2.5 Limitations and Applications of Pulse Oximetry

There are certain situations in which data processed by a pulse oximeter can be misinterpreted or difficult to acquire. Significant reduction in peripheral vascular pulsation due to hypotension, vasoconstriction or hypothermia can cause a small signal to be processed unreliably by a pulse oximetry [1]. Also, due to the small signal that is analyzed, only 1 to 2% of the PPG signal can be processed, motion artifacts can interfere with a proper PR signal reading if the patient is shivering or having a seizure. Increase in venous pulsations may also interfere with pulse oximetry resulting in artificially low SpO_2 readings [13]. Furthermore, large amounts of dysfunctional Hb, which is Hb derivatives that do not bind reversibly with O_2 like HbCO and MetHb, can lead to an incorrect oxygen saturation interpretation by the pulse oximeter

[1]. Compromised blood circulation, excessive contact pressure or weak PPG signals resulting from insufficient contact pressures may also yield to measurement errors [14]. Finally, one of the greatest limitations of transmittance pulse oximetry is movement of the patient. By being attached to the finger and the fact that extraneous movements can cause a change in absorbance of light by arterial blood flow, a conventional pulse oximeter hinders the user to perform regular daily activities [14;15].

2.3 Reflectance vs. Transmittance Pulse Oximetry

With recent achievements in pulse oximetry, the devices are generally characterized as transmission based and reflectance based. In transmission based pulse oximetry, LED and a photodiode are placed on opposite sides of a substrate, which in turn can be attached across the fingertip, earlobe, and foot.

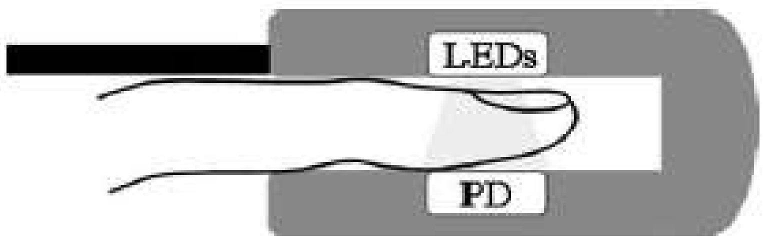

Figure 2.3: Transmittance pulse oximetry

In reflectance-based oximeters, the LED are placed together on the same probe surface. This method is mainly intended to be used on body locations where pulse oximetry through transmission is not feasible.

Figure 2.4: Reflectance pulse oximetry

Forehead reflection pulse oximetry is one example and is generally more accurate than transmission type pulse oximeters on patients with a low cardiac index or poor peripheral perfusion.[1]

Figure 2.5: Forehead pulse oximeter

2.4 New Studies for Pulse Oximeters

One such wrist based prototype relying on reflectance based oximetry is the AMON [19]. This prototype endeavored to measure blood oxygen saturation, pulse, blood pressure, skin temperature and ECG data using a single ECG lead. However, after conducting a study on 33 healthy volunteers, and comparing the data gathered by AMON to that of two commercially available pulse oximeters, the results weren't promising and not every type of measurement was able to be used. Results showed that blood pressure data and pulse measurements from SpO_2 were satisfactory and as expected, however SpO_2 measurements were far from expected due to significant deviation. As for ECG, although PR results could be obtained, there was no conformity in the QRS and QT complexes of the ECG as results, as well as high levels of measurement noise which degraded the results. The lack of conformity and noise made it difficult to distinguish the ECG as a waveform. The temperature sensor on the other hand was unsuccessful since the study showed no reliable correlation between the reading at the wrist and the core body temperature. [19]

A second wrist based pulse oximeter that showed potential is a prototype by Coker et al. in which the results were far more promising. For pulse measurements, Coker's prototype had an accuracy error of less than 2% as compared to two different commercial pulse oximeters while the averaged SpO_2 measurements had an accuracy error of less than 1%. However, it is noted that while the prototype provided accuracy competitive to that of commercial pulse oximeters, motion artifacts cause signal integrity issues and needs to be addressed. Some possible methods of addressing motion artifacts are through the use of a motion sensor to account for user movement or much more refined signal processing using filters to minimize noise and find the highest signal to noise ratio. [16]

Lastly, a sensor consisting of a multiple photodiode array was arranged concentrically around 4 LED's was tested on the forearm and calf [20]. This sensor however also utilizes a heating unit. Previous research has shown that heating the skin under the sensor increases the magnitude of the detected pulsatile component four- to five-fold. The purpose of this study however was to measure the effectiveness of the sensor under controlled hypoxia. Ten volunteers were studied and the inspired fraction of oxygen in the breathing gas mixture was gradually lowered from 100 to 12%. Measurements were simultaneously taken from the forearm and calf then compared to SpO_2 measurements obtained by a finger sensor. Though the experiment was done while the volunteers were standing still and the results are not as ideal as the forehead reflectance oximeters [20].

3 Design Approach

Applying pulse oximetry technology to the chest and the wrist can provide the opportunity to create new noninvasive devices that will be less restrictive to a wears' movements and more comfortable. The combination of a different placement and design could further the monitoring of vital signs in settings other than hospitals.

3.1 Initial Client Statement

Develop a wearable, noninvasive reflectance-based pulse oximeter prototype that demonstrates accurate and precise measurements of arterial oxygen saturation and heart rate from the chest and/or wrist on healthy volunteers.

3.2 Clinical Need

Reflectance-based pulse oximetry allows measurements to be taken from areas of the body in which transmittance-based pulse oximetry cannot be used. Using reflectance-based pulse oximetry, the wavelengths are passed through the skin and reflect off the bone and tissue in the area of the measurement. Being able to receive signals from the chest and wrist has not yet been successfully achieved using reflectance-based pulse oximetry. It is difficult to receive signals from the chest and wrist because the light needed to create the signal must be reflected back which makes the signal weaker and more difficult to detect. Creating a method to obtain a PPG signal strong enough to process for SpO_2 and PR from the chest and wrist is the central dilemma behind this project. Achieving this could further the development of new devices that could be worn during daily activities and as a method of protecting servicemen in the field.

3.3 Design Parameters

In this section are outlined the various aspects of project designed to address the clinical need behind a reflectance-based pulse oximeter for the chest and wrist. These design parameters cover both the qualitative and quantitative pieces of the final design.

3.3.1 Objectives

The objectives consisted of three categories: 'Easy to use', 'Marketable', and 'Safe'. 'Easy to use' addresses the user friendly nature needed for the device to be useable by the large audience that is to be targeted. To be easy to use the device must be easy to wear, operate, or read. 'Marketable' addresses the need for the device to be successful and competitive on the market. This means that the device must be cost-efficient, manufacturable, portable, durable, and comfortable. 'Safe' addresses that device must be safe for the users. Thus the device must be secured against the user to avoid false measurements, be composed of biocompatible materials as not to cause the user adverse reactions, and conduct reliable readings.

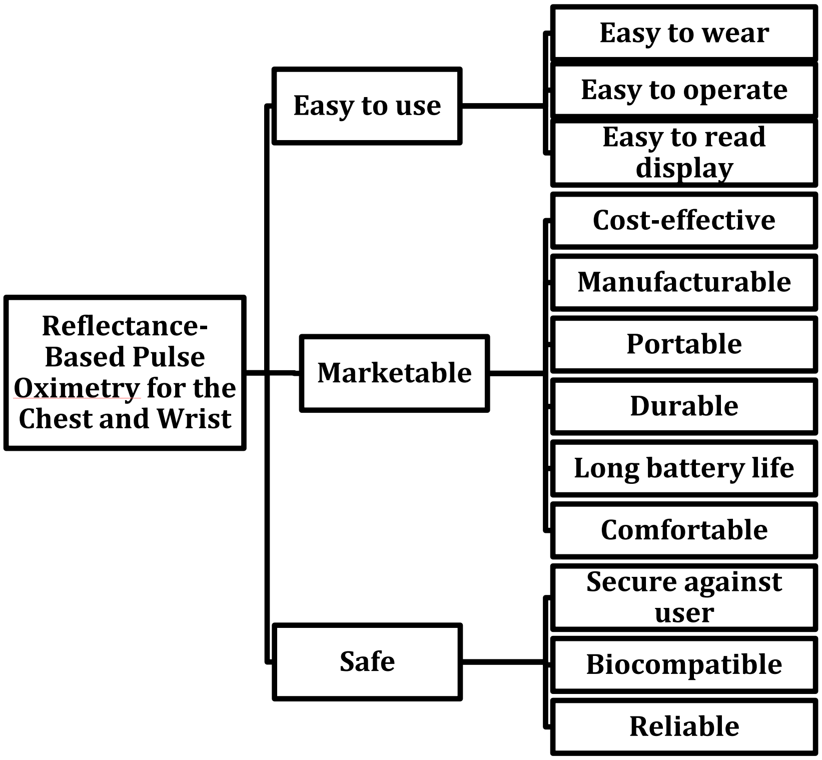

Figure 3.1: Objective tree

3.3.2 Constraints

Throughout the duration of our project, there were many constraints that the device must overcome. First, the device must not restrict the wearer from following their daily activities. There are many sizes the device could potentially be, however in order to keep the device from impacting a patients daily activities, the device must be kept to a small, concealable size. Second, the device must stay in constant contact with the skin. In order for the device to provide accurate results, it must not separate from the wearer at any time. The last constraint that the device must overcome is the regulatory requirements. The FDA has compiled a set of regulations, which include patient safety, performance requirements, and electrical, mechanical and environmental safety. In order for the device to be considered a success it must successfully overcome all of these constraints.

3.3.3 Functions

In this section is discussed the attributes that allow the prototype designed during this project to function properly.

3.3.3.1 Obtain Photoplethysmogram Signal

As dictated in the client statement, reflectance-based pulse oximetry was used to obtain the PPG signal necessary for computing SpO_2 and PR. The theory and method of reflectance-based pulse oximetry will be used to do this from the chest and wrist.

3.3.3.2 Measure Heart Rate

In the AC component from the obtained PPG signal, the pulsatile pattern on the top of the PPG signal reflects the changing blood volume at the site of measurement with each cardiac beat. The signals are passed through a bandpass filter with a cut-off of about 1.5 Hz, to separate the AC pulses from the DC signals. The LabVIEW VI developed to process the PPG signal is then used to average the maximum frequency to determine the rate of the cardiac beat in hertz. This value was then multiplied by 60 to find the PR in beats per minute.

3.3.3.3 Measure Oxygen Saturation

SpO_2 is defined as the ratio of HbO_2 to the total concentration of Hb present in the blood [1]. After the LabVIEW VI processes the PPG signal, it calculates the ratio of red to infrared light used in the calculation for SpO_2.

3.3.4 Design Specifications

The specifications for this prototype were determined from the market standards by selecting several commercially available pulse oximeters specifications and examining them. One such device was the Respironics' WristOx™ Ambulatory Finger Pulse Oximeter which entered the market in October of 2003. Its specifications can be found in Table 3.1. [21]

Table 3.1: Respironic's WristOx Ambulatory Finger Pulse Oximeter Specifications [21]

Effective Measuring Range	
Saturation	0% to 100%
Pulse Rate	18 to 300 bpm
Resolution	1 digit
Accuracy	
Saturation	70 to 100% ± 2 digits
Pulse rate	±3%
Display	
Numerical	3-digit indicators
Pulse indicator	Pulse Strength Bar Graph
Power requirement	Two 1.5V alkaline N-cell batteries
Battery life	Minimum 24 hours continuous
Storage	9 months
Size	

Weight	~0.88 ounces (24.95g)
Dimensions (w/o sensor or strap)	1.75” wide x 2” high x 0.75” deep 4.45cm x 5.08cm x 1.905cm

Another device which is on the market and FDA approved is the Santa Medical’s Finger Pulse Oximeter. Its specifications can be found in Table 3.2. [7]

Table 3.2: Santa Medical's Finger Pulse Oximeter Specifications[7]

Effective Measuring Range	
Saturation	0% to 100%
Pulse Rate	18 to 254 bpm
Resolution	±1 digit
Accuracy	
Saturation	75 to 99% ±2 digits
Pulse rate	± 2bpm
Display	
Numerical	3-digit indicators
Pulse indicator	Pleth bar
Power requirement	Two AAA alkaline batteries or rechargeable batteries
Power consumption	Less than 30Ma 2.6-3.6V
Battery life	30 hours continuous
Size	
Weight	50g including batteries

The final device specifications examined are those of the Crucial Medical System’s Finger Pulse Oximeter which is also FDA approved. Its specifications can be found in Table 3.3. [22]

Table 3.3: Crucial Medical Systems Finger Pulse Oximeter Specifications [22]

Effective Measuring Range	
Saturation	35% to 99%
Pulse Rate	30 to 250 bpm
Resolution	±1 digit
Accuracy	

Saturation	70 to 99% ±2 digits
Pulse rate	± 2bpm
Display	
Numerical	3-digit indicators
Pulse indicator	Bar graph and perfusion index
Power requirement	Two AAA alkaline batteries
Power consumption	Less than 30Ma 2.6-3.6V
Battery life	30 hours continuous
Size	
Weight	1.8oz (50g) including batteries
Dimensions	58.5 x31 x32 mm

The standard parameters to make the prototype in this project competitive by market standards were determined after examining the specifications for the Respironics' WristOx™ Ambulatory Finger Pulse Oximeter, the Santa Medical's Finger Pulse Oximeter, and the Crucial Medical System's Finger Pulse Oximeter. The specifications table for this project's prototype can be found in Table 3.4.

Table 3.4: Project Specifications

Effective Measuring Range	
Saturation	70 to 100%
Pulse Rate	20 to 250 bpm
Resolution	1 digit
Accuracy	
Saturation	± 3% or ± 2 digits
Pulse rate	± 3% or ± 3 digits
Display	
Saturation	2 characters
Pulse Rate	3 characters
Power Requirement	3V lithium battery (coin sized batteries)
Battery Life	Minimum 24 hours continuous

3.4 Revised Client Statement

Develop a wearable, noninvasive reflectance-based pulse oximeter prototype that demonstrated reliably accurate and precise measurements SpO_2 and PR from the chest and wrist. The prototype connects to the computer generated program, LabVIEW, which displays the SpO_2 and PR graphically and numerically. The prototype measures SpO_2 within 70 to 100 percent and PR within 20 to 250 beats per minute having a resolution of 1 digit and accuracy within ±3% or ±3 digits. This prototype should weigh less than 150 grams. The prototype must not cause any harm, such as burning the skin or allergic reactions. In order to provide the best results possible for SpO_2 and PR, the prototype must remain in constant contact with the skin. This prototype should be easy to use, requiring little to no training before use. Once the prototype is completed, testing for this device was conducted on healthy volunteers to test the accuracy and precision as well as proving that SpO_2 and PR can be measured from the chest and wrist.

4 Device Development

4.1 Device Alternatives

4.1.1 Sensor Design 1

This prototype design utilized a dual-wavelength LED surrounded by 4 photodiodes. These photodiodes were positioned at 90° increments around the LED. The LEDs transmitted at 660nm and 940nm. Many studies showed that better signal quality can be achieved when a ring of photodiodes are used to collect light from a central light source [23]. The separation distance between the LED and each photodiode were approximately 1 cm. As a result, the LED required a larger driving current so that more tissue is able to absorb and reflect light [5]. A bandpass filter was utilized at a cut off frequency of 2Hz and bandwidth of 3Hz. This sensor was compatible with flash memory and utilizes a serial connector interface so as to make it possible to connect the device to LabVIEW for signal analysis. Further signal processing was accomplished by using LabVIEW in order to minimize motion artifacts and noise.

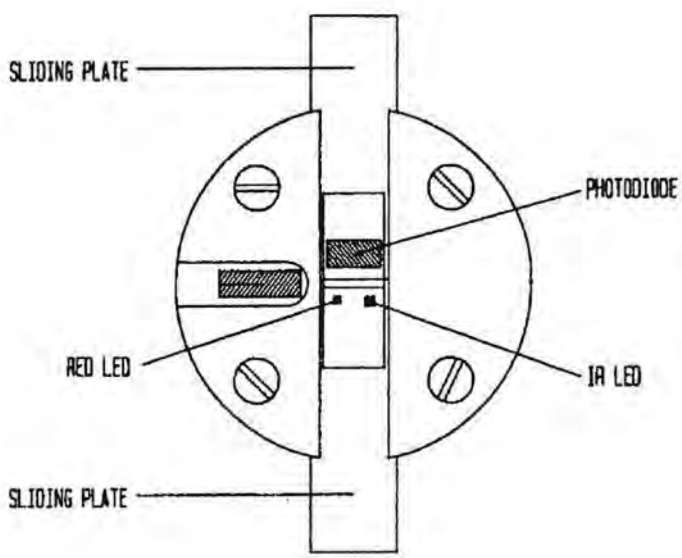

Figure 4.1: Sensor design 1.[5]

4.1.2 Sensor Design 2

The other prototype also utilized a dual-wavelength LED surrounded by 4 photodiodes. These photodiodes were positioned at 90° increments around the LED. The LEDs transmitted at 730nm and 880nm. These wavelengths have been shown to provide a more linear relationship for SpO_2 values less than 70%. Many studies showed that better signal quality can be achieved when a ring of photodiodes is used to collect light from a central light source [23]. The separation distance between the LED and each photodiode was approximately 1 cm. As a result, the LED required a larger driving current so that more tissue is able to absorb and reflect light [5]. A bandpass filter was utilized at a cut off frequency of 2Hz and bandwidth of 3Hz. This sensor was compatible with flash memory and utilized a serial connector interface so as to make it possible to connect the device to LabVIEW for signal analysis. Further signal processing was implemented using LabVIEW in order to minimize motion artifacts and noise.

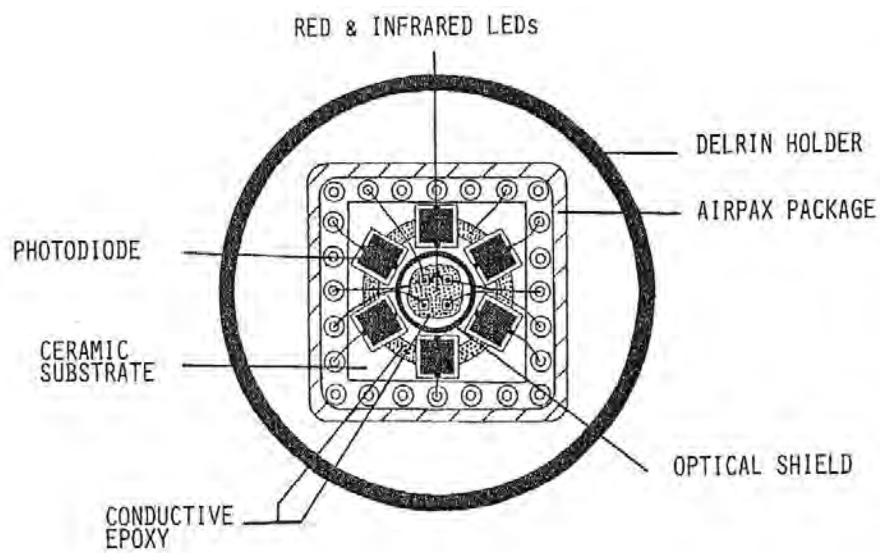

Figure 4.2: Diagram of sensor design 2.[5]

4.1.2.1 Evaluating Alternative Designs

The most significant difference between the two alternative designs above was the difference in wavelengths. In design 1, the most commonly wavelengths, 660nm and 940nm, for oximetry were used for the LEDs since they have been proven to work efficiently. In design 2, wavelengths 730nm and 880nm were explored and investigated to determine if these wavelengths would serve as more efficient substitutes. Nogawa showed that with a 730/880nm sensor, a linear relationship could be established for the oxygen saturation between 30-100% with the greatest improvement seen at oxygen saturation levels between 30-70% [12]. For the purpose of this project, the most commonly used wavelengths, 660nm and 940nm were selected. For a chest based pulse oximeter, research showed that the upper sternum provides decent readings when the user is still [24]. For the wrist based pulse oximeter, the desired measurement location was the radial artery which has shown some success over the ulnar artery on the wrist [25].

4.2 Software Design

The program used to compute SpO_2 and PR from the PPG signals gathered by the sensor is LabVIEW System Design Software from National Instruments. Each program created within LabVIEW is known as a virtual instrument (VI).

5 Methods

5.1 Photodetection Unit

The photodetection unit used in this project utilizes LEDs and photodiodes to collect backscattered light that travels from the LED, through skin and tissue and is reflected off the bones and subcutaneous tissues back into the photodiode. Our ability to measure the PPG and calculate SpO_2 comes from the varying absorption that occurs as the heart pumps blood through the arteries. For the photodetection unit to properly work, the LED and photodiode must be close enough to each other so the photodiode can pick up the greatest fraction of backscattered light for the highest possible output and signal to noise ratio.

5.2 PPG

The pulse oximeter makes it possible to observe the PPG signal due to the changing of absorbance because of arterial blood pulsating throughout the body. In Figure 5.1 below we can see that the PPG which is commonly referred to as the pulsatile component or the AC component, is a small percentage of the total signal output which is generally riding on top of a large DC offset. This DC offset occurs due to absorbencies that are not changing such as skin or other non-arterial tissues which maintain a constant absorbance. When attempting to amplify the PPG for closer inspection, it is generally the case that the DC component is also amplified and as a result ends up saturating the signal. To properly amplify the PPG signal it is best to filter out the DC component through the use of a bandpass or high pass filter. Once amplified, the PPG signal can then be used to calculate heart rate either visually or with the aid of special software that can calculate the frequency or count the number of peaks in a certain time interval.

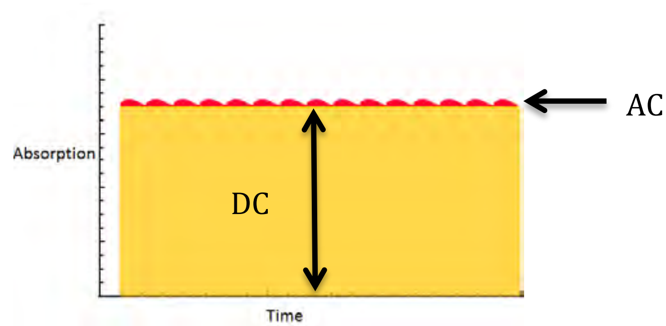

Figure 5.1: Unfiltered output of a PPG signal with an AC component riding on top of a DC component

5.3 Filter Design

To separate the PPG from the output of the photodiodes, it is necessary to filter the signal in such a way so that the PPG signal is preserved while other unwanted parts of the signal are attenuated. In the case of the PPG and the average pulse rate of a healthy patient, a bandpass filter with a cutoff frequency of 1.5-2Hz and a narrow bandwidth of 2-3Hz. This will allow for the separation of the AC and DC components which is necessary for SpO_2 and PR calculations.

5.4 Software

Signals were digitized and sampled using LabVIEW DAQ Assistant with analog inputs collected by a National Instrument's Data Acquisition Board with a sampling frequency of 100Hz. The functions of the software are described in Appendix A and can provide further detail into the design of the VI used for this prototype.

Figure is the summarized sequence of software processes which are applied to both the red and infrared PPGs.

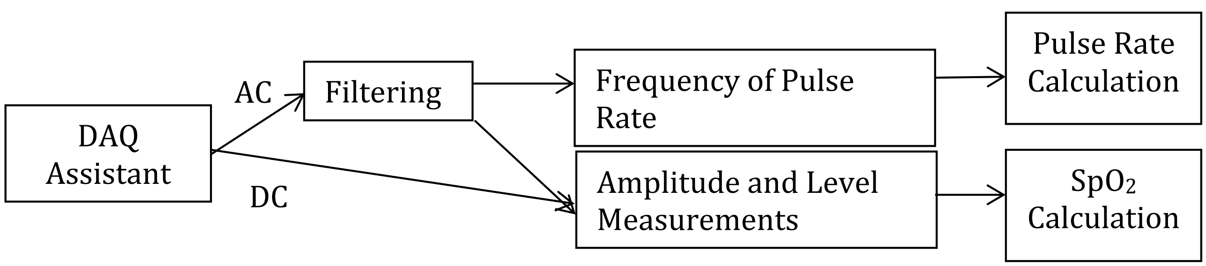

Figure 5.2: Software flow chart

5.4.1 Incoming Signals

The first block in the Software Flow Chart, in Figure 5.2 is to address the installation of the external DAQ Assistant and the completion of its internal task which includes identifying the connected external DAQ Assistant with the DAQ Assistant function in the Block Diagram, each of the incoming signal channels, and the sampling rate. Since the DAQ Assistant function combines the four incoming signals created by the sensor into a single output called data, four Select Signals functions are used to separate and identify the incoming signals. The Select Signal functions were used instead of a simple Split Signal function because they could be set to single out a one specific signal while a Split Signal would separate the signals, but provide no indication of which signal was being produced. To ensure that the DAQ Assistant external and internal system was receiving the signals correctly, Waveform Graphs were implemented at the output of each Select Signals which when the prototype was running would plot the AC and DC components of the red and infrared signals and be compared to the readings of an oscilloscope.

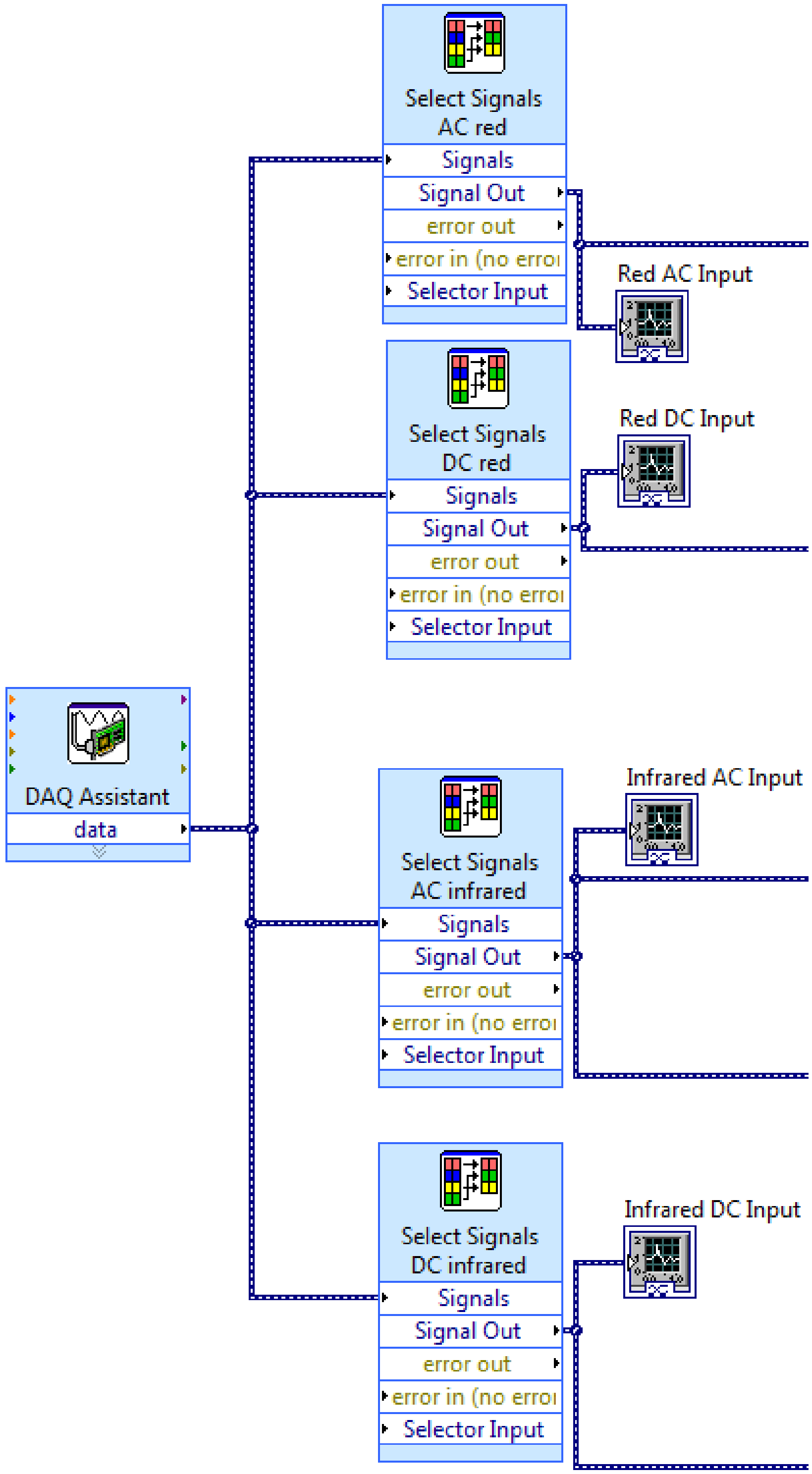

Figure 5.2: Configuration of functions to separate incoming signals

5.4.2 Filtering

Next, is the filtering of the red AC signal because of the extra noise that accompanies this signal. The infrared AC signal was not filtered digitally because it was a stronger signal due to infrared light not being as blood absorbent as red light. A bandpass filtering type was selected because it was necessary to eliminate extraneous signal samples above and below the main signal. Since an average pulse rate is approximately 60bpm, the amplitude of the signal necessary to produce the average pulse rate is between 1.5 -2 Hz. This provides the low cutoff with 0.75Hz which is about 40bpm and the high cutoff with 2.5Hz which is about 130bpm. The Chebyshev filter topology of the 7th order was implemented because it provides a steeper roll-off and minimizes the error between the idealized and the actual filter characteristic over the range of the filter. The impact of removing the noise from the signal by using these filter parameters can be seen on the sample graphs provided in the Configure Filter menu as seen below.

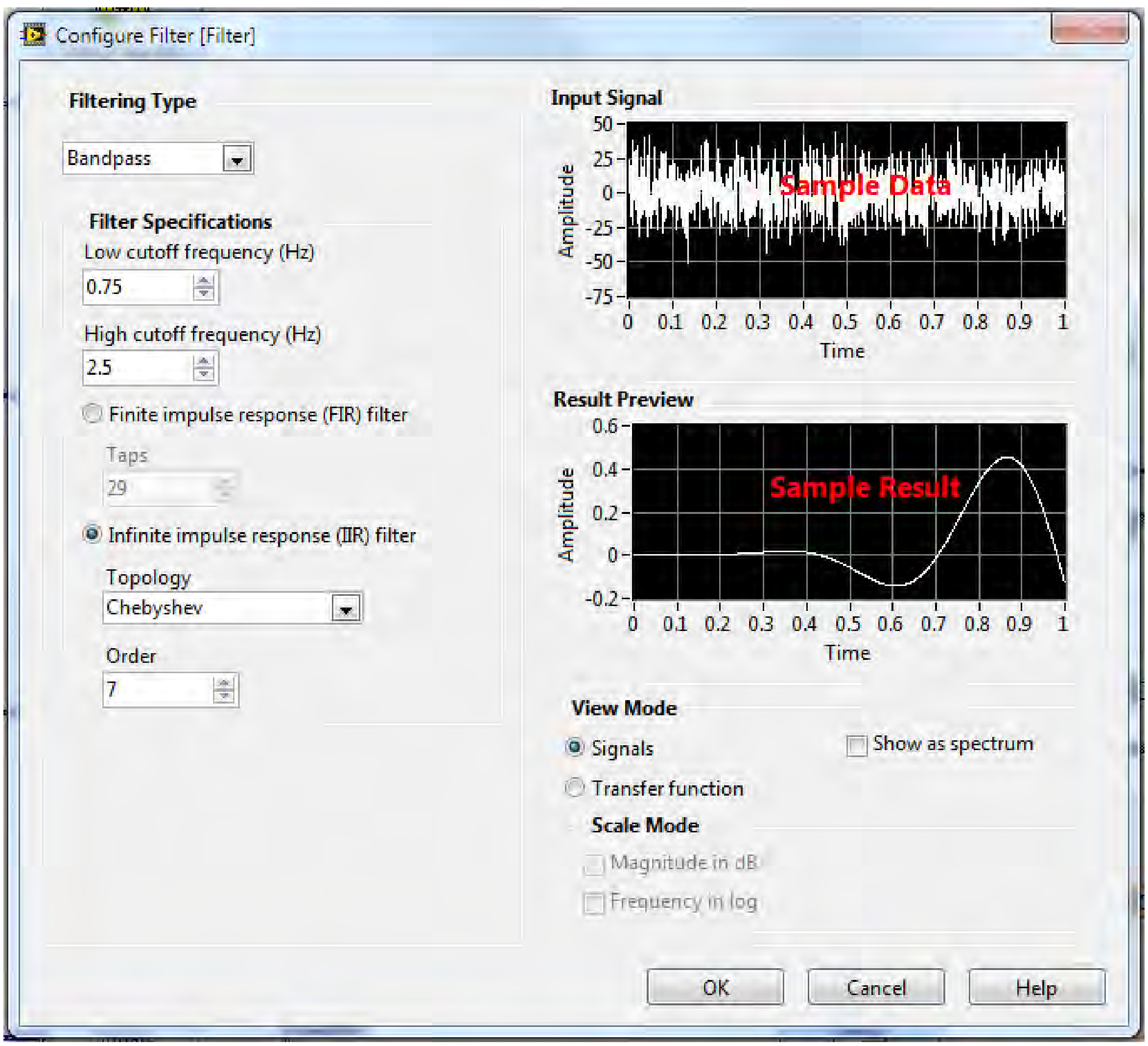

Figure 5.3: Configure filter menu

In Figure 5.4, the Filter function can be seen connected to a Waveform Graph which allows for the visualization of the change of the digital signal after it passes through the filter and confirmation that the filter was working.

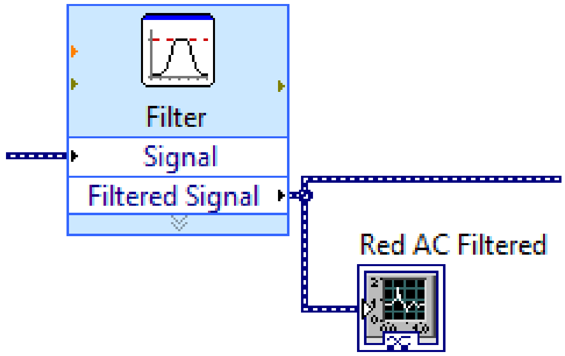

Figure 5.4: Filter function and graph

5.4.3 Frequency of Pulse Rate

Tone Measurements are the function used to determine the frequency of the Infrared AC signal which is needed to determine PR. This function has several measurements that it can perform, but for this VI, it is only used to measure frequency. Tone Measurements achieves this by searching for the set frequency, which is 2±50Hz. This range was chosen because a 2 Hz signal results in the average pulse rate of approximately 60bpm, but pulse rate can vary from 40bpm to 150bpm thus the ±50Hz range. In Figure 5.5, the Tone Measurement function can be seen connected to both a Numeric Indicator and Waveform Chart. In Figure 5.67, the configuration display for the Tone Measurement function is displayed with the settings used to measure frequency and plots of the signal before and after the function is applied.

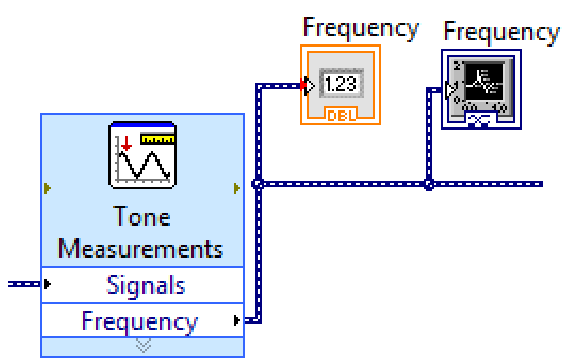

Figure 5.5: Tone measurements output frequency

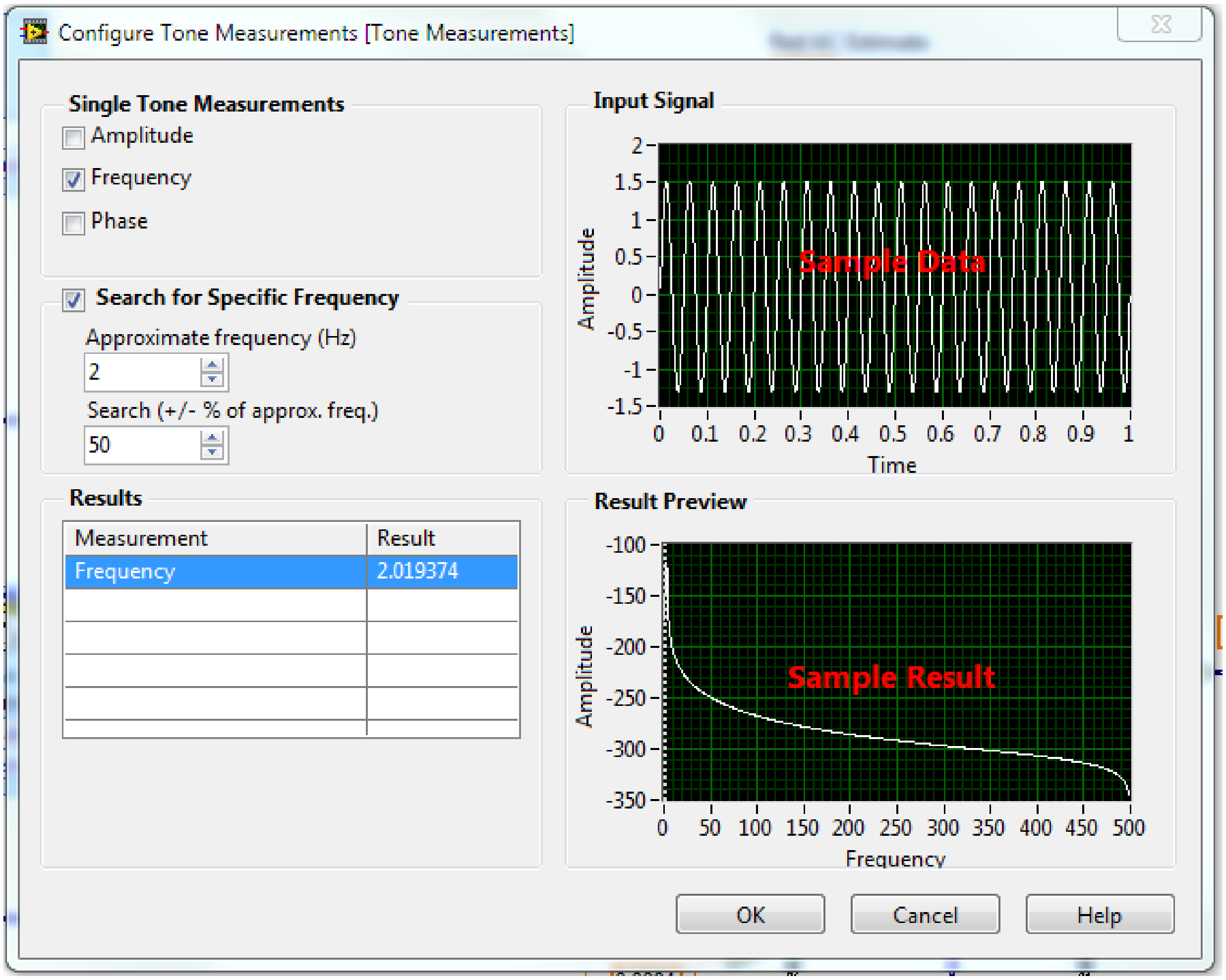

Figure 5.6: Configure tone measurements parameters

5.4.4 Pulse Rate Calculation

The PR calculation is the maximum average frequency of the infrared AC signals around 1.5 Hz with a ±50% search. The highest peaks can be assumed to be the PR because the raw graph of the AC signal, while having has some noise, is mostly representative of a clean PPG of the PR. The signal to noise ratio is very high resulting in the maximum average frequency measured being the PR.

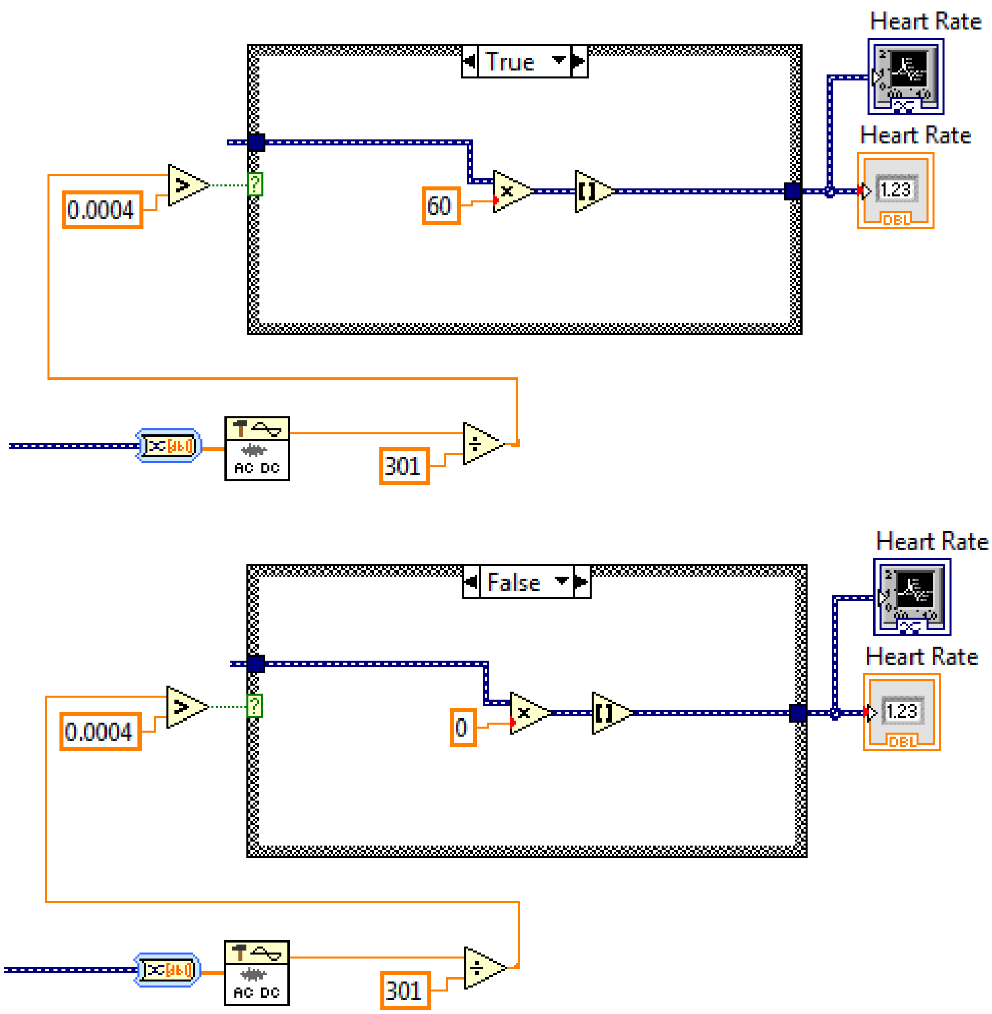

Figure 5.7: Functions used to calculate pulse rate

5.4.5 Spectral Measurements

Both the DC components of the red and infrared signals were averaged using the Amplitude and Level Measurement function and had these averages displayed with numeric indicators. This is necessary because to use the DC components of the signals, they need to be quantified into a signal value to be used in the SpO_2 calculation.

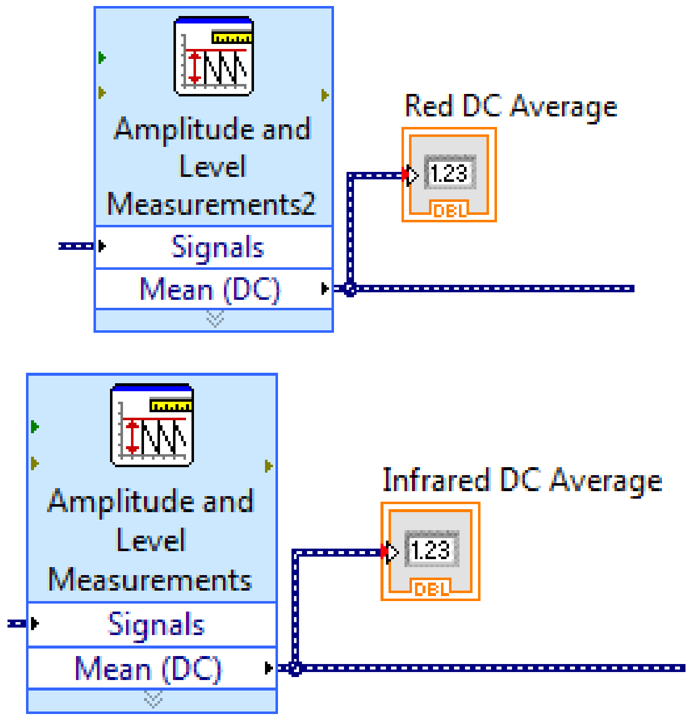

Figure 5.8: Amplitude and level measurements functions with numeric indicators

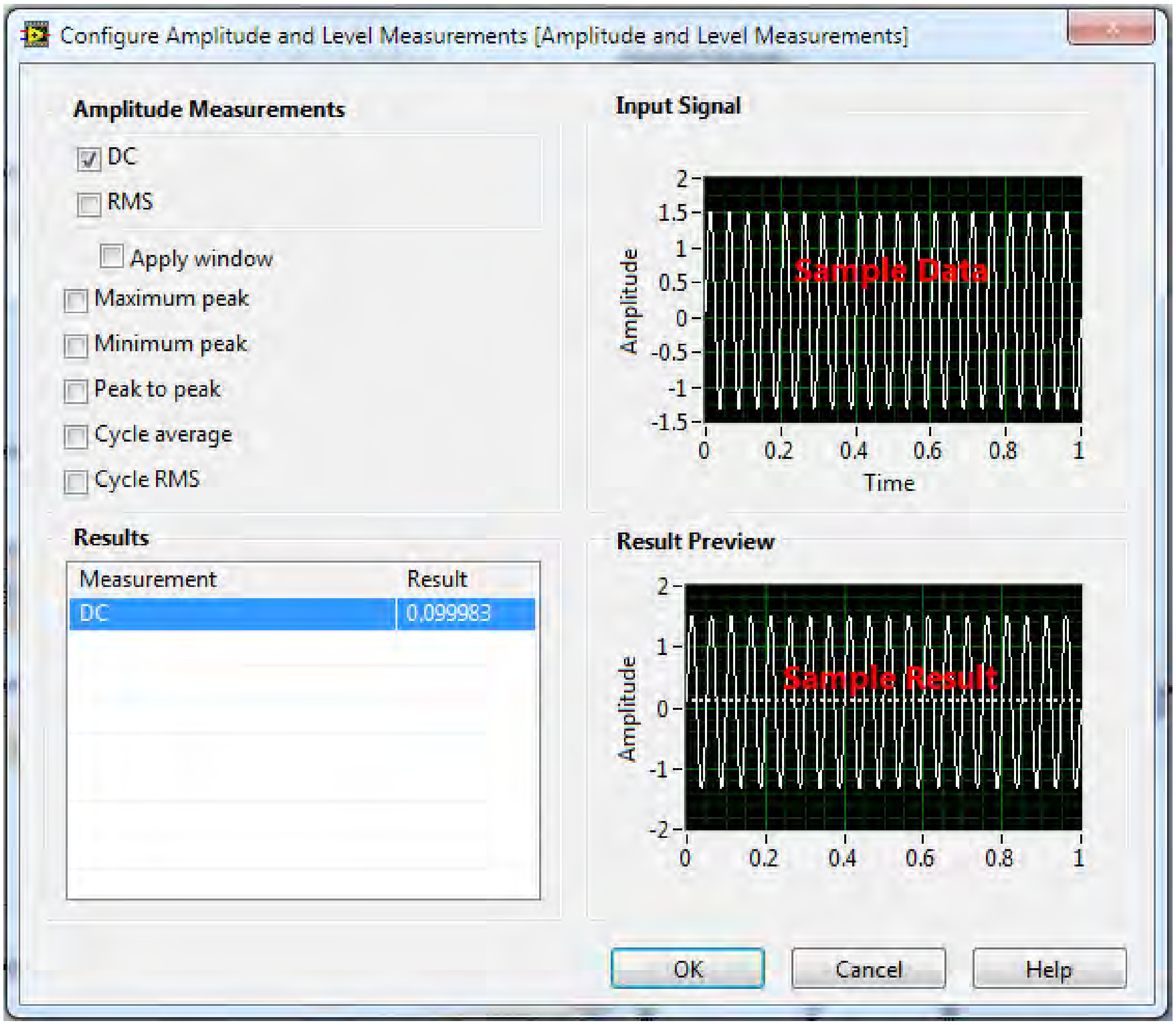

Figure 5.9: Configure amplitude and level measurements set to mean (DC)

5.4.6 SpO_2 Calculation

As mentioned previously, the SpO_2 calculation, with A = 110 and B = -25, is:

$$A + B\left(\frac{\left(\frac{AC}{DC}\right)_{Red}}{\left(\frac{AC}{DC}\right)_{IR}}\right) \qquad (4)$$

To create this equation in LabVIEW, the divide, add, and multiply functions were used on the already processed AC and DC components of the red and infrared signals. At the end of the configuration of functions used to create the SpO_2 equation in LabVIEW, which can be seen in *Figure 5.11*, there is a numerical indicator and waveform chart so that the ratio $\left(\frac{\left(\frac{AC}{DC}\right)_{Red}}{\left(\frac{AC}{DC}\right)_{IR}}\right)$ is displayed on the Front Panel and monitored to ensure that this section of the VI is working.

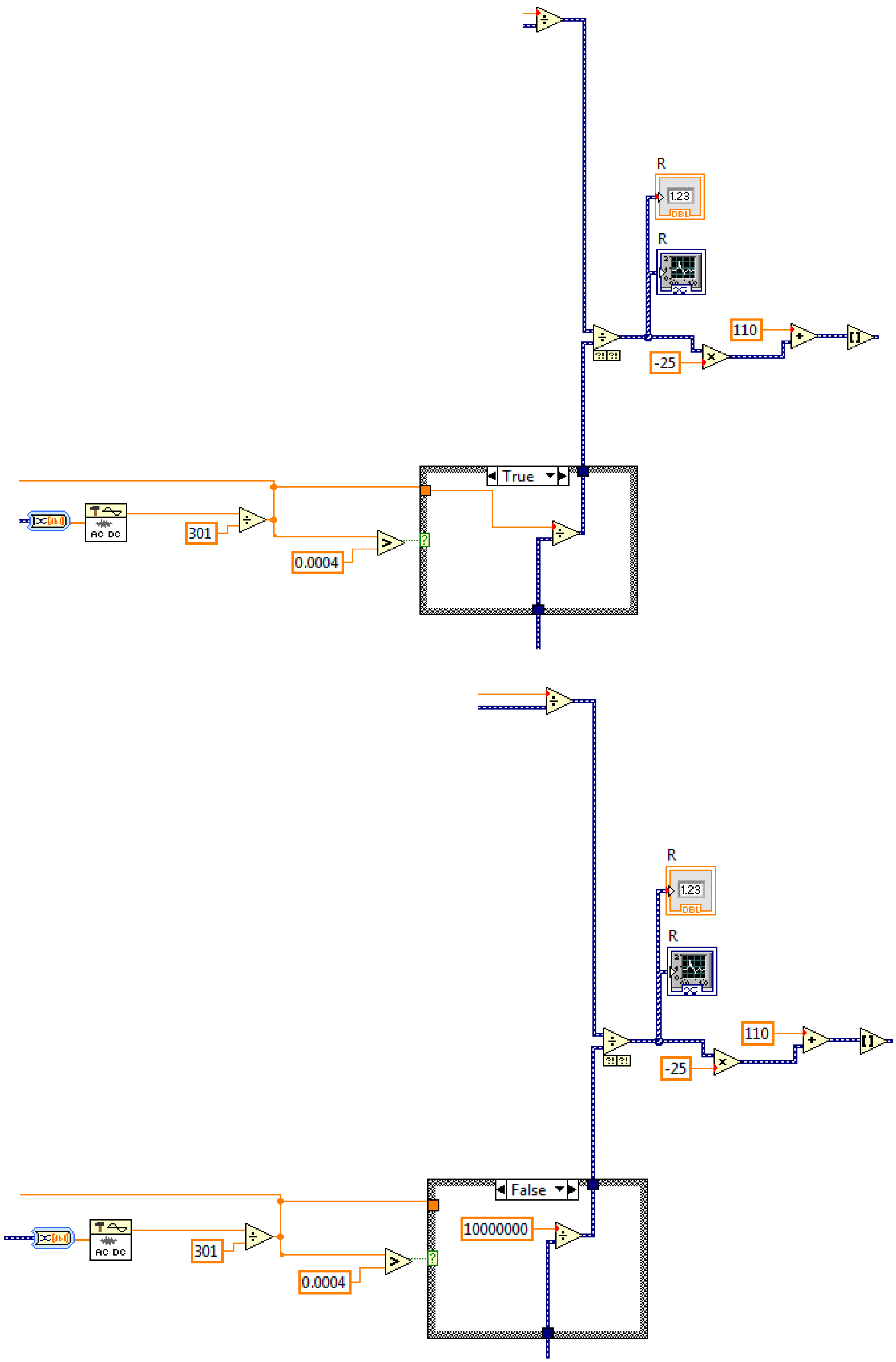

Figure 5.10: SpO_2 calculation

5.4.6.1 Limiting Range of SpO_2 Measurement

To receive the desired measurement range of 0-100 for SpO_2, the SpO_2 equation is first normalized by dividing the value produced by the SpO_2 equation by 110 and multiplying by 100. This value is then passed through a simple logic test. The logic test states if the value is greater than 0 and less than 100 it will be displayed on the SpO_2 gauge and waveform chart. Otherwise, the value is multiplied by 0 and then displayed on the SpO_2 gauge and waveform chart.

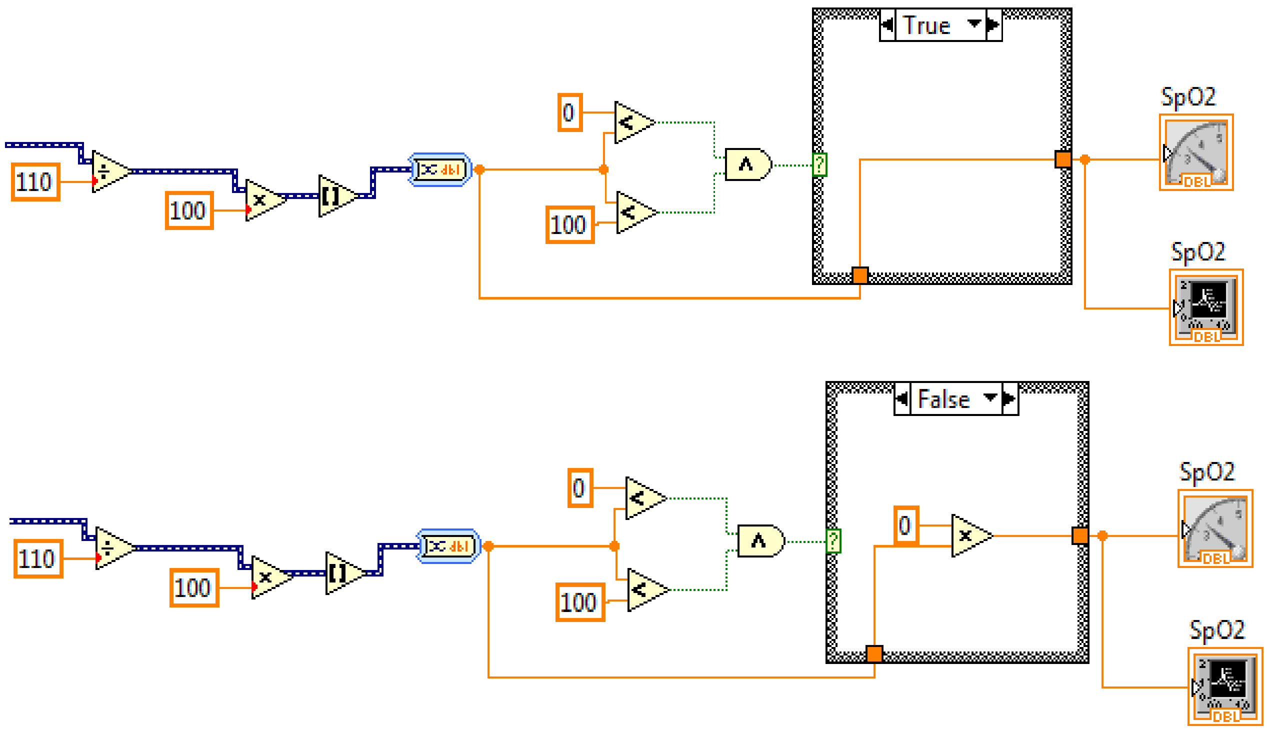

Figure 5.11: The configuration of function that limit the displayed SpO_2

Below are images of the block diagram and front panel of the full VI used in this project.

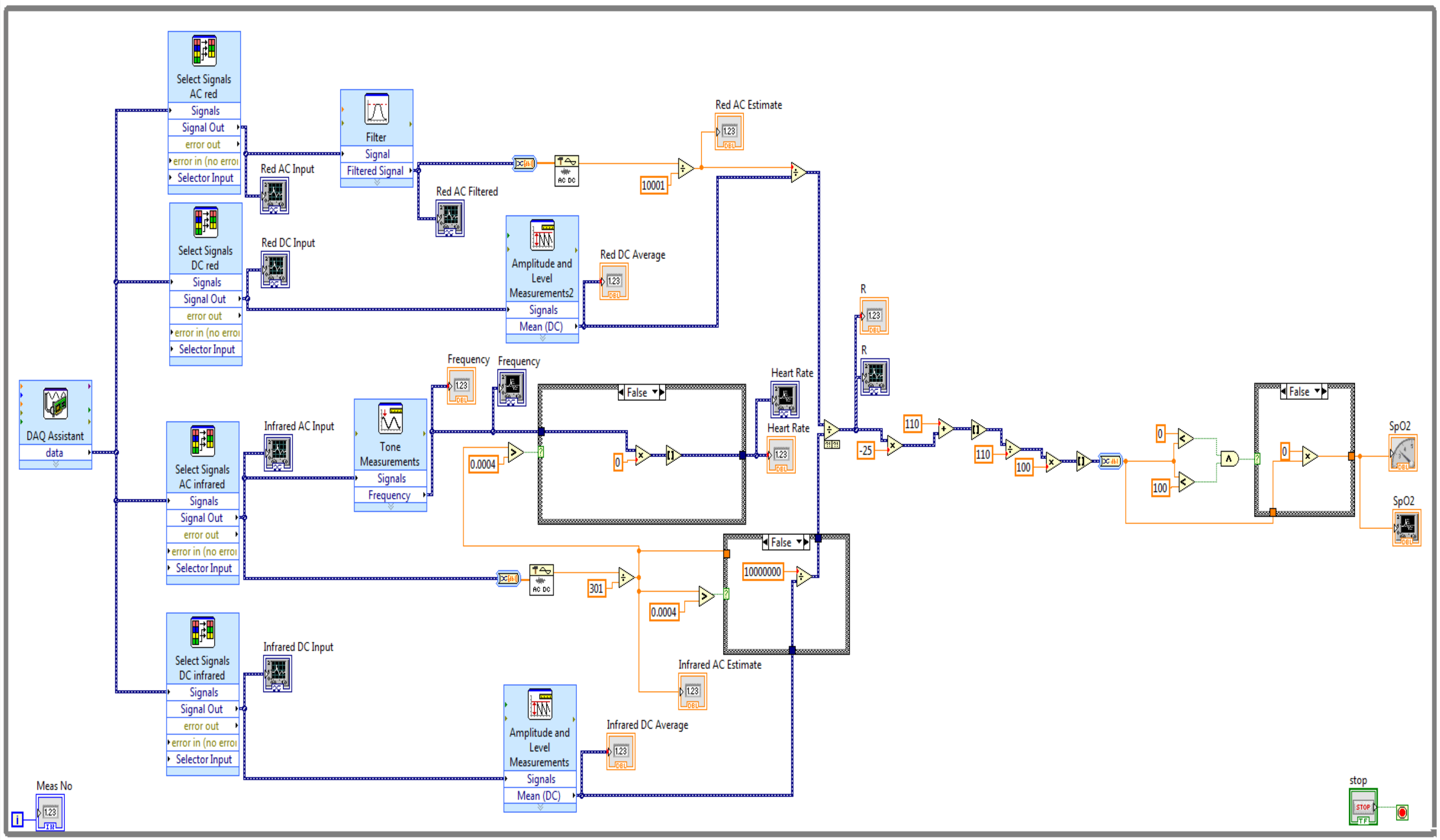

Figure 5.12: VI Block Diagram

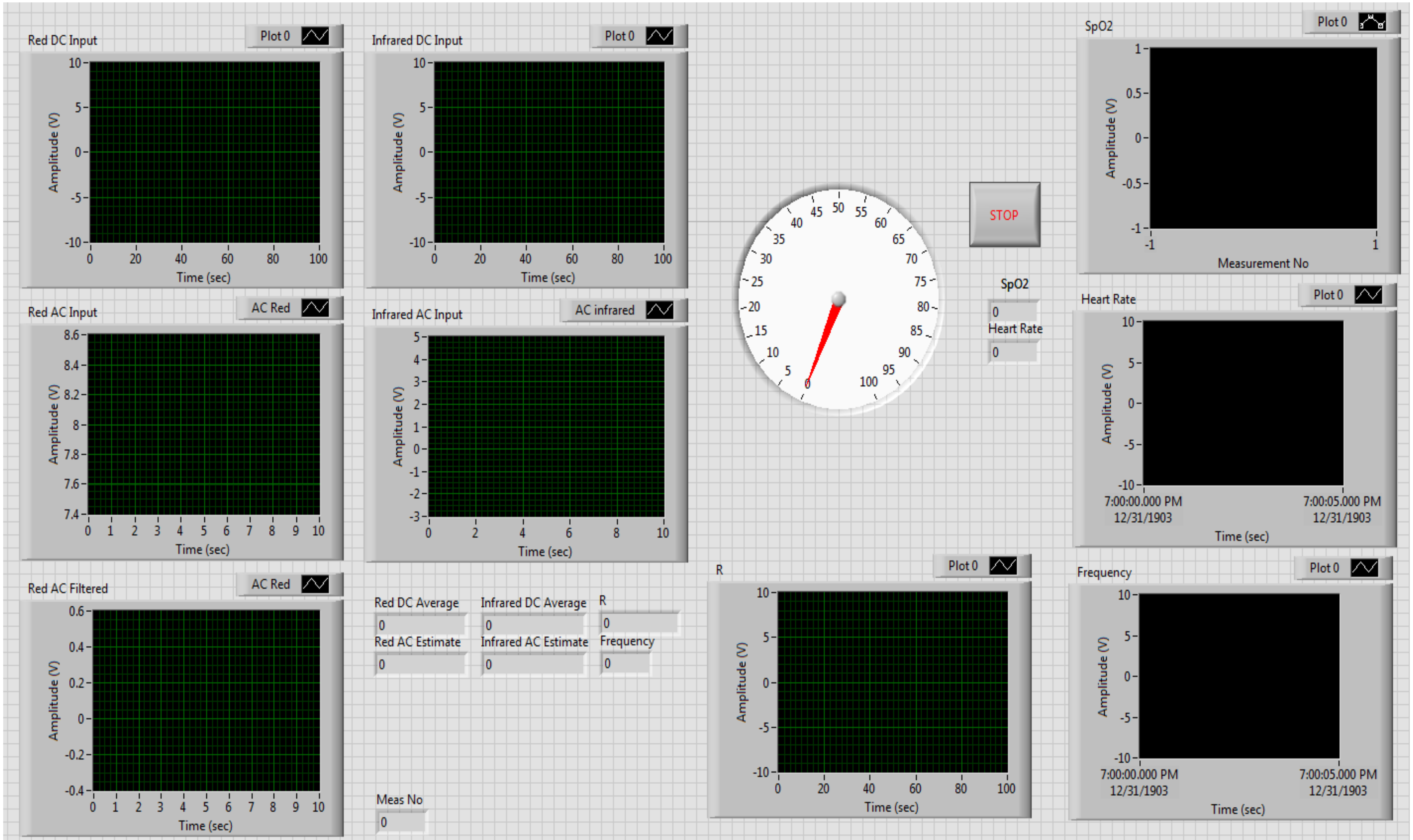

Figure 5.13: VI Front Panel

5.4.7 Preliminary VI Test

To test the VI, four digitally simulated signals were used with a control, a function in LabVIEW that will allow the manipulation of a variable while the VI is running, was placed on the amplitude of the red AC signal. This control was used to manually increase the red AC signal's amplitude causing the SpO_2 to decrease. This test of the VI replicated the oxygen decrease in the blood of a person who was hypoxic.

Below are images that demonstrate the success of this preliminary test of the VI. Figure 5.15, depicts the VI at the start of the test with the amplitude control at 0.5, the control can be seen below the SpO_2 gage and to the left of the LabVIEW stop button. Since the amplitude control has not been changed yet the SpO_2 graph in the upper right of the figure is a straight line and the AC Red Input and Red AC Filtered graphs have the relatively large amplitudes of 20Hz. As the amplitude control is slowly increased to 21, the SpO_2 graph in the upper right of Figure 5.16 shows a steady decrease and the AC Red Input and Red AC Filtered graphs now have amplitudes of 0.4Hz.

The "R" indicator, which displays the ratio value calculated during the SpO_2 calculation, is seen to increase between the two figures, as it was expected, because it is necessary for the ratio to increase for the resulting SpO_2 to decrease. The other graphs and indicators do not show a change in between Figure 5.15 and 5.16 because this was a controlled tested with simulated input signals.

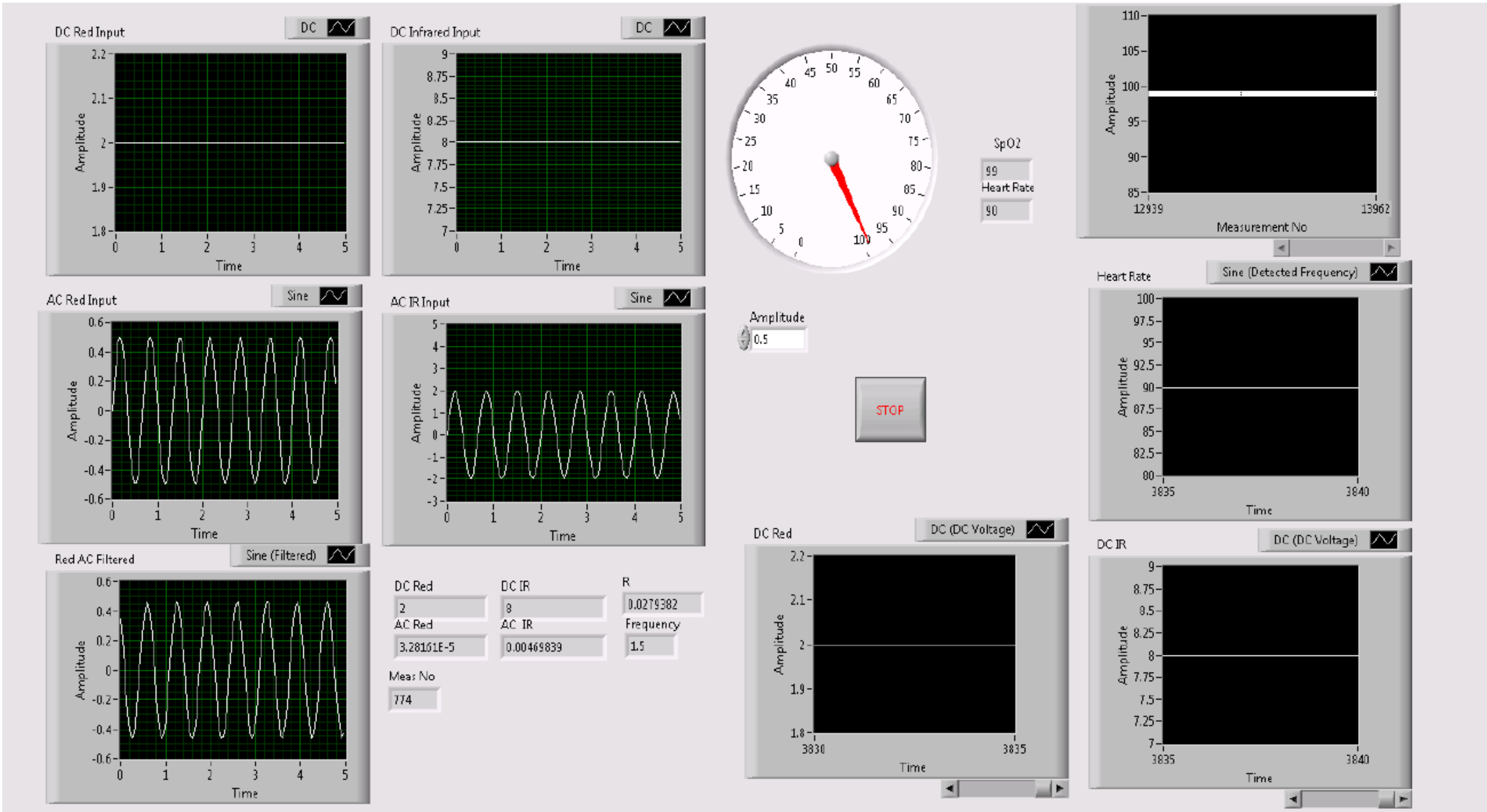

Figure 5.14: Front panel for the simulated hypoxia test with low amplitude

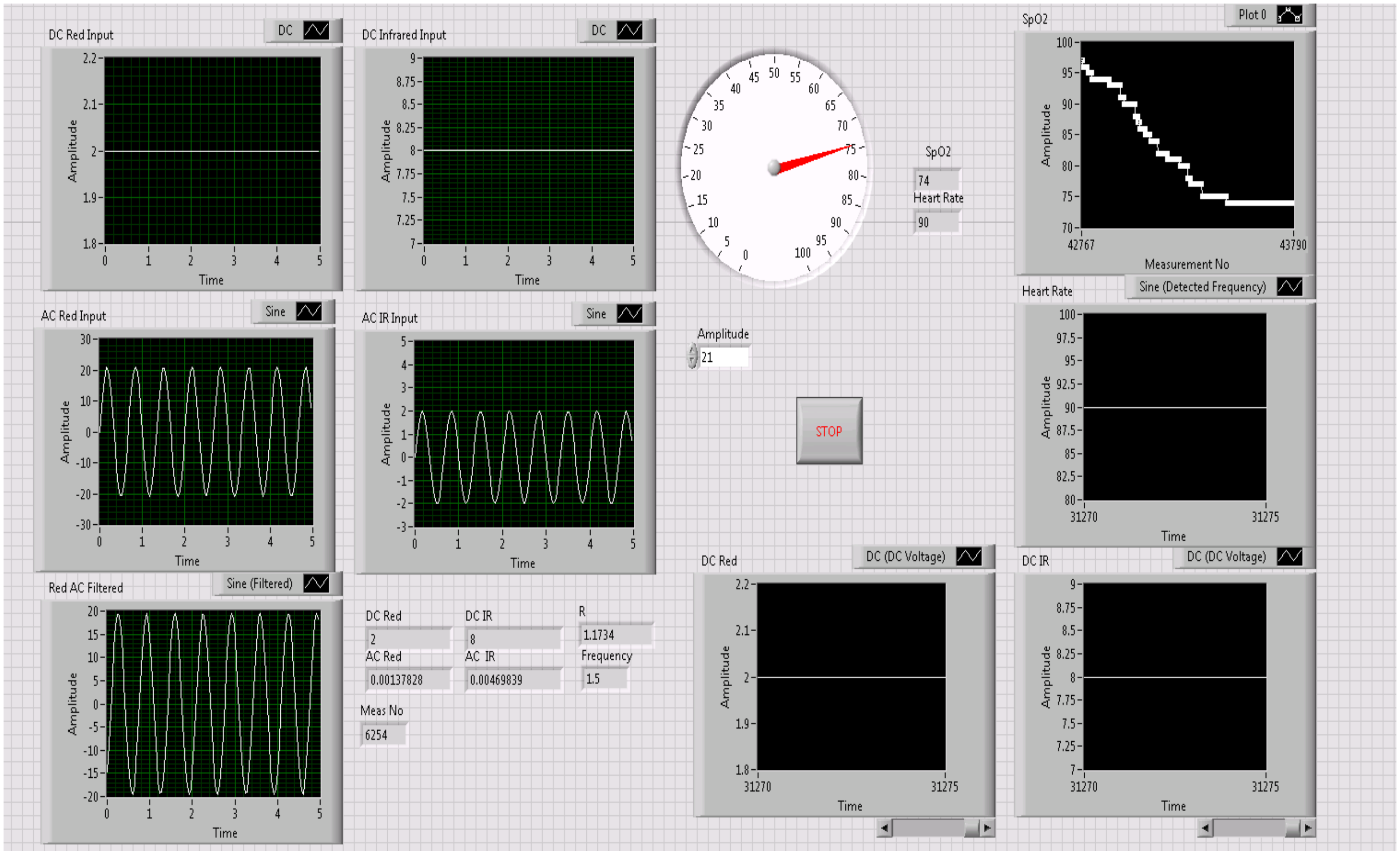

Figure 5.15: Front panel for the simulated hypoxia test with high amplitude

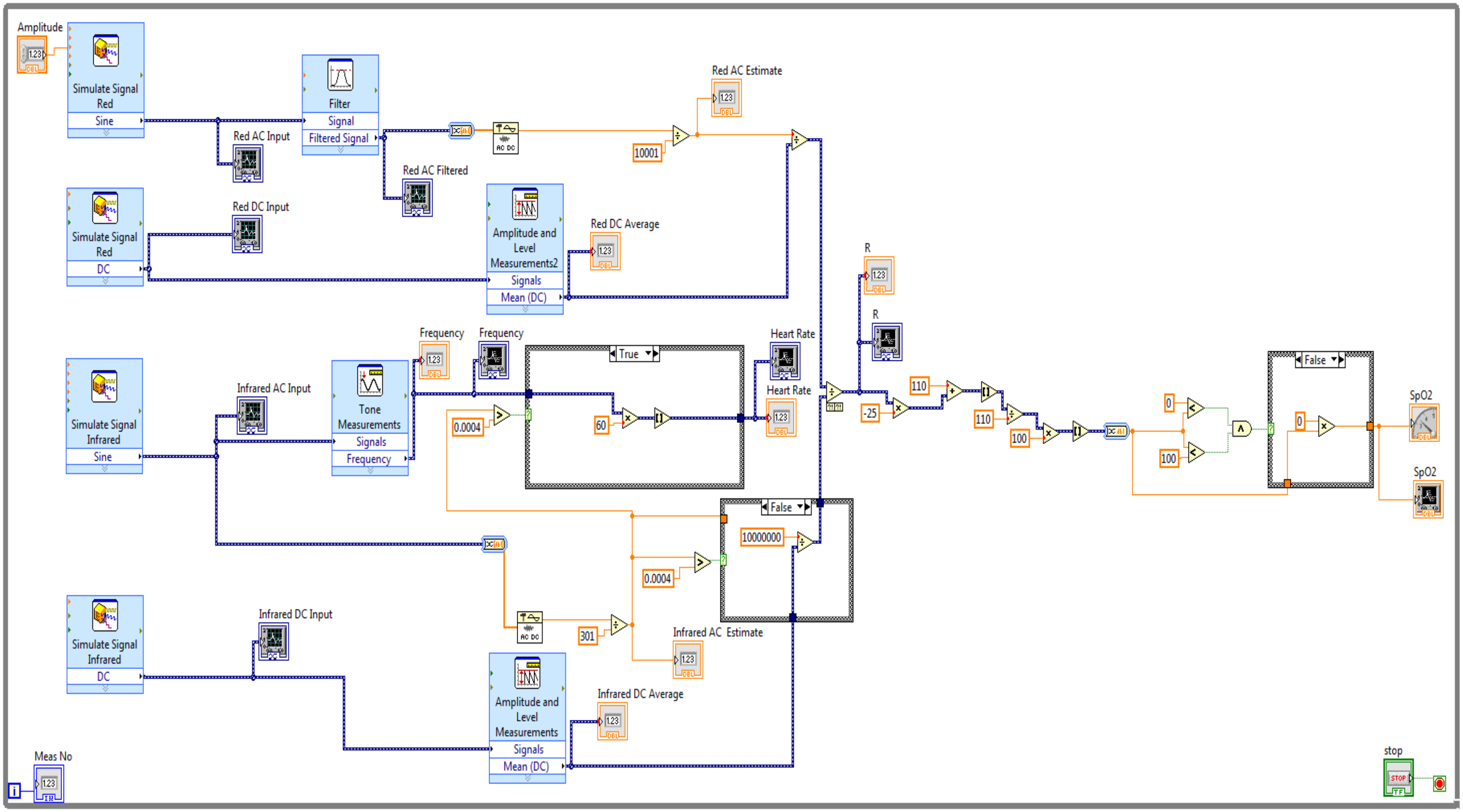

Figure 5.16: Block diagram for the simulated hypoxia test

5.5 Experimentation/Testing

5.5.1.1 ECG and Reference Pulse Oximeter Reliability Test

For measurement and comparison purposes a HOMEDICS Deluxe Pulse Oximeter with transmission method for the finger was utilized as a reference along with our pulse oximeter prototype. The reliability of the reference pulse oximeter was tested against an ECG Biopac module model 100C.

Three ECG electrodes were connected to each subject's right arm, left arm and left leg. Data collected from the ECG electrodes were displayed by the AcqKnowledge software and changes in PR were monitored on the screen using peak to peak analysis. The pulse oximeter was placed on the subject's index finger. The ECG Biopac module was turned on and one minute of data were collected while the PR was monitored by the finger pulse oximeter at the same time. Accuracy and error percentages were calculated from each measurement. We calculated the error to be less than $\pm 3\%$, which matches the finger pulse oximeter's specification sheet and deems it suitable to use as a reference.

5.5.1.2 Wrist Measurements

The probe of an oscilloscope was connected to the AC infrared outlet of the circuit and to common ground. The display of the oscilloscope was set up to segments of 500 milliseconds with amplitude of 2 volts so the blood pressure wave was clearly visualized. Since the AC component of the infrared outlet from the circuit showed a more defined representation of the blood pressure curve than the AC red component, the AC infrared component was utilized as a second visual reference for the testing phase of the prototype.

The sensor was strapped tightly to the wrist of the subject by means of a Velcro strap to maintain constant pressure while the subject was sitting with his/her arm resting on a table. Although we encouraged the subjects to place the sensor directly over the radial artery, the specific location and orientation of the sensor varied for each individual since PPG intensity can vary from person to person.

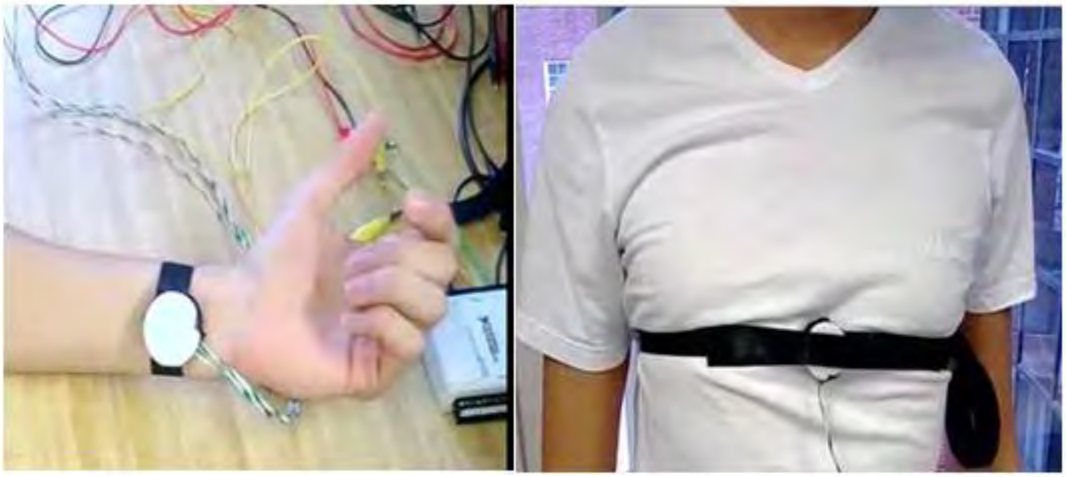

Figure 5.17: Application of the sensor to the wrist (left) and the chest (right)

The VI is setup to collect data in ten seconds intervals during six minutes. Measurements from the reference pulse oximeter, which was worn on the subject's finger, were taken at the same time that a new measurement appeared on our prototype VI. These results were recorded in an excel spreadsheet for the corresponding time. Measurants were recorded using the described procedure while sitting and standing.

5.5.1.3 Chest Measurements

The sensor was then attached to the chest using a longer Velcro strap and positioned directly over the sternum to obtain a strong PPG signal. The oscilloscope was set again with a window of 500 milliseconds and amplitude of 2 Volts. The pressure applied to the sensor on the chest varies depending on the subject's ability to display a continuous PR wave on the oscilloscope and their comfort level. The chest test was performed while the subjects were sitting and standing over six minutes.

5.5.1.4 Hypoxia Testing

The ability of the prototype to reproduce accurate low SpO_2 levels was also tested. Here, the sensor was strapped around the wrist and data were collected right after asking the subject to self-induce hypoxia by not breathing for 45 seconds. Hypoxia test were performed on four different sitting individuals. Only one individual was able to show a drop in SpO_2 levels after 45 seconds. The lowest SpO_2 value observed on the reference pulse oximeter was 91% while the VI displayed a value of 93%.

5.5.1.5 Hyperventilation Testing

The final test performed was a hyperventilation test in which we measured how well our prototype responding the changing values of PR. During this test four different subjects were asked to strap the sensor to the wrist and remain calm with their arm extended and relaxed on a table with the reference device attached to the finger. The subjects were asking to breathe normally for a 1-minute period to obtain a stable PR. After the initial minute, each subject was then asked to begin hyperventilating for about 4 minutes. After the hyperventilation period the subjects were asked to breathe normally again for an additional minute to conclude the 6 min test and to show a declining PR. The results were compared to the reference device and plotted data were produced and shown in the results section.

6 Final Design

6.1 Device Hardware

For our final design, we took alternative design 1 and modified parts of it for efficiency. For the sensor block we increased the number of photodiodes surrounding the LEDs in order to obtain a lower degree of sensitivity that would otherwise be present with a smaller amount of photodiodes. More photodiodes also results in an increase in the total photodiode surface area which can capture reflected light.

6.1.1 Sensor

The design for the sensor module was based on the need for a concentric photodiode arrangement around two LEDs, one infrared and one red. Since that a larger number of photodiodes would only benefit the device, the group decided to utilize 8 surface photodiodes instead of the 4 that was designated in alternative design 1. In Figure 6.1 Figure 6.1 below, we can see the top view of the sensor module that the group developed. The red and infrared LEDs are placed in the center of 8 photodiodes which are able to pick up light from nearly every angle. The added effect of the photodiodes is also a benefit since summing up the current from all eight photodiodes maximizes the fraction of total backscattered light collected by the sensor.

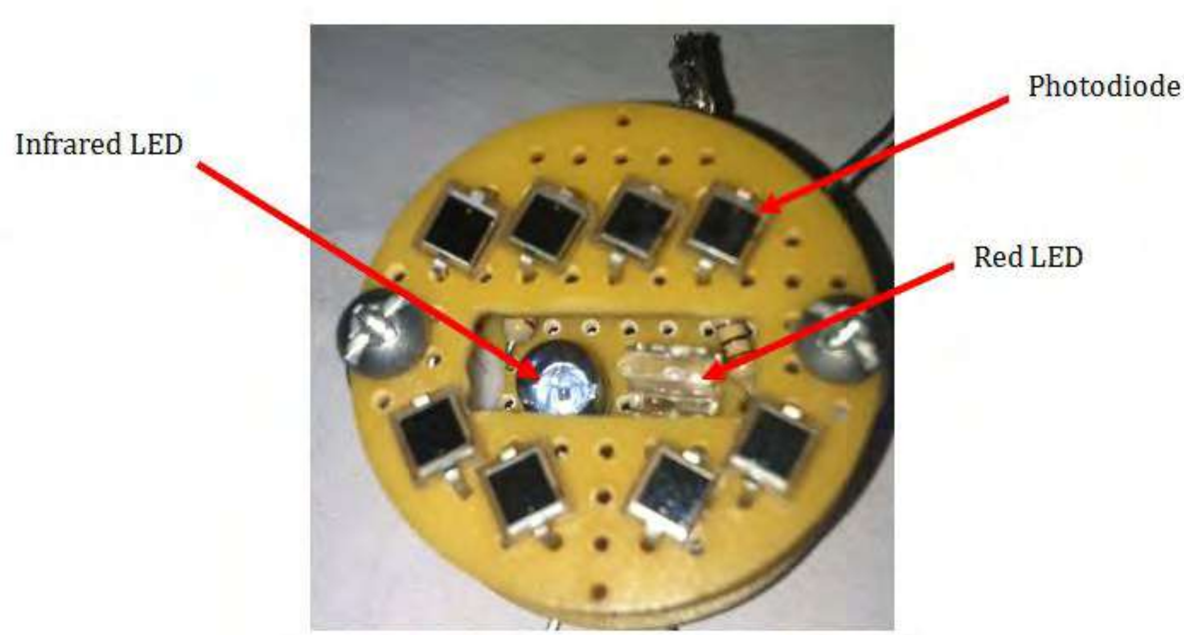

Figure 6.1: Top View of sensor module with photodiodes and LEDs.

The placement of the LEDs relative to the photodiodes was also important. Since the LEDs were much larger than the photodiodes, we had to consider how we could design the sensor so that the LEDs and photodiodes were the same level when placed on the skin. Our solution for this was using a two platform design. In Figure 6.2Figure 6.2, we present a side view image of our sensor module with each platform labeled.

Figure 6.2: Platform view of sensor module

The top platform, which is the surface of the device that is placed against the skin, was used primarily for the placement of the photodiodes. A rectangular opening was then made in the center of the board to allow for the LEDs placed on the bottom platform to protrude through and allow the light to pass through the skin. To allow for portability and to reduce the weight of the sensor, we separated the sensor module from the actual circuitry and connected 4 wires from the sensor to the circuitry board.

6.1.2 Circuitry

To process the signals obtained from the sensor module, we implemented several different signal processing techniques which helped to simplify the programming required in the VI. The block diagram in Figure 6.3Figure 6.3 shows a simplified view of our circuitry and how it is connected.

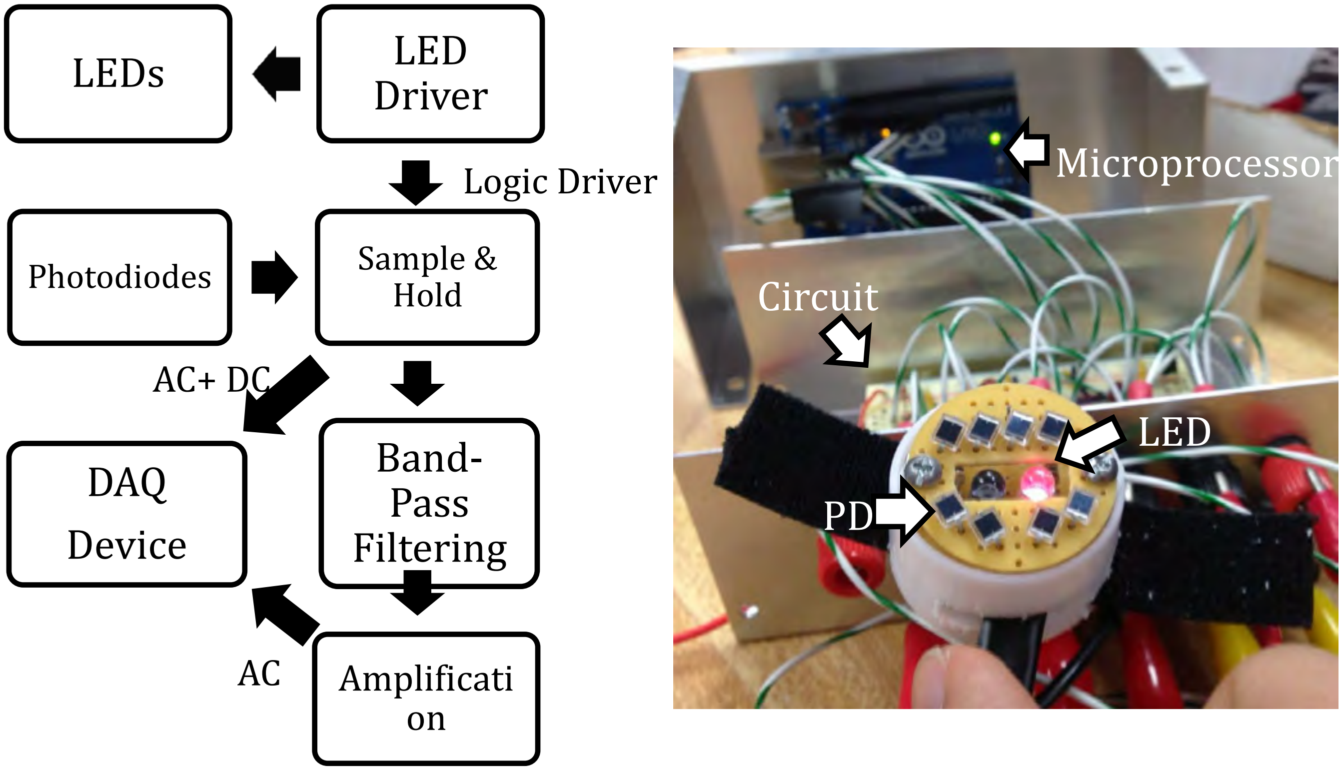

Figure 6.3: Block diagram of the prototype pulse oximeter

The LEDs in the sensor module are driven at alternating frequencies of 100Hz with a 2.5ms delay between each LED as it is turned on. Figure 6.4 displays the timing diagram of the Arduino Microcontroller which is used as an LED driver. The board was programmed so that the first channel (in yellow) is ON for 2.5ms and OFF for 7.5ms while the second channel (in green) is OFF for 5ms, ON for 2.5ms and then OFF for 2.5ms.

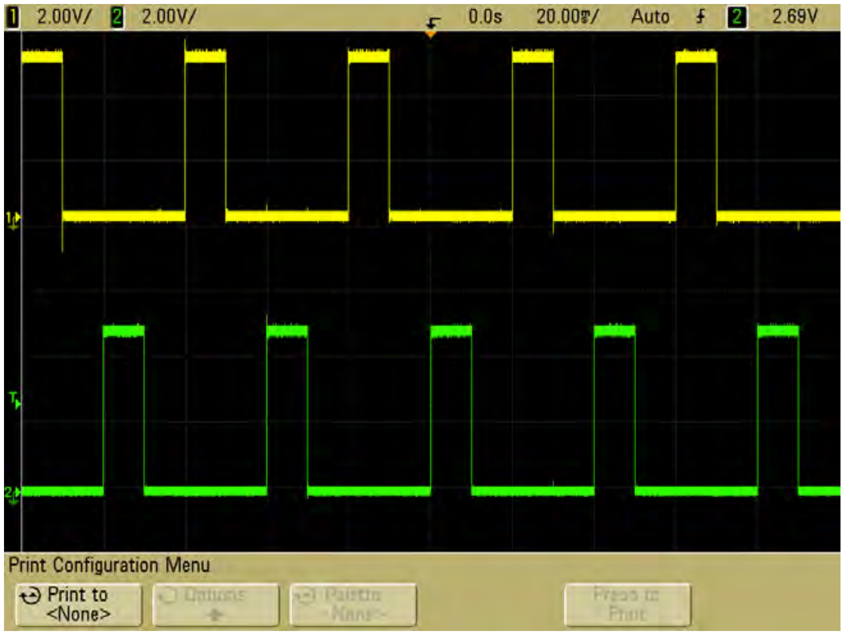

Figure 6.4:LED driver timing diagram with 2.5ms time increments

For the photodiodes, we used an op-amp in photovoltaic mode so that the current output of the photodiodes is converted to a voltage. The voltage, which is directly related to the amount of light collected, is then sent through two Sample-and-Hold ICs (LF398) (S/H) to separate the red and infrared signals. To accomplish this, the voltage output by the photodiodes were connected simultaneously connected to both S/H and used the LED driver signals for the red and infrared LEDs as the logic driver for each S/H respectively. Each S/H is able to sample the respective LED to which they are connected to and hold that value until the next time the LED is turned on. The output of each S/H provided the AC and DC components of the PPG required for calculating oxygen saturation. However, because the AC component is generally very tiny compared to the DC component, it was necessary to filter this signal further so that the DC component can be removed and the AC component is amplified. The circuit in Figure 6.55 Figure 6.5a detailed diagram for each signal processing stage in the block diagram.

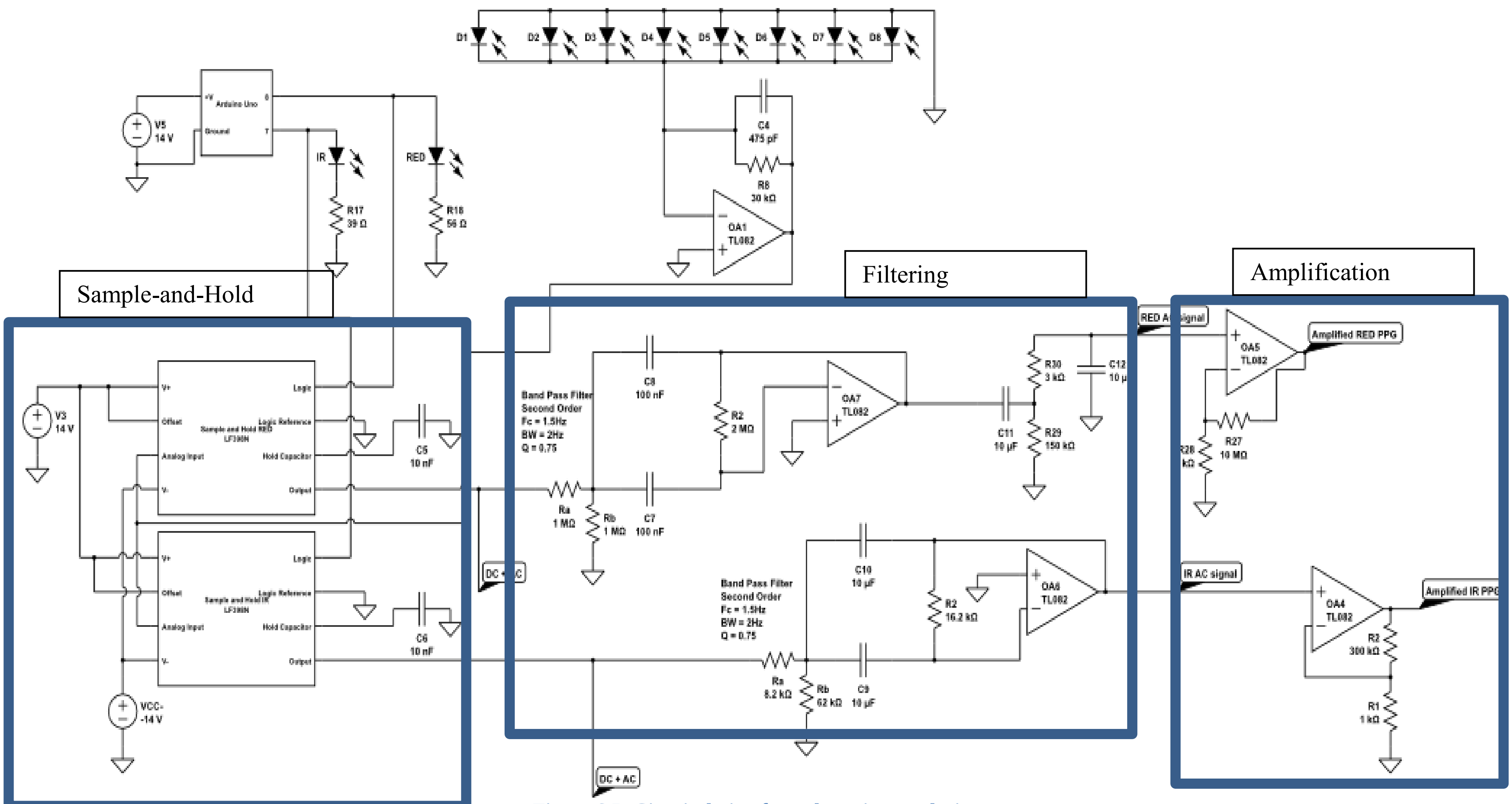

Figure 6.5: Circuit design for pulse oximeter device

To filter and separate the AC component from the AC and DC components, obtained from the S/H, each respective signal red and infrared was processed through a 2nd order bandpass filter. Both bandpass filters were designed with a frequency cutoff of 1.5Hz and bandwidth of 1.5Hz. The rationale behind the selected characteristics is that a range between 0.75Hz and 2.25Hz should be enough to capture and amplify the signals of almost any individual who is at rest. Although the ideal use for any pulse oximeter is to work efficiently at rest and in motion, we felt for the purpose of this project this frequency range would be enough to prove a concept and provide accurate enough readings for individuals with PR between 45bpm and 135bpm.

Seeing a lot of high frequency noise riding on top of a DC offset present in the red signal, we then implemented an additional high pass and low pass filter for the red AC signal so that the DC offset could first be removed and then second so that the high frequency noise could also be filtered out. The last stage in the signal processing is the amplification of the respective red and infrared AC signals at which point they are ready to be interfaced with the DAQ and processed by the VI.

6.2 Software

The final design of the block diagram and front panel of the VI can be seen below. The VI starts by accessing the signals from the sensor with the DAQ Assistant and then separating the signals by implementing select signals. Once the signals are separated and identified the AC components of the red and infrared signals are measured using the peak-to-peak method while the DC components were measured by finding their respective averages. The peak-to-peak method was chosen for the AC components because it is a straightforward measurement which can be compared to the readings of an oscilloscope. Averaging the DC components was necessary because it provided a single value to be used in the SpO_2 calculation for each data set sampled.

Once the signals are processed SpO_2 can be calculated as the ratio of the red AC/DC divided by the infrared AC/DC multiplied by -25 and added to 110. To provide a SpO_2 measurement between 0 and 100, the SpO_2 calculation is then divided by110 and multiplied by 100 so that the value is normalized. To calculate the PR, the frequency of the AC infrared signal was measured using the tone measurements function and then multiplied by 60 to calculate the PR in beats per minute.

Since the VI is constantly sampling data as long as the sensor and a power supply is connected to it, the VI samples noise and runs the computations for PR and SpO_2 even if the sensor is not being worn. To avoid this, case structures were used to introduce thresholds which allow the VI to calculate measurements when the amplitude of the red and IR AC signals were above a certain level and to output 0 when these conditions were not met.

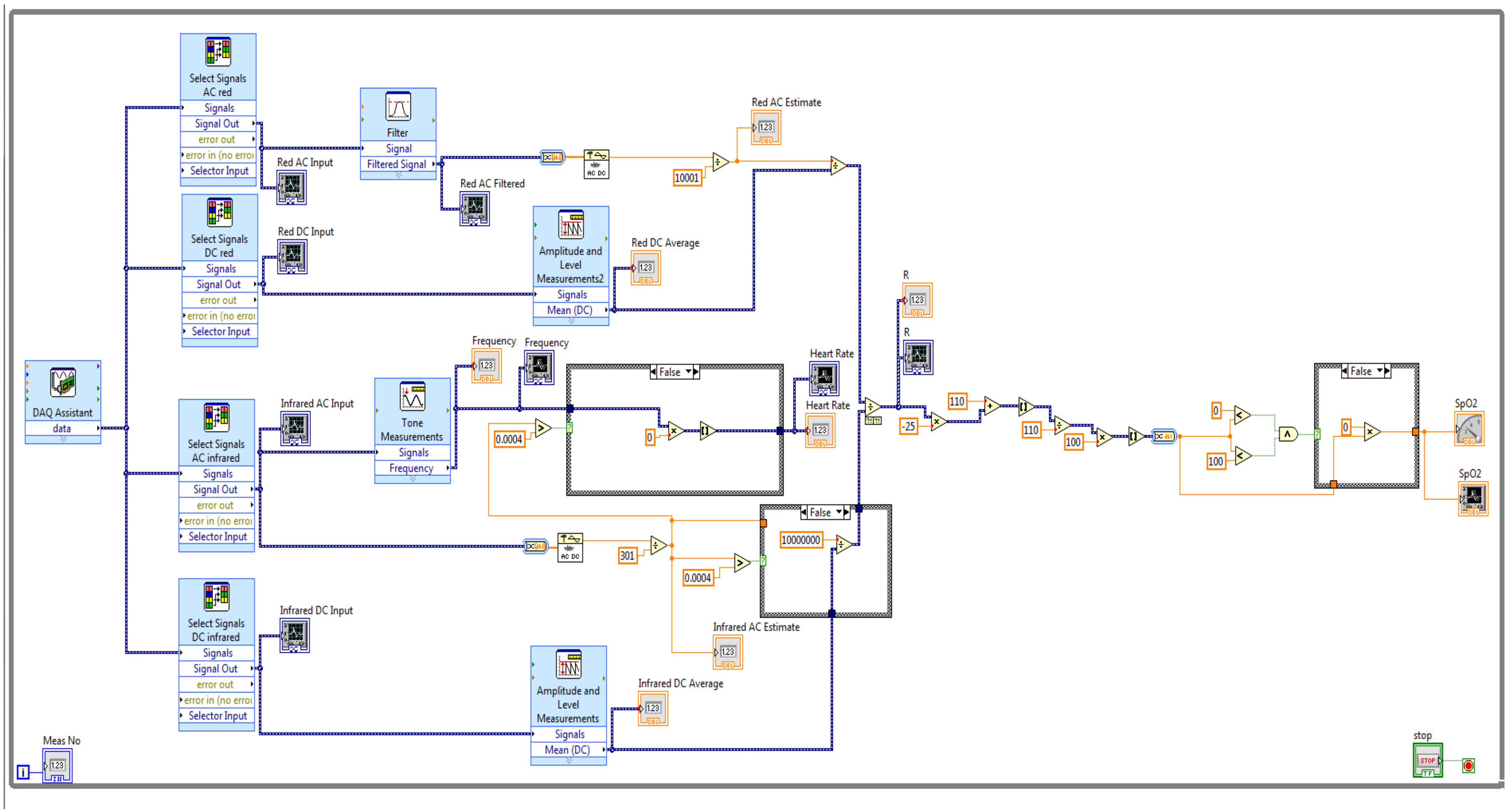

Figure 6.6: Block Diagram of Final VI

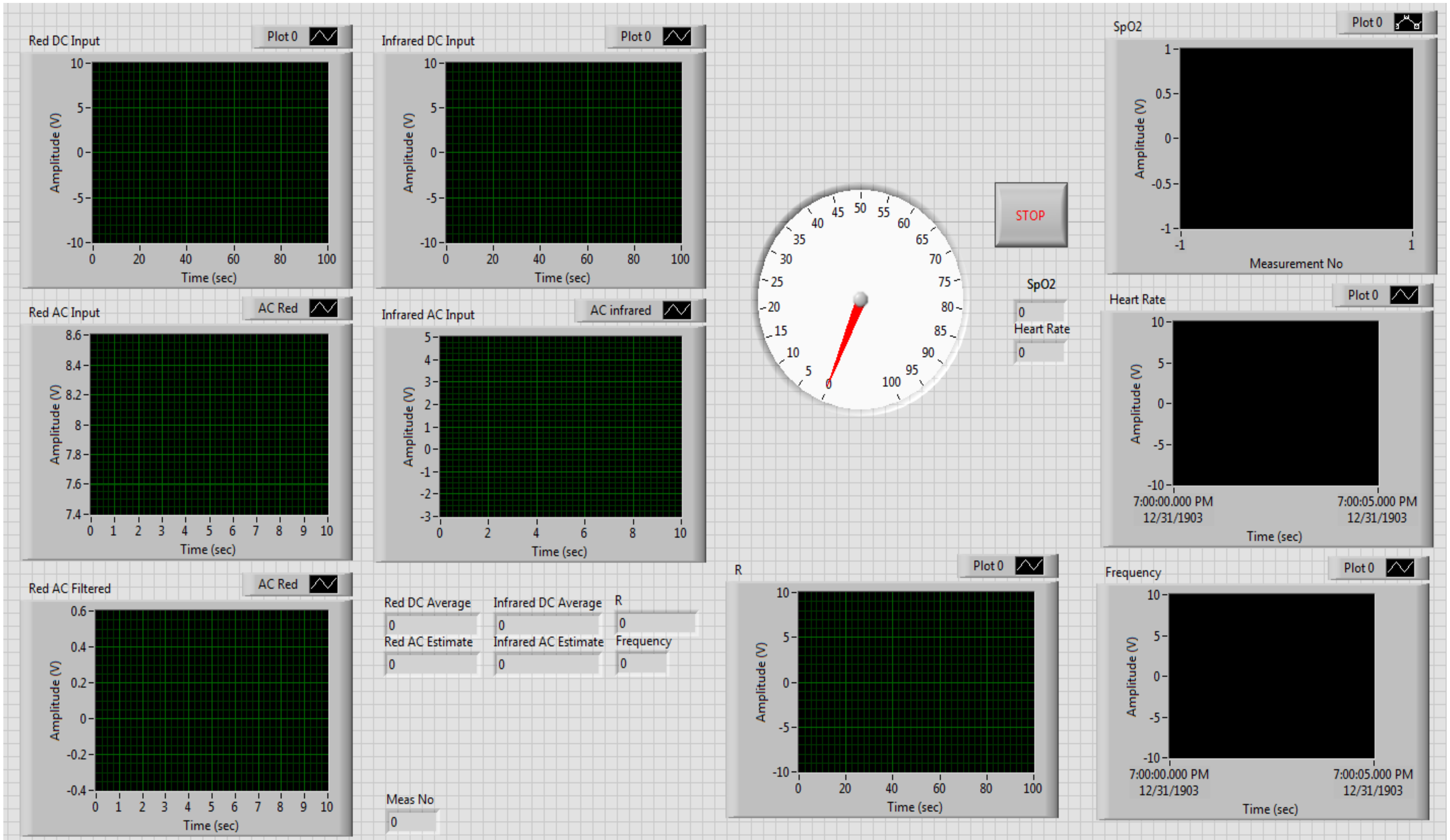

Figure 6.7: Front Panel of Final VI

7 Results

The VI was set to collect and average data every 10 seconds throughout a 6 minute timespan accounting for 36 measurements per data set. The VI was programmed to output SpO_2 and PR every 10 seconds at which point a second individual that was monitoring the control device recorded the corresponding SpO_2 and PR values displayed by the HOMEDICS pulse oximeter. Subjects were tested while sitting, standing, hyperventilating, and during self-induced hypoxia. PPG readings were acquired from both the chest and wrist. Each subject was asked to hyperventilate to mimic an increase in pulse rate and each of the subjects was also asked to hold their breath for 30 to 40 seconds after a full exhale to induce hypoxia. These tests showed the devices ability to detect increasing and decreasing levels of PR and SpO_2 respectively. To compare the accuracy of our prototype to that of the reference pulse oximeter we calculated the average SpO_2 and PR for each data set, and then calculated the percent error using the accuracy equation below summarized in Table 7.1.

$$Percent\ Accuracy = \frac{X_{actual} - X_{measured}}{X_{actual}} * 100 \qquad (5)$$

Table 7.1: Calculated accuracy for the average SpO_2 and PR for each data set

Average Measurements	Reference		Prototype		Percent Errors	
	SpO_2 (%)	PR (bpm)	SpO_2 (%)	PR (bpm)	SpO_2	PR
Wrist Standing	97.9	92.6	97.3	92.8	0.6	0.2
Wrist Sitting	98.2	82.4	98.4	83.3	0.2	1.1
Chest Standing	98.1	96.7	98.5	96.5	0.4	0.1
Chest Sitting	97.8	83.8	98.1	83.9	0.3	0.1

This method was only used for the standing and sitting positions for both chest and wrist readings. To calculate the percent error for all the data collected with our prototype, we first used the accuracy equation on every individual measurement taken for each data set and averaged the percent error per measurement. To calculate the prototype's accuracy, we then averaged the percent error for each data set to obtain a single value. The accuracy of each data set and the prototype's final accuracy are shown in Table 7.2. Due to the fact that we were focusing primarily on SpO_2 for hypoxia and PR for hyperventilation, we chose to collect only those measurants during our testing and did not take measurements for PR and SpO_2 respectively.

Table 7.2: Prototype accuracy based on all data collected

Measurement	Position	Accuracy (Percent Error %)	
		SpO₂	***PR***
Chest	Sitting	0.76	3.15
	Standing	0.60	3.09
Wrist	Sitting	0.24	4.14
	Standing	0.76	3.75
Hypoxia		1.50	
Hyperventilation			5.32
Prototype Accuracy		0.77	3.89

As seen in a couple of the graphs in the sections below, there were examples of outliers in some of the data. These outliers were linked to a corrupted PPG signal in which the PPG was somehow affected by factors such as motion artifact or inconsistent pressure. Figure 7.1 shows an example of a corrupted PPG, in turn compromising the accuracy of that data point.

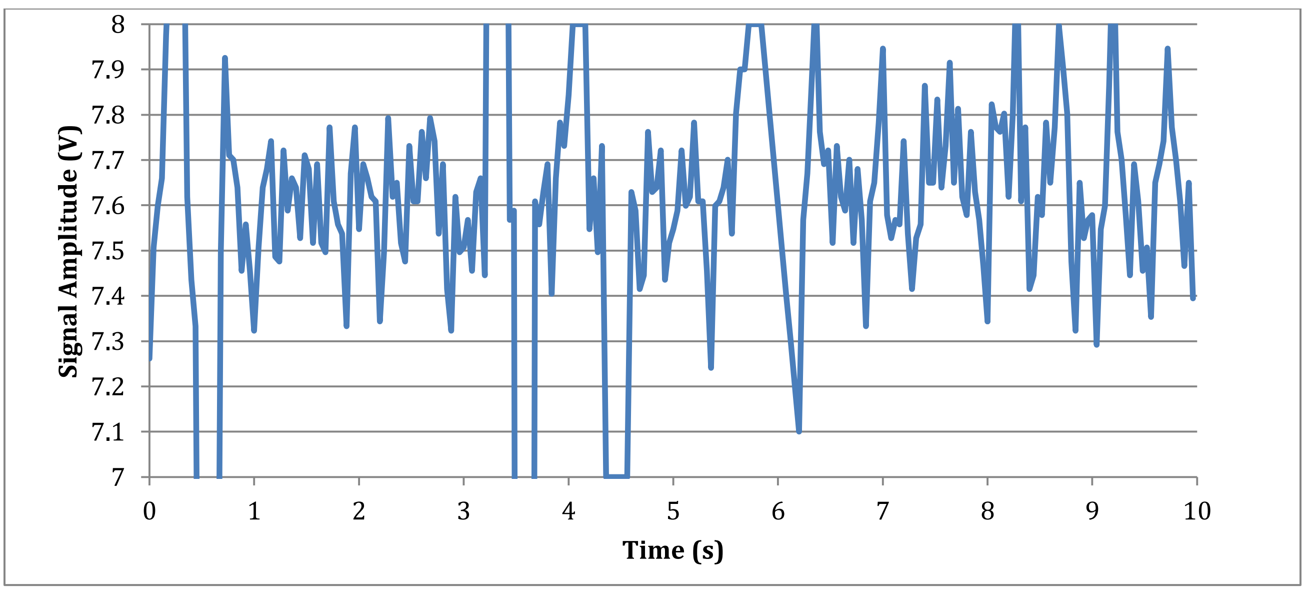

Figure 7.1: Example of corrupted PPG

7.1 Comparison Graphs

Comparison graphs are a useful tool when graphically representing our data because it enables to compare all the data sets for the prototype and reference devices for one test as a whole. Figure 7.2 displays a regression line for the PR data collected from our pulse oximeter prototype on the chest of four different subjects over a six-minute period while sitting. The data are clustered in four different groups, each one having a distinctive symbol corresponding to the subject tested. The total PR data obtained from our prototype for all four subjects ranges from 55 to approximately 105 bpm. The linear regression equation obtained from the data points as well as the statistical coefficient R^2 that determines how well the regression line approximates a linear trend are shown on the upper left corner of the graph. Table 7.1 shows that the PR measurements taken from the chest while sitting has a low percent error of less than 1% when looking at the average of the data and 3% when calculating the accuracy of each individual data point.

The fact that R^2 is close to 1 and the slope of the regression line is also very close to 1 show that the measurements picked up by the prototype appear to be well correlated with the measurements picked up by the reference pulse oximeter. This can also be observed visually by looking at how closely the regression line is to the line of identity.

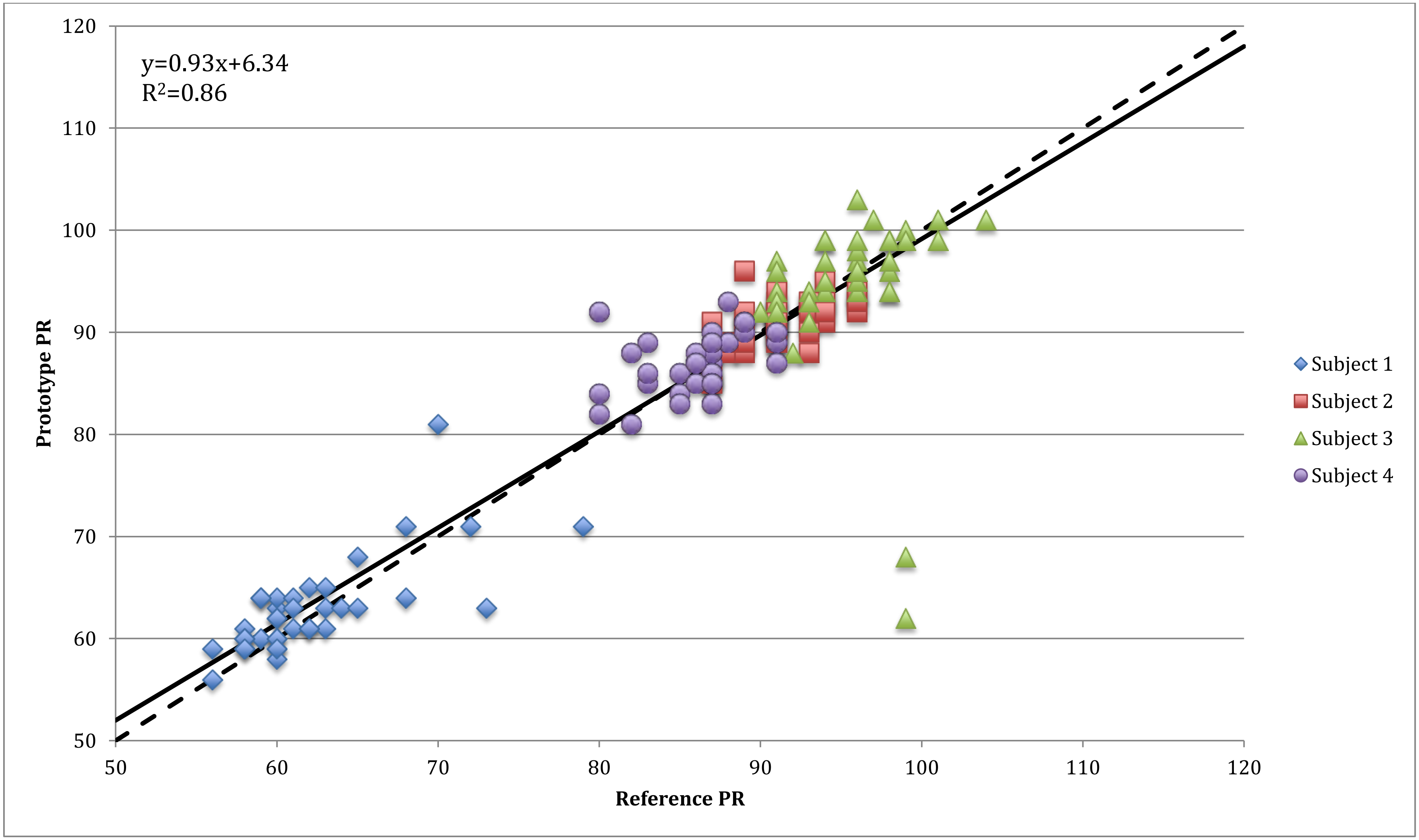

Figure 7.2: Comparison graph for the chest sitting tests. The solid line represents the regression line and the dashed line represents the identity line.

In Figure 7.3, a comparison plot referencing the data collected from our prototype on the chest of four different subjects while standing over a six minute period is displayed. The measuring scale ranges from 80 to 120 bpm with increments of 5 bpm. The linear regression equation and best fit coefficient are shown at the upper left corner. Similar to the regression line presented in Figure 7.2, the regression line in this comparison graph shows a slope very close to 1. The statistical coefficient of determination R^2, which is used in the context of statistical modeling for predictions, is a measure of how good a predicted value might be construed from the modeled values. A lower R^2 also shows that the correlation coefficient denoted as R, is lower than the sitting measurement shown in Figure 7.2.

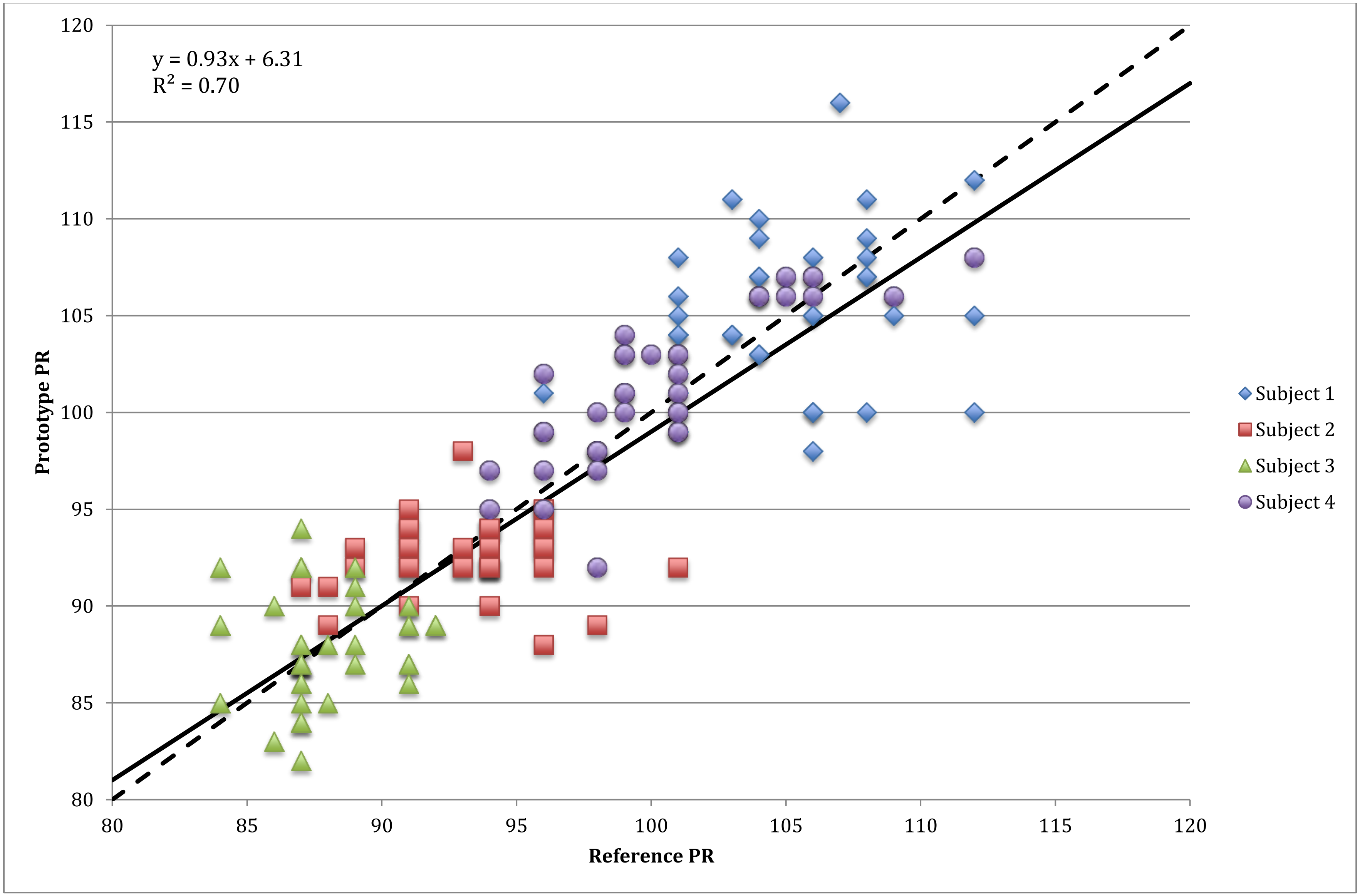

Figure 7.3: Comparison graph for the chest standing tests. The solid line represents the regression line and the dashed line represents the identity line.

Figure 7.4 displays a regression line for the PR data collected from our pulse oximeter prototype on the wrist against the HOMEDICS reference finger pulse oximeter on four different subjects over a six minute period while sitting. The data are clustered in four different groups, each one having a distinctive symbol corresponding to the subject tested. The measuring scale ranges from 50 to 120 bpm with increments of 10 bpm. The total PR data obtained from our prototype for all four subjects ranged from 52 to approximately 105 bpm. The graph displays the linear regression line and R^2 on the upper left corner. In this set of data we observed that the coefficient of variance, R^2, and in turn the coefficient of correlation, R, to be slightly lower than the values observed from the chest while sitting. When visually comparing the regression line to the line of identity, we can conclude that these measurements were not as accurate compared to the reference pulse oximeter.

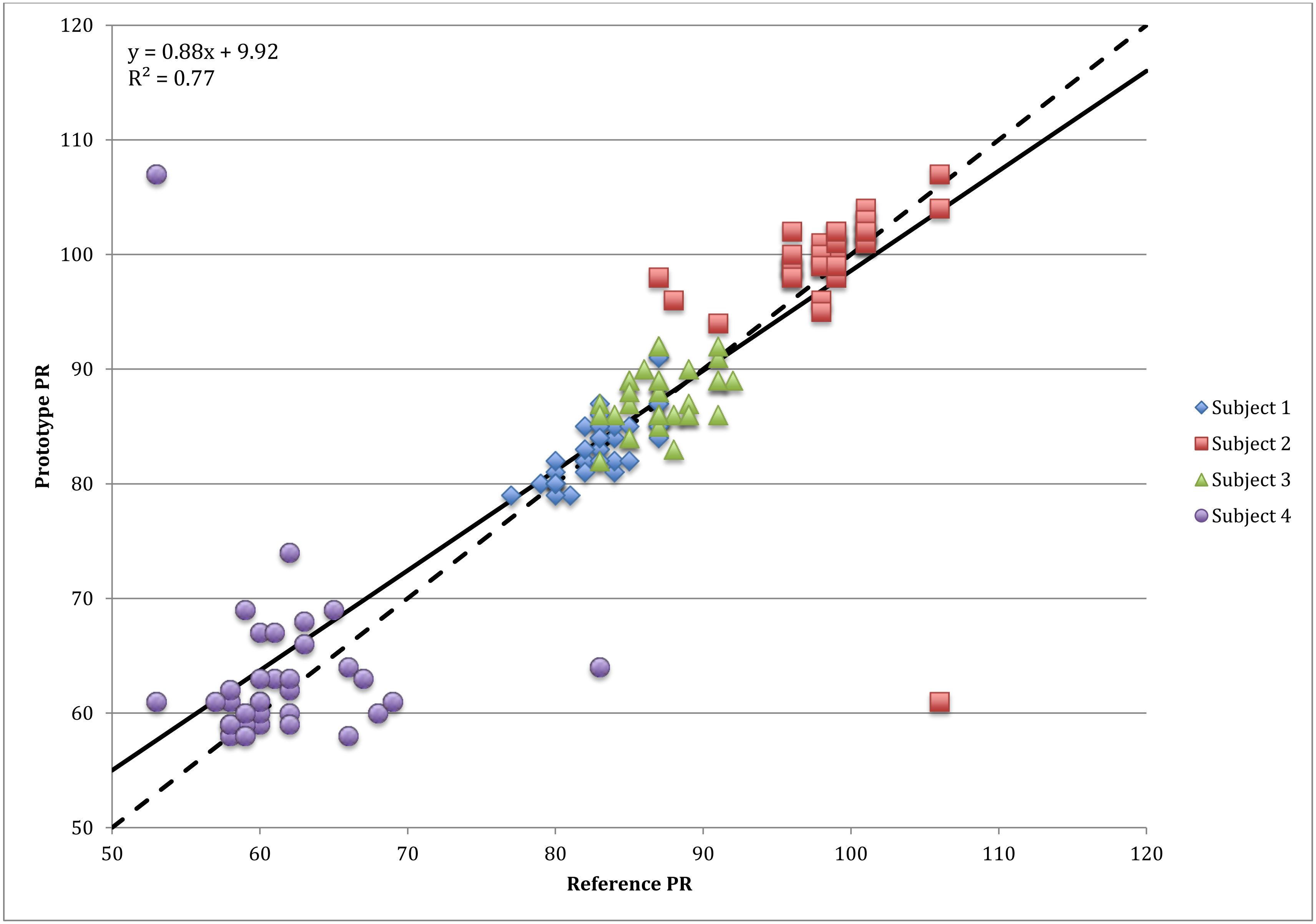

Figure 7.4: Comparison graph for the wrist sitting tests. The solid line represents the regression line and the dashed line represents the identity line.

In Figure 7.5 a comparison plot referencing the data collected from our prototype on the wrist of four different subjects over a six minute period while standing is displayed. The measuring scale ranges from 60 to 120 bpm with increments of 10 bpm. The linear regression equation and best fit coefficient are shown on the upper left corner. When comparing the standing wrist measurements to the sitting wrist measurements shown in Figure 7.4, we saw that the measurements obtained from the wrist while standing appeared to be the least correlated data set. Visually, there appears to be more variations between the identity line and the regression line than in other comparison graphs.

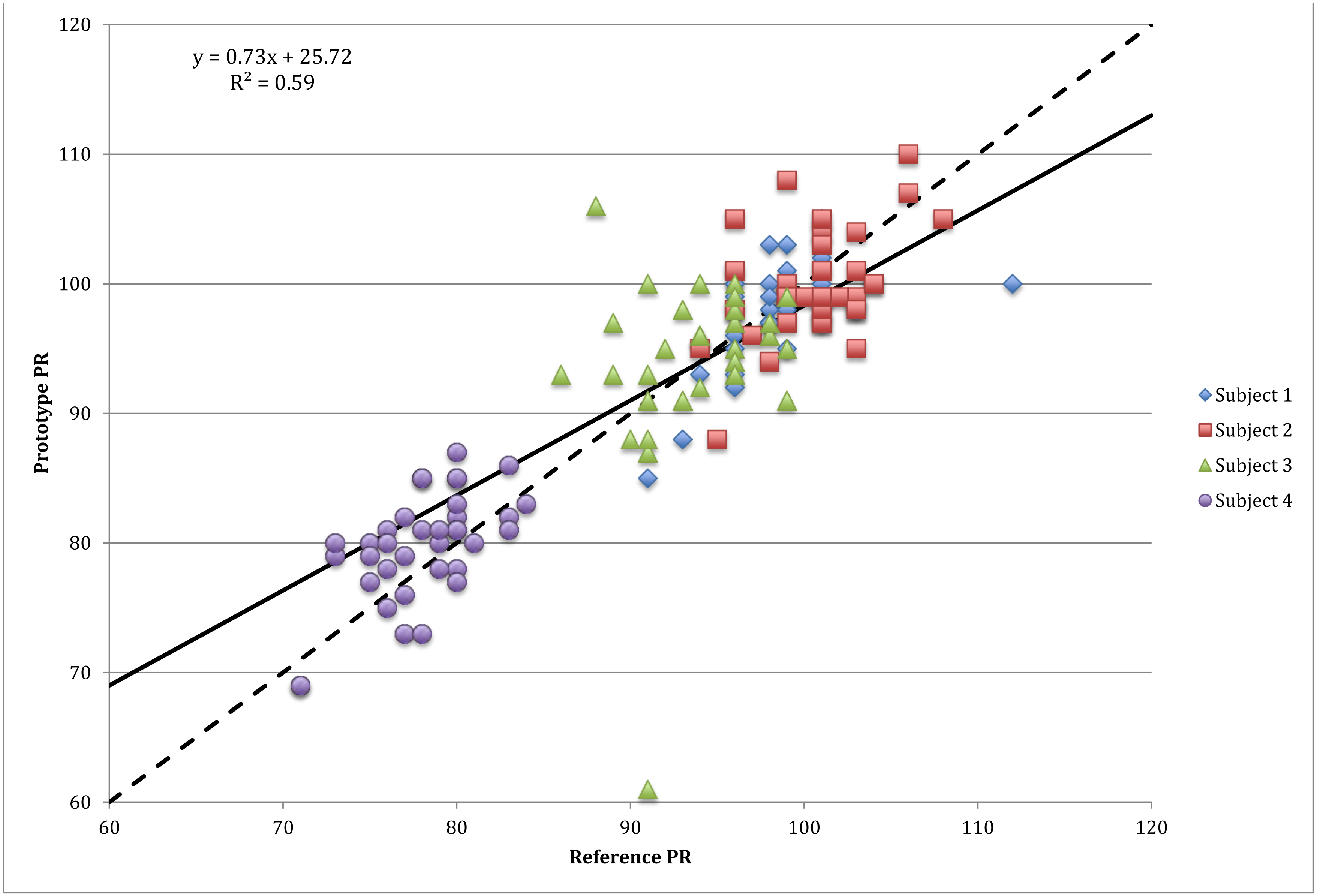

Figure 7.5: Comparison graph for the wrist standing tests. The solid line represents the regression line and the dashed line represents the identity line.

The plot displayed on Figure 7.6 shows the data points collected from our prototype on the wrist of four different subjects over a six minute period with the HOMEDICS reference device attached to the finger while hyperventilating. The measuring scale ranges from 50 to 140 bpm with increments of 10 bpm. The linear regression equation and best fit coefficient are shown at the upper left corner. One characteristic that is quickly observed when looking at this graph is that there is a lower accuracy in these measurements than in the previous graphs. This is visible in how the data points are distributed and the distance between points. Another aspect of these graphs that was noticed was that there appeared to be more outliers present in the data than in the other data sets.

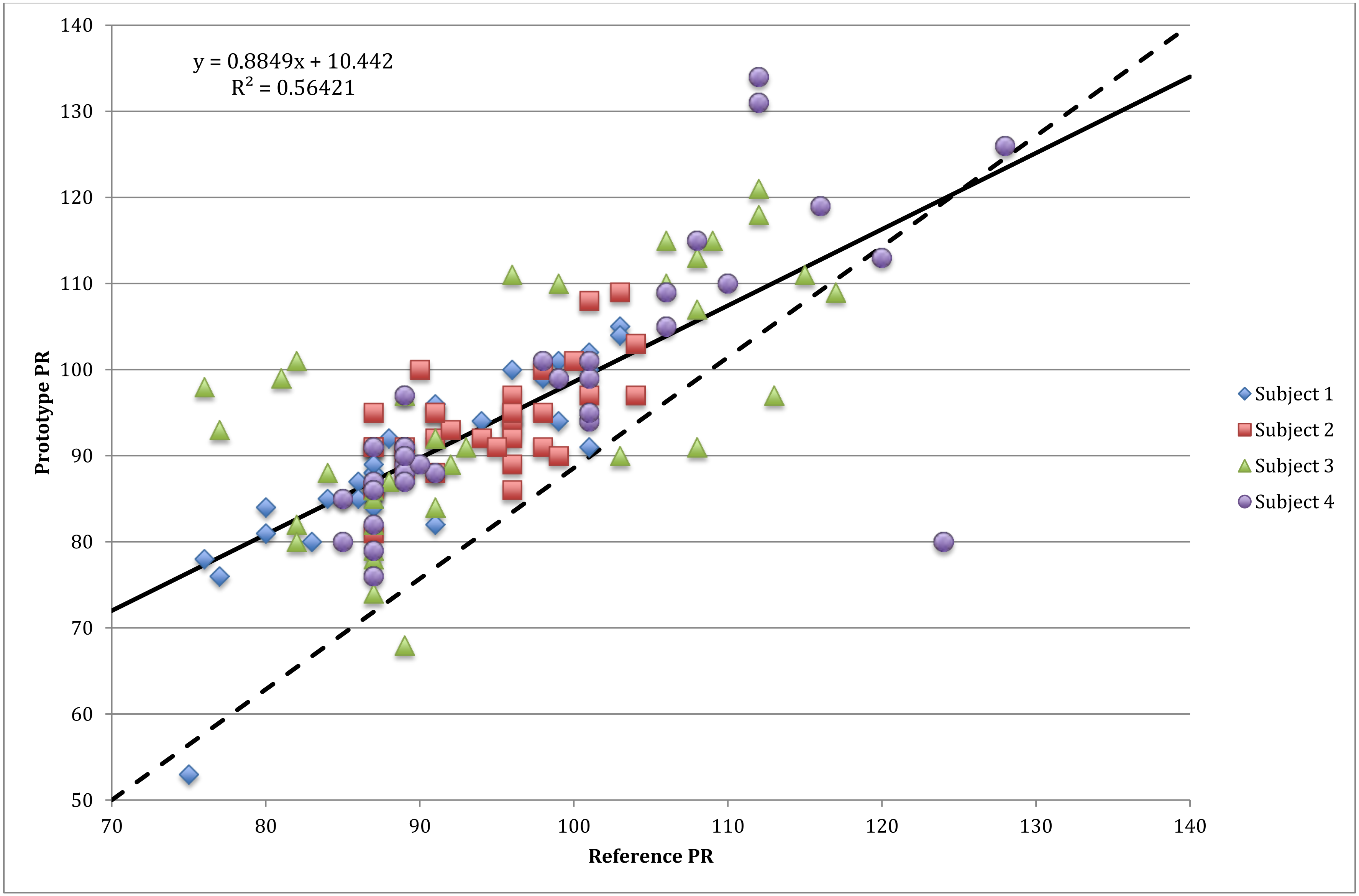

Figure 7.6: Comparison graph for hyperventilation tests

The hypoxia testing graph shown in Figure 7.7 was performed on 2 subjects capable of holding their breath for more than 40 seconds. SpO_2 readings were collected by our prototype pulse oximeter as well as by the reference HOMEDICS device. The measuring percentage scale ranged from 90 to 100 with increments of 1%. Regression line equation and best fit line coefficient are given at the upper left corner. For the purpose of plotting a regression line for SpO_2 we found it very difficult to correctly plot a regression line when the data had only a 10% range. Considering that for the majority of testing the subjects maintained a SpO_2 level of 97 or 98% we were only able to measure several small dips to assess the responsiveness of our device to changing SpO_2 levels. To correctly plot a regression line, one would need to change the SpO_2 levels over a larger range such as 70-100% in order to have a better idea of how well our device compares to the reference pulse oximeter.

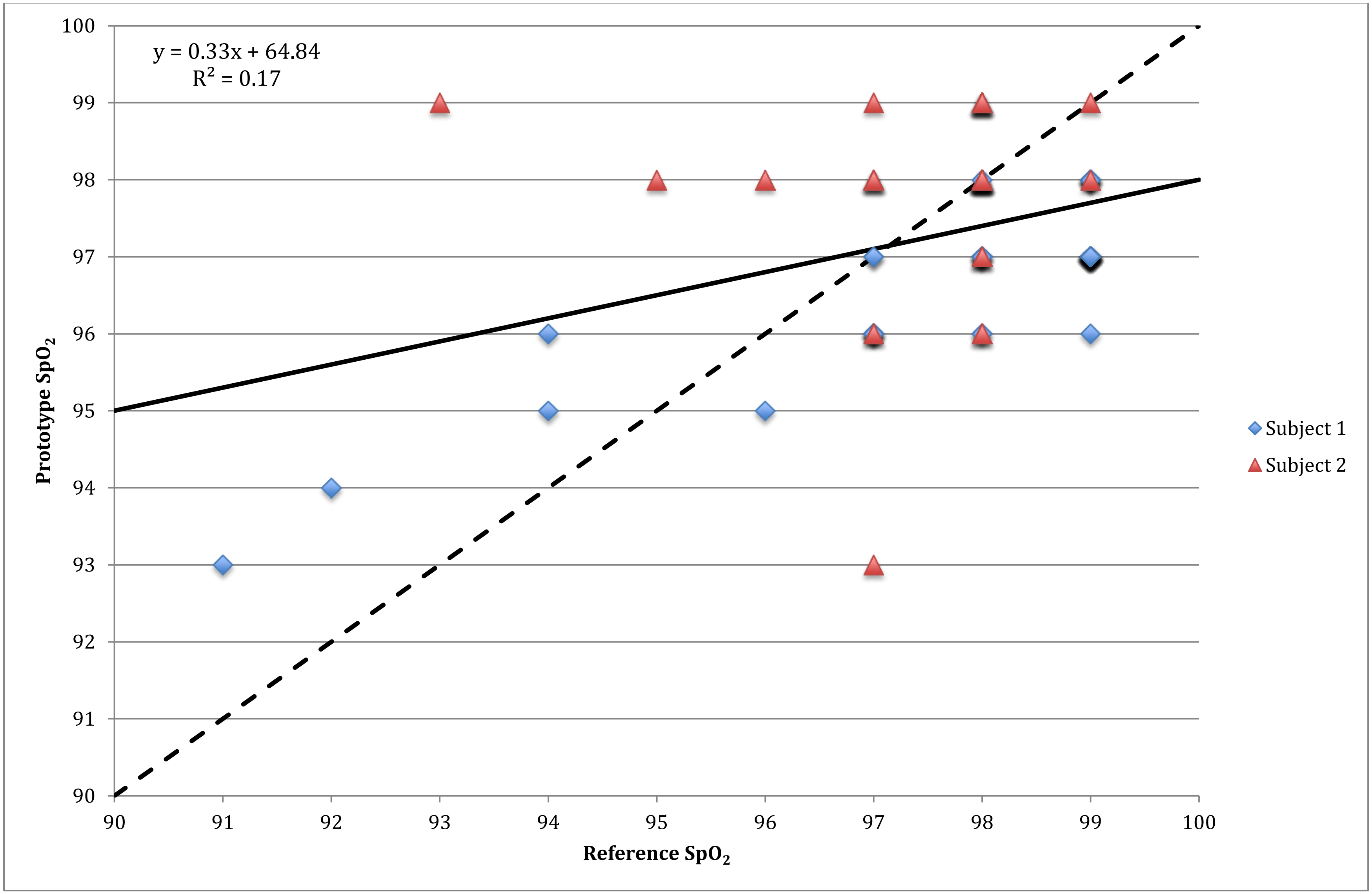

Figure 7.7: Comparison graph for hypoxia tests. The solid line represents the regression line and the dashed line represents the identity line.

7.2 Dynamic Response Plots

Dynamic response plots were utilized in analyzing the data because they show the prototype's response to changing levels of PR and SpO_2 over time. These plots in particular were utilized for all of the measurements to better understand how our device reacts to varying PR. The fact that the SpO_2 levels varied very little in most of the measurements doesn't provide any real indication as to whether the prototype is able to response to changing levels of SpO_2. To address this, we performed hypoxia tests in which we saw the SpO_2 level drop to around 90 and plotted those results.

Figures 7.8 and 7.9 depict the SpO_2 and PR measurements during the 6 minute testing period respectively. Although the only information we can obtain from Figure 7.8 is that the SpO_2 remained constant throughout the entire measurement, Figure 7.9 shows the prototypes response to changing levels of PR. One feature that was observed was that at times when the PR would ramp up, the prototype would instead ramp downwards towards a smaller PR. In fact, it was observed that this occurred 5 times during the measurement period.

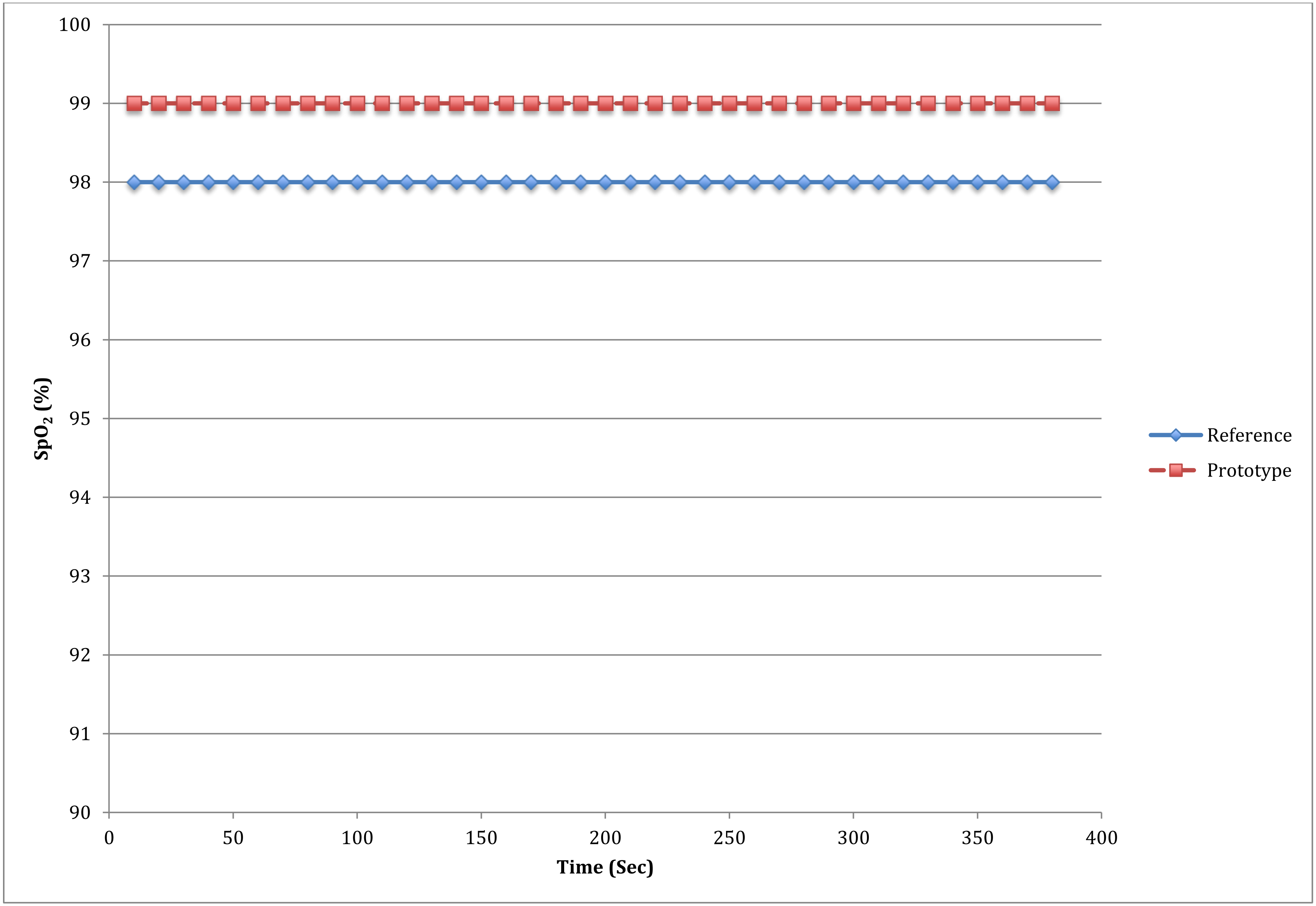

Figure 7.8: Oxygen saturation measurement validation plot for the chest standing test

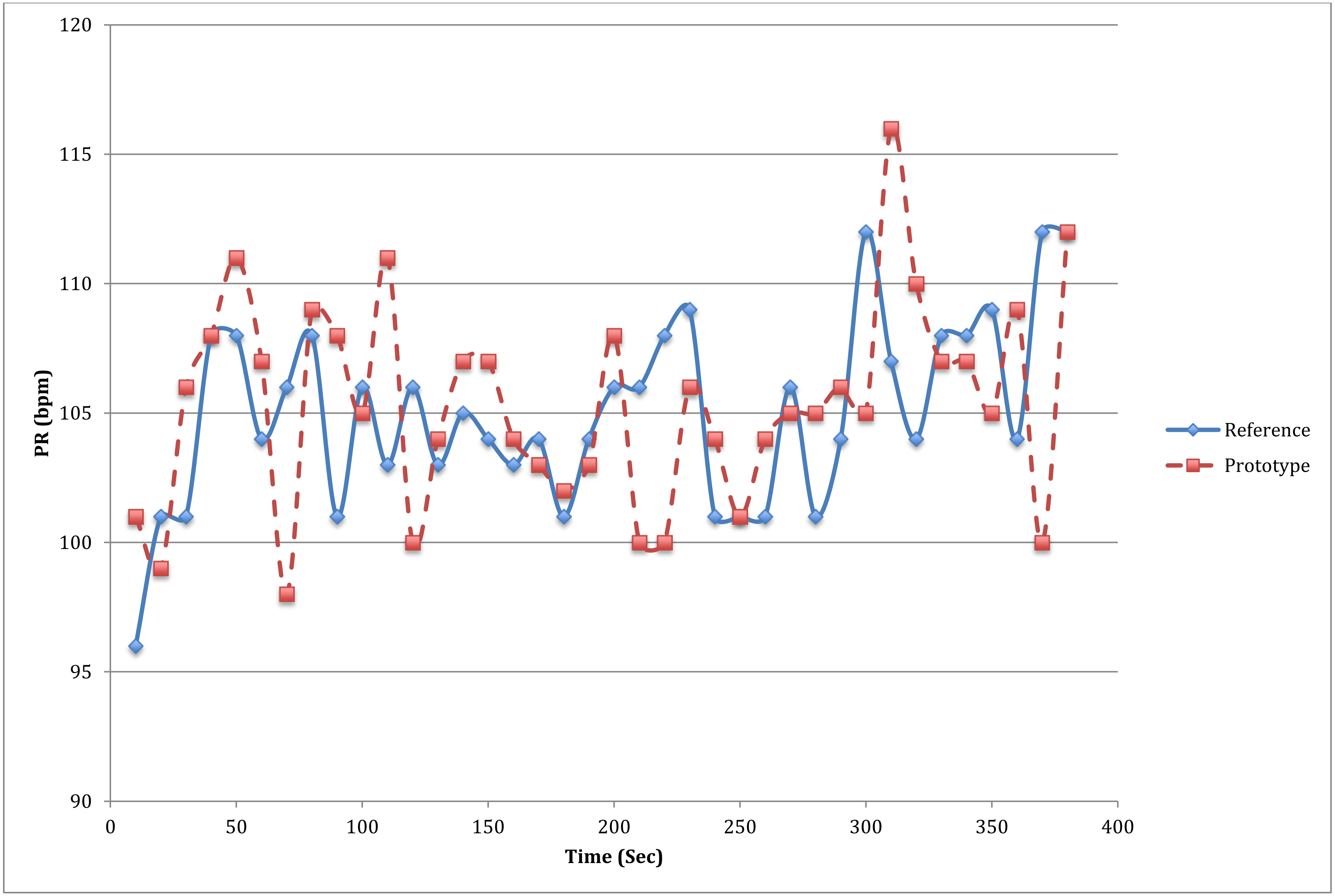

Figure 7.9: Pulse rate measurement validation plot for the chest standing test

Figures 7.10 and 7.11 display the dynamic response plots for the chest measurements of one subject while sitting. Although it was observed that the prototype's measurements bounced around 98% and 99%, this still doesn't give us any real interpretations as to how the prototype can handle different values of SpO_2. Figure 7.11 displays the changing PR measurements over time, depicts the variations in PR of an individual at rest. We did notice from this chart that while our prototype appeared to be following the general trend of data and PR variability, there was indeed quite a number of errors in the measurements. Some cases of overshooting and undershooting were observed as well as certain data points which appeared to almost be delayed PR values of the reference pulse oximeter.

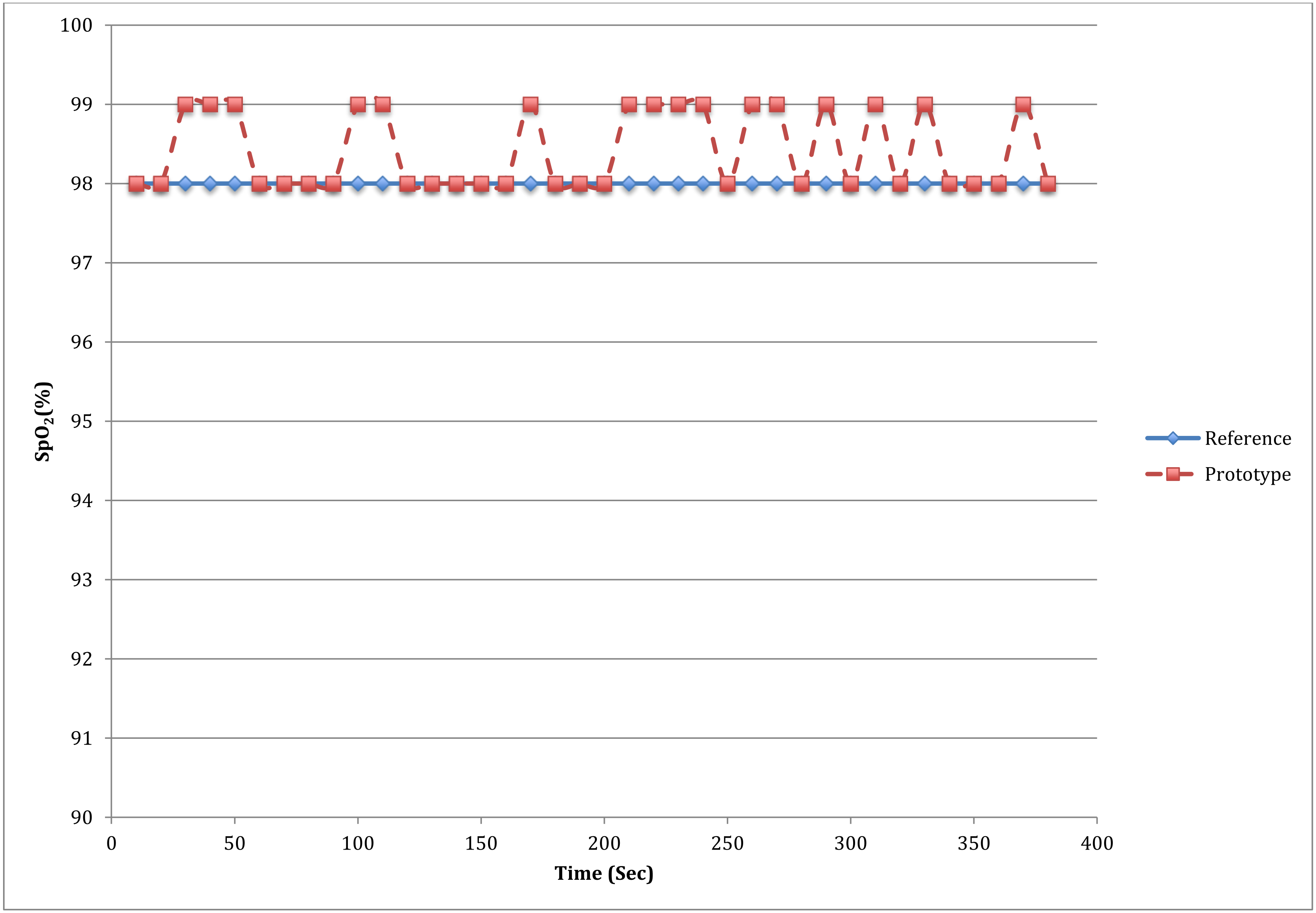

Figure 7.10: Oxygen saturation measurement validation plot for the chest sitting test

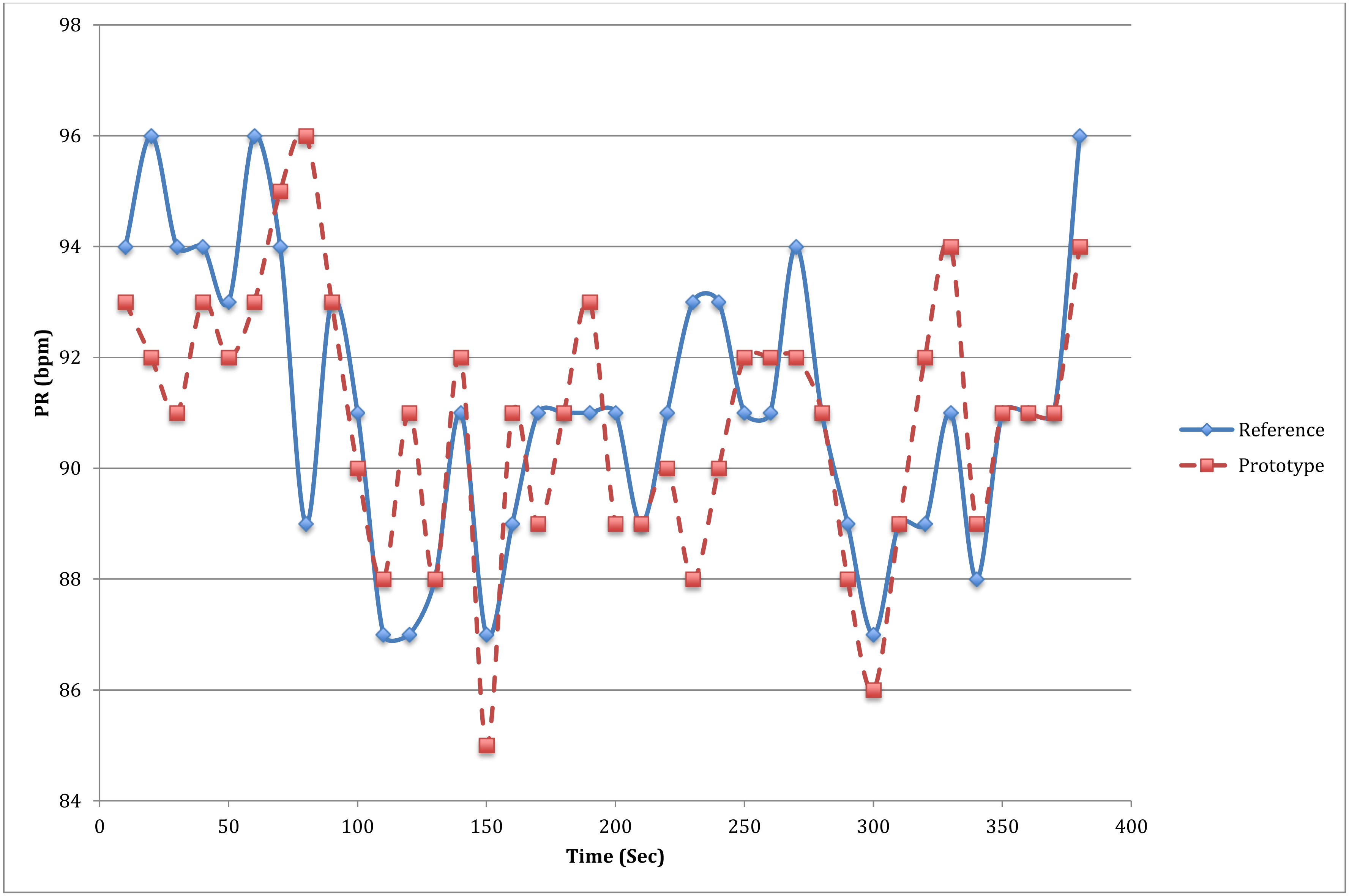

Figure 7.11: Pulse rate measurement validation plot for the chest sitting test

Figures 7.12 and 7.13 display the dynamic response plots for the hyperventilation trials. Both figures display varying PR's for two subjects during the 6 minute measurement period. Plot 1, depicted as Figure 7.12 shows a very high correlation between the prototype and the reference pulse oximeter. This is evident in the proximity of the data points between the prototype and reference pulse oximeter as well as the general trend that the chart follows. However, it was noticed that at 80 seconds, there was an unexplained drop in PR from the 75-80 range to a PR value of 53. The reason for this was believed to be due to corrupted PPG signals during that 10 second duration of measurements. Figure 7.1 shows how a corrupted PPG signal appears. Since our method for calculating PR is by searching for the highest amplitude around a specific frequency, any high frequency noise presented either through ambient light picked up by the sensor or by motion artifacts would slant the power spectrum of the signal which in turn would provide false PR calculations for that interval of data. Figure 7.13 shows similar drops in PR as well due to corrupted PPG signals. One difference observed in Figure 7.13 was that the data were not as closely correlated as in Figure 7.12.

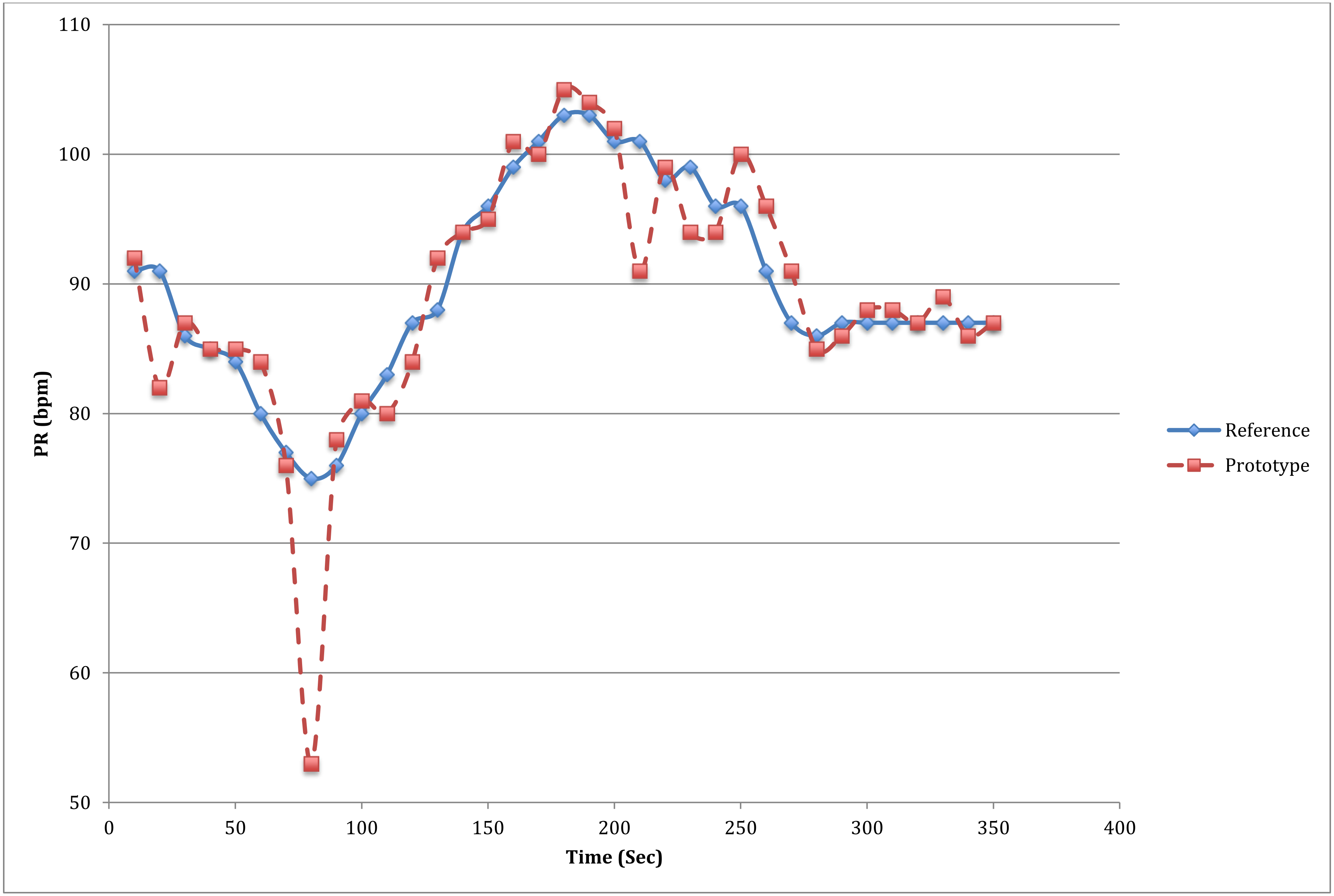

Figure 7.12: Pulse rate measurement validation plot 1 for hyperventilation test

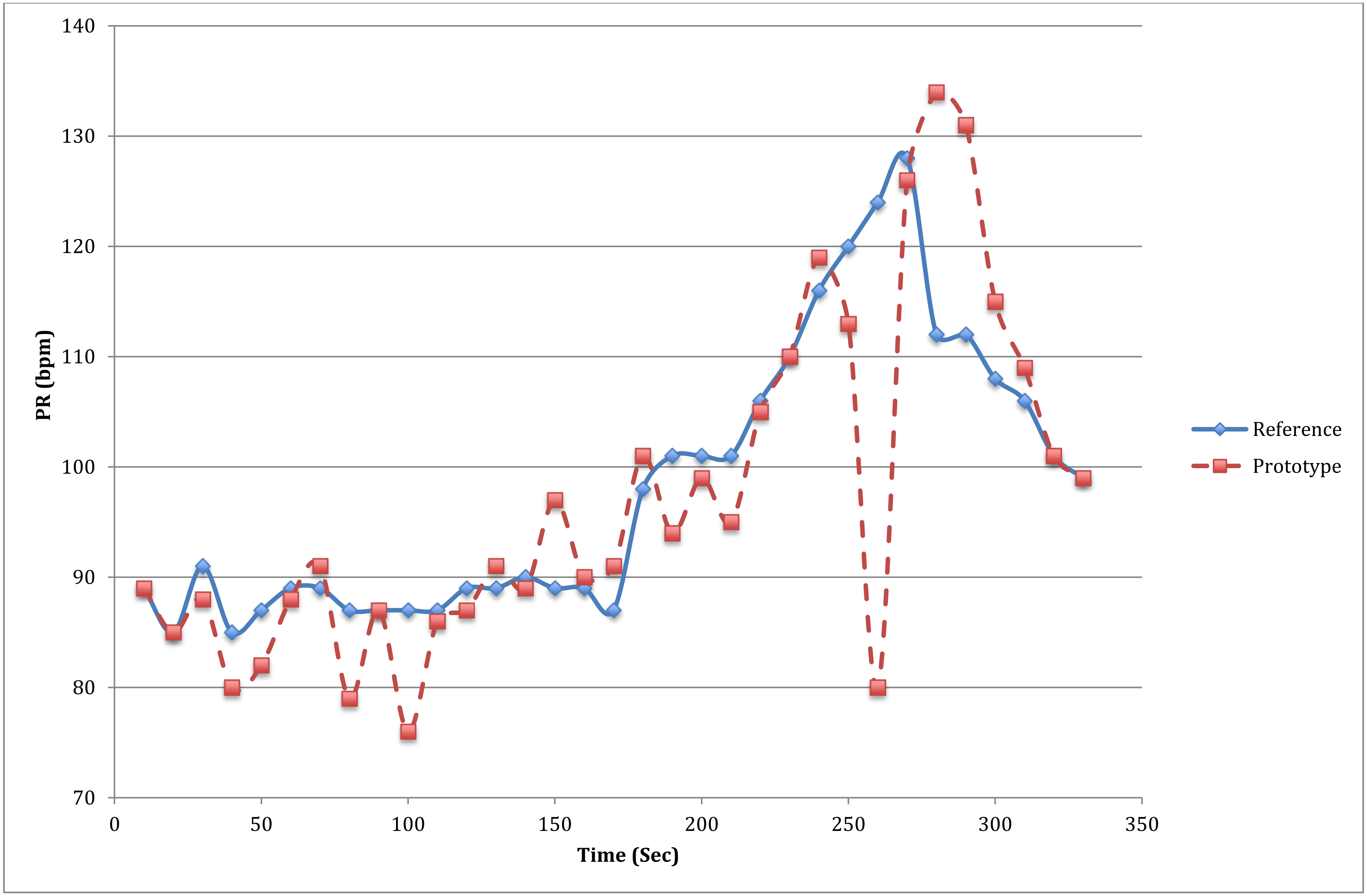

Figure 7.13: Pulse rate measurement validation plot 2 for hyperventilation test

Figures 7.14 and 7.15 depict the PR and SpO_2 measurements during the 6 minute testing period from the wrist as the subject was sitting, respectively. Figure 7.14 shows the prototypes response to changing levels of PR. In general this set of data appears to be very closely correlated and only contains one measurement in which the PR overshoots the reference by about 4bpm. In Figure 7.15 we can observe a small dip at the beginning of the measurements in the SpO_2 but otherwise, the SpO_2 levels stayed constant throughout the entire measurement.

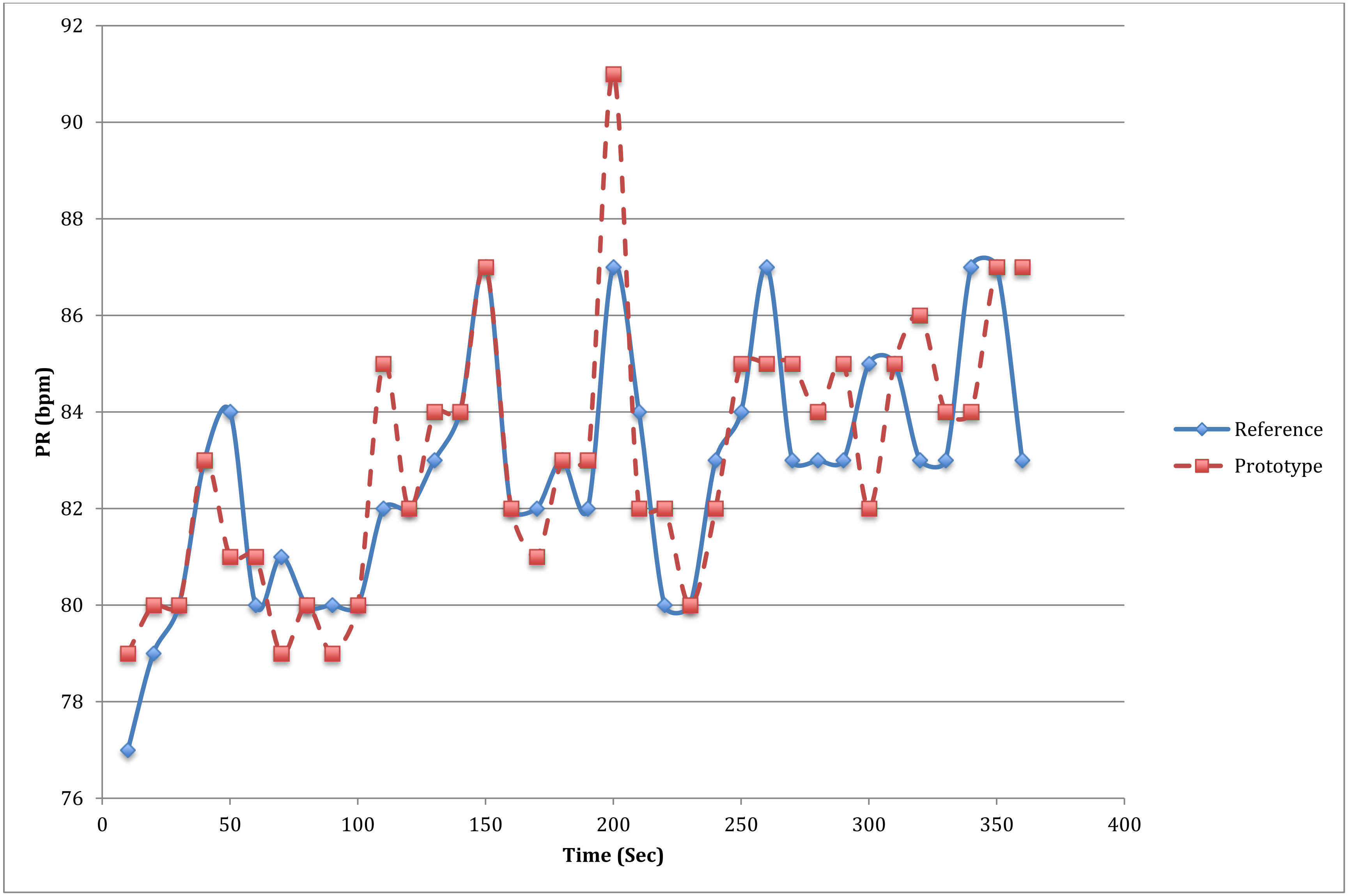

Figure 7.14: Pulse rate measurement validation plot for the wrist sitting test

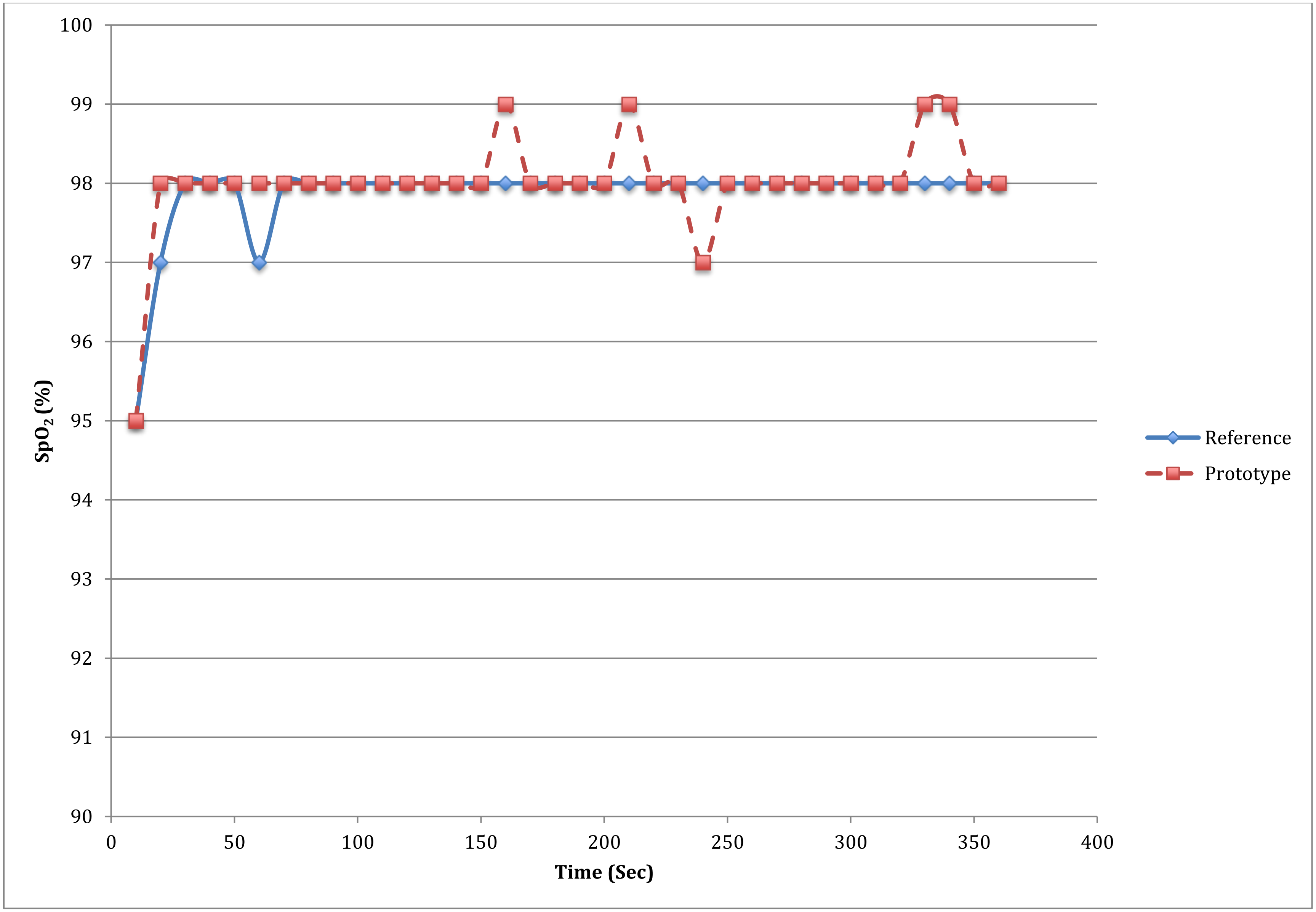

Figure 7.15: Oxygen saturation measurement validation plot for the wrist sitting test

Figures 7.16 and 7.17 depict the SpO_2 and PR measurements during the 6 minute testing period from the wrist as the subject was standing. In Figure 7.16 we observe a constant bouncing of SpO_2 between 98 and 99% for our prototype and a dip in SpO_2 at around 2 minutes into the measurements. Figure 7.17 shows the prototypes response to changing levels of PR while the subject was standing. Apart from two moments of undershooting in which the value displayed on the prototype was lower than the value displayed on the reference device, the rest of the data appeared to be slightly less well correlated than when the subject was sitting.

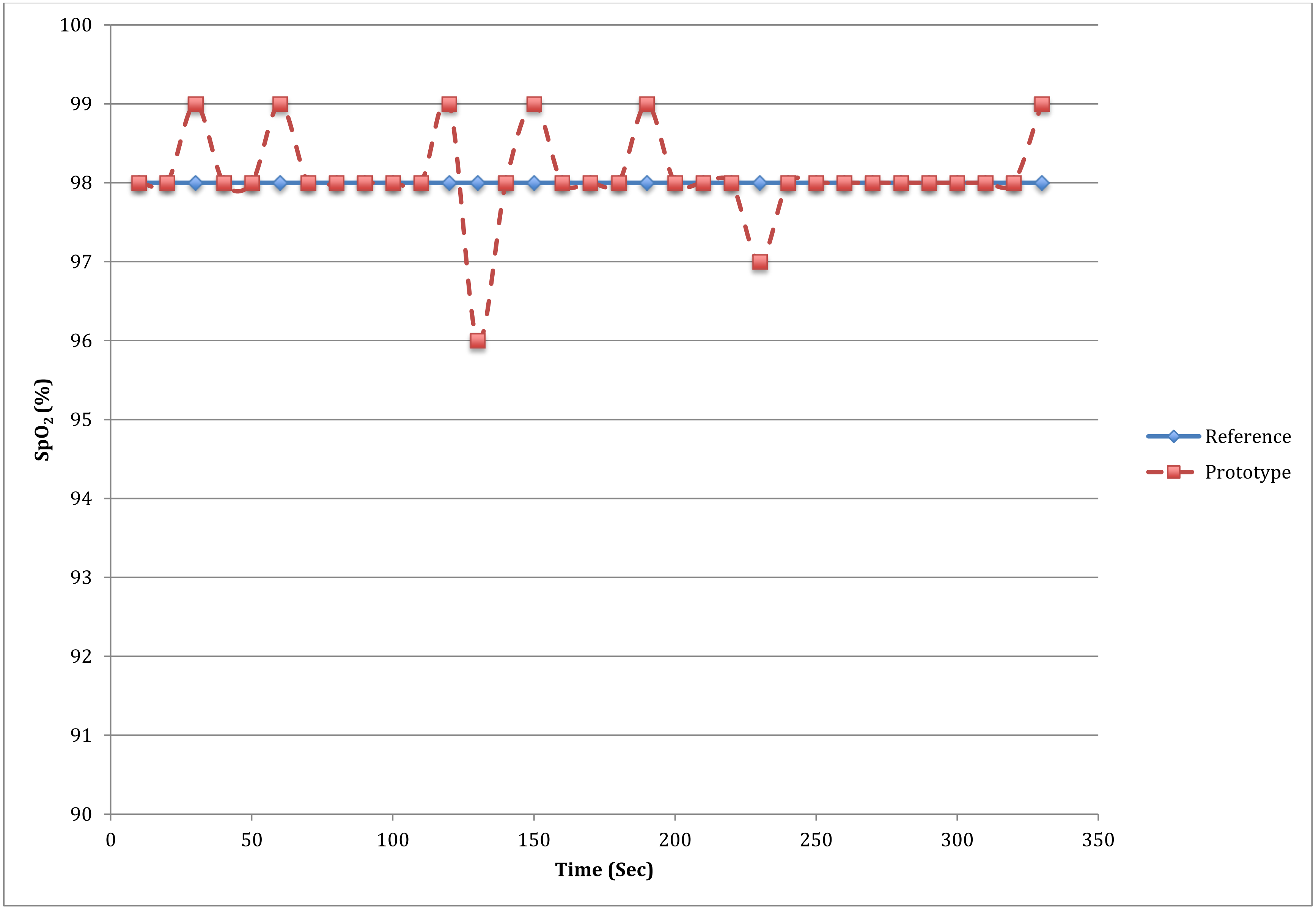

Figure 7.16: Oxygen saturation measurement validation plot for the wrist standing test

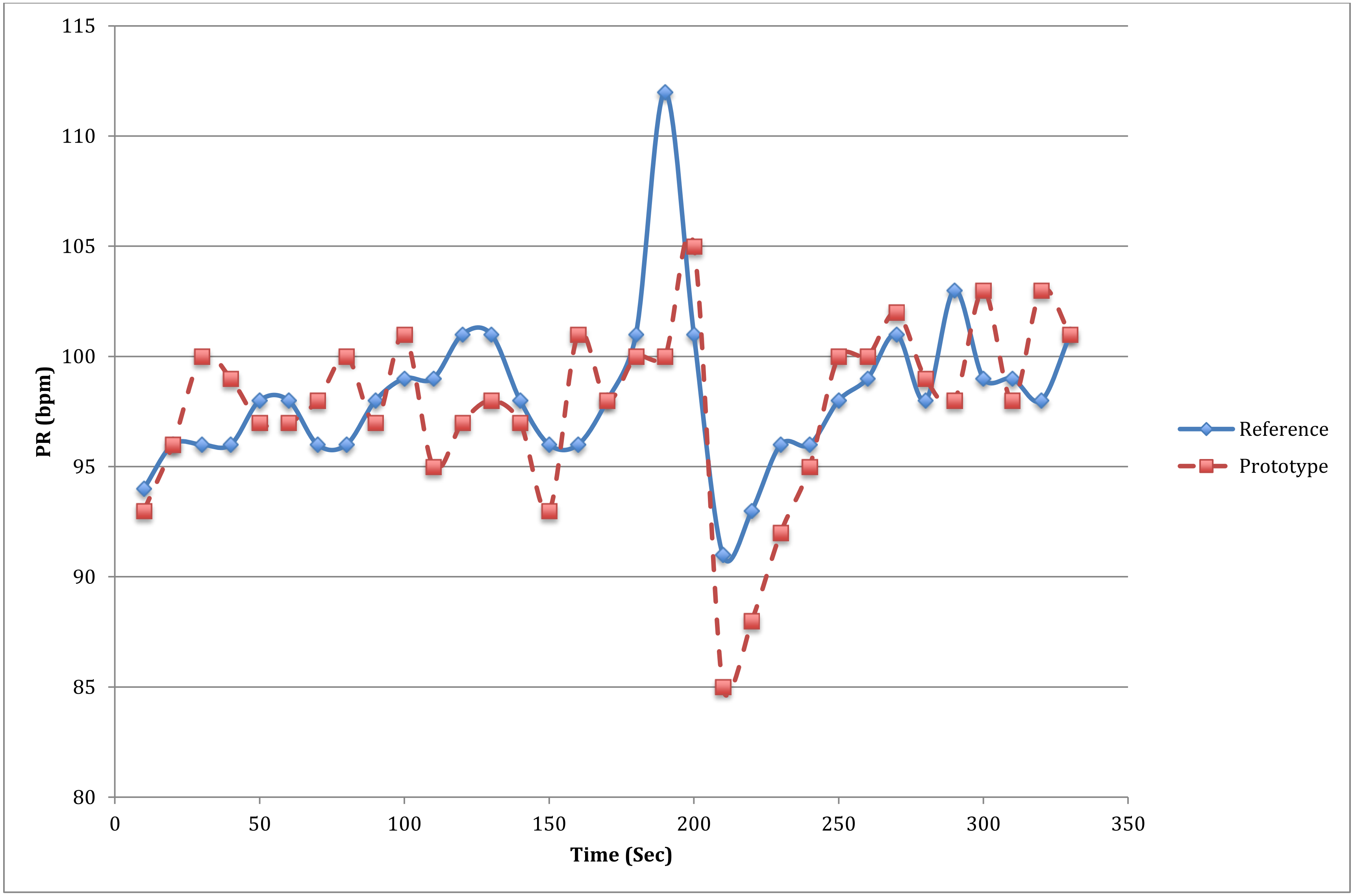

Figure 7.17: Pulse rate measurement validation plot for the wrist standing test

To accurately see how well our device responded to sudden drops in SpO_2 we asked our subjects to hold their breaths for 45 seconds in hopes that a drop in SpO_2 could be observed. Figures 7.18 and 7.19 display two separate plots for induced hypoxia. In Figure 7.18 the moment of induced hypoxia can be observed at around 120-160 seconds in which the SpO_2 dropped from 99 to 91% in the reference pulse oximeter and 97 to 93% for the prototype. While the drop in SpO_2 for the prototype was not as sudden as it was for the reference pulse oximeter, it does in fact validate the claim that our prototype does respond to changing levels of SpO_2. In Figure 7.19 we observe two moments of induced hypoxia, once at 150 seconds and later at 230 seconds. We also observed what appeared to be a delay between our prototype and the reference pulse oximeter when the drops in SpO_2 occurred.

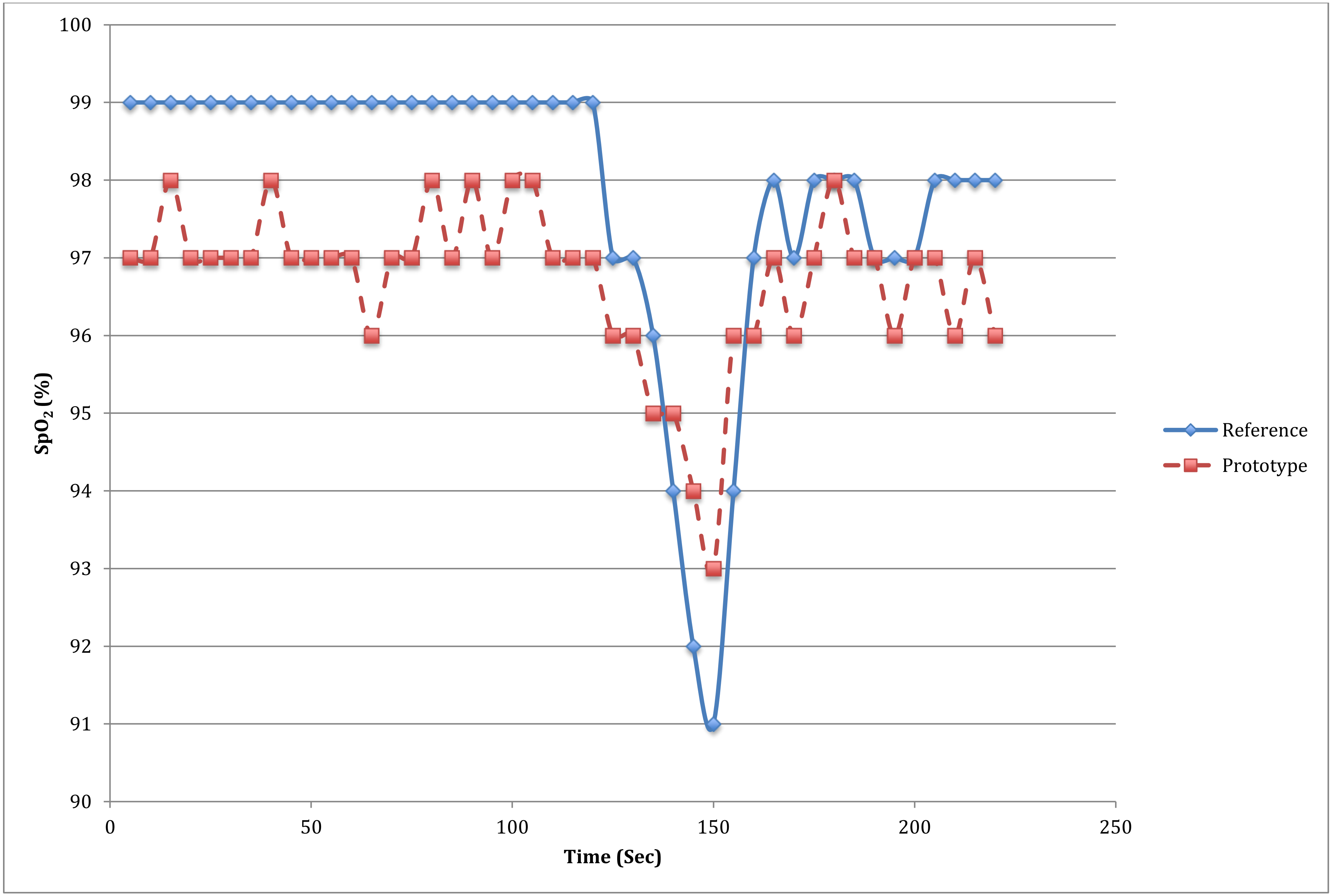

Figure 7.18: Oxygen saturation measurement validation plot 1 for hypoxia test

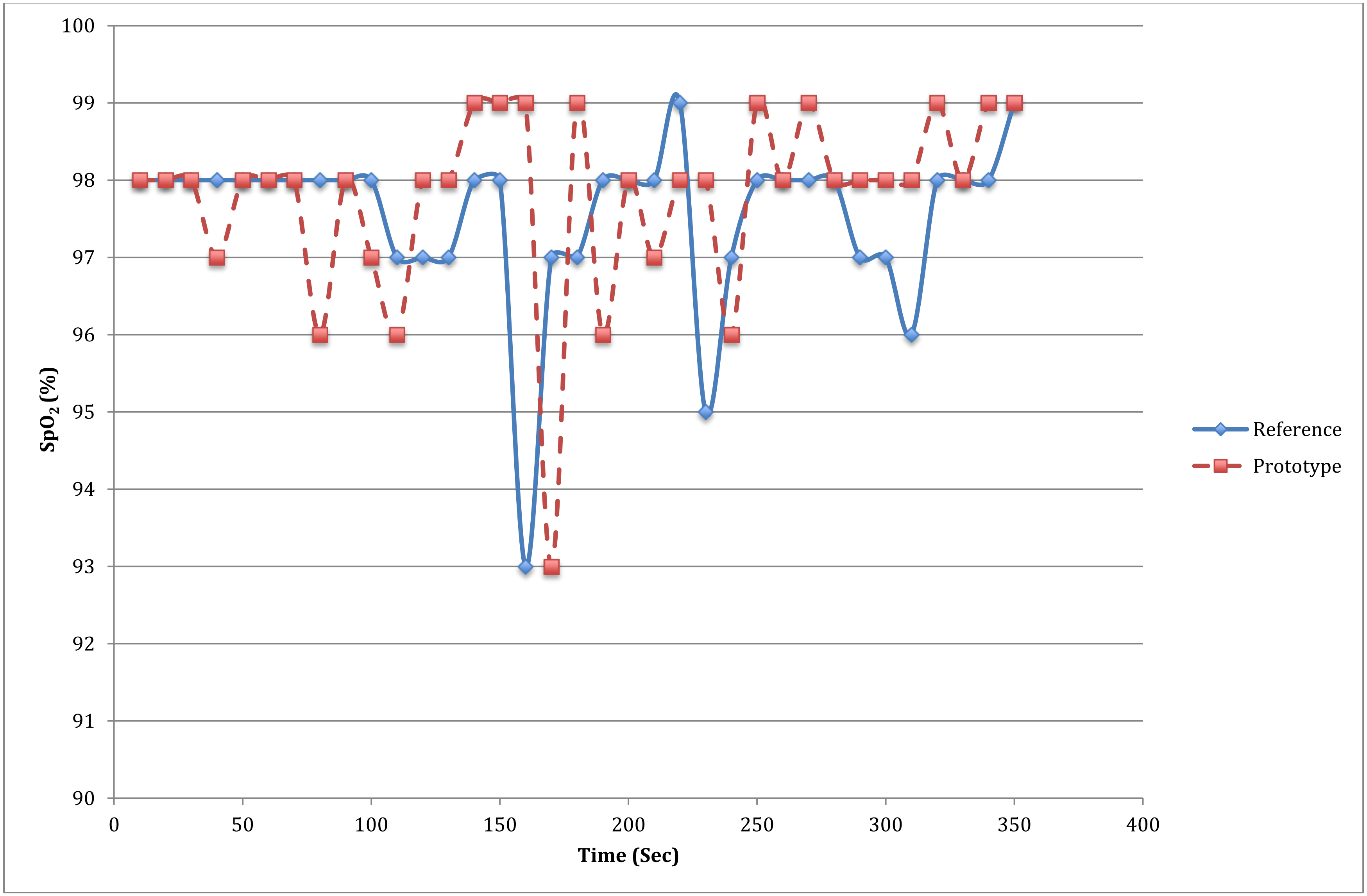

Figure 7.19: Oxygen saturation measurement validation plot 2 for hypoxia test

7.3 Residual Plots

Residual plots were also utilized in analyzing the hypoxia and hyperventilation tests. To graph the residual plots, we calculated the average between the observed measurements from the reference device and our prototype, the difference between each observed measurement, the average of the difference between each observed measurement number, and the standard deviation of the differences. Using these calculations we then plotted the averages of the individual measurements on the horizontal axis and the difference between measurements on the vertical axis. A solid black line was then plotted to represent the average of the differences, and two dashed black lines to represent $\pm$ 2 standard deviations around the average of the difference of measurements. Figures 7.20, 7.21 and 7.22 show the residual plots for the hyperventilation testing. All of these plots show that at least 95% of the data falls within the two standard deviations meaning that the differences between the reference device and the prototype are normally distributed. Although 95% of the data in each figure does fall within the two standard deviations, Figure 7.22 shows the best representation of a high correlation between the reference device and the prototype. Most of the data shown in that plot is much closer to the average of the differences, shown as the black solid line.

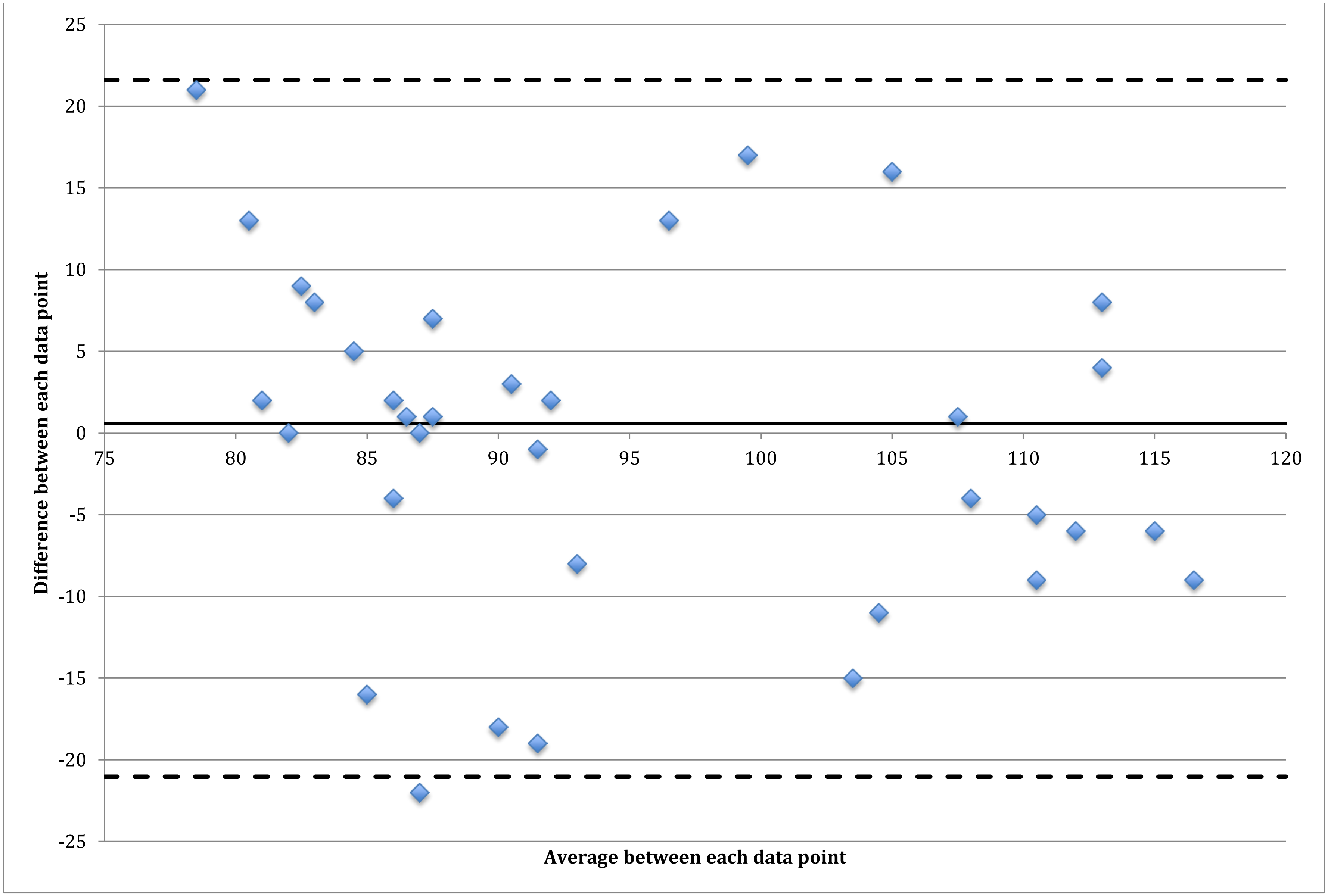

Figure 7.20: Residual plot for hyperventilation testing for data set 1 (dotted lines: $\underline{+}$ 2SD, solid line: average of differences)

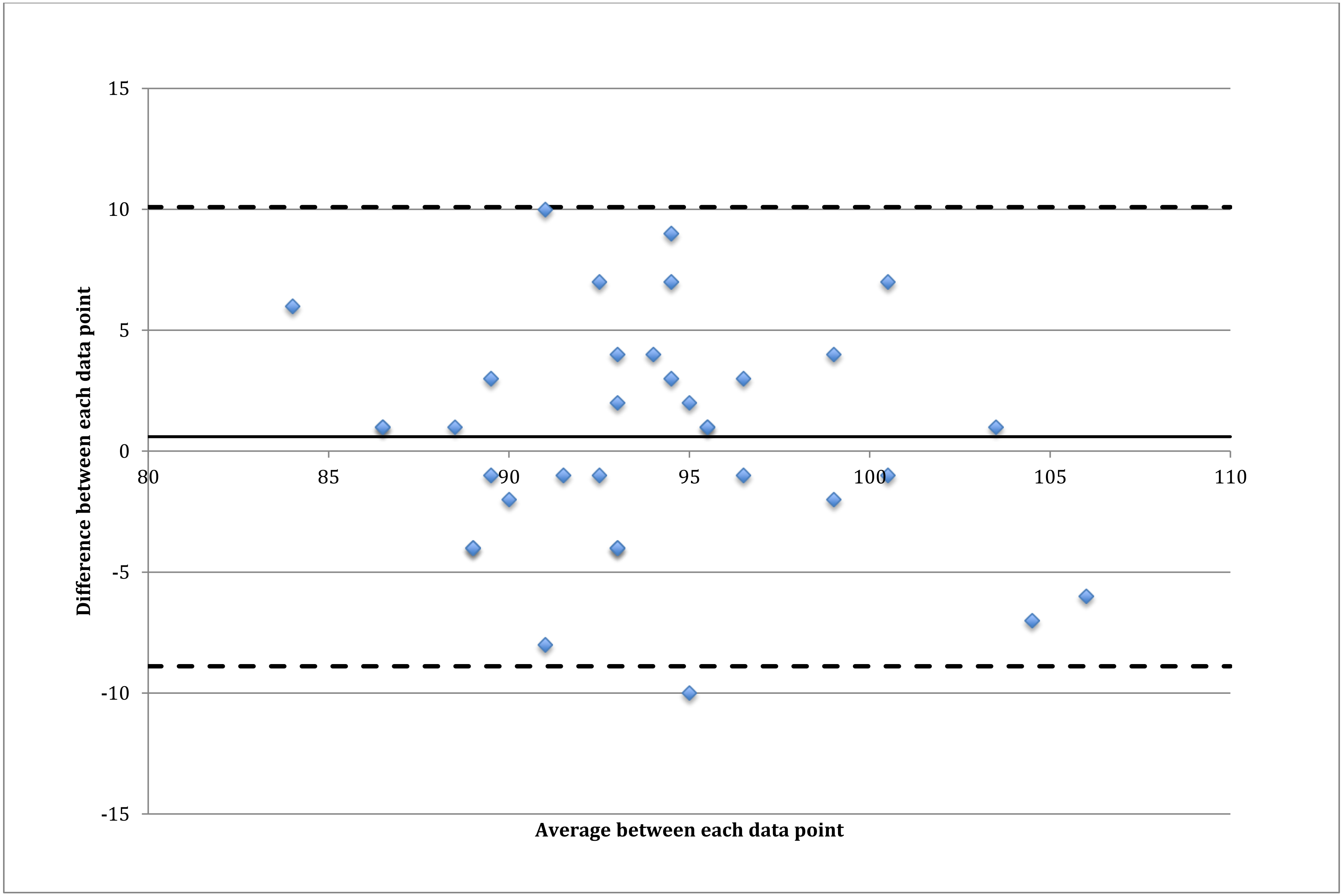

Figure 7.21: Residual plot for hyperventilation testing for data set 2(dotted lines: ± 2SD, solid line: average of differences)

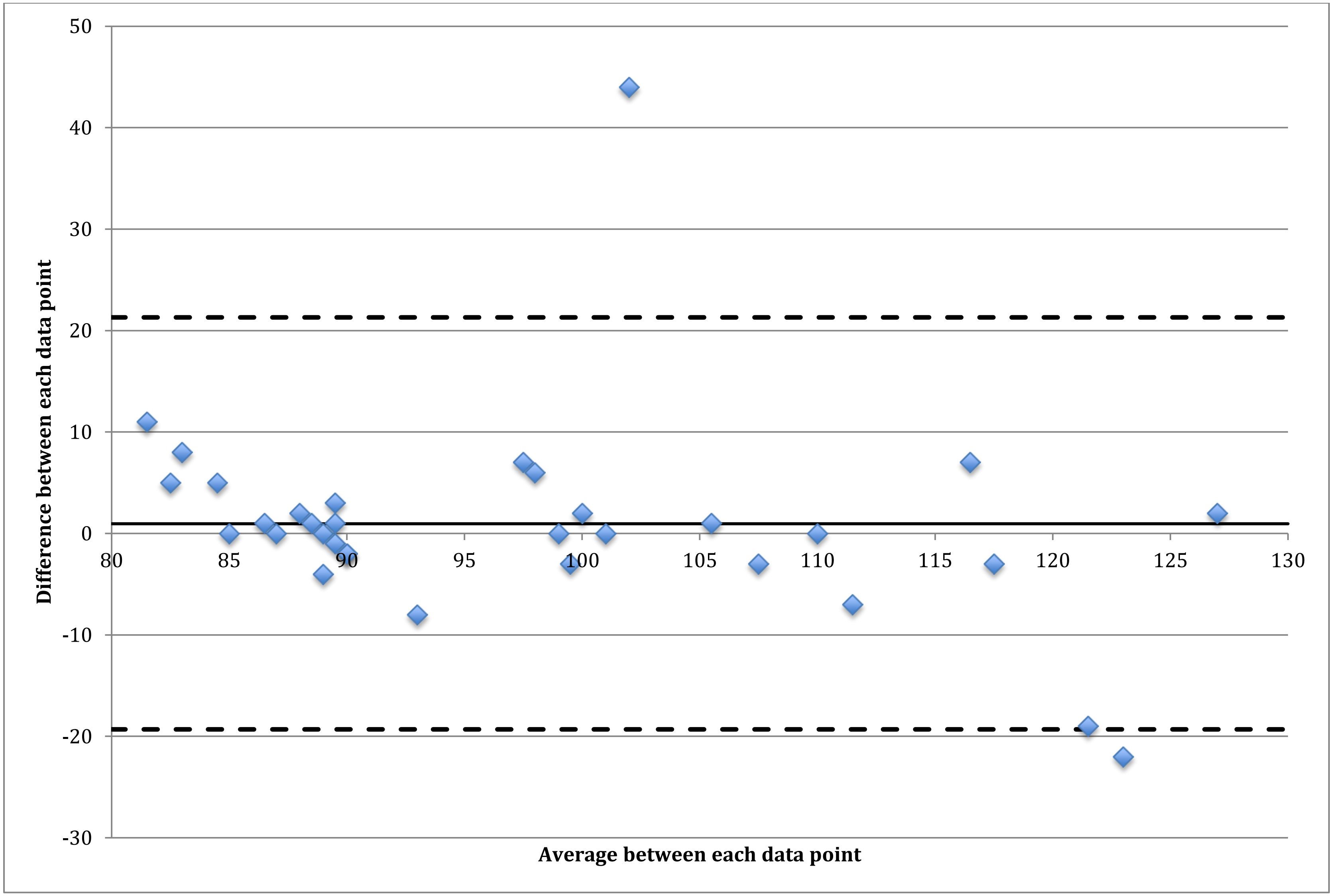

Figure 7.22: Residual plot for hyperventilation testing for data set 3 (dotted lines: $\pm$ 2SD, solid line: average of differences)

Figures 7.23 and 7.24 show the residual plots for the hypoxia testing. The data in both plots appear to be slanted to one side due to there not being a large enough SpO_2 range to effectively measure. However, one positive to note from these plots is that the majority of the residuals in both plots appear to fall within two standard deviations of the average difference.

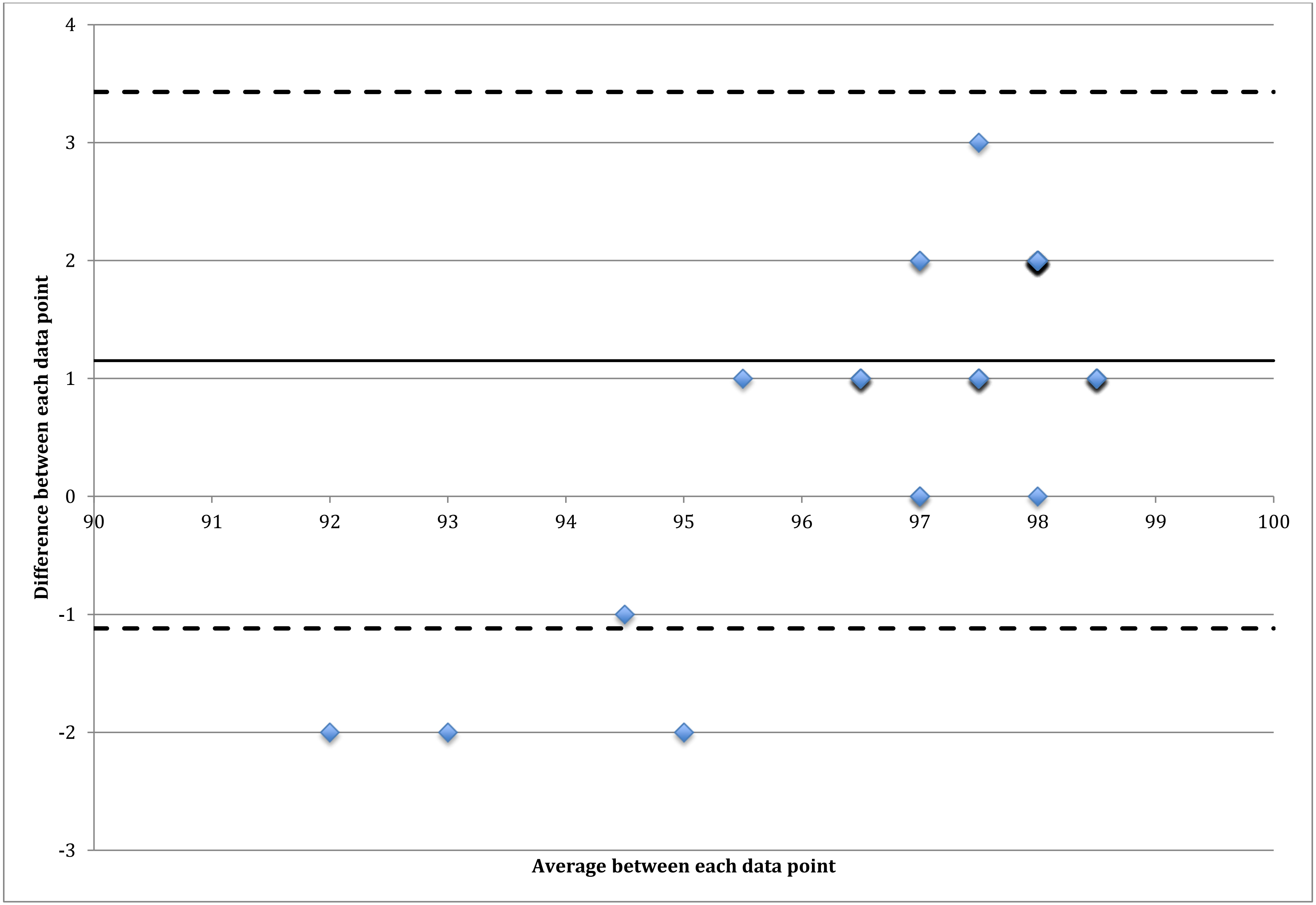

Figure 7.23: Residual plot for hypoxia testing for data set 1 (dotted lines: $\pm$ 2SD, solid line: average of differences)

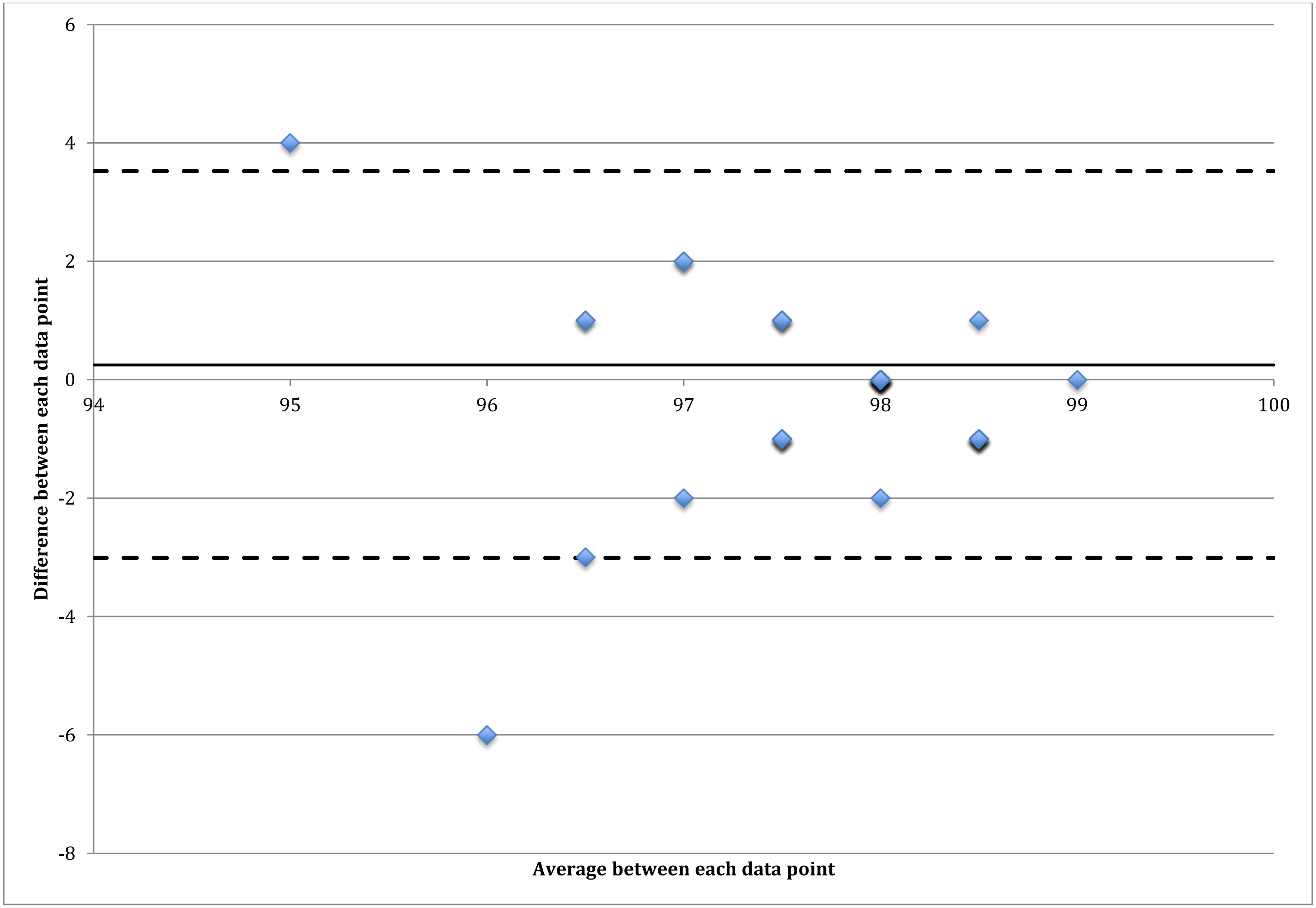

Figure 7.24: Residual plot for hypoxia testing for data set 2 (dotted lines: ± 2SD, solid line: average of differences)

8 Discussion

When creating a device such as a pulse oximeter which requires the acquisition of signals such as PPGs, it is difficult to ensure the integrity of the signals that are acquired. This causes the placement of the sensor on the wrist and chest to be very important. We were able to obtain fairly strong PPGs from the wrist and chest because of the stronger signals due to the high levels of bone and subcutaneous tissues in these locations.

The summarized results suggest that recorded wrist measurements were more accurate than chest measurements. For the standing and sitting measurement tests obtained from the wrist, the errors obtained were 0.6%, and 0.2% for SpO_2 and 0.2%, 1.1% for the PR, respectively. While the measurements from the chest obtained errors of 0.4% and 0.3% for SpO_2 and 0.1%, and 0.7% for the PR, respectively for the same test conditions. There are many factors that could contribute to the difference in the percent errors for the two different locations. When the sensor was placed on the wrist, it was placed over the radial artery which could have given stronger signals as opposed to those gathered from the chest where the sensor was simply placed over the sternum. One factor noticed was when the sensor is placed on the chest, the device became subject to increased motion artifact from breathing. The motion the chest makes when each subject took a breath in some cases moved the device on the skin and could have also prevented it from being in constant contact with the skin. Another factor that could have affected this is the pressure at which the device was strapped on. If there was too much or too little pressure, the signal strength could change, in turn changing the results. For this device to be considered a success, the percent error for all tests must remain at ±3. Although these factors did not affect the accuracy of the device in an extremely negative way as displayed in the results, they were cause for a slightly higher percent error in data taken from the chest. In these cases it was noticed the sensor would allow ambient light to be picked up by the photodetectors. It was observed that when this occurred, the sensor output would completely saturate due to the high amplification we utilized for signal analysis.

The standard tests of standing and sitting while taking measurements from the chest and wrist showed that the prototype could accurately and continuously measure SpO_2 and PR. While the hypoxia and hyperventilation tests demonstrated that the prototype can respond to various SpO_2 and PR measurements respectively. The comparison graphs were used to plot each set of data for each test on one graph together. In these graphs, the reference device was plotted against our prototype to see the correlation between the two. Each different marker corresponds to a different subjects' data taken. The identity line represents a line with a slope of 1. This was useful to plot in the comparison charts because it represents the slope our data is expected to follow when comparing devices as such. The regression line in these plots models the relationship between the reference device and our prototype. In figures 7.2 and 7.3

displaying PR data, the regression line has a slope of .93 and .93 respectively. These slopes show the high correlation between the reference device and our prototype for both the chest sitting and standing results when measuring PR. In figures 7.4 and 7.5 displaying PR data, the regression lines have a slope of .89 and .73 respectively, also showing a high correlation between the reference device and our prototype for the wrist sitting and standing when measuring PR. When testing the devices ability to detect changing PR and SpO_2, the group only took measurements from the wrist. This was decided because of the increased accuracy in the measurements taken from the wrist. Figure 7.6 displays the PR data for the hyperventilation testing. The slope of the regression line here is .88 showing that our device is able to accurately detect changes in PR that would mimic those of exercise. Figure 7.7 displays the SpO_2 data for hypoxia testing. The slope of the regression line here is .33 which would normally indicate that the device does not have a high correlation with the reference device however, because SpO_2's measurements are on such a small scale, even the slightest of discrepancies would cause a big change in the slope of the regression line. It is for examples like this that it was necessary to analyze the data in more than one way and to have more than one form of graphical representation.

The dynamic response plots were used to see the prototypes response to PR and SpO_2 as opposed to the reference devices response over time. Each graph contains a line representing the prototype and a line representing the reference device. While the plots here for the chest while sitting and standing and the wrist while sitting and standing show that the measurements from our prototype remain in close proximity to those of the reference device, the most valuable plots are those done for hyperventilation and hypoxia. Figures 7.12 and 7.13 show that the prototype can react to changing levels of PR as fast as the reference device does and with high accuracy. In figure 7.12 at about 75 seconds in and in figure 7.13 at about 250 seconds there are noticeable outliers in the PR measurement from the prototype. The outliers for each subject went from a regular PR, around 90bpm, to values of about 40 or 50bpm. To verify whether this was due to abnormal PPG data or the software, the PPG data gathered by the VI was re-examined for the specific periods of time in which the outliers occurred. It was discovered that these outliers were primarily due to corrupted PPG data. Figure 7.1 shows a portion of the PPG data with corrupted readings which could be due to motion artifacts introduced by the subject through sudden movements. Another possibility for the corrupted data could be related to the amount of pressure applied to the sensor when it was placed on the subject. Figure 7.18 shows one drop in SpO_2 during induced hypoxia at about 150 seconds while figure 7.19 shows two drops in SpO_2 during induced hypoxia at 160 seconds and at 230 seconds. Both the prototype and the reference oximeter registered the drops in oxygen saturation, though the drop observed by our prototype was less than that of the reference device. This test demonstrated the prototype's ability to detect a decrease in SpO_2 with some degree of accuracy.

Residual plots were used to show by how much the prototype is likely to differ from the reference device. These plots allow us to see if there are any large discrepancies between the reference device and the prototype that would otherwise not be seen in the comparison charts. Figure 7.22 shows one of the residual plots for hyperventilation testing. In this plot we can see that there is not a large difference in the data gathered from the reference device and the prototype as all the data is fairly close to 0 and well within the 2 standard deviation limits showing that our data is normally distributed. Figures 7.20 and 7.21 show the remaining two residual plots for hyperventilation. These two plots show a much larger range of difference between the reference device and the prototype however, 95% of the values are within the 2 standard deviation limits and that the data is normally distributed as well. Figures 7.23 and 7.24 show the residual plots for hypoxia testing. These two plots show that the differences between the reference device and the prototype are very small ranging from a difference of either 1 or 2 and shows that 95% of these data points are also within the 2 standard deviation limit showing that our data is normally distributed.

From the data presented in Table 7.2, the accuracy of the PR measurements ranged in percent error between 3-5% for every single data set. From this it was concluded that while the tone measurements function in LabVIEW is a simple and effective method for calculated PR, it introduces a high degree of error since it is programmed to seek the highest amplitude frequency. For SpO_2 a low percent error was maintained for all the stationary measurements, but there was a decrease in accuracy when the prototype was experiencing changing SpO_2 levels. To ascertain a more precise accuracy for the prototype, further testing should be done in which the SpO_2 levels range from 70-100%.

10 Summary

This project started with the goal of designing and building a wearable reflectance-based pulse oximeter that could measure SpO_2 and PR accurately from the chest and wrist. A literature search was the conducted exploring pulse oximetry theory, application methods, and commercial products. After which, alternative designs for a reflectance-based pulse oximeter were considered. Assessing the benefits of each alternative design, a design consisting of 8 photodiodes positioned concentrically around 2 LEDs, one red and one infrared at wavelengths of 660nm and 940nm, respectively, was selected. In the circuitry, an Arduino Duo microprocessor was used as the LED driver and the logic driver. Sample-and-Hold circuits were utilized to separate the appropriate signals for red and infrared light with analog bandpass filters implemented to isolate the AC component of the PPG waveforms from the DC component. Stages of operational amplifiers were also used to amplify the original signal created by the sensor and amplify the AC signals which were representative of the PPG fluctuations.

The software for this project was developed in the program LabVIEW to further filter the signals and calculate SpO_2 and PR. For the calculation of PR, tone measurement function was used inside of LabVIEW which searches for the highest amplitude signal around a custom set frequency. Expecting the frequency of the range of PRs to lie between 1Hz and 3Hz, the function was set to search around 2Hz with a window of $\pm$ 50%. This method was very effective in calculating the PR frequency and chose to stay with it rather than opting for a peak to peak analysis. The PR frequency was then multiplied by 60 to have the final PR values in beats per minute.

For the calculation of SpO_2 several functions inside of LabVIEW were used to obtain these values. For the AC signals, a function called AC & DC estimator which effectively measured the amplitude of every single amplified PPG fluctuation and then averaged this amplitude over 10 seconds worth off PPG data. To obtain a DC value for both red and infrared signals, the amplitude and level measurements function was used to average 10 seconds worth of data and come up with a constant value for the DC. These methods were found to be satisfactory for calculating the red and infrared AC and DC values due to the small variation in the signal once placed on the skin of an individual. Variations in the signal were only noticeable if the sensor was moved or if the subject moved during testing. For calculating SpO_2, equation 2 was used with variables A= 110 and B = -25. The value for SpO_2 was then normalized so that it is out of 100% and then plotted on a chart as well as having a visual gauge as a reference with a range from 0-100% SpO_2.

Tests were performed using our prototype and a HOMEDICS Deluxe Pulse Oximeter as a reference. For the chest measurements, the sensor was placed directly over the sternum while for the wrist measurements the sensor was worn on the left arm over the radial artery. Depending on the signal intensity for each subject there were variations in the specific location over the radial artery in which the sensor was placed on to collect measurements. The pressure of the sensor on the skin was adjusted using a Velcro strap which went around the wrist and chest. The testing performed allowed for the collection of measurements from the chest and wrist while sitting and standing. Tests of hypoxia and hyperventilation were also performed to observe the responds of the prototype to changing levels of SpO_2 and PR. Many of the subjects had trouble holding their breaths for the allotted 45 seconds thus the lowest SpO_2 levels observed were 91%. From the gradual increase and decrease of PR, the prototypes response to changing PRs was observed. The VI was set to sample at 25 samples per second for 250 samples each measurement. Every 10 seconds, the VI would display 10 seconds worth of PPG waveforms, as well as the calculated PR and SpO_2 for the last 10 seconds. To maintain the same sampling rate as the prototype, the SpO_2 was also sampled and PR values of the reference pulse oximeter every 10 seconds to coincide with the results picked up by the VI.

Once all of the measurements were taken, the data were analyzed using several different techniques. The averages of each data set were taken for both measurants from which the accuracy of the prototype to that of the reference pulse oximeter was calculated and comparative graphs were created. Regression lines were also calculated and plotted for each set of measurements and compared to an identity line with a slope of 1 and a y-intercept of 0.

The hypoxia and hyperventilation measurements demonstrated how the device would perform with changing SpO_2 and PR levels. To this effect, dynamic response graphs were plotted for each measurement. For the hypoxia and hyperventilation tests, respective prototype and reference pulse oximeter SpO_2 values over time were plotted. Induced hypoxia resulted in lowered levels of SpO_2 and showing a similar response in both the prototype and the reference pulse oximeter. During hyperventilation, rising PR on each subject were observed with the prototype and reference pulse oximeter. Lastly, residual plots were also created for the hypoxia and hyperventilation tests to investigate how our device differs from the reference device. This was accomplished by calculating the difference between the prototype and reference pulse oximeter for each measurement.

11 Conclusion

Based on the experimental results derived several conclusions can be drawn. Through the testing performed on the prototype pulse oximeter we observed that it is in fact possible to measure SpO_2 and PR from the wrist and chest with a reasonable level of accuracy. The SpO_2 measurement contained an error of less than $\pm$1% and the PR measurements less than $\pm$4%. However the prototype does still need some improvement to increase the accuracy of the PR. Though simple to implement, the algorithm currently being used in calculating PR did not provide the level of accuracy required for a FDA regulated commercial device.

12 Future Improvements

While the hardware and software components of this project met the project goals in that they were able to measure PR and SpO_2, there are several improvements we could make in the future for the device to meet industry standards. One aspect of the hardware construction which we never really tackled was designing a PCB model. For the purposes of our project it was simpler to use a breadboard since adjustments were constantly being made with the hardware components to test different settings and for troubleshooting. A factory fabricated PCB board would give us the possibility to start planning for portability and how the device could be attached to the patient. While our design for this project involved a separate module for the LED and photodiode sensor from the actual circuitry, it could be possible to integrate everything in one board once a PCB design is fabricated. A PCB design would allow us to use smaller components in the circuit and minimize the size of the sensor as well as the accompanying circuitry.

Another future improvement which could be implemented is the use of a National Instruments LabVIEW embedded microcontroller. This would not only minimize the amount of components used in the circuitry but would also remove our prototypes dependency on being connected to a desktop PC running LabVIEW in order for the device to work. An embedded microcontroller would allow us to add an LCD display which could show both SpO_2 and PR to the patient. Another benefit for using an embedded microcontroller would be that circuit designs such as the Sample-and-Hold and the bandpass filters would no longer be necessary as analog components since these functions can be programmed digitally in LabVIEW.

The hardware casing should also be redesigned to be not only more aesthetically pleasing but also fully wireless so that it can be worn anywhere. Currently as it stands, our prototype is fairly bulky and requires a constant connection to a desktop PC. Weight is also an issue since the enclosure for our circuitry is an aluminum box with dimensions of 5” x 3” x 3”. We feel that with the development of a PCB design, the overall size requirement for the casing would also dramatically decrease. Another aspect of the casing we would like to see changed is using a hard polymer shell instead of an aluminum box. A plastic casing would be easier to design in any modeling software and would be more easily manufactured with the use of molding techniques. Current developments in 3D printers with plastics would also make a plastic casing an easier option for manufacturing.

To make the device fully portable, wireless connectivity should be considered for future improvements. Wireless connectivity, whether through WIFI, Bluetooth or NFC would not only remove from the user the burden of having wires running through the body but would also provide easier access of SpO_2 and PR measurements. Although battery consumption might be an issue, a wireless pulse oximeter would be more user friendly and increase mobility for the user. The possibility of being able to display these measurements on any smartphone or other portable wireless devices is another advancement that could make this device increasingly valuable for patients and clinicians.

References

(1) Mendelson, Y. “Pulse Oximetry.” Wiley Encyclopedia of Biomedical Engineering (2006): vol. 5. Hoboken, NJ: John Wiley & Sons, Inc. Print.
(2) Pole, Yash. "Evolution of the Pulse Oximeter." International Congress Series 1242 (2002): 137-44. Print.
(3) "Hemoglobin." Encyclopædia Britannica. Encyclopædia Britannica Online Academic Edition. Encyclopædia Britannica Inc., 2012. Web. 15 Sep. 2012. <http://www.britannica.com/EBchecked/topic/260923/hemoglobin>.
(4) Brinkman R., Zijlstra W.G., and Koopmans R.K, “A Method For Continuous Observation Of Percentage O2 Saturation In Patients,” Arch. Chir. Neerl. 1 (1950): 333 - 444. Print.
(5) Mendelson, Y., and B. D. Ochs. "Noninvasive Pulse Oximetry Utilizing Skin Reflectance Photoplethysmography." IEEE transactions on bio-medical engineering (1988): 35, 10, 798-805. Print.
(6) Mendelson, Duckworth, and Comtois. “A wearable reflectance pulse oximeter for remote physiological monitoring.” Conference Proc. IEEE Engineering Medical Biology Soc. (2006): 1:912-5. Print.
(7) Santa Medical. Finger pulse oximeter SM-110 with carry case and neck wrist cord.
(8) Mendelson, Y., et al. "Design and Evaluation of a New Reflectance Pulse Oximeter Sensor." Medical instrumentation 22.4 (1988): 167. Print.
(9) Shelley K. and Shelley S., “Pulse Oximeter Waveform: Photoelectric Plethysmography,” Clinical Monitoring, Carol Lake, R. Hines, and C. Blitt, Eds.: W.B. Saunders Company, (2001): 420-428. Print.
(10) Shelley K. H., Jablonka D. H., Awad A. A., Stout R. G., Rezkanna H., and Silverman D. G., “What Is the Best Site for Measuring the Effect of Ventilation on the Pulse Oximeter Waveform?” Anesth Analg, (2006): vol. 103, 372-377. Print.
(11) Reisner A, Shaltis. P. A., McCombie D., and Asada, H. H., “Utility of the Photoplethysmogram in Circulatory Monitoring, Anesthesiology,” Anesthesiology, (2008): vol. 108, pp. 950-958. Print.
(12) Nogawa, M., Kaiwa, T., and Takatani, S., "A Novel Hybrid Reflectance Pulse Oximeter Sensor With Improved Linearity And General Applicability to Various Portions of the Body," Engineering in Medicine and Biology Society, (1998). Proceedings of the 20th Annual International Conference of the IEEE, vol.4,.1858-1861.
(13) Tilakaratna, Prasanna. "Pulse Oximeter." Equipmentexplained.com. N.p., n.d. Web. 15 Sept. 2012. <http://www.equipmentexplained.com/physics/respi_measurements/oxygen/oximeter/pulse_oximeter.html>.
(14) Dresher RP, Mendelson Y., “Reflectance Forehead Pulse Oximetry: Effects of Contact Pressure During Walking.” Conf Proc IEEE Eng Med Biol Soc. (2006); 1: 3529-32.
(15) Mardirossian, G., and Schneider R. E.. "Limitations of Pulse Oximetry." Anesthesia Progress 39.6 (1992): 194-6. Print.
(16) Cocker, B., Leung J., Cohen C., Goska B., Albright R., House S., and Chiang P.. "Wearable, Wireless Reflectance-Sensing Pulse Oximeter." (2012): 2017-020.
(17) "Neonatal Pulse Oximetry Archives Tag Archive for Baby Heart Screening- Newborn Heart Defect Screening." *Baby Heart Screening Newborn Heart Defect Screening*. N.p., n.d. Web. 23 Apr. 2013.
(18) Online Courses: Medical Equipment Technology, Support and Management. N.p., n.d. Web. 23 Apr. 2013.
(19) Anliker et al. “AMON: A Wearable Multiparameter Medical Monitoring and Alert System.” IEEETrans Inf Technology Biomedical (2004): (4) 415-27. Print.
(20) Mendelson, Y., and M. J. McGinn. "Skin reflectance pulse oximetry: In vivo measurements from the forearm and calf." Journal of Clinical Monitoring and Computing 7.1 (1991): 7-12.
(21) Respironics. WristOx™ Ambulatory Finger Pulse Oximeter.
(22) Crucial Medical Systems. Oled cms50d fingertip pulse oximeter and oxygen meter.
(23) Mendelson Y. and Pujary. “Photodetector Size Considerations in the Design of a Noninvasive Reflectance Pulse Oximeter for Telemedicine Applications.” IEEE Xplore, (2003): 148-149. Print.
(24) Schreiner, C., Catherwood, P., & Anderson, J. “Blood Oxygen Level Measurement with a Chest-Based Pulse Oximetry Prototype System.” Computing in Cardiology (2010). Print.
(25) Li, K., & Warren, S. “A Wireless Reflectance Pulse Oximeter with Digital Baseline Control for Unfiltered Photoplethysmograms.” IEEE Transactions on Biomedical Circuit and Systems (2010). Print.

Appendix A: Description of LabVIEW

Discussed below are the functions used in the construction of the program that was used in this study.

While loop is a structure that allows for the continuous sampling of input signals and the application of the diagrams placed within it.

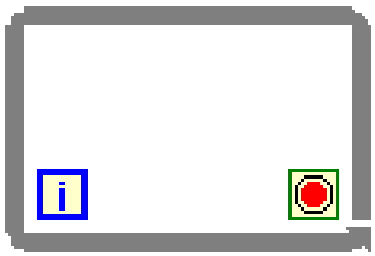

Figure A.1: While loop

When placed in the block diagram, the DAQ assistant launches creating a new task. The task was to identify the signal provided by the external DAQ and set sampling parameters.   The task can be edited by double-clicking the DAQ assistant. For continuous measurement a while loop should be placed around the DAQ assistant.

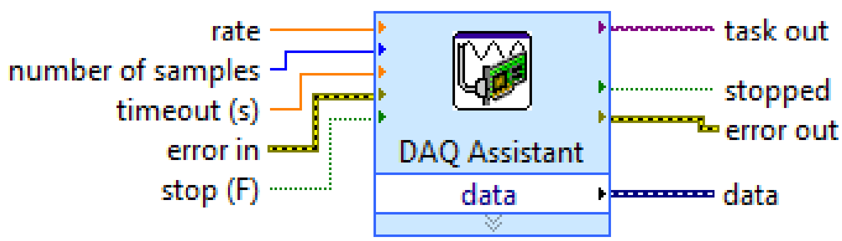

Figure A.2: DAQ Assistant

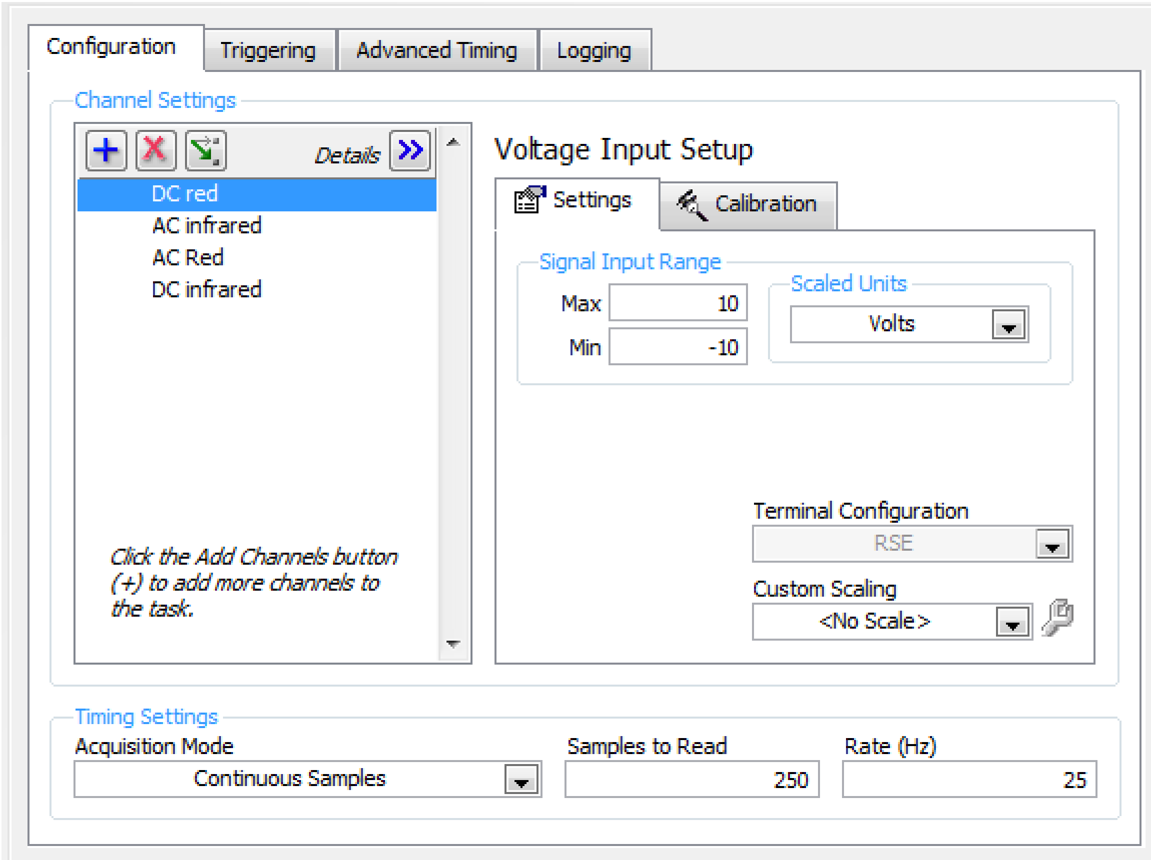

Figure A.3: DAQ assistant task

108

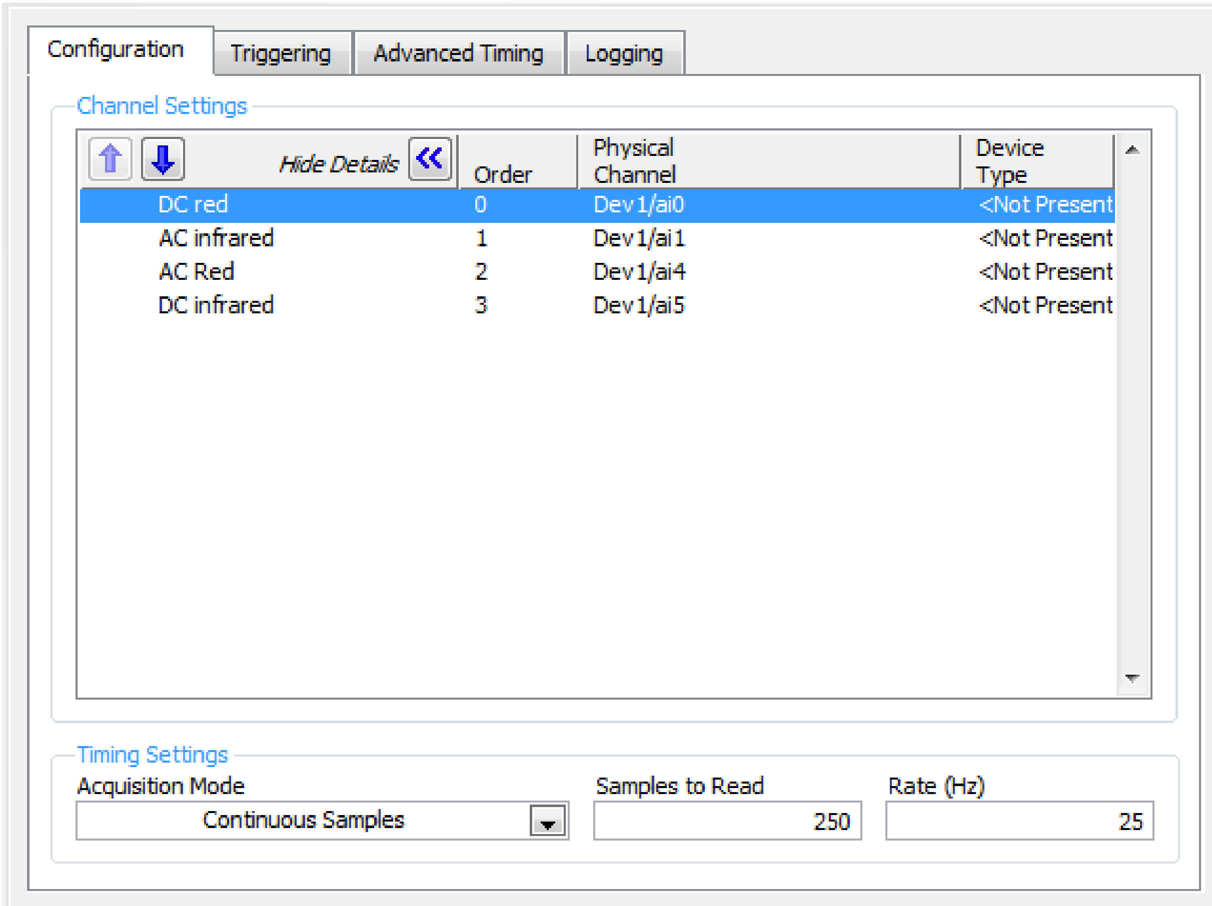

Figure A.4: DAQ assistant task with open details

Select signals accepts multiple signals as inputs and returns only the signals selected allowing the user to specify which signals to include in the output.

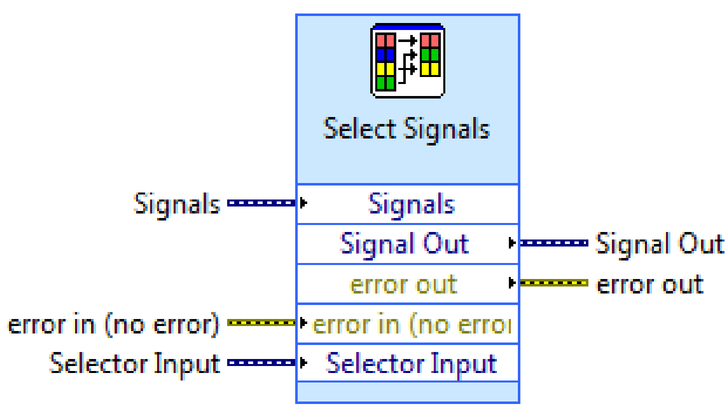

Figure A.5: Select signals

The filter function filters a signal using an infinite impulse response or finite impulse response filter which removes or attenuates unwanted frequencies from a signal using various standard filter types and topologies continuously. In this instance the Chebyshev filter was used because Chebyshev filters minimize the error between the idealized and the actual filter characteristic over the range of the filter.

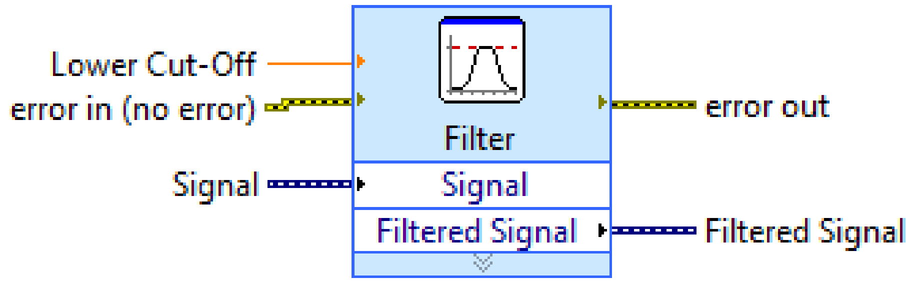

Figure A.6: Filter function

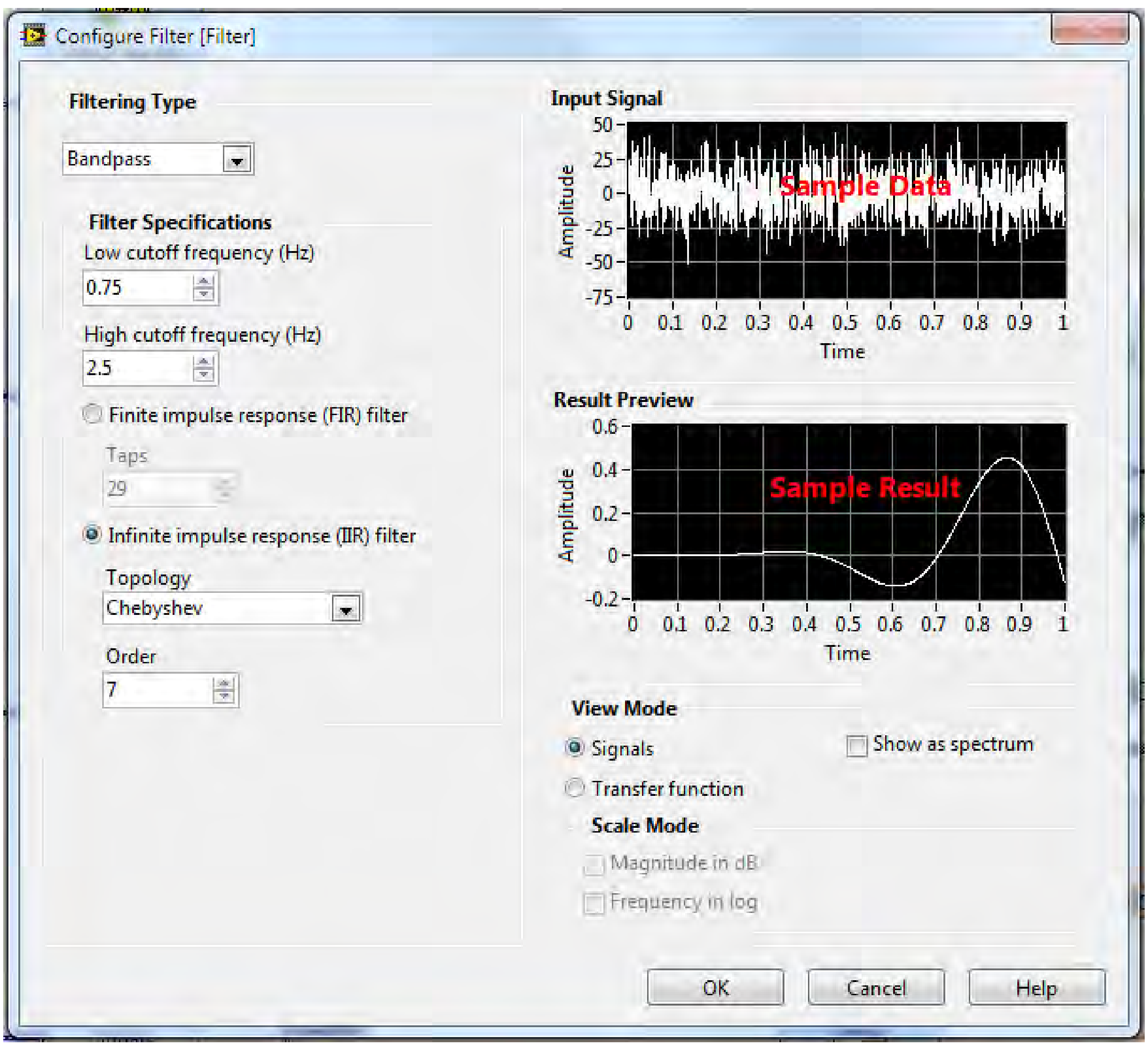

Figure A.7: Filter function parameters

The *tone measurements* function finds the signal with the highest amplitude or searches a specified frequency range to find the single tone with the highest amplitude and also can find the frequency and phase. In this instance, this function is used to find frequency.

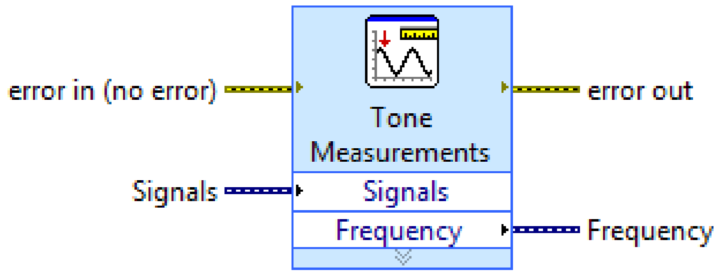

Figure A.8: Tone measurements function

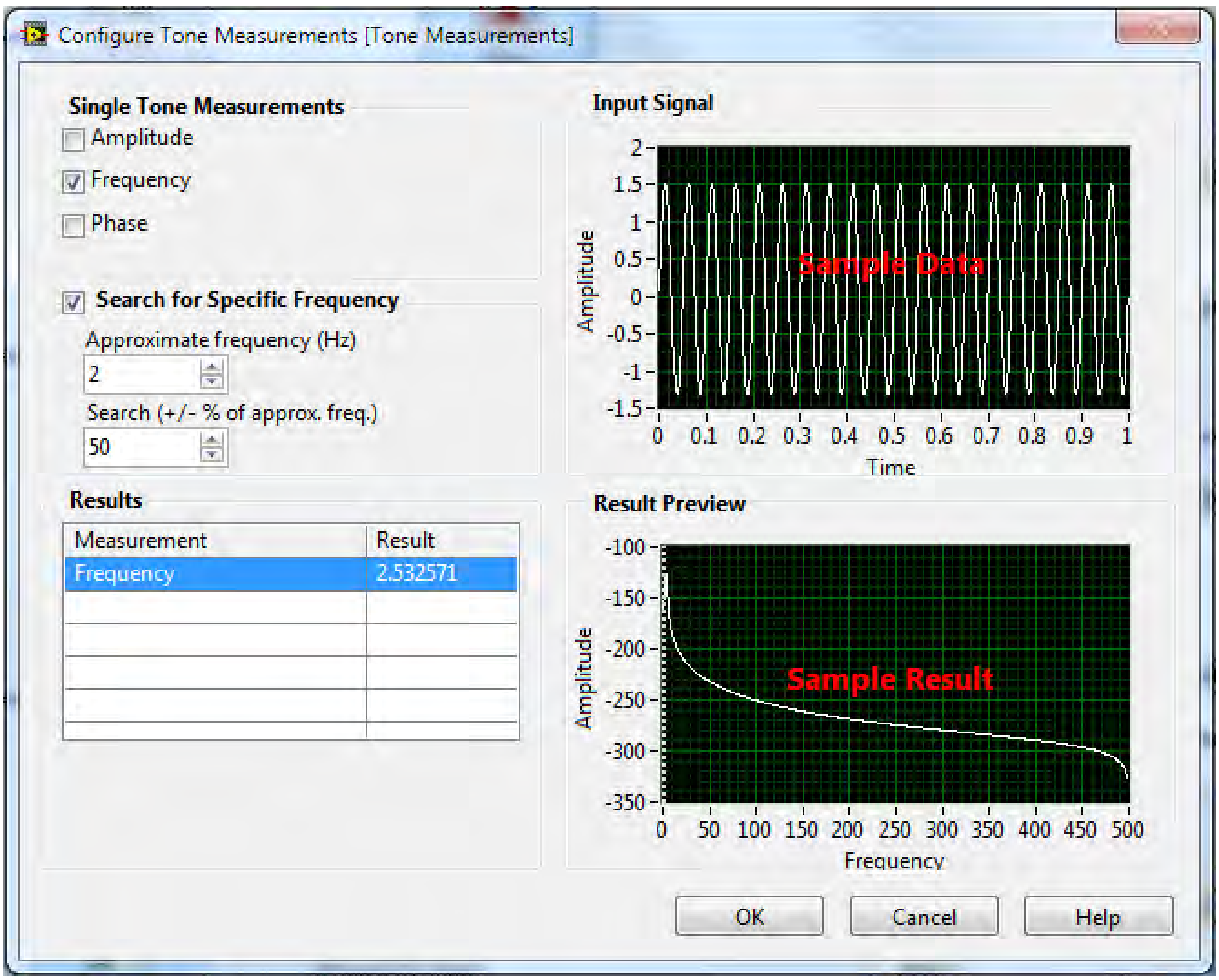

Figure A.9: Configuration of the tone measurements function

Amplitude and level measurements performs voltage measurements on a signal, such as an average of the DC component of the signal, the maximum peaks, and the mean level of one complete period of a periodic input signal.

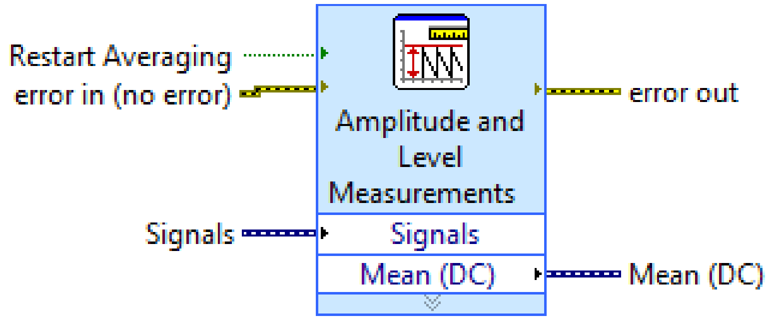

Figure A.10: Spectral measurement function

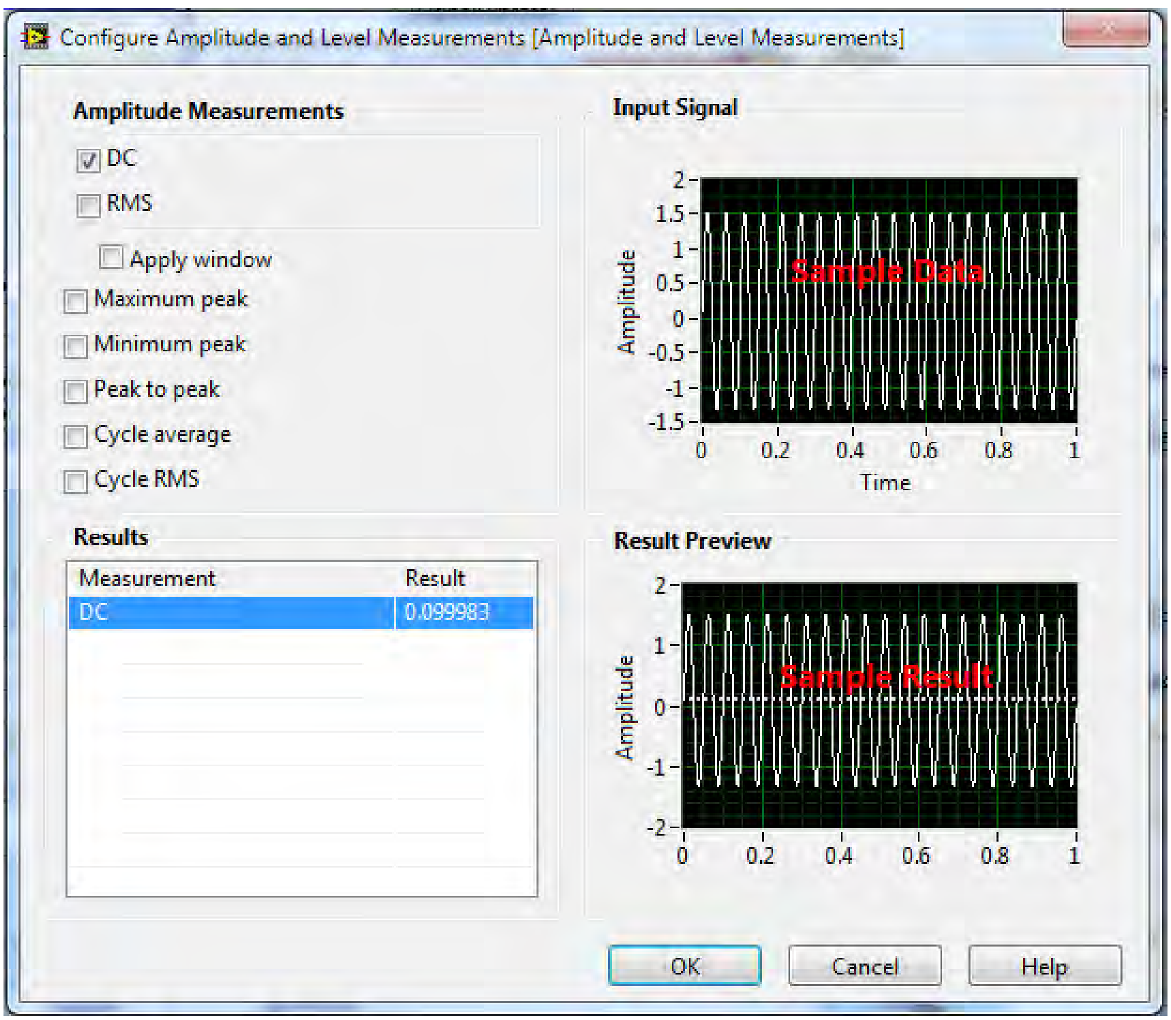

Figure A.11: Configuration of the spectral measurements

112

The AC&DC estimator.vi applies the Hanning window, which separates most of the AC energy from the DC bin, allowing the estimation the AC and DC levels of the input signal.

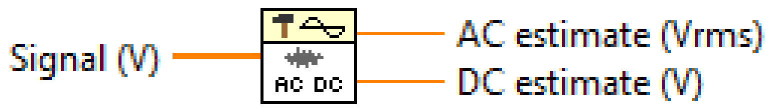

Figure A.12: AC & DC estimator.vi

Divide computes the quotient of the inputs.

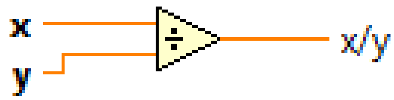

Figure A.13: Division

Round to nearest integer rounds the input to the nearest integer. If the value of the input is midway between two integers, the function returns the nearest even integer.

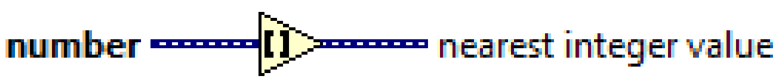

Figure A.14: Round to nearest integer

Multiply returns the product of the inputs.

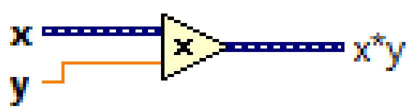

Figure A.15: Multiply

Add computes the sum of the inputs.

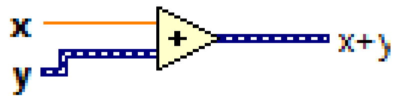

Figure A.16: Add

The *greater than function* returns TRUE if x is greater than y and returns FALSE if y is greater than x.

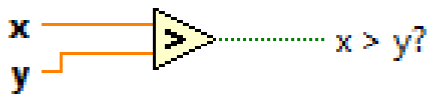

Figure A.17: Greater than function

The *less than function* returns TRUE if x is less than y and returns FALSE if y is greater than x.

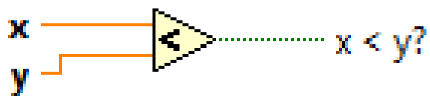

Figure A.18: Less than function

The *and function* computes the logical AND, meaning if both inputs are TRUE, the function returns TRUE and otherwise it returns FALSE.

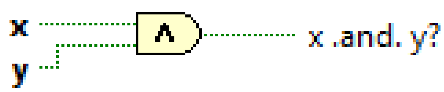

Figure A.19: And function

Case structure has multiple sub diagrams, or cases, with only one case executing when the structure executes. The execution can be controlled by wiring a value to the case structure which will determine which case to use.

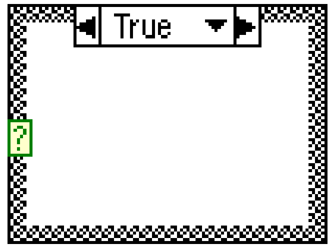

Figure A.20: Case structure

Above is the *numeric indicator* that displays values continuously. The image on the left represents the function in the block diagram while the image on the right represents the function in the front panel that displays the commuted values.

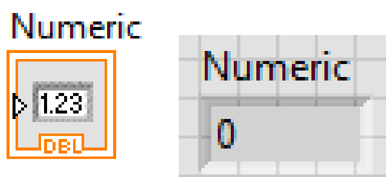

Figure A.21: Numeric indicator (left: block diagram, right: front panel)

The *gauge indicator* is a continuous numeric indicator. The image on the left represents the function in the block diagram while the image on the right represents the function in the front panel that displays the commuted values.

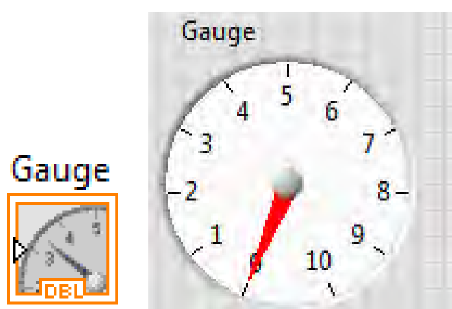

Figure A.22: Gauge indicator (left: block diagram, right: front panel)

Waveform graph is a graphic indicator that evenly plots sampled measurements. The image on the left represents the function in the block diagram while the image on the right represents the function in the front panel that graphs the commuted values.

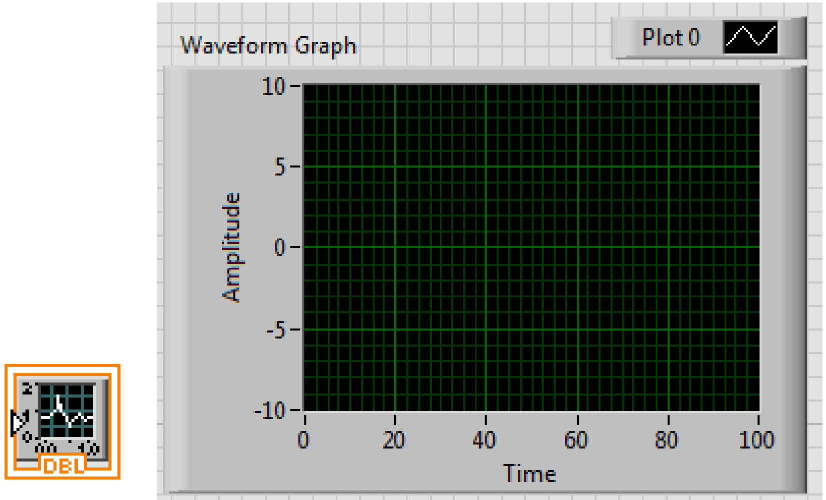

Figure A.23: Waveform graph (left: block diagram, right: front panel)

Waveform chart is a numeric indicator that plots data at a constant rate and maintains a history of the data. The image on the left represents the function in the block diagram while the image on the right represents the function in the front panel that graphically records the commuted values.

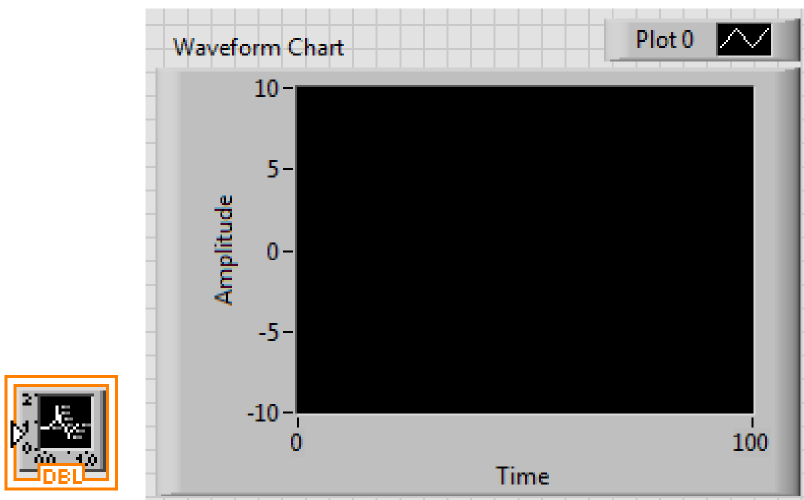

Figure A.24: Waveform chart (left: block diagram, right: front panel)

Appendix B: Bill of Materials

Item	Vendor	Part Number	Quantity	Price
Photodiodes	Allied Electronics	BPW34	8	$18.80
940nm Infrared LED	Radioshack	276-143	1	$2.49
660nm Red LED	Radioshack	55050641	1	$1.44
Round Fiberglass Copper Boards	Radioshack	276-004	1	$5.49
Bread Board	Radioshack	276-003	1	$9.99
LF398LN	Mouser	LF398N/NOPB	2	$3.08
LM348 Quad Op-Amp	Obtained from BME Lab		3	$1.99
Velcro Strap	Home Depot	90340	1	$9.27
Aluminum Box Enclosure	Radioshack	270-238	1	$3.49
Double sided tape	Home Depot	285189	1	$6.97
Arduino Duo Microcontroller	Radioshack	276-128	1	$29.99
			SUM	$93.00

Appendix C: Data Sets

Table C.1: Sitting chest data set

Subject 1 Sitting Chest				Subject 2 Sitting Chest				Subject 3 Sitting Chest				Subject 4 Sitting Chest			
Reference Oximeter		Prototype		Reference Oximeter		Prototype		Reference Oximeter		Prototype		Reference Oximeter		Prototype	
SpO2	PR	SpO2	PR	SpO2	PR	SpO2	PR	SpO2	PR	SpO2	PR	SpO2	PR	SpO2	PR
98	62	99	65	98	94	98	93	97	92	99	88	98	80	96	92
98	60	99	63	98	96	98	92	98	94	99	99	98	80	98	82
98	59	99	60	98	94	99	91	97	90	96	92	98	83	98	85
98	60	99	60	98	94	99	93	98	93	95	91	98	86	98	87
98	61	99	61	98	93	99	92	98	94	95	94	98	87	98	88
98	60	99	62	98	96	98	93	97	91	95	94	98	87	98	87
98	60	99	64	98	94	98	95	97	93	96	93	98	87	98	86
98	63	99	63	98	89	98	96	97	93	95	94	98	85	98	86
98	64	99	63	98	93	98	93	97	91	95	93	98	87	98	85
98	61	99	64	98	91	99	90	97	91	96	92	98	91	98	89
98	65	99	63	98	87	99	88	98	96	96	94	98	87	98	88
98	68	99	64	98	87	98	91	98	98	95	94	98	89	98	91
98	65	99	68	98	88	98	88	97	96	94	94	98	91	98	87
98	61	99	63	98	91	98	92	97	94	95	97	98	83	98	89
98	58	99	61	98	87	98	85	97	99	95	62	98	87	98	88
98	60	99	59	98	89	98	91	97	97	98	101	98	82	98	81
98	60	99	60	98	91	99	89	97	96	97	97	98	87	98	83
98	59	99	64	98	91	98	91	97	96	97	95	98	87	98	86
98	58	99	60	98	91	98	93	97	96	98	98	98	85	98	84
98	58	99	59	98	91	98	89	97	91	97	97	98	86	98	88
98	60	99	58	98	89	99	89	97	91	97	96	98	88	99	89

98	63	99	61	98	91	99	90	97	93	98	93	98	91	98	90
98	73	99	63	98	93	99	88	97	94	98	99	98	87	98	89
98	72	99	71	98	93	99	90	97	96	98	96	98	87	98	90
98	79	99	71	98	91	98	92	97	99	98	68	98	87	98	85
98	70	99	81	98	91	99	92	97	96	99	103	98	86	98	85
98	68	99	71	98	94	99	92	97	98	97	96	98	88	98	93
98	63	99	65	98	91	98	91	97	99	97	100	98	83	99	86
98	59	99	64	98	89	99	88	97	96	98	99	98	85	98	83
98	58	99	60	98	87	98	86	97	98	98	97	98	87	99	85
98	56	99	59	98	89	99	89	98	98	97	99	98	82	98	88
98	56	99	56	98	89	98	92	98	94	98	95	98	80	99	84
98	58	99	59	98	91	99	94	98	98	98	94	98	89	98	90
98	60	99	59	98	88	98	89	97	99	99	99	98	86	98	87
98	60	99	62	98	91	98	91	97	101	98	99	98	87	99	89
98	62	99	61	98	91	98	91	97	104	99	101	98	89	98	91
98	62	99	61	98	91	99	91	97	101	98	101				
				98	96	98	94	97	98	99	99				

Table C.2: Standing chest data set

Subject 1 Standing Chest				Subject 2 Standing Chest				Subject 3 Standing Chest				Subject 4 Standing Chest			
Reference Oximeter		Prototype		Reference Oximeter		Prototype		Reference Oximeter		Prototype		Reference Oximeter		Prototype	
SpO2	PR	SpO2	PR	SpO2	PR	SpO2	PR	SpO2	PR	SpO2	PR	SpO2	PR	SpO2	PR
98	96	99	101	98	96	96	93	98	91	99	87	98	98	98	98
98	101	99	99	98	94	98	92	98	91	99	89	98	94	98	97
98	101	99	106	98	98	98	89	98	87	98	92	98	100	97	103
98	108	99	108	98	101	98	92	98	87	99	94	98	99	95	100

98	108	99	111	98	93	97	93	97	87	99	82	98	98	98	98
98	104	99	107	98	94	99	92	98	87	99	87	98	96	98	97
98	106	99	98	98	96	99	94	98	88	99	85	98	96	99	102
98	108	99	109	98	91	99	93	98	91	99	87	98	99	98	104
98	101	99	108	98	96	99	95	98	84	99	89	98	96	98	95
98	106	99	105	98	96	99	93	97	84	98	92	98	98	98	100
98	103	99	111	99	94	99	93	98	86	99	83	98	99	98	103
98	106	99	100	99	91	99	94	98	87	99	88	98	99	98	101
98	103	99	104	99	91	98	90	98	84	99	85	98	98	98	97
98	105	99	107	98	91	99	92	98	87	98	86	98	94	99	95
98	104	99	107	98	91	99	92	98	87	99	84	98	99	98	103
98	103	99	104	98	89	99	93	98	86	98	90	98	101	98	101
98	104	99	103	98	89	99	92	98	87	99	88	98	99	98	101
98	101	99	102	99	88	99	89	98	87	98	87	98	96	98	99
98	104	99	103	98	87	99	91	98	91	98	86	98	98	98	98
98	106	99	108	99	88	99	91	98	87	98	92	98	101	98	103
98	106	99	100	99	94	99	90	98	89	98	92	98	101	97	99
98	108	99	100	99	93	98	92	98	91	98	90	98	98	98	92
98	109	99	106	98	96	99	95	98	87	98	87	98	101	98	100
98	101	99	104	99	96	98	92	98	89	98	87	98	101	97	103
98	101	99	101	99	96	99	94	98	87	99	84	98	104	97	106
98	101	99	104	99	96	99	88	98	87	98	85	98	105	98	107
98	106	99	105	99	94	99	92	98	87	98	87	98	106	98	106
98	101	99	105	99	93	99	98	98	89	98	88	98	106	98	107
98	104	99	106	99	91	99	95	98	92	98	89	98	112	99	108
98	112	99	105	99	93	99	92	98	91	98	89	98	96	97	99
98	107	99	116	99	94	98	92	98	87	98	92	98	101	98	99
98	104	99	110	99	91	99	94	98	89	98	91	98	101	98	102

98	108	99	107	99	94	99	94	98	89	98	90	98	104	98	106
98	108	99	107	99	94	99	94	98	92	98	89	98	105	98	106
98	109	99	105	99	93	99	69	98	87	99	87	98	109	97	106
98	104	99	109	99	94	99	94	98	88	99	88	98	101	98	100
98	112	99	100	98	96	98	74					98	106	97	107

Table C.3: Sitting wrist data set

Subject 1 Sitting Wrist				Subject 2 Sitting Wrist				Subject 3 Sitting Wrist				Subject 4 Sitting Wrist			
Reference Oximeter		Prototype		Reference Oximter		Prototype		Reference Oximeter		Prototype		Reference Oximeter		Prototype	
SpO2	PR	SpO2	PR	SpO2	PR	SpO2	PR	SpO2	PR	SpO2	PR	SpO2	PR	SpO2	PR
95	77	95	79	98	106	98	104	98	85	99	84	99	62	98	60
97	79	98	80	98	106	98	107	98	87	99	88	99	61	99	63
98	80	98	80	98	101	98	103	98	85	99	89	99	62	99	62
98	83	98	83	98	101	98	101	98	85	99	89	99	62	99	59
98	84	98	81	98	96	98	102	98	87	98	86	99	66	99	64
97	80	98	81	98	98	98	101	98	87	99	89	99	62	99	74
98	81	98	79	98	99	98	102	98	88	99	86	99	58	99	61
98	80	98	80	98	96	98	99	98	91	99	91	99	58	99	58
98	80	98	79	98	98	98	99	98	91	98	92	99	59	99	59
98	80	98	80	98	99	98	101	98	92	98	89	99	58	99	59
98	82	98	85	98	101	98	102	98	87	98	86	99	60	99	59
98	82	98	82	98	106	99	61	98	87	99	89	99	63	99	66
98	83	98	84	98	96	98	98	98	87	98	92	99	62	99	63
98	84	98	84	98	96	98	99	98	87	99	86	99	67	99	63
98	87	98	87	98	101	98	102	98	86	99	90	99	83	99	64
98	82	99	82	98	87	98	98	98	89	99	90	99	60	99	63

98	82	98	81	98	88	98	96	98	91	98	89	99	60	99	61
98	83	98	83	97	91	98	94	98	89	98	87	99	68	99	60
98	82	98	83	98	101	98	104	98	85	99	87	99	59	99	69
98	87	98	91	98	99	98	98	98	89	99	86	99	58	99	62
98	84	99	82	98	96	98	99	98	91	98	86	99	59	99	59
98	80	98	82	98	96	98	100	98	87	98	92	99	59	99	59
98	80	98	80	98	99	98	100	98	88	98	83	99	60	99	60
98	83	95	82	98	101	98	101	98	87	99	85	99	60	99	61
98	84	98	85	98	101	98	101	98	83	99	87	99	57	99	61
98	87	98	85	98	99	98	101	98	85	98	88	99	58	99	59
98	83	98	85	98	101	98	103	98	91	98	89	99	66	99	58
98	83	98	84	98	98	98	96	98	89	98	86	99	60	99	67
98	83	98	85	98	98	97	100	98	85	99	84	99	59	99	60
98	85	98	82	98	98	98	99	98	83	99	82	99	59	99	58
98	85	98	85	98	96	98	98	98	84	99	86	99	53	99	61
98	83	98	86	98	99	98	101	98	87	99	86	99	53	99	107
98	83	99	84	98	98	98	95	98	83	98	86	99	63	99	68
98	87	99	84	98	99	98	99	98	87	98	89	99	69	99	61
98	87	98	87	98	99	98	102	98	87	99	86	99	65	99	69
98	83	98	87	98	101	98	102	98	87	99	92	99	61	99	67

Table C.4: Standing wrist data set

Subject 1 Standing Wrist				Subject 2 Standing Wrist				Subject 3 Standing Wrist				Subject 4 Standing Wrist			
Reference Oximeter		Prototype		Reference Oximeter		Prototype		Reference Oximeter		Prototype		Reference Oximeter		Prototype	
SpO2	PR	SpO2	PR	SpO2	HR	SpO2	PR	SpO2	HR	SpO2	PR	SpO2	Heart Rate	SpO2	PR
98	94	98	93	98	99	98	108	98	98	98	96	98	71	94	69

98	96	98	96	98	101	98	99	98	98	95	97	98	77	98	73
98	96	99	100	98	99	98	99	98	94	95	100	98	71	98	69
98	96	98	99	98	103	98	98	98	96	95	100	98	79	98	80
98	98	98	97	98	103	98	101	98	99	95	91	98	84	98	83
98	98	99	97	98	96	98	101	98	99	95	99	98	76	98	75
98	96	98	98	98	101	98	97	98	94	95	96	98	75	98	77
98	96	98	100	98	94	96	95	98	96	97	97	98	80	98	82
98	98	98	97	98	95	97	88	98	94	95	96	98	77	98	79
98	99	98	101	98	96	97	98	98	96	95	98	98	80	98	78
98	99	98	95	98	97	98	96	98	96	96	99	98	80	98	81
98	101	99	97	98	99	98	97	98	91	95	100	98	79	98	78
98	101	96	98	98	101	98	101	98	94	95	92	98	75	98	80
98	98	98	97	98	100	98	99	98	99	95	95	97	83	98	82
98	96	99	93	98	98	99	94	98	93	95	91	98	83	98	81
98	96	98	101	98	101	98	97	98	91	95	87	98	80	98	85
98	98	98	98	98	103	98	99	98	88	97	106	98	77	98	82
98	101	98	100	98	101	97	104	98	89	96	93	97	78	98	85
98	112	99	100	98	99	97	100	98	93	95	98	97	78	98	85
98	101	98	105	98	102	98	99	98	92	95	95	97	80	98	83
98	91	98	85	98	103	98	104	98	96	96	95	98	78	98	73
98	93	98	88	98	101	97	103	98	96	95	93	98	76	98	78
98	96	97	92	98	99	98	99	98	91	96	88	98	78	98	81
98	96	98	95	98	101	98	98	98	96	95	94	98	77	98	76
98	98	98	100	98	104	98	100	98	90	97	88	98	83	98	86
98	99	98	100	98	106	98	107	98	91	98	61	98	80	98	77
98	101	98	102	98	101	98	99	98	86	99	93	98	75	98	79
98	98	98	99	98	99	96	99	97	96	96	93	98	80	98	87
98	103	98	98	98	99	97	99	97	91	96	91	98	76	98	81

98	99	98	103	98	103	98	98	97	91	95	93	98	80	98	81
98	99	98	98	98	101	97	105	98	89	95	97	98	80	97	85
98	98	98	103	98	104	98	100					98	79	98	81
98	101	99	101	98	108	98	105					98	76	98	80
				98	106	98	110					98	73	98	79
				98	96	98	105					98	73	98	80
				98	103	98	95					98	81	98	80

Table C.5: Standing wrist data set

Subject 1 Hyperventilation		Subject 2 Hyperventilation		Subject 3 Hyperventilation		Subject 4 Hyperventilation	
Reference Oximeter	Prototype	Reference Oximeter	Prototype	Reference Oximeter	Prototype	Reference Oximeter	Prototype
PR	PR	PR	PR	PR	PR	PR	PR
91	92	91	92	82	82	89	89
91	82	89	88	81	99	85	85
86	87	89	91	82	80	91	88
85	85	87	86	88	87	85	80
84	85	87	86	84	88	87	82
80	84	87	91	87	87	89	88
77	76	87	91	87	85	89	91
75	53	89	90	87	78	87	79
76	78	94	92	87	86	87	87
80	81	96	95	87	74	87	76
83	80	96	93	87	82	87	86
87	84	98	100	87	79	89	87
88	92	100	101	77	93	89	91
94	94	96	89	76	98	90	89
96	95	96	94	82	101	89	97

99	101	96	92	96	111	89	90
101	100	91	95	99	110	87	91
103	105	91	88	106	110	98	101
103	104	87	95	108	107	101	94
101	102	87	81	108	113	101	99
101	91	92	93	106	115	101	95
98	99	95	91	109	115	106	105
99	94	96	97	112	118	110	110
96	94	96	95	112	121	116	119
96	100	98	95	115	111	120	113
91	96	98	91	117	109	124	80
87	91	99	90	113	97	128	126
86	85	104	97	108	91	112	134
87	86	104	103	103	90	112	131
87	88	103	109	93	91	108	115
87	88	101	108	91	92	106	109
87	87	101	97	89	97	101	101
87	89	91	95	91	84	99	99
87	86	90	100	92	89		
87	87	96	86	89	68		

Table C.6: Hyperventilation data set

Subject 1		Subject 2	
Reference Oximeter	Prototype	Reference Oximeter	Prototype
SpO2	SpO2	SpO2	SpO2
99	97	98	98
99	97	98	98
99	98	98	98

99	97	98	97
99	97	98	98
99	97	98	98
99	97	98	98
99	98	98	96
99	97	98	98
99	97	98	97
99	97	97	96
99	97	97	98
99	96	97	98
99	97	98	99
99	97	98	99
99	98	93	99
99	97	97	93
99	98	97	99
99	97	98	94
99	98	98	98
99	98	98	97
99	97	99	98
99	97	95	98
99	97	97	96
97	96	98	99
97	96	98	98
96	95	98	99
94	95	98	98
92	94	97	98
91	93	97	98
94	96	96	98

97	96	98	99
98	97	98	98
97	96	98	99
98	97		
98	98		
98	97		
97	97		
97	96		
97	97		
98	97		
98	96		
98	97		
98	96		

Appendix D: Filter Bode Plots

The bode plot in *Figure D.1* was generated online using an online filter calculator which allows you to input the filter characteristics and the calculator will output appropriate resistor and capacitor values. In the case above, the filter was a bandpass filter utilized in analog form in the circuitry directly after the Sample-and-Hold circuits. The filters consisted of a frequency cutoff of 2Hz and a bandwidth of 2Hz to effectively cover a range between 1Hz and 3Hz.

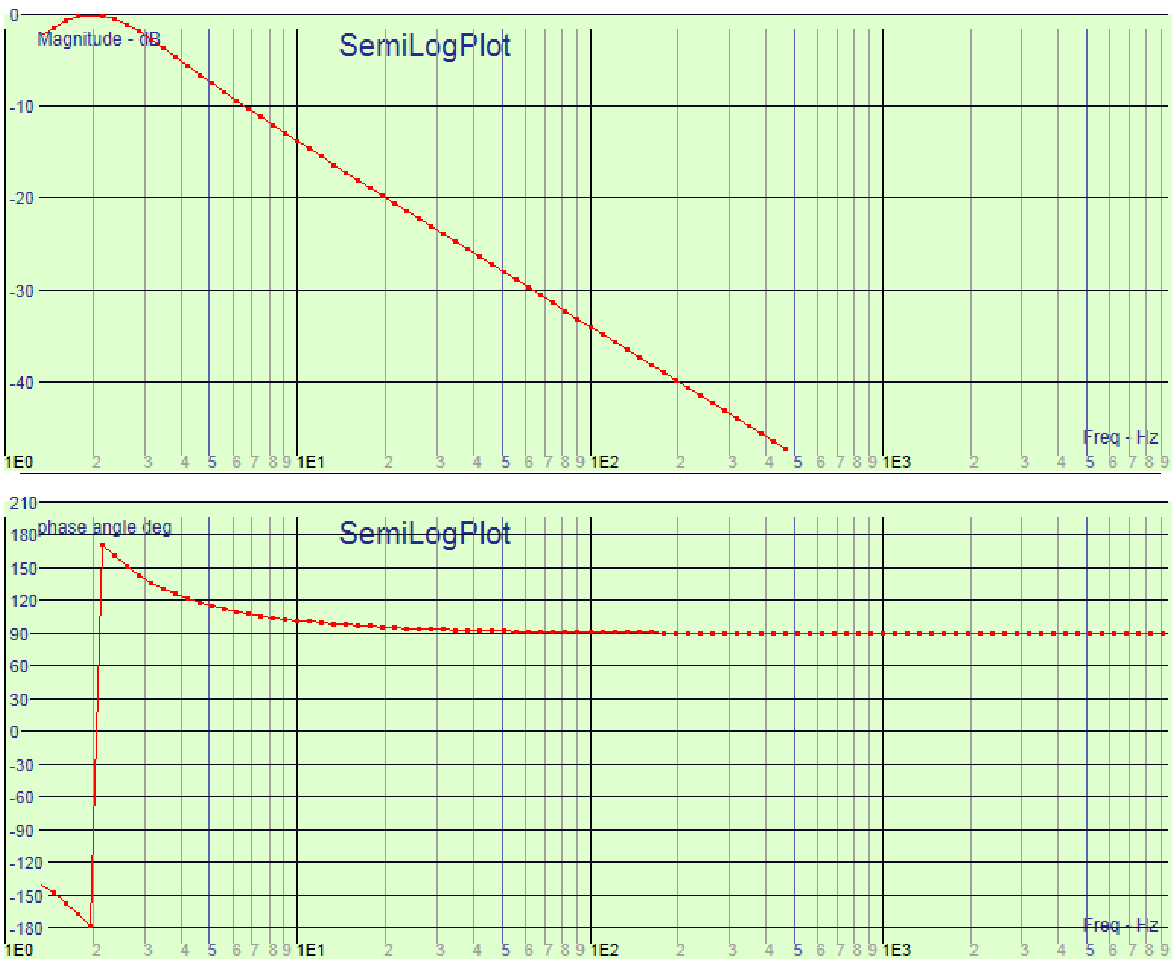

Figure D.1: Active analog bandpass filter plot

In *Figures D.2* and *D.3* we show two analog filters that were implemented in the circuitry for the red AC signal. We noticed that the red AC signal still contained a DC offset even after the bandpass filter and as a result decided to implement two more analog passive filters, one a high pass filter with an fc of 0.1Hz and the other a low pass filter with a fc of 5.3Hz. This not only reduced the DC offset that was present in the red AC signal but also reduced any noise present.

Both Bode plots and phase diagrams were generated online through a similar calculator for RC Lowpass and RC High pass filters. The calculations for these filters were also done to check for errors.

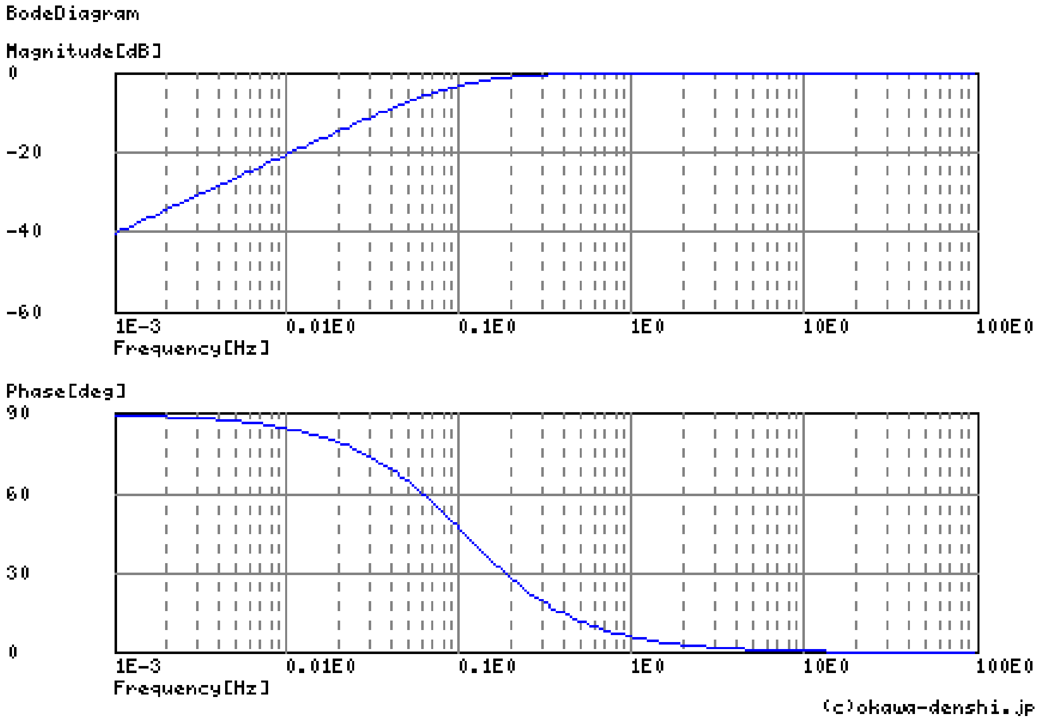

Figure D.2: High pass filter with fc of 0.1 Hz

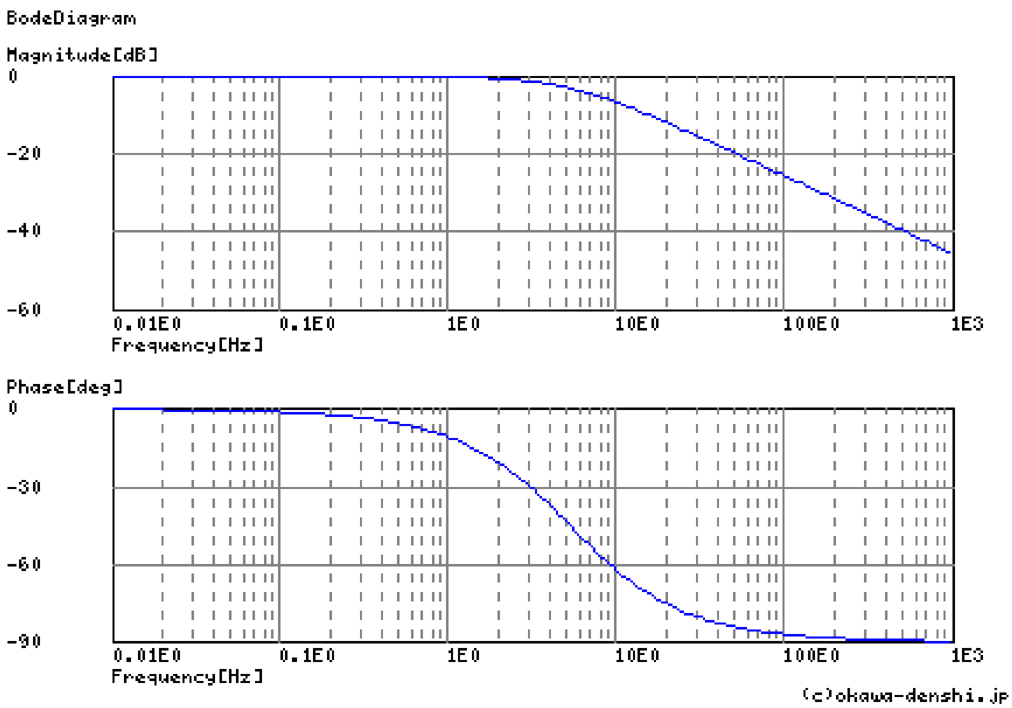

Figure D 3: Low pass filter with fc of 5.3 Hz

In *Figure D.4* we show the magnitude response and the phase response of a 7th order Chebyshev digital filter which was implemented in LabVIEW for the purpose of cleaning up the red AC signal to a further extent. This Bode Plot and phase diagram was generated using the Signals Toolbox in LabVIEW which allows one to see the magnitude response and the phase response of a filter as its being developed.

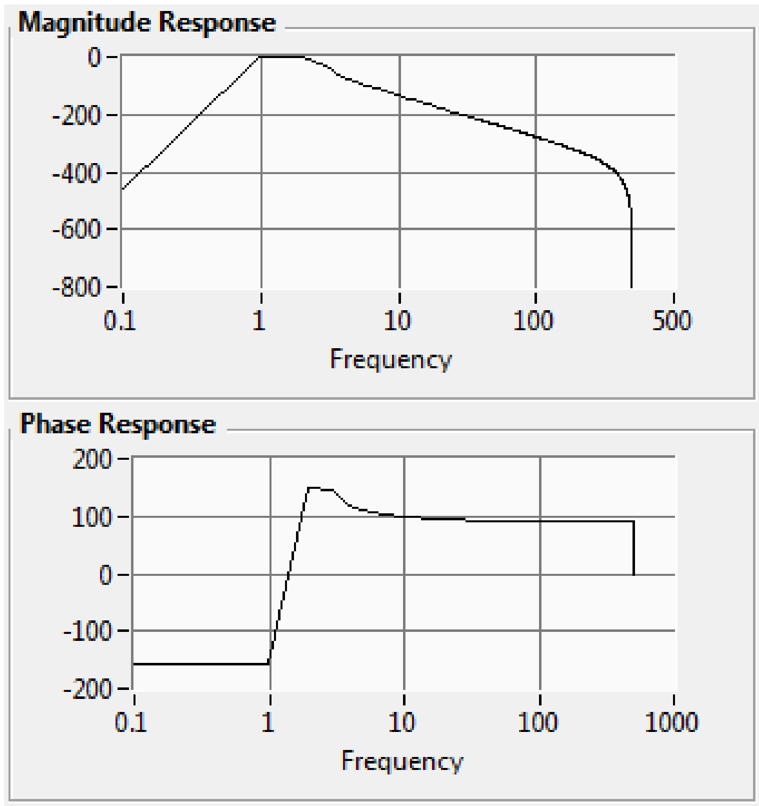

Figure D.4: 7th order Chebyshev digital filter with low fc of 0.75 and high fc of 2.5

APPENDIX Q

US007468036B1

(12) **United States Patent**
Rulkov et al.

(10) **Patent No.: US 7,468,036 B1**
(45) **Date of Patent: *Dec. 23, 2008**

(54) **MONITORING DEVICE, METHOD AND SYSTEM**

(75) Inventors: **Nikolai Rulkov**, San Diego, CA (US); **Mark Hunt**, San Diego, CA (US); **Donald Brady**, Las Vegas, NV (US); **Steve Lui**, San Diego, CA (US); **Sammy I. Elhag**, San Diego, CA (US)

(73) Assignee: **Impact Sports Technology, Inc.**, Las Vegas, NV (US)

(*) Notice: Subject to any disclaimer, the term of this patent is extended or adjusted under 35 U.S.C. 154(b) by 37 days.

This patent is subject to a terminal disclaimer.

(21) Appl. No.: **11/762,078**

(22) Filed: **Jun. 13, 2007**

Related U.S. Application Data

(63) Continuation-in-part of application No. 11/566,229, filed on Dec. 3, 2006, which is a continuation-in-part of application No. 11/388,707, filed on Mar. 24, 2006, which is a continuation-in-part of application No. 11/085,778, filed on Mar. 21, 2005.

(60) Provisional application No. 60/829,679, filed on Oct. 17, 2006, provisional application No. 60/843,967, filed on Sep. 12, 2006, provisional application No. 60/665,116, filed on Mar. 25, 2005, provisional application No. 60/613,785, filed on Sep. 28, 2004.

(51) **Int. Cl.**
A61B 5/00 (2006.01)

(52) **U.S. Cl.** **600/485**; 600/500; 600/503

(58) **Field of Classification Search** .... None
See application file for complete search history.

(56) **References Cited**

U.S. PATENT DOCUMENTS

4,380,240	A	4/1983	Jobsis et al.	
4,800,495	A	1/1989	Smith	
4,807,630	A	2/1989	Malinouskas	
4,825,879	A	5/1989	Tan et al.	
5,213,099	A	5/1993	Tripp, Jr.	
5,431,170	A	7/1995	Mathews	
5,735,800	A	4/1998	Yasukawa et al.	
6,018,673	A	1/2000	Chin et al.	
6,241,684	B1 *	6/2001	Amano et al.	600/531
6,470,199	B1	10/2002	Kopotic et al.	
6,556,852	B1	4/2003	Schulze et al.	
6,575,912	B1 *	6/2003	Turcott	600/485
6,599,251	B2	7/2003	Chen et al.	
6,605,038	B1	8/2003	Teller et al.	
6,616,613	B1 *	9/2003	Goodman	600/504
6,678,543	B2	1/2004	Diab et al.	
6,681,454	B2	1/2004	Modgil et al.	

(Continued)

Primary Examiner—Robert L Nasser
(74) *Attorney, Agent, or Firm*—Clause Eight LLP; M. Catania

(57) **ABSTRACT**

A monitoring device (**20**) for monitoring the vital signs of a user is disclosed herein. The monitoring device (**20**) is preferably an article (**25**) having an optical sensor (**30**) and a circuitry assembly (**35**). The optical sensor (**30**) preferably comprises a photodetector (**130**) and a plurality of light emitting diodes (**135**). The monitoring device (**20**) preferably provides for the display of the following information about the user: pulse rate; blood oxygenation levels; calories expended by the user of a pre-set time period; target zones of activity; time; distance traveled; and/or dynamic blood pressure.

6 Claims, 13 Drawing Sheets

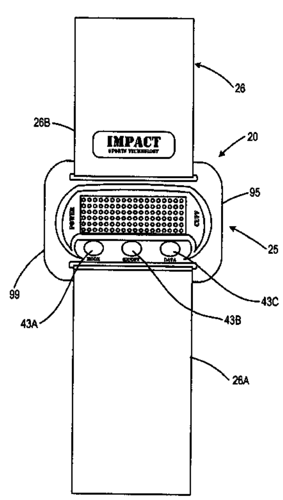

U.S. PATENT DOCUMENTS

6,720,734	B2	4/2004	Norris	
6,808,473	B2	10/2004	Hisano et al.	
6,813,511	B2	11/2004	Diab et al.	
6,866,639	B2 *	3/2005	Causevic et al.	600/559
7,179,228	B2	2/2007	Banet	
2002/0109600	A1	8/2002	Mault et al.	
2006/0084851	A1 *	4/2006	Lee et al.	600/301
2007/0244398	A1 *	10/2007	Lo et al.	600/500
2007/0287923	A1 *	12/2007	Adkins et al.	600/485

* cited by examiner

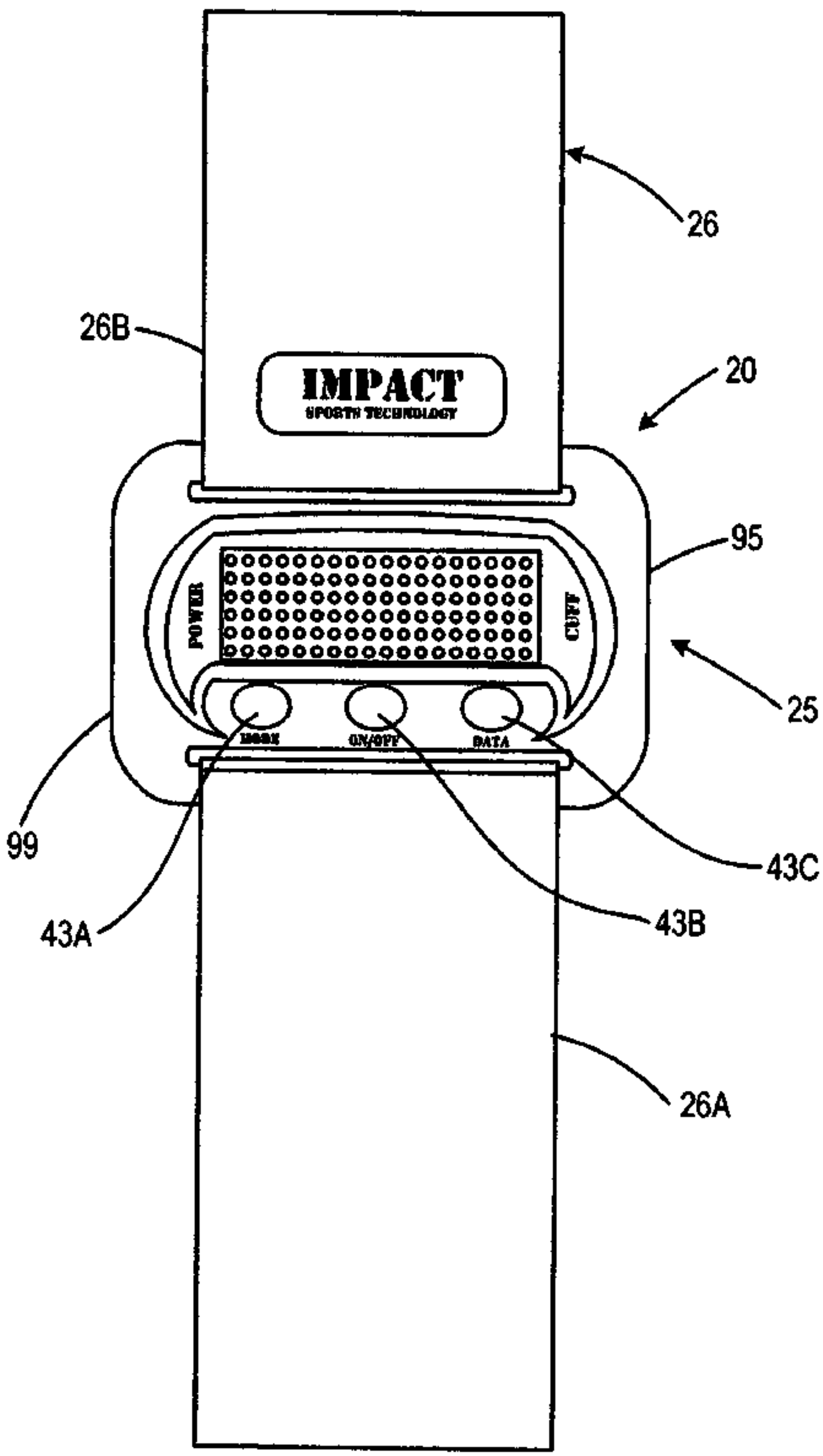
26
26B
IMPACT
SPORTS TECHNOLOGY
20
95
POWER
CUFF
25
MODE
ON/OFF
DATA
99
43C
43A
43B
26A

FIGURE 1

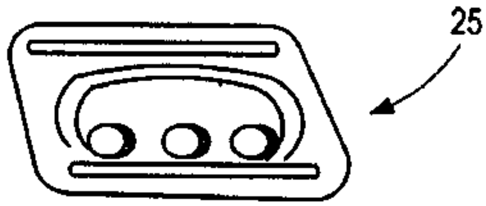

FIGURE 2

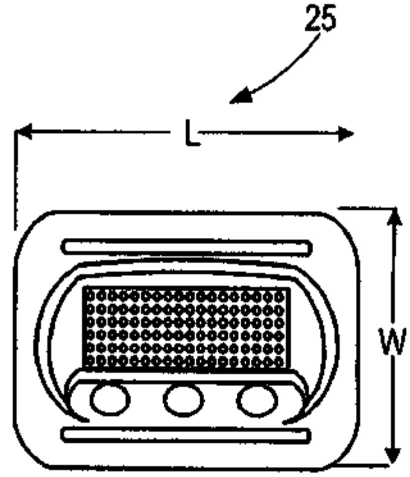

FIGURE 2A

FIGURE 2B

FIGURE 2D

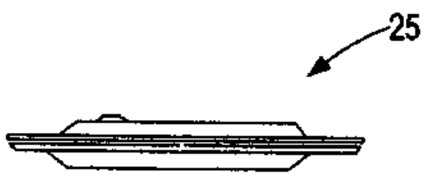

FIGURE 2C

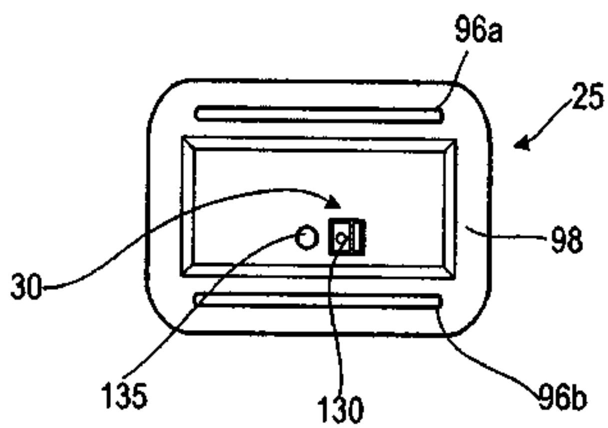

FIGURE 2E

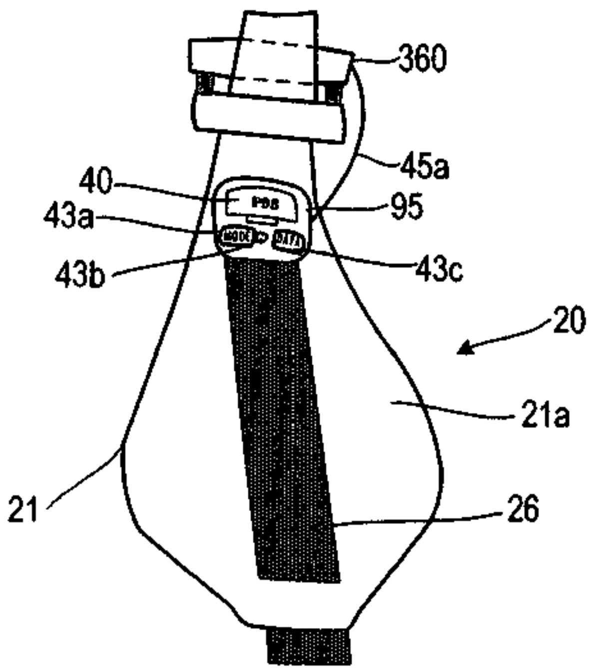

FIGURE 3

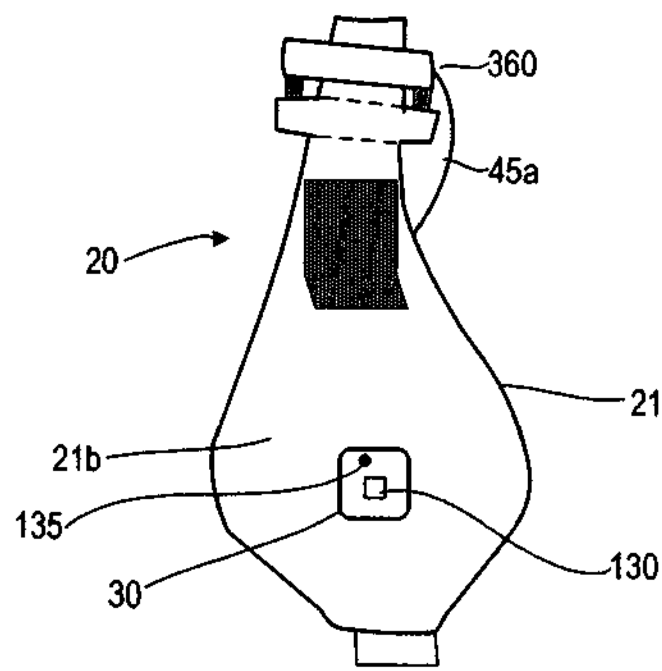

FIGURE 3A

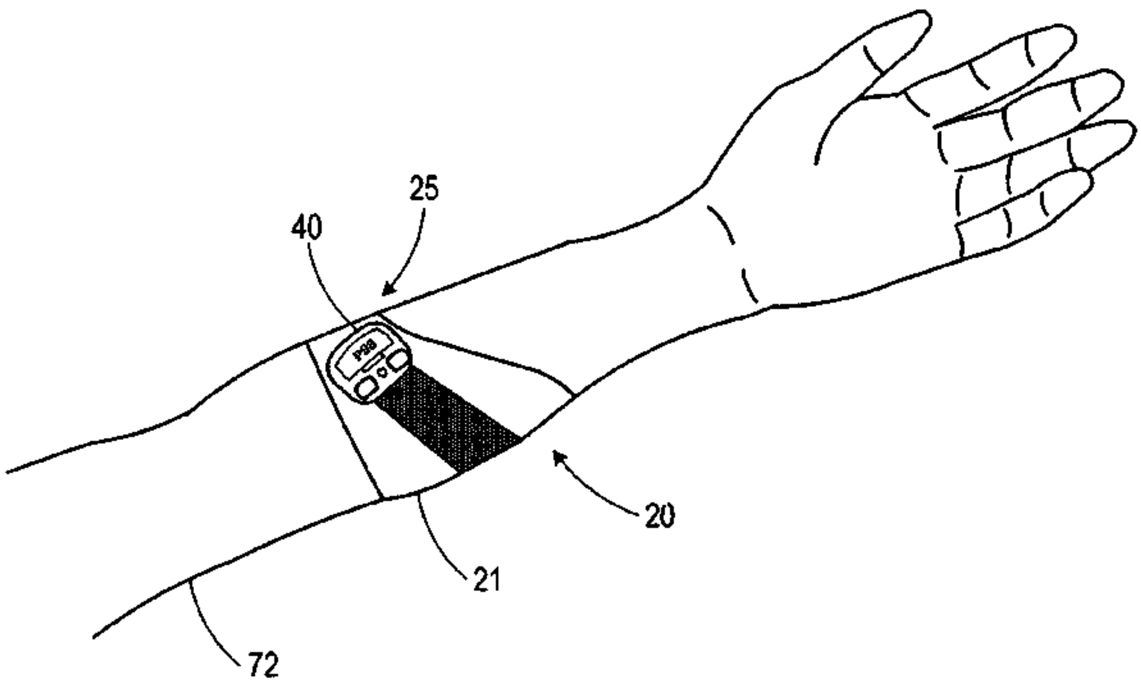

FIGURE 3B

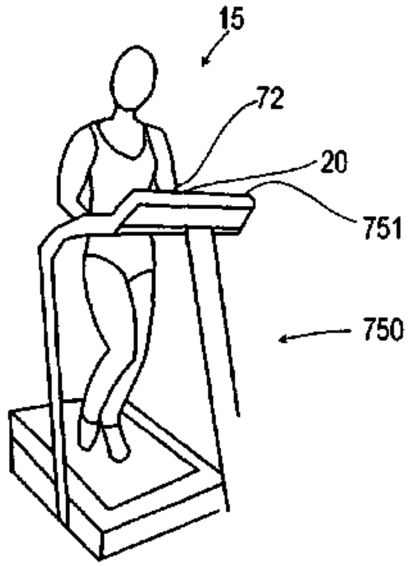

FIGURE 5

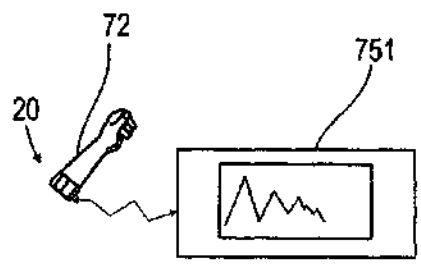

FIGURE 6

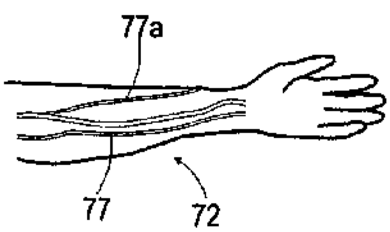

FIGURE 4

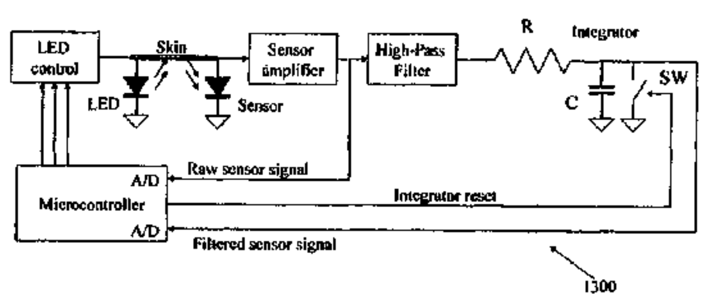

FIGURE 7

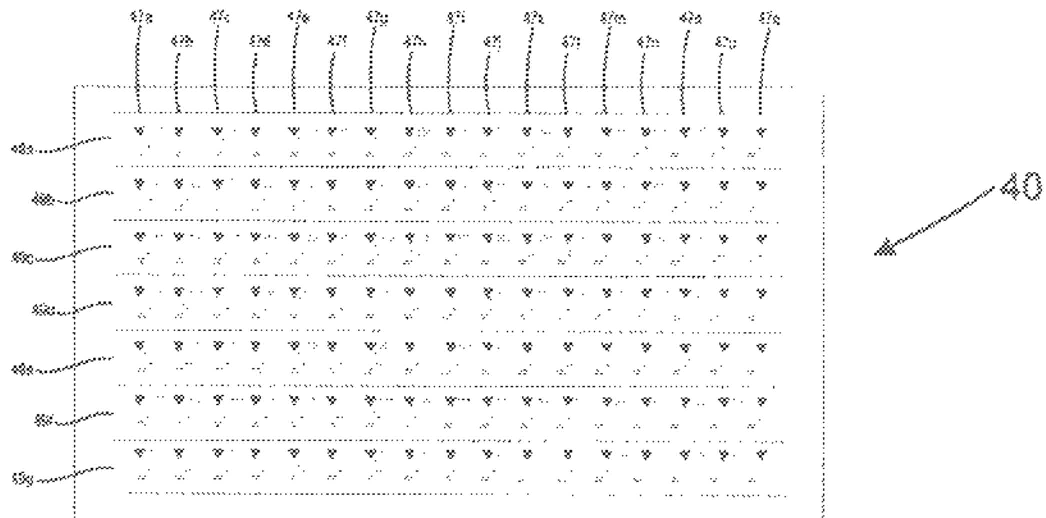

FIGURE 8

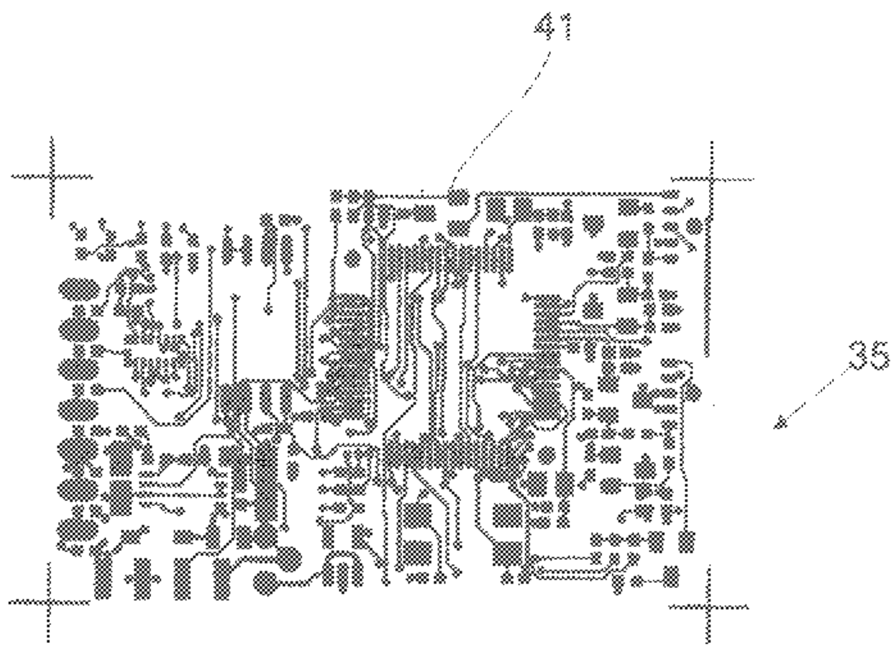

FIGURE 9

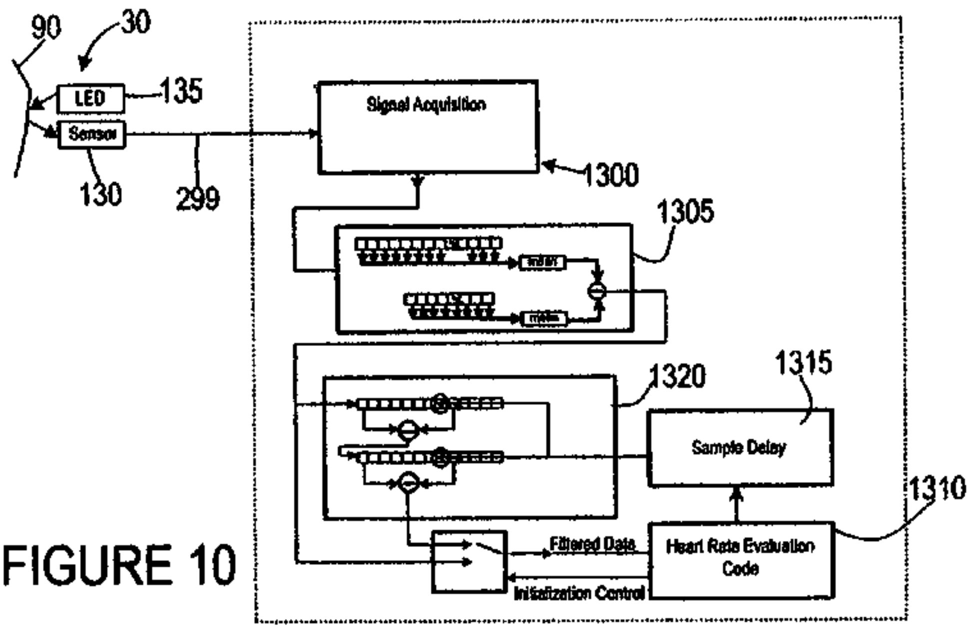

FIGURE 10

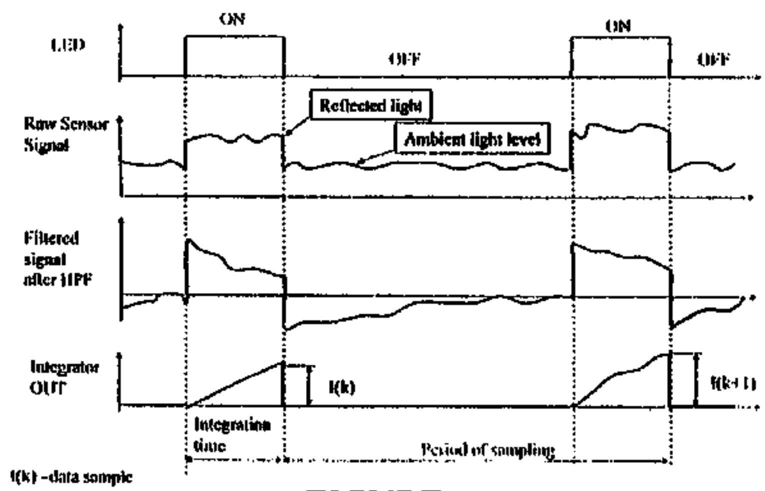

FIGURE 11

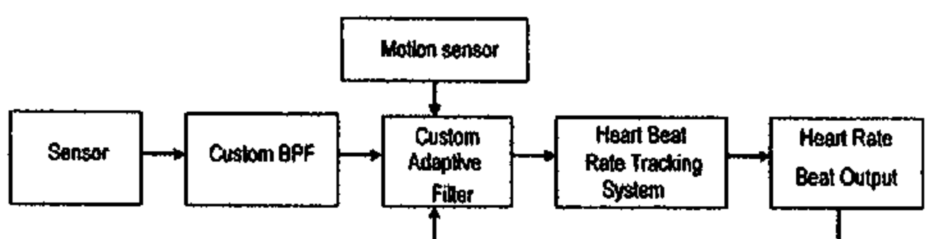

FIGURE 12

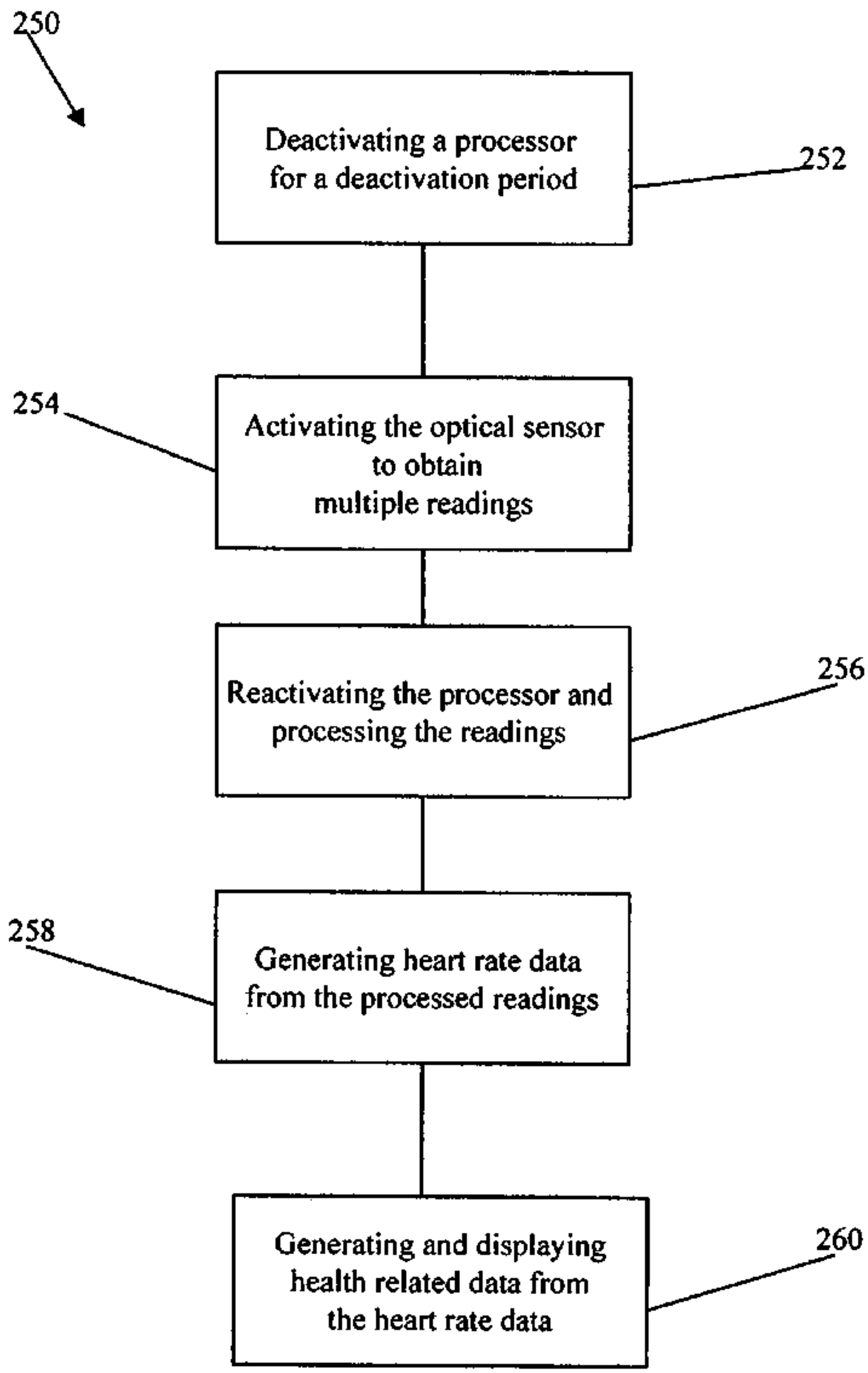
250
Deactivating a processor for a deactivation period
252
254
Activating the optical sensor to obtain multiple readings
Reactivating the processor and processing the readings
256
258
Generating heart rate data from the processed readings
Generating and displaying health related data from the heart rate data
260

FIGURE 13

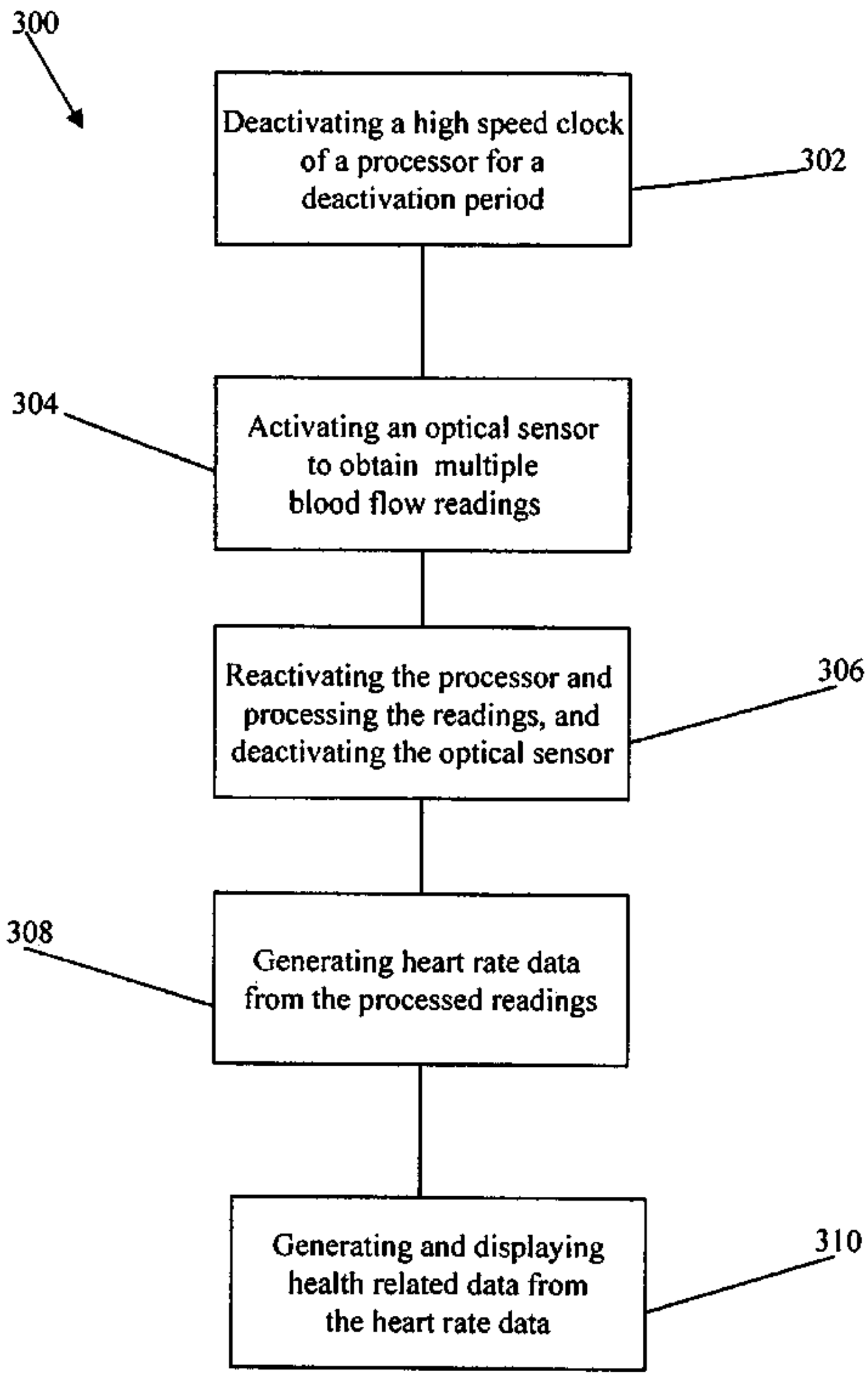
300
Deactivating a high speed clock of a processor for a deactivation period
302
304
Activating an optical sensor to obtain multiple blood flow readings
Reactivating the processor and processing the readings, and deactivating the optical sensor
306
308
Generating heart rate data from the processed readings
Generating and displaying health related data from the heart rate data
310

FIGURE 14

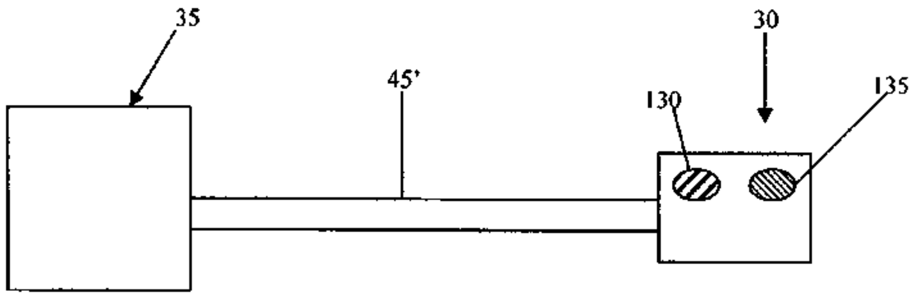

FIGURE 15
(Prior Art)

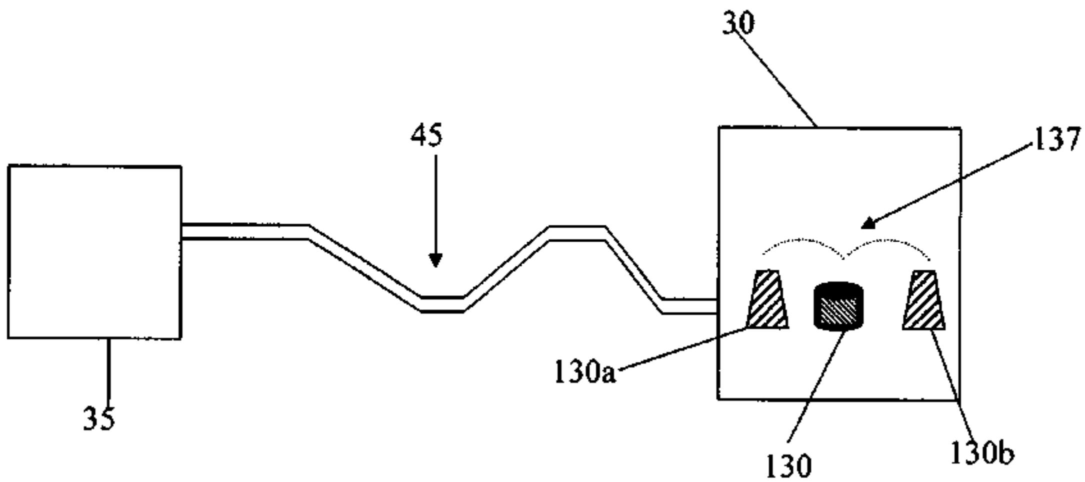

FIGURE 16

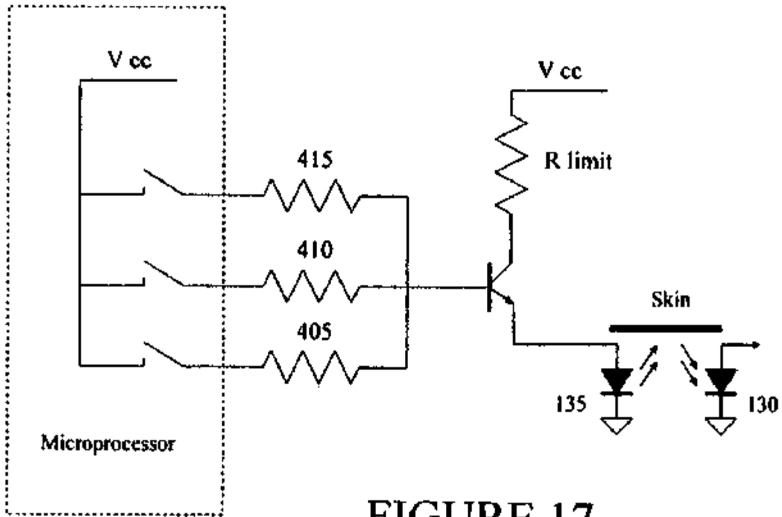

FIGURE 17

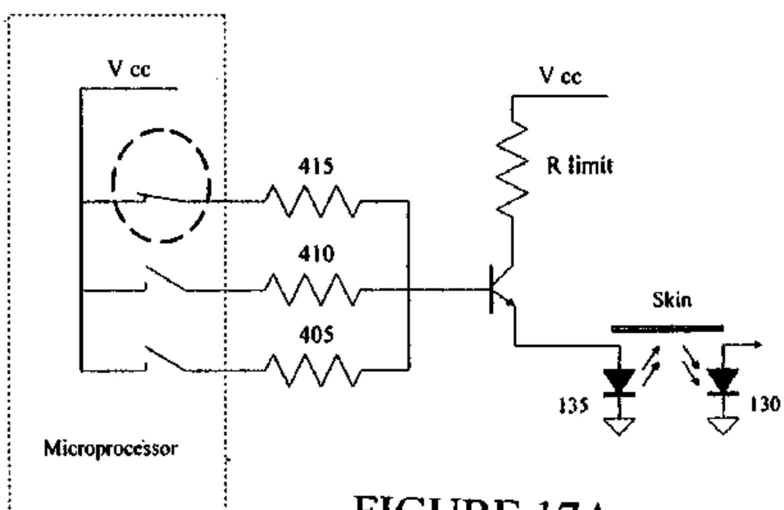

FIGURE 17A

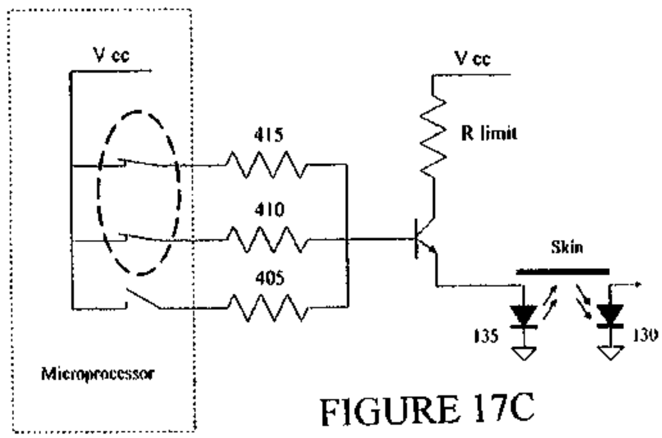

FIGURE 17C

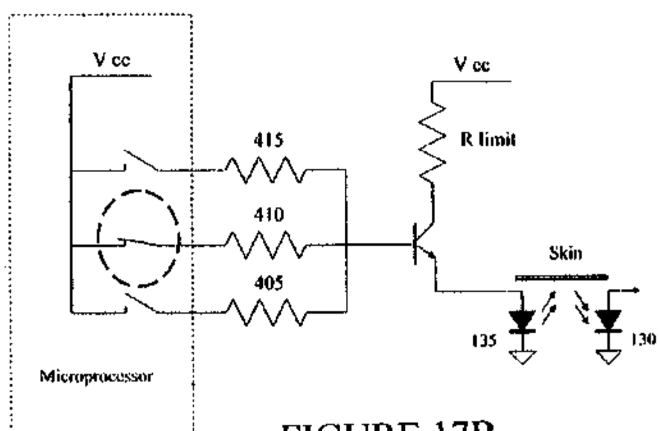

FIGURE 17B

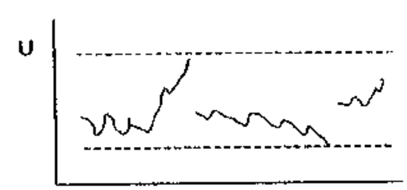

FIGURE 19

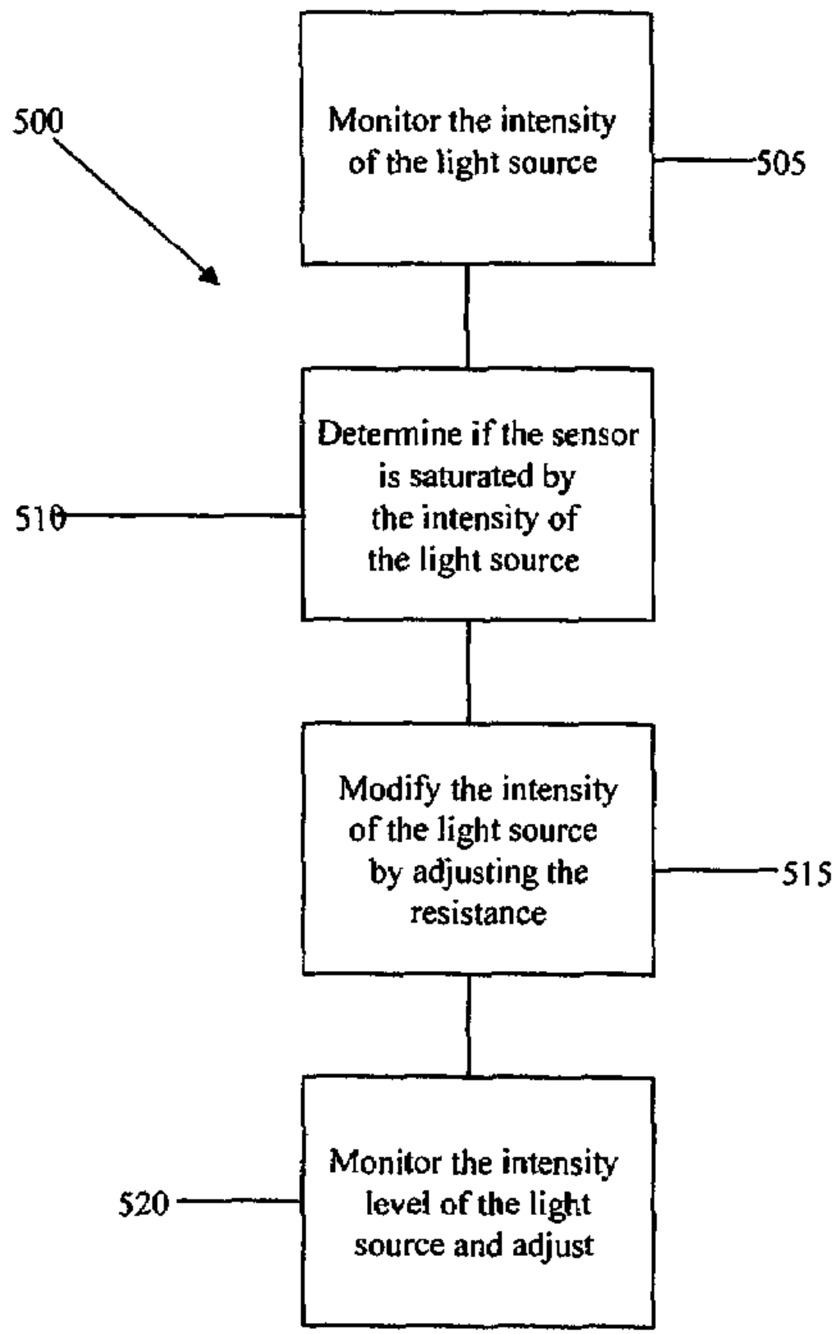
500
Monitor the intensity of the light source
505
Determine if the sensor is saturated by the intensity of the light source
510
Modify the intensity of the light source by adjusting the resistance
515
Monitor the intensity level of the light source and adjust
520

FIGURE 18

MONITORING DEVICE, METHOD AND SYSTEM

CROSS REFERENCES TO RELATED APPLICATIONS

The Present application is a continuation-in-part application of U.S. patent application Ser. No. 11/566,229, filed on Dec. 3, 2006, which is a continuation-in-part application of U.S. patent application Ser. No. 11/388,707, filed on Mar. 24, 2006, which claims priority to U.S. Provisional Application No. 60/665,116, filed on Mar. 25, 2005, now abandoned; and the Present application is a continuation-in-part application of U.S. patent application Ser. No. 11/085,778, filed on Mar. 21, 2005, which claims priority to U.S. Provisional Application No. 60/613,785, filed on Sep. 28, 2004, now abandoned. The Present application also claims priority to U.S. Provisional Application No. 60/843,967, filed on Sep. 12, 2006 and U.S. Provisional Application No. 60/829,679, filed on Oct. 17, 2006.

STATEMENT REGARDING FEDERALLY SPONSORED RESEARCH OR DEVELOPMENT

Not Applicable

BACKGROUND OF THE INVENTION

1. Field of the Invention

The present invention is related to real-time vital sign monitoring devices. More specifically, the present invention relates to a device for monitoring a user's vital signs.

2. Description of the Related Art

There is a need to know how one is doing from a health perspective. In some individuals, there is a daily, even hourly, need to know one's health. The prior art has provided some devices to meet this need.

One such device is a pulse oximetry device. Pulse oximetry is used to determine the oxygen saturation of arterial blood. Pulse oximeter devices typically contain two light emitting diodes: one in the red band of light (660 nanometers) and one in the infrared band of light (940 nanometers). Oxyhemoglobin absorbs infrared light while deoxyhemoglobin absorbs visible red light. Pulse oximeter devices also contain sensors that detect the ratio of red/infrared absorption several hundred times per second. A preferred algorithm for calculating the absorption is derived from the Beer-Lambert Law, which determines the transmitted light from the incident light multiplied by the exponential of the negative of the product of the distance through the medium, the concentration of the solute and the extinction coefficient of the solute.

The major advantages of pulse oximetry devices include the fact that the devices are non-invasive, easy to use, allows for continuous monitoring, permits early detection of desaturation and is relatively inexpensive. The disadvantages of pulse oximetry devices are that it is prone to artifact, it is inaccurate at saturation levels below 70%, and there is a minimal risk of burns in poor perfusion states. Several factors can cause inaccurate readings using pulse oximetry including ambient light, deep skin pigment, excessive motion, fingernail polish, low flow caused by cardiac bypass, hypotension, vasoconstriction, and the like.

Chin et al., U.S. Pat. No. 6,018,673 discloses a pulse oximetry device that is positioned entirely on a user's nail to reduce out of phase motion signals for red and infrared wavelengths for use in a least squares or ratio-of-ratios technique to determine a patient's arterial oxygen saturation.

Smith, U.S. Pat. No. 4,800,495 discloses an apparatus for processing signals containing information concerning the pulse rate and the arterial oxygen saturation of a patient. Smith also discloses maintaining the position of the LEDs and detectors to prevent motion-artifacts from being produced in the signal.

Another method for using a pulse oximeter to measure blood pressure is disclosed in U.S. Pat. No. 6,616,613 to Goodman for a 'Physiological Signal Monitoring System'. The '613 patent discloses processing a pulse oximetry signal in combination with information from a calibrating device to determine a patient's blood pressure.

Chen et al, U.S. Pat. No. 6,599,251 discloses a system and method for monitoring blood pressure by detecting pulse signals at two different locations on a subjects body, preferably on the subject's finger and earlobe. The pulse signals are preferably detected using pulse oximetry devices.

Schulze et al., U.S. Pat. No. 6,556,852, discloses the use of an earpiece having a pulse oximetry device and thermopile to monitor and measure physiological variables of a user.

Malinouskas, U.S. Pat. No. 4,807,630, discloses a method for exposing a patient's extremity, such as a finger, to light of two wavelengths and detecting the absorbance of the extremity at each of the wavelengths.

Jobsis et al., U.S. Pat. No. 4,380,240 discloses an optical probe with a light source and a light detector incorporated into channels within a deformable mounting structure which is adhered to a strap. The light source and the light detector are secured to the patient's body by adhesive tapes and pressure induced by closing the strap around a portion of the body.

Tan et al., U.S. Pat. No. 4,825,879 discloses an optical probe with a T-shaped wrap having a vertical stem and a horizontal cross bar, which is utilized to secure a light source and an optical sensor in optical contact with a finger. A metallic material is utilized to reflect heat back to the patient's body and to provide opacity to interfering ambient light. The sensor is secured to the patient's body using an adhesive or hook and loop material.

Modgil et al., U.S. Pat. No. 6,681,454 discloses a strap that is composed of an elastic material that wraps around the outside of an oximeter probe and is secured to the oximeter probe by attachment mechanisms such as Velcro, which allows for adjustment after initial application without producing excessive stress on the spring hinge of the oximeter probe.

Diab et al., U.S. Pat. No. 6,813,511 discloses a disposable optical probe suited to reduce noise in measurements, which is adhesively secured to a patient's finger, toe, forehead, earlobe or lip.

Diab et al., U.S. Pat. No. 6,678,543 discloses an oximeter sensor system that has a reusable portion and a disposable portion. A method for precalibrating a light sensor of the oximeter sensor system is also disclosed.

Tripp, Jr. et al., U.S. Statutory Invention Registration Number H1039 discloses an intrusion free physiological condition monitor that utilizes pulse oximetry devices.

Hisano et al., U.S. Pat. No. 6,808,473, discloses a headphone-type exercise aid which detects a pulse wave using an optical sensor to provide a user with an optimal exercise intensity.

Mathews, U.S. Pat. No. 5,431,170 ("Mathews"), discloses a pulse responsive device, which has a pulse oximetry device (10) attached to a headband (12) and a separate read-out device (14) that may be attached to a glove and worn on the user's hand. Mathews discloses that the read-out device (14) has a digital display and an analogue display, however, Mathews provides no further detail.

Mault et al, U.S. Patent Application Publication Number 2002/0109600 ("Mault") discloses a smart activity monitor ("SAM") which is a pedometer based device which includes an electronic clock, a sensor, entry means for recording food consumption and exercise activities and a memory for storing such information. Mault fails to disclose the details of the display other than to mention that the SAM has a time display, an exercise display and a food display, with the exercise and food displays having a bar-graph style. Mault fails to disclose an optical sensor in detail, and only states that photo-plethysmography may be used to determine the heart rate by a sensor provided on the rear of a wrist mounted SAM.

Kopotic et al, U.S. Pat. No. 6,470,199, discloses a sock for positioning an optical probe.

Yasukawa et al., U.S. Pat. No. 5,735,800 ("Yasukawa"), discloses a wrist-worn device which is intended for limited motion about the user's wrist. Yasukawa discloses an optical sensor that uses a blue LED with a phototransistor in conjunction with an analog to digital converter to provide a digital signal to a data processing circuit.

In monitoring one's health there is a constant need to know how many calories have been expended whether exercising or going about one's daily routine. A calorie is a measure of heat, generated when energy is produced in our bodies. The amount of calories burned during exercise is a measure of the total amount of energy used during a workout. This can be important, since increased energy usage through exercise helps reduce body fat. There are several means to measure this expenditure of energy. To calculate the calories burned during exercise one multiplies the intensity level of the exercise by one's body weight (in kilograms). This provides the amount of calories burned in an hour. A unit of measurement called a MET is used to rate the intensity of an exercise. One MET is equal to the amount of energy expended at rest.

For example, the intensity of walking 3 miles per hour ("mph") is about 3.3 METS. At this speed, a person who weighs 132 pounds (60 kilograms) will burn about 200 calories per hour ($60\times3.3=198$).

The computer controls in higher-quality exercise equipment can provide a calculation of how many calories are burned by an individual using the equipment. Based on the workload, the computer controls of the equipment calculate exercise intensity and calories burned according to established formulae.

The readings provided by equipment are only accurate if one is able to input one's body weight. If the machine does not allow this, then the "calories per hour" or "calories used" displays are only approximations. The machines have built-in standard weights (usually 174 pounds) that are used when there is no specific user weight.

There are devices that utilize a watch-type monitor to provide the wearer with heart rate as measured by a heartbeat sensor in a chest belt.

However, the prior art devices often suffer from noise, light and motion related problems. These problems are increased when the user participates in an athletic activity such as running. Further, attempting to correct one problem often creates additional problems such as increasing a sensor output which results in a shorter battery life.

The prior art has failed to provide a means for monitoring one's health that is accurate, easy to wear on one's body for extended time periods, allows the user to input information and control the output, and provides sufficient information to the user about the user's health. Thus, there is a need for a monitoring device that can be worn for an extended period and provide health information to a user.

BRIEF SUMMARY OF THE INVENTION

The present invention provides a solution to the shortcomings of the prior art. The present invention is accurate, comfortable to wear by a user for extended time periods, allows for input and controlled output by the user, is light weight, and provides sufficient real-time information to the user about the user's health.

One aspect of the present invention is a monitoring device for monitoring the health of a user. The monitoring device includes an article, an optical device for generating a pulse waveform, a circuitry assembly embedded within the article, a display member positioned on an exterior surface of the article, and a control means attached to the article.

The article is preferably a band to be worn on a user's wrist or ankle. The article preferably has a minimal mass, one to five ounces, and is flexible so that the user can wear it the entire day if necessary. The monitoring device allows the user to track calories burnt during a set time period, monitor heart rate, blood oxygenation levels, distance traveled, target zones and optionally dynamic blood pressure.

Yet another aspect of the present invention is a system for real time monitoring of a user's vital sign during a live event within a playing environment. The system includes a monitoring device, a computing device and an electro-optical display. The monitoring device is attached to an arm, wrist or ankle of the user. The monitoring device comprises means for generating a real-time vital sign signal corresponding to the heart rate of the user, and means for transmitting the real-time vital sign signal outside of the playing environment. The computing device is positioned outside of the playing environment. The computing device comprises means for receiving the real-time vital sign signal from the monitoring device, and means for processing the real-time vital sign signal for transmission to and image on the electro-optical display.

Yet another aspect of the present invention is a monitoring device for monitoring the health of a user. The monitoring device includes an article to be worn on the user's wrist, arm or ankle. The monitoring device also includes an optical sensor, a circuitry assembly, a display member and a control component. The optical sensor is disposed on the interior surface of the article. The circuitry assembly is preferably embedded within the annular body of the article. The display member is preferably attached to an exterior surface of the annular body of the article. The control component is disposed on the exterior surface of the annular body of the article. The control component controls the input of information and the output of information displayed on the display member.

Having briefly described the present invention, the above and further objects, features and advantages thereof will be recognized by those skilled in the pertinent art from the following detailed description of the invention when taken in conjunction with the accompanying drawings.

BRIEF DESCRIPTION OF THE SEVERAL VIEWS OF THE DRAWINGS

FIG. **1** is a plan view of a preferred embodiment of a monitoring device worn by a user.

FIG. **2** is a perspective view of the article of the monitoring device worn by a user.

FIG. **2**A is a plan view of the article of the monitoring device.

FIG. **2**B is a front side view of the article of the monitoring device.

FIG. 2C is a rear side view of the article of the monitoring device.

FIG. 2D is an edge side view of the article of the monitoring device.

FIG. 2E is a bottom plan view of the article of the monitoring device.

FIG. 3 is a top view of an alternative embodiment of the monitoring device of the present invention.

FIG. 3A is bottom view of the monitoring device of FIG. 3.

FIG. 3B is a top perspective view of the monitoring device of FIG. 3 worn on a user's arm.

FIG. 4 is a schematic view of arteries within a human arm.

FIG. 5 is a front view of a user running on exercise equipment with the monitoring device on her arm.

FIG. 6 is an isolated view of a display unit of the exercise equipment of FIG. 5.

FIG. 7 is a schematic flow chart of the signal acquisition step of the flow chart of FIG. 10.

FIG. 8 is a schematic view of the display member circuitry.

FIG. 9 is a schematic view of the circuitry assembly.

FIG. 10 is a flow chart of a signal processing method of the present invention.

FIG. 11 is an illustration of the waveforms of the data sampling during the signal processing method.

FIG. 12 is a flow chart of a portion of the signal processing step utilizing a motion sensor to reduce the affect of motion.

FIG. 13 is a flow chart of a noise reduction method of the present invention.

FIG. 14 is a flow chart of a specific noise reduction method of the present invention.

FIG. 15 is a schematic diagram of a prior art connection of a processor to an optical sensor.

FIG. 16 is a schematic diagram of a connection of a processor to an optical sensor utilized by the present invention.

FIG. 17 is a schematic diagram of a light source intensity controlling mechanism of the present invention.

FIG. 17A is a schematic diagram of the light source intensity controlling mechanism of FIG. 17 with a single resistor connected.

FIG. 17B is a schematic diagram of the light source intensity controlling mechanism of FIG. 17 with a single resistor connected.

FIG. 17C is a schematic diagram of the light source intensity controlling mechanism of FIG. 17 with two resistors connected.

FIG. 18 is a flow chart of a light source intensity controlling method of the present invention.

FIG. 19 is a graph illustrating the method and mechanism of controlling the intensity of the light source over time.

DETAILED DESCRIPTION OF THE INVENTION

As shown in FIGS. **1**-**2**E, monitoring device is generally designated **20**. The monitoring device **20** preferably includes an article **25** and an attachment band **26**, preferably composed of first strap **26***a* and second strap **26***b*. The straps **26***a* and **26***b* are preferably attached to each other with a VELCRO® hook and loop material. The article **25** preferably includes an optical sensor **30**, a circuitry assembly **35**, control components **43***a*-**43***c* and optionally a display member **40**. The monitoring device **20** is preferably worn on a user's wrist **71**, arm **72** or ankle **73**. The article **25** preferably has a housing **95** that is sized to securely attach to a user's wrist **71**, arm **72** or ankle **73**, and the housing has an interior surface **98** and an exterior surface **99**. The housing **95** also preferably has a pair of slots **96***a* and **96***b* for placement of the straps **96***a* and **96***b* therethrough for attachment purposes.

It is desirous to adapt the monitoring device **20** to the anatomy of the user's arm **72** or even the user's ankle. The strap **96** is preferably composed of neoprene, leather, synthetic leather, LYCRA, another similar material, or a combination thereof. The article **25** is preferably composed of a semi-rigid or rigid plastic with a rubber-like or semi-flex plastic bottom layer for contact with the user's body. The bottom layer of the housing **95** may have a curve surface for contact with a user's body. The article **25** preferably has a mass ranging from 5 grams to 50 grams. Preferably, the lower the mass of the article **25**, the more comfort to the user. The article **25** preferably has a thickness ranging from 5 mm to 10 mm, and is most preferably 6.5 mm. The bottom layer **95***a* preferably has a thickness ranging from 3.0 mm to 5.0 mm, and most preferably is 3.3 mm. A top layer **95***a* preferably has a thickness ranging from 2.0 mm to 5.0 mm, and most preferably is 2.63 mm. A mid-layer **95***c* preferably has a thickness ranging from 0.25 mm to 1.0 mm, and most preferably is 0.5 mm. The housing **95** preferably has a width, W, ranging from 30 mm to 50 mm, more preferably from 35 mm to 45 mm, and is most preferably approximately 40 mm. The housing **95** preferably has a length, L, ranging from 40 mm to 65 mm, more preferably from 50 mm to 60 mm, and is most preferably approximately 55 mm. The article **25** preferably has a mass ranging from 5 grams to 50 grams, and more preferably from 10 grams to 40 grams. The light weight of the article **25** provides for more comfort to the user. The optical sensor **30** is preferably positioned on the interior surface **98** of the housing **95** and electrically connected to the circuitry assembly **35**.

Although the monitoring device **20** is described in reference to an article worn on a user's arm, wrist or ankle, those skilled in the pertinent art will recognize that the monitoring device **20** may take other forms such as eyewear disclosed in U.S. patent application Ser. No. 11/566,228, which is hereby incorporated by reference in its entirety or a glove such as disclosed in U.S. patent application Ser. No. 11/473,641, which is hereby incorporated by reference in its entirety.

The optical sensor **30** of the monitoring device **20** is preferably positioned over the radial artery **77** or ulnar artery **77***a* (as shown in FIG. **4**) if the article **25** is worn on the user's arm **72**. The optical sensor **30** of the monitoring device **20** is preferably positioned over the posterior tibial artery of a user if the article **25** is worn on the user's ankle. However, those skilled in the pertinent art will recognize that the optical sensor may be placed over other arteries of the user without departing from the scope and spirit of the present invention. Further, the optical sensor **30** need only be in proximity to an artery of the user in order to obtain a reading or signal.

In a preferred embodiment, the optical sensor **30** is a plurality of light emitting diodes ("LED") **135** based on green light wherein the LEDs **135** generate green light (wavelength of 500-570 nm), and a photodetector **130** detects the green light. Yet in an alternative embodiment, the optical sensor **30** is a photodetector **130** and a single LED **135** transmitting light at a wavelength of approximately 900 nanometers as a pulsed infrared LED. Yet further, the optical sensor is a combination of a green light LED and a pulsed infrared LED to offset noise affects of ambient light and sunlight. As the heart pumps blood through the arteries in the user's arm, ankle or wrist, the photodetector **130**, which is typically a photodiode, detects reflectance/transmission at the wavelengths (green, red or infrared), and in response generates a radiation-induced signal.

A preferred optical sensor **30** utilizing green light is a TRS1755 sensor from TAOS, Inc of Plano Tex. The TRS1755 comprises a green LED light source (567 nm wavelength) and a light-to-voltage converter. The output voltage is directly proportional to the reflected light intensity. Another preferred photodetector **130** is a light-to-voltage photodetector such as the TSL260R and TSL261, TSL261R photodetectors available from TAOS, Inc of Plano Texas. Alternatively, the photodetector **130** is a light-to-frequency photodetector such as the TSL245R, which is also available from TAOS, Inc. The light-to-voltage photodetectors have an integrated transimpedance amplifier on a single monolithic integrated circuit, which reduces the need for ambient light filtering. The TSL261 photodetector preferably operates at a wavelength greater than 750 nanometers, and optimally at 940 nanometers, which would preferably have a LED that radiates light at those wavelengths.

In a preferred embodiment, the circuit assembly **35** is flexible to allow for the contour of the user's arm, wrist or ankle, and the movement thereof. The circuitry assembly and display member **40** are preferably separate components electrically connected within the housing **95**. In one embodiment, discussed below, the display member **40** is removed and the signal is sent to a device such as a personal digital assistant, laptop computer, mobile telephone, exercise equipment, or the like for display and even processing of the user's real-time vital signs information. Alternatively, the circuitry assembly **35** includes a flexible microprocessor board which is a low power, micro-size easily integrated board which provides blood oxygenation level, pulse rate (heart rate), signal strength bargraph, plethysmogram and status bits data. The microprocessor can also store data. The microprocessor can process the data to display pulse rate, blood oxygenation levels, calories expended by the user of a pre-set time period, target zone activity, time and dynamic blood pressure. Further, microprocessor preferably includes an automatic gain control for preventing saturation of the photodetector, which allows for the device to be used on different portions of the human body.

The display member **40** is preferably a light emitting diode ("LED"). Alternatively, the display member **40** is a liquid crystal display ("LCD") or other similar display device. As shown in FIG. **8**, the display member **40** is an LED array which preferably has seven rows **49***a*-**49***g* and seventeen columns **47***a*-**47***q*. Further, LED array is angled to allow for a greater aspect ratio. The LED array allows for each column to be illuminated separately thereby giving the appearance of a moving display. For example, if the term "200 calories expended" is displayed on the display member **40**, the "2" of the "200" would preferably first appear in column **47***q* and then subsequently in each of the other columns **47***p*-**47***a*, from the right-most column to the left-most column thereby giving the appearance of the term scrolling along the display member **40**. The terms or words alternatively scroll from left to right. Still alternatively, all of the columns are illuminated at once or all flash in strobe like manner. Further, the user's real-time pulse waveform is displayed in motion on the display member **40** as a default setting. Those skilled in the pertinent art will recognize alternative methods of displaying information on the display member **40** without departing from the scope and spirit of the present invention.

As shown in FIG. **9**, a microprocessor **41** processes the signal generated from the optical sensor **30** to generate the plurality of vital sign information for the user which is displayed on the display member **40**. The control components **43***a-c* are connected to the circuit assembly **35** to control the input of information and the output of information displayed on the display member **40**.

The monitoring device **20** is preferably powered by a power source **360** positioned on the article **25**. Preferably the power source is a battery. The power source **360** is preferably connected to the circuit assembly **35** by positive wire **45***a* and ground wire **45***b*, and the ground wire **45***b* and positive wire **45***c* are embedded within the article **25**. The power source **360** is preferably an AA or AAA disposable or rechargeable battery. The power source **360** is alternatively a lithium ion rechargeable battery such as available from NEC-Tokin. The power source **360** preferably has an accessible port for recharging. The circuit assembly **35** preferably requires 5 volts and draws a current of 20- to 40 milliamps. The power source **360** preferably provides at least 900 milliamp hours of power to the monitoring device **20**.

As shown in FIGS. **3**, **3**A and **3**B, an alternative embodiment of the monitoring device **20** comprises a light shield **21** with the article **25** disposed on an exterior surface **21***a* of the light shield **21**, and the optical sensor **30** disposed on an interior surface **21***b* of the light shield **21**. The light shield **21** is preferably composed of a light-weight, non-transparent (preferably opaque) cloth material. The light shield **21** prevents or substantially eliminates environmental light from interfering with the optical sensor **30** thereby reducing interference with the signal. In a preferred embodiment, the light shield **21** is black in color. A user preferably wears the monitoring device **20** on the user's arm **72** as shown in FIG. **3**B, with a display member **40** visible to the user. In this embodiment, the article **25** contains a circuitry assembly **35**, as discussed above, within the housing **95** of the article **25**. The display member **40** is preferably a LED display monitor, and alternatively a LCD display monitor.

A connection wire arrangement **45** is shown in FIG. **16**, wherein the connection **45** between the microprocessor **41** of the circuitry assembly **35** and the optical sensor **30** is preferably non-planar or non-straight in order to reduce noise in the signal. The optical sensor **30** preferably comprises a photodetector **130**, and first and second LEDs **130***a* and **130***b*, which transmit light **137**. Using two LEDs on each side of a photodetector creates a more mechanically stable optical sensor **30**. The prior art connection assembly is shown in FIG. **15** wherein the connection wire **45'** is straight and prone to noise due to movement of the circuitry assembly **35** relative to the optical sensor **30**, especially lateral movement. The present invention has a non-straight or non-planar connection wire **45** which reduces noise due to movement of the circuitry assembly **35** relative to the optical sensor **30**. The alternating portions of the connection wire **45** absorb the shock of lateral movement and oscillating movement of the circuitry assembly **35** relative to the optical sensor **30**.

The monitoring device **20** alternatively has a short-range wireless transceiver **36***b* which is preferably a transmitter operating on a wireless protocol, e.g. BLUETOOTH, part-15, or 802.11. "Part-15" refers to a conventional low-power, short-range wireless protocol, such as that used in cordless telephones. The short-range wireless transmitter **36***b* (e.g., a BLUETOOTH transmitter) receives information from the microprocessor and transmits this information in the form of a packet through an antenna. An external laptop computer or hand-held device features a similar antenna coupled to a matched wireless, short-range receiver that receives the packet. In certain embodiments, the hand-held device is a cellular telephone with a Bluetooth circuit integrated directly into a chipset used in the cellular telephone. In this case, the cellular telephone may include a software application that receives, processes, and displays the information. The secondary wireless component may also include a long-range wireless transmitter that transmits information over a terrestrial, satellite, or 802.11-based wireless network. Suitable networks include those operating at least one of the following protocols: CDMA, GSM, GPRS, Mobitex, DataTac, iDEN, and analogs and derivatives thereof. Alternatively, the handheld device is a pager or PDA.

As shown in FIGS. **5** and **6**, in yet an alternative system utilizing the monitoring device **20**, a user **15** wears the monitoring device **20** on the user's arm while exercising on exercise equipment **750**. In this embodiment, a wireless signal is transmitted to the exercise equipment **750** to be displayed on a display **751** of the exercise equipment **750**. In this embodiment, it is unnecessary for the monitoring device **20** to have a display **40** since the information is transmitted to the exercise equipment **750**. As shown in FIG. **5**, a user **15** preferably wears the monitoring device **20** on her arm **72** over the radial artery.

A general method is as follows. The light source **135** transmits light through at least one artery of the user. The photodetector **130** detects the light. The pulse rate is determined by the signals received by the photo-detector **130**. An optical sensor **30** with a photodetector **130** and LEDs **135** are preferably utilized.

This information is sent to the circuitry assembly **35** for creation of user's real-time pulse rate. The microprocessor **41** further processes the information to display pulse rate, calories expended by the user of a pre-set time period, target zones of activity, time and/or dynamic blood pressure. The information is displayed on a display member or electro-optical display.

In a preferred embodiment, the housing **95** has three control buttons **43***a-c*. The control buttons **43***a-c* are preferably positioned in relation to the display member **40** to allow the user immediate visual feedback of the user's inputted information. The middle control button **43***b* preferably activates and deactivates the article **25**. The left button **43***a* is preferably used to scroll through the different modes. The right button **43***c* is preferably used to input data. The control buttons **43***a-c* allow for the user's personal data to be entered and for choices to be selected by the user. The left button **43***a* preferably allows for the user's calories burned to be displayed on the display member **40** and for the activity to be reset, and allows for other fitness monitoring features to be displayed.

To activate the article **25**, the middle button **43***b* is depressed for preferably 0.5 seconds and then released. The display member will appear with a current pulse of the user and a calories burned display. The microprocessor preferably stores the calories burned and accumulates the values for a daily calories burned value and a total calories burned value until the activity is reset.

To enter the user's personal data, the middle button **43***b* is depressed for 2 seconds and then released. The user will enter gender, age, mass, height and resting heart rate. Entering the data entails pushing the middle button to select a category (gender, age, . . .) and then pushing the right or left button to scroll through the available options or to enter a value (e.g. age of the user). The middle button **43***b* is pressed again to save the entry. This process is preformed until the user's has entered all of the data that the user wishes to enter into the microprocessor. The display member **40** will then display a heart rate and current calories burned value. A preset resting heart rate for men and women is preferably stored on the microprocessor, and used as a default resting heart rate. However, the user may enter their own resting heart rate value if the user is aware of that value. To access daily calories, the left button **43***a* is pushed by the user and the display member **40** will illustrate the value for daily calories burned by the user. If the left button **43***a* is pushed again, the value for total calories burned by the user will be displayed on the display member **40**. The left button **43***a* is pushed again to return to a heart rate value on the display member **40**.

The right button **43***c* is pushed to scroll through the choices of other output values, which comprises: basal metabolic rate; average heart rate; minimum heart rate; maximum heart rate; fat burn heart rate exercise target zone; cardio burn heart rate exercise target zone; and, summary of daily calories burned. The basal metabolic rate (displayed as "BMR") is an estimate of the total calories burned by the user in one day without exercise, and is based on the user inputted personal data. The average heart rate (displayed as "avHR") is the average heart rate of the user between resets, and is an overall indicator of fitness. The lower the average heart rate, the healthier the heart. The average heart rate is also a measure of the effectiveness of the exercise program employed by the user since a decrease in the average heart rate of the user will indicate the user's fitness has improved. The minimum heart rate (displayed as "mnHR") of the user is typically measured during sleep and periods of relaxation. The maximum heart rate (displayed as "mxHR") is typically measured during intense workouts. The fat burn heart rate exercise target zone (displayed as "fatB") displays a low and high range for the heart rate of the user to optimize fat burning during exercise. The cardio burn heart rate exercise target zone provides a high and low range for the heart rate of the user to optimize cardio conditioning during exercise. The summary of daily calories burned (displayed as "cal") displays the daily calories burned by the user.

In yet an alternative embodiment, an accelerometer, not shown, is embedded within the article **25** and connected to the circuitry assembly **35** in order to provide information on the distance traveled by the user. In a preferred embodiment, the accelerometer is a multiple-axis accelerometer, such as the ADXL202 made by Analog Devices of Norwood, Mass. This device is a standard micro-electronic-machine ("MEMs") module that measures acceleration and deceleration using an array of silicon-based structures.

In yet another embodiment, the monitoring device **20** comprises a first thermistor, not shown, for measuring the temperature of the user's skin and a second thermistor, not shown, for measuring the temperature of the air. The temperature readings are displayed on the display member **40** and the skin temperature is preferably utilized in further determining the calories expended by the user during a set time period. One such commercially available thermistor is sold under the brand LM34 from National Semiconductor of Santa Clara, Calif. A microcontroller that is utilized with the thermistor is sold under the brand name ATMega 8535 by Atmel of San Jose, Calif.

The monitoring device **20** may also be able to download the information to a computer for further processing and storage of information. The download may be wireless or through cable connection. The information can generate an activity log or a calorie chart.

The microprocessor can use various methods to calculate calories burned by a user. One such method uses the Harris-Benedict formula. Other methods are set forth at www.unu.edu/unupress/food2/ which relevant parts are hereby incorporated by reference. The Harris-Benedict formula uses the factors of height, weight, age, and sex to determine basal metabolic rate (BMR). This equation is very accurate in all but the extremely muscular (will underestimate calorie needs) and the extremely overweight (will overestimate caloric needs) user.

The equations for men and women are set forth below:

Men: $BMR=66+(13.7\times mass(kg))+(5\times height(cm))-(6.8\times age(years))$

Women: $BMR=655+(9.6\times mass)+(1.8\times height)-(4.7\times age)$

The calories burned are calculated by multiplying the BMR by the following appropriate activity factor: sedentary; lightly active; moderately active; very active; and extra active.

Sedentary=BMR multiplied by 1.2 (little or no exercise, desk job)

Lightly active=BMR multiplied by 1.375 (light exercise/sports 1-3 days/wk)

Moderately Active=BMR multiplied by 1.55 (moderate exercise/sports 3-5 days/wk)

Very active=BMR multiplied by 1.725 (hard exercise/sports 6-7 days/wk)

Extra Active=BMR multiplied by 1.9 (hard daily exercise/sports & physical job or 2× day training, marathon, football camp, contest, etc.)

Various target zones may also be calculated by the microprocessor. These target zones include: fat burn zone; cardio zone; moderate activity zone; weight management zone; aerobic zone; anaerobic threshold zone; and red-line zone.

Fat Burn Zone=(220−age)×60% & 70%

An example for a thirty-eight year old female:

i. (220−38)×0.6=109

ii. (220−38)×0.7=127

iii. Fat Burn Zone between 109 to 127 heart beats per minute.

Cardio Zone=(220−your age)×70% & 80%

An example for a thirty-eight year old female:

i. (220−38)×0.7=127

ii. (220−38)×0.8=146

iii. Cardio zone is between 127 & 146 heart beats per minute.

Moderate Activity Zone, at 50 to 60 percent of your maximum heart rate, burns fat more readily than carbohydrates. That is the zone one should exercise at if one wants slow, even conditioning with little pain or strain.

Weight Management Zone, at 60 to 70 percent of maximum, strengthens ones heart and burns sufficient calories to lower one's body weight.

Aerobic Zone, at 70 to 80 percent of maximum, not only strengthens one's heart but also trains one's body to process oxygen more efficiently, improving endurance.

Anaerobic Threshold Zone, at 80 to 90 percent of maximum, improves one's ability to rid one's body of the lactic-acid buildup that leads to muscles ache near one's performance limit. Over time, training in this zone will raise one's limit.

Red-Line Zone, at 90 to 100 percent of maximum, is where serious athletes train when they are striving for speed instead of endurance.

EXAMPLE ONE

Female, 30 yrs old, height 167.6 centimeters, weight 54.5 kilograms.

The BMR=655+523+302−141=1339 calories/day.

The BMR is 1339 calories per day. The activity level is moderately active (work out 3-4 times per week). The activity factor is 1.55. The TDEE=1.55×1339=2075 calories/day. TDEE is calculated by multiplying the BMR of the user by the activity multiplier of the user.

The heart rate may be used to dynamically determine an activity level and periodically recalculate the calories burned based upon that factor. An example of such an activity level look up table might be as follows:

Activity/Intensity Multiplier Based on Heart Rate

Sedentary=BMR×1.2 (little or no exercise, average heart rate 65−75 bpm or lower)

Lightly active=BMR×3.5 (light exercise, 75 bpm-115 bpm)

Mod. active=BMR×5.75 (moderate exercise, 115-140 pm)

Very active=BMR×9.25 (hard exercise, 140-175 bpm)

Extra active=BMR×13 (175 bpm−maximum heart rate as calculated with MHR formula)

For example, while sitting at a desk, a man in the above example might have a heart rate of between 65 and 75 beats per minute (BPM). (The average heart rate for an adult is between 65 and 75 beats per minute.) Based on this dynamically updated heart rate his activity level might be considered sedentary. If the heart rate remained in this range for 30 minutes, based on the Harris-Benedict formula he would have expended 1.34 calories a minute×1.2 (activity level)×30 minutes, which is equal to 48.24 calories burned.

If the man were to run a mile for 30 minutes, with a heart rate ranging between 120 and 130 bpm, his activity level might be considered very active. His caloric expenditure would be 1.34 calories a minute×9.25 (activity level)×30 minutes, which is equal to 371.85.

Another equation is weight multiplied by time multiplied by an activity factor multiplied by 0.000119.

FIG. **10** illustrates a block diagram of a flow chart of a signal processing method of the present invention. As shown in FIG. **10**, the photodetector **130** of the optical sensor **30** receives light from the light source **135** while in proximity to the user's artery. The light source **135** is preferably a plurality of LEDs **135**. In a preferred embodiment, the optical sensor **30** is a TRS1755 which includes a green LED light source (567 nm wavelength) and a light-to-voltage converter. The output voltage is directly proportional to the reflected light intensity. The signal **299** is sent to the microprocessor **41**. At block **1300**, the signal acquisition is performed. As shown in FIG. **7**, in the pulse mode the LED **135** is periodically activated for short intervals of time by a signal from the microcontroller. The reflected pulse of light is received by the sensor, with the generation of a voltage pulse having an amplitude proportional to the intensity of the reflected light. When the LED is activated, the switch, SW, is open by the action of the control signal from the microcontroller, and the capacitor, C, integrates the pulse generated from the sensor by charging through the resistor R. Immediately prior to deactivation of the LED, the analog-to-digital converter acquires the value of the voltage integrated across the capacitor, C. The analog-to-digital converter generates a data sample in digital form which is utilized by the microcontroller for evaluation of the heart rate the wearer. Subsequent to the sample being acquired by the analog-to-digital converter, the LED is deactivated and the capacitor, C, is shortcut by switch, SW, to reset the integrator, RC. A signal indicating sensor saturation is also sent to the microcontroller for light control of the LEDs. This states remains unchanged for a given time interval after which the process is repeated, which is illustrated in FIG. **11**. The signals are shown in FIG. **11**, with the raw sensor signal received from the sensor amplifier shown as varying between reflected light when the LEDs are on and an ambient light level when the LEDs are off. The filtered signal from the high pass filter ("HPF") is shown as the filtered sensor signal in FIG. **7**. The integrator reset signal is shown as integrator out signal in FIG. **11**, and the integrator reset signal in FIG. **7**. A noise reduction and power reduction process is discussed below in reference to FIGS. **13** and **14**.

At block **1305**, a band pass filter is implemented preferably with two sets of data from the analog-to-digital converter. At block **1305**, an average of the values of data samples within each of a first set of samples is calculated by the microprocessor. For example, the values of data samples within forty-four samples are summed and then divided by forty-four to generate an average value for the first set of samples. Next, an average of the values of data samples within a second set of samples is calculated by the microprocessor. For example, the values of data samples within twenty-two samples are summed and then divided by twenty-two to generate an average value for the second set of samples. Preferably, the second set of samples is less than the first set of samples. Next, the average value of the second set of samples is subtracted from the average value for the first set of samples to generate a first filtered pulse data value.

At block **1310**, the filtered pulse data value is processed using a heart rate evaluation code to generate a first heart rate value. In a preferred method, the heart rate evaluation code obtains the heart rate by calculating the distance between crossing points of the voltage through zero. Once the first heart rate value is known, then an adaptive resonant filter is utilized to generate a filtered second heart rate value by attenuating interference caused by motion artifacts. At block **1315**, a sample delay is computed as the period of evaluated heart rate divided by two.

At block **1320**, preferably a two cascade adaptive resonant filter generates a second filtered pulse data value which is processed at block **1310** using the heart rate evaluation code to generate a second heart rate value. Those skilled in the pertinent art will recognize that three, four, or more, cascade adaptive resonant filters may be utilized in generating the second filtered pulse data value. Essentially, the highest and lowest values are disregarded in calculating the filtered second heart rate value. Alternatively, a phase is established and any values outside of the phase are disregarded in calculating the second heart rate value. The filtering is preferably continued during the use of the monitor thereby further refining the heart rate value of the user.

As shown in FIG. **12**, a motion sensor **1100** is included in an alternative embodiment to assist in identifying motion noise and filtering the noise from the signal sent by the sensor **30**. The motion sensor **1100**, such as an accelerometer, is integrated into the circuitry and software of the monitoring device **20**. As the motion sensor detects an arm swinging, the noise component is utilized with the signal processing noise filtering techniques to provide additional filtering to remove the noise element and improve the accuracy of the monitoring device **20**. More specifically, the signal from the sensor **30** is transmitted to the processor where a custom blood pressure filter **41***w* processes the signal which is further processed at by custom adaptive filter **41***x* before being sent to a heart beat tracking system **41***y* and then transmitted to a heart rate beat output **41***z*. The heart rate beat output **41***z* provides feedback to the custom adaptive filter **41***x* which also receives input from the motion sensor **1100**.

Still further, a battery source containing twin AAA batteries is built into a buckle for the straps **26***a* and **26***b*. The battery holder is preferably similar in appearance to a shoe buckle.

FIG. **13** illustrates a noise reduction method of the present invention. Due to the desire to minimize power consumption of the monitoring device **20**, and achieve very accurate signal measurements using the optical sensor **30**, the present invention preferably utilizes the method **200** illustrated in FIG. **13**. At block **202**, the processor **41** is deactivated for a deactivation period in order to conserve power and to eliminate noise for a signal measurement. The deactivation period ranges from 128 to 640 microseconds, more preferably from 200 microseconds to 400 microseconds, and more preferably from 225 microseconds to 300 microseconds. In reference to FIG. **10**, this deactivation period occurs during block **1300**. At block **204**, during the deactivation period, the optical sensor **30** is activated to obtain multiple readings using the light source **135** and the photodetector **130**. Preferably 4 to 25 sub-readings or sub-samples are obtained during the deactivation period. The sub-readings or sub-samples are averaged for noise reduction to provide a reading or sample value. In a single second, from 500 to 1500 sub-readings or sub-samples are obtained by the optical sensor **30**. At block **206**, the processor **41** is reactivated and the reading values are processed by processor **41**. At block **208**, heart rate data is generated from the readings by the processor **41**. At block **210**, health related data is generated from the heart rate data, and the health related data and the heart rate data are displayed on the display member **40**.

FIG. **14** illustrates a more specific method **300** for noise reduction during a signal reading. At block **302**, a high speed clock of a processor **41** is deactivated for a deactivation period as discussed above. At block **304**, the optical sensor **30** is activated during the deactivation period to obtain multiple readings as discussed above. At block **306**, the processor **41** is reactivated and the readings are processed. The optical sensor **30** is also deactivated. At block **308**, heart rate data is generated from the readings by the processor **41**. At block **310**, health related data is generated from the heart rate data, and the health related data and the heart rate data are displayed on the display member **40**.

FIG. **17** illustrates a mechanism for controlling the intensity of the light source **135** using a plurality of resistors **405**, **410** and **415** in parallel. Usually, an optical sensor **30** has a light source **135** set for a single intensity for placement at a single location on a user. However, if the optical sensor **30** is placed at a different location, e.g. from the lower arm to the upper arm, the intensity of the light source **135** may be too great for the photodetector **130** and lead to saturation of the photodector **130** which terminates the signal reading. The present invention preferably adjusts the intensity of the light source **135** using feedback from the photodetector **130** to indicate whether the light intensity is too high or too low. As shown in FIGS. **17**,**17**A, **17**B and **17**C, the current flow through the resistors **405**, **410** and **415** is changed, which results in changes in the light intensity of the light source **135**. Equation A below illustrates the resistance:

$$1/R_{eff}=S_1(1/R_1)+S_2(1/R_2)+S_3(1/R_3)$$

where S_n=Switch$_n$ having a value of 0 or 1, and R_n=resistor, in ohms. In one embodiment, resistor **405** has a resistance of 400 Ohms, resistor **410** has a resistance of 200 Ohms and resistor **415** has a resistance of 100 Ohms. Various combinations of the resistors can be switched on to control the light intensity.

FIG. **17**A has current flowing through a single line and a single resistor. FIG. **17**C has current flowing through all of the lines. Although FIG. **17**C utilizes the most resistors **410** and **415**, it has the greatest current flow and the highest intensity. The current flow is given by the equation B:

$$(V_{cc}-V)/R_{eff}=I_{LED}$$

where I_{LED} is the current flow. Although only three resistors are shown, those skilled in the pertinent art will recognize the more or fewer resistors may be used without departing from the scope and spirit of the present invention.

FIG. **18** is a preferred method **500** for controlling the light intensity of the optical sensor **30**. At block **505**, the light intensity of the light source **135** is monitored. At block **510**, the sensor/phototdetector is determined to be saturated by the light source. At block **515**, the intensity of the light source is modified by adjusting the resistance and the flow of current to the light source **135**. At block **520**, the light intensity is again monitored and adjusted if necessary. In a preferred embodiment, this automatic gain mechanism prevents the green light from overwhelming the photodetector thereby maintaining an accurate reading no matter where the optical sensor is placed on the user.

FIG. **19** illustrates how the control mechanism operates to maintain a proper light intensity. As the signal reaches the upper limit, the photodetector becomes saturated and the processor lowers the current flow, which results in a break in the signal. Then as the signal is lowered it becomes too low and the processor increases the light intensity resulting in a break in the signal.

From the foregoing it is believed that those skilled in the pertinent art will recognize the meritorious advancement of this invention and will readily understand that while the present invention has been described in association with a preferred embodiment thereof, and other embodiments illustrated in the accompanying drawings, numerous changes modification and substitutions of equivalents may be made therein without departing from the spirit and scope of this invention which is intended to be unlimited by the foregoing except as may appear in the following appended claim. Therefore, the embodiments of the invention in which an exclusive property or privilege is claimed are defined in the following appended claims.

We claim as our invention:

1. A method of monitoring a user's vital signs, the method comprising:

deactivating a processor for a deactivation period of 128 to 640 microseconds;

activating an optical sensor during the deactivation period to generate a signal corresponding to the flow of blood through at least one artery of the user, the optical sensor comprising a photodetector and a plurality of light-emitting diodes;

reactivating the processor to process the signal to obtain an average pulse value of a first set of time periods;

processing the signal to obtain an average pulse value of a second set of time periods, the second set of time periods less than the first set of time periods;

subtracting the average pulse value of the second set of time periods from the average pulse value of the first set of time periods to generate a first filtered pulse data value;

processing the first filtered pulse data value to obtain a first heart rate value;

using the first heart rate value to filter the subsequent average pulse values generated from the digital signal to obtain a real-time heart rate value of the user;

processing the real-time heart rate data of the user for analysis of real-time calories expended by the user and for real-time display of a plurality of the user's vital signs; and

displaying the plurality of user's vital signs on a display member, the display of the plurality of user's vital signs controlled by the user using a control component.

2. The method according to claim **1** further comprising filtering motion noise from the signal utilizing a motion sensor.

3. The method according to claim **1** wherein the plurality of light emitting diodes comprises a plurality of pulsed infrared light emitting diodes.

4. The method according to claim **1** wherein the plurality of light emitting diodes comprises a pulsed infrared light emitting diode and a green light emitting diode.

5. The method according to claim **1** wherein the real-time heart rate data is based on 60 to 180 sample readings and each of the sample readings is based on 4 to 15 sub-sample readings.

6. The method according to claim **1** wherein the processor, the optical sensor and the display member are disposed on a monitoring device.

* * * * *

APPENDIX R

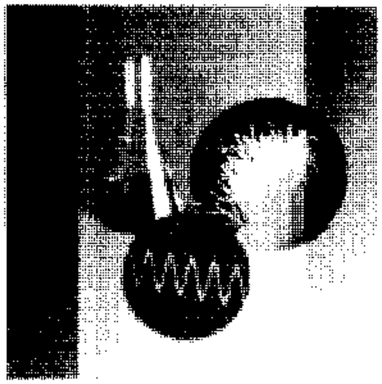

Optical Oximetry Sensors for Whole Blood and Tissue

Setsuo Takatani
Jian Ling
Department of Surgery
Baylor College of Medicine

The oxygen saturation of hemochromes such as hemoglobin, myoglobin, and cytochromes yield useful information for evaluation of patients in various clinical settings. In particular, clinical measurements of hemoglobin saturation in major vessels and cardiac chambers have been reported during catheterization for detection of cardiac shunts [1-2], for estimation of cardiac output from arterio-venous oxygen difference via Fick's principle [3], and for monitoring patients with various cardiac diseases [4-6]. During surgical procedures and recovery from anesthesia, hemoglobin oxygen saturation has been utilized for early detection of hypoxia [7-8]. And in the care of fetuses and neonates, oxygen saturation data are useful [9-12].

The measurement of oxygen saturation in humans goes back to the 1940s, when Millikan devised an instrument to measure arterial saturation from the forehead [13]. This was followed by various workers including Brinkman, Wood, Sekelj, Tait, et al., who noninvasively estimated arterial saturation as well as tissue oxygen saturation [14-17]. The works by Wood and co-workers resulted in ear oximeters, and the contributions by Sekelj, et al. advanced this device. In the 1960s, solid state devices such as the light emitting diode and photodiode were introduced to make a miniature skin reflectance sensors and also intravascular measurement systems by utilizing fiber optic guides. The fiber optic intravascular oximeter developed by Polanyi and Hehir [18] became the basis for the modern invasive oximeter.

In the 1970s, Cheung and Reynolds [19-20] modeled the optical fiber system in blood, based on the photon diffusion theory developed by Johnson [21]. Noninvasive skin and tissue reflectance oximeters were also developed by Cohen and Takatani [22-23] in the late 1970s, with optical propagation in the medium modeled utilizing one-dimensional and three-dimensional photon diffusion theory. Contrary to the transport theory approach, Lubbers, et al. [24-25] utilized the multi-component approach in combination with Monte-Carlo simulation in analyzing the tissue spectra. However, problems of the earlier workers included 1) lack of adequate calibration procedure in vivo, 2) unknown distribution of arterial-to-venous blood volume in tissue, 3) unknown optical path-length in tissue, and 4) lack of an appropriate mathematical relation to calculate tissue hemoglobin saturation in vivo.

In the early 1980s, the innovative approach of pulse oximetry, which combined the principle of conventional optical oximetry with the plethysmographic principle, offered a means of noninvasively estimating arterial blood oxygen saturation [26-30]. This instrument assumes that the forward scattered plethymographic pulsatile signals are due to arterial blood, and noninvasively measures arterial saturation from the finger tip or the ear lobe. Most operating rooms and intensive care units today are equipped with this device. Another innovative approach is the use of a very narrow light pulse (on the order of picoseconds) or ultra high frequency signal (on the order of 500 MHz) to measure transit time of light signals through tissues. These techniques characterize the tissue optical properties of absorption and scattering, from which absolute tissue oxygen saturation can be estimated [31-34]. Although this approach is still in the experimental state, it offers an absolute determination of tissue oxygen saturation as well as an image of the tissue oxygen field in a three dimensions [35-36].

This article reviews the optical techniques applied to the determination of intravascular hemoglobin oxygen saturation as well as the noninvasive estimation of arterial and tissue saturation. Although in skeletal muscles and brain tissues myoglobin and cytochrome analyses have been demonstrated [37-38], their effects upon absorption and reflection spectra of tissues are small. Thus, this review is focused only upon measurement of hemoglobin saturation.

Basis of Optical Oximetry

Optical oximetry can be classified into a) transmission or forward scattering and b) reflection or back scattering type (Fig. 1). In forward scattering, a target area is illuminated with a light source, and transmitted or forward scattered light is analyzed. In the reflection mode,

 0739-5175/94/$4.00©1994

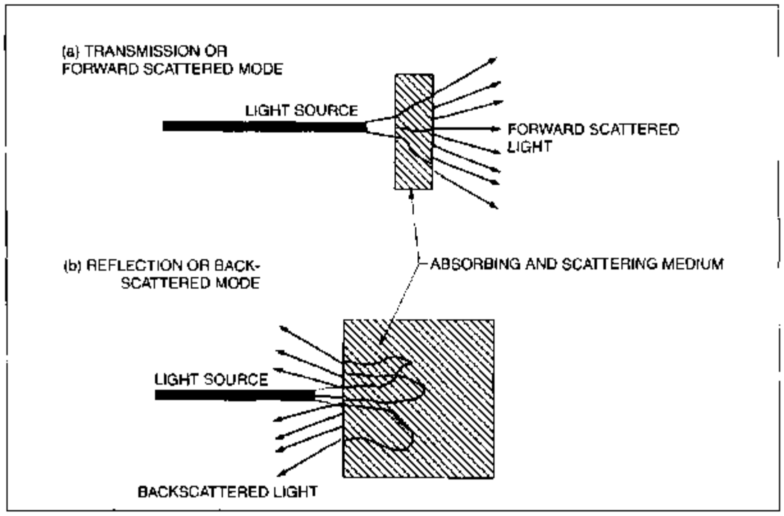

1. Principle of (a) transmission or forward scattered, and (b) reflection or backward scattered optical spectroscopy.

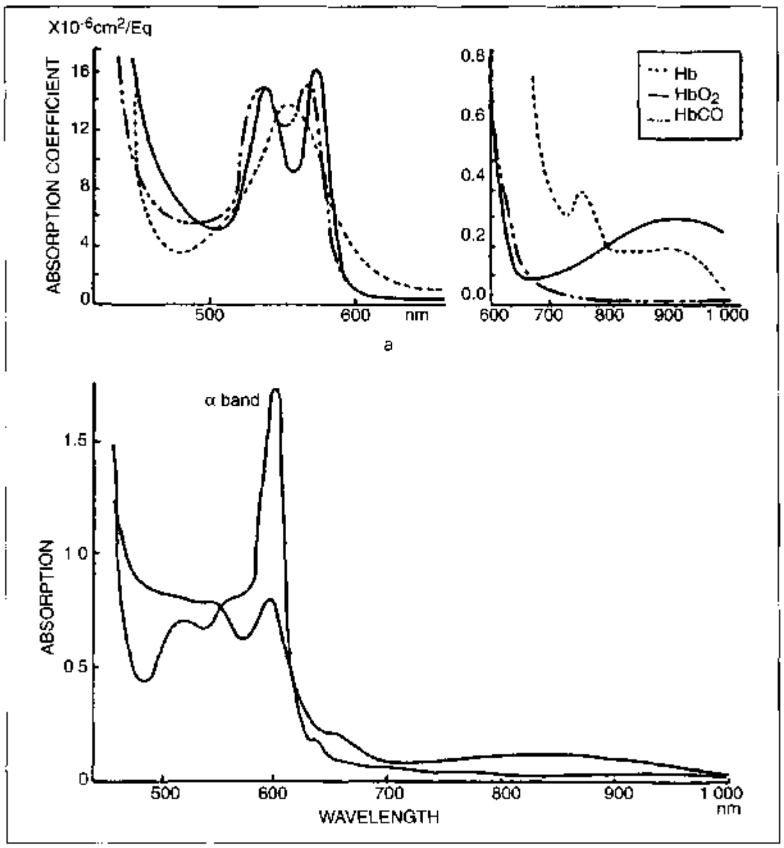

2. Absorption spectra of hemoglobin, myoglobin, bilirubin and cytochrome aa3 in visible and near-infrared wavelength.

backscattered light from the specimen is sampled to estimate the oxygen saturation. In both methods, absorption (K) and scattering (S) properties of the tissue sample plays a major role. In particular, wavelength dependent absorption properties of various species such as hemoglobin, myoglobin, cytochrome aa3 contained in the tissue sample will affect the measured transmittance and reflectance.

Figure 2 shows the absorption spectra of these hemochromes in the visible and near-infrared regions [39-40]. In normal tissue, when the transmission and reflection spectra are examined, they strongly depend on the absorption spectra of hemoglobin, since the concentration is much greater than other species.

Absorption Constant

In relation to blood and tissue oximetry, absorption of light by hemoglobin in the wavelength ranges between 450 and 550 nm is significantly larger (about 10 times) in comparison to the wavelength range between 650-1000 nm (Fig. 2). Bench top oximeters usually sample absorption spectra at around 550 nm, while intravascular and tissue oximetry utilize the wavelength range of 650-1000 nm. The wavelength of 805 nm is called isosbestic, where there is no absorption difference between the oxy- and deoxy-hemoglobin.

As the hemoglobin is contained inside the red blood cells (RBC), a microscopic absorption cross section of RBCs, σ in μ^2, is usually used to describe absorption properties, either as oxygenated cross section, σ_o or deoxygenated, σ_r. Microscopic absorption cross section of RBCs can be derived from the specific absorption coefficients of hemoglobin using the known absorption cross section at a specific wavelength. The macroscopic absorption constant of blood, K_b in mm^{-1} is obtained by multiplying the microscopic cross section, σ, by concentration of RBCs (hematocrit, $H/\overline{V}$), i.e., $K_b = H\sigma/\overline{V}$. For a given oxygen saturation SO_2 of whole blood, K_b is expressed as a linear sum of σ_o and σ_r as follows:

$$K_b = H\frac{\sigma}{\overline{V}} = \frac{H}{\overline{V}}\left(\sigma_o\, SO_2 + \sigma_r\,(1-SO_2)\right) \quad (1)$$

A compound system of tissue can be treated as a homogeneous mixture of blood and blood-less tissue, and blood volume fraction, V_b, can be used to obtain the net absorption constant of tissue, K_T, as follows:

$$K_T = K_t\,(1-V_b) + K_b V_b \quad (2)$$

where, K_t is the macroscopic absorption constant of the blood-less tissue. Typical K_t values of various tissues range from 0.03 to 10.0 mm^{-1} [37, 41-46]. Further, blood in tissue can be treated as a sum of arterial and venous blood, and V_b can be given as:

$$V_b = V_a + V_v \tag{3}$$

where V_a and V_v are the arterial and venous fractional blood volume in tissue, respectively. Equation 1 can be divided into a component for arterial saturation, S_aO_2, and the one for venous saturation S_vO_2 as follows:

$$K_{ba} = \frac{H}{V}(\sigma_o S_a O_2 + \sigma_r(1 - S_a O_2)) \tag{4}$$

$$K_{bv} = \frac{H}{V}(\sigma_o S_v O_2 + \sigma_r(1 - S_v O_2)) \tag{5}$$

where K_{ba} and K_{bv} are the macroscopic absorption constants of arterial and venous blood, respectively. Then, The net absorption constant due to mixture of the arterial and venous blood, K_b' becomes:

$$K_b' = K_{ba}V_{ba} + K_{bv}V_{bv} \tag{6}$$

Thus, the net absorption constant of the tissue becomes

$$K_T = K_t\,[1-(V_a+V_v)] + K_b' \tag{7}$$

The net tissue oxygen saturation, SO_{2T}, averaged over the arterial and venous blood, can be expressed as:

$$SO_{2T} = S_aO_2V_a + S_vO_2V_v \tag{8}$$

This is the oxygen saturation of tissue when transmitted or reflected light from tissue is analyzed. When we discuss tissue oxygenation utilizing time resolved spectroscopy, SO_{2T} is the target measurement from which venous saturation and arterial to venous blood volume distribution can be derived.

Scattering Constant

Scattering of light by red blood cells and tissue components takes place at interfaces where there is a change in the index of refraction. This scattering is due to microscopic fluctuations in the refractive index of the tissue, corresponding to physical inhomogeneities. The angles through which the light is scattered and the scatter coefficient depend on the size and shape of the optical inhomogeneities relative to the wavelength, and to differences in the refractive index between the inhomogeneities and the surrounding medium. Scattering from molecules or structures whose size is much less than the wavelength (Rayleigh scattering), is weak, nearly equal in all directions (isotropic scattering), and rapidly decreases with wavelength. When the wavelength and inhomogeneities are about the same size, the scattering is stronger, is more forward-directed, and decreases roughly inversely with the wavelength. Scattering from large inhomogeneities is highly forward-directed and only weakly dependent on wavelength (Mie scattering).

The RBC is biconcave in shape, with outer diameter of about 8 μm and average thickness of about 1 μm. The average volume of a human RBC is about 87 μm^3. Again, the microscopic scattering cross section of a RBC is defined as σ_s, where this value denotes total scattering cross section and comprises forward scattering cross sections σ_s^+, and backscattering cross section σ_s^-. The index of anisotropicity is defined as: $w = (\sigma_s^+ - \sigma_s^-)/(\sigma_s^+ + \sigma_s^-)$. When the particle is totally forward scattering, w = 1, while totally backscattering, w= -1. The w of RBC ranges from 0.7 to 0.967, and is strongly forward scattering. The scattering characteristics of RBC and tissue components are wavelength dependent. The backscattering cross section of RBC in the visible and near-infrared regions is approximately constant. In the near-infrared region above 800 nm, since the absorption by the hemoglobin is smaller, the light particle can propagate deeper into tissue. Scattering cross sections of the RBCs have been described theoretically using a sphere model by Mie theory [19,20,47], a disk model by the Rayleigh-Gans method [19,20], and a more complicated discoid model by a WKB method [48]. These values have been compared against experimental values and used to explain experimental results.

Again, the macroscopic scattering constant of the blood can be given by:

$$S_b = \frac{H}{V}\sigma_s \tag{9}$$

where σ_s is the total scattering cross section given by $\sigma = \sigma_s^+ + \sigma_s^-$. However, in a single phase material there will be no scattering, i.e., when RBCs are packed (H = 100%) or when there are no RBCs (H = 0). Thus, Eq. 8 is usually multiplied by (1 - H) [49], giving:

$$S'_b = S_b(1-H) = \frac{H}{V}(1-H)\sigma \tag{10}$$

For a compound system such as tissue, the linear treatment used in the absorption analysis is also applicable. Thus, the net scattering constant of tissue, S_T, is expressed as:

$$S_T = S_t(1-V_b) + S_b'V_b \tag{11}$$

Here, S_t is the scattering constant of the bloodless tissue component. Usually, since the absorption constant of arterial and venous blood do not deviate significantly, that is oxygen saturation does not affect scattering properties of RBCs, Eq. 11 can be used to express the macroscopic scattering constant of compound tissue.

Theoretical Analysis of Optical Propagation in Tissue

Theoretical analysis of optical propagation can be divided into 1) absorbing but no scattering, and 2) both absorbing and scattering.

Absorbing but Non-Scattering Medium

In the case of non-scattering but absorbing medium, the simple Beer-Lambert Law can be applied to analyze the transmitted light intensity in terms of various species concentrations. Here, the transmitted intensity of light, I_t, is related to the incident light intensity, I_o, by:

$$I_t = I_o e^{-\alpha C t} \tag{12}$$

$$OD = \ln(I_o/I_t) = \alpha C t \tag{13}$$

where α is the absorption coefficient, C the concentration of the absorber, and t is the optical pathlength. This equation can be applied to a homogeneous and non-scattering solution. In Eq. 13, OD is the optical density, a linear function of concentration, C, when optical pathlength, t, is fixed. Bench top oximeters usually utilize from 2 to 4 wavelengths, depending on the number of components involved in the system. Equation 13 is utilized to solve for the concentration of the species, from which saturation can be derived. For example, when two wavelengths are used, from Eq. 13, concentrations of oxy- and deoxy-hemoglobin, C_{HbO2} and C_{Hb}, are given as:

$$C_{Hb} = \frac{n}{d}$$

where

$n = OD(\lambda_1)\alpha(\lambda_2 Hb) - OD(\lambda_2)\alpha(\lambda_1 Hb)$

and

$$d = t\,[\alpha(\lambda_1 HbO2)\alpha(\lambda_2 Hb) - \alpha(\lambda_2 HBO2)\alpha(\lambda_1 Hb)] \tag{14}$$

$$C_{Hb} = \frac{n}{d}$$

where

$n = OD\ (\lambda_1)\alpha(\lambda_2 HbO2) - OD(\lambda_2)\ \alpha(\lambda_1 HbO2)$

and

$$d = t\,[\alpha(\lambda_1 Hb)\ \alpha(\lambda_2 HbO2) - \alpha(\lambda_2 Hb)\ \alpha(\lambda_1 HbO2)] \tag{15}$$

In Eqs. 14 and 15, $\alpha(\lambda_1 Hb)$ and $\alpha(\lambda_1 HbO2)$ are the absorption coefficients of Hb and HbO2, respectively, at wavelength λ_1, and $\alpha(\lambda_2 Hb)$ and $\alpha(\lambda_2 HbO2)$ are the absorption coefficients of Hb and HbO2, respectively, at wavelength λ_2. Then, from Eqs. 14 and 15, the oxygen saturation can be derived as:

$$SO_2 = \frac{C_{HbO2}}{C_{HbO2} + C_{Hb}}$$

Absorbing and Scattering Medium

When the medium is both scattering and absorbing, the non-liner effect of scattering becomes important and the result deviates from Eq. 13. The first theoretical treatment of scattering in a random medium was given in 1903 by Schuster [50], who described interactions of radiation with the foggy atmosphere. This one-dimensional theory was based on phenomenological observations of intensity transfer in the medium. It was further heuristically developed in 1931 by Kubelk and Munk [51], by which time it was called the "two-flux theory." Based on the concept of forward and backward traveling fluxes, it adequately describes optical propagation in a medium if the illumination is diffuse and the medium is dull so that light is diffusely scattered (Fig. 3). However, because of its phenomenological and heuristic nature, as well as its one-dimensionality, the theory has serious limitations when applied to optical processes in whole blood and tissue.

The optical process can be classified into a) single scattering, b) multiple scattering and 3) diffusion, depending on the concentration of scatterers as shown in Fig. 4. Various scattering theories are available for a single particle, including Mie theory, which deals with scattering of light by a sphere; and Rayleigh-Gans theory for scattering by a disk. When the particle concentration increases, a phenomenon called "multiple scattering" occurs. The light goes through multiple scatterings because of the existence of numerous particles in the medium. In application to biological samples, such as whole blood and tissue, Twersky developed a forward scattering theorem [49]. It includes both absorption and scattering terms in a modification of Eq. 12, and as given by:

$$I_t = I_o e^{-ST} + q(1-e^{-ST})e^{-\alpha C t} \qquad (16)$$

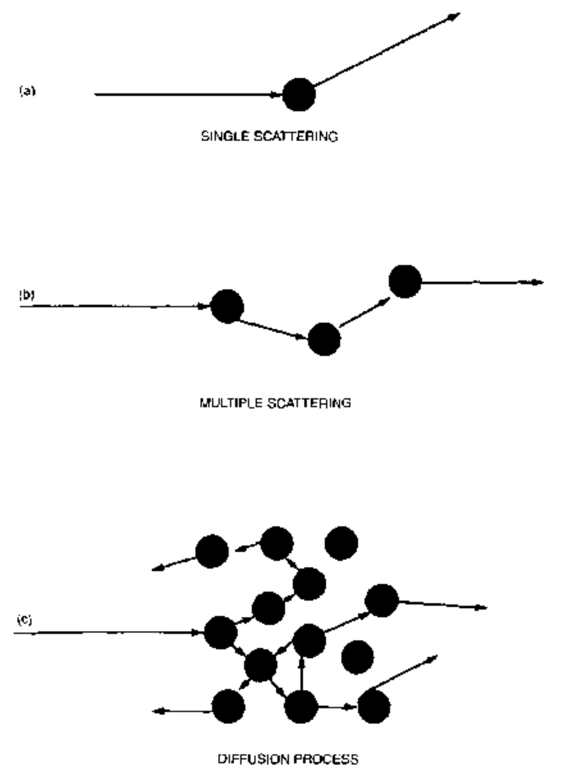

3. Schematic drawing of (a) single scattering, (b) multiple scattering, and (c) diffusion processes.

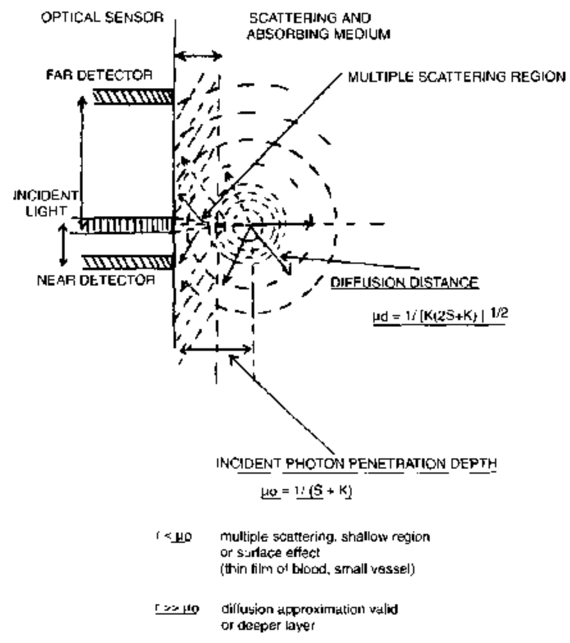

4. Diffusion process in the medium, and underlying assumptions for diffusion process.

Then, OD becomes:

$$OD = B + \alpha C t \tag{17}$$

Here, B is the term related to scattering and the second term is related to absorption. For the multiple scattering analysis to be applicable, the medium thickness must be very thin or the concentration of the particles must be very low, so that the coherence of the incoming light is not lost. Equation 16 has been successfully applied to analysis of light transmitted through a small vessel, through a frozen tissue sample, and in the vicinity of the optical fiber tips.

When the particle concentration increases above 5%, or the medium thickness becomes large so that light will go through repeated multiple scattering, then the coherence of the incident light is lost and it is said the light becomes diffused [52]. This was confirmed in whole blood with an immersed optical fiber. As the hematocrit of blood increased, the light patterns became more and more centered around the tip of optical fiber, and coherence of the incident light was completely lost [21].

Thus, as shown in Fig. 5, diffusion takes place, when the medium satisfies the conditions of a) scattering particle concentration above the critical value, and b) the medium thickness becomes large. We can define two parameters to evaluate the underling assumptions of diffusion theory. First, incident photon penetration depth, δ_0, and defined as $1/(S + K)$, will indicate the average depth, t_D in which the light can penetrate into a particular medium before losing coherence. Thus, it is entirely function of the medium and excitation wavelength, λ. The second parameter is the diffusely scattering condition, called albedo, and defined as $S/(S + K)$. The albedo, as S and K are also wavelength dependent, is determined by the medium and the excitation wavelength . When the albedo of the medium is greater than 0.5, diffusion will take place. When the medium satisfies both conditions, diffusion analysis is valid. Diffusion analysis is a heuristic approach derived from transport theory. Its application to biological media such as whole blood and tissues has been employed by several researchers. The diffusion approach can be divided into two phases: a) steady state continuous case, and b) a time resolved or pulse diffusion case.

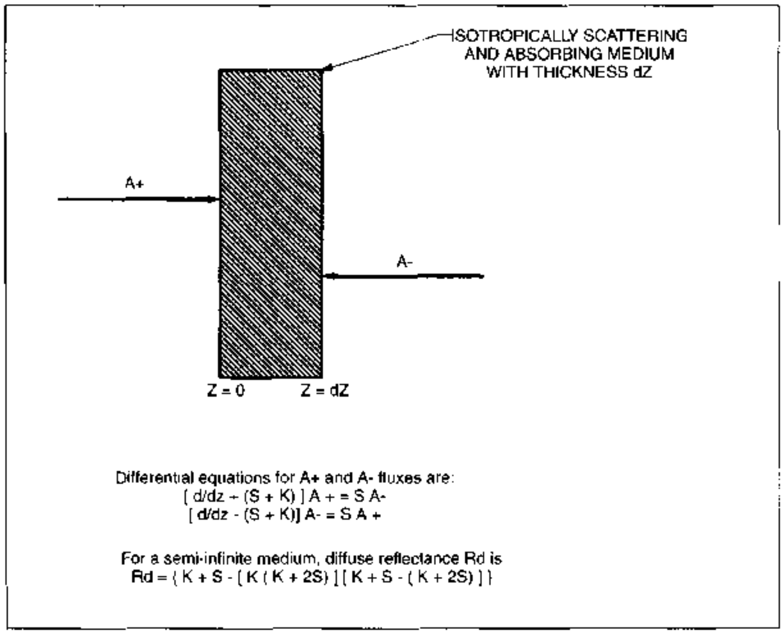

5. Two flux analysis

Diffusion analysis

a. Steady state diffusion equation

For the steady state case, the diffusion equation was derived from the transport theory and given in the cylindrical coordinate by [21]:

$$(\Delta^2 - f_a / D)\, \rho_s(r,\theta,z) = So(r,\theta,z) \tag{18}$$

where So is a source function and ρ_s is the scattered photon density, c is the velocity of light, D is the diffusion constant given by $D = 1/3\,[f_a+(1 - w)f_s]$. f_a and f_s are the absorption and scattering coefficient and related to K and S by

$$c\,K = f_a \tag{19}$$

$$c\,S = f_s \tag{20}$$

The solutions of Eq. 18 for both isotropic and an-isotropic scattering with various boundary conditions have been solved and successfully applied to design fiber optic oximeters in whole blood. The solution obtained by Reynolds for isotropically scattering homogeneous medium is [20]:

$$R(r_a) = (2/d)[S/(S+K)] \times \sum A_n \left[1 - e^{\,d/\delta_o}(-1)^n\right] \times [1-(2r/b)\, M_1 N_1] \tag{21}$$

This equation gives diffuse reflectance for an illuminating optical fiber radius of b separated from the receiving fiber by r_a as a function of tissue thickness, d, and scattering and absorption constants, S and K. M1 and N1 are the first order Bessel functions. This equation can give quantitative diffuse reflectance from an isotropically scattering homogeneous medium such as whole blood.

In application to tissue, one-dimensional solution was applied to reflectance oximetry in blood and tissue by Longini, Cohen, et al. [53-54]. A three-dimensional solution for a two-layer tissue model was obtained by Takatani and Graham for application to reflectance oximetry from gut mucosa [55]. This solution was further extended by Schmitt to a multi-layer model application in pulse oximetry [56].

b. Time resolved case

When a narrow width light pulse, on the order of picoseconds, is injected into the medium, the transmitted pulse's shape and amplitude indicate the scattering and absorbing characteristics of the medium. The diffusion equation for a narrow width pulse through the medium can be written as [57]:

$$[(1/Dc)(\delta / \delta t) - (\Delta^2 - f_a / D)]\rho_s(r,\theta,z,t) = S'(r,\theta,z,t) \tag{22}$$

where, scattered photon density, $\rho_s(r, \theta, z, t)$, is now expressed as a time varying function. The local diffuse reflectance, R (r,t), from a semi-infinite medium irradiated by a pencil beam is given by [57]:

$$R(r,t) = (4\pi Dc)^{-3/2} f_s^{-1} t^{-5/2} e^{-r/4DCt} e^{-f_a ct} \quad (23)$$

In the limit when time approaches infinity, the terminal slope of the $(\delta/\delta t) \log_e R(r, t)$ converges to:

$$\lim_{t \to \infty} (\delta / \delta t) \log_e R(r,t) = -f_a c \quad (24)$$

Thus, from Eq. 24, the absorption properties of the medium can be quantified.

In the frequency domain, the amplitude modulation and phase shift can be directly obtained from the Fourier transform of Eq. 22, with $S'(r, t) = N_0 \sin(\omega + \phi_0)$. Figure 6 shows a one-to-one transformation between the time resolved and frequency domain analyses. At low modulation frequency with $\omega << f_a c$ and $N = 1$, the mean of the distribution of pathlengths, $< L >$, is directly proportional to phase shift, $\phi(r, \omega)$ which is given by [57]:

$$\phi(r,\omega) = (3^{1/2} r\omega / 2\pi c)[(1-w) f_s / f_a]^{1/2} \quad (25)$$

Since $\Delta\varphi = \omega\Delta<L>/c$, then $<L>$ becomes:

$$\begin{aligned} < L > &= \Delta\phi c / \omega \\ &= (3^{1/2} r) / 2\pi[(1-w) f_s / f_a]^{1/2} \\ &= [3(1-w) f_s / f_a]^{1/2} \, r / 2\pi \quad (26) \end{aligned}$$

Since the scattering constant does not vary significantly with small wavelength changes, the ratio of the $<L>^2$ at two wavelengths will become the ratio of the absorption constants, thus giving hemoglobin saturation. Likewise, the phase shift information can also be used to obtain absorption characteristics of tissue that is dependent on hemoglobin oxygen saturation.

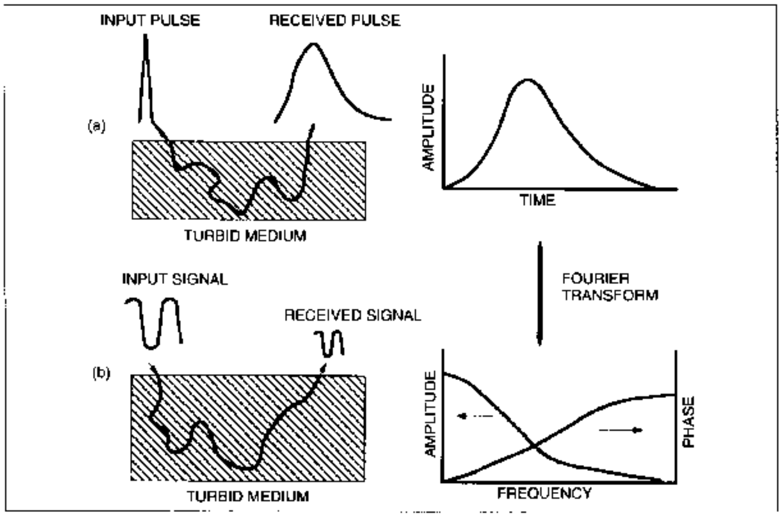

6. (a) Time and (b) frequency domain analysis of picosecond and ultra high frequency spectroscopy.

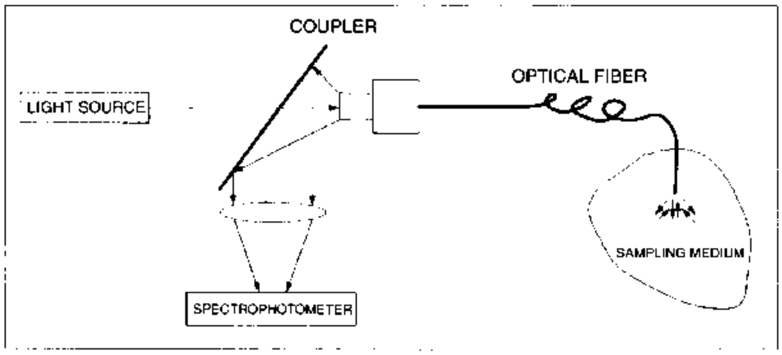

7. Basic block diagram of fiber-optic oximeter.

Invasive and Noninvasive Oximeter Systems

a) Intra- and extra-vascular oximetry

For intra-vascular oximetry, optical fibers are used to guide the light signal inside the vessel and reflected light from red blood cells back to the light detector (Fig. 7). In estimating SO_2, usually the reflectances at the two wavelengths, one in the red and the other in the near-infrared regions, are used with the empirical relation given below:

$$SO_2 = A + B(R\lambda_1 / R\lambda_2) \quad (27)$$

where A and B are the constants that depend on the fiber geometry and physiological parameters of blood. Equation 27 is the basis of modern reflection oximetry, derived empirically by Polany and Hehir [18]. Although the computation of reflectance ratios at wavelengths in the vicinity was suggested to cancel the effects of nonlinearity due to scattering, effects of hematocrit change may become important. Hence, currently available fiber-optic oximeters utilize more than two wavelengths to adjust for hematocrit variation. The fiber-optic oximeter from Oximetric (Oxnard, CA) utilizes three wavelengths to compensate for hematocrit changes.

Current use of intravascular oximeters is aimed at measurement of mixed venous saturation, from which status of circulatory system can be deduced. Mixed venous saturation varies in reflecting the changes of 1) SaO_2, 2) cardiac output, 3) hematocrit or hemoglobin content, and 4) oxygen consumption [6, 58-59]. One of the disadvantages of fiber optic oximeters is that damage to optical fibers results in severe measurement error. In order to circumvent this short-coming, catheter tip type oximeters using hybrid type miniature sensors have also been developed [60-61] (Figure 8).

In extra-vascular oximetry, forward scattered light through small vessels of frozen tissue samples, the messentery have also been analyzed to obtain oxygen saturation [62-64]. Multiple scattering theory (Eq. 18) has been utilized to treat scattering as an additive component to absorption. The oximeter sensor has also been applied to the extra-corporeal circuit used in the heart-lung machine to determine the oxygen saturation of the flowing blood [65-66].

b) Tissue oximetry

Tissue is a complicated medium in which blood vessels, both artery and vein, are distributed non-homogeneously. Red blood cells in arterial blood that flows

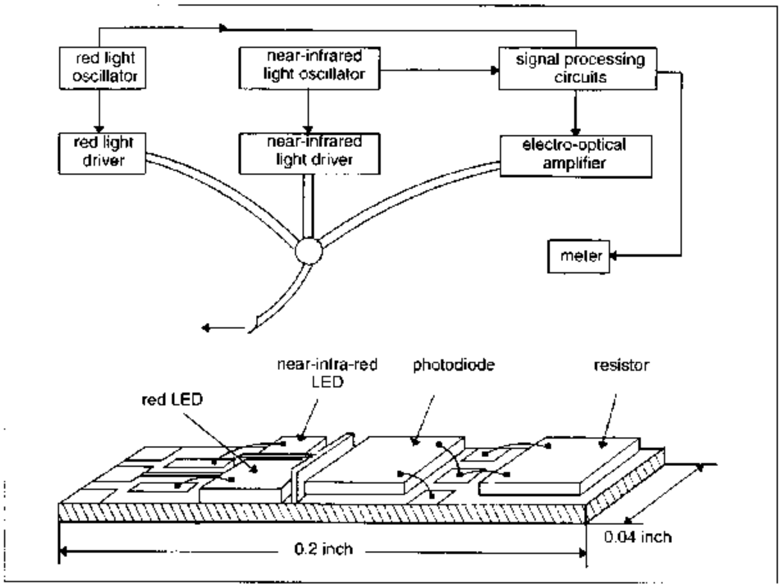

8. Basic illustration of the catheter-tip hybrid circuit oximeter sensor.

through the tissue release oxygen and return via the veinous system to the heart. Because of the unknown and nonhomogeneous distribution of arteries and veins, analysis of optical process in tissue is complex. Ever since the first tissue oximeter by Millikan, researchers have been trying to measure tissue oxygen saturation either in the transmission or reflection mode. The ear oximeter by Hewlett Packard Corp. has acquired some clinical success [67]. However, this instrument was never fully accepted. Arterialization of capillary blood by heating in the sensor created discomfort for patients. More importantly, the oximeter failed in the case of shock or hypo-volemia. The skin reflectance oximeter developed by Cohen [22] utilized solid state devices such as LEDs and photo-transistors. However, again because of a lack of calibration procedure, it did not attain clinical acceptance. Takatani [23,41,55], in 1979, developed a noninvasive tissue reflectance oximeter based on the photon diffusion theory and succeeded in estimation of mucosal oxygen saturation. Because of capillaries high density, the assumption to treat the tissue as a homogeneous mixture of blood and blood-free components was valid. The tissue was cooled to minimize arterial-to-venous saturation difference and tissue blood volume was measured by replacing the blood with saline. The arterial-to-venous saturation difference was minimized to less than 5% by cooling the tissue. The three-dimensional photon diffusion theory was used to compute the reflectances in the visible and near-infrared regions, which were then compared to the sampled tissue reflectances at five wavelengths. The theoretical predicted tissue saturation compared well with the average of the arterial and venous saturations. Approximately 70% of the blood was in the venous system of the gut mucosa.

1) Pulse oximetry

Pulse oximetry utilizes the plethysmographic principle in combination with the optical absorption characteristics of hemoglobin. The signal varies with pulsatile changes in tissue blood volume. The optical signal is usually sampled at two wavelengths and conventional linear regression analysis is applied to obtain arterial saturation. Pulse oximetry thus assumes that the pulsatile signal change is due to arterial blood volume change (Fig. 9). Most pulse oximeters are transmission type, where forward scattered light through the finger tip or the ear lobe is analyzed based on the Beer-Lambert law. An accuracy of 1% or better has been reported for the saturation range above 80%. Usually, the accuracy is less at lower saturation because of non-linear effects of absorption. Reflection type pulse oximeters have also been developed, with more general applicability to any portion of the body, such as forehead, cheek, calf and thigh (Fig. 10) [68-71]. However, in comparison to transmission, the reflection pulse oximeter has poorer signal-to-noise ratio. Mendelson, et al. utilized multiple photodiodes around the light source to enhance signal level, and a heater was incorporated in the sensor to warm the tissue so as to increase local blood flow [72-73]. Excellent correlation in comparison with the transmission oximeter has been shown from the calf and thigh. Takatani, et al. have studied the effect of light source and detector separation, and concluded that the greater the separation, the better the pulsatile to average signal level in the reflectance mode [74]. However, the absolute signal level decreased exponentially as the separation increased, and also the variability from person to person increased due to effects of tissue non-homogeneity. More light sources or light detectors are required to increase the signal level as well as to minimize the effects of tissue non-homogeneity.

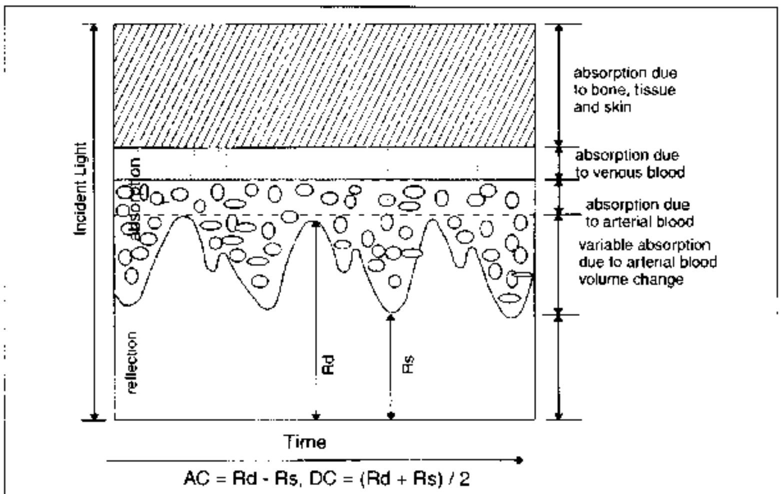

9. Conceptual tissue model for pulse oximetry.

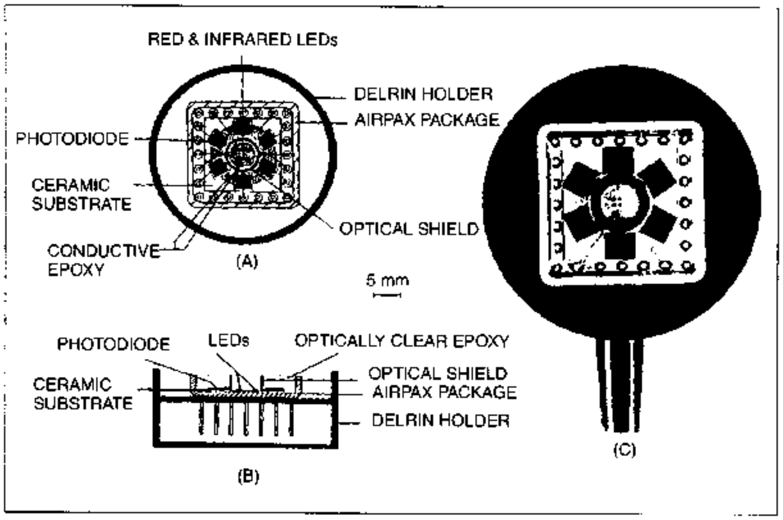

10. Schematic diagram of the reflectance oximeter sensor [68].

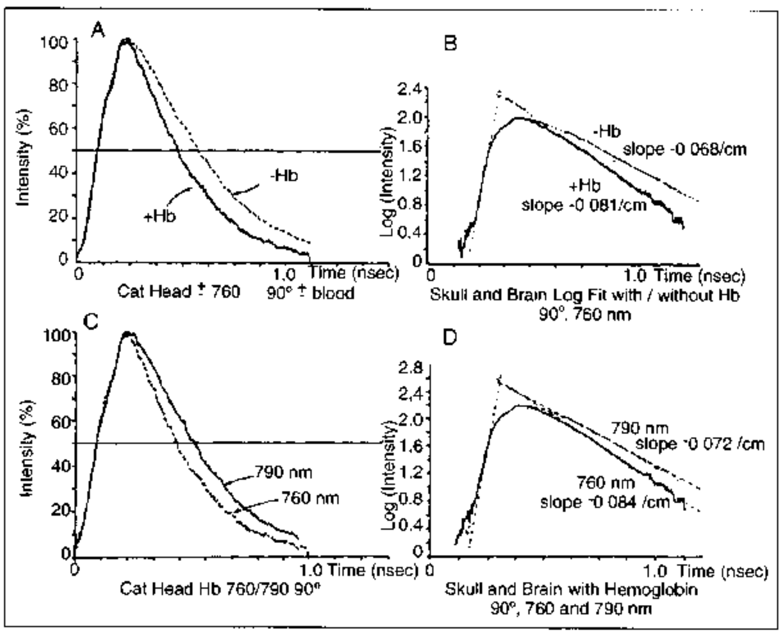

11. Measured pulse waveform of a picosecond light pulse through tissue. (a) Linear scale, (b) logarithmic scale, (c) effect of an alteration of wavelength from 790 to 760 nm in the cat-head model, a point at which the Hb absorbs maximially in this region [33], (d) logarithmic scale.

2) Time resolved spectroscopy

The major problem in analysis of tissue spectroscopy is the unknown pathlength, which precludes application of a simple Beer-Lambert law. When the optical pathlength is determined, optical density measurements based on the Beer-Lambert law allows computation of absorption in the tissue, assuming that the extinction due to scattering is minimal. In order to qunatitate this value, Chance, et al. and later Delpy, et al. applied a very narrow duration (picosecond order) pulse at the near-infrared region, where absorption due to hemoglobin and tissue is low, and measured the transit time of a photon through the tissue [31-35, 75-77]. Figure 11 shows the pulse wave after passing through the tissue. One can estimate the transit time as well as tissue scattering and absorption properties from this wave form. Similarly, frequency modulation, at frequencies on the order of 500 MHz, has been used to measure the phase shift through the tissue, from which transit time is calculated. According to the measurement performed by Delpy, et al., path length through an infant's head and arm is about 4 to 5 times larger than the separation distance of the light source and detector [78].

Time resolved spectroscopy is being applied to the area of neonatal cerebral monitoring [79-82]. A light signal is injected from one side of the head and scattered light through the head is measured at the opposite side. Figure 12 shows the instrumentation system to accomplish such measurement. The Beer-Lambert law is applied to analyze the measured signal in terms of oxy- and deoxy- hemoglobin concentrations. However, this method still lacks calibration. Thus, the result is still qualitative and only change with respect to the initial measurement can be followed. Also, the distribution of arterial and venous blood in the tissue is unknown. If the venous blood volume in tissue is assumed to be about 70-75%, venous saturation can be derived. Once these unknown areas are clarified, a very powerful technique will be available to map the oxygen field deep in the body, without invasive procedures.

In applications to the brain, McCormick, et al. [83] employed dual detectors as proposed also by Takatani, et al. [84]; one placed close to the light source and the other at a distance. Through differential measurement from these detectors, the effect of the skull was minimized and deep layer brain tissue information was obtained. Figure 13 shows how this concept works to eliminate surface or shallow layer effects. In the continous mode, the difference between the receivers one and two can be expressed using Eq. 13 as follows:

$$OD(\#1) = \alpha(bone)\,C(bone)\,d(bone) \tag{28}$$

$$OD(\#2) = \alpha(bone)\,C(bone)\,d(bone) + \alpha(brain)\,C(brain)\,d(brain) \tag{29}$$

$$OD(\#1) - OD(\#2) = \alpha(brain)\,C(brain)\,d(brain) \tag{30}$$

where α(bone) and α(brain) are the absorption coefficients; C(bone) and C(brain) are concentrations; and d(bone), d(brain) are the photon travel distances. Differential measurement allows detection of hemochrome concentration in a

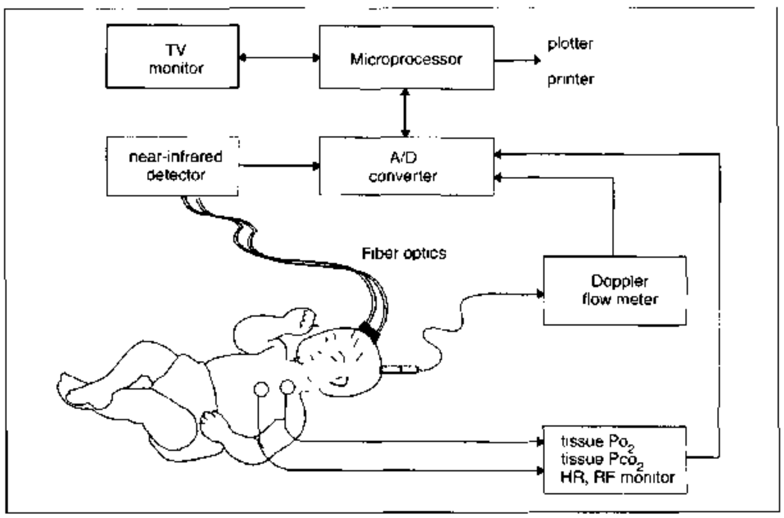

12. Block diagram of the neonatal cerebral monitoring system.

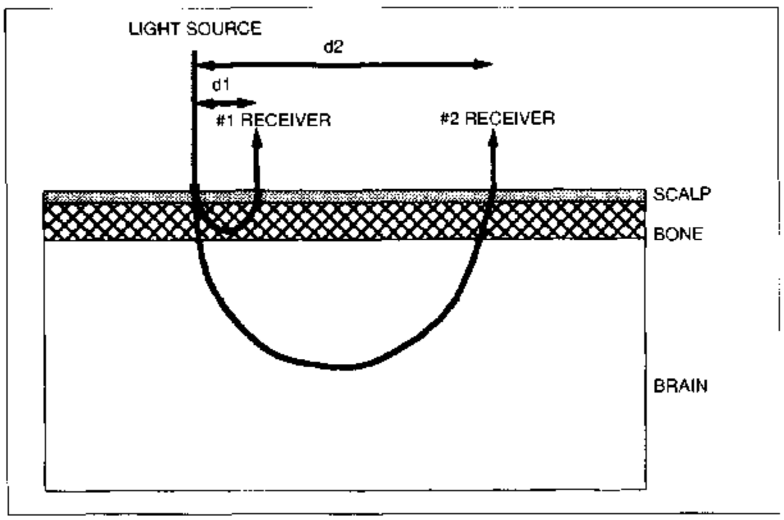

13. Near and far detector approach in estimation of deep layer tissue oxygenation as applied to the head.

deeper layer. Similar analysis is also applicable with time resolved spectroscopy. Transit time difference between detectors #1 and #2 can be obtained from Eqs. 23-24. In general, multiple detectors can be placed to focus at specific depths in tissue, yielding three-dimensional mapping of the oxygen field of tissue using time resolved diffusion equations.

Pulse spectroscopy is also applicable for the measurement of cytochrome aa3 saturation in the brain [38-39]. Although the concentration of cytochrome aa3 is considerably less than hemoglobin, photon counting techniques may yield information related to oxygenation of cytochrome at the mitochondria level. In combination with hemoglobin measurement, cytochrome and myoglobin measurements in tissue using time resolved oximetry will elucidate the mechanism of cell metabolism otherwise unattainable.

Summary

During the last decade, we have experienced two innovative approaches in spectroscopy. The first is pulse oximetry, which revolutionalized the clinical instrumentation. Because of limitations in application sites of the transmission oximeter, research continues on reflection oximeters. In the area of tissue oxygen monitoring, time resolved spectroscopy is gaining the interest of researchers. Picosecond pulse transit time measurements allow characterization of the tissue, from which oxygen saturation can be derived. However, we still lack adequate calibration procedure to quantitate optical measurements through the tissue. We need to build a good tissue model in which we can simulate real tissue with known arterial and venous distribution and oxygen saturation. Theoretical predictions can be compared to measured values in order to verify the applicability of tissue models. In addition to these measurements, imaging of tissue in terms of an oxygen field is becoming realistic. A three-dimensional oxygen field can be obtained through optical measurement, but first we need to quantitate accurately tissue arterial and venous blood volumes and oxygen saturations. Such a breakthrough will bring non-invasive optical spectroscopy into wide use in the diagnosis of circulatory disorders, the evaluation of the cardio-pulmonary system, and to determine the viability of various end-organs.

Setsuo Takatani obtained his B.S. with Distinction and M.S. in Electrical Engineering from the University of Oklahoma in 1971 and from Catholic University of America in 1974, respectively. He earned his Ph.D. in Biomedical Engineering from Case Western in 1978. He was a Fellow and Staff member of the Cleveland Clinic Foundation from 1979 through 1982. From 1982 to 1988, he was a Head of the Biomedical Instrumentation Lab, national Cardiovascular Center, Osaka, Japan. Since 1989, he has been Associate Professor, Department of Surgery, at the Baylor College of Medicine. In 1994, he also obtained the Doctor of Medicine Degree from Tokyo Medical and Dental University. His research interests include biomedical sensors and instrumentation, physiological system analysis, and artificial organs. He is a member of numerous medical societies including IEEE, BME, ASAIO, ISAO, ISOTT, and the Japanese societies of Artificial Organs and Medical Electronics.

Jian Ling received his B.S. degree from East China Normal University in 1986 and the M.S. degree from the University of Houston, both in electrical engineering. His master's research involved EEG signal processing and pattern recognition. He is currently employed as a Research Assistant in the Department of Surgery, Baylor College of Medicine. He is involved in biomedical sensor projects including reflectance pulse oximetry and non-invasive blookd pressor monitoring, as well as the artificial heart project. His research interests include biomedical signal processing, neural networks, and medical instrumentation.

The authors may be reached at the Department of Surgery, Baylor College of Medicine, Houston, TX 77030.

References

1. **Antman EM, March JD, Green LH and Grossman W:** Blood oxygen measurements in the assessment of intracardiac left to right shunts: A critical appraisal of methodlogy. *Am J Cardiol* 46:265-271, 1980.

2. **Hillis LD, Firth BG, Winniford MD:** Variability of right-sided cardiac oxygen saturations in adults with and without left-to-right intracardiac shunting. *Am J Cardiol* 58:129-132, 1986.

3. **Davies GG, Jebson RJ, Glasgow BM and Hess DR:** Continuous Fick cardiac output compared to thermodilution cardiac output. *Critical Care Medicine* 14(10):881-885, 1986.

4. **Maekenzie GJ, Taylor SH, Flenley DC, and McDonald AH:** Circulatory and respiratory studies in myocardial infarction and cardiogenic shock. *Lancet* 2:825-832, 1964.

5. **Scheinman NM, Brown MA and Papaport E:** Critical assessment of use of central venous oxygen saturation as a mirror of mixed venous oxygen in severely ill cardiac patients. *Circulation* 40:165-172, 1969.

6. **Orland R:** Continuous mixed venous oximetry in critically ill surgical patients. *Arch Surg* 121:470-471, 1986.

7. **Valancia MD, and Burgess JH:** Arterial hypoxemia following acute myocardial infarction. *Circulation* 40:641-651, 1969.

8. **Severinghaus JW and Naifeh KH:** Accuracy of response of six pulse oximeters to profound hypoxia. *Anesthesiology* 67:551-558, 1987.

9. **Ryan CA, Barrington KJ, Vaughan D and Finer NN:** Directly measured arterial oxygen saturation in the newborn infant. *The Journal of Pediatrics* 109(3):526-529, 1986.

10. **Harris AP, Sendak MJ, Donham RT:** Changes in arterial oxygen saturation immediately after birth in the human neonate. *The Journal of Pediatrics* 109(1):117-119, 1986.

11. **Johnson N, Johnson V, Bannister J and Lilford RJ:** The accuracy of fetal pulse oximetry in the second stage of labor. *Neonatal Intensive Care* May/June 46-49, 1992.

12. **Brazy JE:** Cerebral oxygen monitoring with near infrared spectroscopy: Clinical application to neonates. *J Clin Monit* 7:325-334, 1991.

13. **Millikan, G.A:** The oximeter, an instrument for measuring continuously the oxygen saturation of arterial blood in man. *Rev of Scientific Instrument*, 13:434-444, 1942.

14. **Wood, EH, and Geraci, JE:** Photoelectric determination of arterial oxygen saturation in man. *J. Lab Clin Med.* 34:387-401, 1949.

15. **Brinkman, R and Sijlstra, WG:** Determination and continuous registration of the percentage oxygen saturation in clinical conditions. *Arch Chir Neerl* 1:177-183, 1949.

16. **Sekelj, P, Johnson, AL, Hoff, HE and Scherch, PM:** A photoelectric method for the determination of arterial oxygen saturation in man. *Amer Heart J.* 42:826-848, 1951.

17. **Tait, GR and Sekelj, P:** Analog computer for ear oximeter. *Med and Biol Engr* 5:463-472, 1967.

18. **Polanyi, ML and Hehir, RM:** New reflection oximeter. *Rev Sci Instru* 31(4):401-403, 1960.

19. **Cheung, PW:** Effects of blood physiological variations on optical scattering and fiberoptic oximetry. PhD. Dissertation, University of Washington, Seattle, WA 1973.

20. **Reynolds, LO:** Optical diffuse reflectance and transmittance from an anisotropically scattering finite blood medium. PhD Dissertation, University of Washington, Seattle, WA 1975.

21. **Johnson, CC:** Optical diffusion in blood. *IEEE Trans Biomed Engr.* BME-17(2):129-133, 1970.

22. **Cohen A and Wadsworth NA:** Light emitting diode skin reflectance oximeter. *Med Biol Eng* 10:385-391, 1972.

23. **Takatani, S, Cheung, PW and Ernst, EA:** Noninvasive tissue reflectance oximeter: An instrument for tissue hemoglobin oxygen saturation in vivo. *Annals of Biomed Engr* 8:1-15, 1980.

24. **Wodick, R and Lubbers, DW:** Quantitative evaluation of reflection spectra of living tissues. Hoppe-Seyler's *Z. Physiol Chem* 355:583-594, 1974.

25. **Lubbers, WD and Wodick R:** The examination of multicomponent systems in biological materials by means of a rapid scanning photometer. *Applied Optics* 8(5):1055-1062, 1969.

26. **Aoyagi, T, Kishi, M, Yamaguchi, K:** Improvement of the ear-piece oximeter. 13th Annual Meeting of Japanese Soc med Electronics and Biomed Eng. 90-91, 1974.

27. **Yelderman, M and New W:** Evaluation of pulse oximetry. *Anesthesiology* 59:349-352, 1983.

28. **Pologe, JA:** Pulse oximetry; technical aspects of machine design. *Int Anesthesiology Clin* 25:137-153, 1987.

29. **Kellerman AL, Cofer CA, Joseph S, Backman BB:** Impact of portable pulse oximetry on arterial blood gas test ordering in an urban emergency department. *Annals of Emergency Medicine* 20(2):130-134, 1991.

30. **Szaflarski NL and Cohen NH:** Use of pulse oximetry in critically ill adults. *Heart and Lung* 18(5):444-455, 1989.

31. **Delpy DT, Cope M, van der Zee P, Arridge S, Wray S and Wyatt J:** Estimation of optical path length. *Phys Med Biol* 33:1433-1442, 1988.

32. **Jacques SL and Flock ST:** Time-resolved reflectance spectroscopy. *SPIE Proceedings* 1525:35-40, 1991.

33. **Chance B, Leigh H, Miyake H, Smith D, Nioka S, et al:** Comparison of time resolved and un-resolved measurements of deoxyhemoglobin in brain. *Proc Natil Acd Sci.* 85:4971-4975, 1988.

34. **Jacques SL:** Principles of phase-resolved optical measurements. *SPIE Proceedings* 1525:143-153, 1991.

35. **Chance B, Haselgrove J, Wang NG, Maris M and Sevick E:** Photon dynamics in tissue imaging. *SPIE* 1525:68-82, 1991.

36. **Singer JR, Grunbaum FA, Kohn P and Zubelli JP:** Image reconstruction of interior of bodies that diffusion radiation. *Science* 248:990-993, 1990.

37. **Jobsis FF, Keizer JH, LaManna JC, Rosenthal M:** Reflection spectrophotometry of cytochrome aa3 in vivo. *J Appl Physiol*: Respirat. Environ. exercise Physiol. 43(5):858-872, 1977.

38. **Kariman K, Jobsis FF and Saltzman H:** Cytochrome aa3 reoxidation: Early indicator of metabolic recovery from hemorrhagic shock in rats. *J Clin Invest* 72:180-191,1983.

39. **Van Assendelft OW:** *Spectrophotometry of hemoglobin derivatives*. Assen, The Netherlands, Royal Vangorcum Ltd. 1970.

40. **Wilson BW:** Optical properties of tissues. *Encyclopedia of Human Biology* 5:587-597, 1991.

41. **Takatani S:** On the theory and development of a non-invasive tissue reflectance oximeter. PhD Dissertation, Case Western Reserve University, Cleveland, OH, 1978.

42. **Bruls WAG and van der Leun JC:** Forward scattering properties of human epidermial layers. *Photochem and photobiol* 40:231-242, 1984.

43. **van Gemert MJC, Henning JPH:** A model approach to laser coagulation of dermal vascular lesions. *Arch Dermatol Res* 270:429-439, 1981.

44. **Wilson BC, Patterson MS and Burns DM:** Effect of photosensitizer concentration in tissue on the penetration depth of phtoactivating light. *Lasers Med Sci* 1:235-244, 1986.

45. **Flock ST, Wilson BC, Patterson MS:** Total attenuation coefficients and scattering function of tissues and phantom materials at 633 nm. *Med Phys* 14:835-841, 1987.

46. **Marynissen JPA and Star WM:** Phantom measurements for light dosimetry using isotropic and small aperture detectors. In Porphyrin Localization and Treatment of Tumors, Doiron DR and Gomen, eds. Liss, New York, 1984. pp 133-138.

47. **Lin JC and Guy AW:** A note on the optical scattering characteristics of whole blood. *IEEE Trans Biomed Engr.* 43-45, 1974.

48. **Ross DA:** Scattering by finite volume dielectric objects. PhD Dissertation, University of Washington, Seattle, WA, 1969.

49. **Twersky V:** Absorption and multiple scattering by biological suspensions. *J Opt Soc Amer* 60:1084-1093, 1970.

50. **Schuster A:** Radiation through a foggy atmosphere. *Astrophys J* 21:1-22, 1905.

51. **Kubelka P and Munk F:** Ein Beitrang zur Optik der Farbanstriche. *Z techn Phys* 12:593-601, 1931.

52. **Ishimaru A:** *Wave Propagation and Scattering in Random Media.* Academic Press, New York, 1978.

53. **Longini RL and Zdrojkowski R:** A note on the theory of backscattering of light by living tissue. *IEEE Trans Biomed Engr.* BME-15(1):4-10, 1968.

54. **Cohen A and Longini RL:** Theoretical deter-

mination of the blood relative oxygen saturation in vivo. *Med and Biol Eng* 9:61-69. 1971.

55. **Takatani S and Graham MD:** Theoretical analysis of diffuse reflectance from a two-layer tissue model. *IEEE Trans Biomed Engr.* BME-26(12):656-664, 1979.

56. **Schmitt JM, Zhou GX, Walker EC and Wall RT:** Multilayer model of photon diffusion in skin. *J Opt Soc Am* 7(11):2141-2153, 1990.

57. **Wilson BC, Sevick EM, Patterson MS, Chance B:** Time-dependent optical spectroscopy and imaging for biomedical applications. *Proceedings of the IEEE* 80(6):918-930, 1992.

58. **Nelson LD:** Continuous venous oximetry in surgical patients. *Ann Surg* 203(3):329-333, 1986.

59. **Takatani S:** Open loop analysis of circulatory system in awake live animals: Relation between mixed venous saturation and hemodynamic and metabolic variables. Artificial Organs 17(2):79-91, 1993.

60. **Yee S, Schibli E and Krishnan V:** A proposed miniature red/infrared oximeter suitable for mounting on a catheter tip. *IEEE Trans Biomed Eng* BME-24(2):195-197, 1977.

61. **Schmitt JM, Meindl JD, Mihm RG:** An integrated circuit-based optical sensor for in vivo measurement of blood oxygenation. *IEEE Trans Biomed Eng* BME-33(2):98-107, 1986.

62. **Pittman RN and Duling BR:** Measurement of percent oxyhemoglobin in the microvasculature. *J Appl Phsiol.* 38(2):321-327, 1975.

63. **Pittman RN and Duling BR:** A new method for the measurement of percent oxygehemoglobin. *J Appl Physiol* 38(2):315-320, 1975.

64. **Sinha AK, Neubauer JA, Lipp JA and Weiss HR:** Blood oxygen saturation determination in frozen tissue. *Micrvascular Research* 14:133-144, 1977.

65. **Vurck GG, Kolobow T, Pegram SE, and Friauf WS:** Oxygen saturation monitor for extracorporeal circulation applications. *Med Instru* 7(4):262-267, 1973.

66. **Takatani S, Noda H, Takano H and Akutsu T:** A miniature hybrid reflection type optical sensor for measurement of hemoglobin content and oxygen saturation of whole blood. *IEEE Trans Biomed Eng* 35:187-198, 1988.

67. **Merrick EB, Bayes TJ:** Continuous, noninvasive measurements of arterial blood oxygen levels. *Hewlett-Packard J* 28:2-9, 1976.

68. **Mendelson Y, Kent JC, Yocum BL, and Birle M:** Design and evaluation of a new reflectance pulse oximeter sensor. *Medical Instrumentation* 22(4):167-173, 1988.

69. **Shimada Y, Nakashima K, Fujiwara Y, Komatsu T, Kawanishi M, et al.,** Evaluation of a new reflectance pulse oximeter for clinical applicability. *Med Biol Eng.* 29:557-561, 1991.

70. **Decker MJ, Dickensheets D, Arnold JL, Cheung PW and Strohl KP:** A comparison of a new reflectance oximeter with the Hewlett-Packard ear oximeter. 24:122-126, 1990.

71. **Takatani S, Davies C, Sakakibara N, Zurick A, Kraenzler E, Golding L, Noon GP, Nose Y and DeBakey ME:** Experimental and clinical evaluation of a noninvasive reflectance pulse oximeter sensor. *J Clin Monit* 8:257-266, 1992.

72. **Mendelson Y and Yocum B:** Noninvasive measurement of arterial oxyhemoglobin saturation with a heated and a non-heated skin reflectance pulse oximeter sensor. *Biomedical Instrumentation and Technology* 25:472-480, 1991.

73. **Mendelson Y and McGinn MJ:** Skin reflectance pulse oximetry: In vivo measurements from the forearm and calf. *J Clin Monit* 7:7-12, 1991.

74. **Ling J, Takatani S, Noon GP and Nose Y:** In vivo studies of reflectance pulse oximeter sensor. *SPIE Proceedings*, 1993 (in press).

75. **Chance B, Wang NG, Maris M, Nioka S and Sevik E:** Quantitation of tissue optical characteristics and hemoglobin desaturation by time and frequency resolved multi-wavelength spectrophotometry. *Oxygen Transport to Tissue* 14:297-304, 1992.

76. **Nomura Y and Tamura M:** Picosecond time of flight measurement of living tissue: Time resolved Beer-Lambert Law. *Oxygen Transport to Tissue* 14: 131-136, 1992.

77. **Kessler FK, Wiesner J and Wokaun A:** Analysis of multiple multipole scattering by time-resolved spectroscopy and angular dependent spectrometry. *Oxygen Transport to Tissue* 14: 261-266, 1992.

78. **van der Zee P, Cope M, Arridge SR, Essenpreis M, Potter LA, et al:** Experimentally measured optical pathlengths for the adult head, calf and forearm and the head of the newborn infant as a function of inter optode spacing. *Oxygen Trasnport to Tissue* 14. 143-153, 1992.

79. **Brazy JE:** Cerebral oxygen monitoring with near infrared spectroscopy. Clinical application to neonates. *J Clin Monit* 7:325-334, 1991.

80. **Hazeki O, Tamura M:** Quantitative analysis of hemoglobin oxygenation state of rat brain in situ by near-infrared spectrophotometry. *J Appl Physiol* 64:796-802, 1988.

81. **Elwell CE, Cope M, Edwards AD, Wyatt JS, Reynolds EOR et al:** Meausrement of cerebral blood flow in adult humans using near infrared spectroscopy - Methodology and possible errors. *Oxygen Transport to Tissue* 14:235-245, 1992.

82. **Kurth CD, Steven JM, Benaron D and Chance B:** Near-infrared monitoring of the cerebral circulation. *J Clin Monit* 9.163-170, 1993.

83. **McCormick PW, Stewart M, Goetting MG, Dujovny M, Lewis G et al:** Noninvasive cerebral optical spectroscopy for monitoring cerebral oxygen delivery and hemodynamics. *Critical Care Medicine* 19(1):89-97, 1991.

84. **Takatani S, Awazu K, Kanda M and Takano H:** Theoretical consideration for design of optical sensor for nonivnasive tissue reflectance oximetry. *Proceedings of Jap Soc of ME & BE* 26:222, 1988.

APPENDIX S

Beam Shaping with Cylindrical Lenses

Cylindrical Lenses focus or expand light in one axis only. They can be used to focus light into a thin line in optical metrology, laser scanning, spectroscopic, laser diode, acousto-optic, and optical processor applications. They can also be used to expand the output of a laser diode into a symmetrical beam.

Generating a Line of Light from a Collimated Laser

A common application of cylindrical lenses is shown in Figure 1. A collimated laser beam of radius r_0 is incident upon a cylindrical plano-concave lens of focal length -f. In this figure, the radius of the laser beam is exaggerated for clarity. The laser beam will expand with a half-angle θ of r_0/f. The laser beam will appear to be expanding from a virtual source placed a distance f behind the lens. At a distance z after the lens, there will be a line with thickness $2r_0$ (ignoring expansion of the Gaussian beam) and length

$$L = 2\,(r_0/f)(z+f)$$

If z is large compared to f, then we have an expansion ratio that is very close to z/f. This is not an imaging problem; we are projecting the laser beam into a line at a particular distance. The length of the line is simply proportional to z.

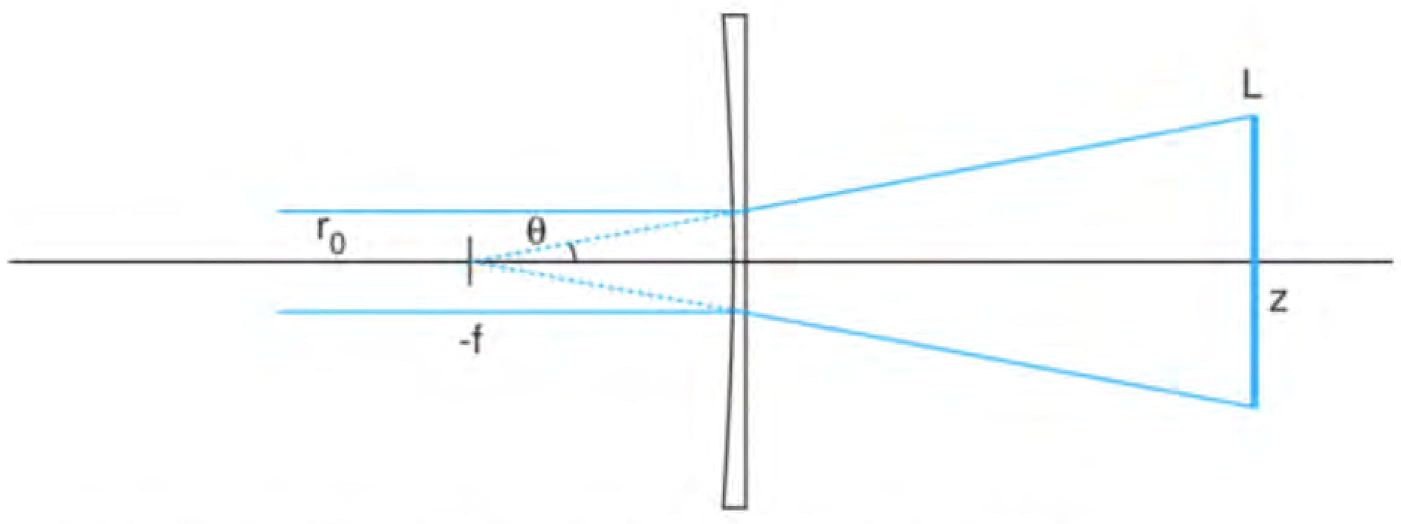

Figure 1. Diagram of line of light generation with a plano-concave cylindrical lens.

If the thinnest possible line is required, then a second lens, this one a cylindrical plano-convex lens of focal length ~ z, can be inserted into the system just before or after the plano-concave lens. When oriented on the orthogonal axis, it will focus the laser at the screen onto which the line is projected

In some cases a sheet of light is required for an application. The projected beam of Figure 1 can be thought of as a sheet of light, but note that the sheet is not square or rectangular. The sheet that is available for use is the isosceles triangle formed by the projected line at the screen and the maximum rays formed at the angles given by θ.

Circularizing the Beam from a Laser Diode

The output of a laser diode diverges in an asymmetrical pattern, making collimating the beam a challenge. Cylindrical lenses can be used to circularize the beam. Consider a laser diode with beam divergence of $\theta_1 \times \theta_2 = 10° \times 40°$. Any attempt to collimate this beam with spherical optics would result in collimation in one direction only, with a diverging or converging beam in the other direction. With cylindrical optics the problem can be approached as two one dimensional problems. The simplest solution would be to collimate the beam in one dimension with a single cylindrical lens, then collimate the orthogonal dimension with a second cylindrical lens (see Figure 2).

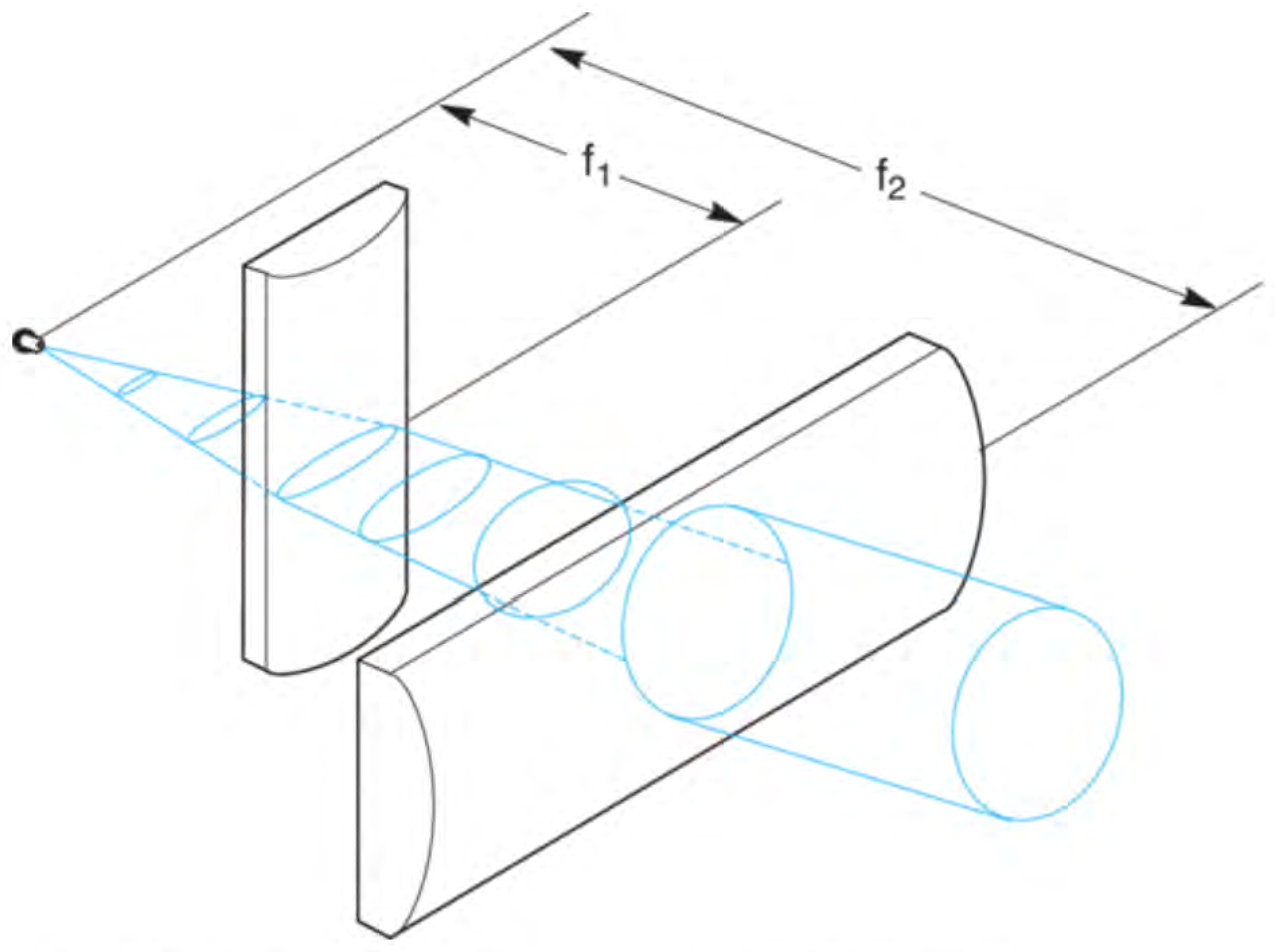

Figure 2. Diagram of circularizing the beam from a laser diode using two cylindrical lenses.

A few observations will guide the selection and placement of the lenses:

1) To achieve a symmetrical beam shape, the ratio of the focal length of the two lenses should be approximately equivalent to the ratio of the beam divergences:

$$\theta_1/\theta_2 = 10°/40° = f_1/f_2$$

2) First, to order, the laser diode is approximated by a point source, so the lenses should be placed at a distance equal to their respective focal lengths from the source to create a collimated output.

3) The principal planes of the two lenses should be spaced at a distance apart equal to the difference of their focal lengths f_2 - f_1. The actual spacing between plano surfaces of the lenses is BFL_2 - BFL_1. As with spherical lenses the convex surfaces should face the collimated rays to minimize aberrations.

4) Because of the rapid divergence of the laser diode beam, care must be taken to make sure the beam width at each lens does not exceed the lens clear aperture. Since each lens is placed one focal distance from the laser diode, the maximum beam width at each lens (d_1 and d_2) can be determined from the following equations:

$$d_1 = 2f_1(\tan(\theta_2/2)),\ \text{and}\ d_2 = 2f_2(\tan(\theta_1/2))$$

For this example a convenient choice of lenses is Newport CKX012 (f_1 = 12.7 mm, BFL_1 = 7.49 mm) and CKX050 (f_2 = 50.2 mm, BFL_2 = 46.03 mm). The nominal spacing between plano surfaces of the lenses is BFL_2 - BFL_1 = 38.54 mm. The beam diameter at the first lens is

$$d_1 = 2 \times 12.7\ \text{mm} \times \tan(20°) = 9.2\ \text{mm}$$

The beam diameter at the second lens is

$$d_2 = 2 \times 50.2\ \text{mm} \times \tan(5°) = 8.8\ \text{mm}$$

so a slight asymmetry remains, but a substantial improvement has been achieved with a simple arrangement of standard lenses.

APPENDIX T

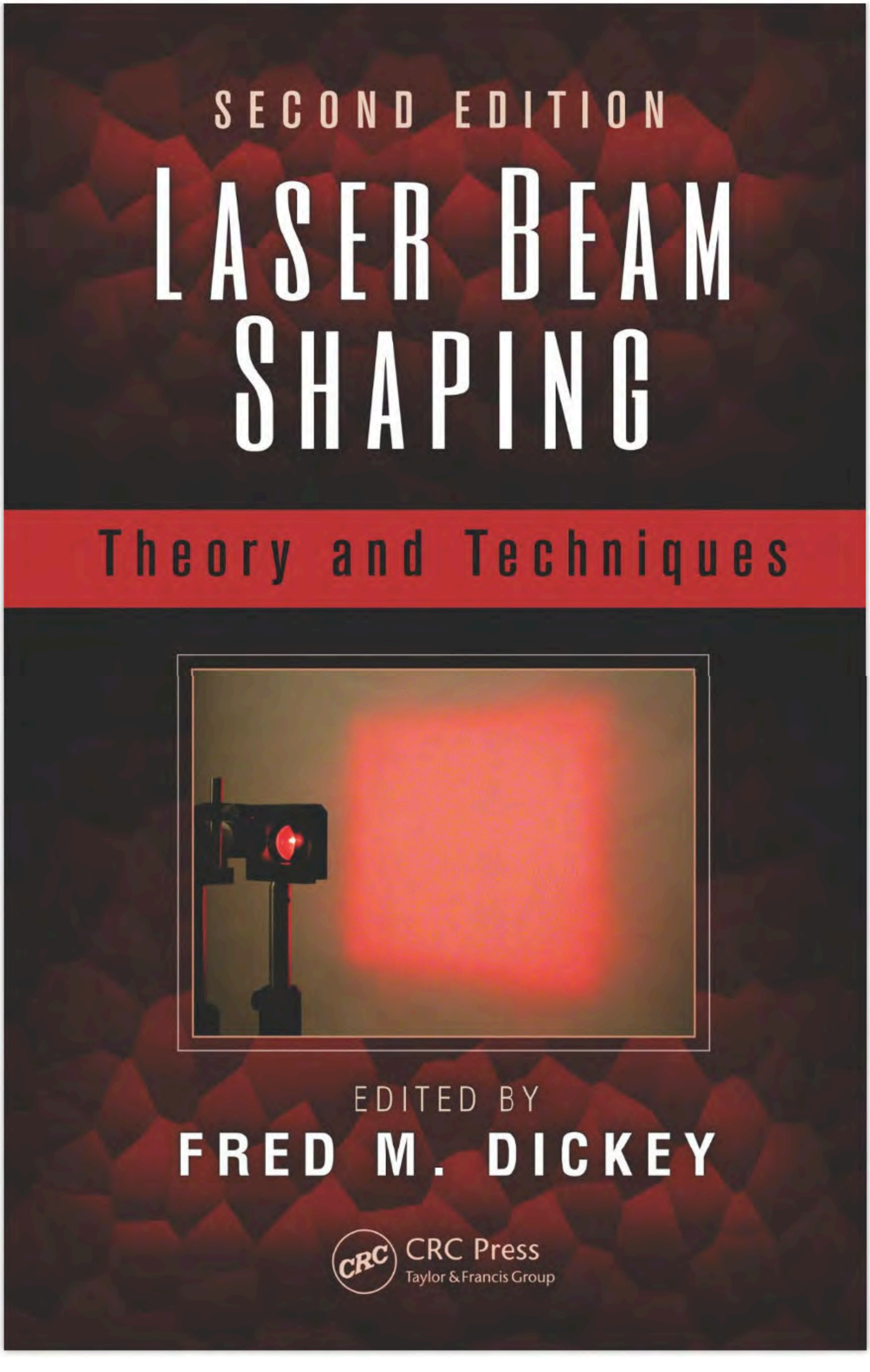
SECOND EDITION
LASER BEAM SHAPING
Theory and Techniques
EDITED BY
FRED M. DICKEY
CRC Press
Taylor & Francis Group

SECOND EDITION

LASER BEAM SHAPING

Theory and Techniques

SECOND EDITION

LASER BEAM SHAPING

Theory and Techniques

EDITED BY
FRED M. DICKEY

CRC Press
Taylor & Francis Group
Boca Raton London New York

CRC Press is an imprint of the
Taylor & Francis Group, an **informa** business

CRC Press
Taylor & Francis Group
6000 Broken Sound Parkway NW, Suite 300
Boca Raton, FL 33487-2742

Version Date: 20140402

International Standard Book Number-13: 978-1-4665-6101-4 (eBook - PDF)

Visit the Taylor & Francis Web site at
http://www.taylorandfrancis.com

and the CRC Press Web site at
http://www.crcpress.com

Dedication

I would like to dedicate this book to Alexander, Ryan, Adrian, Miles, and Leo.

Contents

Preface

At the time of the publication of the first edition of this book, there was a significant interest in laser beam shaping for industrial applications and research. A significant amount of this work was not published for proprietary reasons. At that time, people began to publish their work on beam shaping. The interest in laser beam shaping increased dramatically in the following years. This is due to the increase in the number of laser applications that can benefit from shaping the beam, the increase in research in laser beam shaping techniques and the corresponding increase in the literature, and the advances in optical component fabrication technology. The purpose of this edition is to update the book to include significant developments in laser beam shaping theory and techniques.

After the Introduction chapter, Chapter 2 presents the underlying electromagnetic theory and mathematical techniques applicable to beam shaping. This chapter is very fundamental and has one minor correction or change. Chapter 3 is a new chapter that presents the theory of optimal beam splitting gratings (fan-out gratings). Chapter 4 is a new chapter that addresses the theory and application of vortex beams. Chapter 5 (former Chapter 3) presents the diffraction approach to single-mode Gaussian beam shaping and includes experimental results. The major changes in this chapter are the inclusion of a new section on wavelength dependence of the problem and an expansion of Appendix B. The methods, theory, and application of geometrical optics are discussed in Chapter 6 (former Chapter 4). This chapter is expanded significantly to include the author's research that was not available at the time of the first edition. Optimization-based techniques are presented in Chapter 7 (former Chapter 5). This chapter is greatly revised around the techniques based on the use of current optical software packages. Beam shaping using diffractive diffusers is introduced in Chapter 8 (former Chapter 6). This chapter is significantly revised. Chapter 9 is a new chapter that presents the theory of beam shaping based on the use of microlens diffusers. Multiaperture beam integration systems, including experiment and design, are presented in Chapter 10 (former Chapter 7). The major change in this chapter is the addition of a new section on channel integrators. Chapter 11 is a new chapter that discusses the generation of light ring patterns using axicons. This chapter includes a technique for the generation of rectangular line light patterns. Beam profile measurement technology is addressed in Chapter 12 (former Chapter 9). This chapter is significantly updated. Chapter 13 (former Chapter 8) discusses the application of geometrical optics methods to classical (nonlaser) shaping problems.

The material in these chapters gives the reader a working understanding of the fundamentals of laser beam shaping techniques. It also provides insight into the potential application of laser beam profile shaping in laser system design.

The book is intended primarily for optical engineers, scientists, and students who have a need to apply laser beam shaping techniques to improve laser processes. It should be a valuable asset to someone who researches, designs, procures, or assesses the need for beam shaping with respect to a given application. Due to the broad treatment of theory and practice in the book, we think that it should also appeal to scientists and engineers in other disciplines.

I express my gratitude to the contributing authors whose efforts made the book possible. It was a pleasure working with the staff of Taylor & Francis Group books. Finally, I express my appreciation to the very helpful project coordinator, Laurie Schlags.

Fred M. Dickey
FMD Consulting, LLC

Editor

Fred M. Dickey received his BS (1964) and MS (1965) degrees from Missouri University of Science and Technology, Rolla, Missouri, and his PhD degree (1975) from the University of Kansas, Lawrence, Kansas. He started and chaired the SPIE Laser Beam Shaping Conference, which is in its fifteenth year, for the first 8 years, and is currently a committee member. He heads FMD Consulting, LLC, Springfield, Missouri. He is a fellow of the International Optical Engineering Society (SPIE) and the Optical Society of America, and a senior member of the Institute of Electrical and Electronic Engineers. Dr. Dickey is also the author of over 100 papers and book chapters, and holds 9 patents.

Contributors

Daniel M. Brown
Optosensors Technology, Inc.
Gurley, Alabama

David R. Brown
JENOPTIK Optical System, LLC
Huntsville, Alabama

Jeremiah D. Brown
JENOPTIK Optical Systems, LLC
Huntsville, Alabama

Fred M. Dickey
FMD Consulting, LLC
Springfield, Missouri

Neal C. Evans
PointClear Solutions, Inc.
Innovation Depot
Birmingham, Alabama

Julio C. Gutiérrez-Vega
Photonics and Mathematical Optics Group
Tecnológico de Monterrey
Monterrey, Mexico

John A. Hoffnagle
Picarro, Inc.
Santa Clara, California

Scott C. Holswade
Sandia National Laboratories
Albuquerque, New Mexico

Kevin D. Kirkham
Ophir-Spiricon, LLC
North Logan, Utah

Alexander Laskin
AdlOptica GmbH
Berlin, Germany

Todd E. Lizotte
Via Mechanics USA, Inc.
Londonderry, New Hampshire

Carlos López-Mariscal
US Naval Research Laboratory
Washington, DC

Louis A. Romero
Department of Computational and Applied Mathematics
Sandia National Laboratories
Albuquerque, New Mexico

Carlos B. Roundy
Logan, Utah

Tasso R.M. Sales
RPC Photonics Inc.
Rochester, New York

David L. Shealy
Department of Physics
University of Alabama at Birmingham
Birmingham, Alabama

Louis S. Weichman
Sandia National Laboratories
Albuquerque, New Mexico

1 Introduction

Todd E. Lizotte and Fred M. Dickey

Beam shaping is the process of redistributing the irradiance and phase of a beam of optical radiation. The beam shape is defined by the irradiance distribution. The phase of the shaped beam is a major factor in determining the propagation properties of the beam profile. For example, a reasonably large beam with a uniform phase front will maintain its shape over a considerable propagation distance. Beam shaping technology can be applied to both coherent and incoherent beams.

Arguably, there exists a preferred beam shape (irradiance profile) in any laser application. In industrial applications, the most frequently used profile is a uniform irradiance with steep sides, flat-top beam. This is due to the fact that the same interaction (physics) is accomplished over the illuminated area. Flat-top beams also have applications in laser printing. However, this is not the only profile of interest. Laser disk technology uses a focused beam with minimized side lobes to eliminate cross talk. Other patterns of interest in applications include shaped lines, rings, and array patterns. Some of the major applications of laser beam shaping are discussed in detail in *Laser Beam Shaping Applications*.[1]

Although the laser was invented in 1960, there were only about eight papers on laser beam shaping that appeared in the literature before 1980. A brief history and overview of laser beam shaping is given in the 2003 *Optics & Photonics News* paper "Laser Beam Shaping."[2] The rate of the appearance of laser beam shaping papers grew linearly, but slowly, until about 1995 when the rate increased dramatically. There is evidence that considerable research and development work on laser beam shaping was done in the period before 1995, but was not published for proprietary reasons. Starting in 2000 and continuing to the present, there have been 14 International Society for Optics and Photonics (SPIE) laser beam shaping conferences.[3–16] The history of laser beam shaping is treated by Shealy in Chapter 9 of *Laser Beam Shaping Applications*.

A flat-top laser irradiance profile can be obtained by expanding the beam to obtain a pattern with the desired degree of uniformity. This approach intrudes very large losses in energy throughput. In almost all beam shaping applications, it is desirable to minimize the losses. The two major beam shaping techniques for producing a uniform beam are field mapping and beam integrators (homogenizers). These techniques can be designed to have very low losses.

Field mapping is the technique of using a phase element to map the laser beam into a uniform beam (or other profile) in a given plane. Field mappers are applicable to single-mode (spatially coherent) lasers. Producing vortex beams is also an example of field mapping. The individual lenslets in beam integrators function as field mappers.

Beam integrators break up the input beam into smaller beamlets that are directed to overlap in the output plane with the desired shape. They frequently consist of a lenslet array and a primary lens. Beam integrators can also be implemented using a reflective tube and focusing the laser beam on the input aperture of the tube. This approach is called a channel integrator. Beam integrators are especially applicable to low spatial coherence beams. The low spatial coherence of the input beam reduces the speckle pattern that is inherent in the output of beam integrators. There cases when it is useful to apply beam integrators to spatially coherent beams when the speckle can be tolerated. It is interesting to note that optical configurations that can be considered beam integrators were introduced long before the advent of the laser.[17,18]

The ability to do beam shaping is limited by uncertainty principle of quantum mechanics, or equivalently the time–bandwidth product inequality associated with signal processing. Mathematically, the uncertainty principle is a constraint on the lower limit of the product of the root-mean-square width of a function and its root-mean-square bandwidth. It can be directly applied to the beam shaping problem because of the Fourier transform relation in the Fresnel integral used to describe the beam shaping problem. In fact, the uncertainty principle is generally applicable to diffraction theory. Applying the uncertainty principle to the general diffraction problem associated with laser beam shaping, one obtains a parameter β of the form

$$\beta = C\frac{r_0 y_0}{\lambda z} \tag{1.1}$$

where:

r_0 is the input beam half-width
y_0 is the output beam half-width
C is a constant that depends on the exact definition of beam widths
z is the distance to the output plane

The parameter β is also obtained when applying the method of stationary phase to diffraction problems.

The value of β must be sufficiently large for successful beam shaping to be accomplished. It should be noted that the system designer has some design control over β by specifying r_0 or, possibly, the other three parameters in Equation 1.1. Because of its fundamental nature, β is applicable to field mappers and beam integrators.

It is commonly stated that when β is large the problem can be treated using geometrical optics. This is true for field mapping systems designed to produce flat-top profiles. However, techniques such as diffractive diffusers inherently require the use of diffraction theory in the design process. In addition, diffraction theory is useful in determining some general properties of beam shapers. An example is the wavelength independence of some field mapping configurations (see Chapter 5).

In no case can quality beam shaping be accomplished if β is small. It is suggested that this parameter be considered in the initial stage of any beam shaping system design.

As stated earlier and clearly defined in the subsequent chapters, the theory, calculations, and strategies for designing laser beam shaping systems have come a long way. Although success in the application of beam shaping does not only come from knowing how to calculate a design and understanding the guiding parameters such as β, it simply provides a working baseline of knowledge.

When an engineer or a development team considers the integration of optics into a process, they need to take into account a number of primary as well as ancillary variables that start at the process and work backward through the optical system to the laser source itself. Failure is inevitable if beam shaping is considered simply as an off-the-shelf product that is easy to integrate. Consideration of a new beam shaper design or the purchase of an off-the-shelf beam shaping product must be approached carefully since the beam shaper's performance is dependent on the stability of the laser source itself. Offering a considerable number of challenges due to the dynamic nature of laser processes simple changes to duty cycle often result in pointing instability, divergence shifts, beam intensity distribution, and power fluctuations, to name a few. All of the variables identified need to be scrutinized and prioritized so that the beam shaper can be designed and configured with an appropriate set of preconditioning optics or enough axes of adjustment to provide fine-tuning if required.[19] These items are only part of what it takes to be successful; a willingness to tackle the hardest problems first is the only true guarantee.

Since the introduction of lasers into the industrial marketplace, those of us involved in its application have been in a technology race, whether we like it or not. Driving innovation is the key to success for technologists, but that innovation in many cases is found by simply searching for insight from existing successes within the scientific community or other markets where similar technology is applied. That insight can take many forms such as exposure to existing and past technologies or merely taking calculated risks by blazing a new trail by pulling together various technologies and integrating them into a new solution. Whether applying old or new ideas, innovation of beam shaping technology requires identifying the parameters within the context of a laser process that matter and moving through them systematically to deliver an elegant solution.

Below are two examples that highlight the development of "diffractive and refractive" laser beam shaping technology over the past 20 years and hit upon this theme. From a historical perspective, the examples were selected to illustrate the progression and impact of laser beam shaping on the industrial laser system marketplace. No attempt has been made to select specific technological milestones of equal importance nor should the reader consider these items critical in terms of a grand historical record. These examples are simply moments in time where insight gained by early adopters led to experimentation and the evolution of laser beam shaping within the industrial laser and laser materials processing field. Let us explore a few exemplar beam shaper solutions that were brought to market, which is the point where true innovation ends, as well as demonstrated.

As mentioned earlier, field mappers are phase elements that redistribute laser light to form a new desired irradiance and phase profile. These phase elements commonly take two highly efficient forms, either traditional refractive phase elements, such as custom aspheric lenses (>96% efficient), or diffractive elements, such as diffractive lenses

FIGURE 1.2 An assembled beam shaping and imaging beam delivery for a UV DPSS marking application installed on an automation system.

produce precision ablated microstructures. The demagnification ratio determines the conjugate distances of the optical imaging system, that is to say the object (mask) distance to the lens and the image distance to the target plane. The optical system reduces the mask design by this factor; therefore, when generating the mask artwork, the feature desired on target is multiplied by the magnification factor. Figure 1.2 shows an assembled beam shaping and imaging beam delivery for a UV DPSS marking application installed on an automation system. The UV beam delivery systems geared for UV DPSS laser micromachining applications have four basic functions once the laser beam exits the laser itself: (1) improve the uniformity of the laser beam, (2) illuminate a fixed aperture or mask plane, (3) reduce/demagnify and project the mask image onto the target material, and (4) control the energy density at the target.

In most cases, the output intensity profile of the UV DPSS laser is Gaussian or TEM_{00} mode. For precision micromachining such as drilling or thin-film patterning, the transformation of the Gaussian laser beam into a flat-top intensity profile was the watershed moment, where the quality and accuracy of laser-based processes truly began to be demonstrated. Microvias that are laser-drilled into microelectronic packaging and laser thin-film patterning for solar cells and flat panel displays were key markets where the benefits of laser beam shaping were initially realized in the late 1990s and continue even today.

Two examples of common designs include field mappers for transforming single-mode Gaussian laser beams into a round or square flat-top intensity distribution profile. Figure 1.3 shows a Gaussian and super Gaussian profile. Within the field of microvia drilling of printed circuit boards (PCBs), the Gaussian output of a UV DPSS laser beam is shaped into a round flat-top intensity distribution and demagnified by using an optical imaging system to achieve the appropriate energy density to either ablate a thin metal film or polymer dielectric layers that make up a PCB assembly. Figure 1.4 shows a 30, 40, and 50 μm blind microvia in a PCB. Conversely, a square flat-top intensity profile can be used to pattern thin films to form structures such as pixel arrays or to precisely cut circuits for repairing advanced displays. Figure 1.5 shows an electrical grounding strap that was laser deleted using a square

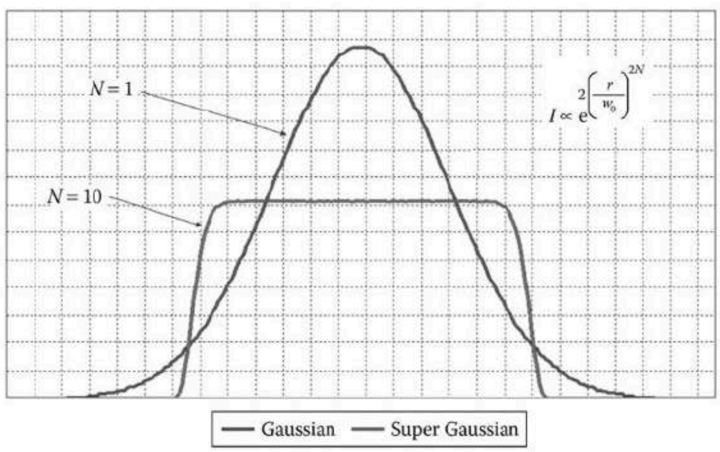

FIGURE 1.3 A Gaussian and super Gaussian profile distribution as an example of the desired transformation for many industrial beam shaping applications.

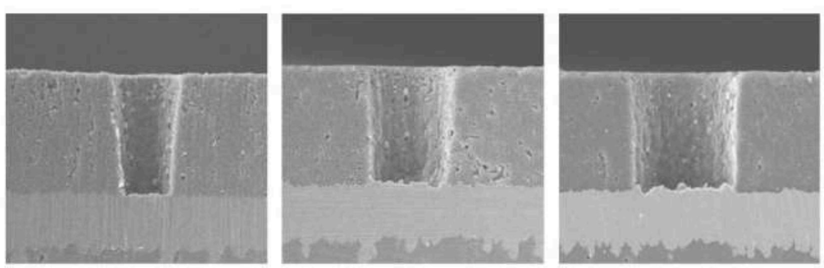

FIGURE 1.4 Microvia hole drilling on a PCB with 30, 40, and 50 μm diameters (left to right). These are possible using a UV DPSS flat-top laser beam.

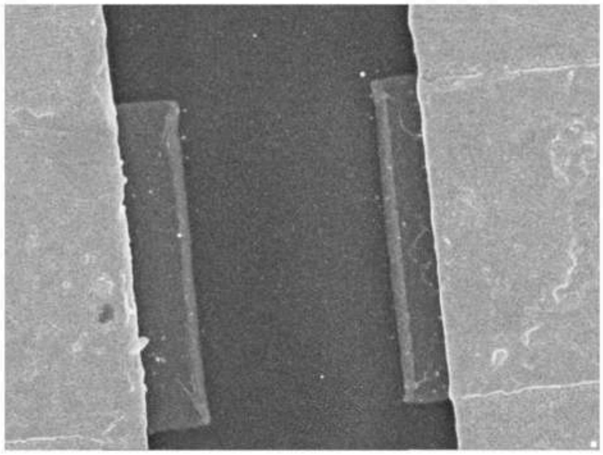

FIGURE 1.5 A grounding strap deletion using a square flat-top laser beam.

flat-top beam and the energy density was tailored so that only the strap was removed leaving the underlying material undamaged.

Depending on the laser system setup, the imaged beam can precisely drill or pattern materials with such finesse as to minimize or negate any thermal damage to the surrounding material. Therefore, precise and tailored to the material being processed, field mappers have enabled new opportunities for precision micromanufacturing that could not have been possible 20 years ago.

The arrival of integrator technology for laser materials processing was under the radar and developed in earnest when major challenges were encountered with the introduction of excimer lasers into the marketplace. During these early years, integrator development was kept secret until patent filings revealed their implementation. Many of these innovations were championed by laser system developers who were seeking solutions to improve excimer laser beam uniformity for large field size high-precision laser processes. In nearly all applications, excimer laser output uniformity is critical for high-precision applications.[21] During the early 1980s, to create a uniform irradiance beam profile, engineers were limited to either improving the performance of the laser itself, at a hefty price, or utilizing optical techniques. Modification of the laser meant trade-offs; increased uniformity at the sacrifice of pulse energy or power and that still did not guarantee the best uniformity.

At this time the excimer laser was finding new applications within semiconductor processing such as lithography and gaining ground in the promising field of laser micromachining. These early adopters were exposed to similar integrator designs used within illumination systems for lamp-based exposure tools, such as those produced by Oriel Instruments Corporation (Stratford, CT), which were generally simple lens array integrator designs.[22] The earliest and relatively successful example of an industrial excimer laser application that would not have been possible without the use of beam integrators, besides the semiconductor lithography market, was laser annealing of silicon. Patented by XMR, Inc. (Houston, TX) in 1986 and issued in 1988 as

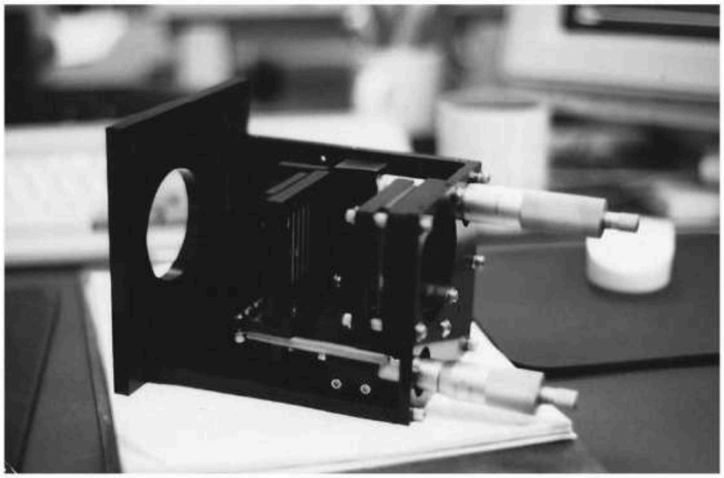

FIGURE 1.6 A beam integrator design from the mid-1980s manufactured by XMR, Inc.

US Patent 4,733,944, the design is one of a handful of instances of an imaging beam integrator for a high-volume industrial laser process requiring absolute stability and uniformity. What was unique about the design at the time was the fact that the spot size produced could be selectively adjusted in size at the working plane. Adjustability allowed variation of the energy density on target, tailoring it to an optimum setting and process area. Figure 1.6 is an example of an XMR design from the actual system.

From this point, the design of laser beam integrators began to take the form of specialized optical configurations with further enhancements and refinements to meet the needs of ever-demanding laser micromachining processes. In 1994 the integration of UV excimer lasers for laser micromachining of fluidic structures was being exploited for consumer and medical device products. One such product was the production of nozzle plates and fluidic channels for inkjet printers. Although personal inkjet printers had entered the marketplace in 1988, it was not until 1991 when inkjet printer manufacturers had begun to seriously consider excimer lasers as a means to reduce the costs of forming precision inkjet nozzle plates, which were upward of $4.00 each to manufacture. Figure 1.7 shows an example of an inkjet nozzle plate with integrated fluidic channels imaged and ablated into polyimide.

At that time, manufacturing nozzle plates to micron accuracies was not an easy task and they were costly to manufacture using traditional lithography and nickel electroforming techniques. It was clear in the early days of process development that the design of excimer beam delivery optics, physical system configuration, methods of optical beam shaping, and laser material interaction would play significant roles in producing inkjet nozzle plates. Due to higher demands for quality and the critical nature of providing consumers with exceptionally reliable products, the excimer processes needed to be robust and repeatable to a 3σ or better level.[23]

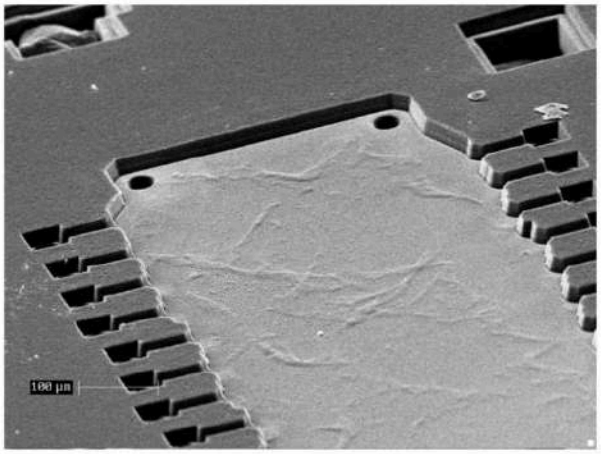

FIGURE 1.7 An inkjet nozzle plate with integrated fluidic channels imaged and ablated into polyimide.

Matching the laser process optics to resolve the nozzle and fluidic channel features to micron tolerances within the desired material was the goal. To complicate matters, inkjet nozzle arrays have dimensional requirements upward of 15 × 2 mm in size (L × W), which made the selection of beam shaping technology to provide uniformity across the entire image plane at a uniform energy density the most critical aspect of the excimer micromachining system. Figure 1.8 shows how the implementation of an imaging lens array beam integrator evolved in less than 10 years (ca. 1994). Larger in size and its zooming feature allowing larger illumination field sizes at the mask plane demonstrates how the integrator design had progressed into a useful and versatile tool for large-field ablation applications. Incorporating beam preconditioning optics, in this case an anamorphic cylindrical lens telescope, the output beam of the excimer was shaped from a rectangular shape into an optimized square configuration for illuminating the zoomable cross-cylindrical lens beam integrator. The beam integrator design was also more advanced than earlier designs, with an adjustable zoom for both axes of the beam, allowing the illumination field at a mask plane to be both uniform in intensity and dimensionally optimum. The shaped beam illuminated a mask that defined the features being produced. The numerical aperture of the beam integrator was designed to match the numerical aperture of the final imaging lens system allowing the mask design to be imaged onto the material to be processed. As the first excimer laser inkjet nozzle drilling system came online, the cost of inkjet nozzle plates had dropped to less than $0.20 a unit—a significant milestone for that industry that would not have been achieved without an integrator-based beam shaper design.

Since that time, further advancements have made it possible to take an excimer beam with a beam size of ~20 × ~10 mm (L × W) and transform it into a uniform beam of ~140 × ~5 mm, another example of how the integrator continues to evolve. Figure 1.9 shows a beam exposed on film at various attenuation factors

FIGURE 1.8 An advanced imaging excimer laser beam integrator design that is zoomable in the short and long axis (*X–Y*), allowing it to be tailored for the illumination field size at the mask plane.

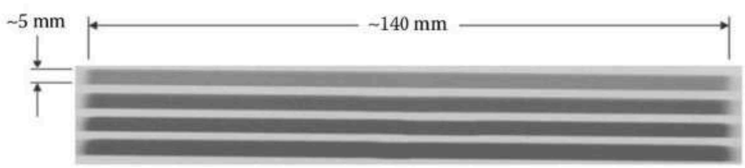

FIGURE 1.9 An integrator-shaped excimer laser beam exposed on a film at various attenuation factors: 25%–100% intensity (top to bottom). The integrator design produces an illumination field size at the mask ~140 × ~5 mm.

25%–100% intensity. This particular design is used in an excimer laser step and scan ablation tool to achieve an on-target ablation field size of ~35 × ~1.25 mm; based on a 4× demagnification the laser beam integrator produced an illumination field size at the mask plane of ~140 × ~5 mm.

When looking for the most dominant market segment that has benefited from beam shaping, you simply need to review history. As a rule of thumb, if you want to understand where technology will be 10 years into the future, you need to only look backward 20 years into the past. Within our optical community we tend to think that beam shaping innovations just came out of nowhere, but in reality there were great challenges that spurred development by pioneers in our field. Each chapter within this book is a testament to those pioneers and represents their continued impact on our laser beam shaping community.

REFERENCES

1. F. M. Dickey, S. C. Holswade, and D. L. Shealy, Editors, *Laser Beam Shaping Applications*, CRC Press, New York, 2005.
2. F. M. Dickey, "Laser beam shaping," *Optics & Photonics News*, 14(4), pp. 30–35, 2003.
3. F. M. Dickey and S. C. Holswade, *Laser Beam Shaping*, *Proceedings of SPIE* 4095, August, San Diego, CA, 2000.
4. F. M. Dickey, S. C. Holswade, and D. L. Shealey, *Laser Beam Shaping II*, *Proceedings of SPIE* 4443, August, San Diego, CA, 2001.
5. F. M. Dickey, S. C. Holswade, and D. L. Shealey, *Laser Beam Shaping III*, *Proceedings of SPIE* 4770, August, Seattle, WA, 2002.
6. F. M. Dickey and D. L. Shealey, *Laser Beam Shaping IV*, *Proceedings of SPIE* 5175, August, San Diego, CA, 2003.
7. F. M. Dickey and D. L. Shealey, *Laser Beam Shaping V*, *Proceedings of SPIE* 5525, August, Denver, CO, 2004.
8. F. M. Dickey and D. L. Shealey, *Laser Beam Shaping VI*, *Proceedings of SPIE* 5876, August, San Diego, CA, 2005.
9. F. M. Dickey and D. L. Shealey, *Laser Beam Shaping VII*, *Proceedings of SPIE* 6290, August, San Diego, CA, 2006.
10. F. M. Dickey and D. L. Shealey, *Laser Beam Shaping VIII*, *Proceedings of SPIE* 6663, August, San Diego, CA, 2007.
11. A. Forbes and T. E. Lizotte, *Laser Beam Shaping IX*, *Proceedings of SPIE* 7062, August, San Diego, CA, 2008.
12. A. Forbes and T. E. Lizotte, *Laser Beam Shaping X*, *Proceedings of SPIE* 7430, August, San Diego, CA, 2009.
13. A. Forbes and T. E. Lizotte, *Laser Beam Shaping XI*, *Proceedings of SPIE* 7789, August, San Diego, CA, 2010.
14. A. Forbes and T. E. Lizotte, *Laser Beam Shaping XII*, *Proceedings of SPIE* 8130, August, San Diego, CA, 2011.
15. A. Forbes and T. E. Lizotte, *Laser Beam Shaping XIII*, *Proceedings of SPIE* 8490, August, San Diego, CA, 2012.
16. A. Forbes and T. E. Lizotte, *Laser Beam Shaping XIV*, *Proceedings of SPIE* 8843, August, San Diego, CA, 2013.
17. J. Mihalyi, "Projection system for color pictures," US Patent Number 1,762,932, June 10, 1930.
18. K. Rantsch, L. Bertlele, H. Sauer, and A. Merz, "Illuminating system," US Patent Number 2,186,123, January 9, 1940.
19. T. Lizotte, F. M. Dickey, and D. Brown, "Laser beam homogenization, splitting and three spot image formation: System design, analysis and testing," *Laser Beam Shaping XIV*, *Proceedings of SPIE* 7789-9, 2010.
20. T. Lizotte and O. Ohar, "UV Nd:YAG laser technology," *Lasers & Optronics*, pp. 17–19, September 1994.
21. K. Weible and T. E. Lizotte, "Adaptation of an existing diffractive mono-mode beam shaping design to compensate a wavelength change," *Laser Beam Shaping X*, *Proceedings of SPIE* 7430, August, San Diego, CA, 2009.
22. T. S. Fahlen, S. B. Hutchison, and T. McNulty, "Optical beam integration system," US Patent Number 4,733,944, March 29, 1988.
23. T. Lizotte and O. Ohar, "Production excimer drilling process for producing micron exit holes in polyimide," *Photon Processing in Microelectronics and Photonics V*, *Proceedings of SPIE* 6106, June, San Jose, CA, 2006.

50095.0045IP3 and 50095.0045IP1

amazon.com

Details for Order # D01-9488553-1129813
Print this page for your records.

Amazon.com order number: D01-9488553-1129813

Order Total: $99.44

Digital Order: September 12, 2023

Items Ordered	Price
Laser Beam Shaping: Theory and Techniques, Second Edition[Kindle Edition] By: Fred M. Dickey Quantity: 1 Sold By: Amazon.com Services LLC	$93.81

Item(s) Subtotal: $93.81

Total Before Tax: $93.81
Tax Collected: $5.63

Total for this Order: $99.44

Payment Information

Payment method
ending in 2628

Billing address
M Jill Strand - Fish & Richardson
1000 MAINE AVE SW STE

Item(s) Subtotal:	$93.81
Total Before Tax:	$93.81
Tax Collected:	$5.63
Grand Total:	**$99.44**

1000
WASHINGT
ON, DC
20024-3446
United
States
612-204-
4621

Return to the Order Summary.

Please note: This is not a VAT invoice.

APPENDIX U

Micro-LED Technologies and Applications

Light-emitting diodes (LEDs) offer extraordinary luminance, efficiency, and color quality, but to date are largely used in displays as backlights or packaged pixel elements in large-area LED billboard displays. Building high-performance emissive displays in a smaller form factor requires a new micro-LED technology separate from what is used for large LED billboards. Several approaches have been proposed to isolate micro-LED elements and integrate these micro-LEDs into active-matrix arrays. Technologies that use micro-LEDs offer the potential for significantly increased luminance and efficiency, unlocking new possibilities in high dynamic range, augmented/mixed reality, projection, and non-display light-engine applications.

by Vincent W. Lee, Nancy Twu, and Ioannis Kymissis

THE luminance and power efficiency of a light source are the key factors for determining suitable applications. Light-emitting diodes (LEDs) offer very high luminance levels, greater than 50,000,000 cd/m^2, giving them a proven ability to perform in high-ambient display applications. LEDs also offer some of the highest efficiencies for converting electrical power to optical power. Depending on the material system, an energy conversion of over 60% can be achieved. Due to these benefits and the small solid-state form factor, emissive LEDs can become a solution for display applications of all sizes.

In today's display applications, LEDs are most commonly used as the illumination source for liquid-crystal displays (LCDs) of practically all sizes, including 100-in. TVs to 0.5-in. microdisplays. Individually packaged LEDs are also used as the direct pixel element in large-area billboard displays, which are currently the only format of directly emissive LED displays. What remains underexploited is the use of LEDs as individual pixel elements in all other smaller display formats.

In large-area displays, discrete packaged LED pixels, each containing a red, green, and blue LED chip in the package, form the active elements in emissive video walls. Emissive video walls are attractive for stadium and advertising applications given the high luminance (excellent viewability under bright ambient light conditions) and energy efficiency of LEDs. Although the size of each packaged LED pixel is relatively large, full-resolution displays are easily achieved in these large-area applications. Building smaller displays with packaged LEDs is more difficult. When using the smallest available packaged LED pixels (approximately 0.75 mm), 70 in. is the current minimum achievable size for a FHD-resolution (1920 × 1080) full-color display. When using packaged LED pixels, displays smaller than 70 in. can be produced, albeit with lower resolution.

New applications such as high-dynamic-range (HDR) television and augmented reality are demanding the same high-performance specifications as that of large-area displays, but at dimensions that are difficult to scale for fully packaged LEDs. For example, TV displays require a peak luminance of 10,000 cd/m^2 for future HDR content, and microdisplays need to reach 100,000 cd/m^2 to support the luminance needs of augmented-reality and mixed-reality (AR/MR) glasses. These requirements are easily satisfied by LEDs, which can have luminances up to 50,000,000 cd/m^2. Like other emissive displays, an emissive LED display offers the luminance and efficiency of the pixel source without the typical loss associated with light selection and modulation elements (polarizers, color filters, *etc*). Emissive LED arrays therefore have a huge luminance advantage

High-luminance emissive FHD-resolution LED displays smaller than 70 in. cannot be made from packaged LED pixels, and thus require the development of new manufacturing techniques and technologies. Specifically, these smaller display formats require fabrication and use smaller LED elements or "micro-LEDs." Loosely defined, micro-LEDs are

***Vincent Lee** is the founder and CEO of Lumiode, a startup company commercializing micro-LED microdisplay technology. He can be reached at vincent@lumiode.com. **Nancy Twu** is a Research and Development Engineer at Lumiode. **Ioannis (John) Kymissis** is a faculty member in the electrical engineering department at Columbia University and a co-founder and scientific advisor to Lumiode.*

0362-0972/6/2016-016$1.00 + .00 © SID 2016

devices in which the LED emission area per pixel is below 50 × 50 µm, or 0.0025 mm^2. An array of micro-LEDs makes up a micro-LED display, which ranges in size from fractions of an inch up to 70 in.

Micro-LED displays take advantage of the exceptional luminance of LEDs by spreading the generated photons over a larger area than the area occupied by the micro-LEDs themselves, either by distributing the LED elements spatially or by dispersing light optically. This is illustrated in Fig. 1. There are wide differences between these two technologies, despite confusing nomenclature that refers to both as "micro-LED." The former technology, shown in Fig. 1(a), distributes LED elements spatially and can be used to build displays ranging from 3 to 70 in. In this article, these are referred to as "direct-view micro-LED displays." The latter technology, shown in Fig. 1(b), disperses light optically and is used to build displays < 2 in., which are referred to as "micro-LED microdisplays."

In direct-view micro-LED displays, micro-LEDs are fabricated with a small pixel pitch, separated into individual dice, and transferred to an active-matrix backplane using pick-and-place methods. This allows for the development of an LED display in which the active LED area occupies only a small fraction of the total area. The area expansion allows for direct viewability of high-luminance micro-LEDs (up to a full 50,000,000 cd/m^2 per LED) because the micro-LEDs are spatially separated, resulting in a lower apparent luminance per pixel. The area unoccupied by micro-LEDs is available for a black matrix and integration of interconnection electronics. With larger current-distribution buses available, this approach allows for passive-matrix display development and integration and also lends itself to active-matrix approaches using large-area electronics.

Micro-LED microdisplays use semiconductor integration techniques to combine an array of small pixel-pitch micro-LEDs with a transistor back plate, which are then integrated with an optical system such as projection lenses or see-through glasses. Because the < 20-µm pixel pitch of micro-LEDs for microdisplays is even smaller than that of direct-view displays, the scaling of micro-LEDs for microdisplays requires full integration at the wafer-fabrication level. There are several strategies to perform the semiconductor integration between micro-LEDs and transistors, including pixel-to-transistor bonding, LED epitaxial transfer to silicon CMOS, and integration with thin-film-transistors (TFTs).

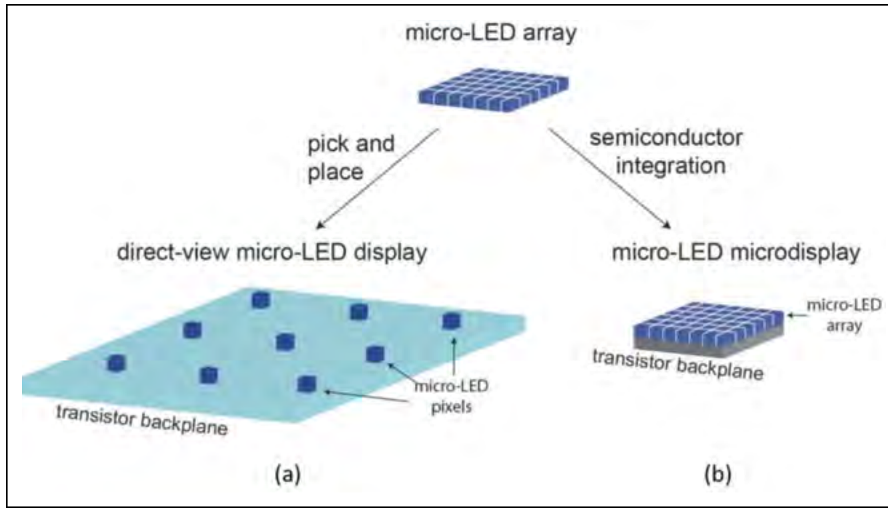

Fig. 1: Shown are two approaches used to build micro-LED displays. Both methods start with a micro-LED array but use either (a) a pick-and-place technology for direct-view displays or (b) semiconductor integration for microdisplays.

Because of fundamental differences in technology approaches and display sizes, micro-LEDs for direct-view displays and micro-LEDs for microdisplays target different markets. Together they offer the promise of replacing all displays now and in the future with the most efficient and highest-luminance systems possible.

Direct-View Micro-LED Displays Using Pick-and-Place Technologies

Today, stadium and large street displays use fully packaged surface-mounted LEDs in a

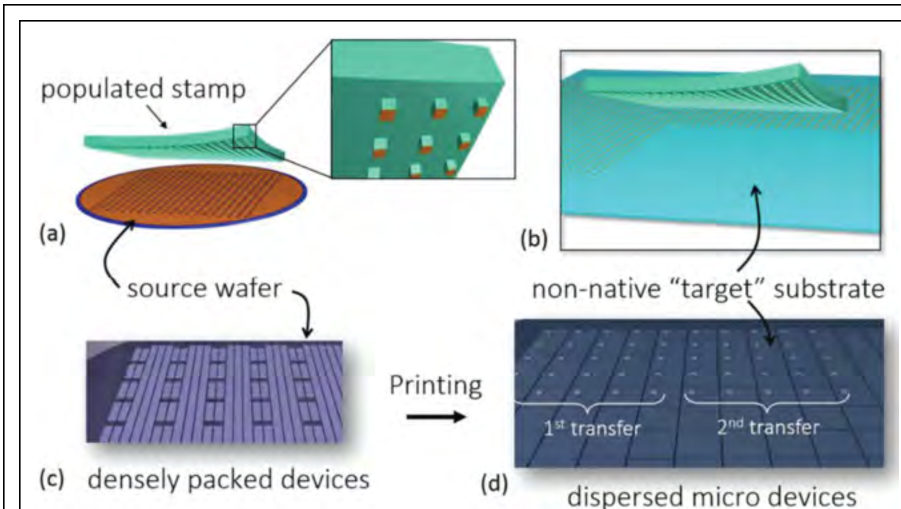

Fig. 2: In (a) and (c), selected individual chips are picked from a wafer using an elastomer stamp. In (b) and (d), the stamp is then moved to a non-native "target" substrate where the devices are placed, typically in a sparse array. Multiple devices are picked and placed in each transfer, and multiple transfers are used to complete a final display.[1]

tiled format. With reductions in packaged LED sizes, large-area tiled displays have scaled to smaller sizes and higher resolution displays, as small as 70 in. with FHD resolution. Direct-view micro-LED technologies are the natural extension of efforts to further shrink stadium-sized LED displays for new applications. Instead of using packaged LEDs, direct-view micro-LED technologies use smaller unpackaged LED dies and pick-and-place techniques to build emissive LED displays in the 3–70-in. size range. The resulting direct-view micro-LED displays show increased luminance and improved color gamut for HDR displays, provide different form factors for wearable and flexible displays, and address the push for ever-increasing power efficiency in these applications.

Several academic groups and companies have demonstrated pick-and-place approaches for transferring LED dies to a substrate board and connecting the elements to each other. All of these techniques begin with fabrication of densely packed small-pitch micro-LEDs. The micro-LEDs are then separated into individual dies, transferred to a secondary substrate, and physically spread out to a large pitch via proprietary pick-and-place processes. The choice of secondary substrate depends on the specific application and resolution. Applications such as flat-panel displays use a secondary glass substrate with active-drive transistors, while wearables such as watches and wristbands can use a flexible secondary substrate.

While several pick-and-place methods are being developed, few are publicly disclosed in detail. One paper by Bower *et al.* from X-Celeprint highlights some key aspects of pick-and-place processes.[1] Figures 2(a) and 2(c) show an array of densely packed devices (micro-LEDs) from which a subset of devices is sparsely picked up by an elastomer stamp. This stamp is moved to a secondary substrate, shown in Figs. 2(b) and 2(d), placing the devices in a dispersed array. The stamp can pick up many micro-LED devices at one time to lower the number of transfers needed to populate a full display.

Figure 3 shows X-Celeprint's process for transferring a small-pitch (~20 μm) micro-LED array to a larger pitch (~200 μm) on a glass substrate.[2] The micro-LEDs have a sacrificial release layer that is engineered into the LED epitaxial growth and later undercut to release the micro-LEDs from the growth substrate [Fig. 3(b)]. The micro-LEDs are then picked up by the elastomer stamp and transferred to a glass substrate with some pre-defined metal lines [Fig. 3(c)]. A second metal layer is then deposited [Fig. 3(d)] to electrically connect the transferred micro-LEDs to the glass substrate. By using this transfer process, X-Celeprint demonstrates a 100 × 100 color passive-matrix display [Fig. 3(e)]. Active-matrix formats can also be achieved by transferring the micro-LEDs to a secondary substrate with indium gallium zinc oxide (IGZO) or low-temperature polysilicon (LTPS) transistors.

Sony's micro-LED technology, initially demonstrated at CES in 2012, was recently released. Based on available technical data,

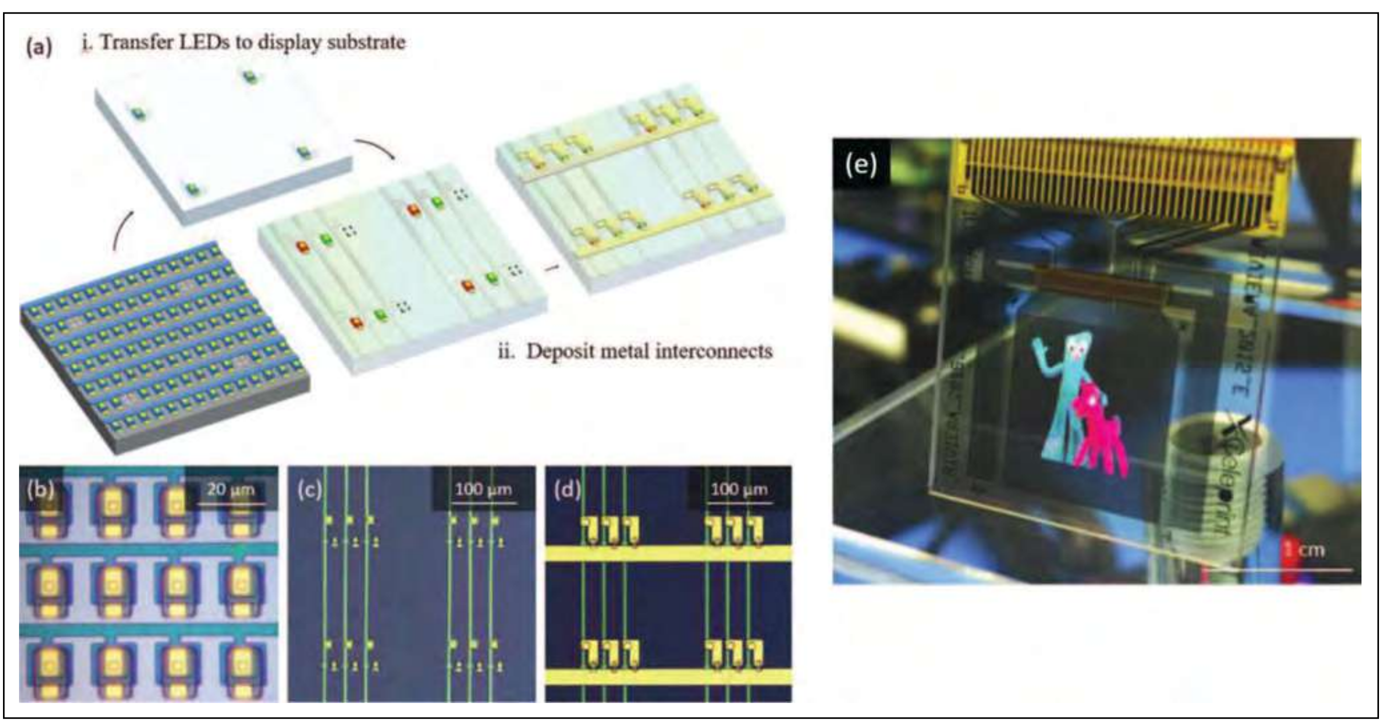

Fig. 3: *Image (a) shows the pick-and-place process of micro-LEDs to a secondary substrate. Image (b) is a micrograph of ready-to-transfer micro-LEDs on a source wafer with an undercut etch of the sacrificial layer. The LED size is approximately 10 x 10 μm. Images (c) and (d) are micrographs of transferred micro-LEDs and deposited metal layer for interconnection between micro-LEDs and a secondary substrate, respectively. Image (e) shows a full-color passive-matrix micro-LED display.*[2]

micro-LEDs approximately 50 × 50 µm in size are placed on a 320 RGB × 360 tile.[3] Much like conventional stadium displays, these micro-LED based tiles are then further arrayed to form the FHD display. Not much is known about the pick-and-place method or the backplanes used in Sony's demonstrations. Two other companies in the space are InfiniLED and LuxVue. InfiniLED's micro-LED technology uses a unique parabolic micro-LED structure for light collimation and light extraction [Fig. 4(a)].[4] This type of shaping allows for control of the micro-LED emission angle and potential improvements to the overall efficiency of the display. LuxVue, recently acquired by Apple, uses a MEMS-based pick-and-place process for micro-LEDs.

For pick-and-place technologies, the manufacturing challenges are similar across all of the techniques. The primary challenge is pixel transfer yield, as modern displays require nearly zero dead pixels across a FHD screen. To reach the needed pixel yields, some groups have proposed transferring redundant micro-LEDs,[4] as shown in Fig. 4(b), or performing individual pixel repair transfers for dead pixels.[2] These workarounds will add to either the base material cost or manufacturing time to build a display, reducing scalability. In addition, each pick-and-place process requires careful engineering of the LED materials, sometimes even custom LED epitaxy, to ensure that the electrical and optical performances are not affected throughout the fabrication process (LED ohmic contacts, undercut etch of the micro-LEDs, transfer of pixels, *etc*).

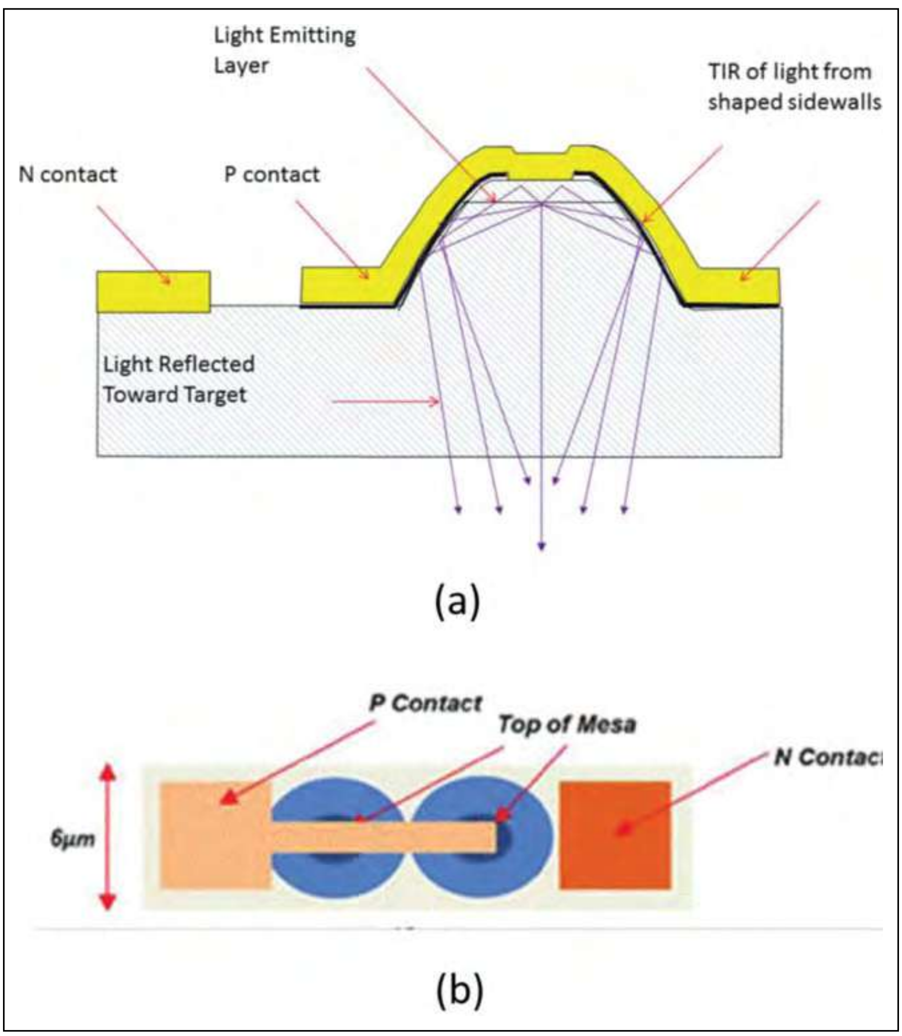

Fig. 4: The top image (a) shows a micro-LED schematic with reflective sidewalls and a curved shape for light collimation and extraction. The lower image (b) demonstrates a top-view design of a twin micro-LED emitter for redundancy and improvement of micro-LED yield.[4]

Micro-LED Microdisplays Using Semiconductor Integration Technologies

For microdisplays with a panel diagonal < 2 in., pick-and-place technologies cannot scale to the smaller pixel pitch required for FHD displays. Microdisplays < 2 in. using passive-matrix schemes also cannot achieve sufficient resolution or luminance, even though small pixel pitches have been demonstrated.[5,6] Building bright high-resolution < 2 in. microdisplays requires direct integration of micro-LED arrays with arrays of transistors that provide active-matrix switching. There are several transistor technologies and approaches to building the integrated active-transistor matrix. At a high level, these technologies can be sorted into the three categories as shown in Fig. 5: (a) chip-level

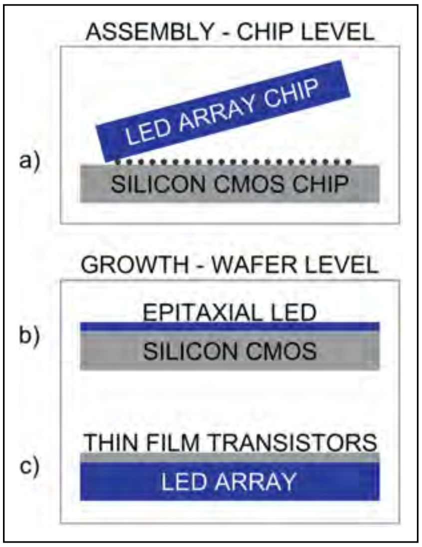

Fig. 5: Shown are three approaches to the integration of silicon transistors and micro-LED arrays for microdisplays: (a) chip-level hybridization of foundry CMOS chip with micro-LED arrays; (b) wafer-level transfer of LED epitaxial layers to CMOS wafer; and (c) wafer-level fabrication of TFTs directly on micro-LED arrays.[7]

micro-LED pixel–to–CMOS-transistor bonding, (b) LED epitaxial transfer to silicon CMOS, and (c) micro-LED array integration with TFTs.

Under first consideration is chip-level micro-LED pixel–to–CMOS-transistor bonding, a process also known as flip-chip bonding. Because of the ubiquity of foundry CMOS processes, many technologies in this category start with a completed silicon chip and work within back-end processes to add functionality, namely, chip-level assembly of micro-LED arrays as shown in Fig. 5(a). The LED arrays are fabricated by lithographic patterning of contacts and mesa etches. Bump bonds are then fabricated either on the silicon CMOS chip or on the micro-LED array. Next, the micro-LED arrays are die separated and bump bonded to the silicon CMOS chip. This fabrication flow offers researchers the advantage of using the highest-performing transistors, demonstrated by researchers at the University of Strathclyde,[8] the Hong Kong University of Science and Technology,[9] the Industrial Technology Research Institute,[10] and mLED.[11] Devices fabricated by mLED with conventional flip-chip bonding have been hybridized and demonstrated up to nHD (640 × 360) resolution with a pixel pitch as low as 20 µm.

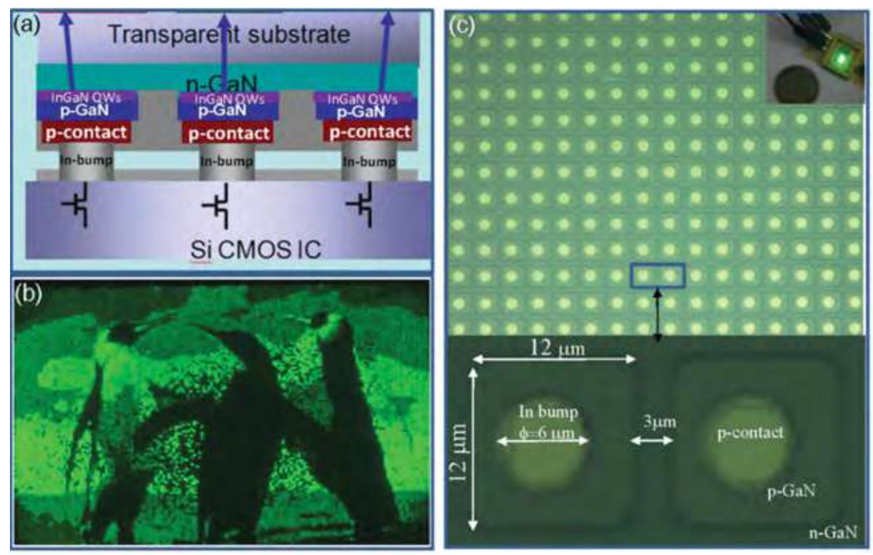

Fig. 6: Image (a) shows a cross-section schematic of a silicon CMOS IC flip-chip bonded with a micro-LED array using indium bump bonds. An image of a monochrome microdisplay appears in (b) and a micrograph of a micro-LED array with indium bonds prior to flip-chip bonding is shown in (c).[12]

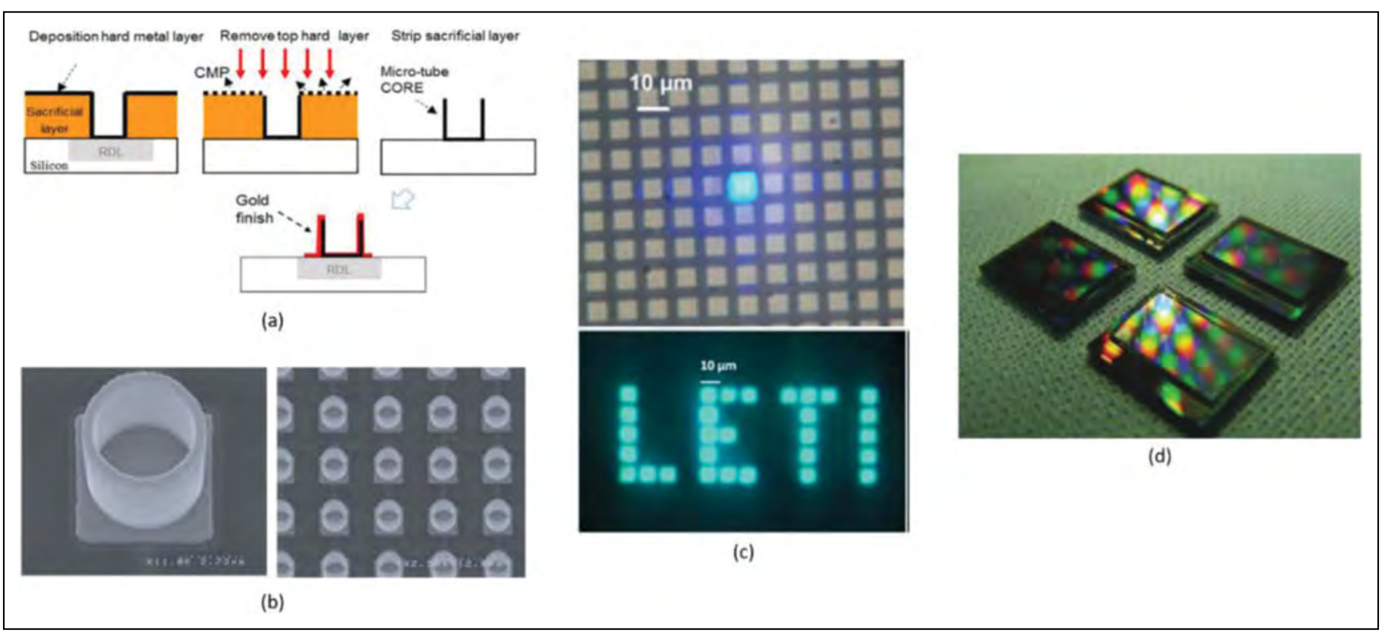

Fig. 7: Image (a) shows a schematic cross section of the micro-tube fabrication process. Image (b) shows a scanning electron micrograph of micro-tubes fabricated on a CMOS wafer. In (c) and (d), micrographs and a photograph of flip-chip bonded micro-LED arrays with a 10-µm pixel pitch are shown.[13,14]

Within flip-chip bonding, as pixel-pitch shrinking becomes more aggressive, non-traditional bonding processes are being developed. Devices by Day *et al*. use indium bumps to bond a 160 × 120 array at a 15-µm pitch [Fig. 6(b)].[12] Fabrication of this device, shown in Fig. 6(a), starts with foundry-silicon CMOS and a micro-LED array. The micro-LED array is then coated with indium through thermal evaporation and lithographically patterned to form indium bumps [Fig. 6(c)]. The indium-patterned micro-LED array is then flipped and mated with the corresponding CMOS silicon contact and heated to reflow each of the LED-transistor contacts.

More recently, Templier *et al*. at CEA-LETI demonstrated an innovative micro-tube technology to perform the bonding process. As in other approaches, a silicon CMOS chip and a micro-LED array are first fabricated separately. The silicon CMOS chip then continues through a series of back-end processes to form micro-tubes, as shown in Figs. 7(a) and 7(b).[13] The micro-tubes are created through the use of a sacrificial layer and deposition of a hard metal layer. This is followed by a chemical mechanical polish and removal of the sacrificial layer to form the micro-tube core. On the micro-LED array, a soft metal is formed to be compressed into the micro-tubes during the die assembly process. The resulting hybridized chip, shown in Figs. 7(c) and 7(d),[14] contains 6-µm micro-LEDs with a 10-µm pitch, a resolution of 873 × 500, demonstrating luminances up to 10,000,000 cd/m^2.

An alternative to flip-chip bonding is been being developed by Ostendo. Here, the process starts with silicon CMOS wafers, but instead of flip-chip bonding a completed array of micro-LEDs, LED epitaxial layers are transferred to the CMOS wafer. The LED material is then patterned and fabricated into the structure shown in Figs. 8(a) and 8(b).[15] In addition, vertical waveguide hole structures are fabricated into the surface, which can define the light-output cone angle. By changing the size of the hole structures, cone angles between ±17° to ±45° can be achieved. Ostendo has shown transfer of three colors (RGB) and a stacked RGB structure yielding a full-color microdisplay. In particular, nHD (640 × 360) and 720p (1280 × 720) resolution displays at 20,000 cd/m^2 have been demonstrated, as shown in Fig. 8(d).

Lumiode, the authors' startup, integrates micro-LEDs with a thin film of silicon transistors in a fully monolithic process, meaning all fabrication work is done on a single wafer. As illustrated in Fig. 5(c), the process starts with the LED substrate, upon which pixels are patterned into a micro-LED array using photolithography.[7] The pixel pitch can ultimately

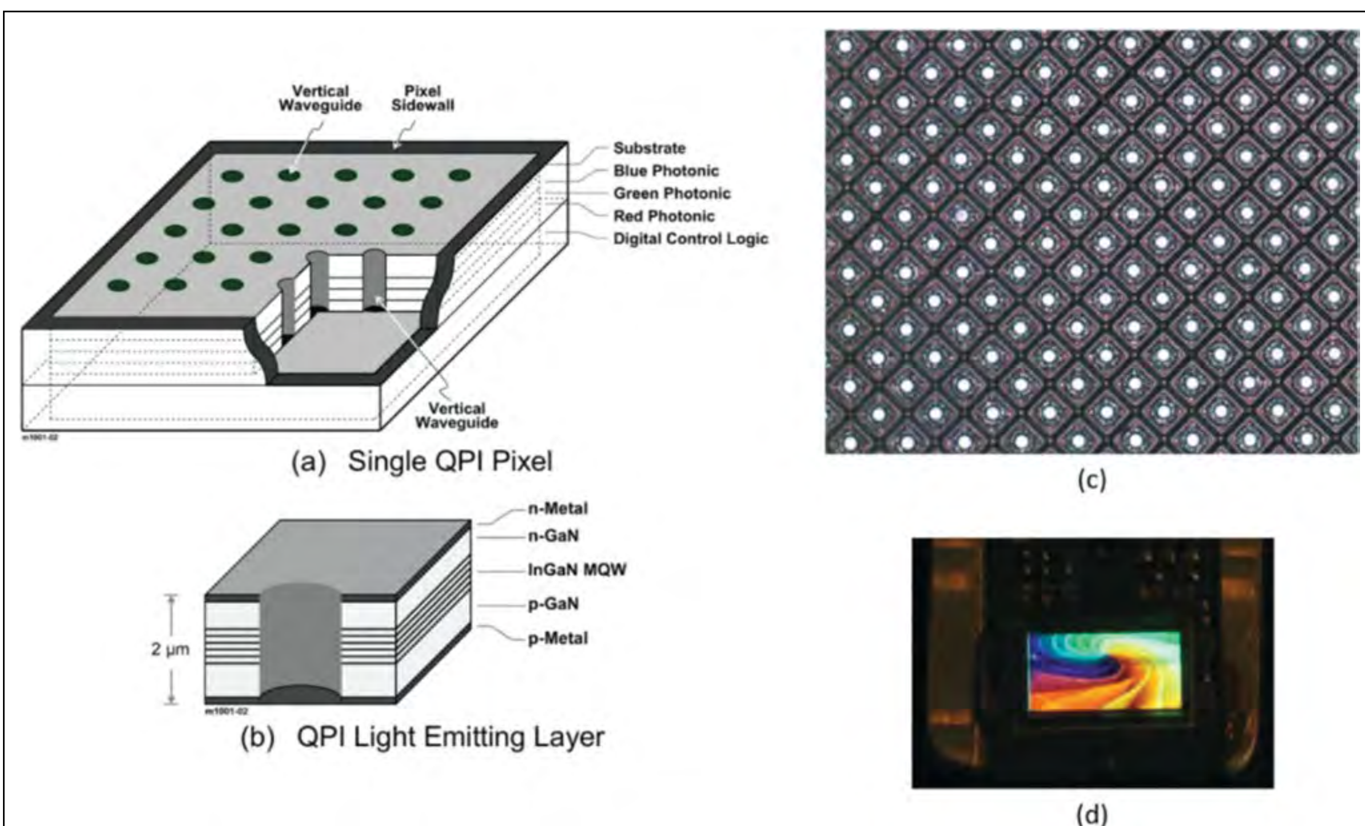

Fig. 8: *A cross-section schematic of a single stacked micro-LED pixel with vertical waveguides appears in (a). Image (b) shows a cross-section schematic of each light-emitting layer within the stacked micro-LED pixel. An image of a micro-LED array after front-side processing appears in (c), and in (d), a photograph of a test image shown on a 720p micro-LED microdisplay is shown.*[15]

scale to the limits of wafer-level photolithography tools. Next, instead of using a foundry CMOS process and bonding to the micro-LEDs, layers of silicon dioxide and silicon are deposited to form the active TFT films. Standard materials from nearly all LED suppliers can be used as the starting LED substrate, with the caveat that the maximum process temperature is limited to what the LEDs can withstand. Thus, the challenge is to build a high-performance low-temperature transistor process. This is achieved by using laser crystallization to convert the low-electron-mobility amorphous silicon to high-mobility polycrystalline silicon. This laser crystallization is similar to low-temperature polysilicon (LTPS) processes employed in flat-panel displays. Transistors are fabricated in the polycrystalline silicon to form the necessary display driving circuits. Figure 9 shows a cross section and top view of an integrated device.

While significant strides have been made with regard to micro-LED microdisplays, much work still remains to be done before commercial products reach the marketplace. The integration of color-generating materials is a challenge, although some work has been demonstrated in using an optical combination of three micro-LED microdisplays[16]; integration of phosphor materials[11]; and stacking of red-, green-, and blue-LED epitaxial layers.[15]

Another challenge for micro-LED microdisplays is the scalability of the integrated semiconductor processes. Flip-chip, LED epitaxial transfer to CMOS, and TFT methods all have unique factors that affect overall scalability and the ability to yield high-resolution displays. Overall, these factors will drive the associated costs and thus associated addressable markets.

Micro-LED microdisplay technologies all aim to address markets where small panels and high luminance are the primary requirement, the largest market being displays for augmented reality and mixed reality (AR/MR). Glasses-based devices for AR/MR require a microdisplay focused through a see-through optic that can be viewed in outdoor environments. This will require luminances well above 100,000 cd/m^2, luminance levels that only emissive micro-LED displays can provide. In addition to AR/MR, micro-LED microdisplays have been demonstrated in a wide range of applications, including projection formats[10,17] and light-field displays,[18] as well as non-display markets such as maskless photolithography,[19] optogenetics,[20] and visible-light communications.[21]

Micro-LEDs Will Maximize LED Usage

Today's consumer markets rely on LEDs as the illumination source for general lighting and nearly all displays. By extending the application of LEDs beyond illumination to directly emissive pixels, the specifications needed for next-generation displays can be satisfied. In this review, we categorized the activity within the micro-LED space by the two display-size regimes: direct-view displays (3–70 in.) which use pick-and-place technologies and microdisplays (< 2 in.) which use semiconductor integration technologies. While the science behind micro-LEDs is straightforward, the success of any particular technology will depend heavily on overcoming the unique engineering and manufacturing challenges associated with each technology. Once commercialized emissive LED displays have the ability to replace all displays and can span the entire size range from 0.5-in. microdisplays all the way up to a 1000-in. stadium displays.

References

[1]C. Bower, M. Meitl, S. Bonafede, and D. Gomez, "Heterogeneous Integration of Microscale Compound Semiconductor Devices by Micro-Transfer-Printing," *IEEE Electronic Components & Technology Conference*, 963–967 (2015).

[2]M. Meitl, E. Radauscher, S. Bonafede, D. Gomez, T. Moore, C. Prevatte, B. Raymond, B. Fisher, K. Ghosal, A. Fecioru, A. Trindade, D. Kneeburg, and C. Bower, "Passive Matrix

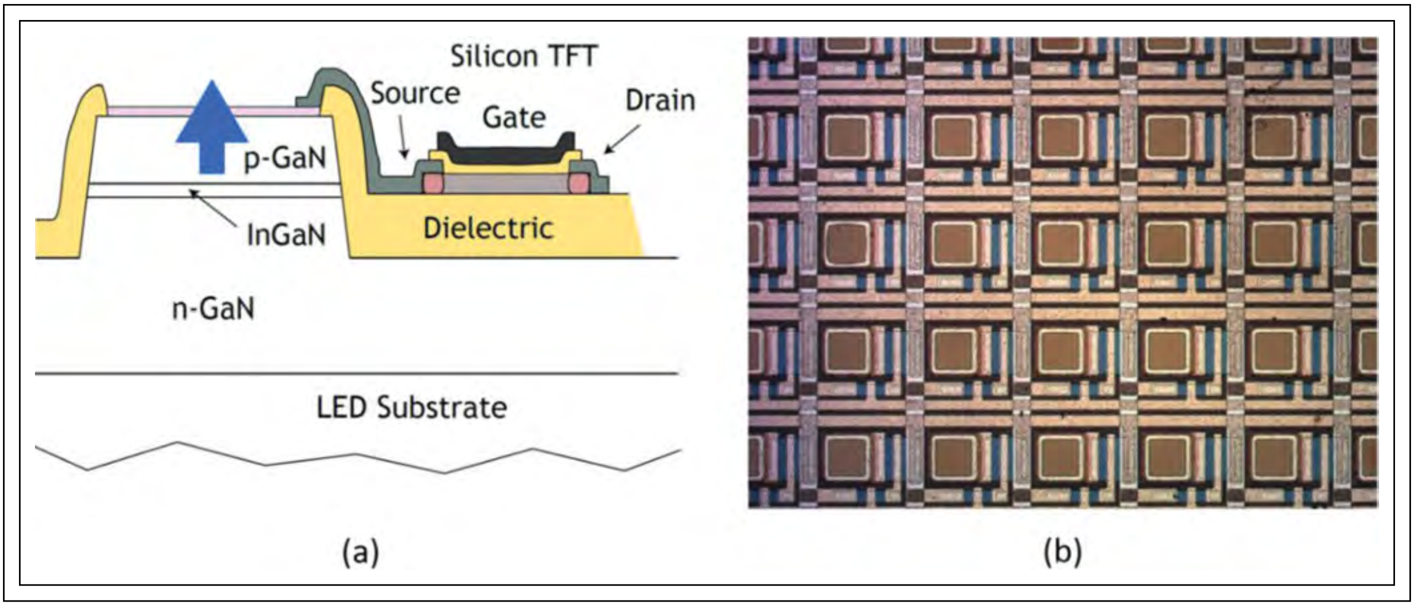

Fig. 9: (a) A schematic cross section of a micro-LED pixel is integrated with a thin-film silicon transistor. Image (b) shows a micrograph of a prototype active-matrix micro-LED microdisplay.[7]

Displays with Transfer-Printed Microscale Inorganic LEDs," *SID Digest of Technical Papers*, 743–746 (2016).
[3]https://blog.sony.com/press/sony-redefines-high-end-visual-display-technology-with-a-new-canvas-for-creativity/
[4]W. Henry and C. Percival, "ILED Displays: Next Generation Display Technology," *SID Digest of Technical Papers*, 747-750 (2016).
[5]H. W. Choi, C. W. Jeon, and M. D. Dawson, "High-Resolution 128 x 96 Nitride Microdisplay," *IEEE Electron Device Letters* **25**(5), 277–279 (2004).
[6]Z. Y. Fan, J. Y. Lin, and H. X. Jiang, "III-Nitride Micro-Emitter Arrays: Development and Applications," *J. Phys. D: Applied Physics* **41**, 094001 (2008).
[7]B. R. Tull, Z. Basaran, D. Gidony, A. B. Limanov, J. S. Im, I. Kymissis, and V. W. Lee, "High Brightness, Emissive Microdisplay by Integration of III-V LEDs with Thin Film Silicon Transistors," *SID Digest of Technical Papers*, 375–377 (2015).
[8]H.X. Zhang, D. Massoubre, J. McKendry, Z. Gong, B. Guilhabert, C. Griffin, E. Gu, P. E. Jessop, J. M. Girkin, and M. D. Dawson, "Individually-addressable flip-chip AlInGaN micropixelated light emitting diode arrays with high continuous and nanosecond output power," *Optics Express* **16**(13), 9918–9926 (2008).
[9]Z. J. Liu, W. C. Chong, K. M. Wong, and K. M. Lau, "360 ppi Flip-Chip Mounted Active Matrix Addressable Light Emitting Diode on Silicon (LEDoS) Micro-Displays," *J. Display Tech.* **9**(8), 678–682 (2013).
[10]C. W. Sun, C. H. Chao, H. Y. Chen, Y. H. Chiu, W.Y. Yeh, M. H. Wu, H. H. Yen, and C. C. Liang, "Development of Micro-Pixellated GaN LED Array Micro-Display System," *SID Digest of Technical Papers*, 1042–1045 (2011).
[11]J. Bonar, G. Valentine, Z. Gong, J. Small, and S. Gorton, "High-brightness low-power consumption microLED Arrays," *Proc. SPIE* **9768**, 97680Y (2016).
[12]J. Day, J. Li, D. Y. C. Lie, C. Bradford, J. Y. Lin, and H. X. Jiang, "III-Nitride full-scale high-resolution microdisplays," *Appl. Phys. Lett.* **99**, 031116 (2011).
[13]F. Marion, S. Bisotto, F. Berger, A. Gueugnot, L. Mathieu, D. Henry, F. Templier, and T. Catelain, "A Room Temperature Flip-Chip Technology for High Pixel Count Microdisplays and Imaging Arrays," *Proceedings of the IEEE 66th Electronic Components and Technology Conference*, 929–935 (2016).
[14]F. Templier, L. Dupré, S. Tirano, M. Marra, V. Verney, F. Olivier, B. Aventurier, D. Sarrasin, F. Marion, T. Catelain, F. Berger, L. Mathieu, B. Dupont, and P. Gamarra, "GaN-based Emissive Microdisplays: A Very Promising Technology for Compact, Ultra-High Brightness Display Systems," *SID Digest of Technical Papers*, 1013–1016 (2016).
[15]H. El-Ghoroury, C. Chuang, and Z. Alpaslan, "Quantum Photonic Imager (QPI): A Novel Display Technology that Enables more than 3D Applications," *SID Digest of Technical Papers*, 371–374 (2015).
[16]Z. J. Liu, W. C. Chong, K. M. Wong, K. H. Tam, and K. M. Lau, "A Novel BLU-Free Full-Color LED Projector Using LED on Silicon Micro-Displays," *IEEE Photonics Technologies Letters* **25**(23), 2267–2270 (2013).
[17]V. W. Lee and I. Kymissis, "A directly addressed monolithic LED array as a projection source," *J. Soc. Info. Display* **18**(10) (2010).
[18]Z. Alpaslan and H. El-Ghoroury, "Small Form Factor Full Parallax Tiled Light Field Display," *Proc. SPIE-IS&T*, 9391 (2015).
[19]B. Guilhabert, D. Massoubre, E. Richardson, J. McKendry, G. Valentine, R. Henderson, I. Watson, E. Gu, and M. Dawson, "Sub-Micron Lithography Using InGaN Micro-LEDs: Mask-Free Fabrication of LED Arrays," *IEEE Photonics Technology Letters* **24**(24), 2221–2224 (2012).
[20]V. Poher, N. Grossman, G. T. Kennedy, K. Nikolic, H. X. Zhang, Z. Gong, E. M. Drakakis, E. Gu, M. D. Dawson, P. M. W. French, P. Degenaar, and M. A. A. Neil, "Micro-LED arrays: a tool for two-dimensional neuron stimulation," *J. Phys. D: Appl. Phys.* **41**, 094014 (2008).
[21]J. McKendry, D. Massoubre, S. Zhang, B. Rae, R. Green, E. Gu, R. Henderson, A. Kelly, and M. Dawson, "Visible-Light Communications Using a CMOS-Controlled Micro-Light-Emitting-Diode Array," *IEEE J. Lightwave Technology* **30**(1), 61–67 (2012). ■